

THE OFFICIAL MAGAZINE OF THE OCEANOGRAPHY SOCIETY

Oceanography

VOL.33, NO.2, JUNE 2020

SPECIAL ISSUE ON

Paleoceanography

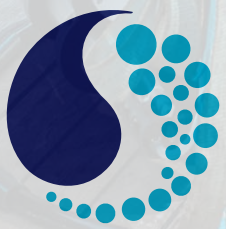
LESSONS FOR A CHANGING WORLD



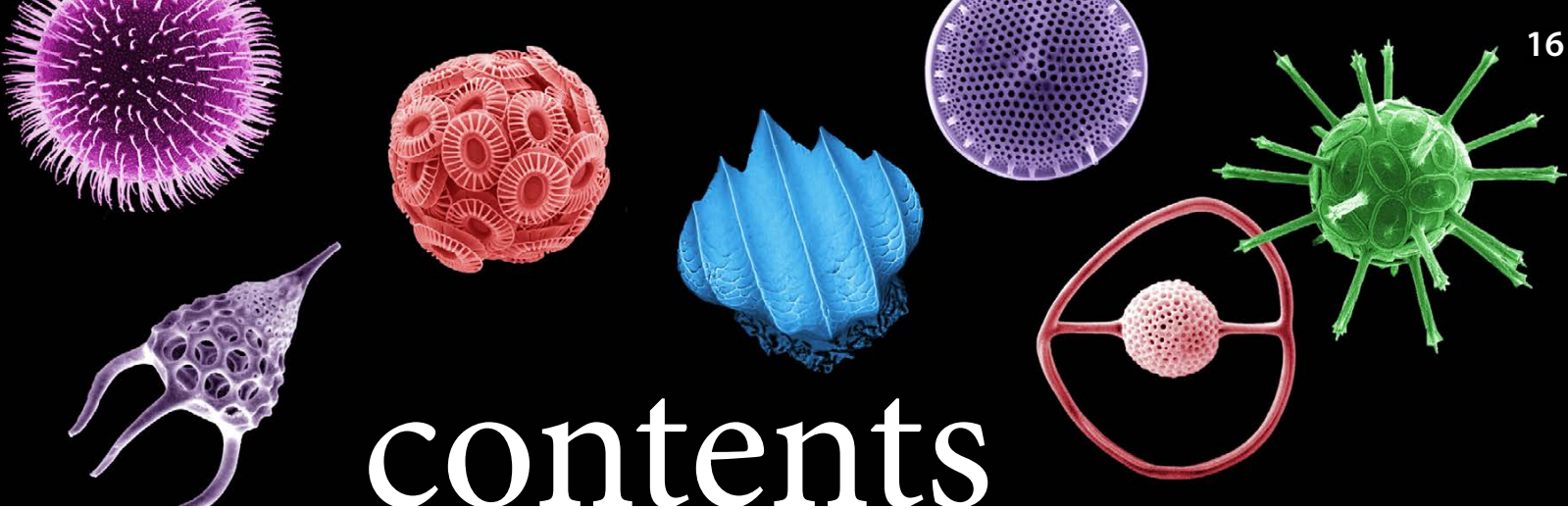
For decades, we have been committed to you and your work of advancing ocean science. That commitment remains—now more than ever.

We're here, and we're ready to partner in **accelerating the understanding of natural waters.**

Join us this October to dive deeper at:
seabird.com/training

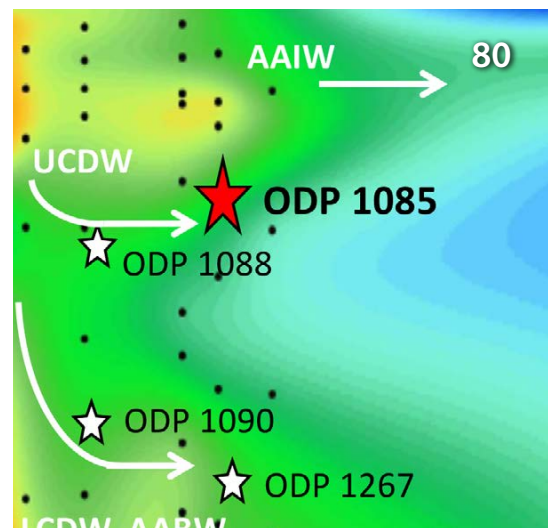
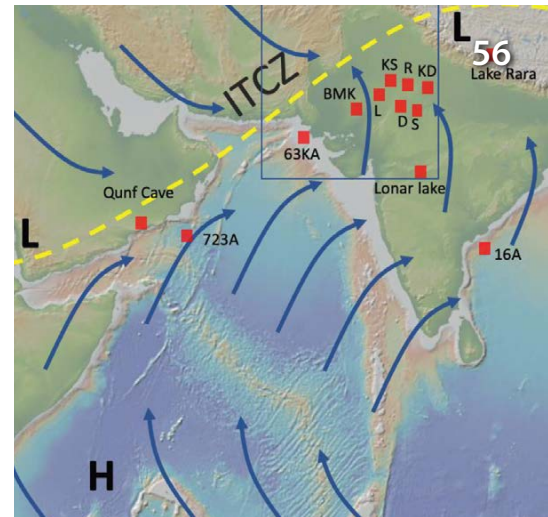


SEA-BIRD
SCIENTIFIC



**SPECIAL ISSUE ON PALEOCEANOGRAPHY:
LESSONS FOR A CHANGING WORLD**

- 13 INTRODUCTION TO THE SPECIAL ISSUE. Paleooceanography—
Lessons for a Changing World**
By A. Shevenell, P. Delaney, K. Meissner, L. Menviel, and A.C. Mix
- 16 Time Machine Biology: Cross-Timescale Integration of Ecology, Evolution,
and Oceanography**
By M. Yasuhara, H.-H.M. Huang, P. Hull, M.C. Rillo, F.L. Condamine, D.P. Tittensor,
M. Kučera, M.J. Costello, S. Finnegan, A. O’Dea, Y. Hong, T.C. Bonebrake,
N.R. McKenzie, H. Doi, C.-L. Wei, Y. Kubota, and E.E. Saupe
- 29 Sidebar | On Quantifying Stratigraphic, Chronologic, and Paleo Flux
Uncertainties in Paleooceanography**
By A.C. Mix
- 32 Ancient Sea Level as Key to the Future**
By K.G. Miller, W.J. Schmelz, J.V. Browning, R.E. Kopp, G.S. Mountain, and J.D. Wright
- 42 Sidebar | Boron Isotopes Provide Insights into Biomineralization,
Seawater pH, and Ancient Atmospheric CO₂**
By J.G.M. Crumpton-Banks and J.W.B. Rae
- 44 Linkages Between Dynamic Phytoplankton C:N:P and the Ocean Carbon
Cycle Under Climate Change**
By K. Matsumoto, T. Tanioka, and R. Rickaby
- 53 Sidebar | Direct Measures of the Vigor of Ocean Circulation via Particle
Grain Size**
By N. McCave
- 56 Regional Character of the “Global Monsoon”: Paleoclimate Insights from
Northwest Indian Lacustrine Sediments**
By Y. Dixit
- 65 Sidebar | Illuminating the Past to See the Future of Western Boundary
Currents: Micropaleontological Investigations of the Kuroshio
Current Extension**
By A.R. Lam, R.M. Leckie, and M.O. Patterson
- 68 Extending the Instrumental Record of Ocean-Atmosphere Variability into
the Last Interglacial Using Tropical Corals**
By T. Felis
- 80 Reconstruction of Ocean Circulation Based on Neodymium
Isotopic Composition: Potential Limitations and Application to the
Mid-Pleistocene Transition**
By K. Tachikawa, W. Rapuc, Q. Dubois-Dauphin, A. Guihou, and C. Skonieczny



CONTACT US

The Oceanography Society
1 Research Court, Suite 450
Rockville, MD 20850 USA
t: (1) 301-251-7708
f: (1) 301-251-7709
info@tos.org

HAVE YOU MOVED?

Send changes of address to info@tos.org or go to <https://tosmc.memberclicks.net>, click on Login, and update your profile.

ADVERTISING INFO

Please send advertising inquiries to info@tos.org or go to <https://tos.org/oceanography/advertise>.

CORRECTIONS

Please send corrections to magazine@tos.org. Corrections will be printed in the next issue of *Oceanography*.

SPECIAL ISSUE SPONSOR

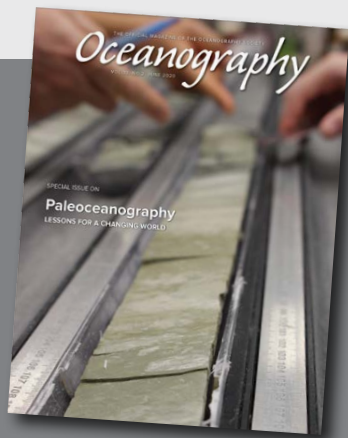
Production of this issue of *Oceanography* was supported by National Science Foundation grant OCE-1912795.

SPECIAL ISSUE GUEST EDITORS

Amelia Shevenell, University of South Florida
Peggy Delaney, UC Santa Cruz
Katrin Meissner, University of New South Wales
Laurie Menviel, University of New South Wales
Alan Mix, Oregon State University

DIY OCEANOGRAPHY GUEST EDITORS

Melissa Omand, University of Rhode Island
Emmanuel Boss, University of Maine



ON THE COVER

A split core set for examination in the D/V *JOIDES Resolution* core laboratory during International Ocean Discovery Program (IODP) Expedition 354: Neogene and Late Paleogene Record of Himalayan Orogeny and Climate: A Transect Across the Middle Bengal Fan. *Photo credit: Petra Dekens and IODP*

88 Sidebar | Amundsen Sea Coastal Ice Rises: Future Sites for Marine-Focused Ice Core Records

By P. Neff

90 The Antarctic Ice Sheet: A Paleoclimate Modeling Perspective

By E.G.W. Gasson and B.A. Keisling

101 Sidebar | The Mid-Pleistocene Enigma

By H.L. Ford and T.B. Chalk

104 Archaeal Membrane Lipid-Based Paleothermometry for Applications in Polar Oceans

By S. Fietz, S.L. Ho, and C. Huguet

115 Sidebar | Diatoms as Sea Ice Proxies

By A. Leventer

116 The Potential of Sedimentary Ancient DNA to Reconstruct Past Ocean Ecosystems

By L.H. Armbrecht

124 Sidebar | A Memory of Ice: The Antarctic Voyage of the *Glomar Challenger*

Reviewed by P.N. Webb and P.J. Barrett

REGULAR ISSUE FEATURES

126 The Origins of Oceanography in France: The Scientific Expeditions of *Travailleur* and *Talisman* (1880–1883)

By J.R. Dolan

134 How Do Advisor Assessments of Diverse Undergraduate Researchers Compare with the Students' Self-Assessments? And What Does This Imply for How We Train and Assess Students?

By B.C. Bruno, C. Heu, and G. Weyenberg

144 Deep Ocean Passive Acoustic Technologies for Exploration of Ocean and Surface Sea Worlds in the Outer Solar System

By R. Dziak, D. Banfield, R. Lorenz, H. Matsumoto, H. Klinck, R. Dissly, C. Meinig, and B. Kahn

DEPARTMENTS

05 QUARTERDECK. Oceanography During the COVID-19 Pandemic

By E.S. Kappel

06 FROM THE PRESIDENT. Ocean Science During the Corona Virus Pandemic: Challenges and Opportunities

By M. Visbeck

08 COMMENTARY. Strategies for Running a Successful Virtual Career Panel

By J. Barr, C. Bean, and J. McDonnell

10 RIPPLE MARKS. Good News Fish Story

By C.L. Dybas

156 DIY OCEANOGRAPHY. The Pressure of In Situ Gases Instrument (PIGI) for Autonomous Shipboard Measurement of Dissolved O₂ and N₂ in Surface Ocean Waters

By R.W. Izett and P.D. Tortell

163 THE OCEANOGRAPHY CLASSROOM. Project EDDIE: Using Real Data in Ocean Science Classrooms

By D. Soule

165 CAREER PROFILES. Stephanie Wear, Senior Scientist and Strategy Advisor, Global Science, The Nature Conservancy • Kim I. Martini, Senior Oceanographer, Sea-Bird Scientific

168 TRIBUTE. A Tribute to Thomas B. Sanford (1940–2020)

By E. Kunze and R.-C. Lien

The Oceanography Society was founded in 1988 to advance oceanographic research, technology, and education, and to disseminate knowledge of oceanography and its application through research and education. TOS promotes the broad understanding of oceanography, facilitates consensus building across all the disciplines of the field, and informs the public about ocean research, innovative technology, and educational opportunities throughout the spectrum of oceanographic inquiry.

OFFICERS

PRESIDENT: Martin Visbeck
PRESIDENT-ELECT: Andone Lavery
PAST-PRESIDENT: Alan C. Mix
SECRETARY: Allison Miller
TREASURER: Susan Banahan

COUNCILORS

AT-LARGE: Richard Crout
APPLIED TECHNOLOGY: Larry Mayer
BIOLOGICAL OCEANOGRAPHY: Charles H. Greene
CHEMICAL OCEANOGRAPHY: Galen McKinley
EDUCATION: Carolyn Scheurle
GEOLOGICAL OCEANOGRAPHY: Amelia Shevenell
PHYSICAL OCEANOGRAPHY: Magdalena Andres
STUDENT REPRESENTATIVE: Christina Hernández

EXECUTIVE DIRECTOR

Jennifer Ramarui

CORPORATE AND INSTITUTIONAL MEMBERS

BAKER DONELSON
» <https://www.bakerdonelson.com>

INTEGRAL CONSULTING INC.
» <https://www.integral-corp.com/>

METOCEAN SOLUTIONS
» <https://www.metocean.co.nz/>

SCIENCE MEDIA
» <http://sciencemedia.nl/>

SEA-BIRD SCIENTIFIC
» <https://sea-birdscientific.com>

SEQUOIA
» <http://www.sequoiasci.com/>

SUBMARINE CABLE SALVAGE
» [https://www.oceannetworks.com/
submarine-cable-salvage](https://www.oceannetworks.com/submarine-cable-salvage)

TELEDYNE RD INSTRUMENTS
» <http://www.teledynemarine.com/rdi>

US ARCTIC RESEARCH COMMISSION
» <https://www.arctic.gov>

EDITOR

Ellen S. Kappel
Geosciences Professional
Services Inc.
ekappel@geo-prose.com

ASSISTANT EDITOR

Vicky Cullen
vcullen@whoi.edu

DESIGN/PRODUCTION

Johanna Adams
johanna-adams@cox.net

ASSOCIATE EDITORS

Claudia Benitez-Nelson
University of South Carolina
cbnelson@geol.sc.edu

Ian Brosnan
NASA Ames Research Center
ian.g.brosnan@nasa.gov

Grace Chang
Integral Consulting Inc.
gchang@integral-corp.com

Margaret L. (Peggy) Delaney
University of California, Santa Cruz
delaney@ucsc.edu

Philip N. Froelich
Duke University
froelich@magnet.fsu.edu

Charles H. Greene
Cornell University
chg2@cornell.edu

William Smyth
Oregon State University
smyth@coas.oregonstate.edu

Kiyoshi Suyehiro
Yokohama Institute for Earth Sciences
JAMSTEC
suyehiro@jamstec.go.jp

Peter Wadhams
University of Cambridge
p.wadhams@damtp.cam.ac.uk

Oceanography contains peer-reviewed articles that chronicle all aspects of ocean science and its applications. The journal presents significant research, noteworthy achievements, exciting new technology, and articles that address public policy and education and how they are affected by science and technology. The overall goal of *Oceanography* is cross-disciplinary communication in the ocean sciences.

Oceanography (ISSN 1042-8275) is published by The Oceanography Society, 1 Research Court, Suite 450, Rockville, MD 20850 USA. *Oceanography* articles are licensed under a Creative Commons Attribution 4.0 International License, which permits use, sharing, adaptation, distribution, and reproduction in any medium or format as long as users cite the materials appropriately, provide a link to the Creative Commons license, and indicate the changes that were made to the original content. Third-party material used in articles are included in the Creative Commons license unless indicated otherwise in a credit line to the material. If the material is not included in the article's Creative Commons license, users will need to obtain permission directly from the license holder to reproduce the material. Please contact Jennifer Ramarui at info@tos.org for further information.

Join TOS

**Make connections,
advance your career,
enrich your research**

The Oceanography Society (TOS) was founded in 1988 to encourage collaboration and innovation among ocean scientists worldwide and across subdisciplines. The Society continues to support this community through publishing *Oceanography* magazine, convening scientific conferences, and recognizing major achievements in ocean sciences through the TOS Honors Program. TOS is fully committed to nurturing the next generation of ocean scientists through mentoring, providing leadership opportunities, and disseminating student-curated newsletters that highlight student members, provide links to resources, and announce opportunities.

The membership period is January 1 through December 31 of each year. Upon joining, new members will receive access to all back issues of *Oceanography* published during this membership period.

Membership Options

Regular Membership [\$70]. Available to oceanographers, scientists, or engineers active in ocean-related fields, or to persons who have advanced oceanography by management or other public service.

Student Membership [Free!]. Available for students enrolled in an oceanography or ocean-related program at the baccalaureate or higher level.

Early Career Membership [\$30]. Available to non-student oceanographers, scientists, or engineers active in ocean-related fields, or to persons who have advanced oceanography by management or other public service who have received their highest degree within the past three years.

Sponsoring Membership [\$125]. Available to individuals who wish to provide enhanced support annually. In the United States, \$50 of the annual dues in this category is tax-deductible as a charitable contribution as are any additional contributions, over and above the annual regular membership dues.

Call for Corporate and Institutional TOS Members

[Starting at \$300] TOS invites all corporate or nonprofit organizations interested in the ocean sciences to join as members in this category. Membership benefits include:

- An active link from the TOS website to the organization's website
- Complimentary inclusion of one quarter-page ad in *Oceanography* magazine
- Organization's name and contact information included in each issue of *Oceanography*
- Discounted rates for employment opportunity postings in the TOS Jobs Center
- Fifteen percent discount on advertising in *Oceanography*

For more information, go to:

<https://tos.org/corporate-and-institutional-members>

**Visit <https://tos.org> and click on join TOS
to complete your application!**

Oceanography During the COVID-19 Pandemic

More than a few years ago, while juggling her young children and her career, Carole King sang, “my baby’s in one hand, I’ve a pen in the other.” Scientists who have been forced by the COVID-19 pandemic to abandon laboratories and classrooms to work and teach from home would surely nod in agreement, even if they might tweak the lyric to substitute a keyboard for a pen.

During the pandemic, *Oceanography* has largely been able to continue operations as usual. The magazine was decades ahead of its time in adopting concepts such as “home office” and “distributed workforce”—before those terms even existed—so unlike other enterprises, we didn’t need to adjust to working remotely. The commitment of June issue authors, reviewers, and guest editors, despite the great disruptions to their lives since March, has allowed us to continue publishing, although on a delayed schedule. *Oceanography* has compensated for the delay by putting all of the special issue articles on its website as early releases as they were completed rather than waiting for full publication of the special issue. This policy will continue indefinitely.

While the most visible short-term consequence for *Oceanography* has been publication delays for special issues that were already in the works, behind the scenes, the development of future special issues is at risk. In-person conferences, workshops, and meetings—the venues where special issues are often conceived and launched—are being canceled, postponed, or conducted virtually. As a result, over the next year or two at least, it is possible that we will publish fewer special issues based on specific scientific themes or programs, the foundation of the magazine. Shortened and/or delayed field seasons may also have an impact on the timing of some potential future special issues. The long-term impact for *Oceanography* of publishing fewer special issues is not yet clear.

The news isn’t all bad. There has been a healthy uptick in the number of unsolicited manuscripts submitted to our regular issue feature and commentaries sections. Right now, we are particularly interested in sharing in *Oceanography* successful strategies for virtual classroom teaching and laboratory activities (in the broadest sense) and for conducting virtual workshops and meetings. Please consider submitting a short article to us (author guidelines at <https://tos.org/oceanography/guidelines>).

I wish everyone good health in these challenging times.



Ellen S. Kappel, Editor

Oceanography

UPCOMING
SPECIAL ISSUES

**Marine Biodiversity
Observation Network:
An Observing System for
Life in the Sea**

**Understanding the Effects
of Offshore Wind Energy
Development on Fisheries**

**GoMRI:
Gulf of Mexico Oil Spill
& Ecosystem Science
2010–2020**

<https://tos.org/oceanography>

CALL FOR IDEAS!

Do you have an idea for a special issue of *Oceanography*? Please send your suggestions to Editor Ellen Kappel at ekappel@geo-prose.com.

Ocean Science During the Corona Virus Pandemic

CHALLENGES AND OPPORTUNITIES

At the beginning of 2020, the World Health Organization announced the outbreak of a new corona virus—SARS-Cov-2—in China. At the time, public health experts issued warnings about the possibility of global pandemic and that the virus that caused the human disease COVID-19 can lead to serious health issues. It was not clear then if the virus outbreak could be contained and remain a regional challenge as similar virus outbreaks during the last decade have suggested. The oceanographic community did not take much note or prepare itself. In late January, I attended the annual meeting of the Partnership for Observation of the Global Ocean (POGO) in Qingdao, China. Many of us left there worried about the local virus situation in China, but not really considering that we all would be in the middle of it six months later. In early February, the three societies that organize the Ocean Sciences Meeting decided to waive the registration fees for attendees from China because the SARS-Cov-2 outbreak was considered a hardship on the participants. However, no measures were taken at the Ocean Sciences Meeting in San Diego to prevent the potential spreading of the virus. Today, we know that the virus was already spreading throughout the US West Coast by then. No reports of virus spreading at the Ocean Sciences Meeting in San Diego reached the organizers. We might have just gotten lucky.

In March, the situation changed rapidly in the Western world. While Asian countries applied their lessons learned during previous virus outbreaks, Europe and North America seemed less concerned and not well prepared. By mid-March, drastic measures such as travel bans and social distancing were implemented. Almost all ocean science was taken “online” and moved to “work from home” operations. Many oceanographic laboratories were closed to visitors, and only essential services were retained. Research vessels around the globe could not exchange crews in foreign ports, and most were called back to their home country base. Dramatic situations emerged, and personal hardships for those at sea and in the field emerged. People spent prolonged times at sea, and return travel options remained uncertain for those far away from home.

With severe restrictions on international travel and stringent health safety measures implemented for seagoing operations, it seemed the tide had turned in favor of robotic systems exploring the ocean. At the end of April, the Global Ocean Observing System (GOOS) community launched a survey on the impacts of the corona pandemic on the global ocean observing system

(Heslop et al., 2020). It became clear that most of the robotic systems used in ocean science need human support from research vessels for deployment and/or servicing equipment. The GOOS survey revealed significant system shortfalls, and further impact is expected as the pandemic prevails. “Despite its significant impacts on the ocean observing system, the COVID-19 crisis can also be an opportunity for us to look at how to build greater resilience into the system,” argues Toste Tanhua from GEOMAR, Co-Chair of the Global Ocean Observing System. “The impacts of Covid-19 have brought to light the inter-reliance of systems and some clear weak points that we can now work on to increase system efficiency and robustness.”

More recently, epidemiologists and public health experts are suggesting that the corona virus pandemic will be around for quite some time and may only be curtailed by a successful vaccine not yet on the horizon. Thus, complex ocean field campaigns have been delayed for at least one year because crew exchanges in foreign ports are essentially impossible. Moreover, health concerns on research vessels, especially from exchanging scientists, have resulted in scaled back operations. Germany, for example, called all its ocean-going research vessels back home in March, then almost immediately permitted operations with reduced science crews. Single cabin occupancy and quarantine and virus testing upfront are now their standard procedure. For the time being, all expeditions have to start and end in Germany. Similar arrangements are reported for some other countries, but many have canceled all large seagoing expeditions with an unknown restart date. Long-distance operations to the South Atlantic, Pacific, and Indian Oceans have been postponed, and the Antarctic field season has been canceled by most nations.

Despite many hardships and setbacks, there are some noteworthy developments and opportunities. First, addressing the global corona virus pandemic requires global cooperation. The same is true for addressing the downturn of “ocean health” and dealing with climate change or the loss of species and biodiversity. The need to work together is apparent and hopefully brings back more global sharing and collaboration. Second, by necessity, we have to conduct most of our teaching virtually. In-person meetings and science conferences have been postponed or reconfigured to online formats. In principle, these changes should spur more equitable and inclusive participation around the globe, reduce scientific travel, and lead to a reevaluation of the way in which we, as scientists, communicate, collaborate, and engage.

These challenging times provide a welcome opportunity for reflection. We are rapidly learning new formats to strengthen and even accelerate global engagement in ocean sciences. However, not all sectors of the ocean science community have the same level of access, abilities, choices, and resilience. Those with stable job situations can weather a pandemic more easily than those on short-term contracts. Those who live in parts of the world where the ability to cope with the pandemic is limited, there is no reliable Internet access, and resources are already scarce for conducting ocean science research are seeing their possibilities rapidly declining. A similar level of inequality is found within the research communities. Those who rely on field- or lab-based science are more affected by the pandemic than those who primarily analyze existing data, do theoretical work, or use ocean model simulations. Recent publications show that the pandemic has disproportionately affected women and those from less-privileged situations (e.g., Myers et al., 2020).

For The Oceanography Society, the pandemic has highlighted the need to reflect on our Society's values. The current, past, and future presidents recently reaffirmed the TOS values (<https://tos.org/diversity>) and committed to ensure that TOS increases its efforts to address issues such as toxic and non-supportive work climates, the lack of role models, a lack of a sense of belonging, and non-alignment of promotion and tenure incentives with aspirations of women and underrepresented minorities in the ocean sciences around the world. We are about to launch a TOS Justice, Equity, Diversity, and Inclusion Committee to develop actions. At the same time, we are evaluating our Society's financial resilience and exploring new ways to increase and diversify income streams. We welcome any suggestions and opportunities you might want to bring to TOS.

Finally, we are looking forward to the launch of the UN Decade of Ocean Science for Sustainable Development with its mission: "Transformative ocean science solutions for sustainable development, connecting people and our ocean." The future of ocean sciences will be more collaborative, more international, more digital, and more inclusive as we build back from the setback of the pandemic to become more resilient and sustainable.



Martin Visbeck, TOS President

REFERENCES

- Heslop, E., A. Fischer, T. Tanhua, D. Legler, M. Belbeoch, M. Kramp, and V. Lindoso. 2020. Covid-19's impact on the ocean observing system and our ability to forecast weather and predict climate change. Briefing note, Global Ocean Observing System, Intergovernmental Oceanographic Commission of UNESCO, June 29, 2020, https://www.gooscean.org/index.php?option=com_oe&task=viewDocumentRecord&docID=26920.
- Myers, K.R., W.Y. Tham, Y. Yin, N. Cohodes, J.G. Thursby, M.C. Thursby, P. Schiffer, J.T. Walsh, K.R. Lakhani, and D. Wang. 2020. Unequal effects of the COVID-19 pandemic on scientists. *Nature Human Behaviour*, <https://doi.org/10.1038/s41562-020-0921-y>.

THE OCEANOGRAPHY SOCIETY'S HONORS PROGRAM

One of the most meaningful aspects of being a member of The Oceanography Society (TOS) is the opportunity to recognize and celebrate our colleagues' accomplishments. Please take this opportunity to recognize a colleague, mentor, team, or peer for their exceptional achievements and contributions to the ocean sciences.

**DON'T MISS THE
NOVEMBER 15, 2020
NOMINATION DEADLINE FOR**

TOS FELLOWS PROGRAM

Recognizing individuals who have attained eminence in oceanography through their outstanding contributions to the field of oceanography or its applications

TOS EARLY CAREER AWARD

For having demonstrated extraordinary scientific excellence and the potential to shape the future of oceanography

TOS MENTORING AWARD

For excellence and/or innovation in mentoring the next generation of ocean scientists

OCEAN OBSERVING TEAM AWARD

Recognizing teams for innovation and excellence in sustained ocean observing for scientific and practical applications





STRATEGIES FOR RUNNING A SUCCESSFUL VIRTUAL CAREER PANEL

By Janine Barr, Christine Bean, and Janice McDonnell

ABOVE. Screenshots of students participating in the Rutgers virtual REU experience.

As part of an eight-week virtual Research Experiences for Undergraduates (REU) program, oceanographers and outreach specialists at Rutgers, the State University of New Jersey, conducted a Virtual Marine Science Career Panel (Ocean Data Labs, 2020). Instead of canceling summer REU programs across the United States (NSF, 2020b), the National Science Foundation (NSF) supported and encouraged academic leadership to develop virtual programming in keeping with each institution's organizational policies concerning the pandemic (NSF, 2020a). Here, we highlight facilitation strategies for running a successful virtual career panel as well as lessons learned that may serve as inspiration for others working to create similar virtual experiences in their own REU programs and beyond.

FACILITATION STRATEGY: USING ONLINE TOOLS AND BUILDING MENTOR-MENTEE RELATIONSHIPS VIRTUALLY

The Rutgers team invited six marine science professionals from around the United States to participate in the Virtual Marine Science Career Panel. They represented careers from the education and outreach, federal government, industry,

nonprofit, research, and state government sectors. To maximize the time students had to interact with each panelist in the limited virtual environment, the one-hour panel was structured differently than a traditional career panel where panelists summarize their work trajectories and then respond to questions. Here, the Rutgers team adopted a structure that matched small groups of students with panelists to help make the virtual environment as conversational as possible and foster meaningful connections between students and panelists. This structure was implemented using the video breakout room feature in Zoom Meetings available through a paid Pro account.

To match students with panelists, the Rutgers team asked each panelist to complete a questionnaire prior to the virtual event (see online supplemental materials). The seven questions presented were geared toward understanding the panelists' career paths and how their backgrounds in marine science brought them to their current positions. Students were provided the completed questionnaires a couple days in advance of the panel and were asked to provide feedback to the Rutgers team on their priorities regarding whom they wished to speak with in the

small breakout sessions. Students submitted their rankings through a short survey created for free using Google Forms.

The panel itself began with the panelists providing brief overviews of their career disciplines. The panelists were then placed in breakout rooms where they each interacted with three different groups of two to three students for periods of 13 minutes. With 15 participants, each student got to interact with three panelists (Figure 1). Once the three breakout sessions had concluded, all the panelists and students returned to the main Zoom room for concluding remarks. For additional details regarding the logistics of the panel, please contact the authors.

KEY INGREDIENTS FOR THE VIRTUAL MARINE SCIENCE CAREER PANEL

The Rutgers team has identified three key ingredients that helped make this Virtual Marine Science Career Panel a success.

1. **Recruiting panelists from a wide geographic range.** An advantage of running a virtual career panel was that the Rutgers team was able to invite professionals who work in geographically distant locations (e.g., Houston, Texas, and Washington, DC) and

who represent a more diverse range of career paths and experiences than would be possible for a one-hour in-person panel.

2. Engaging panelists and students before the panel using a standardized questionnaire.

Instead of preparing slides or formal introductory remarks, each panelist was asked to fill out a standardized questionnaire nine days prior to the panel (see online supplementary materials). The questionnaires were shared with the students two days prior to the panel, allowing them to make informed choices about which panelist they wanted to speak with, and there was more time to engage with each panelist because introductory remarks were not extensive.

3. Setting up smaller conversations using breakout rooms.

Panelists and students provided positive feedback regarding the structure of the virtual career panel's breakout rooms. Each 13-minute breakout session yielded unique conversations focused on that smaller group of students' interests. This structure also offered an opportunity for students to build their pro-

fessional networks. It provided each student with a personal connection to a panelist, helping the student see that panelist's career path as more attainable.

LESSONS LEARNED

While the Virtual Marine Science Career Panel was largely a success at Rutgers, we offer several additional considerations that would improve similar career panels conducted at other institutions.

If the virtual career panel is one component of a longer online program, institutions may benefit from creating a list of "norms" with their students to help them feel more comfortable in a new virtual space and to provide a sense of community (KONU, 2020). Norms here refer to online etiquette that students and their instructors can brainstorm and agree to follow together (e.g., deciding if everyone should always have their video on, or if calling in is okay, and committing to ending each session on time). It may be helpful to designate funds for purchasing Wi-Fi hotspots to distribute to students who do not have access to high-speed Internet. The availability of hotspots

facilitates the students' use of video conferencing and helps them fully participate in the virtual experience. Finally, consider holding a virtual career panel for at least one hour and 15 minutes when following the structure discussed above. A slightly longer time devoted to a career panel would ensure sufficient time to move students between breakout rooms without compromising their time with each panelist.

Although it was only a small part of the eight-week summer REU program at Rutgers, the successful implementation of our virtual career panel can be used as a template for other career panels in the ocean sciences, whether associated with REUs, large conferences, university alumni programs, or scientific societies. 📍

ONLINE SUPPLEMENTARY MATERIALS

The supplementary materials are available online at <https://doi.org/10.5670/oceanog.2020.220>.

REFERENCES

KONU. 2020. *Enabling Humanity on Zoom—How to Facilitate Deep Learning Virtually*. <https://konu.org/blog-en/2020/3/16/enabling-humanity-on-zoom-how-to-facilitate-deep-learning-virtually>.

NSF (National Science Foundation). 2020a. *Frequently Asked Questions (FAQs) About the Coronavirus Disease 2019 (COVID-19) for Research Experiences for Undergraduates (REU) Sites, Research Experiences for Teachers (RET) Sites, International Research Experiences for Students (IRES) Sites, and Similar Activities*. https://www.nsf.gov/bfa/dias/policy/covid19/covid19faqs_reu.pdf.

NSF. 2020b. *Research Experiences for Undergraduates (REU)*. https://www.nsf.gov/funding/pgm_summ.jsp?pims_id=5517.

Ocean Data Labs. 2020. *Data Labs 2020 Virtual Research Experience for Undergraduates (REU)*. <https://datalab.marine.rutgers.edu/2020-virtual-reu/>.

ACKNOWLEDGMENTS

The authors would like to thank the students and mentors for their participation, Lisa Auermuller, and their fellow Rutgers team members for making this program a reality: Josh Kohut, Sage Lichtenwalner, Daphne Munroe, and Anthony Vastano. This project was funded by National Science Foundation Grant No. OCE-1831625.

AUTHORS

Janine Barr (jmb883@hsrl.rutgers.edu) is a graduate student pursuing a master of science degree in oceanography at Rutgers University and is a trainee in the Rutgers Coastal Climate Risk and Resilience Program. **Christine Bean** (bean@marine.rutgers.edu) is STEM Program Administrator at Rutgers University. **Janice McDonnell** (mcdonnel@marine.rutgers.edu) is a STEM agent in the Department of Youth Development, and Associate Professor, Rutgers Cooperative Extension, Rutgers University.

Timeslot	4:00 – 4:10pm	4:10 – 4:23pm	4:23 – 4:36pm	4:36 – 4:49pm	4:49 – 5:00pm
Main Zoom Room					
Breakout Room One					
Breakout Room Two					
Breakout Room Three					
Breakout Room Four					
Breakout Room Five					
Breakout Room Six					
Floating Between Breakout Rooms					

FIGURE 1. Locations of the Rutgers team (gray boxes, n = 3), panelists (orange boxes, n = 6), and students (blue boxes, n = 15) as they participated in the Virtual Marine Science Career Panel. Each box represents a unique individual. The panel began at four in the afternoon with 10 minutes of introductory remarks, followed by three 13-minute breakout sessions, and 11 minutes for concluding remarks. Panelists remained in their breakout rooms for the three breakout sessions, and the students were moved between rooms. Two Rutgers team members remained in the main Zoom meeting room to coordinate moving students to their assigned breakout rooms while the third team member moved between breakout rooms to ensure there were no technical difficulties or other issues.

Good News Fish Story

By Cheryl Lyn Dybas

It's a fish story with a happy ending. At least for now.

On the US West Coast, the Dungeness crab (*Cancer magister*) fishery supports a valuable annual harvest of seafood. And, year after year, it's a fishery that keeps on giving.

In the last few decades, fishers from California to Washington have caught almost all available legal-size male Dungeness crabs each season. Yet, the crab population has remained stable or increased, according to a new population estimate of US West Coast Dungeness stocks.

"Catches and abundance, in central California especially, are increasing," said Kate Richerson, a researcher at NOAA's Northwest Fisheries Science Center in Seattle. "There's reason to be optimistic that this fishery will continue to be one of the most productive on the West Coast." Richerson is the lead author of a paper published in February in the journal *Fisheries Research*.

Other studies have suggested that, in the future, ocean acidification and climate change could impact the West Coast's signature shellfish. That's a concern, Richerson said, but the group's work didn't detect obvious signs of population-level impacts—yet.

FROM EELGRASS BED TO MARKET

Dungeness crabs live in eelgrass beds and other benthic habitats along the west coast of North America. They range from Unalaska, Alaska, to Santa Barbara County, California. Scientists think that all Dungeness crabs on the contiguous US West Coast are one evolutionary population.

The crabs play an important role in the California Current ecosystem as predators of bivalves and other benthic species, and as prey, with megalopae (the last larval stage) important in the diets of rockfish, salmon, and other fish, write Gilbert Pauley et al. in *Species profiles: Life histories and environmental requirements of coastal fishes and invertebrates (Pacific Northwest): Dungeness crab*. According to Pauley, eight coho salmon feasted on a combined 1,061 megalopae. A single fish consumed another 1,500 megalopae.

In Washington State waters, megalopae are most abundant in May and June. In Oregon, they peak in April and May. Larval development begins later moving north.

After molting into juveniles, the tiny crabs hitch rides on ocean bottom currents into estuaries, where they remain for 11 to 15 months. Dungeness crab growth proceeds in steps through a series of molts. At about four years old, most adult Dungeness males are market size.

A PRIZED FISHERY

Dungeness crabs have been commercially harvested since the mid-1800s and today are one of the most profitable fisheries on the West Coast. They are caught in circular steel traps called pots that are baited with squid or razor clams. The average crab boat fishes 300 to 500 pots set in depths up to 180 m. After the pots are retrieved, crabs are kept alive in circulated seawater until they are delivered to shore-based processing plants.

In recent years, total West Coast Dungeness crab revenues have exceeded 200 million USD. "While *C. magister* landings have generally been trending upward since the 1980s," Richerson et al. report, "it is unknown whether this is due to increased [fishing] effort, changes in abundance, or both."

The researchers estimated pre-season abundance of the coastal population of legal-size male Dungeness crabs from 1970 to 2016 in California, and from 1982 through 2016 in Washington and Oregon. They found that the fishery takes 9% to 98% of the legal-size male population each year, averaging 66%.

Despite that high rate of exploitation, pre-season abundance appears to be stable or increasing in all areas, the biologists say. In central California, abundance rapidly increased over the past decade after

Lone Dungeness crab on an Oregon beach at low tide. Dungeness crabs usually travel less than 16 km. Larvae can be transported up to 6 km offshore before returning to near-shore waters or estuaries as juveniles. Credit: [iStock.com/Claudia_Kuenkel](https://www.iStock.com/Claudia_Kuenkel)





(above) A beached by-the-wind sailor (*Velella velella*). *Velella* may help ferry Dungeness crab megalopae (the last larval stage) from place to place and offer protection from predation. Credit: Evan Baldonado/AquariumKids.com (right) Live Dungeness crabs for sale at a Seattle market. Credit: iStock.com/Maxvis



a long period of low numbers. From 1950 to 1980, catches in northern California, Oregon, and Washington followed decadal cycles. Catches in central California also fluctuated. Since 1980, central California “landings don’t appear to have a strong periodicity,” the researchers found.

Some scientists believe the change could be linked with an increase in the crab fishing fleet’s capacity. But Richerson and colleagues say that “environmental and biological factors, rather than harvest, are the most likely drivers.”

Those drivers include the El Niño-Southern Oscillation, the Pacific Decadal Oscillation, and the timing of the spring transition. The spring transition, an annual shift of coastal winds and currents, is linked to the number of megalopae returning to the shallows to settle after their pelagic stage. That translates to commercial catch numbers four years later.

TICKET TO FISH

Richerson’s main data source in Washington and Oregon was “fish tickets,” or landing receipts, from the Pacific States Marine Fisheries Commission’s PacFin database. In California, fish tickets were obtained from the California Department of Fish and Wildlife.

Fish tickets note the date, port, species, gear, and weight of catch landed by a commercial vessel. In California and Washington, a description of the catch area is included. In Oregon, only the state where the catch was made is recorded. “Fish tickets cover virtually all commercial landings and thus can be considered an

unbiased measure of total catch,” write the scientists.

They also used information from logbooks kept by crab fishers in Oregon and Washington. The logbooks contain information on the number of pots, depth, estimated catch weight or numbers, and other variables. In Oregon, logbooks cover 78% to 96% of the total weight landed; in Washington, logbooks include almost all landings, excluding tribal landings.

SECRET TO A SUCCESSFUL FISHERY

The success of the Dungeness crab fishery may lie in fishing regulations that protect the crabs’ reproductive potential. Male Dungeness crabs mature and begin reproducing one to two years before they can be caught. Female Dungeness crabs can store sperm for more than a year, allowing them to reproduce even in the absence of numerous males. Fishers must return females to the water, further protecting the reproductive capacity of the population.

West Coast states manage the fishery under a “3S” system: size, sex, and season. Only males with carapace widths greater than 159 mm may be harvested. In central California, the fishery for Dungeness crab usually opens in November; in northern California, Oregon, and Washington, in December. At the start of the season, fishing is intense, with the majority of the total catch often landed in the first six weeks. In summer or early fall, the fishery closes to protect the males during their molt.

“The management system for Dungeness crabs seems to be a perfect fit for their life history because it allows the pop-

ulation to reproduce and grow even with an intensive harvest,” says Richerson.

Crab numbers and reproduction rates vary from year to year, according to Richerson, mostly because of ocean conditions. In central California, numbers have risen over the last two decades, perhaps related to trends in the spring transition, and now average nearly five times the abundance estimates from 1970 to 2000.

Central California crab numbers have increased enough that they are closer to those of Dungeness populations in northern California, Oregon, and Washington, the researchers say. The latter populations don’t show the same growth trends as in central California, but are stable overall.

A previous increase in central California landings from the 1930s to the late 1950s was followed by a dramatic crash about 1960. Catches remained low until the 1980s, then rebounded. Biologists believe the jump reflected changing ocean conditions—and could happen again. The recent increase in central California crab abundance may be reversed when the system again shifts to a period of later spring transitions, scientists say.

The central California population is at the southern end of the *C. magister* range, so changes in ocean ecosystems may have a large impact on the return of larvae, “especially in years when a later spring transition leads to more northward transport of megalopae,” state Richerson et al.

Increasing water temperatures in the region may affect larval recruitment success by disrupting the timing of reproduction, according to the *Dungeness Crab*



Whales are often ill-equipped to avoid obstacles such as Dungeness crab fishing gear, and so get tangled up in crab pot lines. Credit: iStock.com/Larry Crain

Enhanced Status Report of the California Department of Fish and Wildlife, published in November 2019. “Adults may move to deeper waters, causing females to extrude eggs earlier in the year. That may shift larvae outside the critical upwelling period that drives their nearshore transport.”

Scientists are modeling future sea surface temperature scenarios expected by 2080 and comparing them to historical Dungeness crab landings and ocean conditions in the California Current (lagged three to five years to represent larval recruitment). Results indicate detrimental impacts to the future fishery from ocean warming, with the most significant changes occurring with decreasing latitude.

Dungeness crabs, like other cold water species, may contract their southern geographic range. In the long term, the central California fishery may have reduced production, according to the status report.

CANARY IN THE CALIFORNIA CURRENT

Future changes in the California Current ecosystem may alter the Dungeness crab population and “the effectiveness of the current management regime,” states Richerson. Harmful algal blooms, especially of the diatom *Pseudonitzschia*, which produces toxic domoic acid, have affected the fishery. The blooms are linked with warming ocean waters.

The opening of the commercial Dungeness fishery was delayed during the 2015–2016, 2016–2017, and 2018–2019 fishing seasons to mitigate human health risks as a result of high domoic acid concentrations from harmful algal blooms. A federal disaster was declared for the 2015–2016

season due to a four-month delay in the fishery opening, resulting in a shortened fishing season and lost revenue.

Beyond harmful algal blooms, human influences are likely to increase hypoxia and ocean acidification in the California Current System, “which may impact the growth, survival, distribution, and/or population size of *C. magister*,” Richerson et al. write. “Increased frequency of these events and other threats to the fishery have the potential to greatly impact fishers and fishing communities.”

Hypoxic zones in shallow, nearshore environments will likely increase with rises in ocean temperature. Large-scale hypoxia developed during the summers of 2006 and 2007, with scores of Dungeness crabs washing ashore along the Oregon coast. Benthic-dwelling nearshore organisms like Dungeness crabs are especially susceptible to hypoxia. If the zone of depleted oxygen develops quickly or is large, crabs may not be able to escape in time.

WHALES VS. CRAB FISHERS?

The Dungeness crab fishery faces another challenge: whale entanglements in fishing gear. The issue resulted in an early closure of the California fishery in 2019.

Since 2014, whale entanglements have sharply increased along the US West Coast, especially “entanglements between humpback whales and commercial Dungeness crab gear,” report Kaitlin Lebon and Ryan Kelly of the University of Washington in a 2019 paper in *Global Ecology and Conservation*.

“Whales may come into contact with fishing gear because of unfamiliarity with it, difficulties detecting certain shapes or

materials in the water column, or because their health or oceanographic conditions inhibit their sensory abilities,” Lebon and Kelly state.

Entanglement is an all-too-common event for many whale populations. Some 72% of North Atlantic right whales on the US East Coast have scars from entanglements. Even populations in remote Arctic waters show impacts, with 10% of bowhead whales taken by subsistence harvesters having rope scars from pot or trap fishing gear.

Lebon and Kelly compared alternative ways of reducing entanglements and found “a small number of high-ranking policy options.” Among them: Galvanic Timed Releases (GTRs), devices that keep lines submerged until crab pots are ready to be picked up. GTRs minimize the time crab pot lines are in the water.

Fixed-gear fisheries in Australia and New Zealand use GTRs. GTRs are inexpensive, Lebon and Kelly found, and help keep vertical float lines out of the water column until fishers can retrieve their pots. Anchoring float lines near crab pots eliminates the possibility of whales encountering the lines.

GTRs, the researchers say, are one more way to help this fish story keep its happy ending. 🐳

ABOUT THE AUTHOR

Cheryl Lyn Dybas (cheryl.lyn.dybas@gmail.com), a Fellow of the International League of Conservation Writers, is a contributing writer for *Oceanography* and a marine ecologist. She also writes about science and the environment for *National Geographic*, *BioScience*, *Ocean Geographic*, *ON Nature*, and many other publications.

Paleoceanography

LESSONS FOR A CHANGING WORLD

By Amelia Shevenell, Peggy Delaney, Katrin Meissner,
Laurie Menviel, and Alan C. Mix

This special issue of *Oceanography* on “Paleoceanography—Lessons for a Changing World” celebrates the field of paleoceanography and paleoclimatology at a time when future climate changes are projected to be larger than within the range of instrumental variation detected to date. The Intergovernmental Panel on Climate Change (IPCC) Assessment Report 6 (AR6), due for release in 2022, is integrating paleoceanography and paleoclimatology studies across all of its chapters, rather than featuring them in one chapter, in order to integrate what we know about the past and what we need to know about processes that will impact our future. The research highlighted in this special issue provides evidence of past large-scale climate changes preserved in marine and terrestrial sediment archives and documents associated impacts on carbon and nutrient cycles. Studying the impacts of such past climate variability at geologic timescales helps us to better understand how projected future increases in air and ocean temperatures will affect the Earth system, including ocean circulation, sea level, marine ecosystem health, and the occurrence and intensity of flooding and droughts, storms, and wildfires.

Much of what we know about the response of the Earth system during warm climate intervals comes from studying ice cores and the chemistry and assemblages of phytoplankton and zooplankton preserved in marine sediments. From these records, we are learning that the long-term sensitivity of the global climate system to greenhouse forcing (known as Earth system sensitivity)

is substantially greater than the short-term sensitivity (Charney sensitivity). A combination of these processes on different timescales is now being included in Earth system models. Although the exact mechanisms involved in this higher sensitivity remain poorly constrained, they likely include the slow-responding components of the Earth system, such as the ocean and the cryosphere—topics highlighted in this special issue of *Oceanography*. These slower processes don’t occur in isolation, however, and may influence the way shorter-term climate changes operate.

Every three years, the paleoceanographic community gathers to highlight research advances that reflect the current status of the field and to take a forward look at research opportunities (Box 1). Many of the papers and sidebars in this special issue are written by speakers and presenters at the Thirteenth International Conference on Paleoceanography (ICP13), held in Sydney, Australia, in September 2019. The meeting focused on several broad topics that served to organize the special issue, including: (1) tool development, (2) geobiology, (3) carbon-climate feedbacks, (4) ocean circulation and climate system dynamics, and (5) ice-ocean interactions. The papers presented here highlight major advances and document unresolved controversies within the paleoceanographic discipline. They also identify opportunities for new research paths and collaborations and point out important insights gained from studies of past climate that can inform studies of future climate.

BOX 1. History of the International Conference on Paleoceanography (ICP)



2–6 SEPTEMBER 2019
SYDNEY, AUSTRALIA

- ICP1**
1983, Zürich, Switzerland
- ICP2**
1986, Woods Hole, USA
- ICP3**
1989, Cambridge, UK
- ICP4**
1992, Kiel, Germany
- ICP5**
1995, Halifax, Canada
- ICP6**
1998, Lisbon, Portugal
- ICP7**
2001, Sapporo, Japan
- ICP8**
2004, Biarritz, France
- ICP9**
2007, Shanghai, China
- ICP10**
2010, La Jolla, USA
- ICP11**
2013, Sitges, Spain
- ICP12**
2016, Utrecht, The Netherlands
- ICP13**
2019, Sydney, Australia
- ICP14**
2022, Bergen, Norway (pending)

Proxy Development, New Models, and Statistical Tools

Paleoceanography has made steady progress since the middle of the twentieth century, developing new tools that include the calibration and application of new proxies (Crumpton-Banks and Rae, McCave) and emerging statistical evaluation and chronologic modeling approaches (Mix). Each new tool expands our ability to interpret paleoenvironmental information and quantify uncertainties in available archives and model experiments. Of particular interest to the IPCC assessment is the potential for paleo-model simulations and sensitivity tests to constrain the long-term sensitivity of climate change and to illuminate the roles of ocean, cryosphere, and carbon-cycle feedbacks in past large-scale climate changes and those projected for the future. It is important to leverage more complete process information from paleo data that may have some gaps in space or time.

Geobiology—New Frontiers in Paleoceanography Linking Paleoclimatic Changes with Biology and Evolution

Geobiology describes the interaction between the physical Earth and the biosphere. By combining information about the past development of more than one species, geobiology offers opportunities to explore the dynamics of biological communities and its relation to climate change. Papers in this special issue address the evolution of marine biological communities and their environments based on many types of biological proxy records that range from standard paleoecological methods to new proxy developments (Yasuhara et al., Fietz, Armbrrecht, Lam, Leventer). This topic is of special interest to policymakers as they consider the likely ecosystem impacts of large-scale climate change that will inescapably modify the distribution and diversity of life on Earth and bring together new and unprecedented associations of species at the same time that the results of human activities impose a global mass extinction event.

Carbon-Climate Feedbacks Across Timescales

Earth's climate history is characterized by long-term gradual changes interrupted by more abrupt transitions, referred to as tipping points. The potential for crossing practically irreversible thresholds is difficult to address beyond the hypothetical absent historical examples of such events. Here, paleo records provide essential insights into extreme changes that have occurred in Earth's history. Abrupt climate changes were, in some cases, accompanied by significant variations in atmospheric $p\text{CO}_2$ related to carbon cycle perturbations. However, in spite of dramatic progress in some areas, the mechanistic links and feedbacks between climate and reorganizations of the carbon cycle remain elusive. The special issue highlights contributions that improve understanding of carbon-climate feedbacks across all timescales (Matsumoto et al., Crumpton-Banks and Rae). Understanding the natural variations of the carbon cycle is an essential part of projecting long-term future changes, changes which may be initiated by anthropogenic emissions but which may also trigger natural feedback mechanisms that will either exacerbate or mitigate change (Miller et al.).

Ocean Circulation and Climate System Dynamics

Climate variability is largely governed by ocean dynamics over a wide range of spatial and temporal scales. In particular, ocean circulation plays a central role in climate dynamics through air-sea interactions, global transport of heat and salt in ocean currents, and storage of heat and carbon in the subsurface ocean. Reconstructing the ocean's past is critical for understanding the dynamics of the climate system as a whole. Contributions to this special issue synthesize knowledge about changes in ocean circulation and its links with climate system dynamics. They encompass observational, theoretical, and modeling studies of ocean circulation in the past, present, and future,

with a particular focus on: (1) paleoceanographic reconstructions on various timescales derived from marine paleoproxies (Tachikawa et al., McCave), (2) key processes that could force or generate changes in ocean circulation, (3) the impact of changes in oceanic circulation on climate system dynamics (e.g., El Niño-Southern Oscillation, monsoons; Dixit), and (4) development and application of numerical models to simulate changes in ocean circulation and its impact on climatic changes (Felis, Ford and Chalk). The paleo record illustrates how variability, in particular extreme events, may dominate impacts on regional and global systems.

Ice-Ocean Interactions: Drivers and Impacts

Sea level rise is perhaps one of the most alarming repercussions of present-day climate change, one that we are beginning to experience in coastal communities, where the majority of the human population lives. Now that it has started, sea level rise may become unstoppable for centuries or millennia. The early stages of sea level rise we are currently experiencing relate mostly to thermal expansion of seawater associated with warming and changes in net ocean heat content, as well as regional differences in sea level changes due to dynamic circulation effects. These phenomena are superimposed on slower effects such as glacial isostatic rebound, both as residuals from the end of the last ice age and as new impacts related to ongoing loss of ice. Due to thermal expansion and ice melting, current sea level rise is accelerating. It is therefore imperative that we gain a more thorough understanding of the dynamics of changes in global ocean heat content and the responses of continental ice sheets, including the complex interactions between buttressing ice shelves, ocean circulation, and warming ocean waters in polar regions. It is particularly important to determine the rates of change in these systems, which will increase our confidence in future sea

level and climate projections and better inform policy decisions. The responses we make as human societies to environmental changes, for example, whether we strive to protect coastal cities from sea level rise or begin the process of moving some of our activities out of harm's way, depend on detailed process-level understanding of the rates and magnitudes of changes. Moreover, the slow changes to the sizes and geographic distributions of continental ice sheets determine an important feedback in the radiative balance of climate. This topic is a focal point for studies of ice sheet variability, ice-ocean interactions, crustal deformation, and ice sheet impacts on climate, from radiative feedbacks to changes in ocean and atmospheric circulation, marine productivity, and the carbon cycle. Articles included in this special issue highlight contributions from both reconstruction and modeling studies to shed light on the role of ice sheets in climate sensitivity and ice-ocean interactions from regional to global scales, on rates of change, and on potential long-term irreversibility of sea level rise originating from ice loss (Miller et al., Gasson and Keisling, Neff, Leventer).

Finally, this issue also includes a book review of *A Memory of Ice: The Antarctic Voyage of the Glomar Challenger* by Elizabeth Truswell. Webb and Barrett describe how the book interleaves diary-based personal recollections of scientific ocean drilling from five decades ago, the significant events in polar exploration and science of the preceding two centuries, and the significant south polar Earth science achievements that have occurred since 1973. Some of us have been in the field all of those nearly five decades, and it is easy to forget that our early work in such a quickly changing field on a fast-changing planet is rapidly becoming instructive history.

We hope this special issue of *Oceanography* provides a useful “touchstone” of interest to research paleoceanographers, to students who may build the

future of paleoceanography and paleoclimatology, and to the broader community of scientists and policymakers who can witness the progress made as the field of paleoceanography and paleoclimatology has advanced. These state-of-the-art contributions also provide a signpost toward future research directions and highlight the value of paleoceanography in illuminating key processes that must be understood by humanity in order to coexist with a world that is changing, both naturally and due to the impact of human activities. 

AUTHORS

Amelia Shevenell (ashevenell@usf.edu) is Associate Professor, University of South Florida College of Marine Science, St. Petersburg, FL, USA.

Peggy Delaney is Professor Emerita, University of California, Santa Cruz, CA, USA. **Katrin Meissner** is Professor and Director, Climate Change Research Centre, University of New South Wales, Sydney, Australia. **Laurie Menviel** is Australian Research Council Future Fellow and UNSW Scientia Senior Lecturer, Climate Change Research Centre, University of New South Wales, Sydney, Australia.

Alan C. Mix is Professor, College of Earth, Ocean, and Atmospheric Sciences, Oregon State University, Corvallis, OR, USA.

ARTICLE CITATION

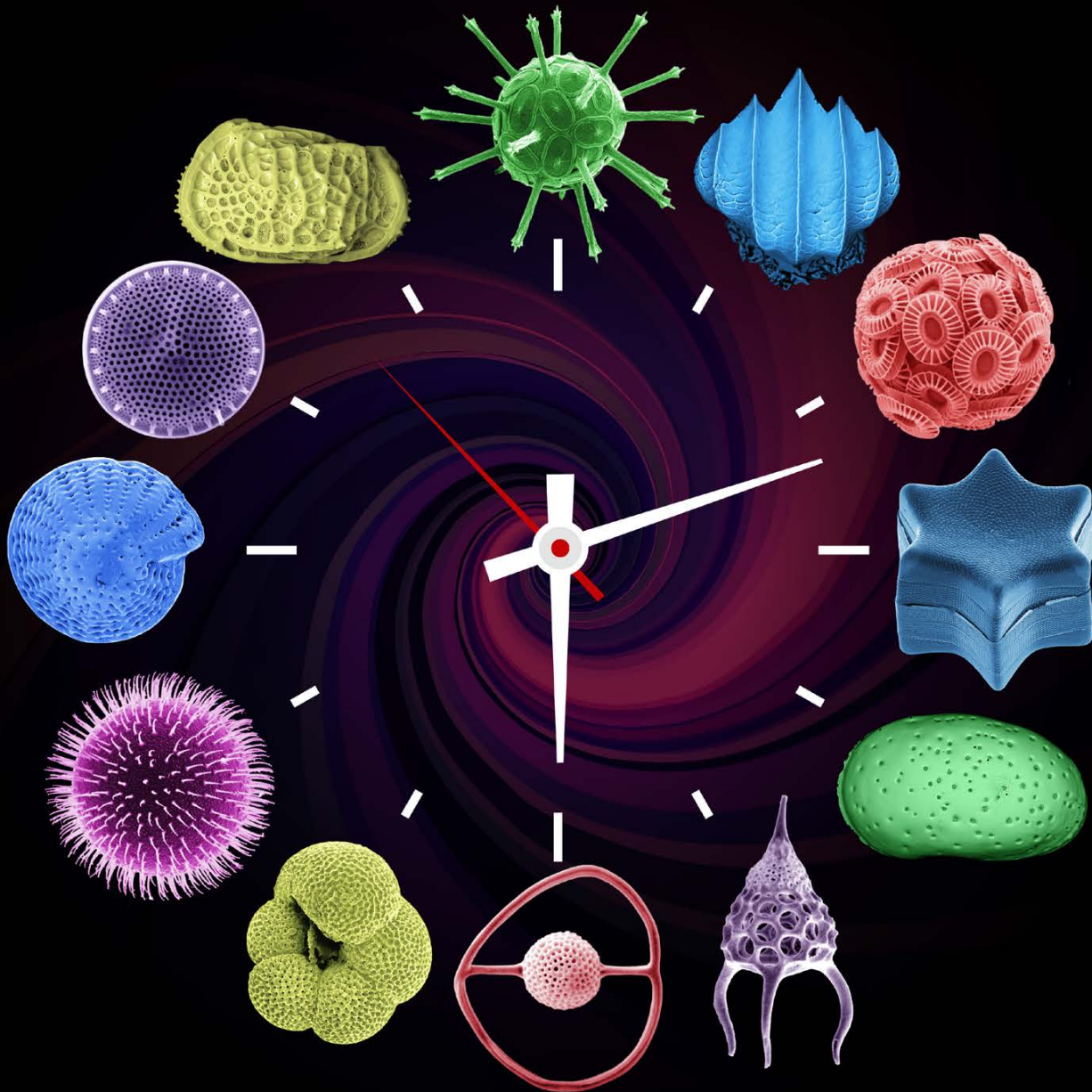
Shevenell, A., P. Delaney, K. Meissner, L. Menviel, and A.C. Mix. 2020. Introduction to the special issue: Paleooceanography—Lessons for a changing world. *Oceanography* 33(2):13–15, <https://doi.org/10.5670/oceanog.2020.226>.

COPYRIGHT & USAGE

This is an open access article made available under the terms of the Creative Commons Attribution 4.0 International License (<https://creativecommons.org/licenses/by/4.0/>), which permits use, sharing, adaptation, distribution, and reproduction in any medium or format as long as users cite the materials appropriately, provide a link to the Creative Commons license, and indicate the changes that were made to the original content.

TIME MACHINE BIOLOGY

CROSS-TIMESCALE INTEGRATION OF ECOLOGY, EVOLUTION, AND OCEANOGRAPHY



By Moriaki Yasuhara, Huai-Hsuan May Huang, Pincelli Hull, Marina C. Rillo, Fabien L. Condamine,
Derek P. Tittensor, Michal Kučera, Mark J. Costello, Seth Finnegan, Aaron O'Dea, Yuanyuan Hong, Timothy C. Bonebrake,
N. Ryan McKenzie, Hideyuki Doi, Chih-Lin Wei, Yasuhiro Kubota, and Erin E. Saupe

*Marine geology and marine biology have common origins.
The iconic founding hero of this connection was Charles Darwin.*

– Berger, 2011

ABSTRACT. Direct observations of marine ecosystems are inherently limited in their temporal scope. Yet, ongoing global anthropogenic change urgently requires improved understanding of long-term baselines, greater insight into the relationship between climate and biodiversity, and knowledge of the evolutionary consequences of our actions. Sediment cores can provide this understanding by linking data on the responses of marine biota to reconstructions of past environmental and climatic change. Given continuous sedimentation and robust age control, studies of sediment cores have the potential to constrain the state and dynamics of past climates and ecosystems on time-scales of centuries to millions of years. Here, we review the development and recent advances in “ocean drilling paleobiology”—a synthetic science with potential to illuminate the interplay and relative importance of ecological and evolutionary factors during times of global change. Climate, specifically temperature, appears to control Cenozoic marine ecosystems on million-year, millennial, centennial, and anthropogenic time-scales. Although certainly not the only factor controlling biodiversity dynamics, the effect size of temperature is large for both pelagic and deep-sea ecosystems.

INTRODUCTION

Ever since the voyage of HMS *Beagle* (1831–1836), ocean expeditions have provided novel insights into geological and biological processes. The HMS *Challenger* expedition (1872–1876) was one of the first to systematically collect numerous marine sediment and organismal samples from around the world (Figure 1), setting the scene for contemporary oceanography, paleoceanography, and marine biology (Macdougall, 2019). The Swedish *Albatross* expedition (1947–1948) expanded on *Challenger* insights by extracting the first deep-ocean sediment cores, which encompassed hundreds of thousands of years of sedimentation and facilitated pioneering paleoceanographic and micropaleontological studies (Arrhenius, 1952; Emiliani, 1955; Parker, 1958; Olausson, 1965; Benson and Sylvester-Bradley, 1971; Benson, 1972; Berger, 2011). Sediment cores are vertical columns of sediment recovered by techniques designed to penetrate the seafloor (Figure 1). The *Albatross* expedition made use of a prototype piston core designed by Kullenberg that was capable of recovering

>10 m of sediment (Revelle, 1987).

Since the *Albatross* expedition, numerous seafloor sediment samples have been collected from coring expeditions and accumulated at oceanographic institutions (Berger, 2011). These collections have facilitated global-scale analyses of past climate change, such as reconstruction of global ocean conditions during the last ice age by the CLIMAP project (Climate: Long range Investigation, Mapping, and Prediction; CLIMAP Project Members, 1976, 1984). The same material also made it possible to investigate species and community dynamics across temporal scales. For instance, Ruddiman (1969), a geologist, used planktonic foraminiferal records in surface sediments from the North Atlantic to reveal large-scale spatial patterns in present-day species, a pioneering contribution to the field now known as macroecology (Brown and Maurer, 1989; Brown, 1995; Yasuhara et al., 2017b). Ruddiman’s analysis of planktonic foraminiferal diversity was feasible because many paleoclimatic reconstructions, such as CLIMAP, use the present-day

distribution and relative abundance of microfossil species as environmental proxies (Box 1). As a result, CLIMAP and related efforts (e.g., the mid-Pliocene PRISM project or Pliocene Research, Interpretation and Synoptic Mapping) have built comprehensive, global data sets of microfossil community censuses for several time periods in Earth history, including the present day, the Last Glacial Maximum, and the Pliocene (CLIMAP Project Members, 1976, 1984; Dowsett et al., 1994, 2013). These data were seldom studied from a biological perspective initially but later proved critical for gaining insight into present (Rutherford et al., 1999; Fenton et al., 2016; Tittensor et al., 2010) and past (Yasuhara et al., 2012c, 2020) biodiversity patterns on global and regional scales.

Scientific ocean drilling began with the launch of the international Deep Sea Drilling Project (DSDP) in 1968, followed by the Ocean Drilling Program (ODP) in 1983, the Integrated Ocean Drilling Program (IODP) in 2003, and the International Ocean Discovery Program (IODP) in 2013 (Becker et al., 2019). These projects allowed scientists to recover sediment sequences up to several kilometers in length, spanning ~170 million years (Figure 1; Becker et al., 2019; Clement and Malone, 2019). Scientific ocean drilling has been deemed one of the most successful international scientific collaborations ever undertaken (Berger, 2011) and has provided unparalleled marine data on a global scale that has resulted in numerous publications (>11,000 peer-reviewed papers; Clement and Malone, 2019; Koppers et al., 2019).

Integration of paleoceanographic and paleobiological data from deep-sea sediments has provided improved under-

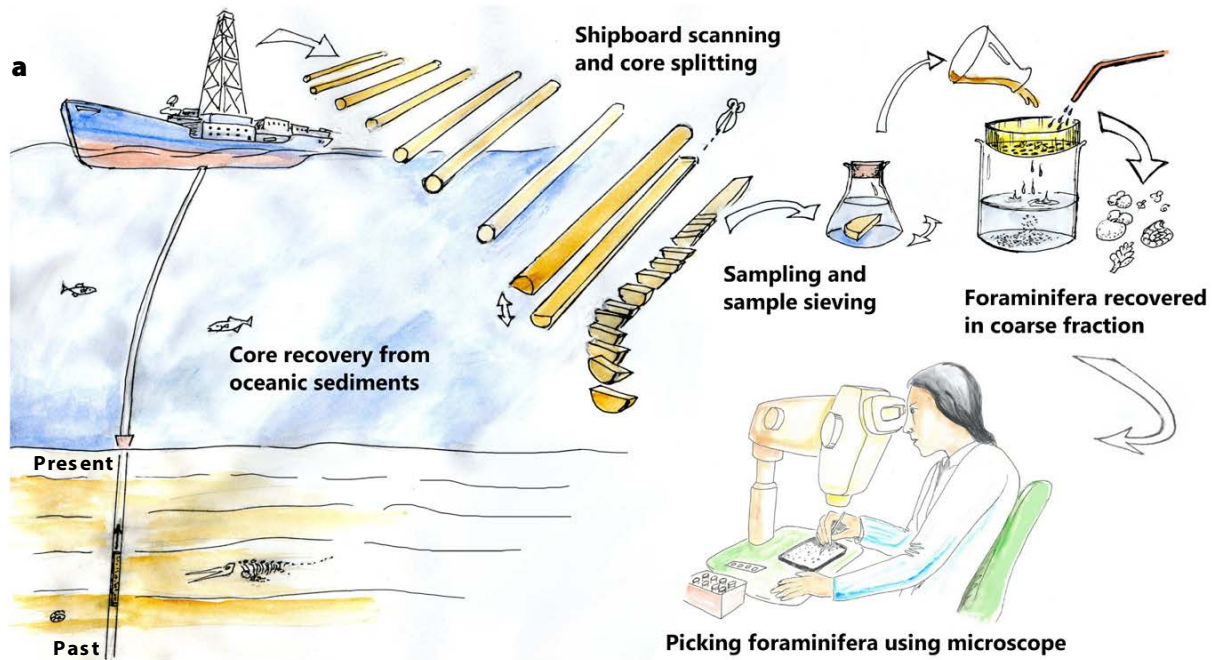


FIGURE 1. (a) An overview of sediment core collection and processing for micropaleontological research. *Illustrations by Simon J. Crowhurst and the Godwin Laboratory.* (b) Ocean-floor sediment samples collected with a dredge during the HMS *Challenger* expedition on March 21, 1876, in the South Atlantic. Sample number M.408 from the Ocean-Bottom Deposit (OBD) Collection held by the Natural History Museum in London (for more information, see Rillo et al., 2019). (c) Sand-sized residue of a Pleistocene deep-sea sediment from ODP Site 925 in the equatorial Atlantic Ocean consisting of numerous microfossil shells. Scale bar: 1 mm.

standing of the co-evolution of marine systems and their biota over the last ~10 years. Here, we review these efforts to understand the interaction between climate change and the marine biosphere on both long and short timescales. Our review is time structured and focuses on the influence of climate on biodiversity on million-year, millennial, centennial, and more recent timescales. We end with a discussion of how deep-sea biodiversity dynamics on the most recent timescales can inform our understanding of the changes expected in the Anthropocene.

BIOTIC DYNAMICS OVER MILLIONS OF YEARS

Quantifying how and why biodiversity levels have changed over Earth history is fundamental to macroecology and macroevolution. Scientific ocean drilling samples have allowed for unprecedented insight into these dynamics on million-year timescales, particularly in response to large-scale global climate and tectonic changes (Figure 2; Kucera and Schönfeld, 2007; Norris, 2000; Fraass et al., 2015; Lowery et al., 2020). The general correspondence between Cenozoic

climate change and biodiversity levels across multiple marine clades suggests that climate, particularly temperature, controls diversification dynamics on long timescales (Box 2 and Figure 3). Higher temperatures generally correspond with higher levels of biodiversity (Box 2). However, the precise mechanisms responsible for this coupling are debated. One potential explanation is that higher temperatures can enhance metabolic efficiency and resulting reproduction, with such enhancements potentially resulting in increased speciation and

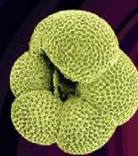
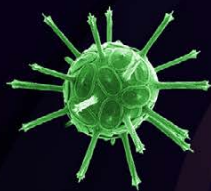
therefore species richness (Allen et al., 2002; Yasuhara and Danovaro, 2016).

In addition to regulating temporal patterns of biodiversity, climate change over the Cenozoic has affected spatial patterns of marine biodiversity. For example, large-scale climatic shifts have modified one of the foremost patterns in ecology, the latitudinal biodiversity gradient (LBG), in which the number of species decreases from the equator to the poles (Hillebrand, 2004a,b; Saupe et al., 2019). In the ocean, LBGs are often characterized by an equatorial dip, resulting in a bimodal biodiversity pattern (Rutherford et al., 1999; Worm et al., 2005; Chaudhary et al., 2016, 2017; Worm and Tittensor, 2018; Rogers et al., 2020; Yasuhara et al., 2020). Growing evidence suggests the LBG was flatter during warm periods (e.g., Eocene, Pliocene) and steeper during cold periods (e.g., Last Glacial Maximum of 20,000 years ago; Yasuhara

et al., 2012c; Fenton et al., 2016; Lam and Leckie, 2020; Meseguer and Condamine, 2020), potentially reflecting degree of climatic heterogeneity (Saupe et al., 2019). The standard tropical-high and extratropical-low LBG can be traced back at least to the Eocene for both deep-sea benthos (~37 million years ago [Ma]; Thomas and Gooday, 1996; **Figure 3**) and pelagic plankton (~48–34 Ma; Fenton et al., 2016). Notably, initiation of the LBG observed today in the deep sea predates the Eocene-Oligocene transition (Thomas and Gooday, 1996), suggesting that it began with the opening of the Drake Passage (Scher and Martin, 2006; **Figure 2**) rather than with climatic changes at the Eocene-Oligocene transition (**Figure 3**). Indeed, the opening and closing of major seaways (**Figure 2**) has been shown to alter the distribution of both shallow-marine and deep-sea organisms throughout the Cenozoic,

both longitudinally (e.g., Tethyan and Central American Seaways) and latitudinally (e.g., Arctic gateways) (O’Dea et al., 2007; Renema et al., 2008; Yasuhara et al., 2019b).

Although evidence supports climate as a primary control on Cenozoic biodiversity change, it is certainly not the only driver of biodiversity dynamics (e.g., Ezard et al., 2011; Condamine et al., 2019; Lam and Leckie, 2020). Ecological interactions in addition to climate, for example, have been found to influence the macroevolution of planktonic foraminifera (Ezard et al., 2011). Continued study of biotic traits will allow for examination of the relative roles of abiotic (e.g., climate) versus biotic factors in shaping ecosystems and their changes through time (Schmidt et al., 2004), as well as of the relationship between biodiversity and ecosystem function (Henehan et al., 2016; Yasuhara et al., 2016; Alvarez et al., 2019).



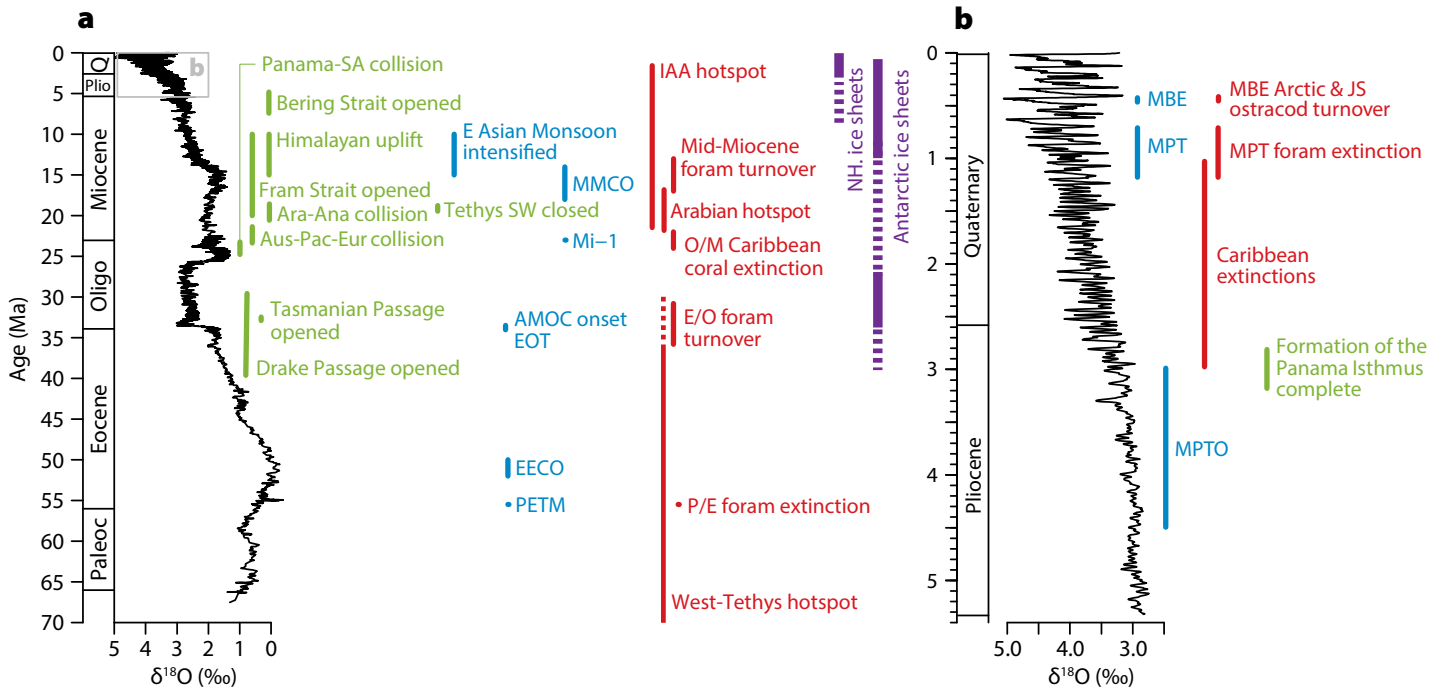
BOX 1. MICROFOSSILS

Microfossils are microscopic remains of organisms or their parts preserved in the fossil record. The most widely studied microfossils are biomineralized structures with high fossilization potential produced by a range of organisms, including photosynthetic plankton such as coccolithophores and diatoms, various mixo- to heterotrophic protists such as planktonic and benthic foraminifera and planktonic radiolarians, and small metazoans such as benthic ostracods (small bivalved crustaceans; Yasuhara et al., 2017b). Dinoflagellates (auto-, mixo-, and heterotrophic plankton) also leave abundant microfossils in the form of resistant organic (and occasionally biomineralized) resting cysts (de Vernal, 2013). Many microfossils represent parts of larger organisms, such as the scales and teeth of fish (Field et al., 2009; Sibert et al., 2017) and shark denticles (Dillon et al., 2017), referred to as ichthyoliths. Although pollen and spores have terrestrial origins, they can also be preserved in both marine and freshwater sediments (Sánchez Goñi et al., 2018).

Microfossils are abundant in deep-sea sediment cores and, in many cases, constitute a large portion of the sediment itself (**Figure 1**; e.g., see Marsaglia et al., 2015). Thus, hundreds of thousands to millions of plankton specimens can be found in a gram of deep-sea sediment. Microfossils are key tools for interpreting age and environment in sediment cores due to their excellent preservation and high abundance. The first and last appearance of key species and groups are used to determine the ages of sed-

iments in cores (Berggren et al., 1995; Motoyama, 1996), whereas the trace element and isotopic compositions of microfossils are used to reconstruct the paleoceanographic history of sediment cores with regard to, for example, temperature, salinity, and polar ice volume (**Figure 2**; e.g., Zachos et al., 2001; Lisiecki and Raymo, 2005; Norris et al., 2013). At the same time, the high abundance and diversity of microfossil groups preserved in small amounts of sediment (**Figure 1**) allow for quantitative assessment of the composition and dynamics of past communities across a range of spatial and temporal scales, as reviewed here.

Although microfossils are ideal subjects for macroecological and macroevolutionary analyses, their study is limited by poor understanding of the life histories and ecology of most species and by evolving species concepts, limited phylogenetic hypotheses for most clades, and the poor preservation potential of other organisms in the community aside from microfossils (i.e., the majority of the ecosystem is not fossilized). In spite of these limitations, almost every trophic or functional group in marine communities is represented by (at least) one well-fossilized microfossil group, providing a basis for macroecological and macroevolutionary synthesis. Notable exceptions are the prokaryotes and viruses, which leave no body fossils. Obtaining information on the history of these groups requires alternative approaches, such as the use of organic biomarkers in the case of some prokaryote clades or ancient DNA (Armbrecht, 2020, in this issue).



The major tectonic events include:

- Tasmanian Passage opened (33.5–33.7 Ma; Cronin, 2009)
- Drake Passage opened (shallow water connection started at ~41 Ma and deepwater connection established by ~30 Ma; Scher and Martin, 2006; Yasuhara et al., 2019b)
- Australia-Pacific-Eurasia (Aus-Pac-Eur) collision (~23 Ma; Renema et al., 2008)
- Arabia-Anatolia (Ara-Ana) collision (~20 Ma; Renema et al., 2008)
- Fram Strait opened (20–10 Ma; Yasuhara et al., 2019b)
- Himalayan uplift latest phase (15–10 Ma; Tada et al., 2016)
- Tethys Seaway closed (~19 Ma; Harzhauser et al., 2007; Yasuhara et al., 2019b)
- Bering Strait opened (7.4–4.8 Ma; Yasuhara et al., 2019b)
- Panama-South America (SA) collision (~24 Ma; Farris et al., 2011)
- Formation of the Panama Isthmus complete (~3 Ma; O’Dea et al., 2016; Jaramillo, 2018)

The major climatic events include:

- PETM: Paleocene-Eocene Thermal Maximum (55.5 Ma; Cronin, 2009)
- EECO: Early Eocene Climatic Optimum (52–50 Ma; Cronin, 2009)
- EOT: Eocene-Oligocene transition (~34 Ma)
- AMOC: Atlantic Meridional Overturning Circulation onset (~34 Ma; Hutchinson et al., 2019)
- Mi-1 event (23 Ma; Cronin, 2009)
- MMCO: Mid-Miocene Climatic Optimum (18–14 Ma; Cronin, 2009)
- East Asian Monsoon intensified (15–10 Ma; Tada et al., 2016)

- MPTO: Mid-Pliocene Thermal Optimum (4.5–3 Ma; Cronin, 2009)
- MPT: Mid-Pleistocene transition (1.2–0.7 Ma; Elderfield et al., 2012)
- MBE: Mid-Brunhes Event (0.43 Ma; Holden et al., 2011)

The major biotic events include:

- Paleocene/Eocene (P/E) deep-sea foraminifera extinction (55.5 Ma; Thomas, 2007)
- Eocene/Oligocene (E/O) deep-sea foraminifera turnover (36–31 Ma; Thomas, 2007)
- Oligocene/Miocene (O/M) Caribbean coral extinction (~23 Ma; Johnson et al., 2009)
- Mid-Miocene deep-sea foraminifera turnover (~15 Ma; Thomas, 2007)
- West Tethys hotspot (Mesozoic to ~30 Ma; Renema et al., 2008)
- Indo-Australian Archipelago (IAA) hotspot (23–0 Ma; Renema et al., 2008; Yasuhara et al., 2017a)
- Arabian hotspot (23–16 Ma; Renema et al., 2008)
- Caribbean extinctions (3–1 Ma; O’Dea et al., 2007; O’Dea and Jackson 2009)
- MPT deep-sea foraminifera extinction (1.2–0.7 Ma; Hayward et al., 2007)
- MBE Arctic (0.43 Ma; Cronin et al., 2017) and Japan Sea (JS) deep-sea ostracod turnover (0.43 Ma; Huang et al., 2018)

Ice sheets:

- The durations of the Northern Hemisphere (NH) and Antarctic ice sheets are from Zachos et al. (2001)

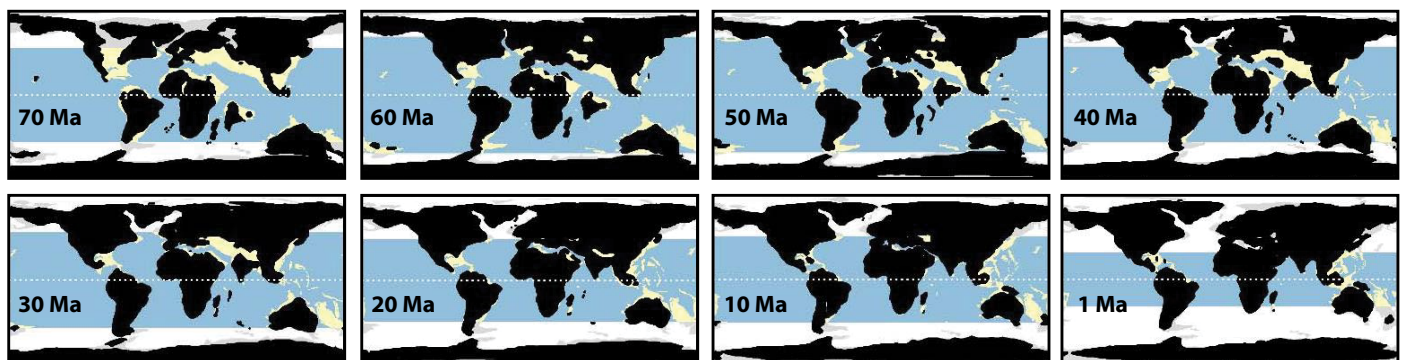


FIGURE 2. Cenozoic global changes and major events. (a) Cenozoic summary and (b) Plio-Pleistocene closeup. Global deep-sea oxygen isotope records (smaller value indicates warmer climate) are from Zachos et al. (2001) for (a), and from the LR04 stack of Lisiecki and Raymo (2005) for (b). Major tectonic (green), climatic (blue), biotic (red), and ice-sheet (purple) events are shown. (c) Paleogeographic maps from Leprieur et al. (2016). Light blue: deep tropical ocean. Yellow: tropical shallow reefs. White and light gray: deep ocean and shallow waters outside the tropical boundary, respectively.

BIOTIC DYNAMICS ON MILLENNIAL TIMESCALES

In addition to million-year timescales, sediment core data provide insight into biodiversity-climate dynamics on millennial timescales. Orbital variations have resulted in changes in climate on 10,000- to 100,000-year timescales throughout Earth history, as is well documented in benthic $\delta^{18}\text{O}$ records (Figure 2B; Raymo et al., 2004; Lisiecki and Raymo, 2005). Surface-ocean and deep-ocean conditions change in pace with orbital forcing of global climate, as do the locations of oceanic currents and bio-provinces (Cronin, 2009). These oceanic changes are matched by changes in the composition of marine microfossil communities that mirror orbital-scale climatic changes (Cronin et al., 1996, 1999; Cronin and Raymo, 1997). Orbital forcing provides repeated experiments on community assembly, with microfossil assemblages demonstrating that similar communities come together repeatedly under similar environmental conditions (Cronin et al., 1996; Beaufort et al., 1997; Yasuhara and

Cronin, 2008; Huang et al., 2018). This close association supports climate, and particularly temperature, as a key driver of marine biodiversity, with the formation of similar assemblages reflecting the process of species tracking their preferred temperature conditions. Orbital-scale time-series studies, for example, consistently show that temperature rather than productivity is the best predictor of deep-sea biodiversity patterns (Hunt et al., 2005; Yasuhara et al., 2009, 2012b). Temperature likely controls biodiversity because fewer species can physiologically tolerate conditions in colder places than in warmer places on these ecological timescales (Currie et al., 2004; Yasuhara and Danovaro, 2016).

Changes in the dominant mode of orbital cyclicity can, by contrast, permanently disturb marine ecosystems (Hayward et al., 2007; DeNinno et al., 2015; Cronin et al., 2017; Huang et al., 2018, 2019), such as during the transition from 41,000- to 100,000-year cycles in the Mid-Pleistocene Transition (MPT) and the Mid-Brunhes Event (MBE). For

example, deep-sea benthic foraminifera show a prominent global extinction event during the MPT (Hayward et al., 2007). Similarly, ostracod taxa with affinity for warm temperatures were abundant both in the Arctic and the North Atlantic Oceans before the MBE (DeNinno et al., 2015; Cronin et al., 2017). However, after the MBE warm-adapted taxa went extinct regionally in the Arctic, with shrinking distributions to the south (DeNinno et al., 2015; Cronin et al., 2017). In the Sea of Japan, endemic cool water species replaced circumpolar species after the MBE, and many circumpolar species went extinct regionally (Ozawa and Kamiya, 2005; Cronin and Ikeya, 1987; Huang et al., 2018, 2019). In sum, when orbital cyclicity is consistent, microfossil species seem to show evidence of repeated community assembly that matches prevailing conditions, indicating that community assembly may be deterministic. Changes in the expression of orbital forcing, however, can lead to extinction. How and why such changes instigate widespread biotic disturbance is not well understood, but

BOX 2. MICROFOSSIL BIODIVERSITY TRENDS OVER THE CENOZOIC

The Cenozoic biodiversity curve for planktonic foraminifera (Ezard et al., 2011; Fraass et al., 2015) is surprisingly similar to those for other global marine groups, such as sharks (Condamine et al., 2019) and calcareous nannofossils (Lowery et al., 2020; Rabosky and Sorhannus, 2009), and to a regional curve of Neotropical terrestrial plants (Jaramillo et al., 2006) (Figure 3). Commonalities among these curves include: (1) peak biodiversity in the Eocene (56–34 Ma), (2) a major extinction event at the Eocene-Oligocene boundary, (3) a Miocene diversification phase (for planktonic foraminifera and sharks), and (4) a Pliocene biodiversity high (for planktonic foraminifera and sharks) (Figure 3). Dinoflagellates also show a similar Eocene diversity peak (Katz et al., 2005; Stover et al., 1996).

In contrast to calcareous microfossil groups such as planktonic foraminifera and calcareous nannofossils, siliceous microfossil groups such as diatoms and radiolarians show contrasting biodiversity trends (Lowery et al., 2020). For example, diatom diversity increased during cooling periods, peaked at the Eocene-Oligocene transition, and reached highest levels during the Plio-Pleistocene (Figure 3; Katz et al., 2005, 2007; Lazarus et al.,

2014; Lowery et al., 2020). Cetaceans show trends similar to those of diatoms, and the two may have coevolved (Berger, 2007; Marx and Uhen, 2010). The contrast between calcareous and siliceous microfossil biodiversity patterns may occur because calcareous microfossils tend to be dominant and diverse in tropical and subtropical latitudes, whereas siliceous groups are dominant in polar, high latitude seas (Rutherford et al., 1999; Powell and Glazier, 2017; Dutkiewicz et al., 2020; Lowery et al., 2020). Thus, colder periods may allow for higher biodiversity in siliceous microfossil groups, given their preference for cooler waters. Alternatively, the differences could also reflect biases resulting from preservation and sampling of siliceous microfossils (Lowery et al., 2020).



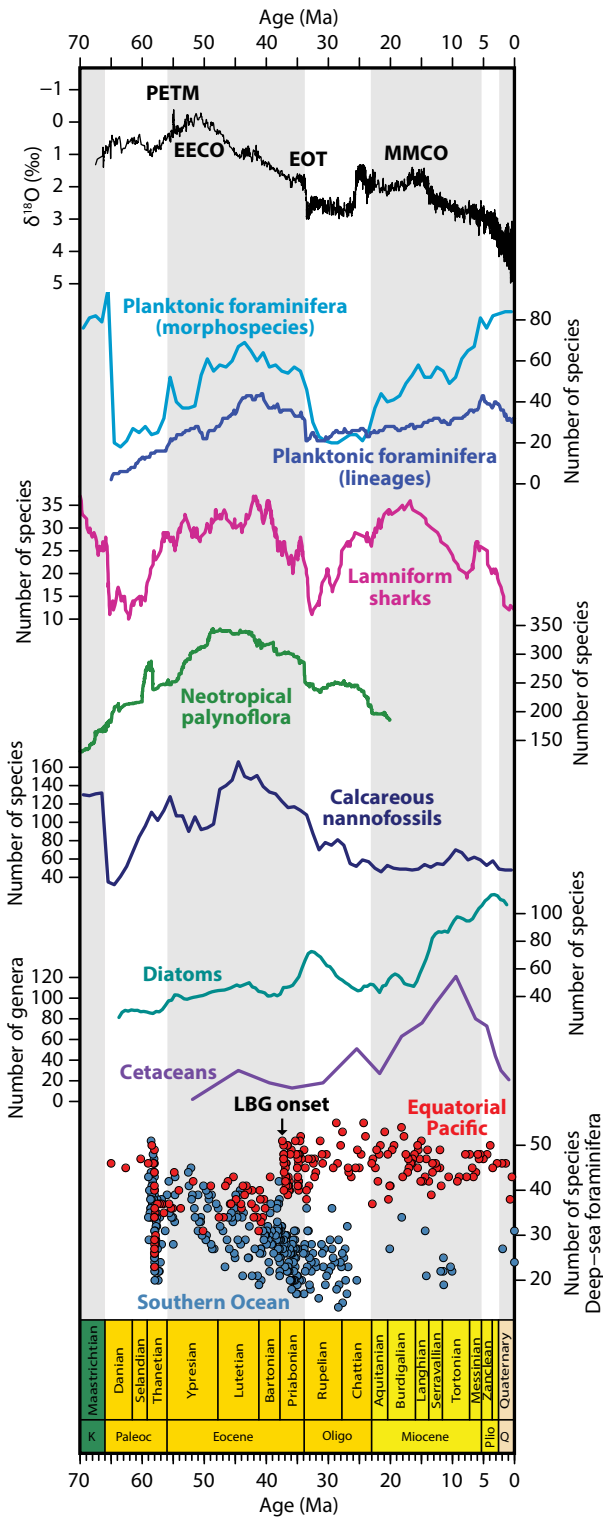


FIGURE 3. Cenozoic climate and biodiversity estimates of multiple taxonomic groups. From top to bottom: oxygen isotopic records (Zachos et al., 2001; smaller value indicates warmer climate) and biodiversity curves of global planktonic foraminifera morphospecies (Lowery et al., 2020) and lineages (Ezard et al., 2011), global lamniform sharks (Condamine et al., 2019), neotropical palynoflora (Jaramillo et al., 2006), global calcareous nannofossils (Lowery et al., 2020), global diatoms (Lazarus et al., 2014), global cetacean genera (Marx and Uhen, 2010; Uhen, 2020), and Southern Ocean and equatorial Pacific deep-sea benthic foraminifera (Thomas and Gooday, 1996). The onset of the deep-sea benthic foraminifera latitudinal biodiversity gradient (LBG) is indicated at ~37 million years ago.

may be explained by the scale of environmental perturbation; larger-scale changes could exceed species' tolerances and/or eliminate potential refugia (Hayward et al., 2012).

BIOTIC DYNAMICS ON CENTENNIAL TIMESCALES

Recent advances in high-resolution paleoceanographic studies (Bond et al., 1997; Bianchi and McCave, 1999; deMenocal et al., 2000; Oppo et al., 2003; McManus et al., 2004; Yasuhara et al., 2019a) have improved understanding of centennial-scale biotic responses to climate change, bridging the gap between geological timescales and the timescales of ecological studies. The centennial timescale has long been a “blind spot” in ecological analysis, lodged between the range of biological monitoring without historical reconstruction and the resolution attainable in most paleontological research (Yasuhara, 2019). Paleobiological records on this timescale can be garnered from microfossils preserved in sediments deposited under high sedimentation rates and/or conditions that minimize post-depositional sediment mixing. Such records can be found in sediment drifts (e.g., sediments collected from a sediment drift at ODP Site 1055 on the Carolina Slope show sedimentation rates of ~23 cm per thousand years; Yasuhara et al., 2008) or in enclosed settings in marginal oceanic basins that act as natural sediment traps and where local anoxia prevents sediment mixing (such as the basins of the Californian borderland, Cariaco Basin, or silled fjords; see Yasuhara et al., 2019c). Although seasonal and annual signals are likely smoothed by bioturbation in many of these sediment cores, it is minimized in cores from anoxic basins. By using these minimally disturbed cores, decadal community changes can be reconstructed to bridge the gaps across timescales (Kuwae et al., 2017; Salvatelli et al., 2018; see the next section).

Pioneering studies using records from the Gulf of Mexico and the Santa Barbara Basin off California have documented responses of biodiversity to centennial-scale abrupt climatic changes (Flower and Kennett, 1995; Cannariato et al., 1999). Initial findings documenting the response of benthic foraminifera to centennial-scale deoxygenation events in the Santa Barbara Basin (Cannariato et al., 1999) have been complemented by data from various benthic groups, including molluscs, foraminifera, ostracods, and ophiuroids (Moffitt et al., 2015; Myhre et al., 2017). Centennial-scale records spanning the last 20,000 years in the North Atlantic Ocean have revealed that deep-sea benthic ostracod diversity responded to changes in deepwater circulation and temperature during the abrupt climatic changes of the Heinrich I (17,000–14,600 yr BP), the Younger Dryas (12,900–11,700 yr BP), and the 8.2 ka event (8200 yr BP) without recognizable time lags (Yasuhara et al., 2008, 2014; Yasuhara, 2019). These studies also documented rapid rearrangement of local communities following the abrupt climatic changes. Thus, even on centennial timescales, climate, and more specifically temperature, has dramatic effects on marine biodiversity. At least locally, the dominant response to climate change seems to involve range shifts and recolonization from the same species pool (Yasuhara and Cronin, 2008; Yasuhara et al., 2009; Yasuhara and Danovaro, 2016). Excessive extinctions in the future may therefore affect the resilience of these ecosystems.

MICROFOSSILS AND THE BRAVE NEW ANTHROPOCENE

The sediment layer on the surface of the ocean floor represents a time-averaged assemblage of microfossils. Because of slow sedimentation in the deep sea (typically less than 10 cm per 1,000 years) and sediment mixing down to a depth of 10 cm (bioturbation), a typical 1 cm thick surface-sediment sample represents average deposition over centuries to millennia (Jonkers et al., 2019). Thus, the proportion of microfossils recording conditions of the Anthropocene (typically >~1950) in surface sediments is negligible, which means core-top sediments typically provide a global pre-industrial baseline for the state of marine communities in fossilized organisms (Jonkers et al., 2019; Yasuhara et al., 2020).

Recently, Jonkers et al. (2019) compared planktonic foraminifera assemblages collected from surface sediments that provide a pre-industrial baseline with assemblages collected from sediment traps that monitored particle flux to the seafloor over the last 40 years. The authors examined whether anthropogenic climate change modified the com-

position of marine plankton communities. They found that Anthropocene assemblages differ from their pre-industrial equivalents, and the observed differences in species composition are consistent with the expected effect of current temperature change trends (Jonkers et al. 2019). Similarly, Moy et al. (2009) used shells of planktonic foraminifera from surface sediments as a benchmark for calcification intensity in living planktonic foraminifera. These authors discovered that shells of modern *Globigerina bulloides* are about a third lighter than those from the sediments, consistent with reduced calcification induced by ocean acidification in the Anthropocene. Their results were recently confirmed by Fox et al. (2020), who observed shell thinning when comparing planktonic foraminifera specimens collected from historical (HMS *Challenger*, 1872–1876) to recent (*Tara* Oceans, 2009–2016) plankton samples. Large collections of surface sediment samples, both modern and historical (Rillo et al., 2019), are available to study, providing an opportunity to quantify anthropogenic impacts on the composition of a range of marine ecosystems

and on traits of their constituent species.

Areas with particularly high rates of sedimentation (e.g., ~50–100 cm per hundred years in Osaka Bay and >120 cm per thousand years in the Santa Barbara Basin; Barron et al., 2010; Field et al., 2006; Yasuhara et al., 2007) can provide insight into the effects that humans are having on marine ecosystems on even finer temporal scales. Study of these sediments has revealed significant marginal marine ecosystem degradation caused by human-induced eutrophication and resulting bottom water hypoxia (Barmawidjaja et al., 1995; Cooper, 1995; Cronin and Vann, 2003; Weckström et al., 2007; Willard and Cronin, 2007; Yasuhara et al., 2007, 2019c; Tsujimoto et al., 2008).

Although anthropogenic forcing is the primary driver of current biodiversity change (Díaz et al., 2019), natural variability in community composition is also at play, and its overprinting can prevent quantification of anthropogenic effects. Measuring this baseline temporal variability is crucial to partition the human signal, but is difficult to accomplish without long ecological time series that precede the Anthropocene. Microfossils

BOX 3. AUTOMATION



Another advantage of the microfossil record is that it is increasingly possible to automate key steps in gathering and processing data, due in part to the small size of samples and specimens. Once a core is obtained, the major data-gathering steps are washing and sieving sediment; picking, identifying, and mounting specimens; and, for studies of phenotypic evolution, measuring morphological traits of specimens. Recent technological and methodological advances can substantially reduce the time and effort required for some of these steps.

Automated picking systems that take sieved size fractions, separate them into individual particles, and image each particle may greatly reduce picking times (de Garidel-Thoron et al., 2017; Itaki et al., 2020). With samples that have already been picked and mounted, hundreds or thousands of individual microfossils can be imaged simultaneously in three dimensions and algorithmically parsed into individual images from which basic morphometric traits and features can be automatically extracted and ana-

lyzed at the assemblage scale (Beaufort et al., 2014; Elder et al., 2018; Hsiang et al., 2018, 2019; Kahanamoku et al., 2018).

These efforts build on decades of previous automation work that either extracted coarser (size related) data or was relatively more labor intensive (Bollmann et al., 2005; Knappertsbusch et al., 2009). Given sufficient training data sets, convolutional neural nets can now identify planktonic foraminifera, coccolithophores, and radiolarians with accuracy similar to that of taxonomic specialists (Beaufort and Dollfus, 2004; de Garidel-Thoron et al., 2017; Hsiang et al., 2019; Itaki et al., 2020). Given these ongoing developments, it is becoming possible to envision a near future in which the entire sample processing and data extraction workflow is streamlined and largely automated, with taxonomic experts guiding and overseeing the process but spending the majority of their time analyzing data sets that may be far larger, denser, and more data-rich than is currently feasible.

provide these time-series data on community composition across multiple temporal scales, albeit for a limited set of taxa. For example, using planktonic foraminifera data, Lewandowska et al. (2020) compared the magnitude of biodiversity change across temporal scales from decades to millions of years. They found that, as expected, biodiversity change was greatest across the longest multi-million-year timescale and decreased at shorter timescales. However, they observed relatively large changes in community composition, comparable to the magnitude of changes over the longest timescale, most recently. The magnitude of recent turnover is suggestive of a large anthropogenic effect but may also reflect “noisy” annually averaged sediment trap time series.

Fish-scale paleobiological studies have similarly provided insight on baseline variability in fish populations. For example, marginal marine and continental margin sediments in the Pacific extended population dynamics for anchovy and sardines back to the nineteenth century and past millennia (Baumgartner et al., 1992; Field et al., 2009; Checkley et al., 2017; Kuwae et al., 2017; Salvattecchi et al.,

especially in the tropics (Dornelas et al., 2018; Blowes et al., 2019), but those that are available are extremely valuable for comparing the magnitude of biodiversity change observed in the fossil record to that observed in response to anthropogenic and recent climatic forcing.

FUTURE OUTLOOK

The continuity and duration of marine sediment core data make it possible to assess the relative importance of abrupt versus gradual, secular changes in climate to species and communities, tied to a refined (and ever improving) understanding of past climate change. The importance of spatial and temporal scales in (macro)ecology and (macro)evolution is well known (Brown and Maurer, 1989; Benton, 2009; Blois et al., 2013), with the patterns and drivers differing across space (Chiu et al., 2019; Jöst et al., 2019; Kusumoto et al., 2020) and time (Huang et al., 2018; Yasuhara et al., 2016, 2019b). Marine sediment cores permit interrogation of these dynamics at multiple temporal scales (Lewandowska et al., 2020). Biotic interactions generally tend to control dynamics on smaller spatial and tem-

particularly with concerted comparisons among Anthropocene, centennial, millennial, and million-year timescales.

Regardless of timescale, paleobiological studies, especially those that examine the relationship between climate and biodiversity and ecosystem functioning, provide insight into the potential response of biodiversity to ongoing climate change. The pace and scale of anthropogenic impacts on ecosystems and ecosystem services remain of great concern (Díaz et al., 2019). Climate change is expected to have an accelerating effect on the ocean, yet the challenges of using relatively short-term ecological data to understand long-term consequences to biodiversity and ecosystems remain significant. Sediment cores and associated microfossils can help elucidate links between climate and spatial biodiversity (e.g., Yasuhara et al., 2012c, 2020), extinction risks (e.g., Harnik et al., 2012; Finnegan et al., 2015), natural baselines (e.g., Yasuhara et al., 2012a, 2017b), and biotic consequences on evolutionary timescales (e.g., Ezard et al., 2011).

Yet, linking paleoecological insights to modern-day ecological change is relatively unexplored, and such insights do not necessarily make their way into informing global policy. Identifying and circumscribing the limits of such transposition remain challenging, particularly given the taxonomic biases of preservation and the rapidity of modern-day change. The opportunity remains to address such challenges and ensure that paleoecological data complement modern ecological data and, where appropriate, contribute to assessments and policy (e.g., IPBES [Intergovernmental Science-Policy Platform on Biodiversity and Ecosystem Services], the post-2020 Global Biodiversity Framework of the CBD [Convention on Biological Diversity]). Studies of sediment cores provide a long-term perspective on climate/biodiversity links that can contextualize modern marine ecological change and provide insights that would otherwise remain absent. 🌐

“While we lack a true time machine, the opportunity provided by this “biological time machine” remains unique.”

2018). These records show that fish population dynamics are more complex and region-specific than those perceived based on twentieth-century fishery data, with a clear Pacific-wide correlation between anchovy and sardine populations and Pacific Decadal Oscillations (Chavez et al., 2003; Kuwae et al., 2017; Salvattecchi et al., 2018). In sum, modern and historical time series of long-term biological monitoring are limited (e.g., Chavez et al., 2003; Engelhard, 2005; Lotze and McClenachan, 2014),

poral scales, while physical climatic factors, particularly temperature as reviewed here, appear to dominate biotic dynamics on larger scales (Benton, 2009; Yasuhara et al., 2016). However, there are gaps in our theoretical understanding of why this occurs, of the temporal scales on which physical factors begin to dominate, and of the relative importance of short abrupt events, cyclical changes, and long-term secular trends in shaping species and ecosystems. Continued study of marine sediment cores can help to fill these gaps,

REFERENCES

- Allen, A.P., J.H. Brown, and J.F. Gillooly. 2002. Global biodiversity, biochemical kinetics, and the energetic-equivalence rule. *Science* 297:1,545–1,548, <https://doi.org/10.1126/science.1072380>.
- Alvarez, S.A., S.J. Gibbs, P.R. Bown, H. Kim, R.M. Sheward, and A. Ridgwell. 2019. Diversity decoupled from ecosystem function and resilience during mass extinction recovery. *Nature* 574(7777):242–245, <https://doi.org/10.1038/s41586-019-1590-8>.
- Ambrecht, L.H. 2020. The potential of sedimentary ancient DNA to reconstruct past ocean ecosystems. *Oceanography* 33(2):116–123, <https://doi.org/10.5670/oceanog.2020.211>.
- Arrhenius, G.O.S. 1952. Sediment cores from the east Pacific. *Reports of the Swedish Deep-Sea Expedition 1947–1948* 5(1):1–227.
- Barmawidjaja, D.M., G.J. van der Zwaan, F.J. Jorissen, and S. Puskaric. 1995. 150 years of eutrophication in the northern Adriatic Sea: Evidence from a benthic foraminiferal record. *Marine Geology* 122:367–384, [https://doi.org/10.1016/0025-3227\(94\)00121-2](https://doi.org/10.1016/0025-3227(94)00121-2).
- Barron, J.A., D. Bukry, and D. Field. 2010. Santa Barbara Basin diatom and silicoflagellate response to global climate anomalies during the past 2200 years. *Quaternary International* 215:34–44, <https://doi.org/10.1016/j.quaint.2008.08.007>.
- Baumgartner, T.R., A. Soutar, and V. Ferreira-Bartrina. 1992. Reconstruction of the history of Pacific sardine and northern anchovy populations over the past two millennia from sediments of the Santa Barbara Basin, California. *CalCOFI Reports* 33:24–40.
- Beaufort, L., Y. Lancelot, P. Camberlin, O. Cayre, E. Vincent, F. Bassinot, and L. Labeyrie. 1997. Insolation cycles as a major control of equatorial Indian Ocean primary production. *Science* 278(5342):1,451–1,454, <https://doi.org/10.1126/science.278.5342.1451>.
- Beaufort, L., and D. Dollfus. 2004. Automatic recognition of coccoliths by dynamical neural networks. *Marine Micropaleontology* 51(1–2):57–73, <https://doi.org/10.1016/j.marmicro.2003.09.003>.
- Beaufort, L., N. Barbarin, and Y. Gally. 2014. Optical measurements to determine the thickness of calcite crystals and the mass of thin carbonate particles such as coccoliths. *Nature Protocols* 9(3):633–642, <https://doi.org/10.1038/nprot.2014.028>.
- Becker, K., J.A. Austin, N. Exon, S. Humphris, M. Kastner, J.A. McKenzie, K.G. Miller, K. Suyehiro, and A. Taira. 2019. 50 years of scientific ocean drilling. *Oceanography* 32(1):17–21, <https://doi.org/10.5670/oceanog.2019.110>.
- Benson, R.H., and P.C. Sylvester-Bradley. 1971. Deep-sea ostracodes and the transformation of ocean to sea in the Tethys. *Bulletin du Centre de recherches de Pau - SNPA* 5 supplément:63–91.
- Benson, R.H. 1972. The *Bradleya* problem, with descriptions of two new psychrospheric ostracode genera, *Agrenocythere* and *Poseidonamicus* (Ostracoda: Crustacea). *Smithsonian Contributions to Paleobiology* 12:1–138, <https://doi.org/10.5479/si.00810266.12.1>.
- Benton, M.J. 2009. The Red Queen and the Court Jester: Species diversity and the role of biotic and abiotic factors through time. *Science* 323(5915):728–732, <https://doi.org/10.1126/science.1157719>.
- Berger, W.H. 2007. Cenozoic cooling, Antarctic nutrient pump, and the evolution of whales. *Deep Sea Research Part II* 54:2,399–2,421, <https://doi.org/10.1016/j.dsr2.2007.07.024>.
- Berger, W.H. 2011. Geologist at sea: Aspects of ocean history. *Annual Review of Marine Science* 3:1–34, <https://doi.org/10.1146/annurev-marine-120709-142831>.
- Berggren, W.A., F.J. Hilgen, C.G. Langereis, D.V. Kent, J.D. Obradovich, I. Raffi, M.E. Raymo, and N.J. Shackleton. 1995. Late Neogene chronology: New perspectives in high-resolution stratigraphy. *Geological Society of America Bulletin* 107(11):1,272–1,287, [https://doi.org/10.1130/0016-7606\(1995\)107<1272:LNCNPI>2.3.CO;2](https://doi.org/10.1130/0016-7606(1995)107<1272:LNCNPI>2.3.CO;2).
- Bianchi, G.G., and I.N. McCave. 1999. Holocene periodicity in North Atlantic climate and deep-ocean flow south of Iceland. *Nature* 397(6719):515–517, <https://doi.org/10.1038/17362>.
- Blois, J.L., P.L. Zarnetske, M.C. Fitzpatrick, and S. Finnegan. 2013. Climate change and the past, present, and future of biotic interactions. *Science* 341(6145):499–504, <https://doi.org/10.1126/science.1237184>.
- Blowes, S.A., S.R. Supp, L.H. Antão, A. Bates, H. Bruehlheide, J.M. Chase, F. Moyes, A. Magurran, B. McGill, and I.H. Myers-Smith. 2019. The geography of biodiversity change in marine and terrestrial assemblages. *Science* 366(6463):339–345, <https://doi.org/10.1126/science.aaw1620>.
- Bollmann, J., P.S. Quinn, M. Vela, B. Brabec, S. Brechner, M.Y. Cortés, H. Hilbrecht, D.N. Schmidt, R. Schiebel, and H.R. Thierstein. 2005. Automated particle analysis: Calcareous microfossils. Pp. 229–252 in *Image Analysis, Sediments and Paleoenvironments*. P. Francus, ed., Springer, Dordrecht, The Netherlands, https://doi.org/10.1007/1-4020-2122-4_12.
- Bond, G.C., W. Showers, M. Cheseby, R. Lotti, P. Almasi, P. deMenocal, P. Priore, H. Cullen, I. Hajdas, and G. Bonani. 1997. A pervasive millennial-scale cycle in North Atlantic Holocene and glacial climates. *Science* 278(5341):1,257–1,266, <https://doi.org/10.1126/science.278.5341.1257>.
- Brown, J.H., and B.A. Maurer. 1989. Macroecology: The division of food and space among species on continents. *Science* 243(4895):1,145–1,150, <https://doi.org/10.1126/science.243.4895.1145>.
- Brown, J.H. 1995. *Macroecology*. The University of Chicago Press, Chicago.
- Cannariato, K.G., J.P. Kennett, and R.J. Behl. 1999. Biotic response to late Quaternary rapid climate switches in Santa Barbara Basin: Ecological and evolutionary implications. *Geology* 27(1):63–66, [https://doi.org/10.1130/0091-7613\(1999\)027<0063:BRTLQR>2.3.CO;2](https://doi.org/10.1130/0091-7613(1999)027<0063:BRTLQR>2.3.CO;2).
- Chaudhary, C., H. Saeedi, and M.J. Costello. 2016. Bimodality of latitudinal gradients in marine species richness. *Trends in Ecology & Evolution* 31(9):670–676, <https://doi.org/10.1016/j.tree.2016.06.001>.
- Chaudhary, C., H. Saeedi, and M.J. Costello. 2017. Marine species richness is bimodal with latitude: A reply to Fernandez and Marques. *Trends in Ecology & Evolution* 32(4):234–237, <https://doi.org/10.1016/j.tree.2017.02.007>.
- Chavez, F.C., J. Ryan, S.E. Lluch-Cota, and M. Niñuen. 2003. From anchovies to sardines and back: Multidecadal change in the Pacific Ocean. *Science* 299:217–221, <https://doi.org/10.1126/science.1075880>.
- Checkley, D.M. Jr., R.G. Asch, and R.R. Rykaczewski. 2017. Climate, anchovy, and sardine. *Annual Review of Marine Science* 9:469–493, <https://doi.org/10.1146/annurev-marine-122414-033819>.
- Chiu, W.T.R., M. Yasuhara, T.M. Cronin, G. Hunt, L. Gemery, and C.L. Wei. 2019. Marine latitudinal diversity gradients, niche conservatism and out of the tropics and Arctic: Climatic sensitivity of small organisms. *Journal of Biogeography* 47:817–828, <https://doi.org/10.1111/jbi.13793>.
- Clement, B., and M. Malone. 2019. Published scientific ocean drilling results. *Oceanography* 32(1):119, <https://doi.org/10.5670/oceanog.2019.132>.
- CLIMAP Project Members. 1976. The surface of the Ice Age earth. *Science* 191:1,131–1,137, <https://doi.org/10.1126/science.191.4232.1131>.
- CLIMAP Project Members. 1984. The last interglacial ocean. *Quaternary Research* 21:123–224, [https://doi.org/10.1016/0033-5894\(84\)90098-X](https://doi.org/10.1016/0033-5894(84)90098-X).
- Condamine, F.L., J. Romieu, and G. Guinot. 2019. Climate cooling and clade competition likely drove the decline of lamniform sharks. *Proceedings of the National Academy of Sciences of the United States of America* 116(41):20,584–20,590, <https://doi.org/10.1073/pnas.1902693116>.
- Cooper, S.R. 1995. Chesapeake Bay watershed historical land use: Impact on water quality and diatom communities. *Ecological Applications* 5:703–723, <https://doi.org/10.2307/1941979>.
- Cronin, T.M., and N. Ikeya. 1987. The Omma-Manganji ostracod fauna (Plio-Pleistocene) of Japan and the zoogeography of circumpolar species. *Journal of Micropaleontology* 6:65–88, <https://doi.org/10.1144/jm.6.2.65>.
- Cronin, T.M., M.E. Raymo, and K.P. Kyle. 1996. Pliocene (3.2–2.4 Ma) ostracode faunal cycles and deep ocean circulation, North Atlantic Ocean. *Geology* 24(8):695–698, [https://doi.org/10.1130/0091-7613\(1996\)024<0695:PMOFCA>2.3.CO;2](https://doi.org/10.1130/0091-7613(1996)024<0695:PMOFCA>2.3.CO;2).
- Cronin, T.M., and M.E. Raymo. 1997. Orbital forcing of deep-sea benthic species diversity. *Nature* 385(6617):624–627, <https://doi.org/10.1038/385624a0>.
- Cronin, T.M., D.M. DeMartino, G.S. Dwyer, and J. Rodriguez-Lazaro. 1999. Deep-sea ostracode species diversity: Response to late Quaternary climate change. *Marine Micropaleontology* 37(3–4):231–249, [https://doi.org/10.1016/S0377-8398\(99\)00026-2](https://doi.org/10.1016/S0377-8398(99)00026-2).
- Cronin, T.M., and C.D. Vann. 2003. The sedimentary record of climatic and anthropogenic influence on the Patuxent estuary and Chesapeake Bay ecosystems. *Estuaries* 26:196–209, <https://doi.org/10.1007/BF02695962>.
- Cronin, T.M. 2009. *Paleoclimates: Understanding Climate Change Past and Present*. Columbia University Press, New York.
- Cronin, T.M., G.S. Dwyer, E.K. Caverly, J. Farmer, L.H. DeNinno, J. Rodriguez-Lazaro, and L. Gemery. 2017. Enhanced Arctic amplification began at the mid-Brunhes event ~400,000 years ago. *Scientific Reports* 7:14475, <https://doi.org/10.1038/s41598-017-13821-2>.
- Currie, D.J., G.G. Mittelbach, H.V. Cornell, R. Field, J.F. Guegan, B.A. Hawkins, D.M. Kaufman, J.T. Kerr, T. Oberdorff, E. O'Brien, and others. 2004. Predictions and tests of climate-based hypotheses of broad-scale variation in taxonomic richness. *Ecology Letters* 7(12):1,121–1,134, <https://doi.org/10.1111/j.1461-0248.2004.00671.x>.
- de Garidel-Thoron, T., R. Marchant, E. Soto, Y. Gally, L. Beaufort, C.T. Bolton, M. Bouslama, L. Licari, J.-C. Mazur, and J.-M. Brutti. 2017. Automatic picking of foraminifera: Design of the Foraminifera Image Recognition and Sorting Tool (FIRST) prototype and results of the image classification scheme. *AGU Fall Meeting Abstracts*: PP43C-1369.
- deMenocal, P., J. Ortiz, G.T., and S.M. 2000. Coherent high- and low-latitude climate variability during the Holocene warm period. *Science* 288:2,198–2,202, <https://doi.org/10.1126/science.288.5474.2198>.
- DeNinno, L.H., T.M. Cronin, J. Rodriguez-Lazaro, and A. Brenner. 2015. An early to mid-Pleistocene deep Arctic Ocean ostracode fauna with North Atlantic affinities. *Palaeogeography, Palaeoclimatology, Palaeoecology* 419:90–99, <https://doi.org/10.1016/j.palaeo.2014.07.026>.
- de Vernal, A., A. Rochon, T. Radi. 2013. Dinoflagellates. Pp. 800–815 in *Encyclopedia of Quaternary Science*, 2nd ed. S.A. Elias and C.J. Mock, eds. Elsevier, Amsterdam.
- Díaz, S., J. Settele, E.S. Brondizio, H.T. Ngo, M. Guèze, J. Agard, A. Arneeth, P. Balvanera, K.A. Brauman, S.H.M. Butchart, and others. 2019. Summary for policymakers of the global assessment report on biodiversity and ecosystem services of the Intergovernmental Science-Policy Platform on Biodiversity and Ecosystem Services. IPBES secretariat, Bonn, Germany.
- Dillon, E.M., R.D. Norris, and A.O. Dea. 2017. Dermal denticles as a tool to reconstruct shark communities. *Marine Ecology Progress Series* 566:117–134, <https://doi.org/10.3354/meps12018>.

- Dornelas, M., L.H. Antao, F. Moyes, A.E. Bates, A.E. Magurran, D. Adam, A.A. Akhmetzhanova, W. Appeltans, J.M. Arcos, H. Arnold, and others. 2018. BioTIME: A database of biodiversity time series for the Anthropocene. *Global Ecology and Biogeography* 27(7):760–786, <https://doi.org/10.1111/geb.12729>.
- Dowsett, H., R. Thompson, J. Barron, T. Cronin, F. Fleming, S. Ishman, R. Poore, D. Willard, and T. Holtz Jr. 1994. Joint investigations of the Middle Pliocene climate I: PRISM paleoenvironmental reconstructions. *Global and Planetary Change* 9(3-4):169–195, [https://doi.org/10.1016/0921-8181\(94\)90015-9](https://doi.org/10.1016/0921-8181(94)90015-9).
- Dowsett, H.J., M.M. Robinson, D.K. Stoll, K.M. Foley, A.L.A. Johnson, M. Williams, and C.R. Riesselman. 2013. The PRISM (Pliocene palaeoclimate) reconstruction: Time for a paradigm shift. *Philosophical Transactions of the Royal Society A* 371(2001):20120524, <https://doi.org/10.1098/rsta.2012.0524>.
- Dutkiewicz, S., P. Cermeno, O. Jahn, M.J. Follows, A.E. Hickman, D.A.A. Taniguchi, and B.A. Ward. 2020. Dimensions of marine phytoplankton diversity. *Biogeosciences* 17:609–634, <https://doi.org/10.5194/bg-17-609-2020>.
- Elder, L.E., A.Y. Hsiang, K. Nelson, L.C. Strotz, S.S. Kahanamoku, and P.M. Hull. 2018. Sixty-one thousand recent planktonic foraminifera from the Atlantic Ocean. *Scientific Data* 5:180109, <https://doi.org/10.1038/sdata.2018.109>.
- Elderfield, H., P. Ferretti, M. Greaves, S. Crowhurst, I. McCave, D. Hodell, and A. Piotrowski. 2012. Evolution of ocean temperature and ice volume through the mid-Pleistocene climate transition. *Science* 337(6095):704–709, <https://doi.org/10.1126/science.1221294>.
- Emiliani, C. 1955. Pleistocene temperatures. *Journal of Geology* 63(6):538–578, <https://doi.org/10.1086/626295>.
- Engelhard, G.H. 2005. *Catalogue of Defra Historical Catch and Effort charts: Six Decades of Detailed Spatial Statistics for British Fisheries*. Science Series Technical Report no. 128, Centre for Environment Fisheries and Aquaculture Science, 42 pp.
- Ezard, T.H.G., T. Aze, P.N. Pearson, and A. Purvis. 2011. Interplay between changing climate and species' ecology drives macroevolutionary dynamics. *Science* 332(6027):349–351, <https://doi.org/10.1126/science.1203060>.
- Farris, D.W., C. Jaramillo, G. Bayona, S.A. Restrepo-Moreno, C. Montes, A. Cardona, A. Mora, R.J. Speakman, M.D. Glascock, and V. Valencia. 2011. Fracturing of the Panamanian Isthmus during initial collision with South America. *Geology* 39(11):1,007–1,010, <https://doi.org/10.1130/G32237.1>.
- Fenton, I.S., P.N. Pearson, T.D. Jones, A. Farnsworth, D.J. Lunt, P. Markwick, and A. Purvis. 2016. The impact of Cenozoic cooling on assemblage diversity in planktonic foraminifera. *Philosophical Transactions of the Royal Society B* 371:20150224, <https://doi.org/10.1098/rstb.2015.0224>.
- Field, D.B., T.R. Baumgartner, C.D. Charles, V. Ferreira-Bartrina, and M.D. Ohman. 2006. Planktonic foraminifera of the California Current reflect 20th-century warming. *Science* 311:63–66, <https://doi.org/10.1126/science.1116220>.
- Field, D.B., T.R. Baumgartner, V. Ferreira, D. Gutierrez, H. Lozano-Montes, R. Salvatelli, and A. Soutar. 2009. Variability from scales in marine sediments and other historical records. Pp. 45–63 in *Climate Change and Small Pelagic Fish*. D. Checkley, J. Alheit, Y. Oozeki, and C. Roy, eds, Cambridge University Press, Cambridge, <https://doi.org/10.1017/CBO9780511596681.006>.
- Finnegan, S., S.C. Anderson, P.G. Harnik, C. Simpson, D.P. Tittensor, J.E. Byrnes, Z.V. Finkel, D.R. Lindberg, L.H. Liow, and R. Lockwood. 2015. Paleontological baselines for evaluating extinction risk in the modern oceans. *Science* 348(6234):567–570, <https://doi.org/10.1126/science.aaa6635>.
- Flower, B.P., and J.P. Kennett. 1995. Biotic responses to temperature and salinity changes during last deglaciation, Gulf of Mexico. Pp. 209–220 in *Effects of Past Global Change on Life*. Panel on Effects of Past Global Change on Life, National Academy Press, Washington, DC.
- Fox, L., S. Stukins, T. Hill, and C.G. Miller. 2020. Quantifying the effect of anthropogenic climate change on calcifying plankton. *Scientific Reports* 10(1):1–9, <https://doi.org/10.1038/s41598-020-58501-w>.
- Fraass, A.J., D.C. Kelly, and S.E. Peters. 2015. Macroevolutionary history of the planktic foraminifera. *Annual Review of Earth and Planetary Sciences* 43:139–166, <https://doi.org/10.1146/annurev-earth-060614-105059>.
- Harnik, P.G., H.K. Lotze, S.C. Anderson, Z.V. Finkel, S. Finnegan, D.R. Lindberg, L.H. Liow, R. Lockwood, C.R. McClain, and J.L. McGuire. 2012. Extinctions in ancient and modern seas. *Trends in Ecology & Evolution* 27(11):608–617, <https://doi.org/10.1016/j.tree.2012.07.010>.
- Harzhauser, M., A. Kroh, O. Mandic, W.E. Piller, U. Gohlich, M. Reuter, and B. Berning. 2007. Biogeographic responses to geodynamics: A key study all around the Oligo-Miocene Tethyan Seaway. *Zoologischer Anzeiger* 246(4):241–256, <https://doi.org/10.1016/j.jcz.2007.05.001>.
- Hayward, B.W., S. Kawagata, H.R. Grenfell, A.T. Sabaa, and T. O'Neill. 2007. Last global extinction in the deep sea during the mid-Pleistocene climate transition. *Paleoceanography* 22(3), <https://doi.org/10.1029/2007PA001424>.
- Hayward, B.W., S. Kawagata, A. Sabaa, H. Grenfell, L. Van Kerckhoven, K. Johnson, and E. Thomas. 2012. *The Last Global Extinction (Mid-Pleistocene) of Deep Sea Benthic Foraminifera (Chrysalogoniidae, Ellipsoidalidae, Glaukulonodosariidae, Plectofrondiculariidae, Pleurostomellidae, Stilostomellidae)*. Their Late Cretaceous-Cenozoic History and Taxonomy. Cushman Foundation for Foraminiferal Research Special Publication 43, 408 pp.
- Henehan, M.J., P.M. Hull, D.E. Penman, J.W. Rae, and D.N. Schmidt. 2016. Biogeochemical significance of pelagic ecosystem function: An end-Cretaceous case study. *Philosophical Transactions of the Royal Society B: Biological Sciences* 371(1694):20150510, <https://doi.org/10.1098/rstb.2015.0510>.
- Hillebrand, H. 2004a. On the generality of the latitudinal diversity gradient. *The American Naturalist* 163(2):192–211, <https://doi.org/10.1086/381004>.
- Hillebrand, H. 2004b. Strength, slope and variability of marine latitudinal gradients. *Marine Ecology Progress Series* 273:251–267, <https://doi.org/10.3354/meps273251>.
- Holden, P., N. Edwards, E.W. Wolff, P. Valdes, and J. Singarayer. 2011. The Mid-Brunhes event and West Antarctic ice sheet stability. *Journal of Quaternary Science* 26(5):474–477, <https://doi.org/10.1002/jqs.1525>.
- Hsiang, A.Y., K. Nelson, L.E. Elder, E.C. Sibert, S.S. Kahanamoku, J.E. Burke, A. Kelly, Y. Liu, and P.M. Hull. 2018. AutoMorph: Accelerating morphometrics with automated 2D and 3D image processing and shape extraction. *Methods in Ecology and Evolution* 9(3):605–612, <https://doi.org/10.1111/2041-210X.12915>.
- Hsiang, A.Y., A. Brombacher, M.C. Rillo, M.J. Mleneck-Vautravers, S. Conn, S. Lordsmith, A. Jentzen, M.J. Henehan, B. Metcalfe, and I.S. Fenton. 2019. Endless forams: >34,000 modern planktonic foraminiferal images for taxonomic training and automated species recognition using convolutional neural networks. *Paleoceanography and Paleoceanology* 34(7):1,157–1,177, <https://doi.org/10.1029/2019PA003612>.
- Huang, H.H.M., M. Yasuhara, H. Iwatani, C.A. Alvarez Zarikian, M.A. Bassetti, and T. Sagawa. 2018. Benthic biotic response to climate changes over the last 700,000 years in a deep marginal sea: Impacts of deoxygenation and the Mid-Brunhes Event. *Paleoceanography and Paleoceanology* 33(7):766–777, <https://doi.org/10.1029/2018PA003343>.
- Huang, H.H.M., M. Yasuhara, H. Iwatani, T. Yamaguchi, K. Yamada, and B. Mamo. 2019. Deep-sea ostracod faunal dynamics in a marginal sea: Biotic response to oxygen variability and mid-Pleistocene global changes. *Paleobiology* 45:85–97, <https://doi.org/10.1017/pab.2018.37>.
- Hunt, G., T.M. Cronin, and K. Roy. 2005. Species–energy relationship in the deep sea: A test using the Quaternary fossil record. *Ecology Letters* 8:739–747, <https://doi.org/10.1111/j.1461-0248.2005.00778.x>.
- Hutchinson, D.K., H.K. Coxall, M. O'Regan, J. Nilsson, R. Caballero, and A.M. de Boer. 2019. Arctic closure as a trigger for Atlantic overturning at the Eocene-Oligocene Transition. *Nature Communications* 10(1):1–9, <https://doi.org/10.1038/s41467-019-11828-z>.
- Itaki, T., Y. Taira, N. Kuwamori, T. Maebayashi, S. Takeshima, and K. Toya. 2020. Automated collection of single species of microfossils using a deep learning–micromanipulator system. *Progress in Earth and Planetary Science* 7, <https://doi.org/10.1186/s40645-020-00332-4>.
- Jaramillo, C., M.J. Rueda, and G. Mora. 2006. Cenozoic plant diversity in the Neotropics. *Science* 311(5769):1,893–1,896, <https://doi.org/10.1126/science.1121380>.
- Jaramillo, C. 2018. Evolution of the Isthmus of Panama: Biological, paleoceanographic and paleoclimatological implications. Pp. 323–338 in *Mountains, Climate and Biodiversity*. C. Hoorn, A. Perrigo, and A. Antonelli, eds, Wiley Blackwell, Oxford.
- Johnson, K.G., M.R. Sánchez-Villagra, and O.A. Aguilera. 2009. The Oligocene-Miocene transition on coral reefs in the Falcón Basin (NW Venezuela). *Palaios* 24(1):59–69, <https://doi.org/10.2110/palo.2008.p08-004r>.
- Jonkers, L., H. Hillebrand, and M. Kucera. 2019. Global change drives modern plankton communities away from the pre-industrial state. *Nature* 570(7761):372–375, <https://doi.org/10.1038/s41586-019-1230-3>.
- Jöst, A.B., M. Yasuhara, C.L. Wei, H. Okahashi, A. Ostmann, P. Martínez Arbizu, B. Mamo, J. Svavarsson, and S. Brix. 2019. North Atlantic Gateway: Test bed of deep-sea macroecological patterns. *Journal of Biogeography* 46(9):2,056–2,066, <https://doi.org/10.1111/jbi.13632>.
- Kahanamoku, S.S., P.M. Hull, D.R. Lindberg, A.Y. Hsiang, E.C. Clites, and S. Finnegan. 2018. Twelve thousand recent patellogastropods from a northeastern Pacific latitudinal gradient. *Scientific Data* 5:170197, <https://doi.org/10.1038/sdata.2017197>.
- Katz, M.E., J.D. Wright, K.G. Miller, B.S. Cramer, K. Fennel, and P.G. Falkowski. 2005. Biological overprint of the geological carbon cycle. *Marine Geology* 217:323–338, <https://doi.org/10.1016/j.margeo.2004.08.005>.
- Katz, M.E., K. Fennel, and P.G. Falkowski. 2007. Geochemical and biological consequences of phytoplankton evolution. Pp. 405–430 in *Evolution of Primary Producers in the Sea*. P.G. Falkowski and A.H. Knoll, eds, Academic Press, Cambridge, <https://doi.org/10.1016/B978-012370518-1/50019-9>.
- Knappertsbusch, M.W., D. Binggeli, A. Hergiz, L. Schmutz, S. Stapfer, C. Schneider, J. Eisenecker, and L. Widmer. 2009. AMOR—a new system for automated imaging of microfossils for morphometric analyses. *Palaeontologia Electronica* 12:1–20.
- Koppers, A.A., C. Escutia, F. Inagaki, H. Pälike, D. Saffer, and D. Thomas. 2019. Introduction to the special issue on scientific ocean drilling: Looking to the future. *Oceanography* 32(1):14–15, <https://doi.org/10.5670/oceanog.2019.108>.
- Kucera, M., and J. Schönfeld. 2007. The origin of modern oceanic foraminiferal faunas and Neogene climate change. Pp. 409–425 in *Deep-*

- Time Perspectives on Climate Change: Marrying the Signal from Computer Models and Biological Proxies*. M. Williams, A.M. Haywood, F.J. Gregory, and D.N. Schmidt, eds, The Micropaleontological Society, Special Publications, The Geological Society, London, <https://doi.org/10.1144/TMS002.18>.
- Kusumoto, B., M.J. Costello, Y. Kubota, T. Shiono, C.L. Wei, M. Yasuhara, and A. Chao. 2020. Global distribution of coral diversity: Biodiversity knowledge gradients related to spatial resolution. *Ecological Research* 35(2):315–326, <https://doi.org/10.1111/1440-1703.12096>.
- Kuwae, M., M. Yamamoto, T. Sagawa, K. Ikehara, T. Irino, K. Takemura, H. Takeoka, and T. Sugimoto. 2017. Multidecadal, centennial, and millennial variability in sardine and anchovy abundances in the western North Pacific and climate-fish linkages during the late Holocene. *Progress in Oceanography* 159:86–98, <https://doi.org/10.1016/j.pocean.2017.09.011>.
- Lam, A.R., and R.M. Leckie. 2020. Late Neogene and Quaternary diversity and taxonomy of subtropical to temperate planktic foraminifera across the Kuroshio Current Extension, northwest Pacific Ocean. *Micropaleontology* 66:177–268.
- Lazarus, D., J. Barron, J. Renaudie, P. Diver, and A. Türke. 2014. Cenozoic planktonic marine diatom diversity and correlation to climate change. *PLoS ONE* 9(1):e84857, <https://doi.org/10.1371/journal.pone.0084857>.
- Leprieur, F., P. Descombes, T. Gaboriau, P.F. Cowman, V. Parravicini, M. Kulbicki, C.J. Melián, C.N. De Santana, C. Heine, and D. Mouillot. 2016. Plate tectonics drive tropical reef biodiversity dynamics. *Nature Communications* 7(1):1–8, <https://doi.org/10.1038/ncomms11461>.
- Lewandowska, A.M., L. Jonkers, H. Auel, J.A. Freund, W. Hagen, M. Kucera, and H. Hillebrand. 2020. Scale dependence of temporal biodiversity change in modern and fossil marine plankton. *Global Ecology and Biogeography* 29(6):1,008–1,019, <https://doi.org/10.1111/geb.13078>.
- Lisiecki, L.E., and M.E. Raymo. 2005. A Pliocene-Pleistocene stack of 57 globally distributed benthic $\delta^{18}\text{O}$ records. *Paleoceanography* 20(1), <https://doi.org/10.1029/2004PA001071>.
- Lotze, H.K., and L. McClenachan. 2014. Marine historical ecology: Informing the future by learning from the past. Pp. 165–200 in *Marine Community Ecology and Conservation*. M.D. Bertness, J.F. Bruno, and B.R. Silliman, and S.J.J. Stachowicz, eds, Sinauer Associates, Inc., Sunderland, Connecticut, USA.
- Lowery, C.M., P.R. Bown, A.J. Fraass, and P.M. Hull. 2020. Ecological response of plankton to environmental change: Thresholds for extinction. *Annual Review of Earth and Planetary Sciences* 48:403–429, <https://doi.org/10.1146/annurev-earth-081619-052818>.
- Macdougall, D. 2019. *Endless Novelties of Extraordinary Interest: The Voyage of H.M.S. Challenger and the Birth of Modern Oceanography*. Yale University Press, New Haven, 288 pp., <https://doi.org/10.2307/j.ctvmd85xk>.
- Marsaglia, K., K. Milliken, R.M. Leckie, D. Tentori, and L. Doran. 2015. IODP smear slide digital reference for sediment analysis of marine mud: Part 2. Methodology and atlas of biogenic components. *IODP Technical Note 2*, <https://doi.org/10.14379/iodp.tn.2.2015>.
- Marx, F.G., and M.D. Uhen. 2010. Climate, critters, and cetaceans: Cenozoic drivers of the evolution of modern whales. *Science* 327(5968):993–996, <https://doi.org/10.1126/science.1185581>.
- McManus, J.F., R. Francois, J.-M. Gherardi, L.D. Keigwin, and S. Brown-Leger. 2004. Collapse and rapid resumption of Atlantic meridional circulation linked to deglacial climate changes. *Nature* 428:834–837, <https://doi.org/10.1038/nature02494>.
- Meseguer, A.S., and F.L. Condamine. 2020. Ancient tropical extinctions at high latitudes contributed to the latitudinal diversity gradient. *Evolution*, <https://doi.org/10.1111/evo.13967>.
- Moffitt, S.E., T.M. Hill, P. Roopnarine, and J.P. Kennett. 2015. Response of seafloor ecosystems to abrupt global climate change. *Proceedings of the National Academy of Sciences of the United States of America* 112:4,684–4,689, <https://doi.org/10.1073/pnas.1417130112>.
- Motoyama, I. 1996. Late Neogene radiolarian biostratigraphy in the subarctic Northwest Pacific. *Micropaleontology* 42(3):221–262, <https://doi.org/10.2307/1485874>.
- Moy, A.D., W.R. Howard, S.G. Bray, and T.W. Trull. 2009. Reduced calcification in modern Southern Ocean planktonic foraminifera. *Nature Geoscience* 2(4):276–280, <https://doi.org/10.1038/ngeo460>.
- Myhre, S.E., K.J. Kroeker, T.M. Hill, P. Roopnarine, and J.P. Kennett. 2017. Community benthic paleoecology from high-resolution climate records: Mollusca and foraminifera in post-glacial environments of the California margin. *Quaternary Science Reviews* 155:179–197, <https://doi.org/10.1016/j.quascirev.2016.11.009>.
- Norris, R.D. 2000. Pelagic species diversity, biogeography, and evolution. *Paleobiology* 26:236–258, [https://doi.org/10.1666/0094-8373\(2000\)26\[236:PSDBAE\]2.0.CO;2](https://doi.org/10.1666/0094-8373(2000)26[236:PSDBAE]2.0.CO;2).
- Norris, R.D., S.K. Turner, P.M. Hull, and A. Ridgwell. 2013. Marine ecosystem responses to Cenozoic global change. *Science* 341(6145):492–498, <https://doi.org/10.1126/science.1240543>.
- O’Dea, A., and J. Jackson. 2009. Environmental change drove macroevolution in cupuladriid bryozoans. *Proceedings of the Royal Society B* 276(1673):3,629–3,634, <https://doi.org/10.1098/rspb.2009.0844>.
- O’Dea, A., J.B. Jackson, H. Fortunato, J.T. Smith, L. D’Croze, K.G. Johnson, and J.A. Todd. 2007. Environmental change preceded Caribbean extinction by 2 million years. *Proceedings of the National Academy of Sciences of the United States of America* 104(13):5,501–5,506, <https://doi.org/10.1073/pnas.0610947104>.
- O’Dea, A., H.A. Lessios, A.G. Coates, R.I. Eytan, S.A. Restrepo-Moreno, A.L. Cione, L.S. Collins, A. De Queiroz, D.W. Farris, and R.D. Norris. 2016. Formation of the Isthmus of Panama. *Science Advances* 2(8):e1600883, <https://doi.org/10.1126/sciadv.1600883>.
- Olausson, E. 1965. Evidence of climatic changes in North Atlantic deep-sea cores, with remarks on isotopic paleotemperature analysis. *Progress in Oceanography* 3:221–252, [https://doi.org/10.1016/0079-6611\(65\)90020-0](https://doi.org/10.1016/0079-6611(65)90020-0).
- Oppo, D.W., J.F. McManus, and J.L. Cullen. 2003. Deepwater variability in the Holocene epoch. *Nature* 422(6929):277–278, <https://doi.org/10.1038/422277b>.
- Ozawa, H., and T. Kamiya. 2005. The effects of glacio-eustatic sea-level change on Pleistocene cold-water ostracod assemblages from the Japan Sea. *Marine Micropaleontology* 54:167–189, <https://doi.org/10.1016/j.marmicro.2004.10.002>.
- Parker, F.L. 1958. Eastern Mediterranean foraminifera. *Reports of the Swedish Deep-Sea Expedition 1947–1948* 8:219–283.
- Powell, M.G., and D.S. Glazier. 2017. Asymmetric geographic range expansion explains the latitudinal diversity gradients of four major taxa of marine plankton. *Paleobiology* 42:196–208, <https://doi.org/10.1017/pab.2016.38>.
- Rabosky, D.L., and U. Sorhannus. 2009. Diversity dynamics of marine planktonic diatoms across the Cenozoic. *Nature* 457(7226):183–186, <https://doi.org/10.1038/nature07435>.
- Raymo, M.E., D.W. Oppo, B.P. Flower, D.A. Hodell, J.F. McManus, K.A. Venz, K.F. Kleiven, and K. McIntyre. 2004. Stability of North Atlantic water masses in face of pronounced climate variability during the Pleistocene. *Paleoceanography* 19(2), <https://doi.org/10.1029/2003PA000921>.
- Renema, W., D. Bellwood, J. Braga, K. Bromfield, R. Hall, K. Johnson, P. Lunt, C. Meyer, L. McMonagle, and R. Morley. 2008. Hopping hotspots: Global shifts in marine biodiversity. *Science* 321(5889):654–657, <https://doi.org/10.1126/science.1155674>.
- Revelle, R. 1987. How I became an oceanographer and other sea stories. *Annual Review of Earth and Planetary Sciences* 15(1):1–24, <https://doi.org/10.1146/annurev.ea.15.050187.000245>.
- Rillo, M.C., M. Kucera, T.H. Ezard, and C.G. Miller. 2019. Surface sediment samples from early age of seafloor exploration can provide a late 19th century baseline of the marine environment. *Frontiers in Marine Science* 5:517, <https://doi.org/10.3389/fmars.2018.00517>.
- Rogers, A., O. Aburto-Oropeza, W. Appeltans, J. Assis, L.T. Ballance, P. Cury, Duarte, C., F. Favoretto, J. Kumagai, C. Lovelock, and others. 2020. *Critical Habitats and Biodiversity: Inventory, Thresholds and Governance*. World Resources Institute, Washington, DC, 87 pp.
- Ruddiman, W.F. 1969. Recent planktonic foraminifera: Dominance and diversity in North Atlantic surface sediments. *Science* 164:1,164–1,167, <https://doi.org/10.1126/science.164.3884.1164>.
- Rutherford, S., S. D’Hondt, and W. Prell. 1999. Environmental controls on the geographic distribution of zooplankton diversity. *Nature* 400:749–753, <https://doi.org/10.1038/23449>.
- Salvattei, R., D. Field, D. Gutierrez, T. Baumgartner, V. Ferreira, L. Ortlieb, A. Sifeddine, D. Grados, and A. Bertrand. 2018. Multifarious anchovy and sardine regimes in the Humboldt Current System during the last 150 years. *Global Change Biology* 24:1,055–1,068, <https://doi.org/10.1111/gcb.13991>.
- Sánchez Goñi, M.F., S. Desprat, W.J. Fletcher, C. Morales-Molino, F. Naughton, D. Oliveira, D.H. Urrego, and C. Zorzi. 2018. Pollen from the deep-sea: A breakthrough in the mystery of the Ice Ages. *Frontiers in Plant Science* 9:38, <https://doi.org/10.3389/fpls.2018.00038>.
- Saupe, E.E., C.E. Myers, A.T. Peterson, J. Soberón, J. Singarayer, P. Valdes, and H. Qiao. 2019. Spatio-temporal climate change contributes to latitudinal diversity gradients. *Nature Ecology & Evolution* 3(10):1,419–1,429, <https://doi.org/10.1038/s41559-019-0962-7>.
- Scher, H.D., and E.E. Martin. 2006. Timing and climatic consequences of the opening of Drake Passage. *Science* 312:428–430, <https://doi.org/10.1126/science.1120044>.
- Schmidt, D.N., H.R. Thierstein, J. Bollmann, and R. Schiebel. 2004. Abiotic forcing of plankton evolution in the Cenozoic. *Science* 303:207–210, <https://doi.org/10.1126/science.1090592>.
- Sibert, E.C., K.L. Cramer, P.A. Hastings, and R.D. Norris. 2017. Methods for isolation and quantification of microfossil fish teeth and elasmobranch dermal denticles (ichthyoliths) from marine sediments. *Palaeontologia Electronica* 20:1–14, <https://doi.org/10.26879/677>.
- Stover, L.E., H. Brinkhuis, S.P. Damassa, L. de Verteuil, R.J. Helby, E. Monteil, A.D. Partridge, A.J. Powell, J.B. Riding, M. Smelror, and others. 1996. Mesozoic-Tertiary dinoflagellates, acritarchs and prasino-phytes. Pp. 641–750 in *Palynology: Principles and Applications. Vol. 2, Applications*. J. Jansonius and D.C. McGregor, eds, American Association of Stratigraphic Palynologists Foundation, College Station, TX.
- Tada, R., H. Zheng, and P.D. Clift. 2016. Evolution and variability of the Asian monsoon and its potential linkage with uplift of the Himalaya and Tibetan Plateau. *Progress in Earth and Planetary Science* 3(1):4, <https://doi.org/10.1186/s40645-016-0080-y>.
- Thomas, E., and A.J. Gooday. 1996. Cenozoic deep-sea benthic foraminifera: Tracers for changes in oceanic productivity? *Geology* 24(4):355–358, [https://doi.org/10.1130/0091-7613\(1996\)024<0355:CDSBFT>2.3.CO;2](https://doi.org/10.1130/0091-7613(1996)024<0355:CDSBFT>2.3.CO;2).

- Thomas, E. 2007. Cenozoic mass extinctions in the deep sea: What perturbs the largest habitat on Earth? *The Geological Society of America Special Paper* 424:1–23, [https://doi.org/10.1130/2007.2424\(01\)](https://doi.org/10.1130/2007.2424(01)).
- Tittensor, D.P., C. Mora, W. Jetz, H.K. Lotze, D. Ricard, E.V. Berghe, and B. Worm. 2010. Global patterns and predictors of marine biodiversity across taxa. *Nature* 466:1,098–1,101, <https://doi.org/10.1038/nature09329>.
- Tsujimoto, A., M. Yasuhara, R. Nomura, H. Yamazaki, Y. Sampei, K. Hirose, and S. Yoshikawa. 2008. Development of modern benthic ecosystems in eutrophic coastal oceans: The foraminiferal record over the last 200 years, Osaka Bay, Japan. *Marine Micropaleontology* 69:225–239, <https://doi.org/10.1016/j.marmicro.2008.08.001>.
- Uhen, M.D. 2020. Paleobiology Database Data Archives 9: Cetacea, https://paleobiodb.org/classic?user=Guest&action=displayPage&page=OSA_9_Cetacea.
- Weckström, K., A. Korhola, and J. Weckström. 2007. Impacts of eutrophication on diatom life forms and species richness in coastal waters of the Baltic Sea. *Ambio* 36:155–160, [https://doi.org/10.1579/0044-7447\(2007\)36\[155:IOEODL\]2.0.CO;2](https://doi.org/10.1579/0044-7447(2007)36[155:IOEODL]2.0.CO;2).
- Willard, D.A., and T.M. Cronin. 2007. Paleoeology and ecosystem restoration: Case studies from Chesapeake Bay and the Florida Everglades. *Frontiers in Ecology and the Environment* 5:491–498, <https://doi.org/10.1890/070015>.
- Worm, B., M. Sandow, A. Oschlies, H.K. Lotze, and R.A. Myers. 2005. Global patterns of predator diversity in the open oceans. *Science* 309:1,365–1,369, <https://doi.org/10.1126/science.1113399>.
- Worm, B., and D.P. Tittensor. 2018. *A Theory of Global Biodiversity*. Princeton University Press, Princeton, 232 pp., <https://doi.org/10.23943/9781400890231>.
- Yasuhara, M., H. Yamazaki, A. Tsujimoto, and K. Hirose. 2007. The effect of long-term spatiotemporal variations in urbanization-induced eutrophication on a benthic ecosystem, Osaka Bay, Japan. *Limnology and Oceanography* 52:1,633–1,644, <https://doi.org/10.4319/lo.2007.52.4.1633>.
- Yasuhara, M., and T.M. Cronin. 2008. Climatic influences on deep-sea ostracode (Crustacea) diversity for the last three million years. *Ecology* 89(sp11):S53–S65, <https://doi.org/10.1890/07-10211>.
- Yasuhara, M., T.M. Cronin, P.B. deMenocal, H. Okahashi, and B.K. Linsley. 2008. Abrupt climate change and collapse of deep-sea ecosystems. *Proceedings of the National Academy of Sciences of the United States of America* 105(5):1,556–1,560, <https://doi.org/10.1073/pnas.0705486105>.
- Yasuhara, M., G. Hunt, T.M. Cronin, and H. Okahashi. 2009. Temporal latitudinal-gradient dynamics and tropical instability of deep-sea species diversity. *Proceedings of the National Academy of Sciences of the United States of America* 106(5):2,171–2,172, <https://doi.org/10.1073/pnas.0910935106>.
- Yasuhara, M., G. Hunt, D. Breitburg, A. Tsujimoto, and K. Katsuki. 2012a. Human-induced marine ecological degradation: Micropaleontological perspectives. *Ecology and Evolution* 2(12):3,242–3,268, <https://doi.org/10.1002/ece3.425>.
- Yasuhara, M., G. Hunt, T.M. Cronin, N. Hokanishi, H. Kawahata, A. Tsujimoto, and M. Ishitake. 2012b. Climatic forcing of Quaternary deep-sea benthic communities in the North Pacific Ocean. *Paleobiology* 38:162–179, <https://doi.org/10.1666/10068.1>.
- Yasuhara, M., G. Hunt, H.J. Dowsett, M.M. Robinson, and D.K. Stoll. 2012c. Latitudinal species diversity gradient of marine zooplankton for the last three million years. *Ecology Letters* 15(10):1,174–1,179, <https://doi.org/10.1111/j.1461-0248.2012.01828.x>.
- Yasuhara, M., H. Okahashi, T.M. Cronin, T.L. Rasmussen, and G. Hunt. 2014. Response of deep-sea biodiversity to abrupt deglacial and Holocene climate changes in the North Atlantic Ocean. *Global Ecology and Biogeography* 23:957–967, <https://doi.org/10.1111/geb.12178>.
- Yasuhara, M., and R. Danovaro. 2016. Temperature impacts on deep-sea biodiversity. *Biological Reviews* 91(2):275–287, <https://doi.org/10.1111/brv.12169>.
- Yasuhara, M., H. Doi, C.L. Wei, R. Danovaro, and S.E. Myhre. 2016. Biodiversity-ecosystem functioning relationships in long-term time series and palaeoecological records: Deep sea as a test bed. *Philosophical Transactions of the Royal Society B* 371, <https://doi.org/10.1098/rstb.2015.0282>.
- Yasuhara, M., H. Iwatani, G. Hunt, H. Okahashi, T. Kase, H. Hayashi, T. Irizuki, Y.M. Aguilar, A.G.S. Fernando, and W. Renema. 2017a. Cenozoic dynamics of shallow-marine biodiversity in the Western Pacific. *Journal of Biogeography* 44(3):567–578, <https://doi.org/10.1111/jbi.12880>.
- Yasuhara, M., D.P. Tittensor, H. Hillebrand, and B. Worm. 2017b. Combining marine macroecology and palaeoecology in understanding biodiversity: Microfossils as a model. *Biological Reviews* 92(1):199–215, <https://doi.org/10.1111/brv.12223>.
- Yasuhara, M. 2019. Marine biodiversity in space and time. *Métophe* 9, <https://doi.org/10.7203/metode.9.11404>.
- Yasuhara, M., P.B. deMenocal, G.S. Dwyer, T.M. Cronin, H. Okahashi, and H.H.M. Huang. 2019a. North Atlantic intermediate water variability over the past 20,000 years. *Geology* 47:659–663, <https://doi.org/10.1130/G46161.1>.
- Yasuhara, M., G. Hunt, and H. Okahashi. 2019b. Quaternary deep-sea ostracods from the north-western Pacific Ocean: Global biogeography and Drake-Passage, Tethyan, Central American and Arctic pathways. *Journal of Systematic Palaeontology* 17(2):91–110, <https://doi.org/10.1080/14772019.2017.1393019>.
- Yasuhara, M., N.N. Rabalais, D.J. Conley, and D. Gutiérrez. 2019c. Palaeo-records of histories of deoxygenation and its ecosystem impact. Pp. 213–224 in *Ocean Deoxygenation: Everyone's Problem: Causes, Impacts, Consequences and Solutions*. D. Laffoley, and J.M. Baxter, eds, IUCN, Gland.
- Yasuhara, M., C.L. Wei, M. Kucera, M.J. Costello, D.P. Tittensor, W. Kiessling, T.C. Bonebrake, C. Tabor, R. Feng, A. Baselga, and others. 2020. Past and future decline of tropical pelagic biodiversity. *Proceedings of the National Academy of Sciences of the United States of America* 117:12,891–12,896, <https://doi.org/10.1073/pnas.1916923117>.
- Zachos, J., M. Pagani, L. Sloan, E. Thomas, and K. Billups. 2001. Trends, rhythms, and aberrations in global climate 65 Ma to present. *Science* 292:686–693, <https://doi.org/10.1126/science.1059412>.

ACKNOWLEDGMENTS

We thank Katsunori Kimoto, Jeremy R. Young, Kotaro Hirose, Tamotsu Nagumo, Yoshiaki Aita, Noritoshi Suzuki, David Lazarus, André Rochon, Erin M. Dillon, and Briony Mamo for help with microfossil images; Simon J. Crowhurst and David A. Hodell for help with coring overview illustrations; Richard D. Norris, R. Mark Leckie, and Peggy Delaney for thoughtful comments; and guest editors Peggy Delaney, Alan C. Mix, Laurie Menviel, Katrin J. Meissner, and Amelia E. Shevenell for editing and for the invitation to contribute to this special issue. This work is a product of the PSEEDS (Paleobiology as the Synthetic Ecological, Evolutionary, and Diversity Sciences) project, and is partly supported by grants

from the Research Grants Council of the Ho-Kong Special Administrative Region, China (Project No. HKU 17302518, HKU 17311316, HKU 17303115), the Seed Funding Programme for Basic Research of the University of Hong Kong (project codes: 201811159076, 201711159057), and the Faculty of Science RAE Improvement Fund of the University of Hong Kong (to M.Y.).

AUTHORS

Moriaki Yasuhara (moriakiyasuhara@gmail.com; yasuhara@hku.hk) is Associate Professor, School of Biological Sciences and Swire Institute of Marine Science, The University of Hong Kong, and a member of State Key Laboratory of Marine Pollution, City University of Hong Kong, Hong Kong SAR. **Huai-Hsuan May Huang** is Postdoctoral Researcher, School of Biological Sciences and Swire Institute of Marine Science, The University of Hong Kong, Hong Kong SAR. **Pincelli Hull** is Assistant Professor, Department of Geology and Geophysics, Yale University, New Haven, CT, USA. **Marina C. Rillo** is Postdoctoral Researcher, Institute for Chemistry and Biology of the Marine Environment, University of Oldenburg, Wilhelmshaven, Germany. **Fabien L. Condamine** is Research Scientist, Institut des Sciences de l'Évolution de Montpellier, CNRS, IRD, EPHE, Université de Montpellier, Montpellier, France. **Derek P. Tittensor** is Associate Professor and Jarilowsky Chair, Department of Biology, Dalhousie University, Halifax, Nova Scotia, Canada. **Michal Kučera** is Professor, MARUM - Center for Marine Environmental Sciences, University of Bremen, Germany. **Mark J. Costello** is Professor, Faculty of Biosciences and Aquaculture, Nord University, Bodø, Norway, and School of Environment, The University of Auckland, New Zealand. **Seth Finnegan** is Associate Professor, Department of Integrative Biology, University of California, Berkeley, CA, USA. **Aaron O'Dea** is Staff Scientist, Smithsonian Tropical Research Institute, Balboa, Republic of Panama. **Yuanyuan Hong** is Postdoctoral Researcher, School of Biological Sciences and Swire Institute of Marine Science, The University of Hong Kong, Hong Kong SAR. **Timothy C. Bonebrake** is Associate Professor, School of Biological Sciences, The University of Hong Kong, Hong Kong SAR. **N. Ryan McKenzie** is Assistant Professor, Department of Earth Sciences, University of Hong Kong, Hong Kong SAR. **Hideyuki Doi** is Associate Professor, Graduate School of Simulation Studies, University of Hyogo, Kobe, Japan. **Chih-Lin Wei** is Associate Professor, Institute of Oceanography, National Taiwan University, Taipei, Taiwan. **Yasuhiro Kubota** is Professor, Faculty of Science, University of the Ryukyus, Okinawa, Japan. **Erin E. Saupe** is Associate Professor, Department of Earth Sciences, University of Oxford, UK.

ARTICLE CITATION

Yasuhara, M., H.-H.M. Huang, P. Hull, M.C. Rillo, F.L. Condamine, D.P. Tittensor, M. Kučera, M.J. Costello, S. Finnegan, A. O'Dea, Y. Hong, T.C. Bonebrake, N.R. McKenzie, H. Doi, C.-L. Wei, Y. Kubota, and E.E. Saupe. 2020. Time machine biology: Cross-timescale integration of ecology, evolution, and oceanography. *Oceanography* 33(2):16–28, <https://doi.org/10.5670/oceanog.2020.225>.

COPYRIGHT & USAGE

This is an open access article made available under the terms of the Creative Commons Attribution 4.0 International License (<https://creativecommons.org/licenses/by/4.0/>), which permits use, sharing, adaptation, distribution, and reproduction in any medium or format as long as users cite the materials appropriately, provide a link to the Creative Commons license, and indicate the changes that were made to the original content.

SIDEBAR. On Quantifying Stratigraphic, Chronologic, and Paleo Flux Uncertainties in Paleoceanography

By Alan C. Mix

Paleoceanography is changing from a qualitative story-telling field to one that is quantitative. This transformation is in part due to the development and adoption of a growing arsenal of statistical tools that evaluate uncertainty. A strength of the field is the illustration of fundamental changes in the Earth/ocean/climate system that are beyond humanity's recent experience. A weakness lurks in the difficulty of telling time well. Precise and accurate geochronology is essential for establishing rates of change and for quantifying physical or biogeochemical fluxes.

Rates and fluxes are important constraints on the impacts of carbon (and other) feedbacks on a warming climate. We know that additional warming of the planet is already “baked into” our future because paleoceanographers and paleoclimatologists have documented how the relatively long response times of the ocean's interior, ice sheets, and some carbon reservoirs slow down the various responses to forcings (e.g., carbon emissions)—but may also eventually amplify them or render them irreversible; thus, we know that new Earth system equilibria will only be approached after millennia. For example, over 90% of the excess heat produced by artificially elevated CO₂ is already in the ocean (Durack et al., 2018). If humanity eventually controls its carbon emissions and reduces atmospheric CO₂, it will take a long time for the excess heat to emerge from, and for the excess carbon to be neutralized in, the ocean (Ehlerlert and Zickfeld, 2018).

But how fast and how much will our planet change? To answer those questions, we need paleo studies that better constrain transient times and feedbacks so models can be adequately tested under extreme change scenarios and better predict the future with confidence. Fischer et al. (2018) summarized various impacts of past warming on the scale of a few degrees of global warming above preindustrial levels, but avoided specifying rates of change, considering them too uncertain with available chronological constraints.

Fortunately, progress is at hand. Radiometric age models are improving. For example, Marine20, a new calibration of marine radiocarbon data into so-called “calendar” ages, is just out and now extends back ~55,000 years (Heaton et al., 2020). The details remain tricky and model-dependent in the ocean because of the need to account for the changing carbon cycle coupled to changes in circulation patterns and rates in the ocean interior, which conspire with changing ¹⁴C production rates to influence regional reservoir ages. The model that projects Marine20's surface-water reservoir ages over the past 55,000 years propagates uncertainties in changing ¹⁴C production and carbon cycling, while satisfying constraints

of limited data available from the ocean. This is a big improvement over previous syntheses. Nevertheless, the representation of changing deep-ocean circulation is inevitably incomplete. We do not yet know this history because various tracers do not yet converge on a single answer without re-evaluation of processes that control the tracer measurements including $\delta^{13}\text{C}$ and ϵNd (Du et al., 2020), and this too has implications for radiocarbon reservoir ages.

Marine20 comes with a clear warning that it applies to the warm surface ocean assumed to be near dynamic equilibrium with respect to ocean mixing and air-sea gas exchange. Application to higher latitudes or regions of changing wind-driven upwelling, where these assumptions break down, requires additional considerations, such as assignment of a deviation from the ideal reservoir age, known as Delta-R, which varies regionally. Delta-R may also vary through time, but for lack of constraints, it is often assumed constant through time. Efforts are underway to use a variety of simple models to begin to address this issue empirically (e.g., Walczak et al., in press).

IIth Commandment: Thou shalt not covet high-resolution results with low-resolution data

A continuous age model based on radiocarbon or other sources of age datums involves finding a logical pathway between dated levels, with quantified uncertainties. Several Bayesian tools are available to assist in this task, such as Bacon (Blaauw and Christian, 2011), Bchron (Haslett and Parnell, 2008; Parnell, 2020), and Oxcal (Bronk Ramsey, 2009). Quantitative correlation also now provides for assessment of the precision of stratigraphic alignment of “wiggly” proxy signals as an adjunct to independent chronologic information (Lee et al., 2019).

These Bayesian methods, now widely used, are not limited to radiocarbon but can be used with many kinds of data for alignment and as smart interpolation tools with propagation of uncertainties. Their solutions are not all identical, however. Tools like this don't absolve us of thinking carefully about the systems we are measuring and the assumptions underlying the methods, which may include ideas about sedimentation patterns and mechanisms.

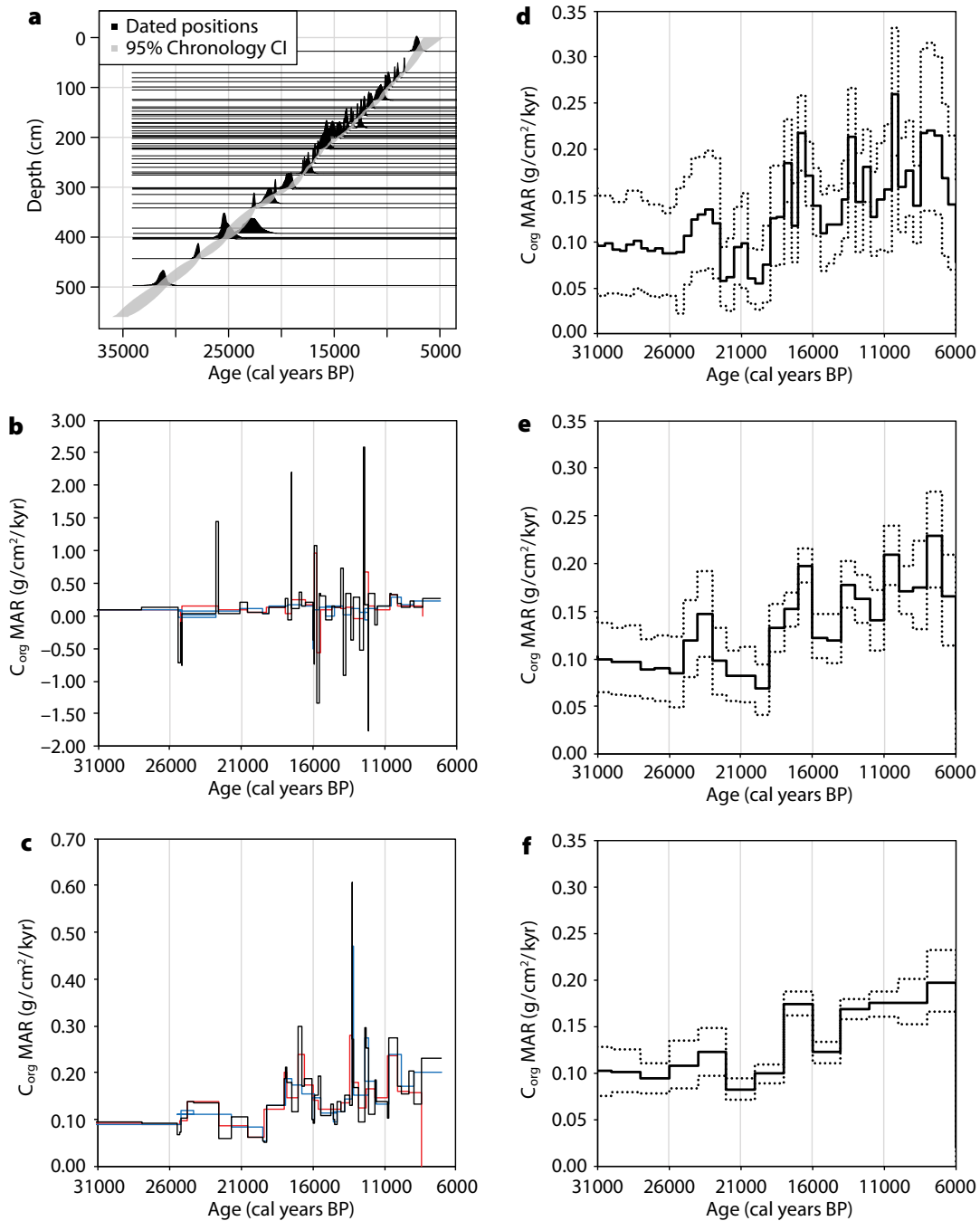


FIGURE 1. Illustration of various model assumptions used in calculating organic carbon mass accumulation rates (MAR: a convolution of sedimentation rate from calibrated dates, dry bulk density, and organic carbon [C_{org}] contents, using data compiled by Lopes et al., 2015, here recalibrated with the Marine20 calibration curve of Heaton et al., 2020). (a) Age-depth curve with Bayesian age model calculated using Bchron (Parnell, 2020). Organic carbon mass accumulation rates calculated using (b) point-to-point MAR changes based on all Marine20 calendar dates (black) and as a sensitivity test every second date odd (red) and even (blue). (c) Point-to-point MAR changes based on Bchron's Bayesian age model at the dated levels, otherwise as in (b). (d, e, f) Bootstrap calculations with full uncertainty propagation for C_{org} MAR in 500-, 1,000-, and 2,000-year bins, respectively. The result in (b) is unstable, and age reversals produce negative MAR, requiring arbitrary decisions about data culling. The result in (c) is better, because the Bayesian model resolves age reversals, but uneven spacing imposes resolution bias. The uniform bins in (d, e, f) allow uncertainty estimation and illustrate the trade-offs between resolution and certainty—coarser time bins give more certain results, but may lose important temporal structure.

Assigning sediment accumulation rates is unfortunately not as simple as taking a first derivative of an age model curve, and may be subject to circular reasoning if sedimentation processes are assumed as part of the age modeling exercise. The sedimentary record's completeness is thought to be a function of the time span over which it is measured (Sadler and Strauss, 1990); specifically, longer time integrations tend to have lower apparent sediment accumulation rates because of a higher probability of missing sediment. Point-by-point flux normalization notwithstanding (e.g., by ^3He or ^{230}Th ; e.g., Costa et al., 2020), a reasonable requirement for minimizing missing-sediment bias is to calculate sediment accumulation rates over fixed and constant time intervals while propagating quantified uncertainties in the age models from the Bayesian age modeling tools. This is relatively straightforward using Monte-Carlo bootstrap methods, but is rarely done.

Calculation of biogeochemical fluxes demands further error propagation of sediment accumulation, bulk densities, and component concentrations. This is accomplished by binning or otherwise assessing proxy data within the boundaries of the time intervals for averaging, and convolving bin uncertainties on dry bulk density with those on property concentrations and sedimentation rates. This too is sufficiently complicated that bootstrap methods are reasonable approaches. The literature is rife with examples of calculated fluxes made with point data applied to interpolated ages between age datums of unequal spacing and without error propagation.

To illustrate how point spacing effects, binning, and changing resolution affect inferred changes in mass accumulation rates and their uncertainties, I calculated carbon burial fluxes (Figure 1) using a published high-resolution data set from a well-characterized core in the Northeast Pacific off Oregon (W98709-13pc, 42.117°N, 125.750°W, 2,712 m depth, with an average spacing between dated levels of 500 years; Lopes et al., 2015). That study showed apparent decoupling between diatom-based primary productivity, export productivity, and organic carbon burial in response to climate change, and it raised questions about how to address issues concerning the effects of biogeochemical fluxes on carbon feedbacks in climate models.

In this case, it appears that variations in carbon burial are not resolved beyond uncertainty in 500-year bins, that some events appear to be resolved in 1,000-year bins, and that most variations are resolved in 2,000-year bins. Armed with this analysis, it is possible to choose at what reasonable temporal resolution and what significance level to evaluate changes in biogeochemical fluxes, or before analysis, we can determine how to design a sampling and analysis program to get the resolution and precision needed to test a hypothesis.

Among paleoceanography's grand challenges for the coming decade is to refine geochronology, and in so doing to quantify rates of change and material fluxes. To do this well demands understanding of biases in the sedimentary record and rigorous estimation of uncertainties. While a variety of

approaches will probably always be needed, widespread adoption of new and emerging Bayesian age modeling tools is essential. Quantitative estimation of uncertainty reveals the need for higher-resolution and higher-precision data sets, which put further demands on our laboratories, and of course on the funding that pays for the analyses. We can expect these approaches to continue to evolve and improve as the relevant literature of theory, tools, and applications expands.

REFERENCES

- Blaauw, M., and J.A. Christen. 2011. Flexible paleoclimate age-depth models using an autoregressive gamma process. *Bayesian Analysis* 6(3):457–474, <https://doi.org/10.1214/11-BA618>.
- Bronk Ramsey, C. 2009. Bayesian analysis of radiocarbon dates. *Radiocarbon* 51(1):337–360, <https://doi.org/10.1017/S0033822200033865>.
- Costa, K.M., C.T. Hayes, R.F. Anderson, F.J. Pavia, A. Bausch, F. Deng, J.C. Dutay, W. Geibert, C. Heinze, G. Henderson, and others. 2020. ^{230}Th normalization: New insights on an essential tool for quantifying sedimentary fluxes in the modern and Quaternary ocean. *Paleoceanography and Paleoeclimatology* 35:e2019PA003820, <https://doi.org/10.1029/2019PA003820>.
- Du, J., B.A. Haley, and A.C. Mix. 2020. Evolution of the global overturning circulation since the Last Glacial Maximum based on marine authigenic neodymium isotopes. *Quaternary Science Reviews* 241:106396, <https://doi.org/10.1016/j.quascirev.2020.106396>.
- Durack, P.J., P.J. Gleckler, S.G. Purkey, G.C. Johnson, J.M. Lyman, and T.P. Boyer. 2018. Ocean warming: From the surface to the deep in observations and models. *Oceanography* 31(2):41–51, <https://doi.org/10.5670/oceanog.2018.227>.
- Ehlert, D., and K. Zickfeld. 2018. Irreversible ocean thermal expansion under carbon dioxide removal. *Earth System Dynamics* 9(1):197–210, <https://doi.org/10.5194/esd-9-197-2018>.
- Fischer, H., K.J. Meissner, A.C. Mix, N.J. Abram, J. Austermann, V. Brovkin, E. Capron, D. Colombaroli, A.-L. Daniau, K.A. Dyez, and others. 2018. Palaeoclimate constraints on the impact of 2°C anthropogenic warming and beyond. *Nature Geoscience* 11:474–485, <https://doi.org/10.1038/s41561-018-0146-0>.
- Haslett, J., and A. Parnell. 2008. A simple monotone process with application to radiocarbon-dated depth chronologies. *Journal of the Royal Statistical Society, Series C* 57(4):399–418, <https://doi.org/10.1111/j.1467-9876.2008.00623.x>.
- Heaton, T.J., P.R. Köhler, M. Butzin, E. Bard, R.W. Reimer, W.E.N. Austin, C. Bronk Ramsey, P.M. Grootes, K.A. Hughen, B. Kromer, and others. 2020. Marine20: The marine radiocarbon age calibration curve (0–55,000 cal BP). *Radiocarbon*, <https://doi.org/10.1017/RDC.2020.68>.
- Lee, T., L.E. Lisiecki, D. Rand, G. Gebbie, C.E. Lawrence. 2019. Dual proxy Gaussian Process stack: Integrating $\delta^{18}\text{O}$ benthic and radiocarbon proxies for inferring ages on ocean sediment cores. *arXiv preprint*, <https://arxiv.org/pdf/1907.08738.pdf>.
- Lopes, C., M. Kucera, and A.C. Mix. 2015. Climate change decouples oceanic primary and export productivity and organic carbon burial. *Proceedings of the National Academy of Sciences of the United States of America* 112(2):332–335, <https://doi.org/10.1073/pnas.1410480111>.
- Parnell, A. 2020. Package 'Bchron', <https://cran.r-project.org/web/packages/Bchron/Bchron.pdf>.
- Sadler, P.M., and D.J. Strauss. 1990. Estimation of completeness of stratigraphical sections using empirical data and theoretical models. *Journal of the Geological Society* 147:471–485, <https://doi.org/10.1144/gsjgs.147.3.0471>.
- Walczak, M.H., A.C. Mix, E.A. Cowan, S. Fallon, L.K. Fifield, J. Alder, J. Du, B. Haley, T. Hobern, J. Padman, and others. In press. Phasing of millennial-scale climate variability in the Pacific and Atlantic Oceans. *Science*, <https://doi.org/10.1126/science.aba7096>.

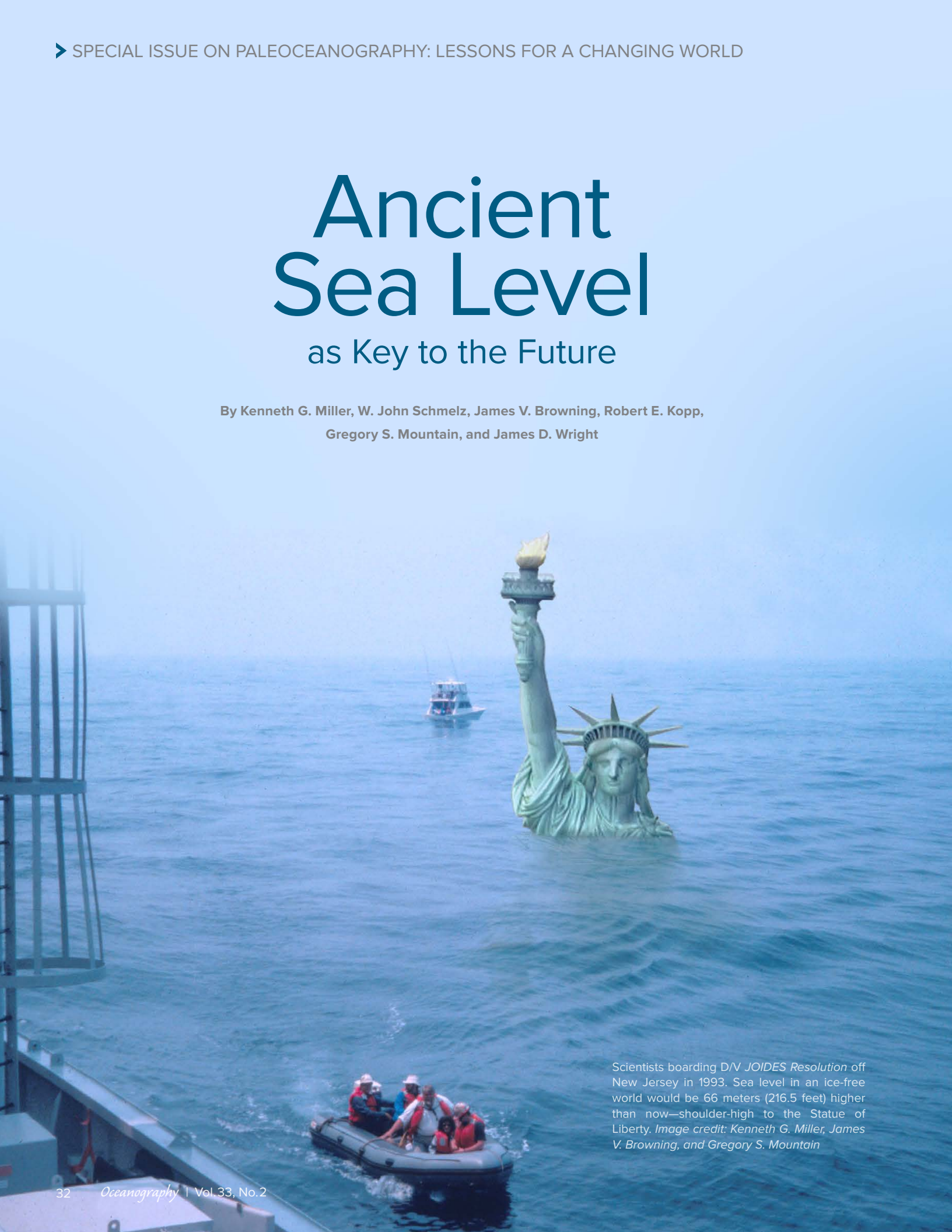
AUTHOR

Alan C. Mix (alan.mix@oregonstate.edu) is Professor, College of Earth, Ocean, and Atmospheric Sciences, Oregon State University, Corvallis, OR, USA.

Ancient Sea Level

as Key to the Future

By Kenneth G. Miller, W. John Schmelz, James V. Browning, Robert E. Kopp,
Gregory S. Mountain, and James D. Wright



Scientists boarding D/V *JOIDES Resolution* off New Jersey in 1993. Sea level in an ice-free world would be 66 meters (216.5 feet) higher than now—shoulder-high to the Statue of Liberty. Image credit: Kenneth G. Miller, James V. Browning, and Gregory S. Mountain

ABSTRACT. Studies of ancient sea levels provide insights into the mechanisms and rates of sea level changes due to tectonic processes (e.g., ocean crust production) and climatic variations (e.g., insolation due to Earth's orbital changes and atmospheric CO₂). Global mean sea level (GMSL) changes since the Middle Eocene (ca. 48 million years ago [Ma]) have been primarily driven by ice volume changes paced on astronomical timescales (2400, 1200, 95/125, 41, and 19/23 thousand years [kyr]), modulated by changes in atmospheric CO₂. During peak warm intervals (e.g., Early Eocene Climatic Optimum 56–48 Ma and the early Late Cretaceous ca. 100–80 Ma), atmospheric CO₂ was high and Earth was more than 5°C warmer and mostly ice-free, contributing ~66 m of GMSL rise from ice alone. However, even in the warmest times (e.g., Early Eocene, ca 50 Ma), growth and decay of small ice sheets (<25 m sea level equivalent) likely drove sea level changes that inundated continents and controlled the record of shallow-water deposits. Ice sheets were confined to the interior of Antarctica prior to the Oligocene and first reached the Antarctic coast at 34 Ma, with the lowest sea levels -20 ± 10 m relative to modern GMSL. Following a near ice-free Miocene Climatic Optimum (17–13.8 Ma), a permanent East Antarctic Ice Sheet (EAIS) developed in the Middle Miocene (ca. 13.8 Ma). During the Pliocene (4–3 Ma), CO₂ was similar to 2020 CE (Common Era) and sea levels stood $\sim 22\pm 10$ m above present, requiring significant loss of the Greenland Ice Sheet (~7 m of sea level), West Antarctic Ice Sheet (~5 m after isostatic compensation), and vulnerable portions of the EAIS. The small Northern Hemisphere ice sheets of the Eocene to Pliocene expanded into continental scale in the Quaternary (past 2.55 million years). Sea level reached its lowest point (~130 m below present) during the Last Glacial Maximum (ca. 27–20 thousand years before 1950 [ka]), episodically rose during the deglaciation (ca. 20–11 ka) at rates that at times were in excess of 47 mm yr⁻¹ (vs. modern rates of 3.2 mm yr⁻¹), and progressively slowed during the Early to Middle Holocene from ca. 11 ka until ~4 ka. During the Late Holocene (last 4.2 kyr, including the CE), GMSL only exhibited multi-centennial variability of ± 0.1 m. The modern episode of GMSL rise began in the late nineteenth century, with most of the twentieth century rise attributable to global warming and ice melt. Under moderate emissions scenarios, GMSL is likely to rise 0.4–1.0 m in this century, with ancient analogs suggesting a longer term (centennial to millennial scale) equilibrium rise of ~10 m. Under higher emissions scenarios, twenty-first century GMSL will rise greater than 2 m, and in the long term, tens of meters cannot be excluded.

SEA LEVEL AS A BAROMETER OF EARTH'S CLIMATE STATES

The state of Earth's climate is reflected by the position of the shoreline globally, both in the modern world as sea level inexorably rises and accelerates, and in ancient worlds of vastly different sea levels that ranged from 130 m below present, when now submerged continental shelves were exposed (e.g., 20 thousand years before

1950 [ka]), to over 150 m above present due to ice-free conditions and long-term tectonics, when large areas of the continents were inundated (e.g., ca. 90 million years ago [Ma] and 55 Ma). Today, humanity looks to its coastlines not only for living space, food, and other resources but also as a barometer of global climate changes that are causing rapidly escalating social and economic impacts. Reading

the record of past sea level changes provides an understanding of processes that control sea level (Figure 1) and shoreline position that are relevant to planning for future rise. Recent advances in data, imaging, and modeling provide fresh constraints and new insights into timing, amplitudes, and rates of ancient sea level changes (Table 1). In this overview, we briefly discuss the history of the timing, rates, and causes of sea level changes (Figures 1–3) during the last 66 million years (with greater uncertainty prior to ca. 48 Ma) and their implications for present and future rise.

Sea level change is not uniform around the world. Relative sea level (RSL) is the difference in height between the sea surface and the solid Earth at a particular place. GMSL change is the global mean of relative sea level change and is the volume of the ocean divided by the ocean surface area (Gregory et al., 2019). In geological literature, GMSL change is sometimes called “eustatic change,” which is defined with respect to some fixed datum level such as the center of the Earth and is more properly termed global mean geocentric sea level change (Gregory et al., 2019). We eschew the terms “eustasy” and “eustatic change” because such datum levels are lacking or equivocal in the geologic record. RSL change at a particular place is controlled both by GMSL change and by regional and local land motion. RSL includes the effects of thermal subsidence, sediment loading, flexure, mantle dynamic topography, and glacial isostatic adjustment (GIA), as well as changes in the height of the geoid driven by the changing distribution of ice and ocean mass and by GIA. In addition, there are short-term (1–1,000-year scale) ocean dynamic sea level changes (e.g., El Niño and Gulf Stream varia-

tions that regionally cause tens of centimeters of transient sea level changes). GMSL variations are caused primarily (Figure 1) by changes in ocean temperature (tens of centimeters on annual to centennial timescales, with up to 10 m over the past 48 million years due to cooling), changes in land ice volume (meter scale operating on decadal to centennial scales and up to 200 m on astronomical timescales of ~20 thousand years [kyr] to 2,400 kyr), and changes in the volumes of ocean basins (100+ m scale primarily on >1 million year timescales; see summary in Miller et al., 2005a).

The yet-to-be formally defined Anthropocene epoch (Zalasiewicz, 2008) can be partly characterized by human-induced modifications of Earth's climate state due to changes in atmospheric CO₂ concentrations from 280 ppm in ~1850 to 414 ppm in 2020 CE, with current trends projected to lead to 600–900 ppm in this century in the absence of strong global climate policy (Riahi et al., 2017; Meinshausen et al., 2020). Other potential markers for the base of the Anthropocene can be as young as the atomic-testing tritium spike that culminated in 1963, though here we use the CO₂ record to place the base at 1850 CE (Figure 3). The Anthropocene will constitute a climate

and sea level state fundamentally different from glacial periods (e.g., 27–20 ka) or the Holocene interglacial (11.3 ka to 1850 CE). Ancient climates range from cold, glacial periods (e.g., Last Glacial Maximum [LGM]) with CO₂ at 180 ppm to warm, ice-free states, the most recent of which are the Early Eocene Climatic Optimum (EECO; 56–48 Ma) and possibly the Miocene Climatic Optimum (17–13.8 Ma), with CO₂ two to three times higher than 1850 CE. Miller et al. (2020) recognize three pre-Anthropocene climate states: Hothouse (very warm, largely ice-free conditions; Late Cretaceous and Early Eocene), cool Greenhouse (Early to Middle Eocene) with small ice sheets (<25 m sea level equivalent), and Icehouse conditions with continental-scale ice sheets at one or both poles (Figure 2). Today, the Greenland Ice Sheet (GIS) contains 7.4 m of sea level equivalent; the West Antarctic Ice Sheet (WAIS) contains 5.6 m of sea level equivalent, including the Antarctic Peninsula; the East Antarctic Ice Sheet (EAIS) contains 52 m of sea level equivalent; and mountain glaciers and ice caps contain <1 m of sea level equivalent (Morlighem et al., 2019). Within the Icehouse of the Oligocene to Holocene (Figure 2), climates varied on glacial and interglacial timescales, with

continental ice sheets waxing and waning in East Antarctica during the Oligocene to Middle Miocene (ca. 34–13.9 Ma), a permanent EAIS developing in the Middle Miocene (ca. 13.8 Ma), and large Northern Hemisphere ice sheets developing in the Quaternary (last 2.55 million years). Changes in ice volume dominate the rise and fall of sea level during Icehouse, cool Greenhouse, and perhaps even Hothouse worlds (Miller et al., 2020).

MEASURING SEA LEVEL CHANGES

Sea level change is determined by measuring time (age) and height of water with respect to datum levels. We refer sea level to the modern mean sea level (MSL) datum level (https://tidesandcurrents.noaa.gov/datum_options.html). Instrumental measurements of RSL are based on data from tide gauges with extensive global coverage after World War II and sparse coverage dating back to the eighteenth century, and from satellites with global coverage since 1993. GMSL is statistically inferred from these records (e.g., Dangendorf et al., 2017). For reconstruction of ancient sea level, proxies (shorelines, fossils, sediment facies) are calibrated to time and MSL, with ages determined from radiometric data (mostly radiocarbon over

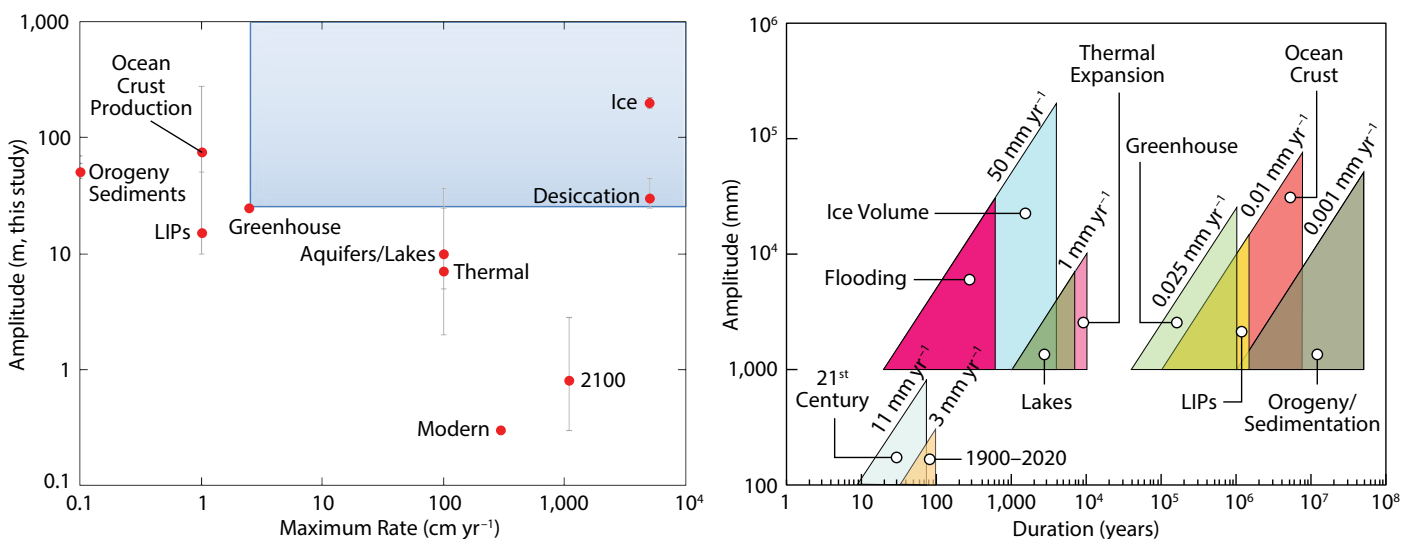


FIGURE 1. Processes affecting sea level change. (left) Log-log plot of maximum amplitudes (in meters with error) versus maximum rates. The blue box encompasses rates that can only be explained by ice volume changes or basin desiccation. (right) Log-log plot of amplitudes versus durations for each process where the length of each hypotenuse gives the maximum rate of change. LIPs = Large Igneous Provinces.

the past 40 kyr, with coral U/Th ages back several 100 kyr), from fossils (biostratigraphy), or from other techniques (magnetostratigraphy, chemostratigraphy, and astrochronology). For the Late Pleistocene to present (last 129 kyr), dating of corals or marshes formed near sea level provides the most accurate means or reconstructing sea level. Measurements of foraminifera $\delta^{18}\text{O}$ records reflect ice volume and temperature changes that can be calibrated to sea level by independent temperature estimates back through the Middle Eocene (e.g., Miller et al., 2020). Flooding (transgressions) and exposure (regressions) of the continents reflect GMSL and tectonic processes, as does the record of sequences (unconformity bounded units; Vail et al., 1977). Continental flooding and sequence stratigraphy provide the longest (billion year) records, though they also record processes of sediment supply, compaction, loading, thermal and flexural subsidence, mantle dynamic topography, and active tectonics.

Various generations of sea level curves produced by Exxon Production Research Company (Vail et al., 1977; Haq et al., 1987) have become entrenched as the Phanerozoic standard. These “cycle” charts provide an excellent record of the

timing of sea level falls but are greatly exaggerated in their sea level amplitudes because they were scaled to sea levels derived from seafloor spreading reconstructions and did not account for processes of compaction, loading, and thermal and flexural subsidence. Even the relative amplitudes are suspect, and thus these curves provide little to no constraints on sea level mechanisms (e.g., Miller et al., 2005a).

Drilling by the International Ocean Discovery Program (IODP) and its predecessors has provided material for independently estimating sea level using sequence stratigraphy and backstripping (progressively accounting for the effects of compaction, loading, and thermal subsidence; John et al., 2004; Miller et al., 2005a), and for combining deep-sea benthic foraminiferal $\delta^{18}\text{O}$ and Mg/Ca records, with the latter providing an independent paleothermometer (Lear et al., 2000; Cramer et al., 2011; Miller et al., 2020). Convergence of these two methods (Figure 2B) allows identification of GMSL changes and inferences about their mechanisms (Miller et al., 2020). In addition, coral drilling in Barbados (Figure 3A; Fairbanks, 1989) and Tahiti by IODP Expedition 310 (Deschamps et al., 2012) provides constraints on

the rates of sea level rise during the last deglaciation. Finally, studies of Holocene marshes have produced pristine chronologies and estimates of the rates of GMSL rise during the Holocene (Figure 3B), including the CE, that can then be linked to instrument records (tide gauge and satellites). Here, we provide a geological perspective on past, present, and future sea level change using published backstripped (Miller et al., 2020), $\delta^{18}\text{O}$ -Mg/Ca (Miller et al., 2020), coral (Peltier and Fairbanks, 2006; Deschamps et al., 2012), marsh (e.g., Kemp et al., 2009, 2018; Kopp et al., 2016; Horton et al., 2018), and instrumental (Dangendorf et al., 2017) sea level records.

HISTORY OF GMSL CHANGES

High-latitude temperatures were remarkably warm in the Late Cretaceous (e.g., Huber et al., 2018) and Early Eocene (e.g., with Arctic surface temperatures $>23^\circ\text{C}$; Sluijs et al., 2006), and there is consensus that Earth was substantially ice-free at these times, with CO_2 concentrations in excess of 1,000 ppm (summary in Foster et al., 2017). However, sea level records indicate large (>25 m) and rapid changes in the Late Cretaceous to the Eocene that can only be explained by ice growth and decay (e.g., Miller et al.,

TABLE 1. Amplitudes and rates of sea level change updated from Pitman and Golovchenko (1983) with best estimates from this study. LIPs = Large Igneous Provinces; the 50 m LIP estimate does not include isostatic loading.

MECHANISMS AND RATES OF SEA LEVEL CHANGE	PITMAN AND GOLOVCHENKO (1983)	AMPLITUDE BEST ESTIMATE (m)	AMPLITUDE ERROR		RATE (mm yr^{-1})	RATE (m Myr^{-1})
			LOWER (m)	UPPER (m)		
Ocean crust production	250	75	50	250	0.01	10
Ice volume changes	200	200	180	220	50	50,000
LIPs	50	15	5	35	0.01	10
Orogeny	70	50	5	20	0.001	1
Global sedimentation	60	50	5	10	0.001	1
Basin flooding/desiccation	15	30	5	15	50	50,000
Lakes and aquifers		7	2	45	1	1,000
Thermal expansion		10	8	15	1	1,000
Greenhouse sea level changes		>25			0.025	25
1900–2020		0.3	0	0	3	3,000
21 st Century		0.8	0.5	2	13	11,000

2005a,b, 2020; Ray et al., 2019; Davies et al., 2020). The solution to this enigma is that there were small (15–25 m sea level equivalent or 25%–40% of modern volume), ephemeral ice sheets during the Late Cretaceous to Eocene in the interior of Antarctica (Miller et al. 2005a;

Huber et al., 2018; Ray et al., 2019; Davies et al., 2020). Remarkable new data show marine-terminating glaciers existed at the Sabrina Coast, adjacent to the Aurora Basin, Antarctica, by the Early to Middle Eocene (Gulick et al., 2017), and modeling studies show that significant ice sheets

(15+ m equivalent) can exist in regions of high Antarctic topography (Deconto and Pollard, 2003) even while subtropical conditions persist along the coast (Pross et al., 2012). We posit that sea level variations on the order of 15±10 m occurred as significant ice sheets grew and decayed,

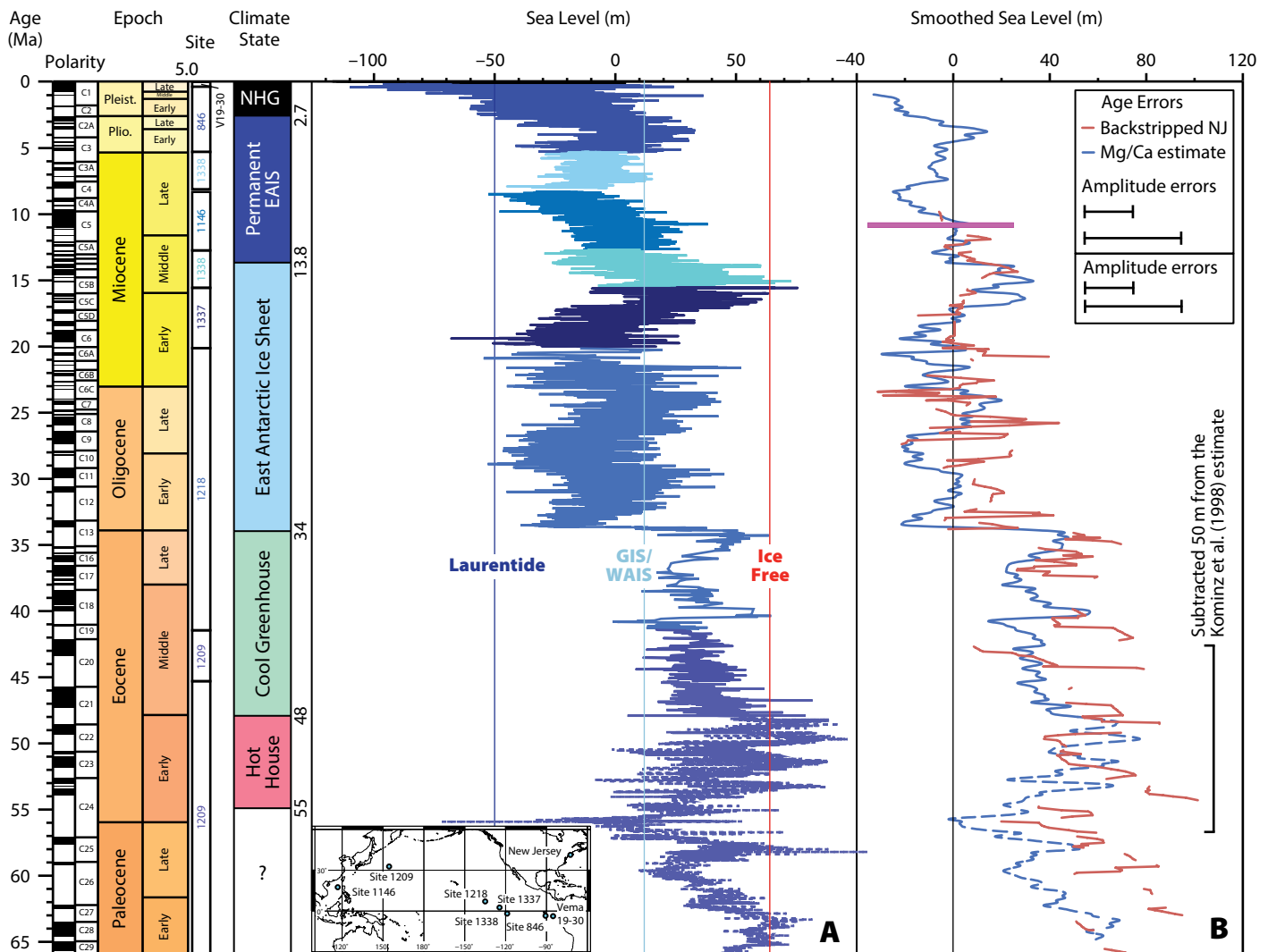


FIGURE 2. Cenozoic (last 66 million years) sea level, modified after Miller et al. (2020). Timescale is GTS2012 (Gradstein et al., 2012). Sites used in construction of curves are color-coded. Climate states as discussed in text. Inset map shows locations of sites used. **(A)** Sea level obtained using benthic (*Cibicidoides*) foraminifer $\delta^{18}\text{O}_{\text{benthic}}$ splice and $\delta^{18}\text{O}_{\text{seawater}}$ using temperatures from Mg/Ca records. The ice-free line (magenta) is drawn 66 m above present, the Greenland Ice Sheet–West Antarctic Ice Sheet (GIS–WAIS; light blue) is drawn at 12 m above present, and the Laurentide Ice Sheet (dark blue) is drawn at –50 m. Each site has a contrasting shade of blue, with the site number indicated in the left column in the corresponding color. The $\delta^{18}\text{O}_{\text{benthic}}$ splice is based on data from Pacific cores obtained at sites 1209 (Leg 198), 1218 (Leg 199), 1337 (Legs 320/321), 1338 (ODP Legs 320/321), 1145 (Leg 184), 846 (Leg 138) by the Ocean Drilling Program (ODP) and the Integrated Ocean Drilling Program (IODP) and piston core V19-30 (Shackleton et al., 1983); full citations for core collection are available in Miller et al., 2020. The sea level record older than 48 million years is dashed because of uncertainties in the Mg/Ca record (Cramer et al., 2011). Long-term Mg/Ca_{seawater} estimates were compiled by Cramer et al. (2011) and a correction for carbonate ion effects was made for the Eocene–Oligocene transition by Miller et al. (2020). Mg/Ca_{seawater} estimates are partly the source of uncertainties older than 48 Ma, though the Mg/Ca record older than 48 Ma from Site 1209 is suspect due to high variability (Cramer et al., 2011). **(B)** Comparison of smoothed sea level estimates from $\delta^{18}\text{O}$ and Mg/Ca (blue; obtained by interpolating to 20 kyr intervals and using a 49-point Gaussian convolution filter, removing periods shorter than 490 kyr) with backstripped (progressive accounting for the effects of compaction, loading, and thermal subsidence; Miller et al., 2005a; John et al., 2004) onshore New Jersey estimates (red; Kominz et al., 2016). The magenta bar is the range of backstripped sea level change on the Marion Plateau, East Australian margin (John et al., 2004). The New Jersey estimates for the Early to Middle Eocene were shifted by –50 m to compensate for long-term (2–10 million years) effects that are likely due to changes in mantle dynamic topography.

even in intervals such as the Early Eocene and Late Cretaceous.

The cool Greenhouse conditions of the Middle to Late Eocene illustrate ice volume control on sea level in what was commonly thought to be an ice-free period. Despite warm bottom water temperatures (8°–12°C), our $\delta^{18}\text{O}$ -Mg/Ca-based estimates show (Figure 2) large (15–30 m) sea level falls at ca. 49, 47.8, 46.9, and 44.5 Ma; smaller falls (~10–20 m) at 43.6, 42.9, and 40.8 Ma; and a major rise of ~40 m to near ice-free conditions at the Middle Eocene Climatic Optimum (40.1 Ma; Bohaty and Zachos, 2003), followed by a ~20 m drop (39.5 Ma). During the Late Eocene, sea level fell 40 m, only to rise in near ice-free conditions again at ca. 35 Ma. The new Middle to Late Eocene sea level record (Figure 2; Miller et al., 2020) indicates dynamic growth and collapse of moderately large ice sheets (0%–75% of modern EAIS), controlled by the 1,200 kyr tilt cycle (Miller et al., 2020). Atmospheric CO_2 proxies show decreasing values accompanied this change in state (Foster et al., 2017) from Hothouse with ephemeral, small ice sheets to cool Greenhouse conditions with moderate-sized ice sheets.

A continental-scale EAIS developed in the Icehouse Early Oligocene associated with Zone Oi1 (ca. 34 Ma; Oi1, Oi2, Mi1 to Mi6 are million-year-scale $\delta^{18}\text{O}$ maxima; Miller et al., 1991), with million year sea level falls of 40–60 m and peak glaciations in the Early Oligocene (Oi1, ca. 34 Ma), middle Oligocene (Mi2, ca. 30 Ma), and spanning the Oligocene/Miocene boundary (Mi1, ca. 22 Ma; Miller et al., 2020). Sea level lowstands were generally lower than present from 34–17 Ma, explaining the poor representation of strata of this age in continental margin sections. During this time, ice growth and decay was paced by the 1,200 kyr tilt cycle (Boullila et al., 2011; Miller et al., 2020), though ice volume was affected by the orbital cycles of precession (19/23 kyr), short tilt (41 kyr), and eccentricity (95/125, 405, and 2,400 kyr).

The cool, glacial climates of the

Oligocene to Early Miocene were punctuated by the Miocene Climatic Optimum (17.0–13.8 Ma), the last time Earth was potentially ice-free (Miller et al., 2020). The Miocene Climatic Optimum is associated with relatively high CO_2 (~500 ppm), high carbon burial (the Monterey event; Vincent and Berger, 1985), and high global $\delta^{13}\text{C}$ values (though these lag the warming). The Miocene Climatic Optimum may be considered an incipient ocean anoxic event, possibly attributed to outgassing of the Columbia River basalts (Kasbohm and Schone, 2018; Sosdian et al., 2020).

A permanent EAIS developed in the Middle Miocene Climate Transition as signaled by Antarctic climates (Lewis et al., 2008) and three major million year-scale $\delta^{18}\text{O}_{\text{benthic}}$ increases, coolings, and attendant sea level falls (Miller et al., 2020): Mi3a (14.8 Ma; ~30 m fall, ~0.7°C cooling), Mi3 (13.8 Ma; ~50 m fall, ~1.2°C cooling), and Mi4 (12.8 Ma; 20–30 m sea level fall, ~1.0°C cooling). GMSL rose after each event but to a lower mean state, stabilizing less than 12 m above present. From 12.8 until ca. 4.5 Ma, the amplitudes of sea level change were muted and ice sheets were mainly paced by the 41 kyr tilt cycle. The large EAIS of the Middle to Late Miocene was less sensitive to precessional and eccentricity forcing. The cause of the Middle Miocene Climate Transition was likely a decrease in atmospheric CO_2 (Greenop et al., 2014), perhaps linked to cessation of Columbia River basalt volcanism and weathering (Sosdian et al., 2020).

The Pliocene recorded the last major warm period (4.5–3 Ma) when (1) global mean surface temperatures were 2°–3°C warmer than 1850 CE (e.g., Dowsett, 2007), (2) CO_2 was similar to 2020 (e.g., Bartoli et al., 2011), and (3) sea levels stood ~22±10 m above present (Miller et al., 2012). Maximum sea level is constrained by $\delta^{18}\text{O}_{\text{benthic}}$ values at ca. 3 Ma to <20 m (Miller et al., 2019), though sea level may have peaked higher earlier in the Pliocene (32±5; Hearty et al., 2020). The ~20–30 m estimates are significant

because they imply absence of the GIS, the WAIS, and vulnerable portions of the EAIS (Miller et al., 2012). Considering the errors, no melting of the EAIS may be required (Rovere et al., 2014; Raymo et al., 2018). However, sea level estimates generally fall into the range of 15–20 m at 3 Ma and 20–35 m at ca. 3.5–4.5 Ma (Miller et al., 2012, 2019, 2020; Hearty et al., 2020), consistent with melting of the EAIS in the Wilkes and Aurora Basins suggested by models (DeConto and Pollard, 2002) and sediment tracer data (e.g., Bertram et al., 2018; see Gasson and Keisling, 2020). This warmer Early Pliocene world was more sensitive to precessional and eccentricity forcing than the cooler Late Miocene, though the 41 kyr tilt cycle still dominated sea level changes.

Small (Greenland-sized) Northern Hemisphere ice sheets existed at least intermittently beginning in the Middle Eocene (St. John, 2008), but the Quaternary (last 2.55 million years) began with development of continental-scale Northern Hemisphere ice sheets signaled by the large Marine Isotope Stage (MIS) 100 $\delta^{18}\text{O}$ increase (>1‰; ~2.5 Ma), sea level fall (~60 m), and appearance of ice rafted sediments in the northern North Atlantic. (MISs are defined as periods of higher [even stages, colder and large ice sheets] and lower [odd stages, warmer, smaller ice sheet] $\delta^{18}\text{O}$ values in deep sea carbonates.) Ice sheets gradually increased in size from ca. 2.8–2.55 Ma, with progressive increase in glacial-interglacial $\delta^{18}\text{O}$ amplitudes. The cause of the beginning of the large Northern Hemisphere ice ages has been variously attributed to closing gateways (e.g., Panamanian seaway, Norwegian-Greenland sill), mountain building, ocean circulation, and CO_2 drawdown (e.g., discussion in Raymo, 1994), though dropping of CO_2 below a critical threshold of 300 ppm is implicated (Willeit et al., 2015; Miller et al., 2020). Sea level was paced by the 41 kyr tilt cycle with amplitudes <100 m.

Sea level amplitudes increased and began to be paced by short eccentric-

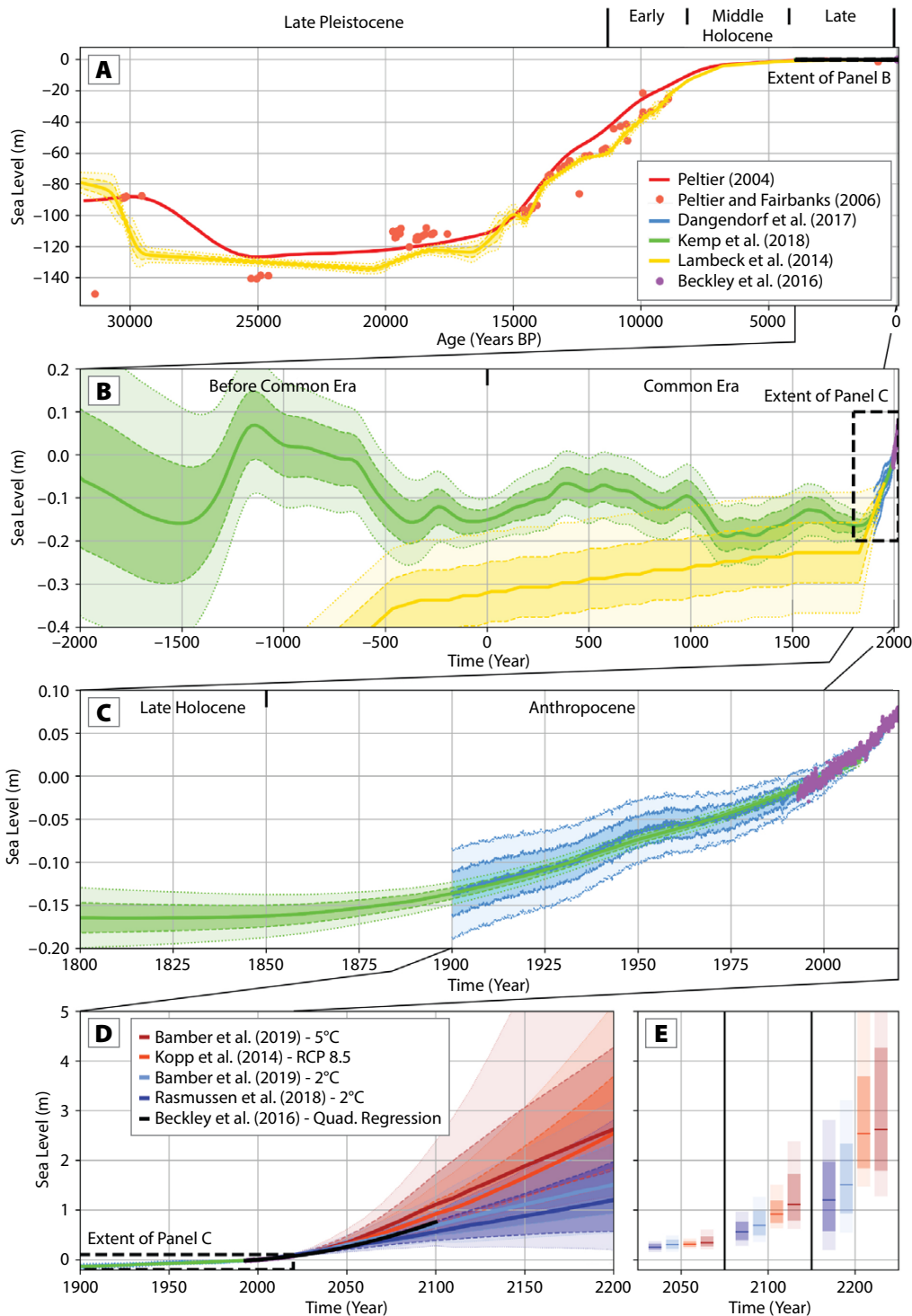


FIGURE 3. Data sets and statistical analyses of variations in sea level from 30,000 calendar years before 1950 (ka), including the Last Glacial Maximum, 27–20 ka to 2200 CE. Gray correlation lines show the relative temporal relationships between panels. Note that the range varies from over 150 m (panel A) to 60 cm (panel B), 30 cm (panel C), and over 5 m (panels D, E).

(A) Time series of global mean sea level (GMSL) estimates from 30,000 calendar years to 1950 (= 0 age). Coral data are from Barbados, corrected for glacial isostatic adjustment (red points; Peltier and Fairbanks, 2006), and the global whole Earth ICE-5G (VM2) model (red line, Peltier, 2004). The GIA-corrected model of Lambeck et al. (2014; yellow line) is shown for comparison. Thick dashed lines/darker shading and thin dashed lines/lighter shading indicate the 1 sigma and 2 sigma errors, respectively, on the statistical estimates of sea level.

(B) Time series of GMSL from 2000 BCE to 2020 CE showing statistical analyses of Kemp et al. (2018). Thick dashed lines/darker shading and thin dashed lines/lighter shading indicate the 1 sigma and 2 sigma errors, respectively, on the statistical estimates of sea level. The yellow line is the GIA-corrected model of Lambeck et al. (2014). Blue lines are drawn based on statistical analysis of satellite and tide gauge records by Dangendorf et al. (2019). Purple points indicate satellite data for 1993–2020.

(C) Time series of GMSL from 1800 to 2020 based on a statistical analysis of satellite and tide gauge records by Dangendorf et al. (2019; blue line). Purple dots record satellite data for 1993–2020 (Beckley et al., 2016). The green line shows processed combined tide and satellite data. The thick dashed blue line/darker shading and thin dashed blue line/lighter shading indicate the 1 sigma and 2 sigma errors, respectively, on the statistical estimates of sea level.

(D) Time series of GMSL from 1900 to 2200, including process-model sea level projections under 2°C (Rasmussen et al., 2018; Bamber et al., 2019) and 5°C representative concentration pathway (RCP) 8.5 warming scenarios (Kopp et al., 2014, updated for consistency with Oppenheimer et al., 2019; Bamber et al., 2019). The black line is a quadratic regression model fit to the Beckley et al. (2016) satellite data. Extrapolation of the acceleration indicates over 0.7 m of sea level rise by 2100 and a $\sim 12.5 \text{ mm yr}^{-1}$ rate of rise in 2100. Thick dashed lines/darker shading and thin dashed lines/lighter shading represent the 17th to 83rd and 5th to 95th percentiles for each of the sea level projections, respectively.

(E) The median 17th to 83rd, and 5th to 95th percentile sea level projections for 2050, 2100, and 2200 from the process-model projection time series displayed in panel D.

ity (quasi 100 kyr), precession, and tilt forcing during the Bruhnes (780 ka) following the Mid-Pleistocene Transition. Precession (19, 23 kyr) and tilt (41 kyr) directly forced sea level lowerings of 10–60 m, but larger sea level rises yielding the distinct sawtooth 100 kyr terminations of the last 780 kyr are likely due to amplification by CO₂ (Shackleton et al., 2000). The cause of the shift to dominant quasi-100 kyr periods and large, rapid (>100 m) sea level rises during the Mid-Pleistocene Transition is unknown, though decreasing atmospheric CO₂ from ~320 to 250 ppm may have reached a threshold, resulting in the return of a 100 kyr beat that had previously been important in the early history of the EAIS (Miller et al., 2020).

Sea level reached its highest points of the last 780 kyr in MIS 11 (9±3 m, ~405 kyr) and MIS 5 (7.5±1.5 m above present, ca 125 kyr), with global mean temperatures about 1°C warmer than 1850 (Dutton et al., 2015). Sea level reached its lowest point of the last 200 million years during the LGM (Peltier and Fairbanks, 2006; Lambeck et al., 2014). The Barbados sea level record of -120±5 m (Fairbanks, 1989) corrected for GIA indicates the LGM occurred from ~27 ka to 20 ka, with GMSL of 122–127 m below present (Peltier and Fairbanks, 2006). An inversion-based analysis using over 1,000 sea level observations from corals proposed an LGM timing of 21 ka and GMSL of 134 m, though the database is sparsely populated between 30 ka and 20 ka (Lambeck et al., 2014). Following the LGM, sea level rose with two large Meltwater Pulses, MWP1A (14.7–14.3 ka, rate >47 mm yr⁻¹) and MWP1B (11.7–11.5 ka, >40 mm yr⁻¹; Fairbanks, 1989; Stanford et al., 2006; Deschamps et al., 2012; Liu et al., 2016; Abdul et al., 2016).

The Holocene (11.3 ka to the beginning of the Anthropocene in 1850 CE) was an epoch of relative stability for global mean temperature and progressive slowing and stabilizing of GMSL. During

the Early Holocene (11.3–8.2 ka), GMSL rise slowed to ~8 mm yr⁻¹ and progressively slowed to 2 mm yr⁻¹ in the Middle Holocene (8.2–4.2 ka) and less than 1 mm yr⁻¹ by 5 ka (Figure 3A; Lambeck et al., 2014). Statistical analysis of a global database of regional sea level records (Figure 3B) shows very little change in Late Holocene GMSL (4.2 ka to the beginning of the Anthropocene), aside from hundred-year scale oscillations of ±0.1 m (Kopp et al., 2016; Kemp et al., 2018). This corroborates the analysis of CE GMSL by Kopp et al. (2016), which exhibited multi-centennial variability of ±0.1 m, but no rising trend. The modern rise is not a remnant of deglaciation but rather due to anthropogenic warming.

The modern period of GMSL rise began in the late nineteenth century, and the rate of rise over the twentieth century was the fastest in at least 3,000 years (Kopp et al. 2016; Kemp et al., 2018). The acceleration of sea level rise continued in the late twentieth and early twenty-first centuries. Statistical analysis of satellite and tide gauge records by Dangendorf et al. (2019) shows a 1.6±0.4 mm yr⁻¹ rate of sea level rise between 1900 and 2015, with the current acceleration beginning in the late 1960s. The rate of sea level rise increased from 2.1±0.1 mm yr⁻¹ to 3.4±0.3 mm yr⁻¹ from 1993 to 2015 (Dangendorf et al., 2017). Using nearly 30 years of satellite data (Nerem et al., 2010; Beckley et al., 2016), a simple regression model (Figure 3C) captures the late twentieth to twenty-first century acceleration of sea level rise. GMSL today is driven primarily by ocean warming (~40%) and the melting of ice sheets (~30%) and mountain glaciers (~20%) (Church et al., 2013; WCRP Global Sea Level Budget Group, 2018).

Though future sea level rise remains a subject of conjecture dependent on future emissions pathways, certain limits can be placed on sea level rise during the twenty-first century and beyond. Simple extrapolation of the acceleration seen in the satellite data (Nerem et al.,

2010; Beckley, 2016) predicts over 0.7 m of GMSL rise by 2100 (Figure 3D, thick black line) and a ~12.5 mm yr⁻¹ rate of rise in 2100. However, whereas the next couple of decades of GMSL rise are independent of emissions pathways, human choices about emissions become an increasingly important driver in the second half of this century and beyond. In a world that eliminates its net carbon dioxide emissions and stabilizes global-mean warming at 2°C above preindustrial temperatures, GMSL is likely (with at least a 66% probability) to be between 0.4 m and 1.0 m by the end of the century (Figure 3D,E; Rasmussen et al., 2018; Bamber et al., 2019). By contrast, in a world of unchecked emissions growth that leads to global-mean warming around 5°C by the end of the century, the currently limited understanding of ice sheet stability on century timescales yields a much broader range of projections. The relatively conservative projections laid out in chapter four of the special report of the Intergovernmental Panel on Climate Change on *The Ocean and Cryosphere in a Changing Climate* indicate a likely rise of 0.6–1.1 m over this century (Oppenheimer et al., 2019), while a structured expert judgment study (Bamber et al., 2019) indicates a broader range of 0.8–1.7 m.

The future beyond 2100 CE is even less certain. Both process modeling (Clark et al., 2016) and ancient sea level analogs discussed here reflecting slow feedback mechanisms suggest that 2°C of warming will lock in ~10 m of GMSL rise over the coming millennia. Under higher emissions scenarios, twenty-first century GMSL rise greater than 2 m cannot be excluded (e.g., Bamber et al., 2019), and equilibrium rise over the next few millennia may be tens of meters. Emissions to date have committed humanity to a world of sea level rise not seen for 3 million years, and our coastal systems, natural and built, need to adapt, roll back, and continue to acclimate to inexorable rise. 🌊

REFERENCES

- Abdul, N.A., R.A. Mortlock, J.W. Wright, and R.G. Fairbanks. 2016. Younger Dryas sea level and meltwater pulse 1B recorded in Barbados reef crest coral *Acropora palmata*. *Paleoceanography* 31:330–344, <https://doi.org/10.1002/2015PA002847>.
- Bamber, J.L., M. Oppenheimer, R.E. Kopp, W.P. Aspinall, and R.M. Cook. 2019. Ice sheet contributions to future sea-level rise from structured expert judgment. *Proceedings of the National Academy of Sciences of the United States of America* 116:11,195–11,200, <https://doi.org/10.1073/pnas.1817205116>.
- Bartoli, G., B. Hönisch, and R.E. Zeebe. 2011. Atmospheric CO₂ decline during the Pliocene intensification of Northern Hemisphere glaciations. *Paleoceanography* 26(4), <https://doi.org/10.1029/2010PA002055>.
- Beckley, B., N.P. Zelensky, S.A. Holmes, F.G. Lemoine, R.D. Ray, G.T. Mitchum, S. Desai, and S.T. Brown. 2016. Global mean sea level trend from integrated multi-mission ocean altimeters TOPEX/Poseidon Jason-1 and OSTM/Jason-2 Version 4.2. Ver. 4.2. PO.DAAC, CA, USA. Data set accessed on July 12, 2020 at <https://doi.org/10.5067/GMSLM-TJ142>.
- Bertram, R.A., D.J. Wilson, T. van de Fliert, R.M. McKay, M.O. Patterson, F.J. Jimenez-Espejo, C. Escutia, G.C. Duke, B.I. Taylor-Silva, and C.R. Riesselman. 2018. Pliocene deglacial event timelines and the biogeochemical response offshore Wilkes Subglacial Basin, East Antarctica. *Earth and Planetary Science Letters* 494:109–116, <https://doi.org/10.1016/j.epsl.2018.04.054>.
- Bohaty, S.M., and J.C. Zachos. 2003. Significant Southern Ocean warming event in the late Middle Eocene. *Geology* 31:1,017–1,020, <https://doi.org/10.1130/G198001>.
- Boullila, S., B. Galbrun, K.G. Miller, S.F. Pekar, J.V. Browning, J. Laskar, and J.D. Wright. 2011. On the origin of Cenozoic and Mesozoic “third-order” eustatic sequences. *Earth-Science Reviews* 109:94–112, <https://doi.org/10.1016/j.earscirev.2011.09.003>.
- Church, J.A., P.U. Clark, A. Cazenave, J.M. Gregory, S. Jevrejeva, A. Levermann, M.A. Merrifield, G.A. Milne, R.S. Nerem, P.D. Nunn, and others. 2013. Sea level change. Pp. 1137–1,216 in *Climate Change 2013: The Physical Science Basis. Contribution of Working Group I to the Fifth Assessment Report of the Intergovernmental Panel on Climate Change*. T.F. Stocker, D. Qin, G.-K. Plattner, M. Tignor, S.K. Allen, J. Boschung, A. Nauels, Y. Xia, V. Bex and P.M. Midgley, eds, Cambridge University Press, Cambridge, UK, and New York, NY, USA.
- Clark, P.U., J.D. Shakun, S.A. Marcott, A.C. Mix, M. Eby, S. Kulp, A. Levermann, G.A. Milne, P.L. Pfister, B.D. Santer, and others. 2016. Consequences of twenty-first-century policy for multi-millennial climate and sea-level change. *Nature Climate Change* 6:360–369, <https://doi.org/10.1038/nclimate2923>.
- Cramer, B.S., K.G. Miller, P.J. Barrett, and J.D. Wright. 2011. Late Cretaceous-Neogene trends in deep ocean temperature and continental ice volume: Reconciling records of benthic foraminiferal geochemistry (^δ18O and Mg/Ca) with sea level history. *Journal of Geophysical Research* 116(C12), <https://doi.org/10.1029/2011JC007255>.
- Dangendorf, S., M. Marco, G. Wöppelmann, C.P. Conrad, T. Frederikse, and R. Riva. 2017. Reassessment of 20th century global mean sea level rise. *Proceedings of the National Academy of Sciences of the United States of America* 114:5,946–5,951, <https://doi.org/10.1073/pnas.1616007114>.
- Davies, A., B. Greselle, S. Hunter, G. Baines, C. Robson, A.M. Haywood, D.C. Ray, M.D. Simmons, and F.S.P. van Buchem. 2020. Assessing the impact of aquifer-eustasy on short-term Cretaceous sea-level. *Cretaceous Research* 112:104445, <https://doi.org/10.1016/j.cretres.2020.104445>.
- DeConto, R.M., and D. Pollard. 2003. A coupled climate-ice sheet modeling approach to the early Cenozoic history of the Antarctic ice sheet. *Palaeogeography, Palaeoclimatology, Palaeoecology* 198:39–52, [https://doi.org/10.1016/S0031-0182\(03\)00393-6](https://doi.org/10.1016/S0031-0182(03)00393-6).
- Deschamps, P., N. Durand, E. Bard, B. Hamelin, G. Camoin, A.L. Thomas, G.M. Henderson, J. Okuno, and Y. Yokoyama. 2012. Ice-sheet collapse and sea-level rise at the Bølling warming 14,600 years ago. *Nature* 483:559–564, <https://doi.org/10.1038/nature10902>.
- Dowsett, H.J. 2007. The PRISM Palaeoclimate reconstruction and Pliocene sea-surface temperature. Pp. 459–480 in *Deep-Time Perspectives on Climate Change: Marrying the Signal from Computer Models and Biological Proxies*. M. Williams, A.M. Haywood, J. Gregory, and D.N. Schmidt, eds, The Micropalaeontological Society, Special Publications, The Geological Society, London, UK.
- Dutton, A., A.E. Carlson, A.J. Long, G.A. Milne, P.U. Clark, R. DeConto, B.P. Horton, S. Rahmstorf, and M.E. Raymo. 2015. Sea-level rise due to polar ice-sheet mass loss during past warm periods. *Science* 349(6244):aa4019, <https://doi.org/10.1126/science.aaa4019>.
- Fairbanks, R.G. 1989. A 17,000-year glacio-eustatic sea level record: Influence of glacial melting rates on the Younger Dryas event and deep-ocean circulation. *Nature* 342:637–642, <https://doi.org/10.1038/342637a0>.
- Foster, G.L., D.L. Royer, and D.J. Lunt. 2017. Future climate forcing potentially without precedent in the last 420 million years. *Nature Communications* 8:1–8, <https://doi.org/10.1038/ncomms14845>.
- Gasson, E.G.W., and B.A. Keisling. 2020. The Antarctic ice sheet: A paleoclimate modeling perspective. *Oceanography* 33:37–46, <https://doi.org/10.5670/oceanog.2020.208>.
- Gradstein, F.M., J.G. Ogg, M.D. Schmitz, and G.M. Ogg. 2012. *The Geologic Time Scale 2012*. Elsevier, New York, NY, 1,176 pp.
- Greenop, R., G.L. Foster, P.A. Wilson, and C.H. Lear. 2014. Middle Miocene climate instability associated with high-amplitude CO₂ variability. *Paleoceanography* 29:845–853, <https://doi.org/10.1002/2014PA002653>.
- Gregory, J.M., S.M. Griffies, C.W. Hughes, J.A. Lowe, J.A. Church, I. Fukimori, N. Gomez, R.E. Kopp, F. Landerer, G. Le Cozannet, and others. 2019. Concepts and terminology for sea level: Mean, variability and change, both local and global. *Surveys in Geophysics* 40:1,251–1,289, <https://doi.org/10.1007/s10712-019-09525-z>.
- Gulick, S.P.S., A.E. Shevenell, A. Montelli, R. Fernandez, C. Smith, S. Warny, S.M. Bohaty, C. Sjunneskog, A. Leventer, B. Frederick, and D.D. Blankenship. 2017. Initiation and long-term instability of the East Antarctic ice sheet. *Nature* 552:225–229, <https://doi.org/10.1038/nature25026>.
- Haq, B., J. Hardenbol, and P.R. Vail. 1987. Chronology of fluctuating sea levels since the Triassic (250 million years ago to present). *Science* 235:1,156–1,167, <https://doi.org/10.1126/science.235.4793.1156>.
- Hearty, P.J., A. Rovere, M.R. Sandstrom, M.J. O’Leary, D. Roberts, and M.E. Raymo. 2020. Pliocene-Pleistocene stratigraphy and sea-level estimates, Republic of South Africa with implications for a 400 ppmv CO₂ world. *Paleoceanography and Palaeoclimatology* 35:7e2019PA003835, <https://doi.org/10.1029/2019PA003835>.
- Horton, B.P., R.E. Kopp, A.J. Garner, C.C. Hay, N.S. Khan, K. Roy, and T.A. Shaw. 2018. Mapping sea-level change in time, space, and probability. *Annual Review of Environment and Resources* 43:481–521, <https://doi.org/10.1146/annurev-environ-102017-025826>.
- Huber, B.T., K.G. MacLeod, D.K. Watkins, and M.F. Coffin. 2018. The rise and fall of the Cretaceous hot greenhouse climate. *Global and Planetary Change* 167:1–23, <https://doi.org/10.1016/j.gloplacha.2018.04.004>.
- John, C.M., G.D. Karner, and M. Mutti. 2004. ^δ18O and Marion Plateau backstripping: Combining two approaches to constrain late middle Miocene eustatic amplitude. *Geology* 32:829–832, <https://doi.org/10.1130/G20580.1>.
- Kasbohm, J., and B. Schoene. 2018. Rapid eruption of the Columbia River flood basalt and correlation with the mid-Miocene climate optimum. *Science Advances* 4(9):eaat8223, <https://doi.org/10.1126/sciadv.aat8223>.
- Kemp, A.C., B.P. Horton, S.J. Culver, D.R. Corbett, O. van de Plassche, W.C. Gehrels, B.C. Douglas, and A.C. Parnell. 2009. Timing and magnitude of recent accelerated sea-level rise (North Carolina, United States). *Geology* 37:1,035–1,038, <https://doi.org/10.1130/G30352A.1>.
- Kemp, A.C., A.J. Wright, R.J. Edwards, R.L. Barnett, M.J. Brain, R.E. Kopp, N. Cahill, B.P. Horton, D.J. Charman, A.D. Hawkes, and others. 2018. Relative sea-level change in Newfoundland, Canada during the past ~3000 years. *Quaternary Science Reviews* 201:89–110, <https://doi.org/10.1016/j.quascirev.2018.10.012>.
- Kominz, M.A., K.G. Miller, J.V. Browning, M.E. Katz, and G.S. Mountain. 2016. Miocene relative sea level on the New Jersey shallow continental shelf and coastal plain derived from one-dimensional backstripping: A case for both eustasy and epeirogeny. *Geosphere* 12:1,437–1,456, <https://doi.org/10.1130/GES01241.1>.
- Kopp, R.E., R.M. Horton, C.M. Little, J.X. Mitrovica, M. Oppenheimer, D.J. Rasmussen, B.H. Strauss, and C. Tebaldi. 2014. Probabilistic 21st and 22nd century sea-level projections at a global network of tide gauge sites. *Earth’s Future* 2:287–306, <https://doi.org/10.1002/2014EF000239>.
- Kopp, R.E., A.C. Kemp, K. Bittermann, B.P. Horton, J.P. Donnelly, W.R. Gehrels, C.C. Hay, J.X. Mitrovica, E.D. Morrow, and S. Rahmstorf. 2016. Temperature-driven global sea-level variability in the common era. *Proceedings of the National Academy of Sciences of the United States of America* 113:E1434–E1441, <https://doi.org/10.1073/pnas.1517056113>.
- Lambeck, K., H. Rouby, A. Purcell, Y. Sun, and M. Sambridge. 2014. Sea level and global ice volumes from the Last Glacial Maximum to the Holocene. *Proceedings of the National Academy of Sciences of the United States of America* 111:15,296–15,303, <https://doi.org/10.1073/pnas.1411762111>.
- Lear, C.H., H. Elderfield, and P.A. Wilson. 2000. Cenozoic deep-sea temperatures and global ice volumes from Mg/Ca in benthic foraminiferal calcite. *Science* 287:269–272, <https://doi.org/10.1126/science.287.5451.269>.
- Lewis, A.R., D.R. Marchant, A.C. Ashworth, L. Hedenäs, S.R. Hemming, J.V. Johnson, M.J. Leng, M.L. Machlus, A.E. Newton, J.I. Raine, and others. 2008. Mid-Miocene cooling and the extinction of tundra in continental Antarctica. *Proceedings of the National Academy of Sciences of the United States of America* 31:10,676–10,680, <https://doi.org/10.1073/pnas.0802501105>.
- Liu, J., G.A. Milne, R.E. Kopp, P.U. Clark, and I. Shennan. 2016. Sea-Level constraints on the amplitude and source distribution of Meltwater Pulse 1A. *Nature Geoscience* 9:130–134, <https://doi.org/10.1038/NGEO2616>.
- Meinshausen, M., Z.R.J. Nicholls, J. Lewis, M.J. Gidden, E. Vogel, M. Freund, U. Beyerle, C. Gessner, A. Nauels, N. Bauer, and others. 2020. The shared socio-economic path-

- way (SSP) greenhouse gas concentrations and their extensions to 2500. *Geoscientific Model Development* 13(8):3,571–3,605, <https://doi.org/10.5194/gmd-13-3571-2020>.
- Miller, K.G., J.D. Wright, and R.G. Fairbanks. 1991. Unlocking the ice house: Oligocene-Miocene oxygen isotopes, eustasy, and margin erosion. *Journal of Geophysical Research* 96:6,829–6,848, <https://doi.org/10.1029/90JB02015>.
- Miller, K.G., M.A. Kominz, J.V. Browning, J.D. Wright, G.S. Mountain, M.E. Katz, P.J. Sugarman, B.S. Cramer, N. Christie-Blick, and S.F. Pekar. 2005a. The Phanerozoic record of global sea-level change. *Science* 310:1,293–1,298, <https://doi.org/10.1126/science.1116412>.
- Miller, K.G., J.D. Wright, and J.V. Browning. 2005b. Visions of ice sheets in a greenhouse world. *Marine Geology* 217:215–231, <https://doi.org/10.1016/j.margeo.2005.02.007>.
- Miller, K.G., J.D. Wright, J.V. Browning, A.A. Kulpecz, M.A. Kominz, T.R. Naish, B.S. Cramer, Y. Rosenthal, R.W. Peltier, and S. Sosdian. 2012. High tide of the warm Pliocene: Implications of global sea level for Antarctic deglaciation. *Geology* 40:407–410, <https://doi.org/10.1130/G32869.1>.
- Miller, K.G., M.E. Raymo, J.V. Browning, Y. Rosenthal, and J.D. Wright. 2019. Peak sea level during the warm Pliocene: Errors, limitations, and constraints. *PAGES Magazine* 27:4–5, <https://doi.org/10.22498/pages.27.1.4>.
- Miller, K.G., J.V. Browning, W.J. Schmelz, R.E. Kopp, G.S. Mountain, and J.D. Wright. 2020. Cenozoic sea-level and cryospheric evolution from deep-sea geochemical and continental margin records. *Science Advances* 6:eaaaz1346, <https://doi.org/10.1126/sciadv.aaz1346>.
- Morlighem, M., E. Rignot, T. Binder, D. Blankenship, R. Drews, G. Eagles, O. Eisen, F. Ferraccioli, R. Forsberg, P. Fretwell, and others. 2019. Deep glacial troughs and stabilizing ridges unveiled beneath the margins of the Antarctic ice sheet. *Nature Geoscience* 13:132–137, <https://doi.org/10.1038/s41561-019-0510-8>.
- Nerem, R.S., D.P. Chambers, C. Choe, and G.T. Mitchum. 2010. Estimating mean sea level change from the TOPEX and Jason altimeter missions. *Marine Geodesy* 33:435–436, <https://doi.org/10.1080/01490419.2010.491031>.
- Oppenheimer, M., B.C. Glavovic, J. Hinkel, R. van de Wal, A.K. Magnan, A. Abd-Elgawad, R. Cai, M. Cifuentes Jara, R.M. DeConto, T. Ghosh, and others. 2019. Sea level rise and implications for low-lying islands, coasts and communities. Chapter 4 in *IPCC Special Report on the Ocean and Cryosphere in a Changing Climate*. H.-O. Pörtner, D.C. Roberts, Y. Masson-Delmotte, P. Zhai, M. Tignor, E. Poloczanska, K. Mintenbeck, A. Alegría, M. Nicolai, A. Okem, and others, eds, Cambridge University Press, Cambridge, UK.
- Peltier, W.R. 2004. Global glacial isostasy and the surface of the ice-age Earth: The ICE-5G (VM2) model and GRACE. *Annual Review of Earth and Planetary Sciences* 32:111–149, <https://doi.org/10.1146/annurev.earth.32.082503.144359>.
- Peltier, W.R., and R.G. Fairbanks. 2006. Global glacial ice volume and Last Glacial Maximum duration from an extended Barbados sea level record. *Quaternary Science Reviews* 25:3,322–3,337, <https://doi.org/10.1016/j.quascirev.2006.04.010>.
- Pitman, W.C. III, and X. Golovchenko. 1983. The effect of sea-level change on the shelf edge and slope of passive margins. Pp. 41–58 in *The Shelfbreak: Critical Interface on Continental Margins*. D.J. Stanley and G.T. Moore, eds, Society of Economic Paleontologists and Mineralogists Special Publication 33.
- Pross, J., L. Contreras, P.K. Bijl, D.R. Greenwood, S.M. Bohaty, S. Schouten, J.A. Bendle, U. Röhl, L. Tauxe, J.J. Raine, and others. 2012. Persistent near-tropical warmth on the Antarctic continent during the early Eocene epoch. *Nature* 488:73–77, <https://doi.org/10.1038/nature11300>.
- Rasmussen, D.J., K. Bittermann, M.K. Buchanan, S. Kulp, B.H. Strauss, R.E. Kopp, and M. Oppenheimer. 2018. Extreme sea level implications of 1.5°C, 2.0°C, and 2.5°C temperature stabilization targets in the 21st and 22nd centuries. *Environmental Research Letters* 13:034040, <https://doi.org/10.1088/1748-9326/aaac87>.
- Ray, D.C., F.S.P. Van Buchem, G. Baines, A. Davies, B. Gréselle, M.D. Simmons, and C. Robson. 2019. The magnitude and cause of short-term eustatic Cretaceous sea-level change: A synthesis. *Earth-Science Reviews* 197:102901, <https://doi.org/10.1016/j.earscirev.2019.102901>.
- Raymo, M. 1994. The initiation of Northern Hemisphere glaciation. *Annual Review of Earth and Planetary Sciences* 22:353–383, <https://doi.org/10.1146/annurev.earth.22.050194.002033>.
- Raymo, M.E., R. Kozdon, D. Evans, L. Liseicki, and H.L. Ford. 2018. The accuracy of mid-Pliocene $\delta^{18}\text{O}$ -based ice volume and sea level reconstructions. *Earth-Science Reviews* 177:291–302, <https://doi.org/10.1016/j.earscirev.2017.11.022>.
- Riahi, K., D.P. Van Vuuren, E. Kriegler, J. Edmonds, B.C. O'Neill, S. Fujimori, N. Bauer, K. Calvin, R. Dellink, O. Fricko, and others. 2017. The Shared Socioeconomic Pathways and their energy, land use, and greenhouse gas emissions implications: An overview. *Global Environmental Change* 42:153–168, <https://doi.org/10.1016/j.gloenvcha.2016.05.009>.
- Rovere, A., M.E. Raymo, J.X. Mitrovica, P.J. Hearty, M.J.O. Leary, and J.D. Inglis. 2014. The mid-Pliocene sea-level conundrum: Glacial isostasy, eustasy and dynamic topography. *Earth and Planetary Sciences Letters* 387:27–33, <https://doi.org/10.1016/j.epsl.2013.10.030>.
- Shackleton, N.J., J. Imbrie, and M.A. Hall. 1983. Oxygen and carbon isotope record of East Pacific core V19-30: Implications for the formation of deep water in the late Pleistocene North Atlantic. *Earth and Planetary Science Letters* 65:233–244, [https://doi.org/10.1016/0012-821X\(83\)90162-0](https://doi.org/10.1016/0012-821X(83)90162-0).
- Shackleton, N.J. 2000. The 100,000-year ice-age cycle identified and found to lag temperature, carbon dioxide, and orbital eccentricity. *Science* 289:1,897–1,901, <https://doi.org/10.1126/science.289.5486.1897>.
- Sluijs, A., S. Schouten, M. Pagani, M. Wolterring, H. Brinkhuis, J.S. Sinninghe Damsté, G.R. Dickens, M. Huber, G.-J. Reichert, R. Stein, and others. 2006. Subtropical Arctic Ocean temperatures during the Palaeocene/Eocene thermal maximum. *Nature* 441:610–613, <https://doi.org/10.1038/nature04668>.
- Sosdian, S.M., T.L. Babila, R. Greenop, G.L. Foster, and C.H. Lear. 2020. Ocean carbon storage across the middle Miocene: A new interpretation for the Monterey Event. *Nature Communications* 11:34, <https://doi.org/10.1038/s41467-019-13792-0>.
- Stanford, J.D., E.J. Rohling, S.E. Hunter, A.P. Roberts, S.O. Rasmussen, E. Bard, J. McManus, and R.G. Fairbanks. 2006. Timing of meltwater pulse 1a and climate responses to meltwater injections. *Paleoceanography and Paleoclimatology* 21(4), <https://doi.org/10.1029/2006PA001340>.
- St. John, K. 2008. Cenozoic ice-rafting history of the central Arctic Ocean: Terrigenous sands on the Lomonosov Ridge. *Paleoceanography and Paleoclimatology* 23(1), <https://doi.org/10.1029/2007PA001483>.
- Vail, P.R., R.M. Mitchum Jr., R.G. Todd, J.M. Widmier, S. Thompson III, J.B. Sangree, J.N. Bubb, and W.G. Hattelid. 1977. Seismic stratigraphy and global changes of sea level: Part 4. Global cycles of relative changes of sea level. Pp. 49–212 in *Seismic Stratigraphy: Applications to Hydrocarbon Exploration*. C.E. Payton, ed., American Association of Petroleum Geologists Memoir 26.
- Vincent, E., and W.H. Berger. 1985. Carbon dioxide and polar cooling in the Miocene: The Monterey Hypothesis. Pp. 455–468 in *The Carbon Cycle and Atmospheric CO₂: Natural Variations Archean to Present*. E.T. Sundquist, and W.S. Broecker, eds, American Geophysical Union, Geophysical Monograph Series, vol. 32, Washington, DC.
- WCRP Global Sea Level Budget Group. 2018. Global sea-level budget 1993–present. *Earth System Science Data* 10(3):1,551–1,590, <https://doi.org/10.5194/essd-10-1551-2018>.
- Willeit, M., A. Ganopolski, R. Calov, A. Robinson, and M. Maslin. 2015. The role of CO₂ decline for the onset of Northern Hemisphere glaciation. *Quaternary Science Reviews* 119:22–34, <https://doi.org/10.1016/j.quascirev.2015.04.015>.
- Zalasiewicz, J., M. Williams, A. Smith, T.L. Barry, A.L. Coe, P.R. Bown, P. Brenchley, D. Cantrill, A. Gale, P. Gibbard, and others. 2008. Are we now living in the Anthropocene? *GSA Today* 18:4–8, <https://doi.org/10.1130/GSAT01802A.1>.

ACKNOWLEDGMENTS

This work was supported by National Science Foundation grants OCE16-57013 (Miller) and the IODP/Texas A&M Research Foundation. We thank the Office of Advanced Research Computing (OARC) at Rutgers University for providing access to the Amarel cluster and associated research computing resources, IODP for samples, and the IODP community for producing the stable isotope, trace metal, and backstripped data used here. We thank Craig Fulthorpe and *Oceanography* Associate/Guest Editor Peggy Delaney for reviews.

AUTHORS

Kenneth G. Miller (kgm@rutgers.edu) is Distinguished Professor, **W. John Schmelz** is PhD Candidate, **James V. Browning** is Assistant Research Professor, **Robert E. Kopp** is Professor, **Gregory S. Mountain** is Professor, and **James D. Wright** is Professor, all in the Department of Earth & Planetary Sciences, Rutgers University, Piscataway, NJ, USA, and the Institute of Earth, Ocean, and Atmospheric Sciences, Rutgers University, New Brunswick, NJ, USA.

ARTICLE CITATION

Miller, K.G., W.J. Schmelz, J.V. Browning, R.E. Kopp, G.S. Mountain, and J.D. Wright. 2020. Ancient sea level as key to the future. *Oceanography* 33(2):32–41, <https://doi.org/10.5670/oceanog.2020.224>.

COPYRIGHT & USAGE

This is an open access article made available under the terms of the Creative Commons Attribution 4.0 International License (<https://creativecommons.org/licenses/by/4.0/>), which permits use, sharing, adaptation, distribution, and reproduction in any medium or format as long as users cite the materials appropriately, provide a link to the Creative Commons license, and indicate the changes that were made to the original content.

SIDEBAR. Boron Isotopes Provide Insights into Biomineralization, Seawater pH, and Ancient Atmospheric CO₂

By Jessica G.M. Crumpton-Banks and James W.B. Rae

Rising atmospheric CO₂ and falling ocean pH place an urgency on our efforts to understand the impact of CO₂ on Earth's ecosystems and climate. Studies of past perturbations of Earth's carbon reservoirs and climate—ranging from glacial-interglacial cycles to mass extinction events—may provide valuable insights, but they require the ability to reconstruct changes in ocean-atmosphere CO₂ chemistry in Earth's past. Here, we provide an overview of the boron isotope pH proxy in marine carbonates and how it can be applied to reconstruct past ocean pH and atmospheric CO₂.

The Boron Isotope pH Proxy

Hemming and Hanson (1992) first suggested using the boron isotopic composition of marine carbonates as a proxy for ocean pH. They proposed a boron isotope pH meter, based on the pH-dependent speciation of the two dominant forms of boron in seawater, boric acid (B(OH)₃) and the borate ion (B(OH)₄⁻). At low pH, boric acid dominates and vice versa (Figure 1a). As there is a constant isotopic offset between the two species, the isotopic signature of each shifts as pH

changes to conserve mass balance and the overall boron isotope composition of seawater (Figure 1b). Empirical calibrations suggest that marine calcifiers—such as foraminifera, corals, and brachiopods—incorporate the tetrahedral borate ion into their carbonate skeletons (e.g., Rae et al., 2011). As a result, the isotopic composition of fossil CaCO₃ may be used to reconstruct that of the borate ion, and in turn pH. While research into the exact mechanism of boron incorporation is ongoing, the original conceptual model described above provides a useful basis for the δ¹¹B pH proxy that is grounded in seawater acid-base chemistry and isotopic equilibria.

With pH established, another carbonate system parameter is needed to quantitatively reconstruct CO₂. Because seawater pH and CO₂ are closely coupled, the resulting pCO₂ record will be mainly driven by pH. Thus, even a broad estimate of alkalinity can result in a well-constrained pCO₂ estimate. The residence time of boron in the ocean is ~10–20 million years, and so changes in seawater δ¹¹B must also be considered when using boron isotopes to reconstruct pH and pCO₂ on multimillion-year timescales.

CO₂ and pH Change Beyond the Ice Cores

While ice cores provide detailed records of past atmospheric CO₂, the records currently only extend back 800,000 years. The boron isotope pH proxy has become one of the key methods paleoceanographers use to extend atmospheric CO₂ reconstructions beyond the timescales of ice core records. Recent studies demonstrate coupling between CO₂ and long-term climate over the last ~66 million years (e.g., Anagnostou et al., 2020), while on shorter timescales, Martínez-Botí et al. (2015) use δ¹¹B to show that, once differences in ice-albedo feedback are accounted for, climate sensitivity in the Pliocene (~5.3–2.6 million years ago) was similar to modern sensitivity. Boron isotopes have also been applied to examining rapid acidification events, including those associated with carbon release during the Paleocene-Eocene Thermal Maximum (~55 million years ago; Penman et al., 2014) and flash acidification associated with the asteroid impact at the Cretaceous–Paleogene boundary (~66 million years ago; Henehan et al., 2019).

Mechanisms of Glacial-Interglacial CO₂ Change

For more recent time periods, boron isotopes can be used to reveal the processes by which CO₂ is transferred between the ocean and the atmosphere during glacial-interglacial transitions. Rae et al. (2018) show that Southern Ocean deep-sea corals recorded lower pH during the Last Glacial Maximum

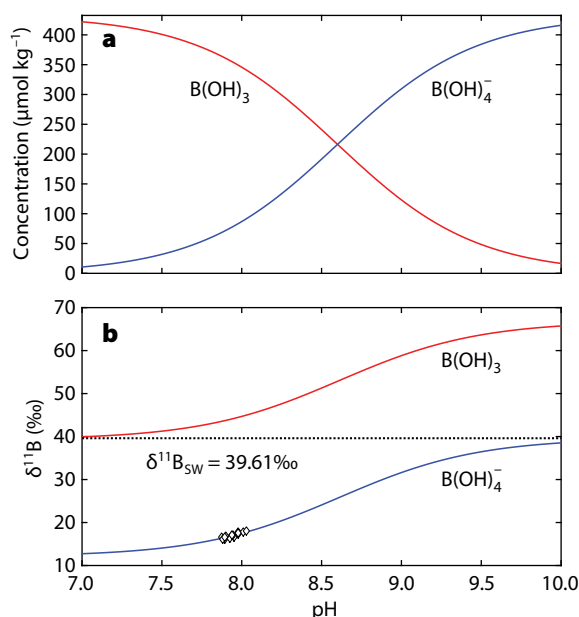


FIGURE 1. (a) Graph of pH-dependent speciation of boric acid (B(OH)₃, red line) and borate ion (B(OH)₄⁻, blue line). (b) Isotopic offset between boric acid and borate ion. Dashed black line = modern seawater (Foster et al., 2010). White diamonds = *Cibicides wuellerstorfi* benthic foraminiferal δ¹¹B (Rae et al., 2011).

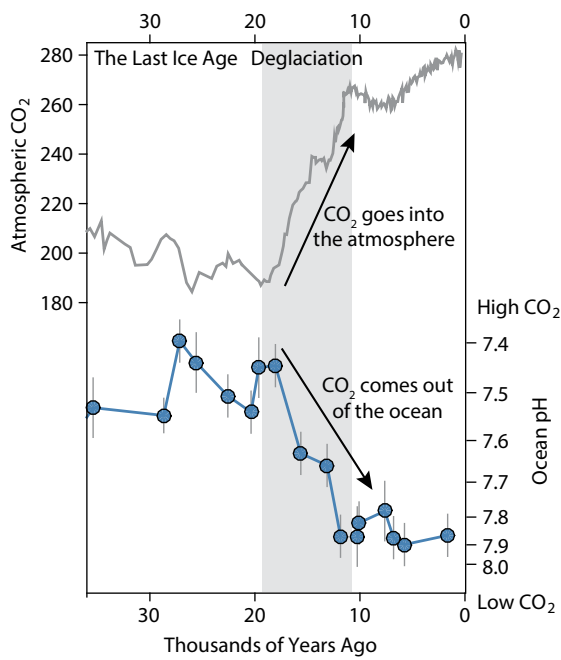


FIGURE 2. Boron isotope analyses of deep-sea corals demonstrates CO₂ release from the deep Southern Ocean to the atmosphere at the end of the last ice age (Rae et al., 2018).

(26,500–19,000 years ago), evidence that CO₂ is stored in the deep ocean during glacial periods (Figure 2), while planktic δ¹¹B (Shao et al., 2019) provides evidence of widespread outgassing of CO₂ via the surface ocean during the last deglaciation.

Biom mineralization

While many calcifiers have δ¹¹B values close to borate at average seawater pH, some genera are notably offset from seawater values, providing insights into the mechanisms of biomineralization. For example, corals consistently record higher δ¹¹B, and thus pH, than that of the water in which they grew, due to internal up-regulation of the calcifying fluid pH (McCulloch et al., 2012). This up-regulation process promotes carbonate precipitation by raising saturation state, and also helps concentrate carbon by creating a pronounced concentration gradient down which CO₂ can diffuse from seawater (Allison et al., 2019). A deeper knowledge of these processes is vital for better understanding the resilience and response of marine calcifiers under rising anthropogenic CO₂ emissions and acidifying ocean conditions.

Outlook

The strength of the boron isotope proxy is its foundation in inorganic acid-base and isotopic equilibria. The key uncertainty for CO₂ system reconstruction on long timescales (>5 million years) is the boron isotopic composition of seawater, which has proved difficult to constrain and thus limits the accuracy of long-term pH and CO₂ estimates (though relative changes

can be reconstructed with more confidence). Despite recent analytical developments, boron isotope analyses also remain challenging. Gaining a better understanding of the CO₂ system will require continued analytical improvements, understanding how boron is incorporated into marine carbonates, and knowledge of the constraints on long-term δ¹¹B of seawater.

REFERENCES

- Anagnostou, E., E.H. John, T.L. Babila, P.F. Sexton, A. Ridgwell, D.J. Lunt, P.N. Pearson, T.B. Chalk, R.D. Pancost, and G.L. Foster. 2020. Proxy evidence for state-dependence of climate sensitivity in the Eocene greenhouse. *Nature Communications* 11:4436, <https://doi.org/10.1038/s41467-020-17887-x>.
- Allison, N., I. Cohen, A.A. Finch, J. Erez, and A.W. Tudhope. 2019. Corals concentrate dissolved inorganic carbon to facilitate calcification. *Nature Communications* 5:5741, <https://doi.org/10.1038/ncomms6741>.
- Foster, G.L., P.A.E. Pogge von Strandmann, and J.W.B. Rae. 2010. Boron and magnesium isotopic composition of seawater. *Geochemistry Geophysics Geosystems* 11:1–10, <https://doi.org/10.1029/2010GC003201>.
- Hemming, N.G., and G.N. Hanson. 1992. Boron isotopic composition and concentration in modern marine carbonates. *Geochimica et Cosmochimica Acta* 56:537–543, [https://doi.org/10.1016/0016-7037\(92\)90151-8](https://doi.org/10.1016/0016-7037(92)90151-8).
- Henehan, M.J., A. Ridgwell, E. Thomas, S. Zhang, L. Alegret, D.N. Schmidt, J.W.B. Rae, J.D. Witts, N.H. Landman, S.E. Greene, and others. 2019. Rapid ocean acidification and protracted Earth system recovery followed the end-Cretaceous Chicxulub impact. *Proceedings of the National Academy of Sciences of the United States of America* 116:22,500–22,504, <https://doi.org/10.1073/pnas.1905989116>.
- Martínez-Botí, M.A., G.L. Foster, T.B. Chalk, E.J. Rohling, P.F. Sexton, D.J. Lunt, R.D. Pancost, M.P.S. Badger, and D.N. Schmidt. 2015. Plio-Pleistocene climate sensitivity evaluated using high-resolution CO₂ records. *Nature* 518:49–54, <https://doi.org/10.1038/nature14145>.
- McCulloch, J. Trotter, P. Montagna, J. Falter, R. Dunbar, A. Freiwald, G. Försterra, M.L. Correa, C. Maier, A. Rüggeberg, and M. Taviani. 2012. Resilience of cold-water scleractinian corals to ocean acidification: Boron isotopic systematics of pH and saturation state up-regulation. *Geochimica et Cosmochimica Acta* 87:21–34, <https://doi.org/10.1016/j.gca.2012.03.027>.
- Penman, D.E., B. Hönisch, R.E. Zeebe, E. Thomas, and J.C. Zachos. 2014. Rapid and sustained surface ocean acidification during the Paleocene-Eocene Thermal Maximum. *Paleoceanography* 29:357–369, <https://doi.org/10.1002/2014PA002621>.
- Rae, J.W.B., G.L. Foster, D.N. Schmidt, and T. Elliott. 2011. Boron isotopes and B/Ca in benthic foraminifera: Proxies for the deep ocean carbonate system. *Earth and Planetary Science Letters* 302:403–413, <https://doi.org/10.1016/j.epsl.2010.12.034>.
- Rae, J.W.B., A. Burke, L.F. Robinson, J.F. Adkins, T. Chen, C. Cole, R. Greenop, T. Li, E.F.M. Littley, D.C. Nita, and others. 2018. CO₂ storage and release in the deep Southern Ocean on millennial to centennial timescales. *Nature* 562:569–573, <https://doi.org/10.1038/s41586-018-0614-0>.
- Shao, J., L.D. Stott, W.R. Gray, R. Greenop, I. Pecher, H.L. Neil, R.B. Coffin, B. Davy, and J.W.B. Rae. 2019. Atmosphere-ocean CO₂ exchange across the last deglaciation from the boron isotope proxy. *Paleoceanography and Paleoeclimatology* 34:1,650–1,670, <https://doi.org/10.1029/2018PA003498>.

AUTHORS

Jessica G.M. Crumpton-Banks (jessica.crumptonbanks@nuigalway.ie) completed her PhD in the School of Earth and Environmental Geosciences, University of St Andrews, UK, and is currently a postdoctoral fellow in the School of Geography and Archaeology, National University of Ireland, Galway, Ireland. **James W.B. Rae** (jwbr@st-andrews.ac.uk) is Professor, School of Earth and Environmental Geosciences, University of St Andrews, UK.

Linkages Between Dynamic Phytoplankton C:N:P and the Ocean Carbon Cycle Under Climate Change

By Katsumi Matsumoto, Tatsuro Tanioka, and Rosalind Rickaby

ABSTRACT. Modelers of global ocean biogeochemistry are beginning to represent a phenomenon that biologists have long observed in laboratory and field settings: that the elemental stoichiometry of phytoplankton is quite flexible. Today, it is well recognized that the C:N:P ratio in phytoplankton and particulate organic matter can vary substantially on ocean basin scales. Recent data show that, compared to the traditional Redfield ratio C:N:P = 106:16:1, the ratio is much higher in the oligotrophic subtropical gyres (~195:28:1) and much lower in eutrophic polar waters (~78:13:1). This pattern of variability, informed by results from phytoplankton incubation experiments, indicates that environmental factors such as nutrient availability and temperature are important drivers. Our model simulations of the global ocean carbon cycle under global warming and glacial conditions suggest that phytoplankton physiology and community composition control global C:N:P export. Model results also indicate the important role that Southern Ocean sea ice plays in determining the global export stoichiometry by altering the proportional contribution of Southern Ocean phytoplankton to global production. Sea ice retreat under warming and expansion under glaciation, while opposite in sign, can both elevate the global export C:N:P ratio by altering phytoplankton physiology and community composition in contrasting ways between each scenario. The global mean export C:N:P ratio increases from 113:16:1 in the control run to 119:17:1 by the year 2100 in the future run and to 140:16:1 in the glacial run. The impact of higher export C:N:P ratios is to strongly buffer carbon export against change for both scenarios.

INTRODUCTION

The world ocean holds vastly more carbon than the atmosphere (~60 times more during preindustrial times). Therefore, a relatively small change in the oceanic carbon inventory can lead to a large change in atmospheric $p\text{CO}_2$ and thus in global climate. Also, the large capacity of the ocean to store carbon means that perturbations to atmospheric $p\text{CO}_2$ can be damped by the ocean through air-sea CO_2 exchange. The timescale of change for the ocean spans decades to centuries, much longer than those for the atmosphere or the land

biosphere. Thus, the ocean has long been considered key to understanding global carbon cycle changes that occurred over glacial-interglacial timescales and that are likely to occur on decadal to centennial timescales in the future.

One of the important drivers of the ocean carbon cycle is the biological pump, the vertical transport of carbon from the surface to the deep ocean by sinking particulate organic matter (POM). This carbon export process can sequester carbon in the ocean interior for centuries until overturning circulation returns it to

the surface. As Broecker (1982) first proposed, changes in the strength of the biological pump can alter the amount of carbon sequestered in the ocean and has the potential to drive large variations in atmospheric $p\text{CO}_2$. For example, strengthening of the pump can reduce $p\text{CO}_2$ and often requires increasing the oceanic inventories or surface supply rates of limiting nutrients such as phosphorus (Broecker, 1982), nitrogen (Falkowski, 1997), and iron (Martin, 1990). Here, we aim to examine a new twist to the biological pump under climate change, namely, how flexible elemental stoichiometry of phytoplankton modifies carbon export as the marine environment changes. This idea was originally suggested by Peter Weyl to Broecker (1982) in the context of glacial $p\text{CO}_2$ and subsequently mentioned infrequently in the literature. Our goal in this work is to introduce how this twist might manifest under glacial conditions (Matsumoto et al., 2020) as well as under future warming conditions (recent work of authors Matsumoto and Tanioka), for which environmental drivers are arguably more easily understood.

REDFIELD RATIO AND FLEXIBLE C:N:P

The possibility that phytoplankton stoichiometry of carbon, nitrogen, and phosphorus (C:N:P) could be flexible on an ocean basin scale has not been considered seriously until recently. The stabil-

ity of the C:N:P ratio has been a central tenet of chemical oceanography since the seminal work by Redfield (1934). He discovered that the stoichiometry in plankton and seawater was very similar. The so-called Redfield ratio of marine organic matter is C:N:P = 106:16:1 (Redfield et al., 1963). Later, L.A. Anderson (1995) extended it to oxygen, -O₂:P = -150:1. The Redfield ratio is very useful in studies of ocean carbon budgeting, and chemical oceanographers have long assumed the Redfield ratio or some variations of it to be fixed. For example, just a decade ago the international modeling community used a fixed ratio in the Ocean Carbon Cycle Model Intercomparison Project (Najjar et al., 2007). However, biologists have long known plankton stoichiometry to be quite variable in individual cells. Indeed, Redfield himself noted stoichiometric flexibility. Furthermore, a strict C:N:P ratio does not seem to be supported by any obvious physiological or biochemical underpinning (Geider and La Roche, 2002).

In recent years, evidence has been mounting of substantial variability in the stoichiometry of phytoplankton and particulate organic matter (POM), even at the ocean basin scale. For example, Martiny et al. (2013) find a clear global pattern that shows an elevated C:N:P ratio of 195:28:1 in the subtropical gyres, 137:18:1 in the warm upwelling zones, and 78:13:1 in the nutrient-rich polar regions (Table 1). An inverse model of ocean biogeochemistry also inferred a similar spatial pattern of global C:N:P ratio (Teng et al., 2014; Wang et al., 2019). This variability is not fully understood, but nutrient availability, especially that of phosphate, is clearly recognized as a driver. Also, stoichiometric measurements on different taxa reveal that eukaryotes have relatively low C:N:P, more consistent with the Redfield ratio, which is perhaps not surprising given that Redfield's original measurements were made on eukaryotes. Modern measurements on much smaller cyanobacteria, not yet discovered in Redfield's day, show distinctly higher ratios, with C:P as high

as 350 and N:P as high as 50.

Today, the global ocean modeling community is transitioning from fixed to dynamic stoichiometry for phytoplankton. For example, the stoichiometric flexibility represented by the state of the art CMIP5/6 models range from none at all (i.e., fixed C:N:P) to partial flexibility (e.g., flexible C:P but fixed C:N) to full flexibility (Bopp et al., 2013; Arora et al., 2019). This flexibility has important implications not only for the glacial carbon cycle but also for future uptake of anthropogenic carbon by the ocean. For example, the traditional view of the future biological carbon pump is that it will become weaker as warming enhances ocean stratification and reduces the vertical supply of nutrients from the subsurface to the sunlit surface layer. However, the concept of flexible stoichiometry allows for the possibility that the biological carbon pump may remain relatively unperturbed in the face of reduced nutrient supply because the reduction should lead to higher phytoplankton C:P.

In other words, changes in phytoplankton stoichiometry could buffer carbon export against change. Previous modeling studies indicate that the ocean's capacity to uptake anthropogenic carbon in the future due to variable C:P alone is quantitatively modest (Tanioka and Matsumoto, 2017).

A major challenge in transitioning to a more fully flexible phytoplankton C:N:P ratio in ocean biogeochemical models is the deficiency in understanding which environmental factors drive the flexibility. A cursory survey of the literature does not give a clear picture (e.g., Moreno and Martiny, 2018). There are numerous reports of laboratory incubation experiments that indicate phytoplankton stoichiometry dependence with a conflicting sense of change (e.g., how temperature affects C:N:P ratio). Also, different studies target different strains of algae, often under dissimilar conditions.

In order to overcome this challenge, we conducted an exhaustive meta-analysis of laboratory studies of marine

TABLE 1. Observed and modeled C:N:P stoichiometry.

		C:N:P TYPE	C:N:P RATIO	SOURCE
OBSERVED				
Redfield Ratio		POM	106:16:1	Redfield et al. (1963)
Biomass-Weighted	Global	POM	146:20:1	Martiny et al. (2013)
	Subtropical Gyres	POM	195:28:1	Martiny et al. (2013)
	Warm Upwelling Waters	POM	137:18:1	Martiny et al. (2013)
	Polar Eutrophic Waters	POM	78:13:1	Martiny et al. (2013)
Global Inverse Model		Export	115:17:1	Wang et al. (2019)
MODEL RESULTS				
Control Run	Global	Uptake	146:19:1	Matsumoto et al. (2020)
	Subtropical Gyres	Uptake	217:25:1	Matsumoto et al. (2020)
	Polar Water	Uptake	69:14:1	Matsumoto et al. (2020)
	Global	Export	113:16:1	Matsumoto et al. (2020)
Global Warming Year 2100		Export	119:17:1	Recent work of authors Matsumoto and Tanioka
Glacial		Export	140:16:1	Matsumoto et al. (2020)

POM = Particulate organic matter/phytoplankton. Wang et al. (2019) provide a data-constrained, global N:P export ratio of 17.3:1 and assume a fixed C:N = 106:16 to calculate the C:P ratio. In the model, the uptake C:N:P ratio is the net primary production (NPP)-weighted, spatially averaged, community phytoplankton uptake ratio over the top 100 m. The export C:N:P ratio in the model is the NPP-weighted, spatially averaged export ratio calculated at 100 m water depth. For data/model comparison, ratios measured for POM should be compared to model uptake ratios.

phytoplankton stoichiometry (Tanioka and Matsumoto, 2020). Meta-analysis is a powerful statistical framework for synthesizing independent studies and identifying trends, and it follows rigorous formal protocols to ensure reproducibility and reduce bias. We analyzed 241 experimental units of P:C and 366 experimental units of N:C from 104 journal articles encompassing seven taxonomic phyla.

Figure 1 illustrates the main findings of the meta-analysis regarding the sensitivities of C:P and C:N uptake as functions of phosphate, nitrate, light, and temperature. Sensitivity to iron was included in the meta-analysis but is excluded here due to a significant but very small signal that was seen in only one class of phytoplankton. Our meta-analysis confirmed that C:P increases as P becomes more limiting (Figure 1a) and also as temperature rises (Figure 1b). Additionally, C:N increases as N becomes more limiting (Figure 1c) and as light increases (Figure 1d). The meta-analysis shows

that the stoichiometric sensitivities differ in terms of their statistical significance, magnitude, and universality across different taxonomic groups. For example, the effect of phosphate on C:P is much larger for eukaryotes than for other phytoplankton types examined, and the effect of temperature is not statistically significant in eukaryotes. The interested reader is referred to the meta-analysis in Tanioka and Matsumoto (2020) for a discussion of the underlying biochemical reasons.

With global warming, water temperatures will rise, and the water column will likely stratify more strongly, providing more light to phytoplankton in a thinner mixed layer and resulting in reduced vertical supply of phosphate and nitrate to the surface. According to the sensitivities of the C:P and C:N ratios (Figure 1), these environmental changes will elevate C:P or C:N so that phytoplankton should become more carbon rich. In this simple thought experiment then, higher carbon content in phytoplankton should lead to

greater carbon export, but coupled with lower overall productivity, global carbon export will be buffered into the future.

FLEXIBLE C:N:P IN THE CONTROL MODEL RUN

Whether and how much this stoichiometric buffering occurs in a more realistic setting can be explored by implementing the C:P and C:N sensitivities shown in Figure 1 in a global model of ocean biogeochemistry. We have employed a coarse resolution three-dimensional Earth system model called MESMO (Minnesota Earth System Model for Ocean biogeochemistry; Matsumoto et al., 2013) for this purpose. Details of the implementation are available in Matsumoto et al. (2020). Here, we note briefly that three phytoplankton functional types (PFTs) are represented in the flexible C:N:P-enabled MESMO: eukaryotes, cyanobacteria, and diazotrophs. Eukaryotes, which include diatoms, are fast and opportunistic growers, especially under nutrient

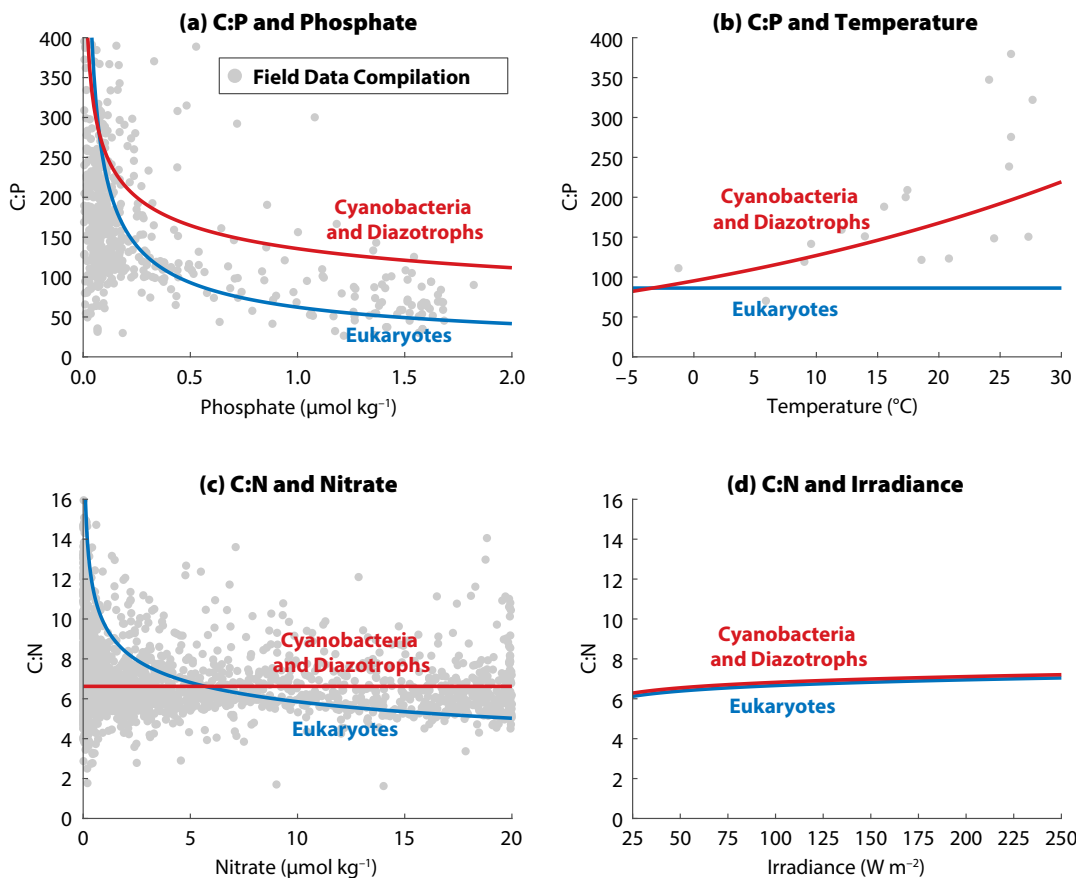


FIGURE 1. C:P and C:N ratios of three phytoplankton groups as functions of four environmental drivers with sensitivities from the meta-analysis of Tanioka and Matsumoto (2020). In each panel, only one driver is changed while others are kept constant at reference values. The gray dots are C:P and C:N data of bulk particulate organic matter from the field. (a) and (c) from Galbraith and Martiny (2015) and (b) from Yvon-Durocher et al. (2015)

replete conditions. Cyanobacteria such as *Prochlorococcus* and *Synechococcus* are smaller cells that do well in oligotrophic waters. Diazotrophs are nitrogen fixers that exhibit slow growth rates but are not limited by nitrate. The growth patterns of these PFTs are limited by temperature, light, and different combinations of nutrients (P, N, Fe, and Si). Base model states for the three PFTs, including nutrient limitation maps, are presented in Matsumoto et al. (2020). In the model, the base C:N:P ratio is set lower for eukaryotes and higher for the other two PFTs as observed, and the three PFTs are given different C:N:P sensitivities, according to the meta-analysis findings. For example, all PFTs have C:P dependence on phosphate, but eukaryotes are the most sensitive compared to the others.

The MESMO control run, prescribed with preindustrial boundary conditions and described by Matsumoto et al. (2020), shows a number of features that indicate good starting points for explor-

ing the effect of flexible stoichiometry on the ocean carbon cycle (Figure 2). For example, in the oligotrophic subtropical gyres of the model, where carbon export production is low, cyanobacteria are dominant (Figure 2a) and C:P is high (Figure 2b). The phytoplankton community C:P is high in the subtropical gyres, because low phosphate concentrations elevate the C:P ratio for all PFTs and because cyanobacteria make the largest contribution to the community. In contrast, the community C:P is low in eutrophic and polar waters because the nutrient replete conditions reduce C:P in all PFTs and eukaryotes are dominant. Community C:P in our model is largely consistent with the observed C:P ratio of particulate organic matter on the global scale (compare black line and squares in Figure 2b).

Globally, the control model predicts C:N:P uptake of 102:14:1 for eukaryotes and much higher uptake ratios for cyanobacteria and diazotrophs

(C:N:P = 198–213:23–32:1) within the production layer. The global mean phytoplankton community C:N:P uptake ratio is 146:19:1 (Table 1). The model predicts the highest C:N:P uptake ratio in the top-most level within the production layer, because the surface is where nutrients are most depleted and light levels and temperatures are the highest. The C:N:P uptake ratio becomes lower with depth in the production layer. Export C:N:P ratio at any site reflects the uptake ratios carried by POM formed at different levels within the production layer. The model currently includes no preferential remineralization of different elements. The global mean export C:N:P in the control model is 113:16:1, which is close to the Redfield ratio (Table 1). The difference between the phytoplankton uptake ratio and the export ratio is thus a consequence of having an environment-driven, flexible stoichiometry. Such a difference does not manifest in the model where phytoplankton C:N:P uptake ratio is fixed.

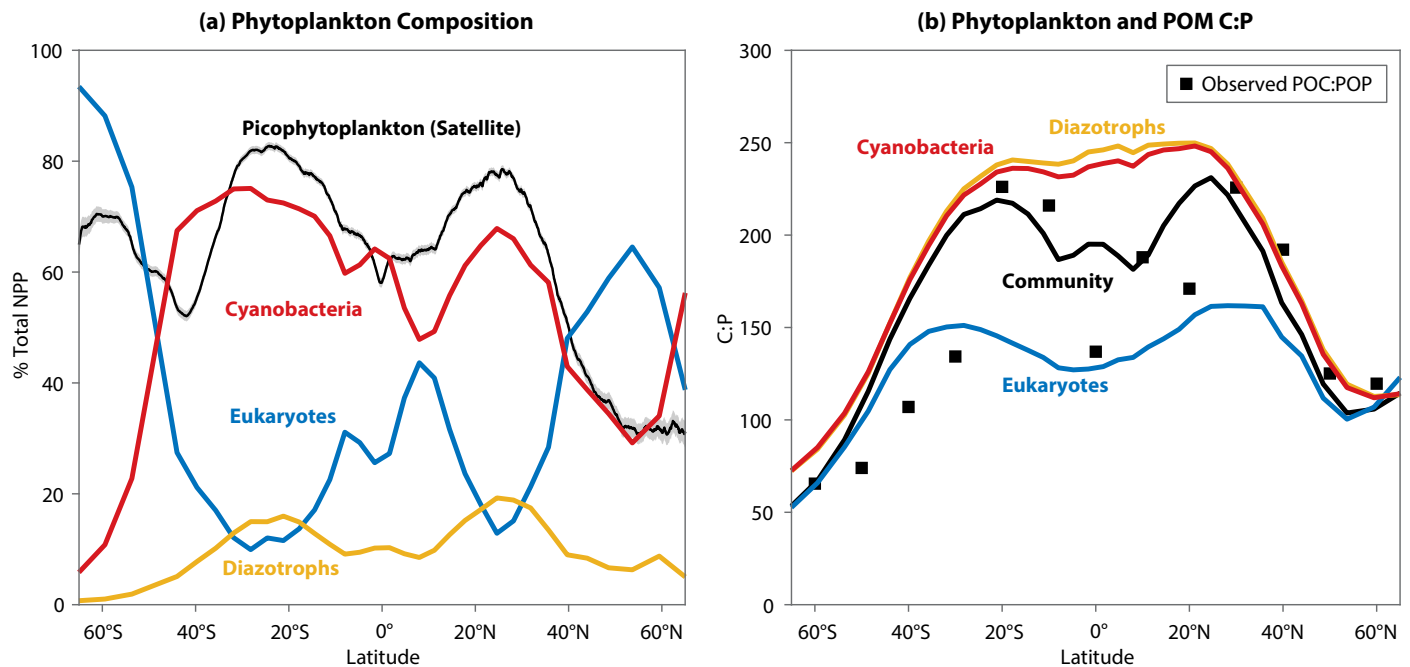


FIGURE 2. Annual mean properties in the control model for the top 100 m of the water column. (a) Zonally averaged, net primary production (NPP)-weighted phytoplankton community composition. The three phytoplankton functional types (PFTs) represented in the model are eukaryotes (blue), cyanobacteria (red), and diazotrophs (yellow). The black line is the remotely sensed contribution of picophytoplankton (0.5–2 μm) to total carbon-based biomass (Kostadinov et al., 2016). (b) Zonally averaged C:P uptake ratios for each PFT (colored lines) and the NPP-weighted community C:P (black line). The community C:P would be reflected in the C:P ratio of organic particles. Black squares are based on data from C:P from Martiny et al. (2013).

FLEXIBLE C:N:P UNDER GLOBAL WARMING

All future MESMO simulations are carried out under a new “middle-of-the-road” scenario for future warming called the Shared Socioeconomic Pathway 2 (Riahi et al., 2017). The summary presented here is based on multiple sensitivity model experiments carried out recently by authors Matsumoto and Tanioka. The model simulates typical climate warming features that include warming of surface air and sea surface, slowdown of the Atlantic meridional overturning circulation, and shallower mixed layer and sea ice retreat in polar waters. Radiative forcing stabilizes at $\sim 4.5 \text{ Wm}^{-2}$ with $p\text{CO}_2$ at around $600 \mu\text{atm}$ by the year 2100. We

show results from our global warming simulation for the year 2100. There are two important drivers of global export C:N:P changes in our model simulation. First, global sea ice coverage retreats from approximately 10% to 6.5%, leading to enhanced biological production in the previously ice-covered Southern Ocean (Figure 3a). This has the effect of depleting surface nutrients there, thus elevating the C:N:P of all Antarctic PFTs and increasing the Southern Ocean’s contribution to global production. Second, higher temperatures increase the C:P ratio for cyanobacteria and diazotrophs. This temperature effect has a significant impact on community C:P outside the Southern Ocean (Figure 3c).

In the warming simulation, the global mean export C:N:P increases for two main reasons. First, physiologically, the global mean C:N:P for eukaryotes increases because of the large reduction in nutrient availability in the Southern Ocean. The same effect is simulated for cyanobacteria and diazotrophs but is smaller due to their lower C:P sensitivities to phosphate limitation. Outside the Southern Ocean, where the nutrients were already much lower or even close to being completely depleted, the temperature effect on cyanobacteria and diazotroph C:P becomes large. The second reason that the global export C:N:P rises is the change in regional production. While biological production declines

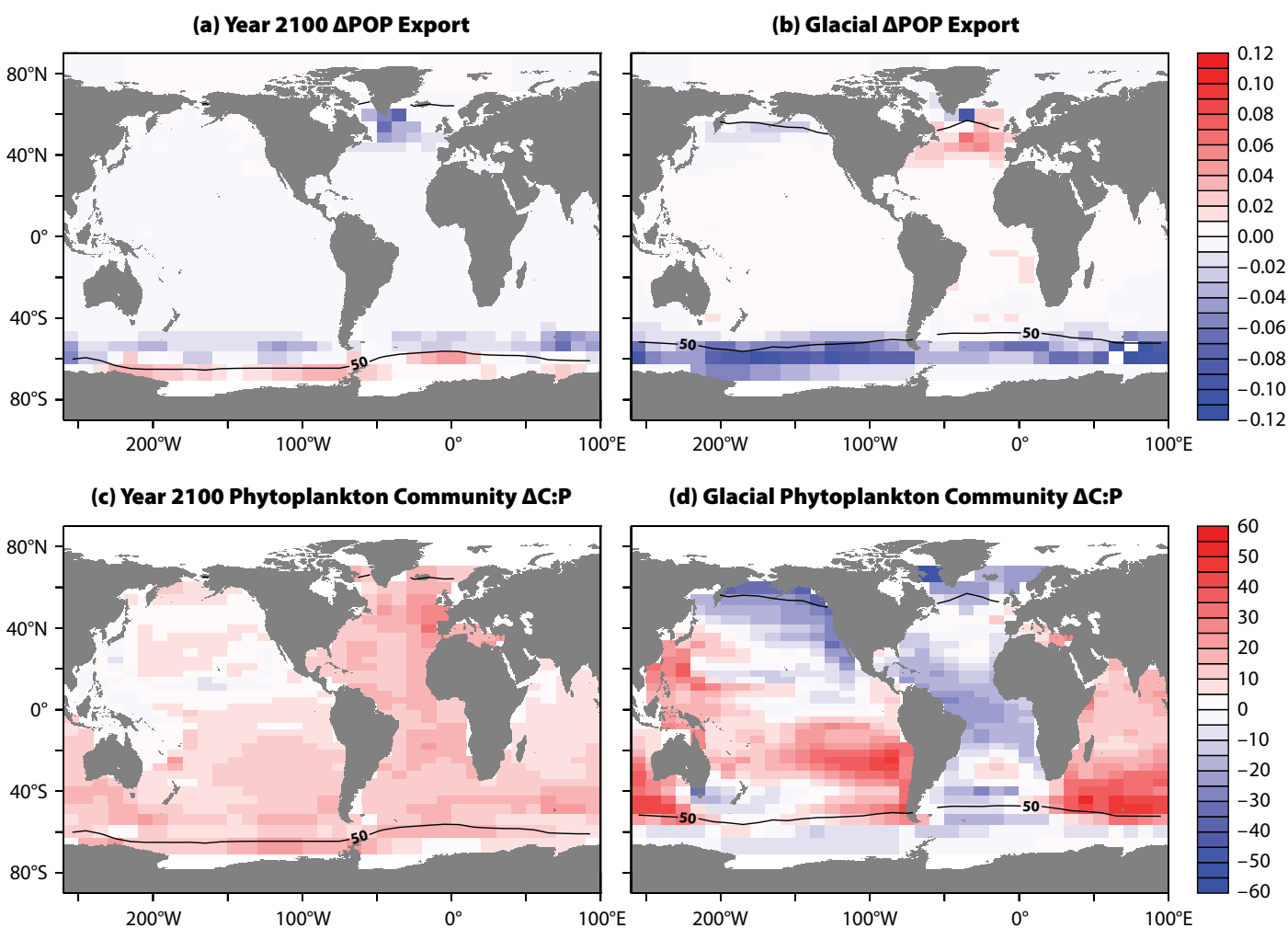


FIGURE 3. Experiment-minus-control changes under global warming and glacial conditions. The change in particulate organic phosphorus (ΔPOP) export (mole-P $\text{m}^{-2} \text{yr}^{-1}$) for (a) year 2100, and (b) glacial. Phytoplankton community $\Delta\text{C:P}$ (molar ratio) for (c) year 2100 and (d) glacial. The black line indicates mean annual sea ice coverage of 50% (e.g., 100% coverage for half a year) predicted by the model under prevailing climate conditions.

globally (due generally to increased stratification), the Southern Ocean is anomalous in showing an increase in production as sea ice retreats. As noted above, the strong, nutrient-driven physiological response of Antarctic phytoplankton stoichiometry, especially by eukaryotes, makes a larger contribution to the global mean. In other words, the stoichiometry of the PFTs from the more productive waters would make a larger contribution to the global mean than the stoichiometry of the PFTs from less productive waters. Interestingly, the shift in community composition under global warming is modest and has little effect on global C:N:P. As expected, a shift in favor of the smaller cyanobacteria occurs at the expense of the larger eukaryotes in the model, as nutrients generally become more depleted. However, the shift is only ~3% globally. In an earlier modeling study with a very different formulation of flexible stoichiometry, Kwiatkowski et al. (2018) also found a similar taxonomic shift by ~2% by the year 2100 and attributed 95% of the global change in C:N:P to physiology.

Under the warming scenario adopted here, MESMO predicts that the global export C:N:P ratio increases from 113:16:1 in the preindustrial state to 119:17:1 by the year 2100 (Table 1). During this period, the global P export by particles (POP) declines by 14%. In a separate model run where phytoplankton C:N:P was fixed, the global carbon export declined by the same proportion as P export, as expected. However, the simulated carbon export decline is only 10% with flexible stoichiometry export. The stoichiometric buffering effect (BE) of carbon export can be quantified as

$$BE = \left(1 - \frac{1 - f_{POC}}{1 - f_{POP}}\right) \times 100,$$

where f_{POC} and f_{POP} are the fractional changes in particulate organic carbon (POC) and POP since preindustrial times. In this case, $1 - f_{POC} = 0.10$ and $1 - f_{POP} = 0.14$. BE is thus 30%. As export C:N:P increases under warming, it facili-

tates a larger uptake of anthropogenic carbon under the prescribed atmospheric pCO_2 . However, the net transport of air-sea CO_2 flux is driven overwhelmingly by the prescribed pCO_2 itself (i.e., large air-sea pCO_2 gradient), so that the effect of flexible C:N:P on anthropogenic carbon is quantitatively insignificant. In our study, the extra anthropogenic carbon uptake due to a higher export C:N:P ratio is just ~1% by the year 2100, similar to the estimate of 0.5%–3.5% by Kwiatkowski et al. (2018).

FLEXIBLE C:N:P UNDER GLACIAL CONDITIONS

We find that the lessons gleaned for the global warming case are generally applicable to the glacial model simulation. In the glacial simulation, the same flexible C:N:P-enabled ocean model was subject to five conditions that are often used in glacial model studies: larger land ice (albedo), reduced radiative forcing from greenhouse gases, insolation changes due to Earth's orbital parameters, increased dust deposition, and weaker Southern Hemisphere westerly winds. A whole suite of glacial model runs with various sensitivities indicated are described in detail in Matsumoto et al., 2020 and are used to draw the general conclusions summarized here.

In the glacial simulation, the application of ice albedo and radiative forcing substantially cools the planetary surface (>5°C in global mean surface air temperature) and has the important effect of expanding the polar sea ice by 64%. In stark contrast to the global warming simulation, the increase in sea ice under glacial conditions has the effect of dramatically reducing biological production in the Southern Ocean (Figure 3b). This reduced contribution in turn leads to an increase in the global export C:N:P, because the Southern Ocean with high nutrients (which drives C:N:P lower) and eukaryote-dominated PFTs (which, again, drives C:N:P lower) now has a reduced influence on the global mean.

A comparison of sensitivity runs with

and without glacial dust flux demonstrates that the increased dust deposition in the glacial model run also has important consequences for global export C:N:P through a chain of events. Iron from dust has a direct fertilization effect on PFTs in places where Fe is limiting. More critically for this study, the iron input impacts the physiology of diatoms as previously suggested in the silicic acid leakage hypothesis (Matsumoto et al., 2002), which predicts that increased iron availability will reduce the Si:N uptake ratio of diatoms, leaving silicic acid underutilized in much of the world's surface ocean. As theorized, this relieves the severe silicic acid limitations that diatoms exhibit in the control model run. As a result, production by the eukaryote PFT is enhanced outside areas of expanded sea ice. Global eukaryote carbon export thus increases substantially from 3.6 Pg-C yr⁻¹ to 6.3 Pg-C yr⁻¹. This eukaryote growth comes at the expense of cyanobacteria growth and depletes surface nutrients because eukaryotes have high growth rates. As a consequence, global mean surface phosphate concentration decreases from 0.31 μmol-P kg⁻¹ to 0.26 μmol-P kg⁻¹ in the model, although phosphate in polar waters increases because the expanded sea ice suppresses biological production. Interestingly, in our model, nitrate becomes decoupled from phosphate in the Southern Ocean surface waters by showing a decline. In the model, the nitrate decline reflects a reduction in the global nitrate inventory, a consequence of weaker southern westerlies reducing deep ocean ventilation, enhancing deoxygenation, and finally promoting a faster rate of denitrification.

The chain of events triggered by the glacial iron input has two important impacts on global C:N:P. First, the depletion of nutrients elevates the C:N:P uptake ratio according to the sensitivities of C:P and C:N illustrated in Figure 1. This physiological response is strongest in eukaryote C:P, which increases everywhere outside the polar waters. The global mean C:N:P for eukaryotes thus increases from

102:14:1 to 152:16:1. Cyanobacteria and diazotrophs exhibit similar, but weaker, stoichiometric responses to nutrients. Also, their C:P becomes lower with cooling. Their overall change in C:N:P is thus mixed, with nutrients raising the ratio and cooling lowering it. Community C:N:P represents a balance of these physiological changes and a general shift in community composition in favor of eukaryotes.

A first glance at the map of experiment-minus-control changes under glacial conditions in [Figure 3d](#) gives the impression that the C:P increase in the Indian and much of the Pacific Oceans is balanced by C:P reduction in the Atlantic and North Pacific. However, the global mean C:N:P is given by the production-weighted average. As already noted, the global mean C:N:P is proportionately influenced by the ratios of the more productive waters, and very little influenced by the low ratios of the largely ice-covered Southern Ocean under glacial conditions. The global mean export C:N:P ratio is therefore decidedly higher under glacial conditions, 140:16:1, compared to the control run, 113:16:1 ([Table 1](#)). There is thus a 24% increase in the carbon content in the sinking POM per unit P.

In terms of the buffer equation presented above, $f_{POP} = 0.77$ and $f_{POC} = 0.95$ for the glacial simulation. That is, while P export decreased by 23%, carbon export only declined by 5%, which indicates $BE = 79\%$, a very strong buffering of carbon export.

The elevated export C:N:P ratio under glacial conditions could help to explain the glacial levels of atmospheric pCO_2 . As first demonstrated in the 1980s with Antarctic ice core records, pCO_2 was lower during peak glacial times by 80–100 μatm than during interglacial periods (e.g., Petit et al., 1999). A comparison of the glacial-minus-control runs with and without flexible C:N:P suggests that having flexible stoichiometry reduces pCO_2 by approximately 20 μatm . This quantification is not without difficulty, but it is on par with the changes in pCO_2 achieved by other mechanisms

such as solubility.

Are the glacial model predictions reasonable? Our model prediction of deep deoxygenation is consistent with recent paleo-proxy studies concluding that many parts of the glacial ocean, including the deep Atlantic and the equatorial Pacific, had substantially lower $[O_2]$ during the last glacial period than today (e.g., Lu et al., 2016; R.F. Anderson et al., 2019). In the Southern Ocean, the literature supports the predictions of sea ice expansion and diminished Antarctic productivity during the last glacial period. A reconstruction of Antarctic sea ice based on fossil diatoms recovered from sediment cores indicates that the maximum limit of Antarctic winter sea ice extended northward by 5°–10° latitude in all sectors of the Southern Ocean (Crosta et al., 1998). It is likely that as sea ice expands, biological production under sea ice will be diminished and surface nutrients will be underutilized and accumulate, as our results indicate. Indeed, a summary of biological production during the glacial period indicates reduced production in Antarctic waters (Kohfeld, 2005). Also, different nutrient proxies in Antarctic waters indicate increases in surface nutrient concentrations, for example, foraminiferal Cd/Ca (Elderfield and Rickaby, 2000), diatom $\delta^{30}Si$ (De La Rocha et al., 1998), and $\delta^{13}C$ of organic matter bound to diatoms (Shemesh et al., 1993).

However, these surface nutrient proxies have long been at odds with sedimentary and diatom-bound $\delta^{15}N$ data, which indicate greater nitrate consumption (François et al., 1997). Interestingly and as noted above, our model shows that nitrate is decoupled from phosphate in Southern Ocean surface waters. While phosphate concentration increases due to underutilization, nitrate concentration decreases, reflecting a globally higher denitrification rate and a declining global ocean inventory of fixed nitrogen. The nutrient decoupling may in fact suggest a possible reconciliation of the apparently contradictory proxy results regarding glacial Southern Ocean nutrient utilization.

TAKE-HOME MESSAGES

There are a few take-home messages. First, there are three important controls on global export C:N:P, namely, the physiological response to environmental changes, a shift in community composition, and the balance in regional production ([Figure 4](#)). Under global warming, the physiological response for all PFTs was production of more carbon-rich organic matter. Under glacial conditions, the physiological response was more mixed, with nutrient depletion raising the C:P uptake ratio for all PFTs, but cooling lowering the C:P ratio in two of three PFTs. The community composition under warming very modestly shifted in favor of cyanobacteria. The shift under glacial conditions favored eukaryotes. The balance in regional production under both climate conditions was driven substantially by sea ice. It shrunk under warming but expanded under glaciation. Surprisingly, both changes had the effect of raising the global mean export C:N:P ratio. Under warming, the increase in production and the depletion of nutrients in previously ice-covered waters increased the contribution of the elevated C:N:P ratio of the Southern Ocean to the global mean. Under glacial conditions, the contribution of the low Southern Ocean C:N:P ratio diminished, raising the global mean.

It is interesting to ponder whether this means the present state is at the lowest C:N:P ratio point in recent Earth history, so that going forward (warming) or backward (glaciation) would lead inevitably to a higher ratio, or whether this is an artifact of the model we used. We do not believe our results show a model artifact, because in different modeling studies, albeit limited in number, the C:P ratio also increased going forward (Kwiatkowski et al., 2018) and backward (Ödalen et al., 2020). Also, the changes in the C:N:P ratio simulated by our model can be understood reasonably in terms of predicted changes in phytoplankton physiology, taxonomy, and regional production. Furthermore, the elevation

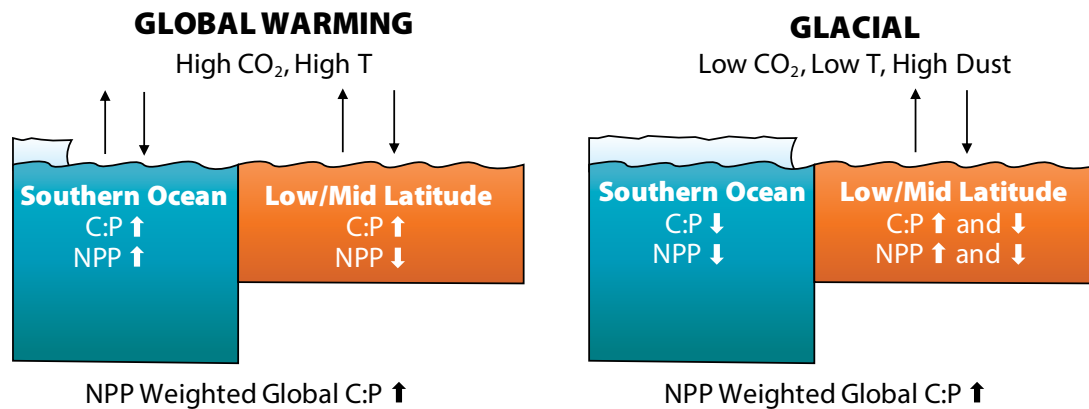


FIGURE 4. A schematic diagram illustrating the differences in two model conditions. In the global warming scenario (left), both C:P and net primary production (NPP) increase in the Southern Ocean as sea ice retreats and nutrient utilization increases. In the low/mid latitudes, C:P rises as nutrient availability decreases and temperatures rise. In the glacial scenario (right), both NPP and C:P in the Southern Ocean decrease as sea ice expands and nutrient utilization decreases. In the low/mid latitudes, the responses of C:P and NPP vary regionally.

of the phytoplankton community C:P uptake ratio under glacial conditions (Figure 3d) is quite nuanced in space. It reflects, for example, a mixture of phosphorus depletion affecting eukaryotes by increasing their C:P uptake ratio and cooling affecting cyanobacteria by lowering their C:P uptake ratio (Figure 4). It seems possible that the balance of such tendencies can result in an overall lower global C:N:P ratio under some set of conditions. If so, it is not obvious that the present state is at the lowest C:N:P ratio point. It may be worth considering what conditions might actually lead to a lower C:N:P ratio compared to the present state. Based on the insights gained in this study, such conditions would include a nutrient replete surface ocean, cooling, lower light levels, and Antarctic sea ice retreat. At least one combination, global cooling plus sea ice retreat, does not seem probable. However, the bipolar seesaw observed between the two hemispheres suggests at least that Northern Hemisphere cooling could be accompanied by Southern Hemisphere warming (Crowley, 1992; Markle et al., 2016) and possibly sea ice retreat. On the other hand, if surface winds were to become substantially stronger, they would deepen the mixed layer and reduce the average light level for phytoplankton there. The same winds would also mix cool and

nutrient-rich subsurface waters upward to the surface. These conditions if prevalent in large areas of the world ocean may lead to a lower global mean C:N:P ratio. Perhaps the question of whether the present state is at the lowest C:N:P ratio point or not can be recast in terms of how realistic such conditions are.

The second take-home message is that, given these results, it is important to have (at least) these three controls properly represented in global models with flexible stoichiometry. Thus, having multiple PFTs is essential to allow for shifts in phytoplankton community composition. Also, formulations of flexible phytoplankton C:N:P uptake ratio that account for a full set of environmental drivers like nutrients and temperature are important. Finally, models that cannot simulate dynamic shifts in regional production would be challenged in predicting the global export C:N:P ratio.

Third, the search for a more complete description of organic matter export C:N:P is an important ongoing goal in ocean biogeochemistry. For example, our model is still missing heterotrophic control on the stoichiometry of sinking POM, an idea that originally prompted Weyl to consider the effect of variable C:P on glacial atmospheric CO₂. Preferential remineralization of N and P by heterotrophy acts not only on POM but on dissolved

organic matter as well.

The final message is to point out that as yet there is no paleo proxy for phytoplankton stoichiometry, although coupling of multiple water column nutrient proxies, together with export proxies, may allow resolution of the resultant change in the water column ratio. Our results suggest that flexible C:N:P is important. It can possibly account for 20 μatm of atmospheric pCO₂ change during a glacial period. Also, it strongly buffers carbon export against change under both warming and cooling. We could therefore hypothesize, perhaps provocatively, that the variability in the export C:N:P ratio under climate change will always act as a buffer against change in carbon export. If a new proxy for phytoplankton stoichiometry were developed, it could be used to test the hypothesis and open a new subfield of paleo research probing ecological change and driving mechanisms for atmospheric CO₂. 

REFERENCES

- Anderson, L.A. 1995. On the hydrogen and oxygen content of marine phytoplankton. *Deep Sea Research Part I* 42(9):1,675–1,680, [https://doi.org/10.1016/0967-0637\(95\)00072-E](https://doi.org/10.1016/0967-0637(95)00072-E).
- Anderson, R.F., J.P. Sachs, M.Q. Fleisher, K.A. Allen, J. Yu, A. Koutavas, and S.L. Jaccard. 2019. Deep-sea oxygen depletion and ocean carbon sequestration during the last ice age. *Global Biogeochemical Cycles* 33(3):301–317, <https://doi.org/10.1029/2018GB006049>.

- Arora, V., A. Katavouta, R. Williams, C. Jones, V. Brovkin, P. Friedlingstein, J. Schwinger, L. Bopp, O. Boucher, P. Cadule, and others. 2019. Carbon-concentration and carbon-climate feedbacks in CMIP6 models, and their comparison to CMIP5 models. *Biogeosciences Discussions*, <https://doi.org/10.5194/bg-2019-473>.
- Bopp, L., L. Resplandy, J.C. Orr, S.C. Doney, J.P. Dunne, M. Gehlen, P. Halloran, C. Heinze, T. Ilyina, R. Séférian, and others. 2013. Multiple stressors of ocean ecosystems in the 21st century: Projections with CMIP5 models. *Biogeosciences* 10(10):6,225–6,245, <https://doi.org/10.5194/bg-10-6225-2013>.
- Broecker, W.S. 1982. Ocean chemistry during glacial time. *Geochimica et Cosmochimica Acta* 46(10):1,689–1,705, [https://doi.org/10.1016/0016-7037\(82\)90110-7](https://doi.org/10.1016/0016-7037(82)90110-7).
- Crosta, X., J.J. Pichon, and L.H. Burckle. 1998. Reappraisal of Antarctic seasonal sea-ice at the Last Glacial Maximum. *Geophysical Research Letters* 25(14):2,703–2,706, <https://doi.org/10.1029/98GL02012>.
- Crowley, T.J. 1992. North Atlantic Deep Water cools the southern hemisphere. *Paleoceanography* 7(4):489–497, <https://doi.org/10.1029/92PA01058>.
- De La Rocha, C.L., M.A. Brzezinski, M.J. DeNiro, and A. Shemesh. 1998. Silicon-isotope composition of diatoms as an indicator of past oceanic change. *Nature* 395(6703):680–683, <https://doi.org/10.1038/27174>.
- Elderfield, H., and R.E.M. Rickaby. 2000. Oceanic Cd/P ratio and nutrient utilization in the glacial Southern Ocean. *Nature* 405(6784):305–310, <https://doi.org/10.1038/35012507>.
- Falkowski, P.G. 1997. Evolution of the nitrogen cycle and its influence on the biological sequestration of CO₂ in the ocean. *Nature* 387(6630):272–275, <https://doi.org/10.1038/387272a0>.
- François, R., M.A. Altabet, E.-F. Yu, D.M. Sigman, M.P. Bacon, M. Frank, G. Bohrmann, G. Bareille, and L.D. Labeyrie. 1997. Contribution of Southern Ocean surface-water stratification to low atmospheric CO₂ concentrations during the last glacial period. *Nature* 389(6654):929–935, <https://doi.org/10.1038/40073>.
- Galbraith, E.D., and A.C. Martiny. 2015. A simple nutrient-dependence mechanism for predicting the stoichiometry of marine ecosystems. *Proceedings of the National Academy of Sciences of the United States of America* 112(27):8,199–8,204, <https://doi.org/10.1073/pnas.1423917112>.
- Geider, R.J., and J. La Roche. 2002. Redfield revisited: Variability of C:N:P in marine microalgae and its biochemical basis. *European Journal of Phycology* 37(1):1–17, <https://doi.org/10.1017/S0967026201003456>.
- Kohfeld, K.E. 2005. Role of marine biology in glacial-interglacial CO₂ cycles. *Science* 308(5718):74–78, <https://doi.org/10.1126/science.1105375>.
- Kostadinov, T.S., S. Milutinović, I. Marinov, A. Cabré, S. Milutinović, I. Marinov, and A. Cabré. 2016. Carbon-based phytoplankton size classes retrieved via ocean color estimates of the particle size distribution. *Ocean Science* 12(2):561–575, <https://doi.org/10.5194/os-12-561-2016>.
- Kwiatkowski, L., O. Aumont, L. Bopp, and P. Ciais. 2018. The impact of variable phytoplankton stoichiometry on projections of primary production, food quality, and carbon uptake in the global ocean. *Global Biogeochemical Cycles* 32(4):516–528, <https://doi.org/10.1002/2017GB005799>.
- Lu, Z., B.A.A. Hoogakker, C.-D. Hillenbrand, X. Zhou, E. Thomas, K.M. Gutchess, W. Lu, L. Jones, and R.E.M. Rickaby. 2016. Oxygen depletion recorded in upper waters of the glacial Southern Ocean. *Nature Communications* 7(7):11146, <https://doi.org/10.1038/ncomms11146>.
- Markle, B.R., E.J. Steig, C. Buizert, S.W. Schoenemann, C.M. Bitz, T.J. Fudge, J.B. Pedro, Q. Ding, T.R. Jones, J.W.C. White, and T. Sowers. 2016. Global atmospheric teleconnections during Dansgaard–Oeschger events. *Nature Geoscience* 10(1):36–40, <https://doi.org/10.1038/ngeo2848>.
- Martin, J.H. 1990. Glacial-interglacial CO₂ change: The Iron Hypothesis. *Paleoceanography* 5(1):1–13, <https://doi.org/10.1029/PA005i001p00001>.
- Martiny, A.C., C.T.A. Pham, F.W. Primeau, J.A. Vrugt, J.K. Moore, S.A. Levin, and M.W. Lomas. 2013. Strong latitudinal patterns in the elemental ratios of marine plankton and organic matter. *Nature Geoscience* 6(4):279–283, <https://doi.org/10.1038/ngeo1757>.
- Matsumoto, K., J.L. Sarmiento, and M.A. Brzezinski. 2002. Silicic acid leakage from the Southern Ocean: A possible explanation for glacial atmospheric pCO₂. *Global Biogeochemical Cycles* 16(3):5–1–5–23, <https://doi.org/10.1029/2001GB001442>.
- Matsumoto, K., K. Tokos, A. Huston, and H. Joy-Warren. 2013. MESMO 2: A mechanistic marine silica cycle and coupling to a simple terrestrial scheme. *Geoscientific Model Development* 6(2):477–494, <https://doi.org/10.5194/gmd-6-477-2013>.
- Matsumoto, K., R. Rickaby, and T. Tanioka. 2020. Carbon export buffering and CO₂ drawdown by flexible phytoplankton C:N:P under glacial conditions. *Paleoceanography and Paleoclimatology*, <https://doi.org/10.1029/2019PA003823>.
- Moreno, A.R., and A.C. Martiny. 2018. Ecological stoichiometry of ocean plankton. *Annual Review of Marine Science* 10(1):43–69, <https://doi.org/10.1146/annurev-marine-121916-063126>.
- Najjar, R.G., X. Jin, F. Louanchi, O. Aumont, K. Caldeira, S.C. Doney, J.-C. Dutay, M. Follows, N. Gruber, F. Joos, and others. 2007. Impact of circulation on export production, dissolved organic matter, and dissolved oxygen in the ocean: Results from Phase II of the Ocean Carbon-cycle Model Intercomparison Project (OCMP-2). *Global Biogeochemical Cycles* 21(3), <https://doi.org/10.1029/2006GB002857>.
- Ödalen, M., J. Nycander, A. Ridgwell, K.I.C. Oliver, C.D. Peterson, and J. Nilsson. 2020. Variable C/P composition of organic production and its effect on ocean carbon storage in glacial-like model simulations. *Biogeosciences* 17(8):2,219–2,244, <https://doi.org/10.5194/bg-17-2219-2020>.
- Petit, J.R., J. Jouzel, D. Raynaud, N.I. Barkov, J.-M. Barnola, I. Basile, M. Bender, J. Chappellaz, M. Davis, G. Delaygue, and others. 1999. Climate and atmospheric history of the past 420,000 years from the Vostok ice core, Antarctica. *Nature* 399:429–413, <https://doi.org/10.1038/20859>.
- Redfield, M.C. 1934. *On the Proportions of Organic Derivatives in Sea Water and Their Relation to the Composition of Plankton*. University Press of Liverpool, James Johnstone Memorial Volume.
- Redfield, A.C., B.H. Ketchum, and F.A. Richards. 1963. The influence of organisms on the composition of sea-water. Pp. 26–77 in *The Sea. Volume 2: The Composition of Sea-Water: Comparative and Descriptive Oceanography*. M.N. Hill, ed., Interscience Publishers, New York.
- Riahi, K., D.P. van Vuuren, E. Kriegler, J. Edmonds, B.C. O'Neill, S. Fujimori, N. Bauer, K. Calvin, R. Dellink, O. Fricko, and others. 2017. The Shared Socioeconomic Pathways and their energy, land use, and greenhouse gas emissions implications: An overview. *Global Environmental Change* 42:153–168, <https://doi.org/10.1016/j.gloenvcha.2016.05.009>.
- Shemesh, A., S.A. Macko, C.D. Charles, and G.H. Rau. 1993. Isotopic evidence for reduced productivity in the glacial Southern Ocean. *Science* 262(5132):407–410, <https://doi.org/10.1126/science.262.5132.407>.
- Tanioka, T., and K. Matsumoto. 2017. Buffering of ocean export production by flexible elemental stoichiometry of particulate organic matter. *Global Biogeochemical Cycles* 31(10):1,528–1,542, <https://doi.org/10.1002/2017GB005670>.
- Tanioka, T., and K. Matsumoto. 2020. A meta-analysis on environmental drivers of marine phytoplankton C:N:P. *Biogeosciences*, <https://doi.org/10.5194/bg-2019-440>.
- Teng, Y.-C., F.W. Primeau, J.K. Moore, M.W. Lomas, and A.C. Martiny. 2014. Global-scale variations of the ratios of carbon to phosphorus in exported marine organic matter. *Nature Geoscience* 7(12):895–898, <https://doi.org/10.1038/NGEO2303>.
- Wang, W.-L., J.K. Moore, A.C. Martiny, and F.W. Primeau. 2019. Convergent estimates of marine nitrogen fixation. *Nature* 566(7743):205–211, <https://doi.org/10.1038/s41586-019-0911-2>.
- Yvon-Durocher, G., M. Dossena, M. Trimmer, G. Woodward, and A.P. Allen. 2015. Temperature and the biogeography of algal stoichiometry. *Global Ecology and Biogeography* 24(5):562–570, <https://doi.org/10.1111/geb.12280>.

ACKNOWLEDGMENTS

This work was funded by the US National Science Foundation (OCE-1827948). KM was supported by the Leverhulme Trust Visiting Professorship at the University of Oxford. RR acknowledges support from ERC Consolidator Grant APPELS: ERC-2015-COG-681746 and a Wolfson Research Merit Award. Numerical modeling and analysis were carried out using resources at the University of Minnesota Supercomputing Institute. Guest editor P. Delaney asked probing questions that motivated us to think deeper about the lowest C:N:P point. All model results presented here are archived at the Biological & Chemical Oceanography Data Management Office and freely accessible (<https://doi.org/10.26008/1912/bco-dmo.810368.1>) for the global warming results and <https://doi.org/10.26008/1912/bco-dmo.784634.1> for the glacial results).

AUTHORS

Katsumi Matsumoto (katsumi@umn.edu) is Professor, and **Tatsuro Tanioka** is Postdoctoral Researcher, both in the Department of Earth & Environmental Sciences, University of Minnesota, Minneapolis, MN, USA. **Rosalind Rickaby** is Professor, Department of Earth Sciences, University of Oxford, Oxford, UK.

ARTICLE CITATION

Matsumoto, K., T. Tanioka, and R. Rickaby. 2020. Linkages between dynamic phytoplankton C:N:P and the ocean carbon cycle under climate change. *Oceanography* 33(2):44–52, <https://doi.org/10.5670/oceanog.2020.203>.

COPYRIGHT & USAGE

This is an open access article made available under the terms of the Creative Commons Attribution 4.0 International License (<https://creativecommons.org/licenses/by/4.0/>), which permits use, sharing, adaptation, distribution, and reproduction in any medium or format as long as users cite the materials appropriately, provide a link to the Creative Commons license, and indicate the changes that were made to the original content.

SIDEBAR. Direct Measures of the Vigor of Ocean Circulation via Particle Grain Size

By Nick McCave

Physical oceanographers measure the intensity or vigor (transport or velocity) of ocean circulation via current meters, geostrophic calculations, satellite-tracked drifters, and modeling of tracer distributions. These techniques are complementary, and none are now used alone.

The vigor of paleocirculation is measured in similar ways, using flow speed from particle grain size, geostrophy from density fields reconstructed from oxygen isotopic data, surface-to-bottom water differences in ^{14}C ages, isotopic tracers with differing particle-related properties (e.g., $^{230}\text{Pa}/^{231}\text{Th}$), and incorporation of nutrient proxy and isotopic tracer fields into box and general circulation models. As with the approaches to measuring modern ocean circulation, these techniques for establishing paleocirculation parameters are not, or should not be, stand-alone, but too many studies currently rely on only one of them.

Starting in the 1970s, particle grain size was used to infer deep-sea flow speed. Using the principles of sediment dynamics, McCave et al. (1995) made this technique more rigorous (see also McCave and Hall, 2006). They proposed that, with particle cohesion becoming less important for sizes $>10\ \mu\text{m}$, material greater than $10\ \mu\text{m}$ would be sorted and deposited as individual particles, depending on their settling velocity and the flow speed at the site of deposition. The basis of the paleoflow inference is that selective particle deposition is controlled by flow speed, with higher speeds suppressing the deposition of finer sizes and slower speeds permitting it, leading to a coarser deposit from a faster flow. Fine material $<10\ \mu\text{m}$ has a strong tendency to form and be deposited as aggregates, whereas medium-to-coarse silt ($>10\ \mu\text{m}$) particles are deposited as individual grains rather than as aggregates. This point is important because sediment has to be disaggregated for analysis, meaning that the measured finer material ($<10\ \mu\text{m}$) size is not the aggregate size (or settling velocity) that was deposited. The distinction was thus made between “sortable silt,” defined as the $10\text{--}63\ \mu\text{m}$ size fraction, as opposed to $2\text{--}10\ \mu\text{m}$ cohesive silt whose inclusion would simply contaminate a record. Sand, coarser than $63\ \mu\text{m}$, is less common than silt and contains much material of biogenic origin. Most deep ocean currents rarely move sand of quartz density.

The parameter of size distributions used for the inference of flow speed is the “sortable silt mean size,” denoted by \overline{SS} , the geometric mean size of $10\text{--}63\ \mu\text{m}$ material. It is usual practice

to remove carbonate and opaline silica because the organisms that make their skeletons out of those materials do so at specific sizes. There are of course locations where we prefer not to do that because detrital carbonate grains are an important component of the sediment, for example, in Heinrich layers.¹ A further parameter of the size distribution is the percentage of sortable silt in the total fine fraction (total $<63\ \mu\text{m}$), $SS\%$. In well current-sorted sediments, the two parameters \overline{SS} and $SS\%$ are highly correlated ($r > 0.9$).

For analysis of particle size, the SediGraph, based on settling velocity, is still the best method, but laser sizers and the Coulter counter are also commonly used. The issue of how particle shape influences grain size determination in clay-rich samples determined from lasers compared with other methods remains a topic requiring further work.

The relationship of grain size to flow speed remained unknown for some time. For many years, the parameters \overline{SS} and $SS\%$ were simply plotted against age where they showed a close correspondence with climatic and hydrographic variables, particularly oxygen isotope ratios (Figure 1). Recently, accumulated data on the grain size of core top material collected adjacent to long-term, near-bottom current meters has been used to establish a calibration of sortable silt mean size (McCave et al., 2017). On several sediment drifts, the bottom sediments become finer down current along the transport path. In such cases, the \overline{SS} value downstream is finer than that for the same flow speed at the upstream end of the drift. This implies that absolute calibration of \overline{SS} to flow speed is not possible. However, the slopes of the relationships between \overline{SS} and flow speed are very similar for the several data sets assembled by McCave et al. (2017), allowing them to be normalized by their means and plotted to give a single line. This has a slope (sensitivity) of $\sim 1.36\ \text{cm s}^{-1}/\mu\text{m}$, permitting us to gauge changes in flow speed implied by shifts in a grain size record. If a record is from a location near a current meter, then the coretop \overline{SS} can be tied to an absolute flow speed.

Recent work in controlled flume experiments by Culp et al. (2020) demonstrated down-current fining and deposited grain size changes at points that are linearly related to flow speed. Their experiments yield sensitivities at locations $4.6\text{--}7.6\ \text{m}$ from the inlet of the $9.1\ \text{m}$ flume of $1.25\text{--}1.38\ \text{cm s}^{-1}/\mu\text{m}$, very similar to the field calibration.

Thick accumulations of sediment, called drifts, are formed along continental margins under deep western boundary

¹ A Heinrich layer is a layer of generally coarser-grained sediments recovered from deep-ocean cores. These sediments provide evidence of increases in iceberg discharges into the North Atlantic and are related to rapid climate events. Six Heinrich layers have been identified and span glacial periods over the last 640,000 years.

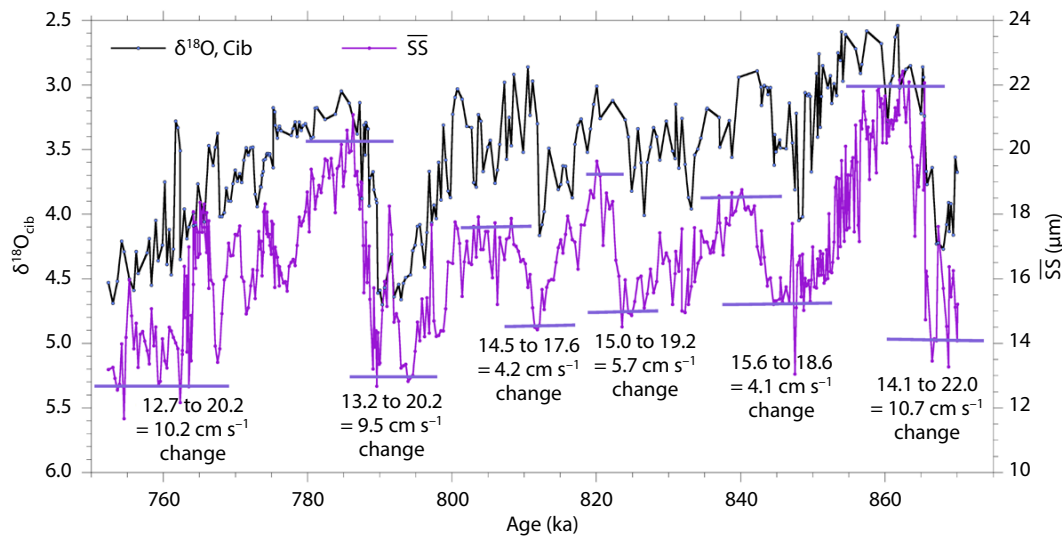


FIGURE 1. This sortable silt record from Gardar Drift south of Iceland under the Iceland-Scotland overflow (Kleiven et al., 2011) spans Marine Isotope Stages 22 to 18 and contains two major glacial-to-interglacial transitions with flow speed changes of $\sim 10 \text{ cm s}^{-1}$ and stadial (colder climate)-to-interstadial (warmer climate) shifts of $4\text{--}6 \text{ cm s}^{-1}$. (Marine isotope stages are alternating warm and cool periods in Earth history deduced from oxygen isotope ratios of fossil foraminifera shells recovered from deep-sea sediments.) Flow speeds closely track climatic (ice volume) changes indexed by bottom water oxygen isotopic values ($^{18}\text{O}/^{16}\text{O}$ ratio per mil relative to the VPDB standard [$\delta^{18}\text{O}$] of the benthic foraminifera *Cibicides wuellerstorfi*). Modern speeds in the region are $\sim 15 \text{ cm s}^{-1}$, so Iceland-Scotland overflow in glacial periods possibly slowed to $\sim 5 \text{ cm s}^{-1}$ but did not cease. SS = sortable silt mean size.

currents (DWBC) in both hemispheres. Away from major sediment sources, typical terrigenous sedimentation rates are of order 2 cm ka^{-1} . These rates increase by at least an order of magnitude in drifts due to the advection of fine sediment from upstream sources, generally the results of downslope movements in slumps and turbidity currents. For flow speeds up to $12\text{--}15 \text{ cm s}^{-1}$, it is thought that accumulation rates increase, but above that range, unsteady peak speeds start to remove material, resulting in reduced accumulation rates. And above mean speeds of $20\text{--}25 \text{ cm s}^{-1}$, strong winnowing sets in and yields a sandy lag, commonly of foraminifera (Figure 2). Because of the high resolution obtainable and their key locations with regard to deep-sea circulation, drifts have been prime targets for acquisition of sedimentary records of paleo-oceanographic importance. DWBCs form a key component of the climatically driven global overturning circulation. Figure 1 shows an example record from Gardar Drift south of Iceland, with calibrated speed changes.

Many such records have now been generated in the North and South Atlantic, Indian, and Southwest Pacific Oceans (McCave and Hall, 2006), but little work has been done in the North Pacific because it lacks sediment drifts. Deep water flows have been the main targets of this work, but major shallow water flows are of considerable climatic interest and require attention—to name a few, these include the Gulf Stream, Kuroshio Current, Antarctic Circumpolar Current (ACC), and East Greenland Current (EGC). The ACC has been targeted because it extends to the seabed and has yielded

small drifts in the Scotia Sea and the Drake Passage (McCave et al., 2014). Work is needed to find suitable sediment targets for monitoring the other major upper ocean western boundary currents. Arctic shelves are deep because of glaciation, and deposits on them have provided material to assess the vigor of the EGC system, but obviously not during glacial periods (McCave and Andrews, 2019).

Grain size proxies for flow speed have an advantage in that they are dominated by local conditions, but a disadvantage in that they do not give an integrated picture of the flux. Thornalley et al. (2013) demonstrated that understanding flux requires acquiring an array of cores across the flow path. Their data show a 20% decrease in the Iceland-Scotland overflow in the past 10,000 years. Further work to collect arrays of cores, known as “dipstick coring,” down slopes where boundary currents are present is required. Upper ocean flows need to be targeted, remembering that the closer they are to the shelf edge, the greater the likelihood that storm and fluctuating sea levels influence the sedimentary record. The grain size proxy is not mediated by biology, and it primarily records depositional flow intensity. It should not be deployed alone but accompanied by hydrographic tracers (e.g., benthic $\delta^{18}\text{O}$, $\delta^{13}\text{C}$, ϵNd). In well-chosen locations such as DWBCs, the grain size proxy is representative of climatically driven major deep ocean flows. As long as the sediments can be disaggregated for size analysis, applications have a time span well beyond short half-life nuclides, already to the Oligocene and potentially back to the Mesozoic.

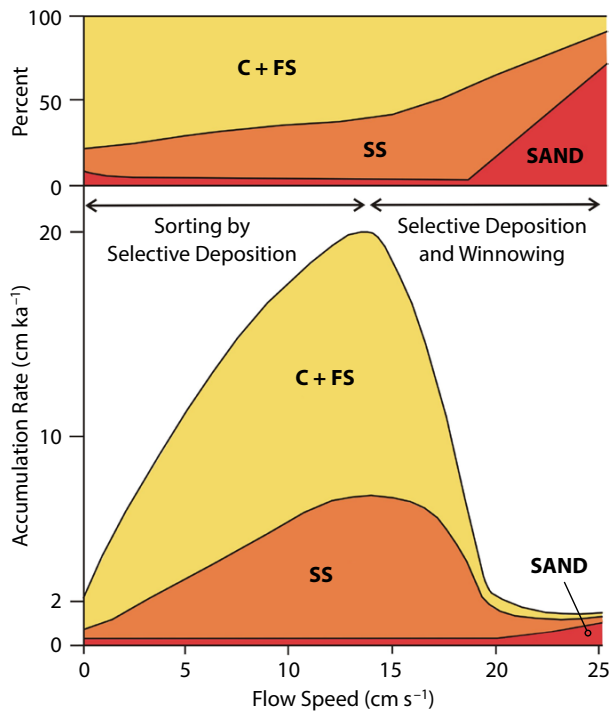


FIGURE 2. Hypothetical variation of accumulation rate and percentage composition of a sediment deposit with increasing current speed advecting sediment to a deposition site. C + FS = clay and fine silt ($<10\ \mu\text{m}$) and SS = sortable silt ($10\text{--}63\ \mu\text{m}$) (McCave and Hall, 2006). The “sand” here is a size term that refers to both terrigenous and carbonate—mainly foraminifera—components. At zero speed, a pelagic rate of $2\ \text{cm ka}^{-1}$ is assumed. From zero to the peak accumulation rate, the sorting process is all selective deposition. Above that point, arbitrarily put at a flow speed of $13\ \text{cm s}^{-1}$, it is a combination of selective deposition and removal of material with a grain size $<63\ \mu\text{m}$. Erosional winnowing and some sand movement is assumed to occur above a flow speed of $20\ \text{cm s}^{-1}$. The curve is shown as peaking between $10\ \text{cm s}^{-1}$ and $15\ \text{cm s}^{-1}$, but this is not at all certain and may well depend on the magnitude-frequency structure of deposition and erosion events. A peak around $10\ \text{cm s}^{-1}$ would be entirely feasible, as some velocity with turbidity records suggest the onset of surface erosion above $10\text{--}12\ \text{cm s}^{-1}$.

No determination of ocean circulation strength, past or present, should rely on a single method. The “sortable silt mean size,” the mean size of $10\text{--}63\ \mu\text{m}$ terrigenous material, is a proxy for local bottom flow speed analogous to the modern current meter. The fact that sediments become finer down current implies that a universal absolute calibration of SS to flow speed is not possible. However, several grain size and near-bottom flow speed data sets normalized by their means yield a slope (sensitivity) of $\sim 1.36\ \text{cm s}^{-1}/\mu\text{m}$, permitting us to estimate changes in flow speed implied by shifts in a grain size record. Biology (fossil content) does not influence the proxy, and it provides a key complement to paleohydrographic tracers of water mass extent. To assess volume transports, arrays of cores across key flow paths are necessary. There is still much to do.

REFERENCES

- Culp, J., K. Strom, A. Parent, and B.W. Romans. 2020. Sorting of fine-grained sediment by currents: Testing the sortable silt hypothesis with laboratory experiments. *EarthArXiv Preprints*, <https://doi.org/10.31223/osf.io/xec2t>, submitted to *Sedimentology*.
- Kleiven, H.F., I.R. Hall, I.N. McCave, G. Knorr, and E. Jansen. 2011. Coupled deep-water flow and climate variability in the middle Pleistocene North Atlantic. *Geology* 39:343–346, <https://doi.org/10.1130/G31651.1>.
- McCave, I.N., B. Manighetti, and S.G. Robinson. 1995. Sortable silt and fine sediment size/composition slicing: Parameters for palaeocurrent speed and palaeoceanography. *Paleoceanography* 10:593–610, <https://doi.org/10.1029/94PA03039>.
- McCave, I.N., and I.R. Hall. 2006. Size sorting in marine muds: Processes, pitfalls and prospects for palaeoflow-speed proxies. *Geochemistry, Geophysics, Geosystems* 7(10), <https://doi.org/10.1029/2006GC001284>.
- McCave, I.N., S.C. Crowhurst, G. Kuhn, C.-D. Hillenbrand, and M.P. Meredith. 2014. Minimal change in Antarctic Circumpolar Current flow speed between the last glacial and Holocene. *Nature Geoscience* 7:113–116, <https://doi.org/10.1038/ngeo2037>.
- McCave, I.N., D.J.R. Thornalley, and I.R. Hall. 2017. Relation of sortable silt grain size to deep-sea current speeds: Calibration of the ‘Mud Current Meter’. *Deep Sea Research Part I* 127:1–12, <http://doi.org/10.1016/j.dsr.2017.07.003>.
- McCave, I.N., and J.T. Andrews. 2019. Distinguishing current effects in sediments delivered to the ocean by ice: Part II. Glacial to Holocene changes in high latitude North Atlantic upper ocean flows. *Quaternary Science Reviews* 223, 105902, <https://doi.org/10.1016/j.quascirev.2019.105902>.
- Thornalley, D.J.R., M. Blaschek, F.J. Davies, S. Praetorius, D.W. Oppo, J.F. McManus, I.R. Hall, H. Kleiven, H. Renssen, and I.N. McCave. 2013. Long-term variations in Iceland-Scotland overflow strength during the Holocene. *Climate of the Past* 9:2,073–2,084, <https://doi.org/10.5194/cp-9-2073-2013>.

AUTHOR

Nick McCave (mccave@esc.cam.ac.uk) is Professor Emeritus, Godwin Laboratory for Palaeoclimate Research, University of Cambridge, UK.

Regional Character of the “Global Monsoon”

PALEOCLIMATE INSIGHTS FROM NORTHWEST INDIAN LACUSTRINE SEDIMENTS

By Yama Dixit

ABSTRACT. The concept of a “global monsoon” proposes that the annual insolation cycle and global-scale atmospheric circulation drive and synchronize regional monsoons. However, model, proxy, and observational studies reveal differences in the regional variability of the summer monsoon and its direct response to solar forcing and glacial boundary conditions. Here, we focus on paleoenvironmental data derived from paleolake sediments in northwest India. These paleolakes straddle a precipitation gradient from sub-humid to semi-arid to arid plains and contain a wealth of information about summer monsoon variability at regional scale over the past 10,000 years. The paleolake records provide compelling evidence of significant regional differences in the timing of monsoon responses to orbital forcings; only sub-humid to semi-arid lakes resemble monsoon reconstructions from marine sediment and speleothem archives, while the arid region lakes contain regional hydroclimate histories. Extracting regional trends from the global signature of monsoon variability is necessary for understanding the regional impact of future climate warming on the monsoon system and human populations. The paleolakes in northwest India highlight the importance of considering the specific location of archive and signal heterogeneity when interpreting monsoon records. Results indicate that detailed records are required from other monsoon regions to improve knowledge of the imprints of the complex monsoon system at regional scales.

INTRODUCTION

With rising global atmospheric greenhouse gas concentrations due to anthropogenic activities, society is increasingly interested in understanding climate variations and their potential effects—past, present, and future—on human civilizations. One of the most significant impacts of climate change is predicted to be on the global hydrological cycle (IPCC, 2014). The Indian summer monsoon (ISM) plays a critical role in the global hydrological cycle by regulating mass and energy exchanges between the atmosphere over the mid-latitudes and the tropics (Gupta et al., 2003). The Indian subcontinent has long depended upon ISM rainfall for the

agricultural activities that are critically important to the Indian economy (Gadgil and Kumar, 2006). India’s burgeoning population depends on agriculture both directly, by using agricultural products, and indirectly, by employment, rural livelihoods, and supplies to other economic sectors that use agricultural products (such as textile and food industries). Therefore, variations in the intensity of the ISM are likely to have widespread socioeconomic impacts in the modern Indian subcontinent. Recent monsoon-related catastrophic events (e.g., Sinha, 2008; Pal and Al-Tabbaa, 2009; Mishra and Nagaraju, 2019) underscore the importance of examining the variabil-

ity of the ISM at various timescales and developing reliable predictions in order to mitigate the catastrophic consequences of monsoon rainfall anomalies.

The ISM is a part of the “global monsoon” that constitutes the coherent responses of all monsoon systems to changes in global-scale atmospheric circulation patterns forced primarily by the annual solar cycle and by land-air-sea interactions (B. Wang and Ding, 2008). This unified global monsoon concept suggests that a single tropical and subtropical atmospheric system influences the Indian subcontinent and Central and East Asia in a similar manner (P.X. Wang et al., 2017). Global monsoon dynamics are shaped by large-scale meridional temperature gradients and the position of the Intertropical Convergence Zone (ITCZ), which is seasonally displaced by cross-equatorial pressure gradients (Donohoe et al., 2013; [Figure 1](#)). A similar mechanism is believed to result in summer rainfall in North Africa and Central and East Asia between June and September. These regional components of the global monsoon system are thought to be closely linked through forcing and feedback processes, suggesting that a change in any component may cause a chain reaction that affects the entire system homogeneously (Kim et al., 2008; P.X. Wang et al., 2017). Consequently, a global perspective is proposed to be more useful for evaluating future variability in monsoon systems (Kim et al., 2008; P.X. Wang et al., 2017).

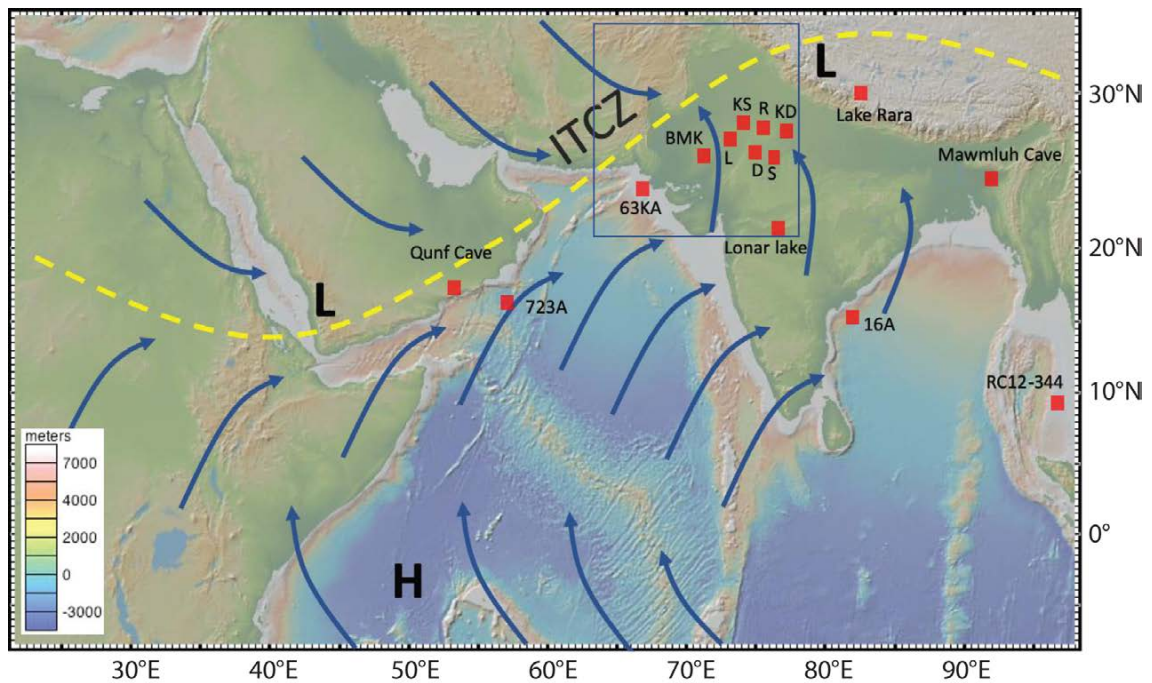


FIGURE 1. Physiographic map of the Indian subcontinent and adjacent ocean regions with a schematic of surface wind patterns. Blue arrows indicate the general directions of the Arabian Sea and Bay of Bengal branches of the Indian summer monsoon. The yellow dashed line denotes the position of the Intertropical Convergence Zone (ITCZ) during Northern Hemisphere summertime, with lower atmospheric pressure on land (L) and higher pressure over the ocean (H). The annual reversal of surface winds caused by the north-south migration of the ITCZ is thought to create a “global monsoon” across the Indian, Asian, tropical African, and Australian landmasses. The map also locates the prominent marine speleothem and lake proxy records discussed in this study. The blue square highlights the northwest Indian lakes. In the sub-humid region, KD = Kotla Dahar (Dixit et al., 2014a). In the semi-arid region, R = Paleolake Riwasa (Dixit et al., 2014b, 2015) and S = Sambhar Lake (Sinha et al., 2006). In the Thar Desert, KS = Karsandi (Dixit et al., 2018), D = Didwana (Singh et al., 1990), L = Lunkaransar (Enzel et al., 1999), and BMK = Bap Malar and Kanod playa (Deotare et al., 2004).

In the last several decades, studies of the longer-term variability in the ISM using natural climate archives, including lake and ocean sediments and speleothems (e.g., Y.J. Wang et al., 2001; Fleitmann et al., 2003; Gupta et al., 2003; Staubwasser et al., 2003; Berkelhammer et al., 2012; Dixit et al., 2014b; Cai et al., 2015; Kathayat et al., 2016, and references therein), together with simulations of past monsoon variability, have revealed that the global monsoon system has a substantial regional character and cannot solely be characterized by the common, global dynamics of monsoon systems at different timescales. Instrumental and paleoclimate data have shown that the interplay of various regional forcings cause the monsoon variability observed at different timescales. Therefore, the concept of a global monsoon has been a topic of recent debate, with an increasing number of regional paleoclimate records revealing

a divergent monsoon history (Caley et al., 2011; Seneviratne and Hauser, 2020). Thus, there is a great need for more studies aimed at investigating regional monsoon variability and the mechanisms that force regional response patterns.

Despite dedicated efforts, a comprehensive picture of monsoon variability has proved elusive, largely due to the absence of long-term, high-resolution regional paleoenvironmental records, the spatial heterogeneity of monsoon precipitation, and the monsoon’s complex forcing mechanisms. Larger regional differences are anticipated in the coming decades, with some regions receiving more rain, despite a projected weakening of monsoon rainfall (IPCC, 2013) and vice versa. ISM rainfall projection remains a key challenge for regional circulation models (Asharaf and Ahrens, 2015). Modern instrumental records (collected since 1871, when the first regional

meteorological station was established) are too short to document the full range of past ISM variability and spatial heterogeneity. Therefore, regional paleoclimate studies of monsoon evolution are essential for improved understanding of how natural and anthropogenic forcing impact the monsoon at local scales.

This paper highlights the regional versus the global signal of monsoon dynamics during the Holocene (the last 10,000 years) using inferences derived from lacustrine sedimentary sequences collected from the northwest Indian plains. Composite data from these lake records fill a knowledge gap and resolve a long-standing debate about whether these lakes record local or global signals of monsoon variability. Because northwest India was one of the most variable regions in terms of environmental conditions and cultural evolution during the Holocene, monsoon variability during this period

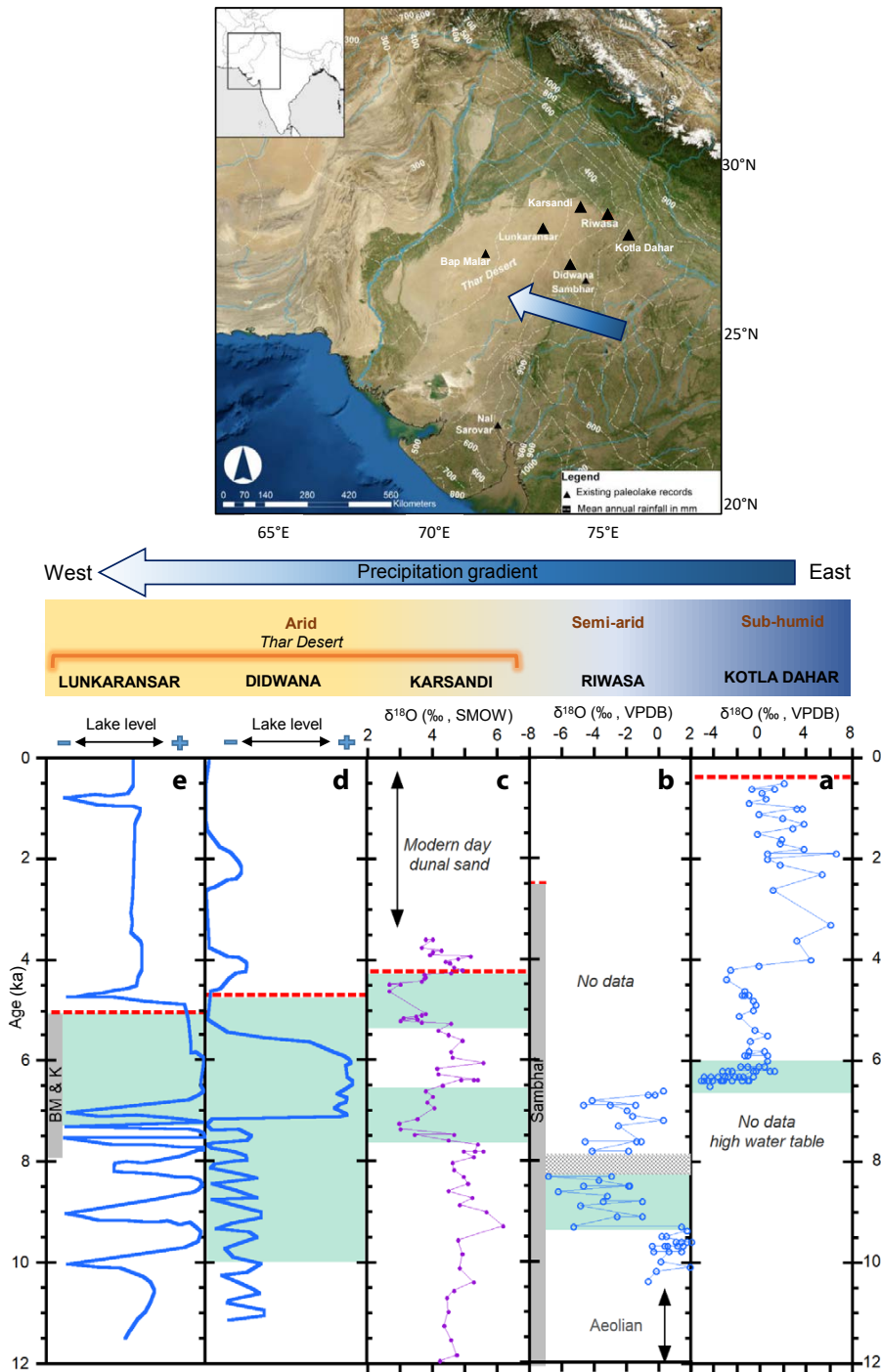


FIGURE 2. Holocene climate reconstructions from lakes in northwest India. Lakes with reasonably robust chronology (that is, each major lithological, sedimentological, and geochemical transition has been age-constrained) were used to infer regional climate history. The lakes and proxies used from east to west (right to left) are: (a) Sub-humid region: Kotla Dahar, with $\delta^{18}\text{O}_{\text{gastropod}}$ reflecting regional evaporation/precipitation (E/P) changes (Dixit et al., 2014a). (b) Semi-arid region: Riwasa, with $\delta^{18}\text{O}_{\text{gastropod}}$ reflecting regional E/P changes (Dixit et al., 2014b). (c) Arid region (Thar Desert): Paleolake Karsandi, with $\delta^{18}\text{O}$ of gypsum hydration water reflecting lake water $\delta^{18}\text{O}$ and regional E/P changes (Dixit et al., 2018). Lake levels are from Prasad and Enzel (2006). (d) Didwana (Singh et al., 1990). (e) Lunkaransar (Enzel et al., 1999). Vertical gray bars in (b) and (e) denote periods with permanent lake levels where age definition is poor: Sambhar Lake (Sinha et al., 2006) and Bap Malar and Kanod playa (BM&K) (Deotare et al., 2004). Green shaded bars denote the wettest periods during the Holocene inferred from geochemical proxies, although these wet periods were interrupted by intervals of aridity. Red dashed lines mark the disappearances of permanent lakes—the sequence of drying follows the east-west path of the Bay of Bengal branch of the modern monsoon: the lakes that lie farthest west dried first, and the easternmost dried last.

has been linked to the evolution of the ancient Bronze Age Indus Civilization (Dixit et al., 2014a; Petrie et al., 2017). The objective here is to critically examine the fidelity of regional terrestrial paleoenvironmental archives as recorders of ISM variability and to compare them with prominent monsoon records from marine and terrestrial archives.

The northwest Indian plains receive over 80% of their rainfall from the Bay of Bengal arm of the strong southwesterly summer monsoon between June and September (Bhattacharya et al., 2003; Sengupta and Sarkar, 2006). The resulting east-west precipitation gradient (Figure 2) lends a distinct character to the region, such that the sedimentology and geochemistry of paleolake archives change every few hundred kilometers. We focus on an east-to-west transect of lake sediment records that record a progressive decrease in monsoon precipitation: Kotla Dahar in the sub-humid region (Dixit et al., 2014a); Riwasa and Sambhar Lake in the semi-arid region (Dixit et al., 2014b, and Sinha et al., 2006, respectively); and in the western arid region, within the Indian state of Rajasthan, the Thar Desert lakes, including Karsandi (Dixit et al., 2018), Didwana (Singh et al., 1990), Lunkaransar (Enzel et al., 1999), and Bap Malar and Kanod playa (Deotare et al., 2004). We appreciate and emphasize that further high-resolution regional terrestrial records are required to develop a complete understanding of monsoon imprints at regional scale.

GLOBAL VERSUS REGIONAL MONSOON VARIABILITY DURING THE HOLOCENE

Because northwest India receives most of its annual rainfall during the summer months via the ISM, regional lake archives should provide relatively independent summer monsoon histories that are similar to those of the global monsoon. When examining lacustrine records, robust chronological control is critical to avoid the possibility of confusing regional vs global monsoon differences. In general,

proxy reconstructions with at least one radiocarbon (^{14}C) age associated with every distinct geochemical and lithological change permits adequate dating. Using this criterion, five well-dated lake records were selected, three from the westernmost Thar Desert region and one each from the semi-arid and sub-humid regions (Figure 2 and Table 1).

Although abundant gastropod and ostracod carbonate shells generally characterize lacustrine sediments, lakes in arid environments often lack well-preserved carbonate tests for ^{14}C dating and isotopic analyses. This is true for most of the Thar Desert lake records. However, lakes in the east (Riwasa and Kotla Dahar) provide robust chronology based on ^{14}C dating of abundant gastropod shells preserved in the lake sediments. In addition, a recent study shows that water isotopes of evaporative salts, such as gypsum, which are often plentiful in arid environment lacustrine sediments, can be used as a novel proxy for lake water conditions (Hodell et al., 2012).

Pioneering work on regional hydroclimate reconstructions for the northwest Indian lakes was carried out using pollen assemblages to determine the relative abundance of C_3 plants (suggesting higher rainfall) versus C_4 plants

(suggesting lower rainfall; Singh et al., 1972). The desert lakes were later revisited, and improved hydroclimate records with robust chronologies were obtained using sedimentological and mineralogical analyses of Lake Didwana sediments (Wasson et al., 1984) and sedimentological and organic matter $\delta^{13}\text{C}$ analyses of Lake Lunkaransar sediments (Enzel et al., 1999). In general, these lakes were formed in several basins as a result of relatively wet conditions that occurred during the early to mid Holocene (Saini et al., 2005; Prasad and Enzel, 2006; Dixit et al., 2018). Paleolakes Lunkaransar, Didwana, and Karsandi in the arid region, and Riwasa and Sambhar in the semi-arid region, all appeared when the monsoon intensified following the precessionally controlled boreal summer insolation (Figure 2). This coherent response of northwest Indian lakes to an intensified summer monsoon after the last glacial period was followed by diverging intensities in monsoon history; the early Holocene ISM maxima, observed as very low $\delta^{18}\text{O}$ values in gastropod shells in paleolakes Kotla Dahar and Riwasa in the east, does not coincide with maximum lake levels in Thar Desert lake records. A very high evaporation/precipitation (E/P) ratio in the Thar Desert and the lack of a large

drainage basin generally led to lower lake levels and formation of ephemeral lakes at Lunkaransar and Didwana during the early Holocene (Prasad and Enzel, 2006). In contrast, eastern lakes were either located in regions with lower E/P or were part of a large lake system whose maximum lake levels occurred during the early Holocene monsoon intensification. The mid-Holocene (~7.0–5.0 ka) was wetter than the early Holocene in the Thar Desert lakes region (Figure 2c–e), because of relatively lower E/P in response to decreasing summer insolation, which in turn led to a net increase in effective moisture (i.e., P–E; Wasson et al., 1984; Prasad and Enzel, 2006; Dixit et al., 2018). An additional source of moisture from the northeast during wintertime is also suggested, and this would have helped to maintain high Thar Desert lake levels during the mid-Holocene (Enzel et al., 1999). The eastern lakes (Kotla Dahar and Riwasa), on the other hand, responded to the progressive decline in general monsoon rainfall following the decreasing summer insolation during the mid-Holocene (Dixit et al., 2014a,b).

Apart from the diachronous response of northwest Indian lakes to general monsoon variability, there are also distinct differences in the way these lake

TABLE 1. Details of records derived from northwest Indian lakes in east-west order. Note that the chronologies of Lakes Sambhar and Bap Malar are poorly defined during the Holocene.

LACUSTRINE ARCHIVES	BAP MALAR	LUNKARANSAR	DIDWANA	KARSANDI	SAMBHAR	RIWASA	KOTLA DAHAR
References	Deotare et al., 2004	Singh et al., 1990; Enzel et al., 1999	Singh et al., 1990; Wasson et al., 1984	Dixit et al., 2018	Sinha et al., 2006	Dixit et al., 2014b	Dixit et al., 2014a
Proxy Used	Palynology and mineralogy	Sediment geochemistry ($\delta^{13}\text{C}$) and palynology	Sedimentology, mineralogy, and palynology	$\delta^{18}\text{O}$ of gypsum hydration water	Sediment geochemistry, mineralogy, $\delta^{18}\text{O}$ of bulk carbonate	$\delta^{18}\text{O}$ of gastropod shells	$\delta^{18}\text{O}$ of gastropod shells
Proxy Indicates	Vegetation changes	Vegetation changes and rainfall variability	Vegetation changes and rainfall variability	Lake water $\delta^{18}\text{O}$ and temperature; (E/P changes)	Rainfall variability	Lake water $\delta^{18}\text{O}$ and temperature; (E/P changes)	Lake water $\delta^{18}\text{O}$ and temperature; (E/P changes)
Record Span	~15 ka–present	~11 ka–present	~13 ka–present	~11 ka–present	~22 ka–present	~11 ka–6 ka	~7 ka–present
# ^{14}C dates	6	12	7	8 + 2 OSL	5	6	8

OSL = Optically stimulated luminescence dating; E/P = Evaporation/precipitation

records exhibit the manifestations of the most prominent abrupt monsoon weakening events of 8.2 ka and 4.2 ka (Dixit et al., 2014a,b). Paleolake Riwasa dried abruptly when lake levels declined and marl sediments were aeri ally exposed to form hardground at ~8.2 ka (Figure 2b; Dixit et al., 2014b). Interestingly, none of the other northwest Indian lake records provide any signs of drying during this period. There is no evidence of complete desiccation throughout the history of Sambhar playa (Sinha et al., 2006), and the Thar Desert lakes—Bap Malar, Kanod playa, Lunkaransar, Didwana, and Karsandi—were ephemeral fluctuating lakes during this period (Figure 2), devoid of massive biogenic carbonates and underlying deep lake marl sediments (a prerequisite for forming hardground). In contrast, Lake Riwasa was in its freshest and deepest phase before the ISM weakened abruptly after ~8.3 ka, causing repeated inundation and aerial exposure of the lake bottom sediments, which formed hardground (Dixit et al., 2014b). Similarly, at Kotla Dahar, a ~4‰ increase in $\delta^{18}\text{O}_{\text{gastropod}}$ occurred at ~4.1 ka, marking an E/P peak in the lake catchment related to the global 4.2 ka abrupt monsoon weakening (Dixit et al., 2014a) that is absent in all the other northwest Indian lake records (Figure 2a). The $\delta^{18}\text{O}$ of gypsum hydration water also indicates drying of Lake Karsandi sometime between 4.4 ka and 3.2 ka (Dixit et al., 2018). However, there is no evidence of abrupt drying, indicating that the lake had already dried out by 4.4 ka due to decreasing summer rainfall (Giesche et al., 2019). Overall, while the drying and permanent decline of lake levels in northwest India mirrors the east-west modern precipitation gradient (Figure 2), significant Holocene monsoon variability is recorded in these lakes, suggesting nonlinear response to monsoon variability and highlighting the importance of local processes and regional monsoon variations. Thus, regional preservation of a global monsoon signal should be treated carefully.

HOLOCENE MONSOON HISTORY FROM TERRESTRIAL AND MARINE ARCHIVES

A comparative assessment of monsoon variability recorded in northwest Indian lakes clearly indicates that the Thar Desert lakes represent more local climate history than global monsoon variability; semi-arid paleolake Riwasa and sub-humid paleolake Kotla Dahar together provide a coherent picture of ISM variability in northwest India. Because none of the northwest Indian lake records offer a continuous Holocene monsoon history, we use records from Riwasa and Kotla Dahar lakes, which have complementary $\delta^{18}\text{O}$ records obtained from the shell carbonates of the gastropod *Melanoides tuberculata*. Together, the Riwasa-Kotla Dahar composite record and the marine and speleothem monsoon records provide a holistic picture of Holocene ISM variability. The intensified monsoon that followed increased boreal summer insolation after the last glacial period is clearly documented in northwest Indian lake records (Figure 3a) as well as in records from the Arabian Sea and the Bay of Bengal branch of the ISM system. For example, early Holocene monsoon intensification (Figure 3) is supported by speleothems from Bitto Cave (North India; Kathayat et al., 2016), Dongge Cave (China; Y.J. Wang et al., 2005; Figure 3b), and Qunf Cave (Oman; Fleitmann et al., 2003; Figure 3c) and by planktonic foraminifera $\delta^{18}\text{O}$ records from Arabian Sea marine sediment core 63KA (Staubwasser et al., 2003; Figure 3d) and Ocean Drilling Program (ODP) Hole 723A (Gupta et al., 2003; Figure 3e). Evidence for increased summer monsoon precipitation in the Bay of Bengal during the early Holocene is found in sediments from Lonar Lake in central India (Prasad et al., 2014) and in marine sediments (Govil and Naidu, 2011; Rashid et al., 2011; Ponton et al., 2012; Figure 3f,g).

Geochemical records from marine sediments and speleothems reveal gradually decreasing ISM strength in the Holocene following Northern Hemisphere sum-

mer insolation (Figure 3a), in line with the Riwasa-Kotla Dahar composite record (Figure 3). This gradually declining monsoon intensity was punctuated by millennial-scale abrupt changes in the composite Riwasa-Kotla Dahar records at ~4.0–4.2 ka, 5.9–6.0 ka, 8.2 ka, 9.4 ka, 10.4 ka, and 11 ka that are also documented in independently dated speleothem records from southern China (Y.J. Wang et al., 2005) and Oman (Fleitmann et al., 2003), and also in marine records from the Arabian Sea (Gupta et al., 2003; Figure 3). The coincident timing of abrupt monsoon variability and North Atlantic cold events (i.e., Bond events) against a backdrop of gradual insolation forcing through the Holocene suggests an atmospheric teleconnection (Gupta et al., 2003). The most prominent cooling event at 8.2 ka in the North Atlantic during the Holocene is consistent with an abrupt monsoon weakening episode recorded in Lake Riwasa and in a stalagmite from southern Oman (Fleitmann et al., 2003; Gupta et al., 2003), in speleothems in China (Y.J. Wang et al., 2005; Cheng et al., 2009) and on the Tibetan Plateau (Cai et al., 2015), and in Arabian Sea sediments (Gupta et al., 2003; Staubwasser et al., 2003; Figure 3).

The 4.2 ka climate event in lake Kotla Dahar (Dixit et al., 2014a) has also been observed in several other terrestrial records on the Indian subcontinent, including the Mawmluh Cave speleothems (Meghalaya) in northeastern India (Berkelhammer et al., 2012; Kathayat et al., 2018). In fact, the most recent of the three subdivisions of the Holocene epoch (beginning at ~4.2 ka) is named Meghalayan Age, a reference to the northeastern Indian state of Meghalaya, where Mawmluh Cave is located (Walker et al., 2019). A less abrupt, yet still arid, period that highlights significant regional variability is also documented in a peat profile from north central India (Phadtare, 2000), at Lonar Lake (~4.6–3.9 ka; Menzel et al., 2013), and in western Nepal at Rara Lake (~4.2–3.7 ka; Nakamura et al.,

2016). Recently, $\delta^{18}\text{O}$ measured on a variety of foraminifera species from a sediment core collected off Pakistan revealed a reduction in both summer and winter monsoon rainfall at ~ 4.1 ka over the general northwest Indian subcontinent (Giesche et al., 2019).

Current understanding of the forcing responsible for the 4.2 ka event highlights a prominent role of tropical Pacific Ocean dynamics, such as El Niño-Southern Oscillation (ENSO) and the Indian Ocean Dipole (IOD; Berkelhammer et al., 2012). The timing of ISM weakening at 4.2 ka coincides, within chronological error, with proxy records from the Pacific Ocean, suggesting increased frequency and intensity of ENSO events (Toth et al., 2012), modulated by the IOD. Increased ENSO activity and the negative phase of the IOD act to suppress summer monsoon circulation via increased subsidence of the Indian subcontinent (Ashok et al., 2004; Berkelhammer et al., 2012; Ishizaki et al., 2012; C. Wang, 2019).

CLIMATE-CULTURAL EVOLUTION IN NORTHWEST INDIA

During the middle Holocene (~ 5.2 – 2.3 ka), northwest India was occupied by the largest Bronze Age civilization, the Indus Civilization (Wright, 2010; Figure 4). There has been a longstanding debate on what led to the collapse of the urban phase of the Indus Civilization. Primarily based on agriculture, its cultural evolution was likely linked with monsoon variability, with the transformation from early (~ 5.2 – 4.5 ka) to urban (4.5–3.9 ka) phase coinciding with a period of high summer and winter rainfall in the region (Dixit et al., 2018; Giesche et al., 2019). Similar to its trading partners in Mesopotamia and Egypt, the collapse of the urban phase of the Indus civilization was likely triggered by an abrupt drying event at ~ 4.2 ka (Possehl, 2003; Staubwasser et al., 2003; Dixit et al., 2014a; Weiss, 2016). A rapid increase in $\delta^{18}\text{O}$ values of gastropod shell carbonate in Lake Kotla Dahar sediments indicates an abrupt monsoon weakening, and corroborates marine sediment and speleothem studies (Gupta et al., 2003; Staubwasser et al., 2003; Berkelhammer et al., 2012; Giosan et al., 2012; Ponton et al., 2012; Kathayat et al., 2016, 2018; Figure 3). Recent paleoclimate data suggests that Indus urbanism was flourishing around 4.2 ka, but

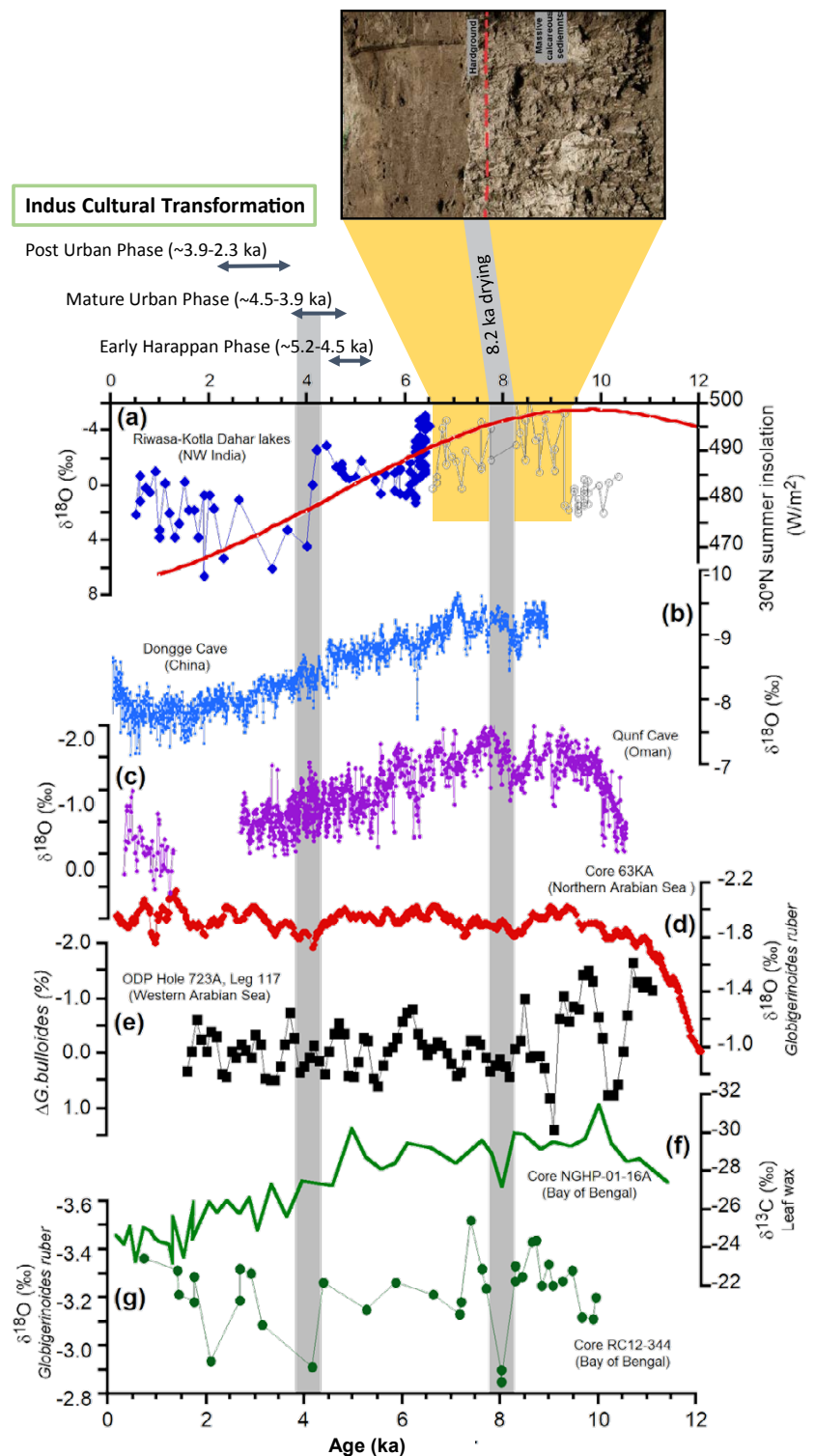


FIGURE 3. Comparison of Holocene summer monsoon history recorded in northwest Indian lakes with prominent distant marine and speleothem records. (a) $\delta^{18}\text{O}_{\text{gastropod}}$ from Rivasa and Kotla Dahar lakes combined reflecting E/P changes in the region and summer insolation at 30°N in red (Berger, 1978). (b) and (c) Speleothem records from Dongge cave (China; Y.J. Wang et al., 2005) and Qunf cave (Oman; Fleitmann et al., 2003) with $\delta^{18}\text{O}$ indicating rainfall changes. (d) and (e) Marine records influenced by the Arabian Sea branch of the ISM: (d) foraminifera $\delta^{18}\text{O}$ from the northern Arabian Sea indicating rainfall changes (Staubwasser et al., 2003). (e) *G. bulloides* abundance (%) indicating upwelling caused by monsoon surface winds (Gupta et al., 2003). (f) and (g) Marine records influenced by the Bay of Bengal branch of the ISM: (f) $\delta^{13}\text{C}$ of leaf wax indicating relative abundance of C_3 (high rainfall) compared to C_4 (lower rainfall) plants (Ponton et al., 2012). (g) Foraminifera $\delta^{18}\text{O}$ indicating rainfall changes (Rashid et al., 2011). Gray bars denote abrupt drying at ~ 8.2 ka (observed as desiccation and formation of a hardground, seen at the top) and at ~ 4.2 ka (coinciding with the end of the mature urban phase of the Indus Civilization). Indus cultural transformations during mid to late Holocene are also shown at top.

that de-urbanization soon followed, with new settlements preferentially located in eastern regions (Giosan et al., 2012; Petrie et al., 2017; Dixit et al., 2018; **Figure 4**). The hydroclimatic stress following the 4.2 ka drying probably led to a decrease in agricultural surpluses that supported the Indus populations, which in turn contributed to diminished social complexity and gradual abandonment of Indus cities (Weber, 2003; Madella and Fuller, 2006; Petrie and Bates, 2017; Pokharia et al., 2017). Archaeobotanical analyses revealed the 4.2 ka drought caused a shift in subsistence practices towards more drought-tolerant, rain-fed crops

and increased reliance on two cropping seasons, Rabi (winter)-Kharif (summer) (Madella and Fuller et al., 2006; Petrie and Bates, 2017). An eastward migration of populations following the 4.2 ka drought and a drastic increase in settlements in the eastern regions, which experienced more reliable and direct summer monsoon rains, is suggested to have ultimately contributed to reduced populations and collapse of the urban Indus region (**Figure 4**; Giosan et al., 2012; Petrie et al., 2017; Dixit et al., 2018). Although the hydroclimatic stress associated with the 4.2 ka event would have been instrumental in shaping Indus cul-

tural transformation, it seems inappropriate to simply attribute the collapse of an entire civilization directly to a single climatic event. As the Indus civilization spanned a wide range of ecological and environmentally diverse regions, more regional studies documenting the local climate history are required to understand the complex human-climate correlation in the Bronze Age era.

RATIONALE FOR EXAMINING REGIONAL VS GLOBAL MONSOON VARIABILITY

The lacustrine records presented here illustrate the variable nature of monsoon signals recorded across northwest India. However, the northwest Indian lake records do not fully document the hydroclimate of the entire Indian subcontinent because of the heterogeneity of monsoon expressions at regional and local scales. Considering the fact that terrestrial records exhibit local climatic conditions more effectively than marine sediment records, it is remarkable that records from the eastern lakes (Riwasa-Kotla Dahar) and marine sediments collectively reflect the global monsoon signal. Both indicate gradual monsoon weakening following boreal summer insolation during the Holocene and abrupt drying at ~8.2 and 4.2 ka. While the work described here focuses on Holocene monsoon variability, marine sediments recovered from International Ocean Discovery Program (IODP) Expedition 353 in the Bay of Bengal will enable further exploration of the coupling of basin-scale monsoon winds and continental precipitation (Clemens et al., 2015).

The divergent climate history of the Thar Desert and the eastern plains of northwest India demonstrate that regional monsoon responses differ in terms of sensitivity and timing. Indeed, the Thar Desert paleoclimate records may help to elucidate the regional characteristics of the monsoon and to better understand the internal feedbacks within the global climate system. Our records demonstrate that it is not appropriate to examine the

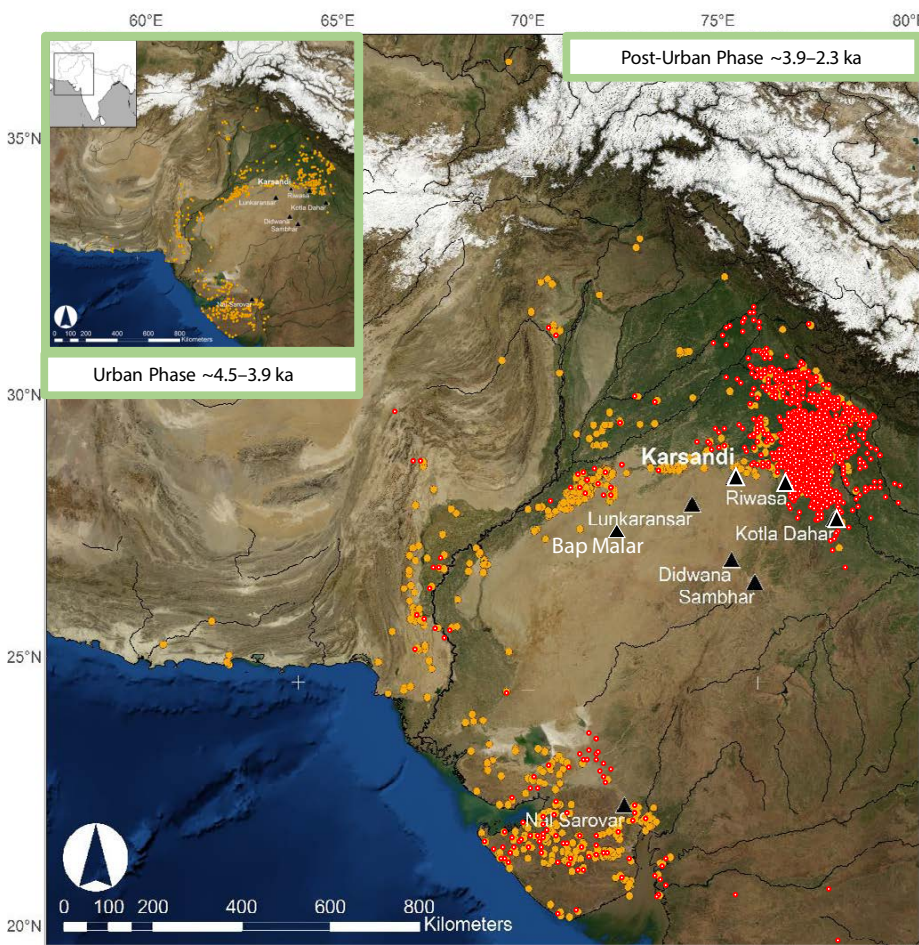


FIGURE 4. Map showing northwest Indian locations of lake records (black triangles) and archaeological sites described in the text along with Indus Civilization population concentrations. Red dots denote the post-urban phase of the Indus Civilization from ~3.9 ka to 2.3 ka. The inset map shows urban phase locations (orange dots) from 4.5 ka to 3.9 ka (Petrie et al., 2017). Notably, a clear concentration of post-urban settlements (mostly village-based) in the east after the ~4.2 ka drying event indicates eastward migration of Indus populations toward more reliable rain-fed regions. The far upper left inset map locates the main map in relation to the Indian subcontinent. Paleolakes Kotla Dahar and Riwasa lie in close proximity to several Indus sites and are well suited for reconstructing regional hydroclimate history in order to examine the climate-cultural relationship in the region.

impacts of past and future climate change on societal changes in the entire region based on an oversimplified global monsoon signal or only from a single regional climate record. In order to understand intricacies within ancient civilizations (e.g., the Bronze Age Indus civilization), it is important to develop a network of well-dated paleoenvironmental records that spans the entire region occupied by that civilization. Regional paleoclimate records are equally important for assessing the ability of climate models to simulate monsoon changes at regional scales and for testing model-derived hypotheses. For example, to translate regional observations into larger, global monsoon dynamics, an integrative approach that superimposes regional energy and moisture conservation on global monsoon dynamics is needed. A recent modeling study designed to examine climate extremes using Coupled Model Inter-comparison Projects (CMIP5 and CMIP6) highlights the need to consider regional climate sensitivity as a distinct feature of Earth system models and a key determinant of regional impacts (Seneviratne and Hauser, 2020). Our data suggest that researchers undertake a coordinated effort to integrate terrestrial and marine paleoclimate and paleoenvironmental records with multi-scale model-based quantifications in order to accurately project future climate changes. Such an approach will aid researchers in identifying the causes of observed mismatches between theory, models, and observations of monsoon dynamics, and ultimately in improving the accuracy of regional climate projections. 

REFERENCES

- Asharaf, S., and B. Ahrens. 2015. Indian summer monsoon rainfall processes in climate change scenarios. *Journal of Climate* 28(13):5,414–5,429, <https://doi.org/10.1175/JCLI-D-14-00233.1>.
- Ashok, K., Z. Guan, N.H. Saji, and T. Yamagata. 2004. Individual and combined influences of ENSO and the Indian Ocean dipole on the Indian summer monsoon. *Journal of Climate* 17(16):3,141–3,155, [https://doi.org/10.1175/1520-0442\(2004\)017<3141:IACIOE>2.0.CO;2](https://doi.org/10.1175/1520-0442(2004)017<3141:IACIOE>2.0.CO;2).
- Berger, A. 1978. Long-term variations of daily insolation and quaternary climatic changes. *Journal of the Atmospheric Sciences* 35(12):2,362–2,367, [https://doi.org/10.1175/1520-0469\(1978\)035<2362:LTVODI>2.0.CO;2](https://doi.org/10.1175/1520-0469(1978)035<2362:LTVODI>2.0.CO;2).
- Berkelhammer, M., A. Sinha, L. Stott, H. Cheng, F.F.S.R. Pausata, and K. Yoshimura. 2012. An abrupt shift in the Indian monsoon 4000 years ago. Pp. 75–87 in *Climates, Landscapes, and Civilizations*. L. Giosan, D.Q. Fuller, K. Nicoll, R.K. Fland, and P.D. Clift, eds, American Geophysical Union, Geophysical Monograph Series, vol. 198, Washington, DC, <https://doi.org/10.1029/2012GM001207>.
- Bhattacharya, S.K., K. Froehlich, P.K. Aggarwal, and K.M. Kulkarni. 2003. Isotopic variation in Indian Monsoon precipitation: Records from Bombay and New Delhi. *Geophysical Research Letters* 30(24), <https://doi.org/10.1029/2003GL018453>.
- Cai, Y., I.Y. Fung, R.L. Edwards, Z. An, H. Cheng, J.-E. Lee, L. Tan, C.-C. Shen, X. Wang, J.A. Day, and others. 2015. Variability of stalagmite-inferred Indian monsoon precipitation over the past 252,000 y. *Proceedings of the National Academy of Sciences of the United States of America* 112(10):2,954–2,959, <https://doi.org/10.1073/pnas.1424035112>.
- Caley, T., B. Malaizé, M. Revel, E. Ducassou, K. Wainer, M. Ibrahim, D. Shoaib, S. Migeon, and V. Marieu. 2011. Orbital timing of the Indian, East Asian and African boreal monsoons and the concept of a 'global monsoon.' *Quaternary Science Reviews* 30(25–26):3,705–3,715, <https://doi.org/10.1016/j.quascirev.2011.09.015>.
- Cheng, H., D. Fleitmann, R.L. Edwards, X. Wang, F.W. Cruz, A.S. Auler, A. Mangini, Y. Wang, X. Kong, and S.J. Burns. 2009. Timing and structure of the 8.2 kyr BP event inferred from $\delta^{18}\text{O}$ records of stalagmites from China, Oman, and Brazil. *Geology* 37(11):1007–1010, <https://doi.org/10.1130/G30126A.1>.
- Clemens, S.C., W. Kuhnt, and L.J. LeVay, and the Expedition 353 Scientists. 2015. Indian monsoon rainfall. *International Ocean Discovery Program Expedition 353 Preliminary Report*, <https://doi.org/10.14379/iodp.pr.353.2015>.
- Deotare, B.C., M.D. Kajale, S.N. Rajaguru, S. Kusumgar, A.J.T. Jull, and J.D. Donahue. 2004. Palaeoenvironmental history of Bap-Malar and Kanod playas of western Rajasthan, Thar desert. *Journal of Earth System Science* 113(3):403–425, <https://doi.org/10.1007/BF02716734>.
- Dixit, Y., D.A. Hodell, and C.A. Petrie. 2014a. Abrupt weakening of the summer monsoon in north-west India ~4100 yr ago. *Geology* 42(4):339–342, <https://doi.org/10.1130/G35236.1>.
- Dixit, Y., D.A. Hodell, R. Sinha, and C.A. Petrie. 2014b. Abrupt weakening of the Indian summer monsoon at 8.2 kyr BP. *Earth and Planetary Science Letters* 391:16–23, <https://doi.org/10.1016/j.epsl.2014.01.026>.
- Dixit, Y., D.A. Hodell, R. Sinha, and C.A. Petrie. 2015. Oxygen isotope analysis of multiple, single ostracod valves as a proxy for combined variability in seasonal temperature and lake water oxygen isotopes. *Journal of Paleolimnology* 53(1):35–45, <https://doi.org/10.1007/s10933-014-9805-3>.
- Dixit, Y., D.A. Hodell, A. Giesche, S.K. Tandon, F. Gázquez, H.S. Saini, L.C. Skinner, S.A.I. Mujtaba, V. Pawar, R.N. Singh, and C.A. Petrie. 2018. Intensified summer monsoon and the urbanization of Indus Civilization in northwest India. *Scientific Reports* 8:4225, <https://doi.org/10.1038/s41598-018-22504-5>.
- Donohoe, A., J. Marshall, D. Ferreira, and D. Mcgee. 2013. The relationship between ITCZ location and cross-equatorial atmospheric heat transport: From the seasonal cycle to the Last Glacial Maximum. *Journal of Climate* 26(11):3,597–3,618, <https://doi.org/10.1175/JCLI-D-12-00467.1>.
- Enzel, Y., L. Ely, S. Mishra, R. Ramesh, R. Amit, B. Lazar, S. Rajaguru, V. Baker, and A. Sandler. 1999. High-resolution Holocene environmental changes in the Thar Desert, northwestern India. *Science* 284(5411):125–128, <https://doi.org/10.1126/science.284.5411.125>.
- Fleitmann, D., S.J. Burns, M. Mudelsee, U. Neff, J. Kramers, A. Mangini, and A. Matter. 2003. Holocene forcing of the Indian Monsoon recorded in a stalagmite from southern Oman. *Science* 300(5626):1,737–1,739, <https://doi.org/10.1126/science.1083130>.
- Gadgil, S., and K.R. Kumar. 2006. The Asian monsoon—Agriculture and economy. Pp. 651–683 in *The Asian Monsoon*. B. Wang, ed., Springer Praxis Books. Springer, Berlin, Heidelberg, https://doi.org/10.1007/3-540-37722-0_18.
- Giesche, A., M. Staubwasser, C.A. Petrie, and D.A. Hodell. 2019. Indian winter and summer monsoon strength over the 4.2 ka BP event in foraminifer isotope records from the Indus River delta in the Arabian Sea. *Climate of the Past* 15(1):73–90, <https://doi.org/10.5194/cp-15-73-2019>.
- Giosan, L., P.D. Clift, M.G. Macklin, D.Q. Fuller, S. Constantinescu, J.A. Durcan, T. Stevens, G.A.T. Duller, A.R. Tabrez, K. Gangal, and others. 2012. Fluvial landscapes of the Harappan civilization. *Proceedings of the National Academy of Sciences of the United States of America* 109(26):E1688–E1694, <https://doi.org/10.1073/pnas.112743109>.
- Govil, P., and P.D. Naidu. 2011. Variations of Indian monsoon precipitation during the last 32 kyr reflected in the surface hydrography of the Western Bay of Bengal. *Quaternary Science Reviews* 30(27–28):3,871–3,879, <https://doi.org/10.1016/j.quascirev.2011.10.004>.
- Gupta, A.K., D.M. Anderson, and J.T. Overpeck. 2003. Abrupt changes in the Asian southwest monsoon during the Holocene and their links to the North Atlantic Ocean. *Nature* 421(6921):354–357, <https://doi.org/10.1038/nature01340>.
- Hodell, D.A., A.V. Turchyn, C.J. Wiseman, J. Escobar, J.H. Curtis, M. Brenner, A. Gilli, A. D. Mueller, F. Anselmetti, and D. Ariztegui. 2012. Late Glacial temperature and precipitation changes in the lowland Neotropics by tandem measurement of $\delta^{18}\text{O}$ in biogenic carbonate and gypsum hydration water. *Geochimica et Cosmochimica Acta* 77:352–368, <https://doi.org/10.1016/j.gca.2011.11.026>.
- IPCC (Intergovernmental Panel on Climate Change). 2013. *Climate Change 2013: The Physical Science Basis. Contribution of Working Group I to the Fifth Assessment Report of the Intergovernmental Panel on Climate Change*. T.F. Stocker, D. Qin, G.-K. Plattner, M. Tignor, S.K. Allen, J. Boschung, A. Nauels, Y. Xia, V. Bex, and P.M. Midgley, eds, Cambridge University Press, Cambridge, UK, and New York, NY, USA, 1,535 pp.
- IPCC. 2014. *Climate Change 2014: Synthesis Report. Contribution of Working Groups I, II and III to the Fifth Assessment Report of the Intergovernmental Panel on Climate Change*. R.K. Pachauri and L.A. Meyer, eds, IPCC, Geneva, Switzerland, 151 pp.
- Ishizaki, Y., K. Yoshimura, S. Kanae, M. Kimoto, N. Kurita, and T. Oki. 2012. Interannual variability of H_2^{18}O in precipitation over the Asian monsoon region. *Journal of Geophysical Research* 117(D16), <https://doi.org/10.1029/2011JD015890>.
- Kathayat, G., H. Cheng, A. Sinha, C. Spötl, R.L. Edwards, H. Zhang, X. Li, L. Yi, Y. Ning, Y. Cai, W.L. Lui, and S.F.M. Breitenbach. 2016. Indian monsoon variability on millennial-orbital timescales. *Scientific Reports* 6(1):24374, <https://doi.org/10.1038/srep24374>.
- Kathayat, G., H. Cheng, A. Sinha, L. Yi, X. Li, H. Zhang, H. Li, Y. Ning, and R.L. Edwards. 2017. The Indian monsoon variability and civilization changes in the Indian subcontinent. *Science Advances* 3(12):e1701296, <https://doi.org/10.1126/sciadv.1701296>.

- Kathayat, G., H. Cheng, A. Sinha, M. Berkelhammer, H. Zhang, P. Duan, H. Li, X. Li, Y. Ning, and R.L. Edwards. 2018. Evaluating the timing and structure of the 4.2 ka event in the Indian summer monsoon domain from an annually resolved speleothem record from Northeast India. *Climate of the Past* 14(12):1,869–1,879, <https://doi.org/10.5194/cp-14-1869-2018>.
- Kim, H.-J., B. Wang, and Q. Ding. 2008. The global monsoon variability simulated by CMIP3 coupled climate models. *Journal of Climate* 21(20):5,271–5,294, <https://doi.org/10.1175/2008JCLI20411>.
- Madella, M., and D.Q. Fuller. 2006. Palaeoecology and the Harappan Civilisation of South Asia: A reconsideration. *Quaternary Science Reviews* 25(11):1,283–1,301, <https://doi.org/10.1016/j.quascirev.2005.10.012>.
- Menzel, P., B. Gaye, M.G. Wiesner, S. Prasad, M. Stebich, B.K. Das, A. Anoop, N. Riedel, and N. Basavaiah. 2013. Influence of bottom water anoxia on nitrogen isotopic ratios and amino acid contributions of recent sediments from small eutrophic Lonar Lake, central India. *Limnology and Oceanography* 58(3):1,061–1,074, <https://doi.org/10.4319/lo.2013.58.3.1061>.
- Mishra, A.K., and V. Nagaraju. 2019. Space-based monitoring of severe flooding of a southern state in India during south-west monsoon season of 2018. *Natural Hazards* 97(2):949–953, <https://doi.org/10.1007/s11069-019-03673-6>.
- Nakamura, A., Y. Yokoyama, H. Maemoku, H. Yagi, M. Okamura, H. Matsuoka, N. Miyake, T. Osada, D.P. Adhikari, V. Dangol, and others. 2016. Weak monsoon event at 4.2 ka recorded in sediment from Lake Rara, Himalayas. *Japanese Quaternary Studies* 39(7):349–359, <https://doi.org/10.1016/j.jquaint.2015.05.053>.
- Pal, I., and A. Al-Tabbaa. 2009. Trends in seasonal precipitation extremes: An indicator of 'climate change' in Kerala, India. *Journal of Hydrology* 367(1–2):62–69, <https://doi.org/10.1016/j.jhydrol.2008.12.025>.
- Petrie, C.A., and J. Bates. 2017. 'Multi-cropping', intercropping and adaptation to variable environments in Indus South Asia. *Journal of World Prehistory* 30(2):81–130, <https://doi.org/10.1007/s10963-017-9101-z>.
- Petrie, C.A., R.N. Singh, J. Bates, Y. Dixit, C.A.I. French, D.A. Hodell, P.J. Jones, C. Lancelotti, F. Lynam, S. Neogi, and others. 2017. Adaptation to variable environments, resilience to climate change: Investigating land, water and settlement in Indus Northwest India. *Current Anthropology* 58(1), <https://doi.org/10.1086/690112>.
- Phadtare, N.R. 2000. Sharp decrease in summer monsoon strength 4000–3500 cal yr BP in the central higher Himalaya of India based on pollen evidence from alpine peat. *Quaternary Research* 53(1):122–129, <https://doi.org/10.1006/qres.1999.2108>.
- Pokharia, A.K., R. Agnihotri, S. Sharma, S. Bajpai, J. Nath, R.N. Kumaran, and B.C. Negi. 2017. Altered cropping pattern and cultural continuation with declined prosperity following abrupt and extreme arid event at ~4,200 yrs BP: Evidence from an Indus archaeological site Khirsara, Gujarat, western India. *PLoS One* 12(10):e0185684, <https://doi.org/10.1371/journal.pone.0185684>.
- Ponton, C., L. Giosan, T.I. Eglington, D.Q. Fuller, J.E. Johnson, P. Kumar, and T.S. Collett. 2012. Holocene aridification of India. *Geophysical Research Letters* 39(3), <https://doi.org/10.1029/2011GL050722>.
- Possehl, G.L. 2003. The Indus Civilization: An introduction to environment, subsistence, and cultural history. Pp. 1–20 in *Indus Ethnobiology: New Perspectives from the Field*. S.A. Weber and W.R. Belcher, eds, Lexington Books, Lanham, MD.
- Prasad, S., and Y. Enzel. 2006. Holocene paleoclimates of India. *Quaternary Research* 66(3):442–453, <https://doi.org/10.1016/j.yqres.2006.05.008>.
- Prasad, S., A. Anoop, N. Riedel, S. Sarkar, P. Menzel, N. Basavaiah, R. Krishnan, D. Fuller, B. Plessen, B. Gaye, and others. 2014. Prolonged monsoon droughts and links to Indo-Pacific warm pool: A Holocene record from Lonar Lake, central India. *Earth and Planetary Science Letters* 391:171–182, <https://doi.org/https://doi.org/10.1016/j.epsl.2014.01.043>.
- Rashid, H., E. England, L. Thompson, and L. Polyak. 2011. Late glacial to Holocene Indian summer monsoon variability based upon sediment records taken from the Bay of Bengal. *Terrestrial, Atmospheric and Oceanic Science* 22:215–228, [https://doi.org/10.3319/TAO.2010.09.17.02\(TibXS\)](https://doi.org/10.3319/TAO.2010.09.17.02(TibXS)).
- Saini, H.S., S.K. Tandon, S.A.I. Mujtaba, and N.C. Pant. 2005. Lake deposits of the northeastern margin of Thar Desert: Holocene(?) Palaeoclimatic implications. *Current Science* 88(12):1,994–2,000.
- Seneviratne, S.I., and M. Hauser. 2020. Regional climate sensitivity of climate extremes in CMIP6 vs CMIP5 multi-model ensembles. *Earth's Future* e2019EF001474, <https://doi.org/10.1029/2019EF001474>.
- Sengupta, S., and A. Sarkar. 2006. Stable isotope evidence of dual (Arabian Sea and Bay of Bengal) vapour sources in monsoonal precipitation over north India. *Earth and Planetary Science Letters* 250(3–4):511–521, <https://doi.org/10.1016/j.epsl.2006.08.011>.
- Singh, G., R.D. Joshi, and A.B. Singh. 1972. Stratigraphic and radiocarbon evidence for the age and development of three salt lake deposits in Rajasthan, India. *Quaternary Research* 2(4):496–505, [https://doi.org/10.1016/0033-5894\(72\)90088-9](https://doi.org/10.1016/0033-5894(72)90088-9).
- Singh, G., R. Wasson, and D. Agrawal. 1990. Vegetational and seasonal climatic changes since the last full glacial in the Thar Desert, north-western India. *Review of Palaeobotany and Palynology* 64(1–4):351–358, [https://doi.org/10.1016/0034-6667\(90\)90151-8](https://doi.org/10.1016/0034-6667(90)90151-8).
- Sinha, R. 2008. Kosi: Rising waters, dynamic channels and human disasters. *Economic & Political Weekly* 43(46).
- Sinha, R., W. Smykatz-Kloss, D. Stüben, S.P. Harrison, Z. Berner, and U. Kramar. 2006. Late Quaternary palaeoclimatic reconstruction from the lacustrine sediments of the Sambhar playa core, Thar Desert margin, India. *Palaeogeography, Palaeoclimatology, Palaeoecology* 233(3):252–270, <https://doi.org/10.1016/j.palaeo.2005.09.012>.
- Staubwasser, M., F. Sirocko, P.M. Grootes, and M. Segl. 2003. Climate change at the 4.2 ka BP termination of the Indus valley civilization and Holocene south Asian monsoon variability. *Geophysical Research Letters* 30(8), <https://doi.org/10.1029/2002GL016822>.
- Toth, L.T., R.B. Aronson, S.V. Vollmer, J.W. Hobbs, D.H. Urrego, H. Cheng, I.C. Enochs, D.J. Combosch, R. van Woessik, and I.G. Macintyre. 2012. ENSO drove 2500-year collapse of eastern Pacific coral reefs. *Science* 337(6090):81–84, <https://doi.org/10.1126/science.1221168>.
- Walker, M., M.J. Head, J. Lowe, M. Berkelhammer, S. Björck, H. Cheng, L.C. Cwynar, D. Fisher, V. Gkinis, A. Long, and others. 2019. Subdividing the Holocene series/epoch: Formalization of stages/ages and subseries/subepochs, and designation of GSSPs and auxiliary stratotypes. *Journal of Quaternary Science* 34(3):173–186, <https://doi.org/10.1002/jqs.3097>.
- Wang, B., and Q. Ding. 2008. Global monsoon: Dominant mode of annual variation in the tropics. *Dynamics of Atmospheres and Oceans* 44(3–4):165–183, <https://doi.org/10.1016/j.jdynatmoce.2007.05.002>.
- Wang, C. 2019. Three-ocean interactions and climate variability: A review and perspective. *Climate Dynamics* 53(7):5,119–5,136, <https://doi.org/10.1007/s00382-019-04930-x>.
- Wang, P.X., B. Wang, H. Cheng, J. Fasullo, Z. Guo, T. Kiefer, and Z. Liu. 2017. The global monsoon across time scales: Mechanisms and outstanding issues. *Earth-Science Reviews* 174:84–121, <https://doi.org/10.1016/j.earscirev.2017.07.006>.
- Wang, Y.J., H. Cheng, R.L. Edwards, Z.S. An, J.Y. Wu, C.-C. Shen, and J.A. Dorale. 2001. A high-resolution absolute-dated Late Pleistocene monsoon record from Hulu Cave, China. *Science* 294(5550):2345, <https://doi.org/10.1126/science.1064618>.
- Wang, Y.J., H. Cheng, R.L. Edwards, Y. He, X. Kong, Z. An, J. Wu, M.J. Kelly, C.A. Dykoski, and X. Li. 2005. The Holocene Asian monsoon: Links to solar changes and North Atlantic climate. *Science* 308(5723):854–857, <https://doi.org/10.1126/science.1106296>.
- Wasson, R.J., G.I. Smith, and D.P. Agrawal. 1984. Late quaternary sediments, minerals, and inferred geochemical history of Didwana Lake, Thar Desert, India. *Palaeogeography, Palaeoclimatology, Palaeoecology* 46(4):345–372, [https://doi.org/10.1016/0031-0182\(84\)90006-3](https://doi.org/10.1016/0031-0182(84)90006-3).
- Weber, S.A. 2003. Archaeobotany at Harappa: Indications for change. Pp. 175–198 in *Indus Ethnobiology: New Perspectives from the Field*. S.A. Weber and W.R. Belcher, eds, Lexington Books, Lanham MD.
- Weiss, H. 2016. Global megadrought, societal collapse and resilience at 4.2–3.9 ka BP across the Mediterranean and West Asia. *PAGES Magazine* 24(2):62–63.
- Wright, R.P. 2010. *The Ancient Indus: Urbanism, Economy, and Society*. Cambridge University Press, Cambridge, 418 pp.

ACKNOWLEDGMENTS

Special issue guest editor Amelia Shevenell and two anonymous reviewers of this article are thanked for constructive reviews. David Hodell, Cameron Petrie, Ayan Bhowmik, and Adam Switzer are acknowledged for insightful discussions at various points in time.

AUTHOR

Yama Dixit (ydixit@ntu.edu.sg) is Research Fellow, Earth Observatory of Singapore, Nanyang Technological University, Singapore.

ARTICLE CITATION

Dixit, Y. 2020. Regional character of the "global monsoon": Paleoclimate insights from northwest Indian lacustrine sediments. *Oceanography* 33(2):56–64, <https://doi.org/10.5670/oceanog.2020.206>.

COPYRIGHT & USAGE

This is an open access article made available under the terms of the Creative Commons Attribution 4.0 International License (<https://creativecommons.org/licenses/by/4.0/>), which permits use, sharing, adaptation, distribution, and reproduction in any medium or format as long as users cite the materials appropriately, provide a link to the Creative Commons license, and indicate the changes that were made to the original content.

SIDEBAR. Illuminating the Past to See the Future of Western Boundary Currents

MICROPALEONTOLOGICAL INVESTIGATIONS OF THE KUROSHIO CURRENT EXTENSION

By Adriane R. Lam, R. Mark Leckie, and Molly O. Patterson

The most prominent features of the marine circulation system, the western boundary currents (WBCs), flow along the western edges of the major ocean basins. These fast-moving, deep, and narrow wind-driven surface currents rim the subpolar and subtropical ocean gyres. WBCs of subtropical gyres transport heat, moisture, salt, and gases from the tropical ocean poleward, creating ocean-atmosphere interactions that impact regional weather patterns. Subtropical WBCs meet their subpolar WBC counterparts in the mid-latitudes, leading to sharp temperature and nutrient gradients (Figure 1a). Mixing of subpolar and subtropical water masses creates an ecotone, a region of overlap between biological communities. The WBC ecotones support rich ecosystems that contain some of the highest biodiversity in today's world ocean (Tittensor et al., 2010), making them regions of significant biologic importance. Due to their high biological abundance and diversity, these currents are vastly important resources for countries with robust fishing industries. Currently, fish stocks are declining in some of these areas, with decreases mostly attributed to the increase in WBC sea surface temperatures (Noto and Yasuda, 2011). Thus, understanding how these complex systems have responded to past warming and will respond to anthropogenic climate change scenarios has significant implications for predicting and mitigating future impacts on weather patterns, local biodiversity, and the human food supply.

Long-term observational and modeling studies confirm that the effects of anthropogenic climate change are significant within WBC systems. Over the past half century, these currents have intensified and shifted poleward, with the surface ocean in WBCs warming two to three times faster than the globally averaged sea surface temperature (Wu et al., 2012). Projections of WBC behavior under increasing CO₂ scenarios mostly forecast continued and increasing intensification, warming, and transport due to strengthening of near-surface winds (with the exception of the Gulf Stream; Yang et al., 2016). However, most WBCs lack long-term monitoring data needed to effectively assess how they behave beyond decadal timescales. One way we can improve our understanding of the response of WBCs to climate change is by examining the behavior of these systems through the lens of the geologic, and especially the paleontological, records. For example, our research on the Kuroshio Current (KC) and its Extension (KCE) using plankton proxies reveals its behavior during periods of prolonged global warmth and climatic transition. This research, then, also has implications for the behavior of regional zooplankton pop-

ulations (specifically, planktic foraminifera), whose domain lies near the base of the oceanic food web.

The KC and KCE in the Northwest Pacific Ocean, a leg of the North Pacific Subtropical Gyre (Figure 1a), is one of the most prominent WBCs in the world ocean. The KC is sourced from the western equatorial Pacific and flows north along the eastern Japanese coast. At approximately 36°N, 141°E, the current turns east and flows into the Pacific as the KCE, with volume transport reaching 130 Sv. The KCE meets the south-flowing Oyashio Current, the WBC of the North Pacific Subpolar Gyre (Figure 1a). The world's highest latitude coral reefs are found within the KCE region at 33°N, and the KCE, along with the KC, serve as a dispersal corridor for some fish species, supporting the large diversity (including planktic foraminifera) and biomass of marine life in the area.

We have characterized the behavior of the KCE using micropaleontological methods, specifically biostratigraphy and paleobiogeography of planktic foraminifera, to better evaluate how this current system responded to prominent tectonic and climate perturbations through the late Neogene and Quaternary periods (~7–0 million years ago). This time interval includes the closure of the Central American Seaway between North and South America (~3.8–2.5 million years ago); the mid-Piacenzian Warm Period (mPWP; 3.2–2.9 million years ago) when global temperatures were >2°C above pre-industrial levels; and the last major climate reorganization, the Mid-Pleistocene Transition (MPT; ~1.2–0.6 million years ago). We analyze deep-sea sediment cores recovered by the Ocean Drilling Program that cross the KCE (Figure 1a) to provide a multi-dimensional view of the current across these important time intervals.

Our research indicates the KCE and the North Pacific Subtropical Gyre expanded and contracted in response to tectonic and climate events. From planktic foraminiferal diversity curves calculated at the three deep-sea sites (Figure 1a), we infer that the KCE was likely a prominent feature through the late Neogene and Quaternary, as foraminifera diversity remained highest on the northern edge of the current, more so than tropical foraminiferal diversity (Lam and Leckie, 2020a). Paleobiogeographic analyses also indicate that throughout the entire time interval, the KCE was used as a corridor for species dispersal into the Northwest Pacific region. The timing and pattern of dispersals varied, but many species reveal a diachronous dispersal pattern from the cooler northern edge of the KCE to the warmer southern edge (Lam and Leckie,

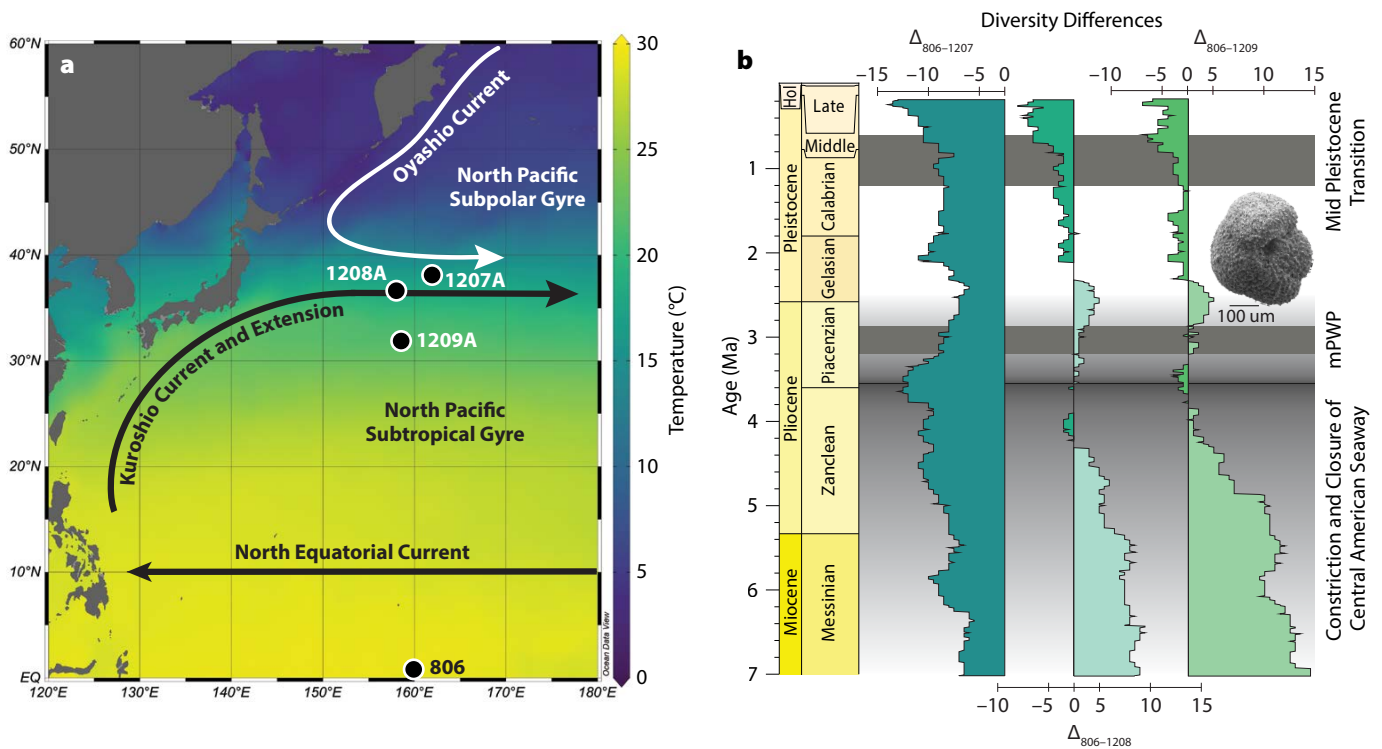


FIGURE 1. (a) Modern sea surface temperature map of the Northwest Pacific region characterized by two western boundary currents, the Kuroshio Current and its Extension (KCE) as part of the North Pacific Subtropical Gyre, and the Oyashio Current as part of the North Pacific Subpolar Gyre. The black dots denote Ocean Drilling Program (ODP) site locations discussed in the text. *Image modified from Lam and Leckie (2020a) under the CC BY 4.0 license (<https://creativecommons.org/licenses/by/4.0/>)* (b) Diversity differences of planktic foraminifera between ODP Site 806 in the western equatorial Pacific and ODP sites in the Northwest Pacific that cross the KCE. Negative values and darker colors indicate higher diversity within the KCE region relative to the western equatorial Pacific, with significant tectonic and paleoclimate events highlighted against the geologic timescale. Note that the difference in diversity between Site 806 in the western equatorial Pacific and Sites 1209 and 1208 on Shatsky Rise is tightly coupled with the effective closure of the Central American Seaway by ~4 million years ago. The scanning electron image is of *Globococcone puncticulata*, a common Pliocene KCE species.

2020b), indicating perhaps that differing water mass properties (e.g., temperature, salinity, nutrients) controlled the timing of species dispersals across the current.

Plankton diversity gradually increased during the final phases of the constriction of the Central American Seaway (~3.8–2.5 million years ago), reaching a diversity apex at the northernmost site (Figure 1b) when surface water exchange was shut off between the Atlantic and Pacific basins. Diversity at the other two sites increased to levels observed in the western equatorial Pacific. We interpret these results to indicate a spin-up and strengthening of the North Pacific Subtropical Gyre, in which warmer waters were brought further north by more vigorous circulation as this important ocean gateway closed. Turnover rates increased within the KCE during final seaway constriction and closure (~5–3 million years ago; Lam and Leckie, 2020b), indicating this tectonic event had profound effects on plankton populations in response to gyre spin-up.

During the mPWP (~3.2–2.9 million years ago), the KCE was incredibly sensitive to warming and cooling. With global warming during the mPWP, the North Pacific Subtropical Gyre

and subtropical waters expanded poleward, with potentially steepened temperature and salinity gradients across the current (Lam, 2020). Planktic foraminiferal data indicate decreasing diversity on the northern edge of the KCE after seaway closure, with a slight uptick in diversity during the mPWP interval (Figure 1b; Lam and Leckie, 2020a). This may indicate another short-lived intensification of the gyre and the KCE in response to warming. During the MPT (~1.2–0.6 million years ago), plankton diversity again increased within the KCE at all three sites (Figure 1b; Lam and Leckie, 2020a), in parallel with long-term cooling over the last 800,000 years and another potential equatorward shift of the KCE.

Micropaleontological data indicate that the KCE was a dynamic feature in the geologic past. It responded to relatively small changes in global mean temperature, with current activity directly influencing the foraminiferal community and biodiversity within the region. Our data support other geologic studies focused on the more recent past (reviewed in Gallagher et al., 2015), observational and modeling studies that show the KCE shifts north and intensifies during warmer periods and shifts south during cooler periods.

As we show here, studies of plankton diversity and paleobiogeography are excellent ways of establishing past KCE behavior and can be used to better assess WBCs and illuminate the response of these systems to climate perturbations. Additional geochemical and X-ray fluorescence data sets utilizing these sedimentary sequences from the Northwest Pacific are underway to expand upon the hypotheses presented here. It is our hope that these studies can test, refine, and generalize findings from the KCE in order to provide a deeper understanding of these currents that can help set a baseline for understanding marine food web dynamics, the extent of WBC sea surface warming, and the latitudinal extent of WBC shifts associated with anthropogenic warming.

REFERENCES

- Gallagher, S.J., A. Kitamura, Y. Iryu, T. Itaki, I. Koizumi, and P.W. Hoiles. 2015. The Pliocene to recent history of the Kuroshio and Tsushima Currents: A multi-proxy approach. *Progress in Earth and Planetary Science* 2:1–23, <https://doi.org/10.1186/s40645-015-0045-6>.
- Lam, A.R. 2020. *Neogene History of the Kuroshio Current Extension and Planktic Foraminifera Evolutionary Implications*. PhD Dissertation, University of Massachusetts Amherst, Amherst.
- Lam, A.R., and R.M. Leckie. 2020a. Late Neogene and Quaternary diversity and taxonomy of subtropical to temperate planktic foraminifera across the Kuroshio Current Extension, Northwest Pacific Ocean. *Micropaleontology* 66(3):177–268.
- Lam, A.R., and R.M. Leckie. 2020b. Subtropical to temperate late Neogene to Quaternary planktic foraminiferal biostratigraphy across the Kuroshio Current Extension, Shatsky Rise, Northwest Pacific Ocean. *PLOS ONE* 15(7):e0234351, <https://doi.org/10.1371/journal.pone.0234351>.
- Noto, M., and I. Yasuda. 2011. Population decline of the Japanese sardine, *Sardinops melanostictus*, in relation to sea surface temperature in the Kuroshio Extension. *Canadian Journal of Fisheries and Aquatic Sciences* 56(6):973–983, <https://doi.org/10.1139/f99-028>.
- Tittensor, D.P., C. Mora, W. Jetz, H.H. Lotze, D. Ricard, E.V. Berghe, and B. Worm. 2010. Global patterns and predictors of marine biodiversity across taxa. *Nature* 466(7310):1,098–1,101, <https://doi.org/10.1038/nature09329>.
- Wu, L., W. Cai, L. Zhang, H. Nakamura, A. Timmermann, T. Joyce, M.J. McPhaden, M. Alexander, B. Qui, M. Visbeck, P. Chang, and B. Giese. 2012. Enhanced warming over the global subtropical western boundary currents. *Nature Climate Change* 2(3):161–166, <https://doi.org/10.1038/nclimate1353>.
- Yang, H., G. Lohmann, W. Wei, M. Dima, M. Ionita, and J. Liu. 2016. Intensification and poleward shift of subtropical western boundary currents in a warming climate. *Journal of Geophysical Research* 121(7):4,928–4,945, <https://doi.org/10.1002/2015JC011513>.

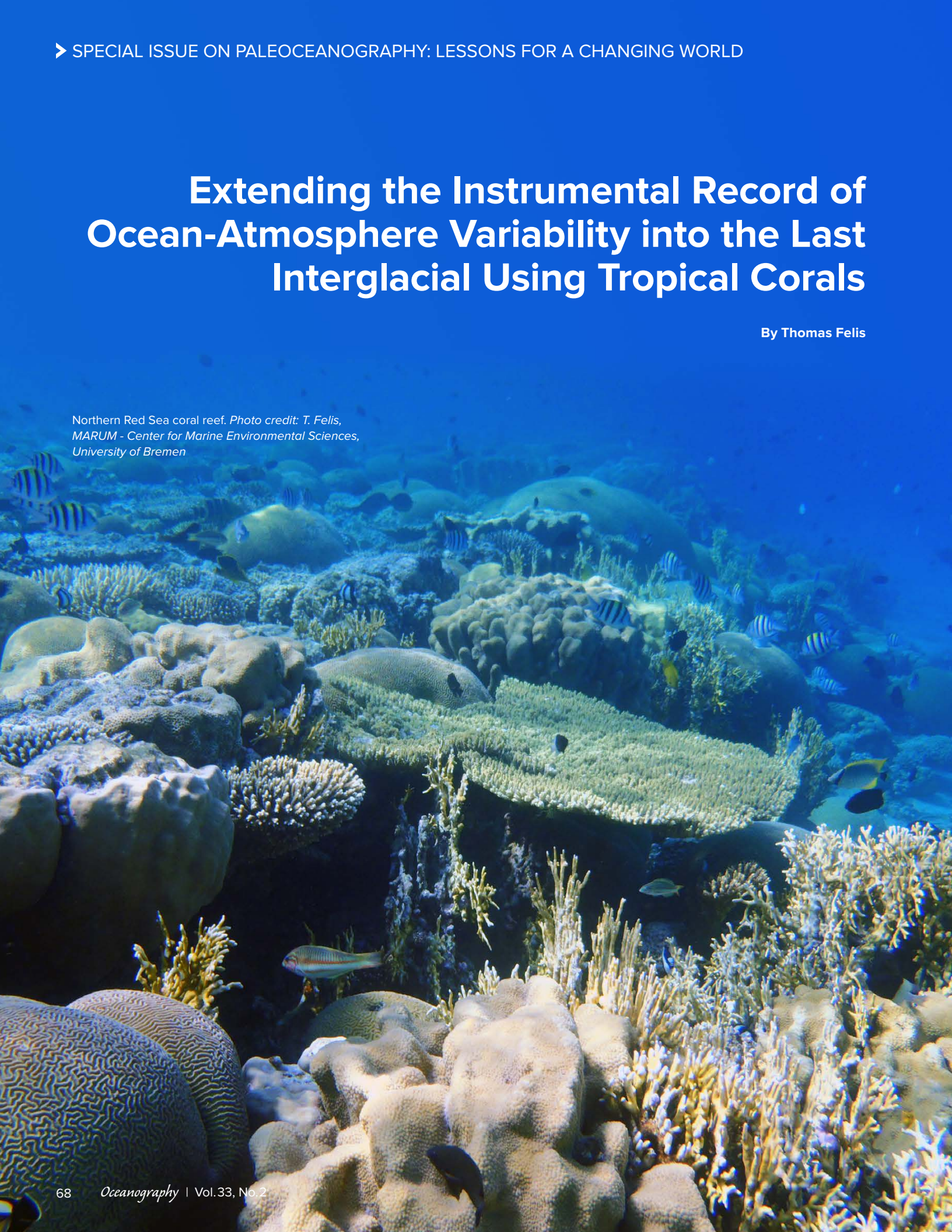
AUTHORS

Adriane R. Lam (alam@binghamton.edu) is Postdoctoral Fellow, Department of Geological Sciences and Environmental Studies, Binghamton University, Binghamton, NY, USA. **R. Mark Leckie** is Professor, Department of Geosciences, University of Massachusetts Amherst, Amherst, MA, USA. **Molly O. Patterson** is Assistant Professor, Department of Geological Sciences and Environmental Studies, Binghamton University, Binghamton, NY, USA.

Extending the Instrumental Record of Ocean-Atmosphere Variability into the Last Interglacial Using Tropical Corals

By Thomas Felis

Northern Red Sea coral reef. Photo credit: T. Felis,
MARUM - Center for Marine Environmental Sciences,
University of Bremen



ABSTRACT. The interaction of warm tropical ocean surface waters with the overlying atmosphere on seasonal, interannual, and decadal timescales is the source of climate extremes throughout the tropics and beyond. Tropical cyclones, heatwaves, flash floods, droughts, and El Niño have severe effects on ecosystems and societies globally. Projecting their amplitude and frequency changes in a warming climate requires knowledge of how the tropical ocean-atmosphere system operated in the past. Tropical shallow-water corals have great potential for extending the short and rather sparse instrumental record of sea surface observations at monthly resolution. Coral records deliver quantitative information about the fluctuations of sea surface temperature and hydrology on seasonal, interannual, and decadal timescales, with precise chronology. They provide a paleo-observational constraint on climate model simulations of past and future tropical ocean-atmosphere variability. This article highlights selected recent achievements in coral-based reconstructions of surface ocean conditions during recent centuries, the Holocene, the last deglaciation, and the last interglacial period. Future work combining ultrahigh-resolution coral reconstructions, novel analytical techniques, advanced statistical methods, and Earth system modeling will contribute to improved projections of tropical marine climate variability and the fates of coral reef ecosystems.

INTRODUCTION

Tropical marine climate variability is an important component of the Earth system. The variability of tropical sea surface temperature and related hydrological changes have substantial climatic impacts throughout the tropics and beyond. The interaction of warm tropical ocean surface waters with the overlying atmosphere modulates global rainfall patterns and climate extremes through atmospheric teleconnections. Climate extremes originating from the tropical ocean include interannual internal climate oscillations such as the El Niño-Southern Oscillation (ENSO) and the Indian Ocean Dipole (IOD) as well as tropical cyclones and hurricanes, marine heatwaves, flash floods, and severe droughts. These climate extremes have severe effects on societies, economies, infrastructures, and marine and terrestrial ecosystems globally and are broadly thought to intensify in amplitude and frequency in a warming climate.

Our current understanding of the tropical ocean-atmosphere system and related climate extremes is limited by the shortness of the instrumental record of observations. Systematic monitoring of tropical surface ocean conditions by ocean observing systems and satellites began less than 40 years ago, in the 1980s. Measurements of sea surface temperature by ships of opportunity extend back

to the late to mid-nineteenth century, but they are mostly located along major shipping lanes and are sparse in key regions of intense tropical ocean-atmosphere interaction such as the equatorial Pacific. Furthermore, these ship-based observations usually do not include sea surface salinity far back in time, limiting our knowledge of surface ocean hydrological changes. Understanding tropical marine climate variability and improving insights into its responses to recent and future climate changes require a long-term perspective beyond the short instrumental record. In particular, warm climate intervals in Earth's recent geologic history as well as periods of substantial or rapid warming are of interest here. Examples of past climate conditions warmer than those of the pre-industrial (~1850 Common Era, CE) can be found during the Holocene thermal maximum (~11,000 to 5,000 years ago) and the last interglacial period (~129,000 to 116,000 years ago). Although these past warm intervals are not strict analogues for future warming because they were orbitally forced and not a result of anthropogenic change, such periods can provide insights into regional climate responses under future warming, and thus provide a paleo-observational constraint on projections of future climate change impacts (Fischer et al.,

2018). Similarly, the last deglaciation (~18,000 to 11,000 years ago), an interval of changing climate following the last glacial period, can be considered a partial analogue for modern warming.

During the last decade, tropical corals have continued to evolve into a powerful archive that extends the instrumental record of oceanic sea surface observations into the pre-instrumental period. These corals grow in shallow waters of warm tropical to subtropical ocean regions. Their massive aragonitic carbonate skeletons commonly reveal annual density banding patterns similar to tree rings. Along with their growth rates of about one centimeter per year or more, these corals can create huge dome-shaped colonies with life spans that may last for centuries. Their continuous growth throughout the year allows precise analysis, using isotopic and geochemical proxies, of their carbonate skeletons for temperature and hydrology at seasonal to monthly resolution. This ultrahigh temporal resolution usually reveals annual cycles in the isotopic and geochemical proxies and enables construction of precise chronologies that can be supported by the annual density banding. Importantly, coral proxy records retrieved from living colonies overlap the instrumental record. Thus, they can be calibrated with instrumental time series of climate parameters of the tropical ocean-atmosphere system. Quantitative proxy records derived from large living coral colonies can extend the instrumental record of tropical marine climate variability back in time for centuries at monthly resolution, with associated uncertainties of reconstructed variables and based on precise chronology.

Most tropical corals have life spans of a few decades to centuries, which limits the use of living ("modern") colonies for extending the instrumental record of tropical marine climate throughout the last millennium and beyond. Using dead ("fossil") corals, for example, from the Holocene or the last interglacial is possible, but requires careful examination of their skeletal preservation. Under rare

circumstances, splicing of coral proxy records derived from living and fossil colonies allows generation of longer records. More commonly, “floating” time windows are derived from fossil corals. These records provide snapshots of past ocean-atmosphere variability with precise internal chronology. The absolute age of fossil corals is established by radiometric methods such as uranium-series dating.

The seasonal to monthly resolution of coral proxy records is exceptional for a marine climate archive. The resolution of coral proxy records, along with their time span of up to centuries, permit us to truly reconstruct tropical marine climate variability in interannual to decadal ranges. Tropical climate variability plays an important role on these timescales in regional projections of recent and future climate change impacts. Furthermore, the seasonal to monthly resolution allows us to truly reconstruct tropical marine climate variability during specific seasons of the year and with respect to changes in the amplitude of the annual cycle. Tropical corals grow throughout remote regions of the tropical oceans, from equatorial waters up to the subtropics, where they provide an important source for insights into past interactions between the tropical ocean-atmosphere system and mid-latitude climate variability (Felis et al., 2004; Felis and Rambu, 2010). This article highlights selected contributions of tropical corals to the field of paleoceanography during the last 10 years and their unique potential for extending the instrumental record of tropical marine climate observations into the more distant past. Particular emphasis is given on proxy records of tropical sea surface temperature and hydrology from paired strontium/calcium (Sr/Ca, for temperature) and oxygen isotope ($\delta^{18}\text{O}$, for temperature and hydrology) measurements in fossil corals of the Holocene, the last deglaciation, and the last interglacial period. For more comprehensive, traditional reviews of various aspects of coral paleoclimatology, see Lough (2010), Sadler et al. (2014), and Saha et al. (2016).

TROPICAL SEA SURFACE TEMPERATURE, EL NIÑO, IOD, AND MARINE HEATWAVES

Tierney et al. (2015) reconstruct tropical sea surface temperatures at annual resolution for the past four centuries from an extensive network of modern coral records. This study, conducted within the Past Global Changes (PAGES) Ocean2K project, suggests that the tropical oceans were cooling until modern warming began around the 1830s CE, especially during the early 1800s CE when there was an exceptionally cool period in the Indo-Pacific region. This coral-based reconstruction of tropical sea surface temperatures was key to the finding of the relatively early onset of industrial-era warming across the ocean and continents (Abram et al., 2016). Decadal-scale variability was determined to be a quasi-persistent feature of all tropical ocean basins, but no evidence was found that either natural or anthropogenic forcings have altered ENSO-related interannual variability in tropical sea surface temperatures (Tierney et al., 2015).

Coral-based reconstructions of Pacific sea surface temperature seasonality and ENSO strength provide fundamental constraints on tropical climate dynamics and may ultimately lead to improved climate model projections of ENSO-related climate extremes under greenhouse warming (Emile-Geay et al., 2016). The two major El Niño event types differ in their impacts on regional temperature and precipitation extremes at a global scale. A higher frequency of central Pacific El Niño events and fewer but more intense “traditional” eastern Pacific El Niño events in recent decades relative to the past four centuries were detected in a tropical coral network by exploiting the seasonal resolution of the coral proxy records (Freund et al., 2019). Climate model simulations suggest sensitivity of ENSO to large volcanic eruptions via aerosol forcing. However, records of modern and fossil corals of the central equatorial Pacific do not reveal a consistent ENSO response to volcanic forcing over the last

millennium, suggesting that some models may overestimate the forced response relative to natural ENSO variability (Dee et al., 2020). An extension of the ENSO proxy record over the past 7,000 years using snapshots provided by modern and fossil corals of the central equatorial Pacific (Cobb et al., 2013) suggests that ENSO variability over the last five decades was stronger than during the pre-industrial era and relatively weak between 3,000 and 5,000 years ago (Grothe et al., 2019). During this mid-Holocene interval of weak ENSO variability, an enhanced annual cycle and delayed seasonal growth was found in a 175-year-long coral record from the central equatorial Pacific from ~4,300 years ago (McGregor et al., 2013).

The Pacific trade winds are an important component of the tropical ocean-atmosphere system and ENSO. These trade winds can modulate global temperatures. Seasonally resolved records of manganese/calcium (Mn/Ca) in tropical Pacific corals from atolls with west-facing lagoons were shown to offer a promising proxy for westerly wind strength, and suggest that early twentieth-century warming was linked to weakening of tropical Pacific trade winds (Thompson et al., 2015). The relationship between trade winds, tropical Pacific temperature, and global temperature may allow reconstructions of tropical Pacific wind strength from coral Mn/Ca to provide important constraints on projections of global temperature evolution under greenhouse warming (Thompson et al., 2015).

The western Indian Ocean has been warming faster than any other tropical ocean during the twentieth century and is the largest contributor to the rise in global mean sea surface temperature. An annually resolved reconstruction of sea surface temperature from a set of western Indian Ocean coral records shows that a methodological bias, the so-called World War II bias, is the main reason for the differences between the various products of instrumental sea surface temperature observations and that it affects western Indian Ocean as well as global mean

temperature trends (Pfeiffer et al., 2017). Such multi-coral reconstructions may help in evaluation of different sea surface temperature products as they are truly independent from historical ship-based observations (Pfeiffer et al., 2017).

The IOD causes hydrological extremes in regions surrounding the Indian Ocean. A proxy record of the IOD over the last millennium based on snapshots provided by modern and fossil corals of the eastern equatorial Indian Ocean demonstrates that extreme positive IOD events were rare before 1960 CE, but that at least one event larger than the most extreme event observed in the instrumental record occurred during the seventeenth century (Abram et al., 2020). The identification of extreme IOD variability, persistent tropical Indo-Pacific climate coupling, and a tendency toward clustering of positive IOD events in the reconstruction may improve projections at seasonal and decadal timescales that will help to improve management of the climate risks associated with future IOD variability in a warming world (Abram et al., 2020).

Increasing intensity of marine heatwaves has caused widespread mass coral bleaching events. An annually resolved reconstruction of sea surface temperature for the past two centuries from multiple southeastern Indian Ocean corals demonstrates the important role of coupling between the western and central Pacific in amplifying thermal stress in the southeastern Indian Ocean (Zinke et al., 2015). Multi-century coral reconstructions provide a long-term perspective on the regional impacts of large-scale climate coupling between ocean basins, which may lead to improved projections of extreme heatwaves and their ecological impacts on coral reef ecosystems at regional scales (Zinke et al., 2015).

The monsoon systems are of critical importance to the densely populated areas of South Asia as they control the amount and intensity of precipitation as well as the severity of winters in some regions. An annually resolved reconstruction of the East Asian Monsoon

based on radiocarbon measurements in a coral of the South China Sea suggests a long-term decline in both summer and winter monsoon variability since the sixteenth century (Goodkin et al., 2019). Coral proxy records from the rim of continental Asia, for example, the South China Sea (Goodkin et al., 2019) and the northern Red Sea (Felis and Rambu, 2010), have the potential to provide

insights into past interactions between tropical marine and higher latitude continental climate variability.

Most centuries-long coral records are based on $\delta^{18}\text{O}$, a proxy that reflects both the temperature and the $\delta^{18}\text{O}$ of the surrounding seawater. This dual control can complicate the interpretation of coral $\delta^{18}\text{O}$ records in terms of temperature through space and time. Furthermore, although seawater $\delta^{18}\text{O}$ is thought to be closely related to salinity, the two variables have a complicated relationship that can vary with time and location. Proxy system models, also known as proxy forward models (Dee et al., 2015; Lawman et al., 2020), can improve the interpretation of coral $\delta^{18}\text{O}$ records and better quantify their uncertainties. Paired with isotope-enabled climate model simulations, they can be used to investigate the dynamics of seawater $\delta^{18}\text{O}$ and salinity variations in relation to coral $\delta^{18}\text{O}$ in different climate regimes (Dee et al., 2015; Stevenson et al., 2018).

Centuries-long coral records based on Sr/Ca, a proxy thought to solely reflect temperature, are becoming increasingly

available (DeLong et al., 2012). Other temperature proxies that are increasingly analyzed in coral skeletons for longer time intervals include uranium/calcium (U/Ca; Felis et al., 2009), lithium/calcium (Li/Ca) and lithium/magnesium (Li/Mg; Hathorne et al., 2013a), as well as a combination of the Sr/Ca and U/Ca proxies termed strontium-uranium (Sr-U; DeCarlo et al., 2016). When paired with

“ Ultrahigh-resolution coral proxy records provide a powerful tool for reconstructing past tropical marine climate and environmental variability and for understanding the temporal response of corals and coral reefs to ongoing climate and environmental changes. ”

coral $\delta^{18}\text{O}$ measurements, temperature proxies such as Sr/Ca and U/Ca provide tools for reconstructing changes in seawater $\delta^{18}\text{O}$ in the surface ocean (Felis et al., 2009), a hydrologically relevant variable that reflects oceanic processes as well as variations in hydroclimate. Such coral-based seawater $\delta^{18}\text{O}$ reconstructions are considered to be an important source of information on hydroclimatic changes for the vast areas of the tropical to subtropical oceans during the pre-instrumental period. They can be used, in combination with terrestrial hydroclimate archives and climate model simulations, to constrain future hydroclimatic risks estimated from climate model projections (PAGES Hydro2k Consortium, 2017).

SURFACE OCEAN FRESHENING DURING THE LAST CENTURIES

Annually resolved reconstructions of seawater $\delta^{18}\text{O}$ changes over recent centuries derived from paired coral Sr/Ca and $\delta^{18}\text{O}$ records provide indications for transitions toward fresher surface conditions since the mid-nineteenth century in regions of the tropical to subtropical Indo-Pacific

(PAGES Hydro2k Consortium, 2017). In the subtropical northern Red Sea (Ras Umm Sidd) and western North Pacific (Ogasawara), apparent regime shifts toward fresher conditions occurred relatively abruptly within about five years after 1850 CE and 1905 CE, respectively (Felis et al., 2009, 2018; **Figure 1**). At both sites, an increase in regional precipitation could be excluded as a cause of the reconstructed surface ocean freshening. While a change in surface evaporation driven by a reorganization of the atmospheric circulation over Europe at the end

of the putative Little Ice Age provides a likely explanation for the arid northern Red Sea (Felis et al., 2018), a change in the Kuroshio Current system and associated westerly winds likely played a role in the western North Pacific (Felis et al., 2009). Reconstruction of seawater $\delta^{18}\text{O}$ and Sr/Ca, U/Ca, or other element/Ca temperature proxies in corals can provide unprecedented insights into the past dynamics of surface ocean hydrology at annual and higher resolution. These reconstructions have the potential to

reveal surprises regarding abrupt changes and unexpected trends even during the last century for which instrumental observations of hydrologically relevant variables such as salinity are sparse. In tandem with corresponding temperature reconstructions (Felis et al., 2010), seawater $\delta^{18}\text{O}$ reconstructions may provide a comprehensive understanding of ocean-atmosphere variability at seasonal and interannual to decadal timescales, including the dynamics of ocean to land moisture transport and related hydrological extremes. The PAGES CoralHydro2k

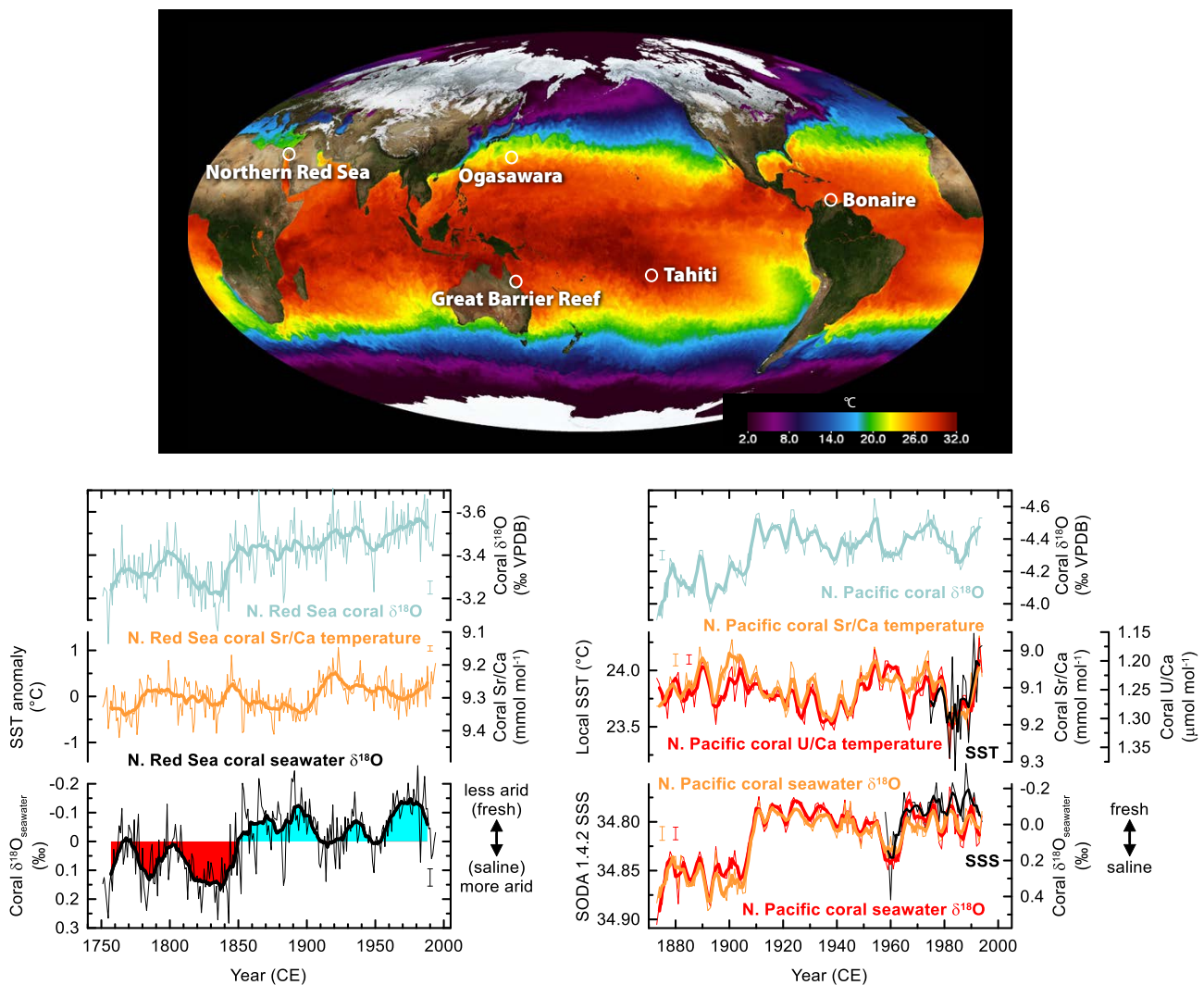


FIGURE 1. (top) Selected tropical and subtropical sites of coral paleoclimate work in the Indo-Pacific and Atlantic Oceans discussed in this paper are indicated on a map showing the multi-scale ultrahigh-resolution (MUR) sea surface temperature (SST) analysis from NASA/Goddard Space Flight Center (downloaded from <https://svs.gsfc.nasa.gov/30008>). The graphs show annual average proxy records of subtropical sea surface temperature and hydrology during recent centuries derived from bimonthly resolved Sr/Ca (and U/Ca) and $\delta^{18}\text{O}$ measurements in modern corals (*Porites* spp.) of (bottom left) the northern Red Sea (Ras Umm Sidd; Felis et al., 2018) and (bottom right) the western North Pacific (Ogasawara; Felis et al., 2009). The corresponding seawater $\delta^{18}\text{O}$ reconstructions suggest abrupt shifts toward fresher conditions after 1850 CE and 1905 CE. Bold lines are 13-year (northern Red Sea) and three-year (western North Pacific) running averages. Modified from Felis et al. (2009) and Felis et al. (2018)

project is a new initiative toward encouraging employment of paired Sr/Ca and $\delta^{18}\text{O}$ measurements in corals for reconstructing tropical ocean hydroclimate and temperature during recent centuries (Hargreaves et al., 2020).

HOLOCENE AND LAST INTERGLACIAL TROPICAL ATLANTIC TEMPERATURE VARIABILITY

The tropical Atlantic Ocean plays a fundamental role in the modulation of ocean-atmosphere variability on interannual to

decadal timescales throughout the basin and adjacent continental areas. The tropical Atlantic is the source of severe climate extremes such as hurricanes, floods, and droughts. Proxy records of tropical North Atlantic sea surface conditions for time intervals back to the mid-Holocene and during the last interglacial provided by fossil corals of the southern Caribbean (Bonaire) allow unprecedented insights into the pre-instrumental period at monthly resolution (Giry et al., 2012, 2013; Felis et al., 2015; Brocas et al., 2016, 2018; Wu et al., 2017). The paired

coral Sr/Ca and $\delta^{18}\text{O}$ records indicate pronounced interannual to decadal variability as well as longer-term trends in tropical Atlantic sea surface temperature and hydrology during the late to mid-Holocene and the last interglacial (Figure 2). The records show some tendency for a positive relationship on these timescales when interpreted as temperature and salinity variations. Quasi-biennial variability is a persistent feature in many records. Pronounced interannual variability at typical ENSO periods $\sim 2,350$ years ago could be indic-

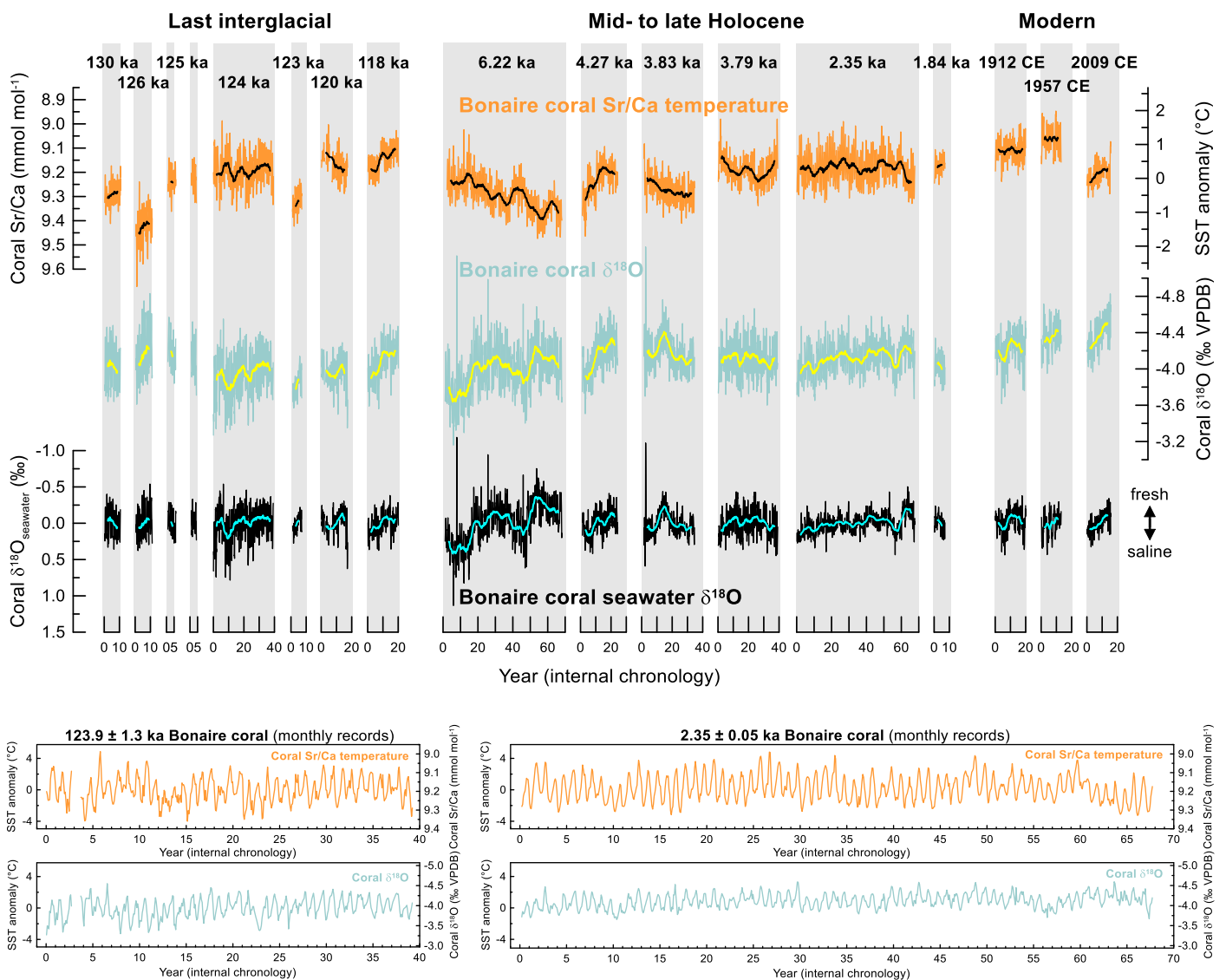


FIGURE 2. (top) Monthly resolved proxy records of tropical Atlantic sea surface temperature (SST) and hydrology for time intervals during the last interglacial ($\sim 130,000$ to $118,000$ years ago) and since the mid-Holocene ($\sim 6,000$ years ago) derived from Sr/Ca and $\delta^{18}\text{O}$ measurements in modern and fossil corals (*Diploria strigosa*) of the southern Caribbean Sea (Bonaire; Giry et al., 2012, 2013; Felis et al., 2015; Brocas et al., 2016, 2018). The corresponding seawater $\delta^{18}\text{O}$ reconstructions are shown. Bold lines are 51-month running averages. (bottom) Enlargement of monthly coral Sr/Ca and $\delta^{18}\text{O}$ records for time intervals around $124,000$ and $2,350$ years ago. Modified from Giry et al. (2012, 2013), Felis et al. (2015), and Brocas et al. (2016, 2018)

ative of a stronger influence of Pacific climate variability on the tropical Atlantic basin at that time (Giry et al., 2012, 2013). Indications for prominent decadal variability in sea surface temperature at a period of ~12 years identified during the peak of the last interglacial ~124,000 years ago (Brocas et al., 2016) are noteworthy. Similar decadal variability has been a typical feature in North Atlantic surface temperatures during the period of instrumental observations.

The monthly resolved Bonaire coral Sr/Ca records indicate that the seasonality of surface ocean temperature in the tropical North Atlantic during the Holocene and the last interglacial was controlled mainly by insolation changes on orbital timescales (Giry et al., 2012; Felis et al., 2015; Brocas et al., 2016). The reconstructed temperature seasonality closely follows the temporal evolution of orbitally controlled changes in insolation seasonality between ~130,000 and 118,000 years ago and from ~6,000 years ago until the present day (Figure 3). The maximum temperature seasonality relative to today reconstructed for 126,000 years ago, during the peak of the last interglacial, is tem-

porally consistent with a corresponding maximum in insolation seasonality at this latitude and in line with climate simulations using a coupled atmosphere-ocean general circulation model (Brocas et al., 2016). It is notable that a time interval of anomalously increased temperature seasonality reached peak last interglacial amplitudes during the late Holocene ~2,350 years ago and cannot be explained by an orbital forcing of insolation seasonality (Giry et al., 2012). Along with pronounced interannual variability at typical ENSO periods, this anomalous time interval might provide a paleo-observational constraint for substantial modulation of tropical Atlantic temperature seasonality through internal variability of the climate system, such as strengthened interactions between the Pacific and Atlantic basins via atmospheric teleconnections (Giry et al., 2012; Felis et al., 2015). Given the important role of tropical surface ocean seasonal temperature changes in the development of hurricanes, floods, and droughts, a better understanding of the dynamics behind such anomalous time intervals of the past might lead to improved projections of future climate extremes and their impacts

on the tropical Atlantic region and adjacent continental areas.

The evolution of tropical ocean temperatures at sub-basin to regional scales during the Holocene and the last interglacial is still not well known. A noteworthy result based on the Bonaire coral records is a reconstructed cooling in the tropical North Atlantic relative to today during the mid-Holocene ~6,000 years ago (Giry et al., 2012) and especially during the peak of the last interglacial ~126,000 years ago (Brocas et al., 2019), with both time intervals accompanied by apparently fresher sea surface conditions (Giry et al., 2013; Brocas et al., 2019). That the tropical Atlantic Ocean did not warm during the peak of the globally warmer-than-pre-industrial last interglacial is at first glance counterintuitive (Brocas et al., 2019). However, this result is consistent with other proxy reconstructions and climate model simulations of the tropical oceans and with the annual orbital forcing of insolation during this time interval (Fischer et al., 2018). This highlights the potential for corals to shed more light on the temperature evolution of the tropical oceans during warm periods of the past.

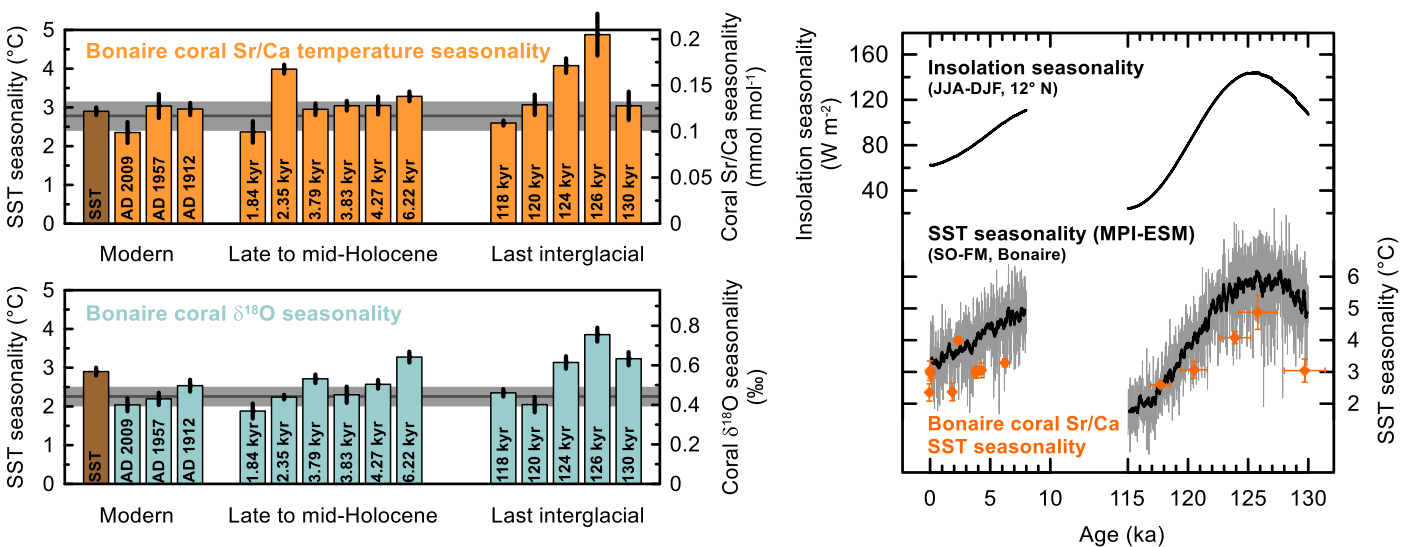


FIGURE 3. (left) Evolution of tropical Atlantic sea surface temperature (SST) seasonality during the last interglacial (~130,000 to 118,000 years ago) and since the mid-Holocene (~6,000 years ago) derived from monthly Sr/Ca and $\delta^{18}\text{O}$ measurements in modern and fossil corals (*Diploria strigosa*) of the southern Caribbean Sea (Bonaire; Giry et al., 2012, 2013; Felis et al., 2015; Brocas et al., 2016, 2018). Deviations of coral $\delta^{18}\text{O}$ seasonality from coral Sr/Ca-temperature seasonality arise from hydrological effects. (right) Reconstructed coral Sr/Ca-temperature seasonality closely follows orbitally controlled changes in insolation seasonality at this latitude and regional SST seasonality from a climate model simulation. Modified from Giry et al. (2012, 2013), Felis et al. (2015), and Brocas et al. (2016, 2018)

LAST DEGLACIAL TEMPERATURES, EAST AUSTRALIAN CURRENT, AND THE GREAT BARRIER REEF

The last deglaciation (~18,000 to 11,000 years ago) is a time interval of substantial global warming and sea level rise following the cold last glacial maximum that culminated 20,500 years ago with a sea level of about 125 m to 130 m lower than today (Yokoyama et al., 2018). Submerged shallow-water reefs that grew during the last deglaciation, however, are difficult to access. In the Great Barrier Reef, along the path of the southward flowing East Australian Current, tropical Pacific corals that grew during the last glacial maximum were successfully recovered for the first time using a mission-specific platform on Integrated Ocean Drilling Program (IODP) Expedition 325 (Felis et al., 2014; Webster et al., 2018; Yokoyama et al., 2018). Average Sr/Ca values of fossil corals from two IODP drilling sites separated by about 3° of latitude indicate a considerably steeper meridional sea surface temperature gradient than that of the present day between ~20,000 and 13,000 years ago, and is supported by the corresponding coral $\delta^{18}\text{O}$ data (Felis et al., 2014; Figure 4). The result was interpreted as an indication for the northward expansion of cooler subtropical waters along the eastern Australian coast during the last glacial maximum and the last deglaciation due to a weakening of the East Australian Current (Felis et al., 2014), the western boundary current of the South Pacific subtropical gyre. These findings also suggest a northward contraction of the southern boundary of the Western Pacific Warm Pool during the last glacial maximum and the last deglaciation. Furthermore, the reduction in the transport of warm tropical waters poleward due to a weakened East Australian Current may have played an important role in dampening the amplitude of cooling in the Western Pacific Warm Pool during the last glacial maximum (Felis et al., 2014). From an ecosystem perspec-

tive, the coral-based temperature reconstructions (Felis et al., 2014) along with the sea level reconstructions (Yokoyama et al., 2018) of IODP Expedition 325 provide the basis for the conclusion that the Great Barrier Reef has been more resilient to past temperature (Felis et al., 2014) and sea level changes than previously thought (Webster et al., 2018), but there is little evidence for resilience during the next decades given the current rates of change (Webster et al., 2018).

The reconstruction of last deglacial temperature gradients at a regional scale from a large number of corals analyzed for Sr/Ca in multiple laboratories within the international context of

an IODP expedition is a challenge. Next to analytical precision, this reconstruction requires well-characterized reference material that is appropriate for the high Sr content of coral skeletons and the corresponding coral matrix. The coral paleoclimatological work arising from IODP Expedition 310 to Tahiti strengthened the need for a direct comparison of coral Sr/Ca temperature proxy data generated in different laboratories (Asami et al., 2009; Hathorne et al., 2011; Felis et al., 2012). The Geological Survey of Japan's JCP-1 coral reference material was identified as appropriate and characterized in an interlaboratory study for coral Sr/Ca and other element/Ca ratio measure-

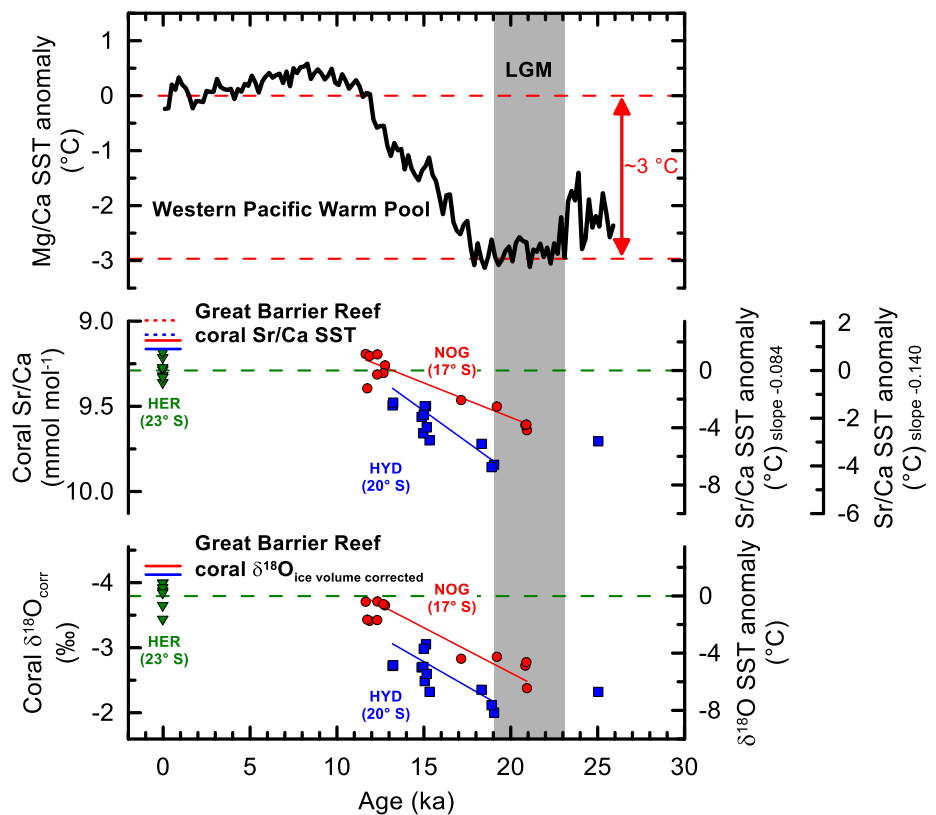


FIGURE 4. Evolution of tropical South Pacific sea surface temperature (SST) during the last deglaciation and last glacial maximum (LGM) derived from average Sr/Ca and $\delta^{18}\text{O}$ values of fossil corals (*Isopora palifera/cuneata*) drilled by Integrated Ocean Drilling Program (IODP) Expedition 325 to the Great Barrier Reef (Felis et al., 2014). Reconstructed coral Sr/Ca temperatures from northern (NOG) and southern (HYD) sites indicate a steeper meridional SST gradient than at present day between ~20,000 years ago and 13,000 years ago, supported by the coral $\delta^{18}\text{O}$ data. The coral Sr/Ca SST anomalies are not adjusted for changes in seawater Sr/Ca, and thus provide upper estimates of the magnitude of cooling. Deviations of coral $\delta^{18}\text{O}$ from coral Sr/Ca temperatures arise from hydrological effects. Coral data for a modern reference site (HER) and scaled relative SST at IODP sites are shown for comparison (short blue and red horizontal lines: solid = Sr/Ca-SST slope -0.084 mmol mol $^{-1}$ per $^{\circ}\text{C}$; dashed = Sr/Ca-SST slope -0.140 mmol mol $^{-1}$ per $^{\circ}\text{C}$). Warm Pool SST data are from Linsley et al. (2010). Modified from Felis et al. (2014)

ments (Hathorne et al., 2013b). It was suggested that future studies reporting coral element/Ca data should also report the average value obtained for a reference such as the JcP-1 (Hathorne et al., 2013b), a procedure that was followed in coral work of subsequent IODP expeditions (Felis et al., 2014) and other studies (Giry et al., 2012; Felis et al., 2015; Zinke et al., 2015; Brocas et al., 2016; DeCarlo et al., 2016; Wu et al., 2017).

TROPICAL PACIFIC TEMPERATURE VARIABILITY DURING HEINRICH STADIAL 1

Fossil corals recovered in the tropical South Pacific at Tahiti by IODP Expedition 310 provide monthly resolved snapshots of sea surface temperature variability during the last deglaciation that coincide with key periods of Northern Hemisphere climate change such as the Younger Dryas cooling, the Bølling-Allerød warming, and the Heinrich Stadial 1 cold interval (Asami et al., 2009; Hathorne et al., 2011; Felis et al., 2012). Average coral Sr/Ca values suggest relative cooling at Tahiti during the Younger

Dryas at 12,400 years ago compared to 14,200 years ago during the Bølling-Allerød, which could indicate the reflection of a Northern Hemisphere-type pattern of deglacial warming at ~17°S in the central tropical South Pacific (Asami et al., 2009).

During the early last glacial termination, the Heinrich Stadial 1 interval (~18,000 to 14,600 years ago) was characterized by intense North Atlantic cooling and weak overturning circulation. Heinrich Stadial 1 was accompanied by a disruption of global climate, but its impact on interannual climate variability in the tropical Pacific is not well known. A monthly resolved Tahiti coral Sr/Ca record indicates pronounced interannual variability in tropical South Pacific sea surface temperatures at typical ENSO periods around 15,000 years ago (Felis et al., 2012), different from today when ENSO influence on Tahiti sea surface temperatures is weak (Figure 5). The results indicate that ENSO was active during Heinrich Stadial 1. Furthermore, greater ENSO influence in the South Pacific at this time is suggested as poten-

tially resulting from a southward expansion or shift of ENSO-related sea surface temperature anomalies (Felis et al., 2012). Such coral proxy evidence of tropical Pacific sea surface temperature characteristics in an extreme climate of the past, at the end of the last glacial period, might help to constrain climate model projections of future climate change.

OUTLOOK

Proxy records derived from tropical shallow-water corals have great potential for extending the instrumental record of sea surface observations into the past throughout the tropical to subtropical oceans. The monthly resolution of coral proxy records provides quantitative information on the fluctuations of sea surface temperature and hydrology on seasonal, interannual, and decadal timescales during the pre-instrumental period, with associated uncertainties and precise chronology. This information can be derived from $\delta^{18}\text{O}$ measurements in modern and fossil corals, paired with analysis of temperature proxies such Sr/Ca and U/Ca (Felis et al., 2009), Li/Ca

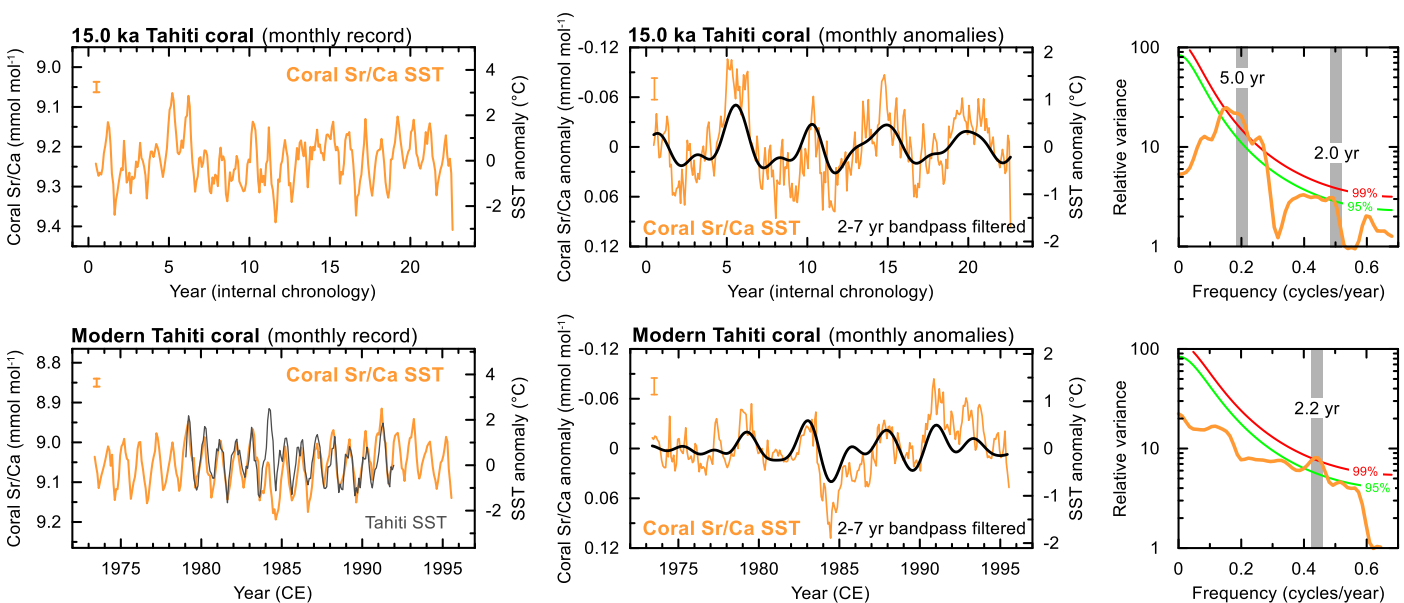


FIGURE 5. (left) Monthly resolved proxy records of tropical South Pacific sea surface temperature (SST) for a time interval during the Northern Hemisphere's Heinrich Stadial 1 cold interval (~18,000 to 14,600 years ago) derived from Sr/Ca measurements in a fossil coral (*Porites* sp.) drilled by IODP Expedition 310 off Tahiti (Felis et al., 2012). (center) Corresponding monthly Tahiti coral Sr/Ca-SST anomaly records (annual cycle removed) filtered in the two- to seven-year band. (right) Results of spectral analysis. Pronounced interannual variability in tropical South Pacific SST at typical El Niño-Southern Oscillation (ENSO) periods is indicated around ~15,000 years ago, which is different from today when the ENSO influence on Tahiti SST is weak. Modern Tahiti coral data is from Cahyarini et al. (2008). Modified from Felis et al. (2012)

and Li/Mg (Hathorne et al., 2013a), and Sr-U (DeCarlo et al., 2016) and clumped isotopes (Saenger et al., 2012). Multi-proxy approaches involving Sr/Ca and Li/Mg show potential for improving coral-based temperature reconstructions (D'Olivo et al., 2018), whereas other emerging proxies such as calcium isotopes ($\delta^{44}/^{40}\text{Ca}$) reveal only a weak temperature dependence (Pretet et al., 2013). Specially designed micromilling techniques for skeleton sampling need to be applied to corals other than the commonly used *Porites* of the Indo-Pacific, such as Atlantic brain corals (Giry et al., 2010). The use of fossil corals requires rigorous screening for potential effects of diagenesis (Hathorne et al., 2011; Felis et al., 2012) as well as identification of appropriate skeletal elements for precise uranium-series dating (Obert et al., 2016).

Paired coral proxy records of sea surface temperature and hydrology are of great importance for better assessment of ongoing and future changes in the tropical ocean-atmosphere system and related climate extremes. They can be used, in combination with proxy system models and isotope-enabled climate models (Dee et al., 2015; Brocas et al., 2018; Stevenson et al., 2018; Lawman et al., 2020), to investigate the fundamental dynamics of tropical ocean-atmosphere variability, investigations that will ultimately lead to a better understanding of how this important component of the Earth system works. Following paleoclimate data reporting and archiving standards agreed on by the scientific community (Khider et al., 2019), the growing network of coral records can serve synthesis studies on various aspects of past tropical marine climate (Tierney et al., 2015; Abram et al., 2016).

Other proxies that are beginning to be frequently analyzed in coral skeletons include boron isotopes ($\delta^{11}\text{B}$) and boron/calcium (B/Ca) for identifying the long-term effects of ocean acidification on coral calcification (McCulloch et al., 2017), nitrogen isotopes ($\delta^{15}\text{N}$) in skeleton-bound organic matter that pro-

vide information about the oceanic nitrogen cycle and the influence of anthropogenic nitrogen on the open ocean (Wang et al., 2018), and barium isotopes ($\delta^{138}/^{134}\text{Ba}$) as a potential proxy for oceanic barium cycling (Liu et al., 2019). The combination of element/Ca and boron isotope records shows promise for detecting the response of coral calcification and calcifying fluid to thermally induced bleaching stress (D'Olivo and McCulloch, 2017), which might contribute to the reconstruction of past bleaching events and a better understanding of coral resilience under current and future warming. These new proxies are important because systematic coral reef monitoring started only a few decades ago and is still absent in many remote reef areas. Consequently, in addition to paleoceanographic and paleoclimatic information, coral reconstructions can provide a long-term perspective on the responses of coral reef ecosystems to environmental stresses. Together, such reconstructions provide the potential for insights into the effects of large-scale oceanographic and atmospheric processes on coral reef ecosystems (Zinke et al., 2015; Felis and Mudelsee, 2019).

Key regions for future coral-based paleoclimatic research include the area of highest ENSO variability in the equatorial Pacific Ocean, including the Western Pacific Warm Pool; the tropical Atlantic Ocean as a source for climate extremes affecting the Americas, Africa, and downstream Europe; and the Indian Ocean, where warming is occurring faster than in any other tropical ocean and whose related climate extremes affect the adjacent continental areas of Africa, Asia, and Australia. Furthermore, subtropical Northern Hemisphere sites that were affected by warming during the last interglacial period are of interest. In addition to the last interglacial, the Holocene thermal maximum is of primary interest as another period warmer than the pre-industrial, as is the Common Era of the last 2,000 years as a time interval immediately preceding the period of instru-

mental observations. Older interglacials that represent time intervals of substantial warming might also provide well-preserved fossil corals, as might the last deglaciation and earlier deglaciations that are of interest to studies of tropical marine climate variability during periods of rapid warming.

In summary, ultrahigh-resolution coral proxy records provide a powerful tool for reconstructing past tropical marine climate and environmental variability and for understanding the temporal response of corals and coral reefs to ongoing climate and environmental changes. Used in conjunction with advanced statistical methods and Earth system modeling, these data can improve projections of tropical climate variability and the fates of coral reef ecosystems. 

REFERENCES

- Abram, N.J., H.V. McGregor, J.E. Tierney, M.N. Evans, N.P. McKay, D.S. Kaufman, and the Pages 2k Consortium. 2016. Early onset of industrial-era warming across the oceans and continents. *Nature* 536:411–418, <https://doi.org/10.1038/nature19082>.
- Abram, N.J., N.M. Wright, B. Ellis, B.C. Dixon, J.B. Wurtzel, M.H. England, C.C. Ummenhofer, B. Philibosian, S.Y. Cahyarini, T.-L. Yu, and others. 2020. Coupling of Indo-Pacific climate variability over the last millennium. *Nature* 579:385–392, <https://doi.org/10.1038/s41586-020-2084-4>.
- Asami, R., T. Felis, P. Deschamps, K. Hanawa, Y. Iryu, E. Bard, N. Durand, and M. Murayama. 2009. Evidence for tropical South Pacific climate change during the Younger Dryas and the Bølling-Allerød from geochemical records of fossil Tahiti corals. *Earth and Planetary Science Letters* 288:96–107, <https://doi.org/10.1016/j.epsl.2009.09.011>.
- Brocas, W.M., T. Felis, J.C. Obert, P. Gierz, G. Lohmann, D. Scholz, M. Kölling, and S.R. Scheffers. 2016. Last interglacial temperature seasonality reconstructed from tropical Atlantic corals. *Earth and Planetary Science Letters* 449:418–429, <https://doi.org/10.1016/j.epsl.2016.06.005>.
- Brocas, W.M., T. Felis, P. Gierz, G. Lohmann, M. Werner, J.C. Obert, D. Scholz, M. Kölling, and S.R. Scheffers. 2018. Last interglacial hydroclimate seasonality reconstructed from tropical Atlantic corals. *Paleoceanography and Paleoclimatology* 33:198–213, <https://doi.org/10.1002/2017PA003216>.
- Brocas, W.M., T. Felis, and M. Mudelsee. 2019. Tropical Atlantic cooling and freshening in the middle of the last interglacial from coral proxy records. *Geophysical Research Letters* 46:8,289–8,299, <https://doi.org/10.1029/2019GL083094>.
- Cahyarini, S.Y., M. Pfeiffer, O. Timm, W.-C. Dullo, and D. Garbe-Schönberg. 2008. Reconstructing seawater $\delta^{18}\text{O}$ from paired coral $\delta^{18}\text{O}$ and Sr/Ca ratios: Methods, error analysis and problems, with examples from Tahiti (French Polynesia) and

- Timor (Indonesia). *Geochimica et Cosmochimica Acta* 72:2,841–2,853, <https://doi.org/10.1016/j.gca.2008.04.005>.
- Cobb, K.M., N. Westphal, H.R. Sayani, J.T. Watson, E. Di Lorenzo, H. Cheng, R.L. Edwards, and C.D. Charles. 2013. Highly variable El Niño–Southern Oscillation throughout the Holocene. *Science* 339:67–70, <https://doi.org/10.1126/science.1228246>.
- D’Olivo, J.P., and M.T. McCulloch. 2017. Response of coral calcification and calcifying fluid composition to thermally induced bleaching stress. *Scientific Reports* 7:2207, <https://doi.org/10.1038/s41598-017-02306-x>.
- D’Olivo, J.P., D.J. Sinclair, K. Rankenburg, and M.T. McCulloch. 2018. A universal multi-trace element calibration for reconstructing sea surface temperatures from long-lived *Porites* corals: Removing ‘vital-effects.’ *Geochimica et Cosmochimica Acta* 239:109–135, <https://doi.org/10.1016/j.gca.2018.07.035>.
- DeCarlo, T.M., G.A. Gaetani, A.L. Cohen, G.L. Foster, A.E. Alpert, and J.A. Stewart. 2016. Coral Sr–U thermometry. *Paleoceanography* 31:626–638, <https://doi.org/10.1002/2015PA002908>.
- Dee, S., J. Emile-Geay, M.N. Evans, A. Allam, E.J. Steig, and D.M. Thompson. 2015. PRYSM: An open-source framework for PROXY System Modeling, with applications to oxygen-isotope systems. *Journal of Advances in Modeling Earth Systems* 7:1,220–1,247, <https://doi.org/10.1002/2015MS000447>.
- Dee, S.G., K.M. Cobb, J. Emile-Geay, T.R. Ault, R.L. Edwards, H. Cheng, and C.D. Charles. 2020. No consistent ENSO response to volcanic forcing over the last millennium. *Science* 367:1,477–1,481, <https://doi.org/10.1126/science.aax2000>.
- DeLong, K.L., T.M. Quinn, F.W. Taylor, K. Lin, and C.-C. Shen. 2012. Sea surface temperature variability in the southwest tropical Pacific since AD 1649. *Nature Climate Change* 2:799–804, <https://doi.org/10.1038/nclimate1583>.
- Emile-Geay, J., K.M. Cobb, M. Carre, P. Braconnot, J. Leloup, Y. Zhou, S.P. Harrison, T. Correge, H.V. McGregor, M. Collins, and others. 2016. Links between tropical Pacific seasonal, interannual and orbital variability during the Holocene. *Nature Geoscience* 9:168–173, <https://doi.org/10.1038/ngeo2608>.
- Felis, T., G. Lohmann, H. Kuhnert, S.J. Lorenz, D. Scholz, J. Pätzold, S.A. Al-Rousan, and S.M. Al-Moghribi. 2004. Increased seasonality in Middle East temperatures during the last interglacial period. *Nature* 429:164–168, <https://doi.org/10.1038/nature02546>.
- Felis, T., A. Suzuki, H. Kuhnert, M. Dima, G. Lohmann, and H. Kawahata. 2009. Subtropical coral reveals abrupt early-twentieth-century freshening in the western North Pacific Ocean. *Geology* 37:527–530, <https://doi.org/10.1130/G25581A1>.
- Felis, T., and N. Rambu. 2010. Mediterranean climate variability documented in oxygen isotope records from northern Red Sea corals: A review. *Global and Planetary Change* 71:232–241, <https://doi.org/10.1016/j.gloplacha.2009.10.006>.
- Felis, T., A. Suzuki, H. Kuhnert, N. Rambu, and H. Kawahata. 2010. Pacific Decadal Oscillation documented in a coral record of North Pacific winter temperature since 1873. *Geophysical Research Letters* 37:L14605, <https://doi.org/10.1029/2010GL043572>.
- Felis, T., U. Merkel, R. Asami, P. Deschamps, E.C. Hathorne, M. Kölling, E. Bard, G. Cabioch, N. Durand, M. Prange, and others. 2012. Pronounced interannual variability in tropical South Pacific temperatures during Heinrich Stadial 1. *Nature Communications* 3:965, <https://doi.org/10.1038/ncomms1973>.
- Felis, T., H.V. McGregor, B.K. Linsley, A.W. Tudhope, M.K. Gagan, A. Suzuki, M. Inoue, A.L. Thomas, T.M. Esat, W.G. Thompson, and others. 2014. Intensification of the meridional temperature gradient in the Great Barrier Reef following the Last Glacial Maximum. *Nature Communications* 5:4102, <https://doi.org/10.1038/ncomms5102>.
- Felis, T., C. Giry, D. Scholz, G. Lohmann, M. Pfeiffer, J. Pätzold, M. Kölling, and S.R. Scheffers. 2015. Tropical Atlantic temperature seasonality at the end of the last interglacial. *Nature Communications* 6:6159, <https://doi.org/10.1038/ncomms7159>.
- Felis, T., M. Ionita, N. Rambu, G. Lohmann, and M. Kölling. 2018. Mild and arid climate in the east–ern Sahara–Arabian Desert during the late Little Ice Age. *Geophysical Research Letters* 45:7,112–7,119, <https://doi.org/10.1029/2018GL078617>.
- Felis, T., and M. Mudelsee. 2019. Pacing of Red Sea deep water renewal during the last centuries. *Geophysical Research Letters* 46:4,413–4,420, <https://doi.org/10.1029/2019GL082756>.
- Fischer, H., K.J. Meissner, A.C. Mix, N.J. Abram, J. Austermann, V. Brovkin, E. Capron, D. Colombaroli, A.-L. Daniau, K.A. Dye, and others. 2018. Palaeoclimate constraints on the impact of 2°C anthropogenic warming and beyond. *Nature Geoscience* 11:474–485, <https://doi.org/10.1038/s41561-018-0146-0>.
- Freund, M.B., B.J. Henley, D.J. Karoly, H.V. McGregor, N.J. Abram, and D. Dommengot. 2019. Higher frequency of Central Pacific El Niño events in recent decades relative to past centuries. *Nature Geoscience* 12:450–455, <https://doi.org/10.1038/s41561-019-0353-3>.
- Giry, C., T. Felis, M. Kölling, and S. Scheffers. 2010. Geochemistry and skeletal structure of *Diploria strigosa*, implications for coral-based climate reconstruction. *Palaeogeography, Palaeoclimatology, Palaeoecology* 298:378–387, <https://doi.org/10.1016/j.palaeo.2010.10.022>.
- Giry, C., T. Felis, M. Kölling, D. Scholz, W. Wei, G. Lohmann, and S. Scheffers. 2012. Mid- to late Holocene changes in tropical Atlantic temperature seasonality and interannual to multidecadal variability documented in southern Caribbean corals. *Earth and Planetary Science Letters* 331–332:187–200, <https://doi.org/10.1016/j.epsl.2012.03.019>.
- Giry, C., T. Felis, M. Kölling, W. Wei, G. Lohmann, and S. Scheffers. 2013. Controls of Caribbean surface hydrology during the mid- to late Holocene: Insights from monthly resolved coral records. *Climate of the Past* 9:841–858, <https://doi.org/10.5194/cp-9-841-2013>.
- Goodkin, N.F., A. Bolton, K.A. Hughen, K.B. Karnauskas, S. Griffin, K.H. Phan, S.T. Vo, M.R. Ong, and E.R.M. Druffel. 2019. East Asian Monsoon variability since the sixteenth century. *Geophysical Research Letters* 46:4,790–4,798, <https://doi.org/10.1029/2019GL081939>.
- Grothe, P.R., K.M. Cobb, G. Liguori, E. Di Lorenzo, A. Capotondi, Y. Lu, H. Cheng, R.L. Edwards, J.R. Southon, G.M. Santos, and others. 2019. Enhanced El Niño–Southern Oscillation variability in recent decades. *Geophysical Research Letters* 47:e2019GL083906, <https://doi.org/10.1029/2019GL083906>.
- Hargreaves, J., K. DeLong, T. Felis, N. Abram, K. Cobb, and H. Sayani. 2020. Tropical ocean hydroclimate and temperature from coral archives. *PAGES Magazine* 28:29, <https://doi.org/10.22498/pages.28.1.29>.
- Hathorne, E.C., T. Felis, R.H. James, and A. Thomas. 2011. Laser ablation ICP-MS screening of corals for diagenetically affected areas applied to Tahiti corals from the last deglaciation. *Geochimica et Cosmochimica Acta* 75:1,490–1,506, <https://doi.org/10.1016/j.gca.2010.12.011>.
- Hathorne, E.C., T. Felis, A. Suzuki, H. Kawahata, and G. Cabioch. 2013a. Lithium in the aragonite skeletons of massive *Porites* corals: A new tool to reconstruct tropical sea surface temperatures. *Paleoceanography* 28:143–152, <https://doi.org/10.1029/2012PA002311>.
- Hathorne, E.C., A. Gagnon, T. Felis, J. Adkins, R. Asami, W. Boer, N. Caillon, D. Case, K.M. Cobb, E. Douville, and others. 2013b. Interlaboratory study for coral Sr/Ca and other element/Ca ratio measurements. *Geochemistry, Geophysics, Geosystems* 14:3,730–3,750, <https://doi.org/10.1002/ggge.20230>.
- Khider, D., J. Emile-Geay, N.P. McKay, Y. Gil, D. Garijo, V. Ratnakar, M. Alonso-Garcia, S. Bertrand, O. Bothe, P. Brewer, and others. 2019. PaCTS 1.0: A crowdsourced reporting standard for paleoclimate data. *Paleoceanography and Paleoclimatology* 34:1,570–1,596, <https://doi.org/10.1029/2019PA003632>.
- Lawman, A.E., J.W. Partin, S.G. Dee, C.A. Casadio, P. Di Nezio, and T.M. Quinn. 2020. Developing a coral proxy system model to compare coral and climate model estimates of changes in paleo-ENSO variability. *Paleoceanography and Paleoclimatology* 35:e2019PA003836, <https://doi.org/10.1029/2019PA003836>.
- Linsley, B.K., Y. Rosenthal, and D.W. Oppo. 2010. Holocene evolution of the Indonesian through-flow and the western Pacific warm pool. *Nature Geoscience* 3:578–583, <https://doi.org/10.1038/ngeo920>.
- Liu, Y., X. Li, Z. Zeng, H.-M. Yu, F. Huang, T. Felis, and C.-C. Shen. 2019. Annually-resolved coral skeletal $\delta^{138}\text{Ba}$ records: A new proxy for oceanic Ba cycling. *Geochimica et Cosmochimica Acta* 247:27–39, <https://doi.org/10.1016/j.gca.2018.12.022>.
- Lough, J.M. 2010. Climate records from corals. *WIREs Climate Change* 1:318–331, <https://doi.org/10.1002/wcc.39>.
- McCulloch, M.T., J.P. D’Olivo, J. Falter, M. Holcomb, and J.A. Trotter. 2017. Coral calcification in a changing World and the interactive dynamics of pH and DIC upregulation. *Nature Communications* 8:15686, <https://doi.org/10.1038/ncomms15686>.
- McGregor, H.V., M.J. Fischer, M.K. Gagan, D. Fink, S.J. Phipps, H. Wong, and C.D. Woodroffe. 2013. A weak El Niño/Southern Oscillation with delayed seasonal growth around 4,300 years ago. *Nature Geoscience* 6:949–953, <https://doi.org/10.1038/ngeo1936>.
- Obert, J.C., D. Scholz, T. Felis, W.M. Brocas, K.P. Jochum, and M.O. Andreae. 2016. $^{230}\text{Th}/\text{U}$ dating of Last Interglacial brain corals from Bonaire (southern Caribbean) using bulk and theca wall material. *Geochimica et Cosmochimica Acta* 178:20–40, <https://doi.org/10.1016/j.gca.2016.01.011>.
- PAGES Hydro2k Consortium. 2017. Comparing proxy and model estimates of hydroclimate variability and change over the Common Era. *Climate of the Past* 13:1,851–1,900, <https://doi.org/10.5194/cp-13-1851-2017>.
- Pfeiffer, M., J. Zinke, W.C. Dullo, D. Garbe-Schönberg, M. Latif, and M.E. Weber. 2017. Indian Ocean corals reveal crucial role of World War II bias for

- twentieth century warming estimates. *Scientific Reports* 7:14434, <https://doi.org/10.1038/s41598-017-14352-6>.
- Pretet, C., E. Samankassou, T. Felis, S. Reynaud, F. Böhm, A. Eisenhauer, C. Ferrier-Pagès, J.-P. Gattuso, and G. Camoin. 2013. Constraining calcium isotope fractionation ($\delta^{44}\text{Ca}$) in modern and fossil scleractinian coral skeleton. *Chemical Geology* 340:49–58, <https://doi.org/10.1016/j.chemgeo.2012.12.006>.
- Sadler, J., G.E. Webb, L.D. Nothdurft, and B. Dechnik. 2014. Geochemistry-based coral palaeoclimate studies and the potential of ‘non-traditional’ (non-massive *Porites*) corals: Recent developments and future progression. *Earth-Science Reviews* 139:291–316, <https://doi.org/10.1016/j.earscirev.2014.10.002>.
- Saenger, C., H.P. Affek, T. Felis, N. Thiagarajan, J.M. Lough, and M. Holcomb. 2012. Carbonate clumped isotope variability in shallow water corals: Temperature dependence and growth-related vital effects. *Geochimica et Cosmochimica Acta* 99:224–242, <https://doi.org/10.1016/j.gca.2012.09.035>.
- Saha, N., G.E. Webb, and J.-X. Zhao. 2016. Coral skeletal geochemistry as a monitor of inshore water quality. *Science of the Total Environment* 566–567:652–684, <https://doi.org/10.1016/j.scitotenv.2016.05.066>.
- Stevenson, S., B. Powell, K.M. Cobb, J. Nusbaumer, M. Merrifield, and D. Noone. 2018. Twentieth century seawater $\delta^{18}\text{O}$ dynamics and implications for coral-based climate reconstruction. *Paleoceanography and Paleoclimatology* 33:606–625, <https://doi.org/10.1029/2017PA003304>.
- Thompson, D.M., J.E. Cole, G.T. Shen, A.W. Tudhope, and G.A. Meehl. 2015. Early twentieth-century warming linked to tropical Pacific wind strength. *Nature Geoscience* 8:117–121, <https://doi.org/10.1038/ngeo2321>.
- Tierney, J.E., N.J. Abram, K.J. Anchukaitis, M.N. Evans, C. Giry, K.H. Kilbourne, C.P. Saenger, H.C. Wu, and J. Zinke. 2015. Tropical sea surface temperatures for the past four centuries reconstructed from coral archives. *Paleoceanography* 30:226–252, <https://doi.org/10.1002/2014PA002717>.
- Wang, X.T., A.L. Cohen, V. Luu, H. Ren, Z. Su, G.H. Haug, and D.M. Sigman. 2018. Natural forcing of the North Atlantic nitrogen cycle in the Anthropocene. *Proceedings of the National Academy of Sciences of the United States of America* 115:10,606–10,611, <https://doi.org/10.1073/pnas.1801049115>.
- Webster, J.M., J.C. Braga, M. Humblet, D.C. Potts, Y. Iryu, Y. Yokoyama, K. Fujita, R. Bourillot, T.M. Esat, S. Fallon, and others. 2018. Response of the Great Barrier Reef to sea-level and environmental changes over the past 30,000 years. *Nature Geoscience* 11:426–432, <https://doi.org/10.1038/s41561-018-0127-3>.
- Wu, H.C., T. Felis, D. Scholz, C. Giry, M. Kölling, K.P. Jochum, and S.R. Scheffers. 2017. Changes to Yucatán Peninsula precipitation associated with salinity and temperature extremes of the Caribbean Sea during the Maya civilization collapse. *Scientific Reports* 7:15825, <https://doi.org/10.1038/s41598-017-15942-0>.
- Yokoyama, Y., T.M. Esat, W.G. Thompson, A.L. Thomas, J.M. Webster, Y. Miyairi, C. Sawada, T. Aze, H. Matsuzaki, J.I. Okuno, and others. 2018. Rapid glaciation and a two-step sea level plunge into the Last Glacial Maximum. *Nature* 559:603–607, <https://doi.org/10.1038/s41586-018-0335-4>.
- Zinke, J., A. Hoell, J.M. Lough, M. Feng, A.J. Kuret, H. Clarke, V. Ricca, K. Rankenburg, and M.T. McCulloch. 2015. Coral record of south-east Indian Ocean marine heatwaves with intensified Western Pacific temperature gradient. *Nature Communications* 6:8562, <https://doi.org/10.1038/ncomms9562>.

ACKNOWLEDGMENTS

I thank guest editors Laurie Menviel, Peggy Delaney, Alan Mix, Amelia Shevenell, and Katrin Meissner, editor Ellen Kappel, and the reviewers for their constructive comments; Cyril Giry, William M. Brocas, Martin Kölling, Ed C. Hathorne, Henning Kuhnert, and Jürgen Pätzold for their contributions to the coral paleoclimatological work at MARUM (University of Bremen); and all collaborators for their contributions to previous publications. Financial support of my research was provided by the Deutsche Forschungsgemeinschaft (DFG, German Research Foundation) – Project numbers 35880301, 42307808, 180346848, 256607970, 408139156.

AUTHOR

Thomas Felis (tfelis@marum.de) is Senior Scientist, MARUM – Center for Marine Environmental Sciences, University of Bremen, Bremen, Germany.

ARTICLE CITATION

Felis, T. 2020. Extending the instrumental record of ocean-atmosphere variability into the last interglacial using tropical corals. *Oceanography* 33(2):68–79, <https://doi.org/10.5670/oceanog.2020.209>.

COPYRIGHT & USAGE

This is an open access article made available under the terms of the Creative Commons Attribution 4.0 International License (<https://creativecommons.org/licenses/by/4.0/>), which permits use, sharing, adaptation, distribution, and reproduction in any medium or format as long as users cite the materials appropriately, provide a link to the Creative Commons license, and indicate the changes that were made to the original content.

RECONSTRUCTION OF OCEAN CIRCULATION BASED ON NEODYMIUM ISOTOPIC COMPOSITION

Potential Limitations and Application to the Mid-Pleistocene Transition

By Kazuyo Tachikawa, William Rapuc, Quentin Dubois-Dauphin,
Abel Guihou, and Charlotte Skonieczny

ABSTRACT. As the ocean is Earth's largest reservoir of carbon, its circulation strongly influences the global carbon cycle. The neodymium (Nd) isotopic composition ($^{143}\text{Nd}/^{144}\text{Nd}$ or ϵ_{Nd}) of seawater has been used as a tracer for ocean circulation. We revisit the capacity of this tracer using compiled modern seawater data sets and recent data ($\leq 10,000$ years, 10 kyr) extracted from the sedimentary record. Empirical equations that predict seawater ϵ_{Nd} values from hydrography parameters can be used to evaluate possible biases in Nd isotopic ratios. The good overall agreement between measured seawater and predicted ϵ_{Nd} values confirms the usefulness of Nd isotopic composition as a tracer of large-scale deepwater circulation in many parts of the modern ocean. Offsets observed between the sedimentary record and predicted values in certain oceanic regions can be partly explained by the contribution of porewater-derived Nd to sedimentary authigenic fractions. We use Nd isotopic composition to study a major climate transition in the middle Pleistocene called the "900 ka event," which is characterized by a major perturbation in ocean carbon chemistry. All available reconstructed seawater ϵ_{Nd} data indicate an increase in isotopic composition at the 900 ka event relative to the present value in the eastern Atlantic Ocean. This shift cannot be explained solely by more active formation of southern-sourced water that has a higher ϵ_{Nd} value than the northern-sourced water. We suggest that a reduction in the Atlantic meridional overturning circulation and/or changes in Nd sources to the North Atlantic were the main cause(s) of the change in ϵ_{Nd} observed during the evolution of the Northern Hemisphere cryosphere.

INTRODUCTION

The ocean contains approximately 60 times more carbon than the atmosphere. About 20%–35% of the carbon dioxide (CO_2) emitted by burning fossil fuels has been absorbed by the ocean (Khatiwala et al., 2009). Changes in the ocean state, such as those that occurred during the last glacial maximum (LGM) and subsequent deglaciation, could significantly affect the carbon cycle by releasing absorbed carbon to the atmosphere in the future. The glacial atmospheric CO_2 concentration was lower than the pre-industrial value mainly because of

increased carbon storage in the ocean via a more active biological pump in the Southern Ocean and/or more efficient carbon storage in the strongly stratified deep ocean (Hain et al., 2010; Adkins, 2013). During the deglaciation, dissipation of old deep water that was rich in respired carbon in the Southern Ocean contributed to CO_2 release to the atmosphere by the upwelling branch of the Atlantic overturning circulation (Skinner et al., 2010).

Although proxy-based reconstructions have provided important insights into past ocean circulation, they do not always tell consistent stories because each

proxy has its own bias. Recent advances in analytical instruments and coordinated international programs such as GEOTRACES have provided abundant high-quality data and contributed to a better understanding of proxy behavior in the modern ocean. Furthermore, the spatial coverage of marine sediment cores has greatly improved over recent decades, thanks to international programs such as the Ocean Drilling Program (ODP)/International Ocean Discovery Program (IODP) and the International MARine Global change Study (IMAGES). Lastly, tremendous progress in climate modeling has revealed the physical and biogeochemical processes involved in climate variability. In particular, proxy-enabled models make it possible to simulate proxy fields, which in turn can be compared to proxy reconstructions (Arsouze et al., 2009; Menviel et al., 2012; Rempfer et al., 2012; Roche and Caley, 2013; Friedrich et al., 2014), allowing evaluation of the capacity of climate models to predict deepwater circulation changes.

The objective of this paper is to revisit the behavior of neodymium (Nd) isotopic composition of seawater as a tracer of water mass provenance and to apply this tracer to a major climate transition, the Mid-Pleistocene transition (MPT, about one million years). In the modern ocean, the Nd isotope composition of seawater follows the global thermohaline circulation (Figure 1), but factors other than water mass mixing influence its distribu-

tion. Using a compiled seawater data set and comparing it with other hydrography parameters, it is possible to identify the oceanic regions significantly affected by local Nd inputs. Processes that may modify Nd isotopic signals recorded in marine sediments are reviewed using compiled archival data. Finally, we use Nd isotopes to infer changes that occurred during the MPT.

DISTRIBUTION OF MODERN SEAWATER Nd ISOTOPIC COMPOSITION

Neodymium is among the rare earth elements (REE) that are characterized by coherent chemical and physical properties. It has seven isotopes, and one of them, ^{143}Nd , is an α -decay product of ^{147}Sm , with a half-life of 1.06×10^{11} years.

Samarium and Nd are fractionated during melting and crystallization, resulting in $^{143}\text{Nd}/^{144}\text{Nd}$ ratios that change in rocks as a function of age and lithology. Continental material is the major Nd source to the ocean (Figure 2), and the seawater Nd isotopic signature reflects the $^{143}\text{Nd}/^{144}\text{Nd}$ values of continents surrounding the ocean basins. Because of the relatively small range of $^{143}\text{Nd}/^{144}\text{Nd}$, the isotopic ratio is typically expressed by the notation ϵ_{Nd} .

$$\epsilon_{\text{Nd}} = \left[\frac{(^{143}\text{Nd}/^{144}\text{Nd})_{\text{sample}}}{(^{143}\text{Nd}/^{144}\text{Nd})_{\text{CHUR}}} - 1 \right] \times 10^4,$$

where CHUR is a chondritic uniform reservoir with a $^{143}\text{Nd}/^{144}\text{Nd}$ ratio of 0.512638 (Jacobsen and Wasserburg, 1980) or of 0.512630 (Bouvier et al., 2008). The advantages of the Nd isotopic composi-

tion of seawater, as compared to the carbon isotopic composition ($^{13}\text{C}/^{12}\text{C}$ or $\delta^{13}\text{C}$) of seawater, another frequently used water mass tracer, is that the former experiences negligible biological fractionation and is not influenced by air-sea exchange.

In modern deep waters ($\geq 1,500$ m), the lowest ϵ_{Nd} values of about -15 are found in an area surrounded by an old craton in the Labrador Sea and area. In contrast, the highest values close to 0 are observed in tropical and North Pacific waters as a result of abundant young volcanogenic material found there (Jeandel et al., 2007; Figure 1). The Southern Ocean and Indian Ocean present deep-water ϵ_{Nd} values intermediate between the North Atlantic and the tropical and North Pacific Oceans, which is consistent with the pattern of global thermo-

FIGURE 1. Distribution of deepwater Nd isotopic composition in the modern ocean (Tachikawa et al., 2017) and schematized global thermohaline circulation (Broecker, 1991). The colored dots indicate ϵ_{Nd} values at 1,500 m depth in the water column or at a water depth closest to 1,500 m but deeper than 1,500 m if ϵ_{Nd} data are not available. The blue and the red curves indicate deep and surface flows, respectively. The figure was created using Ocean Data View (ODV; Schlitzer, 2015).

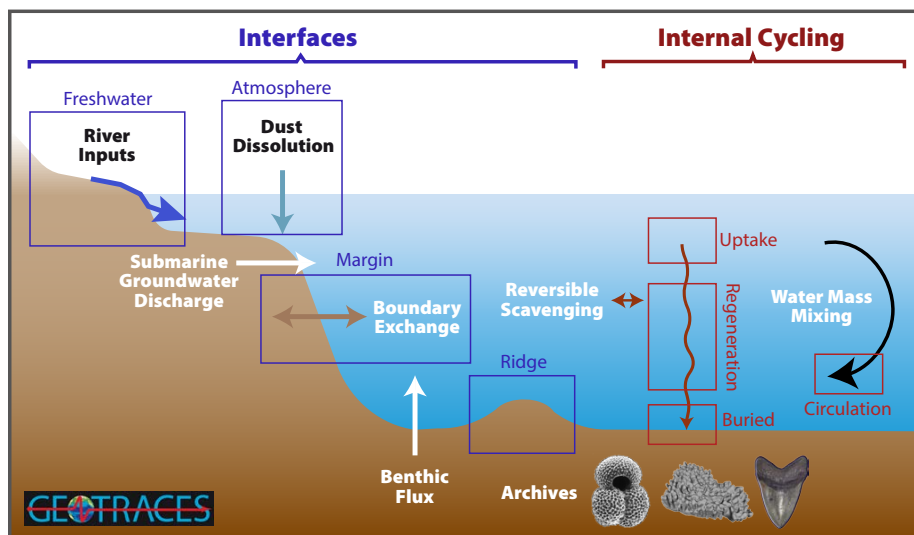
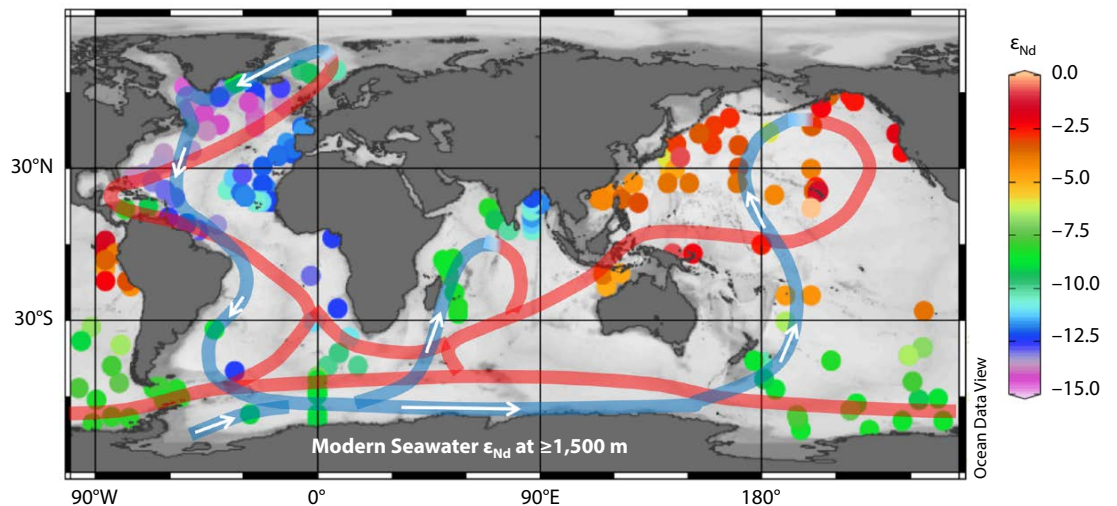


FIGURE 2. Neodymium sources and processes affecting oceanic Nd concentration and isotopic composition as well as possible marine sedimentary records of Nd isotopic composition. Figure based on data from GEOTRACES (<http://www.geotraces.org/>) modified to summarize the oceanic Nd cycle.

haline circulation (Figure 1). The spatial heterogeneity of deepwater ϵ_{Nd} values is also coherent with the estimated residence time of Nd in the ocean of 360 to 700 years (Tachikawa et al., 2003; Siddall et al., 2008; Rempfer et al., 2011), less than the mean mixing time of the deep ocean, which is about 1,500 years in the modern ocean (Broecker and Peng, 1982).

Net Nd sources to the ocean include partial dissolution of atmospheric inputs and of river sediments as well as river water after Nd removal in estuaries (Tachikawa et al., 2003; Figure 2). In reconciling both Nd concentration and isotopic distribution, water-sediment interaction along continental margins, called “boundary exchange,” has been considered the most important Nd source to the ocean (Lacan and Jeandel, 2005; Arsouze et al., 2009; Rempfer et al., 2012).

The precise mechanism of boundary exchange, however, has not yet been fully identified, and it may include submarine groundwater discharge (Johannesson and Burdige, 2007) as well as benthic flux (Abbott et al., 2019, and references therein). In the open ocean, away from continental inputs, reverse scavenging transports Nd isotopic signatures vertically from shallower toward deeper water masses by dissolved/particulate interaction (Bertram and Elderfield, 1993; Figure 2). Even if this process is essential for producing observed depth profiles of seawater Nd concentration, the main control on deepwater ϵ_{Nd} values in the open ocean is estimated to be the mixing of water masses characterized by distinct isotopic signatures (von Blanckenburg, 1999; Frank, 2002; van de Flierdt et al., 2016; Tachikawa et al., 2017).

IS Nd ISOTOPIC COMPOSITION A RELIABLE TRACER OF OCEAN CIRCULATION?

In order to identify oceanic regions significantly affected by local/regional lithogenic inputs that may mask water mass mixing effects, a compiled deepwater ϵ_{Nd} database was compared with the values derived from empirical equations that predict seawater ϵ_{Nd} from hydrography parameters (temperature, salinity, concentration of silicate, phosphate, and oxygen; Tachikawa et al., 2017). Assuming that the offset from the predicted values indicates the local/regional lithogenic influence on deepwater ϵ_{Nd} values, regions with strong local/regional effects were compared with the open ocean (Figure 3a,b). The most striking global feature is the positive offset in the tropical Pacific (Figure 3a,b) that is due to the

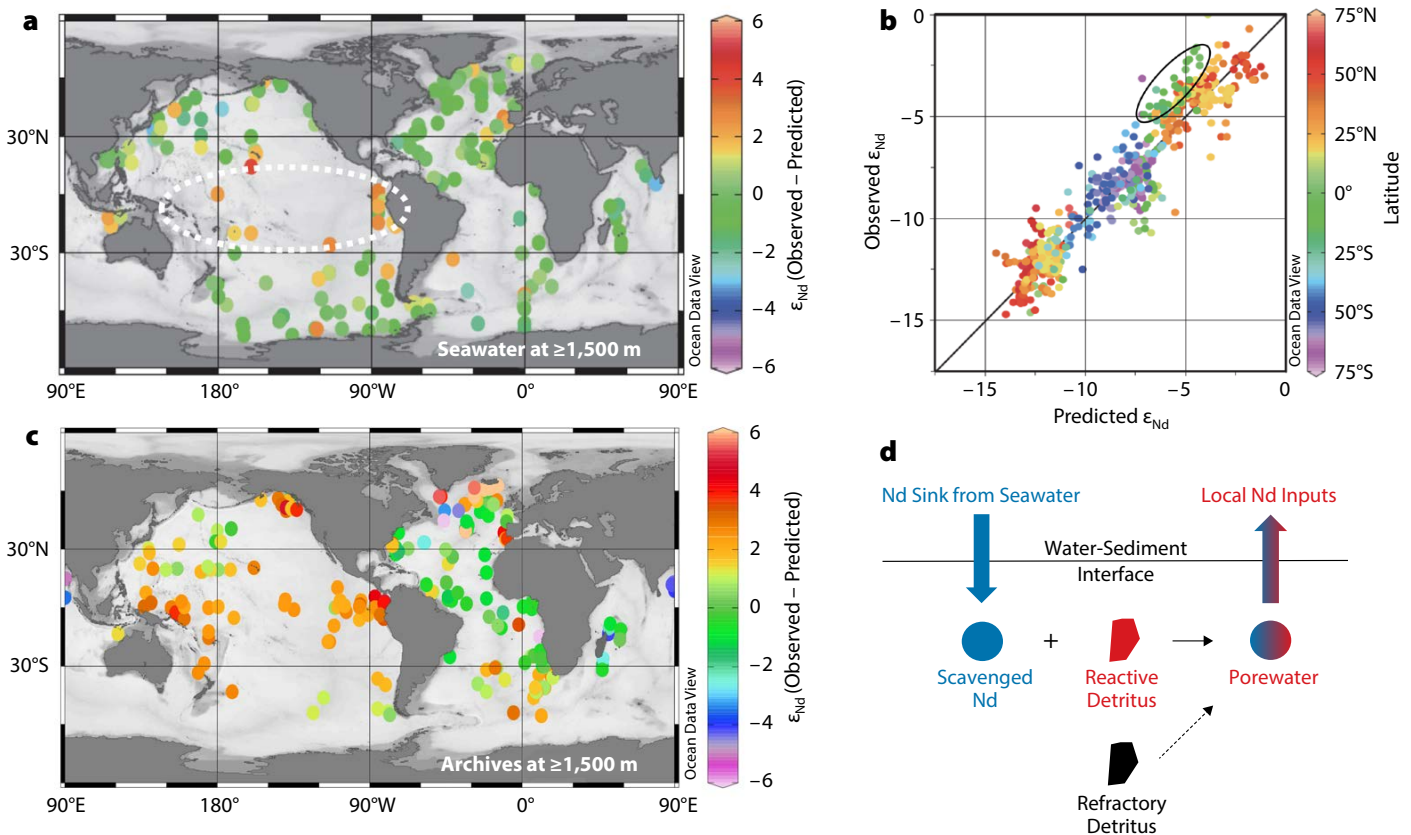


FIGURE 3. Comparison of observed and predicted values for Nd isotopic composition. (a) Spatial distribution of ϵ_{Nd} offsets between modern deepwater ($\geq 1,500$ m depth) and predicted values using empirical equations (Tachikawa et al., 2017). (b) Relationship between measured deepwater Nd isotopic composition and predicted values. (c) Spatial distribution of ϵ_{Nd} offsets between archived Holocene (≤ 10 kyr) sediments and predicted seawater values. (d) Schematic presentation showing the porewater Nd contribution that creates ϵ_{Nd} offsets between archival and predicted values. The white dashed ellipse in (a) and the black solid ellipse in (b) indicate the observed ϵ_{Nd} offsets in the tropical Pacific. (a), (b), and (c) are adapted from Tachikawa et al. (2017) and (d) is adapted from Du et al. (2016)

strong influence of boundary exchange (Lacan and Jeandel, 2001; Grenier et al., 2013). In this region, abundant labile volcanogenic matter releases radiogenic Nd to deep water. Moreover, the deep water in this area is poorly ventilated, increasing the importance of local Nd sources relative to water mass mixing effects.

Predicted ϵ_{Nd} seawater signatures can be compared to marine archives of fish teeth/debris, deep-sea corals, and authigenic fractions associated with foraminiferal tests or bulk sediments (Tachikawa et al., 2017; Figure 3c). The archival ϵ_{Nd} values from the major part of the Atlantic Ocean (except for the northern North Atlantic; Elmore et al., 2011) show general agreement with the predicted values, suggesting that this proxy is reliable. In contrast, some areas of the Pacific Ocean are characterized by positive offsets (Figure 3c). One possible reason for the offsets is the contribution of porewater Nd (Du et al., 2016; Skinner et al., 2019) that is more evident in the Pacific because the Nd isotopic composition of porewater could be significantly higher than that of the bottom water (Figure 3d). The detrital fraction can contain exchangeable Nd such as volcanogenic matter, Fe-Mn coating, and clay minerals that release Nd to porewater during early diagenesis (Abbott et al., 2019; Du et al., 2016).

It is possible that the predicted ϵ_{Nd} values do not perfectly represent bottom water isotopic composition because the equations are based on empirical relationships established using limited seawater data. Nevertheless, a possible porewater Nd contribution should be taken into account in the interpretation of Nd isotopic composition, in particular, at sites where recent marine sediment values significantly differ from the seawater values. Additional process studies and further modeling efforts are required to better understand the possible contribution of local Nd inputs to the ocean. For paleoceanography studies, a multiproxy approach is recommended to obtain robust reconstructions. If proxy response diverges from predicted values,

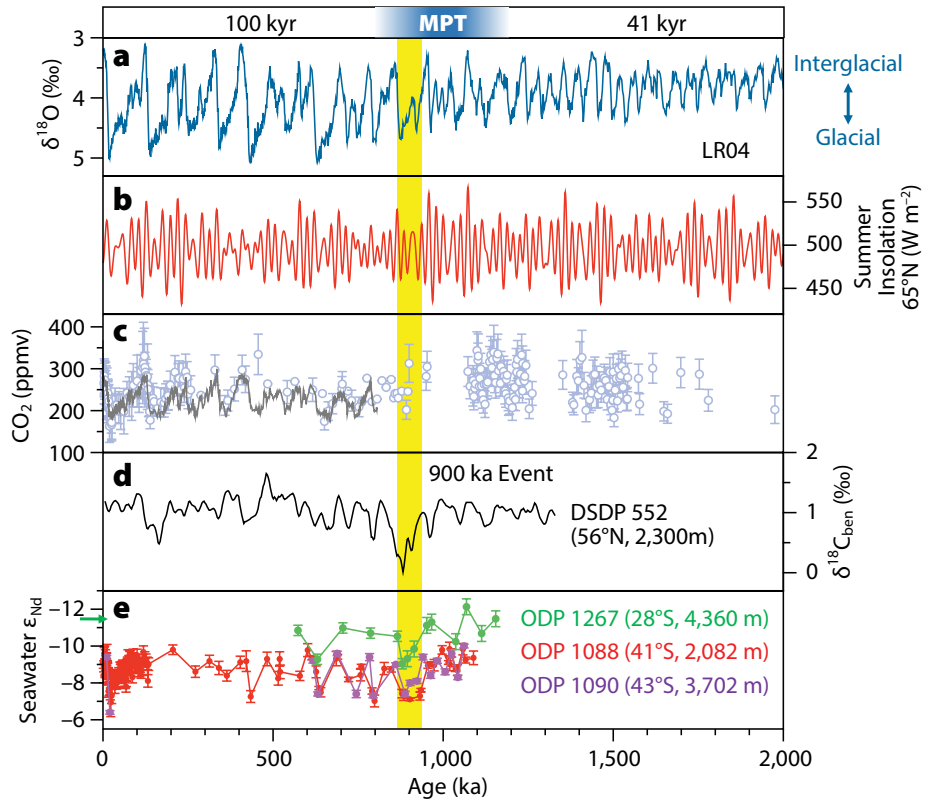


FIGURE 4. Variability across the Mid-Pleistocene transition (MPT). (a) Stack of benthic foraminiferal oxygen isotopic composition ($\delta^{18}O$) over the last 2 million years (Lisiecki and Raymo, 2005) as an indicator of glacial/interglacial cycles. (b) Summer insolation at $65^{\circ}N$ over the last 2 million years (Laskar et al., 2004). (c) Reconstructed atmospheric CO_2 concentration (Hönisch et al., 2009; Bereiter et al., 2015; Higgins et al., 2015; Chalk et al., 2017; Dyez et al., 2018). (d) Benthic foraminiferal carbon isotopic composition ($\delta^{13}C$) record of core from Deep Sea Drilling Project (DSDP) site 552 from the northern Northeast Atlantic ($56^{\circ}N$, $23^{\circ}W$, 2,300 m water depth) over the past 1.3 million years (Raymo et al., 1990) as an example of oceanic $\delta^{13}C$ changes. (e) Previously published seawater ϵ_{Nd} records across the Mid-Pleistocene transition at three sites in the eastern Atlantic: Ocean Drilling Program (ODP) sites 1088 ($41^{\circ}S$, $13^{\circ}E$, 2,080 m) and 1090 ($43^{\circ}S$, $9^{\circ}E$, 3,700 m), and ODP site 1267 ($28^{\circ}S$, $2^{\circ}E$, 4,400 m). Data are from Dausmann et al. (2017); Farmer et al. (2019); Howe et al. (2016); Hu et al., 2016; Pena and Goldstein (2014). The green arrow along the y-axis indicates the present-day seawater ϵ_{Nd} value estimated by the empirical equation using temperature and dissolved oxygen concentration (Tachikawa et al., 2017). The yellow band indicates the “900 ka event.”

a better understanding of proxy behavior will provide new insights into overlooked processes.

CLIMATE TRANSITION DURING THE MID-PLEISTOCENE AND POSSIBLE OCEAN CIRCULATION CHANGES

In this final section, we reconstruct seawater ϵ_{Nd} by studying cores from the eastern Atlantic in order to obtain insight into the role of ocean circulation changes during the MPT (1,200–800 kyr; Figure 4). The MPT is marked by an amplification of the glacial/interglacial cycle with the development of longer and more severe glacial periods and a shift

from a 41 kyr to a 100 kyr cycle (Clark et al., 2006) (Figure 4a). Because insolation forcing does not explain such changes (Figure 4b), internal feedbacks are of primary importance.

Among possible mechanisms explaining the MPT, one hypothesis is regolith removal that allowed the formation of thicker and more stable ice sheets by increasing basal stability (Clark et al., 2006) and subsequent atmospheric circulation changes. A recent study suggests that changes in ice sheet dynamics alone could not explain the MPT and that the combination of regolith removal and reduced atmospheric CO_2 concentration by an efficient biological carbon

pump was necessary (Chalk et al., 2017). In addition to the biological pump, the development of Southern Ocean stratification during glacial periods between 900 ka and 600 ka was suggested as a physical mechanism that permitted the storage of more carbon in the deep ocean and resulted in colder and longer glacials (Hasenfratz et al., 2019). To date, a precise evaluation of the carbon cycle at this transition is not possible because of the scarcity of atmospheric CO₂ reconstruction for the MPT (Hönisch et al., 2009; Bereiter et al., 2015; Higgins et al., 2015; Chalk et al., 2017; Dyez et al., 2018; Figure 4c). Regarding ocean circulation,

benthic foraminiferal δ¹³C records show a prominent decrease centered at 900 ka, called the “900 ka event” on the global scale (Raymo et al., 1990; Clark et al., 2006; Figure 4d). This change is considered to be a major perturbation of oceanic carbon chemistry.

In order to investigate the ocean circulation changes at the 900 ka event, seawater ε_{Nd} values were reconstructed at ODP sites 1267 (28°S, 4,400 m water depth), 1088 (41°S, 2,080 m water depth), and 1090 (43°S, 3,700 m water depth) (Pena and Goldstein, 2014; Farmer et al., 2019) in the southeastern Atlantic (Figures 4e and 5a,b). We combine

these ε_{Nd} records with other reported data at ODP sites 1088 (Hu et al., 2016; Dausmann et al., 2017) and 1090 (Howe et al., 2016) to extract the main features. ODP site 1267 is located north of Walvis Ridge where a bathymetric barrier minimizes the southern-sourced deep-water contribution to the basin. Thus, it is mostly influenced by North Atlantic Deep Water (NADW; Farmer et al., 2019). In contrast, ODP sites 1088 and 1090 are currently bathed by the southern-sourced water masses, Upper Circumpolar Deep Water (UCDW) and Lower Circumpolar Deep Water (LCDW), with a possible contribution of Antarctic Bottom Water

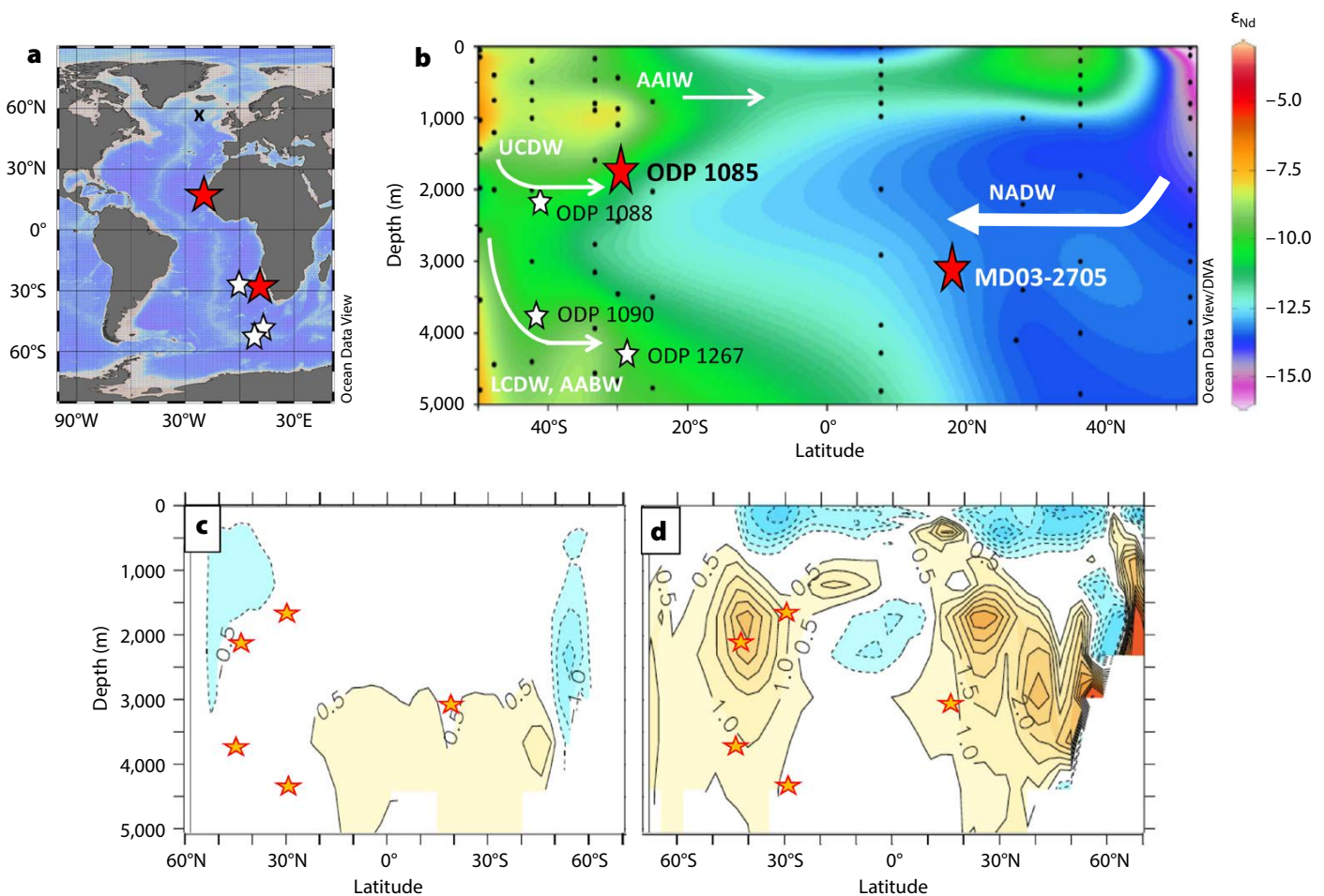


FIGURE 5. Reconstructed seawater ε_{Nd} records from the eastern Atlantic. (a) Core location map in the Atlantic Ocean. The two red stars indicate cores from MD03-2705 (18°N, 21°W, 3,085 m water depth) and ODP site 1085 (29°S, 14°E, 1,725 m) studied here. The three white stars indicate the sites of previous studies: ODP sites 1088, 1090, and 1267. The black x shows DSDP site 552. (b) Latitudinal transect of present-day seawater ε_{Nd} values in the Atlantic Ocean (Howe et al., 2016) with the main water masses: NADW = North Atlantic Deep Water; UCDW and LCDW = Upper and Lower Circumpolar Deep Water, AABW = Antarctic Bottom Water, AAIW = Antarctic Intermediate Water. More seawater ε_{Nd} data are available GEOTRACES IDP2017 (<https://www.bodc.ac.uk/geotraces/data/idp2017/>). (c) Comparison between reconstructed and zonally averaged simulated seawater ε_{Nd} anomalies in the case of enhanced southern-sourced water formation. The orange stars mark the sites of reconstructed seawater ε_{Nd} with positive anomalies at the 900 ka event. Orange and blue shading corresponds to oceanic zones characterized by positive and negative simulated ε_{Nd} anomalies. (d) The same as (c) in the case of reduced northern-sourced water formation. The simulation results are from Friedrich et al., 2014.

(AABW) at 1090 (Figure 5b). Reflecting these water masses, the present-day ϵ_{Nd} value at ODP site 1267 is lower than those at sites 1088 and 1090, and the difference has been maintained for the past 1,200 ka (Figure 4e). In general, glacial ϵ_{Nd} values are higher than interglacial values, and smaller glacial/interglacial ϵ_{Nd} amplitude is observed at the three sites before the 900 ka event compared with the period after the MPT. At the 900 ka event, the reconstructed Nd isotopic composition is as high as in more recent glacial values. We define the high ϵ_{Nd} values at the 900 ka event relative to the modern isotopic ratio as ϵ_{Nd} anomalies.

If we assume that the observed ϵ_{Nd} shift is produced by circulation changes alone, a possible explanation is either a reduction in the formation of northern-sourced water or enhanced formation of southern-sourced water. To evaluate these possibilities, we compare the distribution of the reconstructed ϵ_{Nd} anomalies at the 900 ka event with simulated zonally averaged modeled Nd isotope anomalies using an Earth system model of intermediate complexity LOVECLIM (Friedrich et al., 2014; Figure 5c,d). The enhanced southern-sourced water formation and the reduction in northern-sourced water formation were simulated by removal of

in Nd isotopic composition at the 900 ka event can be explained by changes in Nd sources to the North Atlantic that have higher ϵ_{Nd} values. The northern-sourced water mass with higher ϵ_{Nd} values may have been transported toward the South Atlantic if the Atlantic meridional overturning circulation was not completely shut down. We may infer this possibility by comparing the 900 ka event with the LGM state. The 900 ka event is the first time over the past 1,200 ka when seawater ϵ_{Nd} values were as high as the isotopic ratio of more recent glacial periods including the LGM (Figure 4e), and it is when the first drop in sea level com-

“ The increase in high-quality data concerning seawater Nd isotopic composition in the modern ocean confirms the capacity of this proxy to trace large-scale ocean circulation patterns. ”

We extended the spatial coverage of ϵ_{Nd} anomalies at the 900 ka event by adding two new cores, MD03-2705 (18°N, 3,090 m water depth) and ODP 1085 (29°S, 1,730 m water depth) from the Northeast and Southeast Atlantic (Figure 5a,b). In the modern ocean, the location of core MD03-2705 is occupied by NADW, whereas the core from ODP site 1085 is located at the boundary between NADW and UCDW, with a higher ϵ_{Nd} value (Figure 5b). It is worth mentioning that ϵ_{Nd} values reconstructed from eastern Atlantic Holocene sediment archives generally agree with predicted seawater values (Figure 3c). Our new results and previous studies all indicate positive ϵ_{Nd} anomalies at the 900 ka event. The details of new records are combined with epibenthic foraminiferal stable isotope records and modeling experiments in recent work of author Tachikawa and colleagues.

fresh water from the Southern Ocean and input of excess fresh water to the North Atlantic (Friedrich et al., 2014). The simulation indicates that enhanced deep-water formation in the Southern Ocean has little impact on the ϵ_{Nd} values of intermediate and deep waters in the Atlantic Ocean (Figure 5c), whereas reduced NADW formation increases the seawater Nd isotopic signature in the major part of the Atlantic basin deeper than 1,000 m (Figure 5d). Comparison of the seawater ϵ_{Nd} distribution pattern between the simulated and the reconstructed anomalies clearly demonstrates that the reduction in northern-sourced water formation better explains the change in seawater ϵ_{Nd} . A source for excess freshwater is still to be elucidated. Perturbation of surface hydrology associated with the evolution of the Northern Hemisphere cryosphere could be a key process.

Alternatively, the observed increase

parable to that of the post-MPT glacial levels occurred (Figure 4a). The ϵ_{Nd} value of northern-sourced water has been assumed to be constant during the late Pleistocene glacial/interglacial cycles, but several modeling studies suggest the possibility of a more radiogenic glacial Nd isotopic ratio for northern-sourced water (Arsouze et al., 2008; Menviel et al., 2020). For instance, the contribution of Labrador Sea water with a very low ϵ_{Nd} value (Figure 1) to the northern-sourced water might have declined during the LGM because of sea ice coverage that prevented deep convection in the Labrador Sea, leading to a higher ϵ_{Nd} value in northern-sourced water (Arsouze et al., 2008). If such a modification of northern-sourced water occurred, seawater ϵ_{Nd} becomes generally more radiogenic in both reduced NADW and enhanced Southern Ocean deepwater formation cases (recent work of author Tachikawa

and colleagues). This hypothesis should be further examined with direct evidence for changes in the deepwater convection zone in the North Atlantic at the 900 ka event and reconstruction of sea ice configuration at that period.

The evolution of the Northern Hemisphere cryosphere is estimated to have been involved in the mechanism of the 900 ka event either via reduced deepwater formation or changes in Nd sources to the North Atlantic. Better spatial coverage of records including data from the different ocean basins and the combination of Nd isotopic composition with other proxies will further clarify the processes involved.

CONCLUSIONS

The increase in high-quality data concerning seawater Nd isotopic composition in the modern ocean confirms the capacity of this proxy to trace large-scale ocean circulation patterns. The tropical Pacific Ocean, which is potentially affected by regional/local lithogenic Nd inputs, is characterized by the presence of labile volcanogenic matter and less than vigorous bottom water circulation. The ϵ_{Nd} offsets between the sedimentary record and predicted values can be explained at least partly by a porewater Nd contribution of diagenetic origin that varies spatially.

At the 900 ka event, the eastern Atlantic records indicate a positive shift in the reconstructed seawater ϵ_{Nd} values relative to the modern values in both the northern and the southern basins. This shift can be explained either by a reduction in North Atlantic Deep Water formation and/or by changes in the Nd source to the North Atlantic with higher ϵ_{Nd} values relative to the evolution of the Northern Hemisphere cryosphere. More active southern-sourced water formation alone cannot account for the observed changes in Nd isotopic composition. 

REFERENCES

- Abbott, A.N., S. Löhner, and M. Trethewey. 2019. Are clay minerals the primary control on the oceanic Rare Earth Element budget? *Frontiers in Marine Science* 6:504, <https://doi.org/10.3389/fmars.2019.00504>.
- Adkins, J.F. 2013. The role of deep ocean circulation in setting glacial climates. *Paleoceanography* 28(3):539–561, <https://doi.org/10.1002/palo.20046>.
- Arsouze, T., J.C. Dutay, M. Gageyama, F. Lacan, R. Alkama, O. Marti, and C. Jeandel. 2008. A modeling sensitivity study of the influence of the Atlantic meridional overturning circulation on neodymium isotopic composition at the Last Glacial Maximum. *Climate of the Past* 4(3):191–203, <https://doi.org/10.5194/cp-4-191-2008>.
- Arsouze, T., J.C. Dutay, F. Lacan, and C. Jeandel. 2009. Reconstructing the Nd oceanic cycle using a coupled dynamical, biogeochemical model. *Biogeosciences* 6(12):2,829–2,846, <https://doi.org/10.5194/bg-6-2829-2009>.
- Bereiter, B., S. Eggelston, J. Schmitt, C. Nehrbaas-Ahles, T.F. Stocker, H. Fischer, S. Kipfstuhl, and J. Chappellaz. 2015. Revision of the EPICA Dome C CO₂ record from 800 to 600 kyr before present. *Geophysical Research Letters* 42(2):2014GL061957, <https://doi.org/10.1002/2014GL061957>.
- Bertram, C.J., and H. Elderfield. 1993. The geochemical balance of the rare earth elements and Nd isotopes in the oceans. *Geochimica et Cosmochimica Acta* 57:1,957–1,986.
- Bouvier, A., J.D. Verwoort, and P.J. Patchett. 2008. The Lu–Hf and Sm–Nd isotopic composition of CHUR: Constraints from unequilibrated chondrites and implications for the bulk composition of terrestrial planets. *Earth and Planetary Science Letters* 273(1–2):48–57, <https://doi.org/10.1016/j.epsl.2008.06.010>.
- Broecker, W. 1991. The great ocean conveyor. *Oceanography* 4(2):79–89, <https://doi.org/10.5670/oceanog.1991.07>.
- Broecker, W.S., and T.H. Peng. 1982. *Tracers in the Sea*. Lamont-Doherty Geological Observatory, Columbia University, Palisades, NY, 243 pp.
- Chalk, T.B., M.P. Hain, G.L. Foster, E.J. Rohling, P.F. Sexton, M.P.S. Badger, S.G. Cherry, A.P. Hasenfratz, G.H. Haug, S.L. Jaccard, and others. 2017. Causes of ice age intensification across the Mid-Pleistocene Transition. *Proceedings of the National Academy of Sciences of the United States of America* 114(50):13,114–13,119, <https://doi.org/10.1073/pnas.1702143114>.
- Clark, P.U., D. Archer, D. Pollard, J.D. Blum, J.A. Rial, V. Brovkin, A.C. Mix, N.G. Piasias, and M. Roy. 2006. The middle Pleistocene transition: Characteristics, mechanisms, and implications for long-term changes in atmospheric pCO₂. *Quaternary Science Reviews* 25(23–24):3,150–3,184, <https://doi.org/10.1016/j.quascirev.2006.07.008>.
- Dausmann, V., M. Frank, M. Gutjahr, and J. Rickli. 2017. Glacial reduction of AMOC strength and long-term transition in weathering inputs into the Southern Ocean since the mid-Miocene: Evidence from radiogenic Nd and Hf isotopes. *Paleoceanography* 32(3):265–283, <https://doi.org/10.1002/2016PA003056>.
- Du, J., B.A. Haley, and A.C. Mix. 2016. Neodymium isotopes in authigenic phases, bottom waters and detrital sediments in the Gulf of Alaska and their implications for paleo-circulation reconstruction. *Geochimica et Cosmochimica Acta* 193:14–35, <https://doi.org/10.1016/j.gca.2016.08.005>.
- Dyez, K.A., B. Hönisch, and G.A. Schmidt. 2018. Early Pleistocene obliquity-scale pCO₂ variability at ~1.5 million years ago. *Paleoceanography and Paleoclimatology* 33(11):1,270–1,291, <https://doi.org/10.1029/2018PA003349>.
- Elmore, A.C., A.M. Piotrowski, J.D. Wright, and A.E. Scrivner. 2011. Testing the extraction of past seawater Nd isotopic composition from North Atlantic deep sea sediments and foraminifera. *Geochemistry, Geophysics, Geosystems* 12(9):Q09008, <https://doi.org/10.1029/2011gc003741>.
- Farmer, J.R., B. Hönisch, L.L. Haynes, D. Kroon, S. Jung, H.L. Ford, M.E. Raymo, M. Jaume-Seguí, D.B. Bell, S.L. Goldstein, and others. 2019. Deep Atlantic Ocean carbon storage and the rise of 100,000-year glacial cycles. *Nature Geoscience* 12(5):355–360, <https://doi.org/10.1038/s41561-019-0334-6>.
- Frank, M. 2002. Radiogenic isotopes: Tracers of past ocean circulation and erosional input. *Reviews of Geophysics* 40(1):1–138, <https://doi.org/10.1029/2000RG000094>.
- Friedrich, T., A. Timmermann, T. Stichel, and K. Pahnke. 2014. Ocean circulation reconstructions from ϵ_{Nd} : A model-based feasibility study. *Paleoceanography* 29(11):1,003–1,023, <https://doi.org/10.1002/2014PA002658>.
- Grenier, M., C. Jeandel, F. Lacan, D. Vance, C. Venchiarutti, A. Cros, and S. Cravatte. 2013. From the subtropics to the central equatorial Pacific Ocean: Neodymium isotopic composition and Rare Earth Element concentration variations. *Journal of Geophysical Research* 118(2):592–618, <https://doi.org/10.1029/2012jc008239>.
- Hain, M.P., D.M. Sigman, and G.H. Haug. 2010. Carbon dioxide effects of Antarctic stratification, North Atlantic Intermediate Water formation, and subantarctic nutrient drawdown during the last ice age: Diagnosis and synthesis in a geochemical box model. *Global Biogeochemical Cycles* 24(4):GB4023, <https://doi.org/10.1029/2010gb003790>.
- Hasenfratz, A.P., S.L. Jaccard, A. Martínez-García, D.M. Sigman, D.A. Hodell, D. Vance, S.M. Bernasconi, H.F. Kleiven, F.A. Haumann, and G.H. Haug. 2019. The residence time of Southern Ocean surface waters and the 100,000-year ice age cycle. *Science* 363(6431):1,080–1,084, <https://doi.org/10.1126/science.aat7067>.
- Higgins, J.A., A.V. Kurbatov, N.E. Spaulding, E. Brook, D.S. Introne, L.M. Chimiak, Y. Yan, P.A. Mayewski, and M.L. Bender. 2015. Atmospheric composition 1 million years ago from blue ice in the Allan Hills, Antarctica. *Proceedings of the National Academy of Sciences of the United States of America* 112(22):6,887–6,891, <https://doi.org/10.1073/pnas.1420232112>.
- Hönisch, B., N.G. Hemming, D. Archer, M. Siddall, and J.F. McManus. 2009. Atmospheric carbon dioxide concentration across the Mid-Pleistocene Transition. *Science* 324(5934):1,551–1,554, <https://doi.org/10.1126/science.1171477>.
- Howe, J.N.W., A.M. Piotrowski, T.L. Noble, S. Mulitza, C.M. Chiessi, and G. Bayon. 2016. North Atlantic Deep Water production during the Last Glacial Maximum. *Nature Communications* 7:11765, <https://doi.org/10.1038/ncomms11765>.
- Hu, R., T.L. Noble, A.M. Piotrowski, I.N. McCave, H.C. Bostock, and H.L. Neil. 2016. Neodymium isotopic evidence for linked changes in Southeast Atlantic and Southwest Pacific circulation over the last 200 kyr. *Earth and Planetary Science Letters* 455:106–114, <https://doi.org/10.1016/j.epsl.2016.09.027>.
- Jacobsen, S.B., and G.J. Wasserburg. 1980. Sm–Nd isotopic evolution of chondrites. *Earth and Planetary Science Letters* 50:139–155, [https://doi.org/10.1016/0012-821X\(80\)90125-9](https://doi.org/10.1016/0012-821X(80)90125-9).
- Jeandel, C., T. Arsouze, F. Lacan, P. Téchine, and J.-C. Dutay. 2007. Isotopic Nd compositions and concentrations of the lithogenic inputs into

- the ocean: A compilation, with an emphasis on the margins. *Chemical Geology* 239:156–164, <https://doi.org/10.1016/j.chemgeo.2006.11.013>.
- Johannesson, K.H., and D.J. Burdige. 2007. Balancing the global oceanic neodymium budget: Evaluating the role of groundwater. *Earth and Planetary Science Letters* 253(1–2):129–142, <https://doi.org/10.1016/j.epsl.2006.10.021>.
- Khatiwala, S., F. Primeau, and T. Hall. 2009. Reconstruction of the history of anthropogenic CO₂ concentrations in the ocean. *Nature* 462(7271):346–349, <https://doi.org/10.1038/nature08526>.
- Lacan, F., and C. Jeandel. 2001. Tracing Papua New Guinea imprint on the central equatorial Pacific Ocean using neodymium isotopic compositions and Rare Earth Element concentrations. *Earth and Planetary Science Letters* 186:497–512, [https://doi.org/10.1016/S0012-821X\(01\)00263-1](https://doi.org/10.1016/S0012-821X(01)00263-1).
- Lacan, F., and C. Jeandel. 2005. Neodymium isotopes as a new tool for quantifying exchange fluxes at the continent-ocean interface. *Earth and Planetary Science Letters* 232(3–4):245–257, <https://doi.org/10.1016/j.epsl.2005.01.004>.
- Laskar, J., P. Robutel, F. Joutel, M. Gastineau, A.C.M. Correia, and B. Levrard. 2004. A long-term numerical solution for the insolation quantities of the Earth. *Astronomy & Astrophysics* 428:261–285, <https://doi.org/10.1051/0004-6361:20041335>.
- Lisiecki, L.E., and M.E. Raymo. 2005. A Pliocene-Pleistocene stack of 57 globally distributed benthic δ¹⁸O records. *Paleoceanography* 20, <https://doi.org/10.1029/2004PA001071>.
- Menviel, L., F. Joos, and S.P. Ritz. 2012. Simulating atmospheric CO₂, ¹³C and the marine carbon cycle during the last glacial-interglacial cycle: Possible role for a deepening of the mean remineralization depth and an increase in the oceanic nutrient inventory. *Quaternary Science Reviews* 56(0):46–68, <https://doi.org/10.1016/j.quascirev.2012.09.012>.
- Menviel, L.C., P. Spence, L.C. Skinner, K. Tachikawa, T. Friedrich, L. Missiaen, and J. Yu. 2020. Enhanced mid-depth southward transport in the northeast Atlantic at the Last Glacial Maximum despite a weaker AMOC. *Paleoceanography and Paleoclimatology* 35(2):e2019PA003793, <https://doi.org/10.1029/2019PA003793>.
- Pena, L.D., and S.L. Goldstein. 2014. Thermohaline circulation crisis and impacts during the mid-Pleistocene transition. *Science* 345(6194):318–322, <https://doi.org/10.1126/science.1249770>.
- Raymo, M.E., W.F. Ruddiman, N.J. Shackleton, and D.W. Oppo. 1990. Evolution of Atlantic-Pacific δ¹³C gradients over the last 2.5 my. *Earth and Planetary Science Letters* 97(3):353–368, [https://doi.org/10.1016/0012-821X\(90\)90051-X](https://doi.org/10.1016/0012-821X(90)90051-X).
- Rempfer, J., T.F. Stocker, F. Joos, J.-C. Dutay, and M. Siddall. 2011. Modelling Nd-isotopes with a coarse resolution ocean circulation model: Sensitivities to model parameters and source/sink distributions. *Geochimica Et Cosmochimica Acta* 75(20):5,927–5,950, <https://doi.org/10.1016/j.gca.2011.07.044>.
- Rempfer, J., T.F. Stocker, F. Joos, and J.-C. Dutay. 2012. On the relationship between Nd isotopic composition and ocean overturning circulation in idealized freshwater discharge events. *Paleoceanography* 27(3):PA3211, <https://doi.org/10.1029/2012pa002312>.
- Roche, D.M., and T. Caley. 2013. δ¹⁸O water isotope in the iLOVECLIM model (version 1.0) – Part 2: Evaluation of model results against observed δ¹⁸O in water samples. *Geoscientific Model Development* 6(5):1,493–1,504, <https://doi.org/10.5194/gmd-6-1493-2013>.
- Schlitzer, R. 2015. Ocean data view, <http://odv.awi.de>.
- Siddall, M., S. Khatiwala, T. van de Flierdt, K. Jones, S.L. Goldstein, S. Hemming, and R.F. Anderson. 2008. Towards explaining the Nd paradox using reversible scavenging in an ocean general circulation model. *Earth and Planetary Science Letters* 274(3–4):448–461, <https://doi.org/10.1016/j.epsl.2008.07.044>.
- Skinner, L.C., S. Fallon, C. Waelbroeck, E. Michel, and S. Barker. 2010. Ventilation of the deep Southern Ocean and deglacial CO₂ rise. *Science* 328(5982):1,147–1,151, <https://doi.org/10.1126/science.1183627>.
- Skinner, L.C., A. Sadekov, M. Brandon, M. Greaves, Y. Plancherel, M. de la Fuente, J. Gottschalk, S. Souaneh-Ureta, D.S. Sevilgen, and A.E. Scrivner. 2019. Rare Earth Elements in early-diagenetic foraminifer ‘coatings’: Pore-water controls and potential palaeoceanographic applications. *Geochimica et Cosmochimica Acta* 245:118–132, <https://doi.org/10.1016/j.gca.2018.10.027>.
- Tachikawa, K., V. Athias, and C. Jeandel. 2003. Neodymium budget in the modern ocean and paleo-oceanographic implications. *Journal of Geophysical Research* 108(C8), <https://doi.org/10.1029/1999jc000285>.
- Tachikawa, K., T. Arsouze, G. Bayon, A. Bory, C. Colin, J.-C. Dutay, N. Frank, X. Giraud, A.T. Gourlan, C. Jeandel, and others. 2017. The large-scale evolution of neodymium isotopic composition in the global modern and Holocene ocean revealed from seawater and archive data. *Chemical Geology* 457:131–148, <https://doi.org/10.1016/j.chemgeo.2017.03.018>.
- van de Flierdt, T., A.M. Griffiths, M. Lambelet, S.H. Little, T. Stichel, and D.J. Wilson. 2016. Neodymium in the oceans: A global database, a regional comparison and implications for palaeoceanographic research. *Philosophical Transactions of the Royal Society A* 374(2081), <https://doi.org/10.1098/rsta.2015.0293>.
- von Blanckenburg, F. 1999. Tracing past ocean circulation? *Science* 286(5446):1,862–1,863, <https://doi.org/10.1126/science.286.5446.1862b>.

ACKNOWLEDGMENTS

KT's contribution to this work was supported by two French National LEFE projects, RICH (IMAGO) and NEOSYNMPA (CYBER). Samples were provided by the International Marine Global Change Study (IMAGES) program and the Ocean Drilling Program (ODP). The reviews by two anonymous reviewers were very helpful. The EQUIPEX ASTER-CEREGE project (Pierre Deschamps, one of the Pls) is acknowledged for Nd isotopic measurements. H el ene Mariot and Marta Garcia are thanked for technical support. The joint workshop PAGES-GEOTRACES provided a great opportunity to discuss the behavior of Nd isotopes in modern and past oceans.

AUTHORS

Kazuyo Tachikawa (kazuyo@cerege.fr) is Director of Research, Centre Europ een de Recherche et d'Enseignement des G eosciences de l'Environnement (CEREGE), Aix-Marseille Universit e, CNRS, IRD, INRAE, Coll ege de France, Aix-en-Provence, France. **William Rapuc** was a master's student at CEREGE, Aix-Marseille Universit e, CNRS, IRD, INRAE, Coll ege de France, Aix-en-Provence, France, and is currently a PhD student at EDYTEM, Universit e Savoie Mont Blanc, CNRS, Chamb ery, France. **Quentin Dubois-Dauphin** is Postdoctoral Fellow and **Abel Guihou** is BIATSS, both at CEREGE, Aix-Marseille Universit e, CNRS, IRD, INRAE, Coll ege de France, Aix-en-Provence, France. **Charlotte Skonieczny** is Lecturer, Laboratoire G eosciences Paris-Sud, UMR CNRS, Universit e Paris-Saclay, Orsay Cedex, France.

ARTICLE CITATION

Tachikawa, K., W. Rapuc, Q. Dubois-Dauphin, A. Guihou, and C. Skonieczny. 2020. Reconstruction of ocean circulation based on neodymium isotopic composition: Potential limitations and application to the Mid-Pleistocene Transition. *Oceanography* 33(2):80–87, <https://doi.org/10.5670/oceanog.2020.205>.

COPYRIGHT & USAGE

This is an open access article made available under the terms of the Creative Commons Attribution 4.0 International License (<https://creativecommons.org/licenses/by/4.0/>), which permits use, sharing, adaptation, distribution, and reproduction in any medium or format as long as users cite the materials appropriately, provide a link to the Creative Commons license, and indicate the changes that were made to the original content.

SIDEBAR. Amundsen Sea Coastal Ice Rises

FUTURE SITES FOR MARINE-FOCUSED ICE CORE RECORDS

By Peter Neff

How much sea level rise will come from Antarctica's ice loss and how quickly will it arrive at coastlines worldwide? These are the key questions for scientists seeking to improve projections of sea level rise through gathering of myriad new geophysical, geological, oceanographic, atmospheric, and paleoclimate data.

The Amundsen Sea sector of West Antarctica (~90°W to 130°W) is losing ice at an accelerating rate (Shepherd et al., 2018) through basal melting of ice shelves linked to atmosphere-ocean processes. In a phenomenon first identified by oceanographic and remotely sensed observations in the mid-1990s, it is now established that regional winds drive upwelling of warm, nutrient-rich Circumpolar Deep Water onto the Amundsen Sea continental shelf via glacially carved bathymetric troughs. These troughs focus this relatively warm water beneath ice shelves and at glacial grounding lines, particularly those of Pine Island Glacier, Thwaites Glacier, and Getz Ice Shelf (Jacobs et al., 2012). However, our understanding of these ice-ocean-atmosphere interactions is fundamentally limited in time and space.

Circum-Antarctic weather observations begin during the International Geophysical Year of 1957–58, and spatiotemporally complete climate reanalysis data sets become reliable after 1979. Remotely sensed observations of ice flow and surface elevation begin in the early 1990s, as do Amundsen Sea oceanographic observations. Thus, regional records of climate and ice sheet behavior are limited to a 30-year time span, making observations ineffective for capturing longer-term ocean and ice sheet variability (Steig and Neff, 2018). This lack of knowledge of Amundsen Sea boundary conditions prevents evaluation of model results that suggest recent ice loss is related to regional winds, which have strengthened through the twentieth century, possibly related to anthropogenic warming (Holland et al., 2019). In order to understand the emergence of such trends and confirm anthropogenic linkages, a longer observational perspective is needed.

Ice cores provide the primary extension of our spatiotemporal view of the modern Antarctic environment through continuous, annually dated proxy records that span recent decades, centuries, and millennia (Steig et al., 2013; Thomas et al., 2017). Most Antarctic ice cores have been recovered from the slow-flowing ice sheet interior (Figure 1a) in areas ideal for preserving stratigraphy and that avoid the complexities of coastal climate, including warmer temperatures, orographic effects, faster ice flow, high snowfall, and crevassed transitional zones. A growing number of ice cores have been recovered from coastal ice rises, domes, ridges, promonto-

ries, or islands, including Law Dome, Siple Dome, Berkner Island, Fletcher Promontory, Roosevelt Island, Skytrain Ice Rise, and Sherman Island.

Ice rises are like miniature ice sheets that fringe the larger Antarctic continent. They are independently flowing accumulations of snow and ice grounded on bedrock highs, often within or at the margin of ice shelves. Ice rises are targeted for coring because, despite their coastal locations, they retain relatively simple domed stratigraphy and slow ice flow speed, they have high snow accumulation rates that yield thick annual layers, they are elevated above ice shelves prone to surface melt, they interact with coastal and ice-shelf processes, and their internal structure can record past ice flow dynamics (see Matsuoka et al., 2015).

Along the Amundsen Sea coast, ice rises up to 800 m thick (Figure 1a,b) are bombarded by cyclonic storms, resulting in high annual snow accumulation rates, often in excess 0.5 m ice-equivalent on windward aspects (NASA Operation IceBridge snow radar data, not shown). Thick layering increases temporal resolution but reduces the age of ice preserved at depth. Here, mere kilometers from the ocean, a 100 m ice core may record at least a century beyond modern observations, while deeper cores to bedrock may record thousands of years of regional environmental history. Because ice rises are less than 1,000 m thick, basal melting is limited and Pleistocene-age ice may be preserved where geothermal heating is minimal.

Due to the remote location of the Amundsen Sea coast, its notoriously foul weather and ocean conditions, and the complexities of interacting ice, ocean, and atmospheric dynamics, fieldwork here requires international, interdisciplinary collaboration, such as the ongoing US-UK International Thwaites Glacier Collaboration. However, the paleoclimate rewards likely exceed the logistical risks. From existing near-coastal records, we know that sodium, chloride, and methanesulfonic acid present in ice enable reconstructions of wind strength and sea-ice/polynya conditions, while water stable isotopes reliably reflect temperature and moisture source (Steig et al., 2013), and snow accumulation records reveal spatiotemporal trends in ice sheet surface mass balance driven by the competition of low and high pressure systems in the Ross-Amundsen and Bellingshausen Seas, respectively (Thomas et al., 2017). Two short ice cores, collected in 2017 from Mount Siple and in 2020 from Sherman Island (Elizabeth Thomas, British Antarctic Survey, *pers. comm.*, 2020; Figure 1a), contain multidecadal records that will provide scientists a first glimpse into the utility of Amundsen Sea coastal ice rises for centennial to millennial paleoclimate reconstructions.

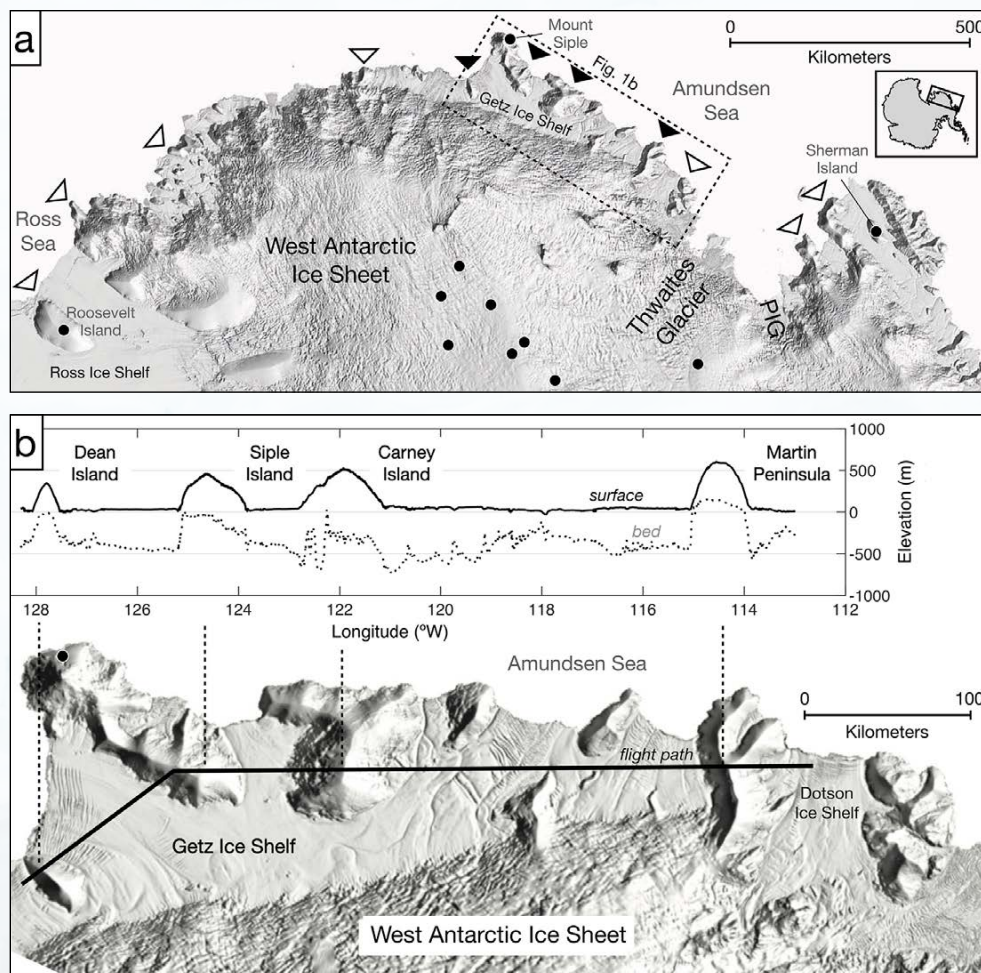


FIGURE 1. (a) West Antarctica. Locations of large ice rises are marked by triangles. Filled triangles indicate ice rises featured in panel (b). Black circles indicate existing ice cores. PIG = Pine Island Glacier. (inset) Antarctica, with the black box denoting location of panel (a). (b) Ice rises near the Getz Ice Shelf. (inset) Radar-derived surface (solid line) and bed (dashed line) elevation data from NASA Operation IceBridge, November 3, 2011. Inset flight path is marked by solid bold line in panel (b). Data available at: ftp://data.cresis.ku.edu/data/rds/2011_Antarctica_DC8/. Basemap: Reference Elevation Model of Antarctica.

To improve our ability to model past and present ice shelf and ice sheet behavior in the dynamic Amundsen Sea sector and beyond, scientists need direct high-resolution paleoclimate records of regional decadal- to millennial-scale atmospheric and oceanic conditions (Jacobs et al., 2012). Previously unstudied coastal ice rises, proximal to the Amundsen Sea, may contain such records. Better understanding of this remote yet globally relevant region is urgently needed to ensure that realistic, actionable sea level projections are available and usable for risk assessments and adaptation plans as society seeks to build resilience for the hundreds of millions of people populating coastal communities worldwide.

REFERENCES

- Holland, P.R., T.J. Bracegirdle, P. Dutrieux, A. Jenkins, and E.J. Steig. 2019. West Antarctic ice loss influenced by internal climate variability and anthropogenic forcing. *Nature Geoscience* 12(9):718–724, <https://doi.org/10.1038/s41561-019-0420-9>.
- Jacobs, S., A. Jenkins, H. Hellmer, C. Giulivi, F. Nitsche, B. Huber, and R. Guerrero. 2012. The Amundsen Sea and the Antarctic ice sheet. *Oceanography* 25(3):154–163, <https://doi.org/10.5670/oceanog.2012.90>.

- Matsuoka, K., R.C. Hindmarsh, G. Moholdt, M.J. Bentley, H.D. Pritchard, J. Brown, H. Conway, R. Drews, G. Durand, D. Goldberg, and others. 2015. Antarctic ice rises and rumpled: Their properties and significance for ice-sheet dynamics and evolution. *Earth-Science Reviews* 150:724–745, <https://doi.org/10.1016/j.earscirev.2015.09.004>.
- Shepherd, A., H.A. Fricker, and S.L. Farrell. 2018. Trends and connections across the Antarctic cryosphere. *Nature* 558(7709):223–232, <https://doi.org/10.1038/s41586-018-0171-6>.
- Steig, E.J., Q. Ding, J.W. White, M. Küttel, S.B. Rupper, T.A. Neumann, P.D. Neff, A.J. Gallant, P.A. Mayewski, and K.C. Taylor. 2013. Recent climate and ice-sheet changes in West Antarctica compared with the past 2,000 years. *Nature Geoscience* 6(5):372–375, <https://doi.org/10.1038/ngeo1778>.
- Steig, E.J., and P.D. Neff. 2018. The prescience of paleoclimatology and the future of the Antarctic ice sheet. *Nature Communications* 9(1):2730, <https://doi.org/10.1038/s41467-018-05001-1>.
- Thomas, E.R., J. Melchior Van Wessel, J. Roberts, E. Isaksson, E. Schlosser, T.J. Fudge, P. Vallelonga, B. Medley, J. Lenaerts, and N. Bertler. 2017. Regional Antarctic snow accumulation over the past 1000 years. *Climate of the Past* 13(11):1491–1513, <https://doi.org/10.5194/cp-13-1491-2017>.

AUTHOR

Peter Neff (pneff@umn.edu) is Research Assistant Professor, Department of Soil, Water, and Climate, University of Minnesota, Saint Paul, MN, USA.

THE ANTARCTIC ICE SHEET

A Paleoclimate Modeling Perspective

By Edward G.W. Gasson and Benjamin A. Keisling



ABSTRACT. The Antarctic Ice Sheet is the largest potential contributor to future sea level rise. Models and paleoceanographic data are often used to examine the past behavior of the ice sheet during both cooler and warmer intervals to understand the forcing and feedbacks that influence ice sheet behavior. Marine geologic studies have focused on understanding ice sheet response during warmer intervals, including the middle Miocene and Pliocene, that have been considered potential analogues to future anthropogenic climate change. Here, we discuss ice sheet modeling and the ways that marine geologic data are used to constrain ice sheet models of the Antarctic Ice Sheet during past warm intervals. We focus on the key challenge of simulating retreat of the “marine” and “terrestrial” sectors of the ice sheet in the geologic past. By integrating ice sheet models and geologic records, we can better characterize the processes that drove past ice sheet retreat. A more complete understanding of these processes, based on continuing engagement between the data and the modeling communities, is the key to predicting the ice sheet’s future.

INTRODUCTION

The Antarctic Ice Sheet is the largest component (by volume) of Earth’s cryosphere. It has a major impact on both regional and global climate through the modification of surface albedo and by altering atmosphere and ocean circulation (DeConto et al., 2007; Bintanja et al., 2013; Colleoni et al., 2018; Golledge et al., 2019). The Antarctic Ice Sheet is the largest store of freshwater on Earth and has the potential to raise global sea level by 58 m if completely melted. Today, it receives 2,100 Gt of annual snowfall that is balanced by mass lost from ice flowing under gravity toward the coast, where it is removed approximately equally by ocean melting of floating ice shelves and the calving of icebergs (Rignot et al., 2019). Unlike the Greenland Ice Sheet, which has an extensive ablation zone, there is minimal melting on the Antarctic Ice Sheet surface at present, although surface meltwater is found in small areas (Trusel et al., 2013; Kingslake et al., 2017; Lenaerts et al., 2017; Banwell et al., 2019).

Much of the ice sheet (~23 m sea level equivalent) is “marine,” meaning that it sits on bedrock currently below sea level (Fretwell et al., 2013) and is often buttressed by floating ice shelves. There are concerns about the role ocean warming plays regarding the future stability of these parts of the ice sheet (Alley et al.,

2015). Of particular concern is the stability of the smaller West Antarctic Ice Sheet if its supporting ice shelves should be lost (Mercer, 1978; Fürst et al., 2016; Pattyn, 2018). There is also growing appreciation that marine portions (~19 m sea level equivalent) of the much larger East Antarctic Ice Sheet may be vulnerable to ocean warming (e.g., Rintoul et al., 2018; Wilson et al., 2018). Although today ~40% of the Antarctic Ice Sheet volume sits on bedrock below sea level, the fraction that is marine has increased through time. This increase is a result of tectonics and glacial evolution, which carved Antarctica’s landscapes, moved sediment to the expanding continental margins, and depressed the bedrock (Bart, 2003; Young et al., 2011; Colleoni et al., 2018; Paxman et al., 2018). Recent reconstructions of past Antarctic bedrock topography for a number of intervals show how the marine fraction of Antarctica has changed through time (Figure 1; Paxman et al., 2019).

The remainder of the Antarctic Ice Sheet is “terrestrial,” that is, grounded on bedrock presently above sea level, so its stability is largely controlled by direct atmospheric melting and buttressing by surrounding ice and the basal topography (e.g., Morlighem et al., 2020). Most importantly, the marine sectors of the ice sheet have the potential to lose mass

through ocean-driven melting and ice-berg calving, as well as surface melting, whereas the terrestrial sectors lose mass when surface melting exceeds snowfall, or by ice flow. Whether retreat occurs in marine or terrestrial sectors can affect the rate at which mass is lost and therefore the rates at which the ice sheet contributes to sea level change. Understanding the style of past ice sheet retreat is therefore critical to understanding possible rates of future sea level rise (DeConto and Pollard, 2016; Rintoul et al., 2018; Dowdeswell et al., 2020; Golledge, 2020).

Our current understanding of the formation and subsequent waxing and waning of the Antarctic Ice Sheet on million-year timescales is largely based on marine sediment records recovered over the past 50 years through scientific ocean drilling (e.g., Kennett and Shackleton, 1976; Barker et al., 1999; Expedition 318 Scientists, 2010). A recently published review in *Oceanography* focused on how scientific ocean drilling of marine sedimentary records from the Antarctic continental margin has revolutionized understanding of the past behavior of the Antarctic Ice Sheet (Escutia et al., 2019). The ice proximal records discussed provide critical data in support of far-field records, which track the pacing of ice sheet change through changes in global ice volume and sea level, and also provide information on the climate drivers that caused these changes (e.g., Littler et al., 2019).

Although Antarctica was partially glaciated during intervals of the Eocene, with glaciation in the high Gamburtsev Mountains (Rose et al., 2013) and glaciers reaching the coast during cooler intervals (Gulick et al., 2017), the onset of continental-sized glaciation occurred during the earliest Oligocene (Miller et al., 1991; Zachos et al., 1992). Immediately after the Eocene-Oligocene boundary, ~32.8 million years ago, a continental-scale ice sheet reached the coast of Antarctica (Stocchi et al., 2013; Galeotti et al., 2016). Throughout the Oligocene and into the early Miocene, ice advanced and retreated across the expanding con-

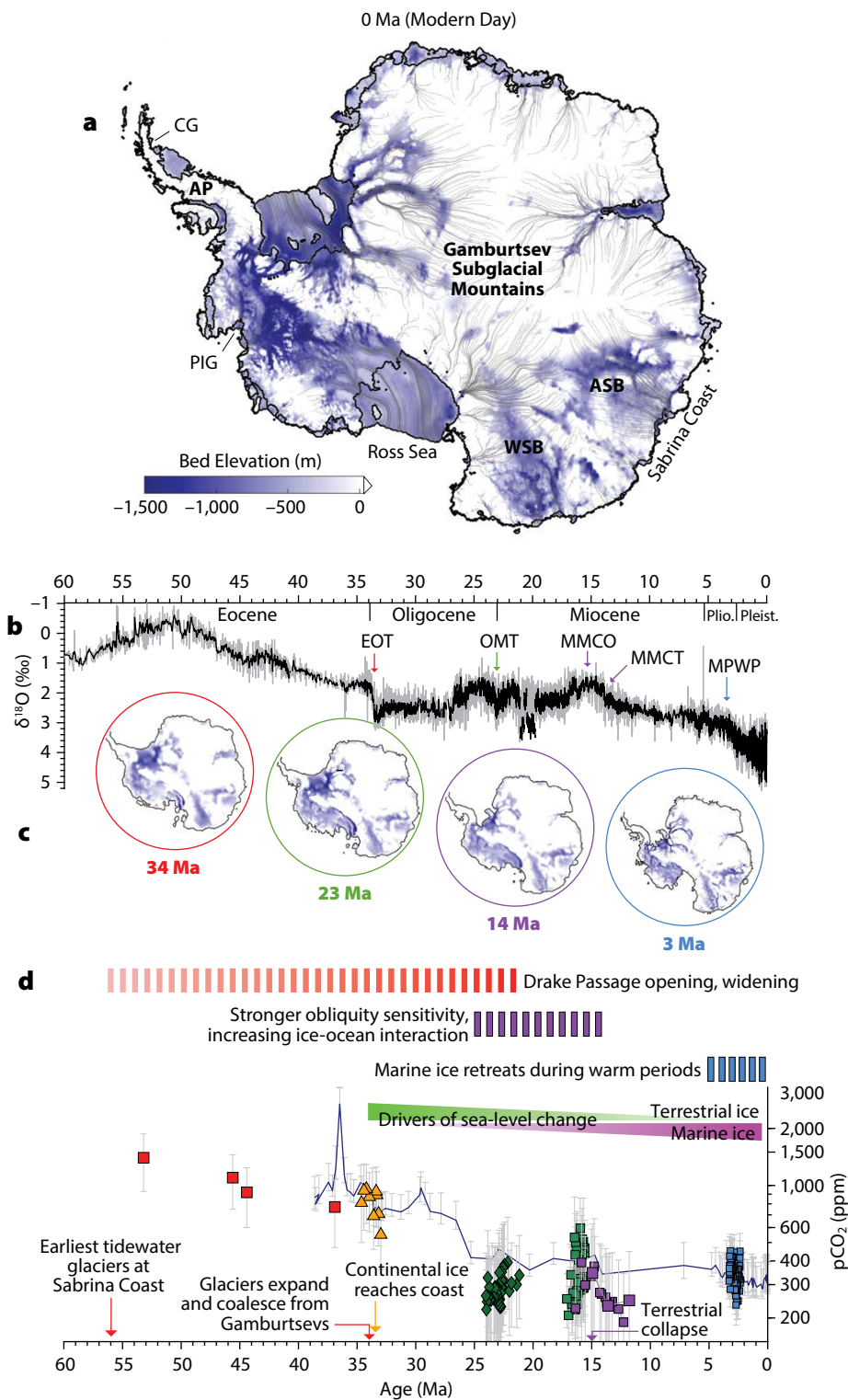


FIGURE 1. (a) Present-day Antarctica. Blue areas indicate marine ice, with topography currently below sea level, and white areas indicate terrestrial ice, grounded on topography above sea level. The black line is the present-day grounding line, the transition between grounded and floating ice. Gray flowlines indicate direction of surface ice flow from an ice sheet model simulation. AP = Antarctic Peninsula. ASB = Aurora Subglacial Basin. CG = Crane Glacier. PIG = Pine Island Glacier. WSB = Wilkes Subglacial Basin. (b) The composite oxygen isotope record from deep-sea foraminifera reveals the general history of the evolution of the Antarctic Ice Sheet, with higher values for increasing ice volume (Zachos et al., 2008). EOT = Eocene-Oligocene transition. OMT = Oligocene-Miocene transition. MMCO = Mid-Miocene climatic optimum. MMCT = Middle Miocene climate transition. MPWP = Mid-Pliocene warm period. (c) Reconstructions of past marine (blue) and terrestrial (white) ice distribution on Antarctica for different time intervals (Paxman et al., 2019). (d) Composite of selected marine-based proxy CO₂ reconstructions (Pearson et al., 2009; Foster et al., 2012; Zhang et al., 2013; Greenop et al., 2014, 2019; Martínez-Botí et al., 2015; Anagnostou et al., 2016).

continental shelf, but the magnitude of these oscillations is still subject to debate (McKay et al., 2016; De Vleeschouwer et al., 2017). Although not a direct measure of ice volume, far-field reconstructions based on oxygen isotope records from benthic foraminifera suggest cycles similar in magnitude to that of modern day Antarctic Ice Sheet volume (de Boer et al., 2010; Liebrand et al., 2017; Miller et al., 2020). The pacing of this early Antarctic Ice Sheet gradually shifted to a stronger sensitivity to obliquity (Earth's axial tilt) toward the mid and then late Miocene, as there was increased ice-ocean interaction (Levy et al., 2019). The ice sheet retreated substantially during the middle Miocene as atmospheric and ocean temperatures increased, and in this warmer and wetter climate, woody plants grew on the Antarctic coast (Warny et al., 2009; Lear et al., 2010; Feakins et al., 2012; Levy et al., 2016; Pierce et al., 2017; Sangiorgi et al., 2018). Immediately following this period, across the middle Miocene climate transition (~14 million years ago), the climate cooled and the ice sheet expanded and became more stable (Shevenell et al., 2004, 2008; Holbourn et al., 2005; Lewis et al., 2008). In the more recent geologic past, the Antarctic Ice Sheet likely retreated during warm intervals of the mid-Pliocene and during some of the warmest interglacials of the late Pleistocene, although this ice was likely sourced only from the marine sectors (Cook et al., 2013; Shakun et al., 2018; Wilson et al., 2018). High sea levels during the last interglacial are often interpreted as evidence for retreat of the Antarctic Ice Sheet, in particular, marine sectors of the West Antarctic Ice Sheet (Dutton et al., 2015; Rohling et al., 2019); however, direct evidence for the loss of the West Antarctic Ice Sheet during the last interglacial is still lacking (e.g., Turney et al., 2020). Note that aspects of this overview are disputed—notably, the magnitude of past Antarctic Ice Sheet retreat has generated many vigorous debates (e.g., Barrett, 2013).

Here, we focus on the separate chal-

allenges of simulating retreat of the marine and terrestrial sectors of the ice sheet by drawing on two intervals: (1) the middle Miocene, an interval that occurred ~15 million years ago, when atmospheric CO₂ concentrations were similar to those projected for the coming decades under intermediate emissions pathways (Foster et al., 2012), and (2) the mid-Pliocene, an interval that occurred ~3 million years ago and likely the last time that atmospheric CO₂ concentrations were as high as they are today (Cook et al., 2013; Martínez-Botí et al., 2015; Shakun et al., 2018). There is evidence for retreat of the terrestrial Antarctic Ice Sheet during the middle Miocene (e.g., Miller et al., 2020), and it is likely that there was retreat of the marine Antarctic Ice Sheet during the mid-Pliocene (Cook et al., 2013; Shakun et al., 2018; Dumitru et al., 2019; Grant et al., 2019). Note that in the rest of this paper, we purposely avoid distinction between the East and West Antarctic Ice Sheets, both of which contain terrestrial and marine sectors.

TERRESTRIAL ICE SHEET RETREAT: COMPLETE COLLAPSE OF THE ANTARCTIC ICE SHEET DURING THE MIDDLE MIOCENE?

Records from around the Antarctic margin (Levy et al., 2016; Gulick et al., 2017; Pierce et al., 2017) and from far-field sea level and ice volume estimates (Shevenell et al., 2008; Miller et al., 2020) support retreat of the Antarctic Ice Sheet during the warm middle Miocene. The change in ice mass led to sea level change on the order of ~60 m (Kominz et al., 2008; John et al., 2011) and fluctuations in the oxygen isotope composition of seawater, an estimate of ice volume, of ~0.5‰ (Lear et al., 2010). These conditions would have required major retreat of the terrestrial-based ice sheet through surface melting—possibly complete collapse of the ice sheet (Pekar and DeConto, 2006; Miller et al., 2020). However, simulating this retreat with coupled climate and ice sheet models with boundary conditions appropriate for the middle Miocene has been chal-

lenging (Pollard and DeConto, 2005). The key middle-Miocene differences in boundary conditions that impact the ice sheets are differences in astronomical parameters, paleogeography (although these differences are relatively small compared with modern), and greenhouse gas concentrations. To generate widespread surface melting and retreat of the terrestrial Antarctic Ice Sheet with global circulation model (GCM)-forced ice sheet models requires a much larger increase in atmospheric CO₂ than can be reconstructed from proxy records (Greenop et al., 2014).

The growth of the Antarctic Ice Sheet cooled the Antarctic continent's climate. Principally, increased albedo reflected more sunlight, and the atmospheric lapse rate led to cooling of the ice surface as the elevation of the growing ice sheet increased (Huybrechts, 1993). These strong positive feedbacks mean that simulating retreat of the Antarctic Ice Sheet requires a magnitude of warming that is inconsistent with proxy reconstructions

of atmospheric CO₂ during the middle Miocene (Pollard and DeConto, 2005; Langebroek et al., 2009). Although simulations of the onset of Antarctic glaciation are largely consistent with proxy reconstructions (DeConto and Pollard, 2003; Pearson et al., 2009), the simulated deglacial CO₂ threshold is much higher than indicated by proxy records and generally outside the error range of these reconstructions (Foster et al., 2012; Foster and Rohling, 2013; shown in red on Figure 2). Following its inception, the simulated Antarctic Ice Sheet is therefore much more stable than the geologic record suggests. This is a fundamental problem because models that cannot capture past collapse will be conservative with respect to projections of future sea level change. Proposed solutions to this conundrum have targeted (a) the proxy records, for example, CO₂ was higher than thought in the middle Miocene (Goldner et al., 2014), or we have been misinterpreting ice volume proxies; (b) climate and ice sheet mod-

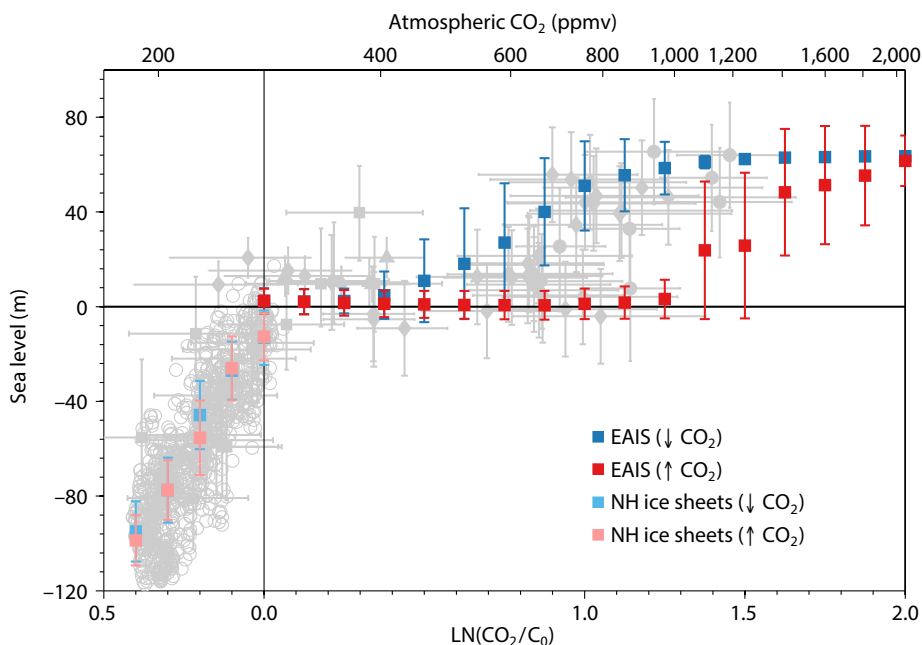


FIGURE 2. Reconstruction of regional sea level against proxy CO₂ for the past 40 million years in gray (Foster and Rohling, 2013, and references therein). Sea level reconstructions are based on a variety of sources and may have local tectonic effects; as such, they should be viewed as relative sea level changes. The red and blue symbols are ice sheet model simulations of the East Antarctic Ice Sheet (EAIS) and Northern Hemisphere (NH) ice sheets; blue indicates a decrease in atmospheric CO₂ and red an increase in atmospheric CO₂. The error bars represent the binning of a perturbed parameter ensemble of simulations. Note that these ice sheet model simulations lack marine ice sheet physics.

els simulating an overly stable ice sheet (Pollard and DeConto, 2005; Langebroek et al., 2009); (c) a missing forcing, for example, a larger role of changes in ocean gateways and changes in paleogeography; or (d) some combination of these effects (e.g., Langebroek et al., 2009; Gasson et al., 2016b; Stap et al., 2019).

The large ice volume changes in the Miocene Climate Optimum are based on assumptions inherent to our understanding of the oxygen isotope composition of benthic foraminifera, which provides a record of both global ice volume and deep ocean temperature that must be deconvolved (Shackleton, 1967). Multiple approaches have been used to extract ice volume from the benthic oxygen isotope records, including using an independent temperature proxy (e.g., Shevenell et al., 2008; Lear et al., 2010), estimating ice volume to temperature partitioning (e.g., Liebrand et al., 2017), and inverse modeling (de Boer et al., 2010). Langebroek et al. (2010) noted that producing an accurate ice volume record also requires knowledge of the changes in oxygen isotope composition of the ice sheets through time. Indeed, such changes, which are caused by changes in atmospheric moisture transport and ice sheet height, could lead to an overestimation of past ice volume changes (Winnick and Caves, 2015). Reconstructions that do not take this process into account (e.g., Miller et al., 2020) should be viewed with caution. Similarly, sea level reconstructions from passive continental margins may also contain signals that are caused by mantle dynamic topography rather than eustasy caused by the waxing and waning of the ice sheets (Moucha et al., 2008).

Alternatively, if ice-proximal reconstructions of past ice sheet extent and past estimates of ice volume change are deemed reliable, and sea level did rise and fall by as much as 60 m, then it is important to determine why current climate and ice sheet models are unable to produce this level of dynamism. Improved representation of ice sheet–climate feedbacks is one way of increasing ice sheet dynamism.

Recent simulations that used an asynchronous ice sheet–climate coupling and that accounted for changes in ice sheet oxygen isotopes are a better match to benthic oxygen isotope estimates and records from the Antarctic margin (Gasson et al., 2016b; Levy et al., 2016), although they still predict a smaller sea level amplitude (~35 m) than some sea level reconstructions (John et al., 2011; Miller et al., 2020). These simulations also include a mechanism for the structural failure of marine ice cliffs, discussed in more detail below.

The problem of simulating the retreat of terrestrial Antarctic ice is linked to another well-studied model-data disagreement in paleoclimate (Barron, 1983)—the reduced temperature gradient between the poles and the tropics during warm periods and, in particular, the strong polar warming shown by temperature proxies that is generally not matched in coupled ocean-atmosphere model simulations (cf. Huber and Caballero, 2011; Sago et al., 2013). Successive generations of GCMs have failed to capture this polar amplification (Lunt et al., 2012); the models that come closest to the proxies require unrealistically high CO₂ forcing or model tuning. However, recent results from the latest generation of GCMs show promise for resolving this long-standing problem (Lunt et al., 2020).

The reduced equator-to-pole temperature gradient is perhaps best associated with the early Eocene, a warm interval when there were no ice sheets on Antarctica. Improvements to climate model cloud physics has led to enhanced Eocene warming at high latitudes through shortwave cloud feedbacks; these results are closer to proxy-derived temperature reconstructions at high latitudes (Zhu et al., 2019), although they may now be too warm in the tropics (Zhu et al., 2020). The new generation of climate models includes a subset of models that have much higher climate sensitivity (the amount of warming for a doubling of atmospheric CO₂) than earlier models, in part because of developments

in the representation of cloud physics (Zelinka et al., 2020). Paleoclimate data are a key test as to whether this higher climate sensitivity is plausible or not (Zhu et al., 2020).

It remains to be seen how the presence of significant ice on Antarctica affects polar amplification and shortwave cloud feedbacks in this new generation of climate models, something missing in studies of the early Eocene. Another modeling target is the Miocene. The advantage of focusing on the Miocene is that it is an interval during which the global continental configuration was fairly similar to today—importantly including the presence of ice on Antarctica (Goldner et al., 2014). It is possible that with greater polar amplification there will be enhanced surface melting and a strong surface mass balance feedback as the ice elevation decreases and melt accelerates at a lower atmospheric CO₂ threshold than previously simulated. Idealized simulations have shown that the ice sheet hysteresis problem can be reduced with an increase in polar amplification, although a mechanism to drive this increase is lacking (Langebroek et al., 2009). It is therefore an exciting time to reassess the long-standing problem of simulating past changes to the terrestrial sectors of the Antarctic Ice Sheet.

There is still much work to be done to understand how the Antarctic Ice Sheet responded to past climate changes and, in particular, what drove past retreat of terrestrial ice. Advances will come from a combined approach targeting both far-field and ice-proximal data (Kennicutt et al., 2015). Clearly defined modeling targets, such as quantitative ice-volume estimates or locations with evidence for meltwater, are incredibly useful (e.g., Lewis et al., 2006; Warny et al., 2009; Mudelsee et al., 2014; Gulick et al., 2017). The recent retrieval of new ice-proximal records from three sectors of Antarctica as part of the International Ocean Discovery Program are already providing some of these key records (Escutia et al., 2019; McKay et al., 2019).

If the retreat of the terrestrial Antarctic Ice Sheet through surface melting did occur under modest atmospheric CO₂ concentrations, we may be forced to reassess long-term future projections (on millennial timescales) of the response of the ice sheet to anthropogenic warming (e.g., Winkelmann et al., 2015).

MARINE ICE SHEET RETREAT: ICE SHEET RESPONSE TO MID-PLIOCENE WARMTH

During the middle Miocene Climate Transition, the climate cooled and the terrestrial Antarctic Ice Sheet became more stable (Kennett, 1977; Shevenell et al., 2004). This scenario is supported by cosmogenic isotope data from the Ross Sea suggesting that for the past 8 million years there has been no retreat of the terrestrial Antarctic Ice Sheet (at least of the sectors draining through the Ross Sea) that would expose land (Shakun et al., 2018). Any ice loss that raised sea levels during this interval would have come from the marine sectors of Antarctica, such as the West Antarctic Ice Sheet, the large basins of East Antarctica, and the Wilkes and Aurora subglacial basins (shown in Figure 1). As mentioned previously, these sectors contain enough ice to raise global sea level by ~23 m. This figure is similar to some estimates of sea level rise during the mid-Pliocene warm interval (3.0–3.2 million years ago; Miller et al., 2012), the last time atmospheric CO₂ concentrations exceeded 400 ppm (Martínez-Botí et al., 2015). The sea level maximum during the mid-Pliocene remains poorly constrained, with large uncertainties (Dutton et al., 2015). However, there is physical evidence for substantial ice retreat in the marine sectors of East Antarctica (Cook et al., 2013) as well as far-field evidence for >10 m sea level fluctuations (Dumitru et al., 2019; Grant et al., 2019).

Marine ice sheets have long been of interest because of their potential vulnerability to ocean warming (Mercer, 1978). A grounded ice sheet and a floating ice shelf connect at the grounding line. The

rate of ice flow from grounded to floating ice is very sensitive to the ice thickness at the grounding line. Analytical solutions suggest that the ice flow across the grounding line increases highly nonlinearly in response to increases in the grounding line ice thickness. In places where the ice sheet bed is on a slope that deepens upstream of the grounding line, including in the large marine basins mentioned above, the geometry of the ice sheet creates the potential for a runaway retreat (Schoof, 2007). As the grounding line retreats backward across this deepening bed, a positive feedback called the “Marine Ice Sheet Instability” (MISI) develops because of the strong increase in ice flow (Mercer, 1978). Restabilization only occurs when the profile of the bed topography changes and the grounding line retreats to sufficiently shallow topography (Figure 3a; Alley and Joughin, 2012). The ability for ice sheet models to correctly simulate the MISI is a key test conducted in inter-model comparison projects (Cornford et al., 2020). The mid-Pliocene warm interval could be considered a real-world test of marine ice sheet behavior, with the caveats that the forcing and the response both have uncertainties (DeConto and Pollard, 2016; Dolan et al., 2018).

Similar to the problem of simulating retreat of the terrestrial Antarctic Ice Sheet, model simulations have largely failed to reproduce retreat in marine sectors of the ice sheet during the Pliocene. This is true for a range of ice sheet models (although they are all relatively low-resolution models with simplified physics) and climate model forcing (de Boer et al., 2015; Dolan et al., 2018). The only models that have successfully simulated retreat have required additional processes that enhance losses from ocean melting (Mengel et al., 2016; Golledge et al., 2017), surface melting (Hill et al., 2007), or calving (Pollard et al., 2015). We next review each of these approaches and their potential limitations.

Golledge et al. (2017) simulated retreat of the Antarctic Ice Sheet by ~9 m during

the early Pliocene. This model includes a parameterization that affects ocean melting at the grounding line. The “sub-grid melt parameterization” applies a reduced ocean melt rate proportional to the fraction of model cells that are floating versus grounded (Figure 3c). This is controversial because it applies an ice shelf melt rate, albeit reduced, to all parts of the cell, including the grounded fraction that is upstream of the grounding line. This parameterization is used to overcome the limitations of using low-resolution ice sheet models in order to perform long-duration simulations that can be compared with paleoclimate data. It also builds on the increasing recognition that ice-ocean interactions occur over a broader grounding “zone” rather than a fixed grounding line. Similar sub-grid schemes are used to calculate the ice flux across the grounding line (Pollard and DeConto, 2009). However, tests of the sub-grid melt parameterization with higher-resolution models that are able to resolve the grounding line in more detail show that this scheme may overestimate mass loss from ice shelf melting (Seroussi and Morlighem, 2018). The sensitivity of ice sheet simulations to the inclusion of this parameterization can be large—the Antarctic Ice Sheet sea level projections for the emissions scenario RCP8.5 of Golledge et al. (2015) vary from 1.6 m to 3.0 m by 2300, with and without sub-grid melt.

Hill et al. (2007) forced an ice sheet model with constant climate forcing from a climate model run with an already partially retreated Antarctic Ice Sheet. This simulation resulted in retreat of the Antarctic Ice Sheet equivalent to ~9 m of sea level, driven by surface melting. This study is one example of a common approach to ice sheet modeling studies in which the ice sheet model and the climate model are not directly coupled. Therefore, the global surface topography, including the ice sheets, is prescribed in the climate model and large differences can develop between ice sheet extent in the ice sheet model and in the climate

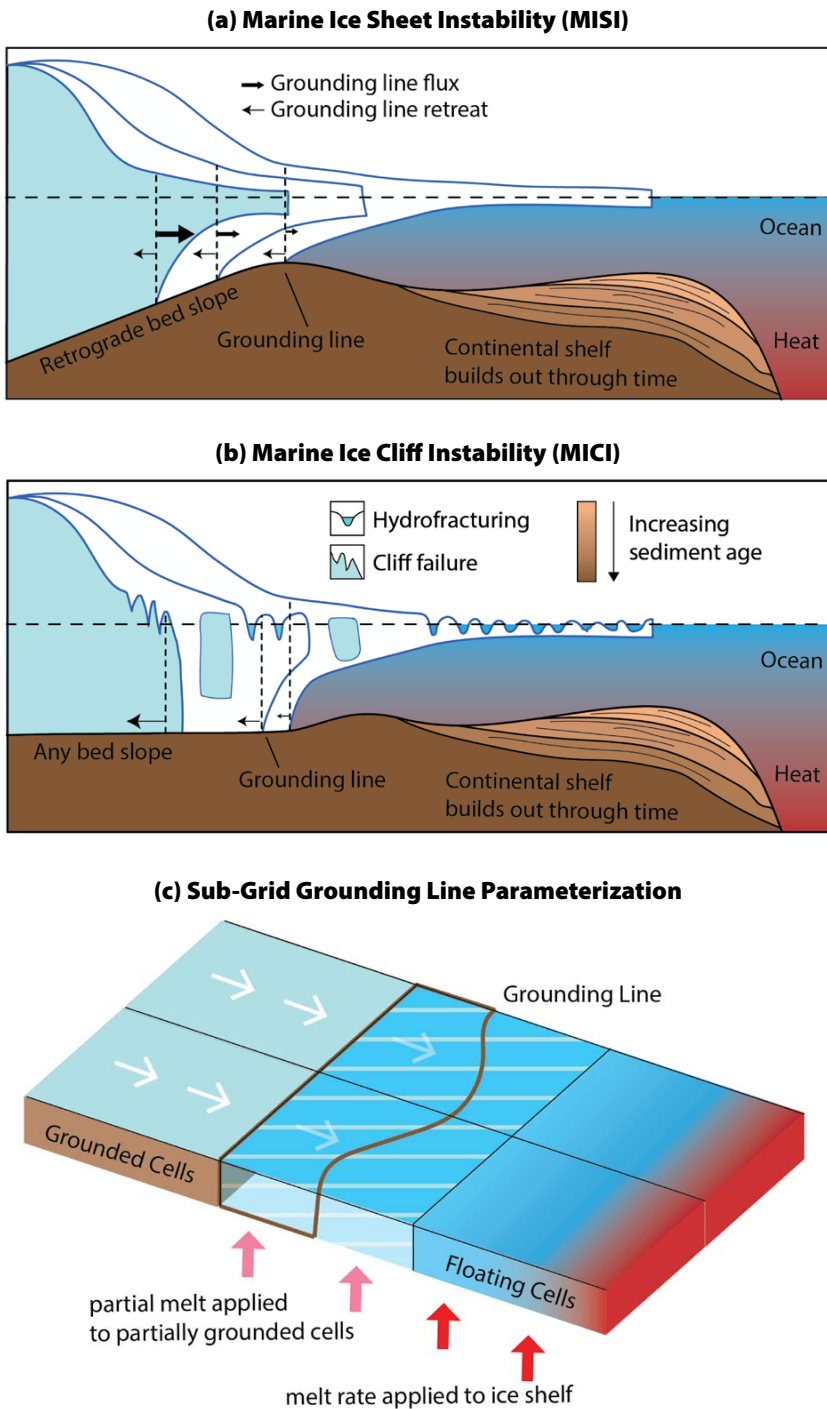


FIGURE 3. Schematics of processes discussed in the text. (a) Marine ice sheet instability on a retrograde slope. (b) Marine ice cliff instability (DeConto and Pollard, 2016). (c) The sub-grid grounding line melt parameterization (adapted from Seroussi and Morlighem, 2018).

model. Any feedbacks from the retreat of the ice sheet are applied to the climate forcing before the ice sheet has retreated. There is therefore concern that the experimental design led to this result. Indeed, tests of alternative climate model forcing, without a collapsed ice sheet, do not produce a similar magnitude of retreat (Dolan et al., 2018). Approaches to forcing ice sheet models are evolving as more attention is paid to direct or asynchronous climate coupling to capture feedbacks between the ice sheets, the ocean, and the atmosphere (e.g., Golledge et al., 2019).

Pollard et al. (2015) introduced a scheme for the structural failure of large marine-terminating ice cliffs in combination with the hydrofracture of ice shelves. This scheme was based on earlier work of Bassis and Walker (2012) and is called “Marine Ice Cliff Instability” (MICI; DeConto and Pollard, 2016). Based on theoretical work, Pollard et al. (2015) introduced an upper limit for the height above water level that ice cliffs can reach. Beyond this limit, stresses exceed the strength of ice and there is brittle failure of the ice cliff. Ice cliffs can form when the buttressing ice shelves are rapidly removed. In the model, this is done using a scheme for hydrofracturing, which is caused by the rapid calving of ice shelves when meltwater and rain drain into surface crevasses. This process is similar to the disintegration of the Larsen B ice shelf, which occurred very rapidly (in ~1 month). Once an ice cliff fails, as long as the grounded ice is thick enough to keep failing, a runaway retreat can occur (Figure 3b).

There are many uncertainties associated with MICI, including the potential rate of ice cliff collapse, what is the failure threshold for subaerial ice cliffs, and whether ice shelves can be removed fast enough to generate sheer cliffs before ice flows into a more stable state (Bell et al., 2017; Clerc et al., 2019; Parizek et al., 2019; Robel and Banwell, 2019). Understanding the potential significance of MICI is limited by a lack of observations because there are only a few locations where MICI-like behavior occurs. Most Antarctic glaciers that have bedrock geometry favorable for MICI are currently protected by ice shelves, with the possible exception of Crane Glacier. In Greenland, the calving fronts of Helheim and Jakobshavn Isbræ Glaciers terminate with subaerial ice cliffs that reach ~100 m in height (Meredith et al., 2019). Observation of

calving events at these glaciers is ongoing to improve understanding of MICI. However, these glaciers are situated in confined valleys and are not perfect analogues to the much wider calving fronts of Antarctica, such as that of Thwaites Glacier (Parizek et al., 2019). This active area of research has been stimulated in part by the rapid rates and high magnitudes of future sea level change in simulations that include these processes—up to ~8 m by 2300 under emission scenario RCP8.5 (DeConto and Pollard, 2016).

An alternative take on the Pliocene sea level problem is that retreat was confined to the marine sectors of the West Antarctic Ice Sheet. This scenario would be consistent with model predictions that do not include MICI (de Boer et al., 2015). When the uncertainties regarding Pliocene sea level estimates are interrogated more closely, this scenario is a possibility for at least some methods (Winnick and Caves, 2015; Gasson et al., 2016a). Indeed, Edwards et al. (2019) suggest that the simulations of DeConto and Pollard (2016) that do not include MICI and ice shelf hydrofracture are consistent with the lowest bounds on Pliocene sea level. The lack of consensus on the Pliocene sea level maximum means that this warm climate interval is currently of debated utility in discriminating between different ice sheet physics (Raymo et al., 2018). This situation was improved recently by the publication of two new studies on Pliocene sea level, one concerning overgrowths on speleothems measured in caves on Mallorca (Dumitru et al., 2019) and another the amplitude of glacial-interglacial sea level cycles based on grain-size analysis of cores drilled in New Zealand (Grant et al., 2019). Both of these support retreat of marine ice throughout Antarctica during the Pliocene. However, the uncertainties are still large and may not alter the conclusions of Edwards et al. (2019). Better constrained sea level estimates of the mid-Pliocene warm period remain critically important to resolving the debate over the stability of Antarctica's marine ice.

OUTLOOK AND CONCLUSIONS

We have described the broad challenges that currently exist in simulating the response of the Antarctic Ice Sheet to climate changes in the geologic past. In sum, proxy records suggest greater ice sheet instability than is often captured by ice sheet modeling studies (Pollard and DeConto, 2005; de Boer et al., 2015). Maintaining a critical view of both data- and model-based histories of the Antarctic Ice Sheet is critical for connecting, and ultimately bridging the two related but often isolated disciplinary communities. We have focused on the separate challenges of simulating retreat of the “terrestrial” and “marine” sectors of the ice sheet and the different styles and mechanisms of ice sheet retreat during the warm intervals of the middle Miocene and the mid-Pliocene. These intervals were chosen as they arguably best characterize the model-data mismatch and provide clear examples of how new modeling approaches are probing longstanding mysteries.

Many other avenues not mentioned in this paper should be further explored by the next generation of ice sheet modelers. The role of opening and widening ocean gateways, in particular Drake Passage, in the inception, fluctuations, and persistence of ice on Antarctica remains debated (Figure 1; Kennett, 1977; Goldner et al. 2014). Coupling of ice sheet and solid Earth models demonstrates how and why different sectors of Antarctica may have become more or less prone to retreat through time (Austermann et al., 2015; Whitehouse et al., 2019). Ice sheets exert local influences on sea level and the surrounding ocean that can affect their stability, and these processes have only recently been included in ice sheet modeling studies (Golledge et al., 2019). Novel observations collected by marine mammals near calving fronts (e.g., Treasure et al., 2017) and autonomous vehicles under floating ice shelves (e.g., Spears et al., 2016) are challenging model parameterizations of the interactions between warm ocean water and the ice sheet. Such

techniques will be critical for understanding active subglacial meltwater features (e.g., Drews et al., 2017) that may extend over a kilometers-wide “grounding zone” beneath the grounded ice sheet (e.g., Christianson et al., 2016). As observations become more detailed, we also find small-scale geological features that can be directly linked to ice sheet processes and thus offer tantalizing targets for models—for example, the observation of corrugation ridges in Pine Island Trough (Wise et al., 2017), “ladders and rungs” on the seafloor of the eastern Antarctic Peninsula (Dowdeswell et al., 2020), and paleo-meltwater channels in the Ross Sea region (Lewis et al., 2006; Simkins et al., 2017) and along the Sabrina Coast (Gulick et al., 2017). In these realms and others, the convergence of geologic data, new observations, and continental-scale models offers many productive paths forward for understanding past fluctuations of the Antarctic Ice Sheet. In further addressing the data-model inconsistencies highlighted in this paper, new developments in ice sheet models may reveal still more mysteries. Close collaboration between data- and model-focused communities will remain critical for moving forward. ☒

REFERENCES

- Alley, R.B., and I. Joughin. 2012. Modeling ice-sheet flow. *Science* 336(6081):551–552, <https://doi.org/10.1126/science.1220530>.
- Alley, R.B., S. Anandakrishnan, K. Christianson, H.J. Horgan, A. Muto, B.R. Parizek, D. Pollard, and R.T. Walker. 2015. Oceanic forcing of ice-sheet retreat: West Antarctica and more. *Annual Review of Earth and Planetary Sciences* 43(1):207–231, <https://doi.org/10.1146/annurev-earth-060614-105344>.
- Anagnostou, E., E.H. John, K.M. Edgar, G.L. Foster, A. Ridgwell, G.N. Inglis, R.D. Pancost, D.J. Lunt, and P.N. Pearson. 2016. Changing atmospheric CO₂ concentration was the primary driver of early Cenozoic climate. *Nature* 533(7603):380–384, <https://doi.org/10.1038/nature17423>.
- Austermann, J., D. Pollard, J.X. Mitrovica, R. Moucha, A.M. Forte, R.M. DeConto, D.B. Rowley, and M.E. Raymo. 2015. The impact of dynamic topography change on Antarctic Ice Sheet stability during the mid-Pliocene warm period. *Geology* 43(10):927–930, <https://doi.org/10.1130/G36988.1>.
- Banwell, A.F., I.C. Willis, G.J. Macdonald, B. Goodsell, and D.R. MacAyeal. 2019. Direct measurements of ice-shelf flexure caused by surface meltwater ponding and drainage. *Nature Communications* 10(1):730, <https://doi.org/10.1038/s41467-019-08522-5>.

- Barker, P.F., P.J. Barrett, A.K. Cooper, and P. Huybrechts. 1999. Antarctic glacial history from numerical models and continental margin sediments. *Palaeogeography, Palaeoclimatology, Palaeoecology* 150(3–4):247–267, [https://doi.org/10.1016/S0031-0182\(98\)00224-7](https://doi.org/10.1016/S0031-0182(98)00224-7).
- Barrett, P. 2013. Resolving views on Antarctic Neogene glacial history – the Sirius debata. *Earth and Environmental Science Transactions of the Royal Society of Edinburgh* 104(1):31–53, <https://doi.org/10.1017/S175569101300008X>.
- Barron, E.J. 1983. A warm, equable Cretaceous: The nature of the problem. *Earth Science Reviews* 19(4):305–338, [https://doi.org/10.1016/0012-8252\(83\)90001-6](https://doi.org/10.1016/0012-8252(83)90001-6).
- Bart, P.J. 2003. Were West Antarctic Ice Sheet grounding events in the Ross Sea a consequence of East Antarctic Ice Sheet expansion during the middle Miocene? *Earth and Planetary Science Letters* 216(1–2):93–107, [https://doi.org/10.1016/S0012-821X\(03\)00509-0](https://doi.org/10.1016/S0012-821X(03)00509-0).
- Bassis, J.N., and C.C. Walker. 2012. Upper and lower limits on the stability of calving glaciers from the yield strength envelope of ice. *Proceedings of the Royal Society A* 468(2140):913–931, <https://doi.org/10.1098/rspa.2011.0422>.
- Bell, R.E., W. Chu, J. Kingslake, I. Das, M. Tedesco, K.J. Tinto, C.J. Zappa, M. Frezzotti, A. Boghosian, and W.S. Lee. 2017. Antarctic ice shelf potentially stabilized by export of meltwater in surface river. *Nature* 544(7650):344–348, <https://doi.org/10.1038/nature22048>.
- Bintanja, R., G.J. Van Oldenborgh, S.S. Drijfhout, B. Wouters, and C.A. Katsman. 2013. Important role for ocean warming and increased ice-shelf melt in Antarctic sea-ice expansion. *Nature Geoscience* 6(5):376–379, <https://doi.org/10.1038/ngeo1767>.
- Christianson, K., R.W. Jacobel, H.J. Horgan, R.B. Alley, S. Anandakrishnan, D.M. Holland, and K.J. DallaSanta. 2016. Basal conditions at the grounding zone of Whillans Ice Stream, West Antarctica, from ice-penetrating radar. *Journal of Geophysical Research* 121(11):1954–1983, <https://doi.org/10.1002/2015JF003806>.
- Clerc, F., B.M. Minchew, and M.D. Behn. 2019. Marine ice cliff instability mitigated by slow removal of ice shelves. *Geophysical Research Letters* 46:12,108–12,116, <https://doi.org/10.1029/2019GL084183>.
- Colleoni, F., L. De Santis, C.S. Siddoway, A. Bergamasco, N.R. Golledge, G. Lohmann, S. Passchier, and M.J. Siegert. 2018. Spatio-temporal variability of processes across Antarctic ice-bed-ocean interfaces. *Nature Communications* 9(1):2289, <https://doi.org/10.1038/s41467-018-04583-0>.
- Cook, C.P., T. Van De Flierdt, T. Williams, S.R. Hemming, M. Iwai, M. Kobayashi, F.J. Jimenez-Spejo, C. Escutia, J.J. González, B.-K. Khim, and others. 2013. Dynamic behaviour of the East Antarctic ice sheet during Pliocene warmth. *Nature Geoscience* 6(9):765–769, <https://doi.org/10.1038/ngeo1889>.
- Cornford, S., H. Seroussi, X. Asay-Davis, and G.H. Gudmundsson. 2020. Results of the third Marine Ice Sheet Model Intercomparison Project (MISMIP+). *Cryosphere Discussions*, <https://doi.org/10.5194/tc-2019-326>.
- de Boer, B., R.S.W. van de Wal, R. Bintanja, L.J. Lourens, and E. Tuenner. 2010. Cenozoic global ice-volume and temperature simulations with 1-D ice-sheet models forced by benthic $\delta^{18}\text{O}$ records. *Annals of Glaciology* 51(55):23–33, <https://doi.org/10.3189/172756410791392736>.
- de Boer, B., A.M. Dolan, J. Bernales, E. Gasson, H. Goelzer, N.R. Golledge, J. Sutter, P. Huybrechts, G. Lohmann, I. Rogozhina, and others. 2015. Simulating the Antarctic ice sheet in the late-Pliocene warm period: PLISMIP-ANT, an ice-sheet model intercomparison project. *The Cryosphere* 9:881–903, <https://doi.org/10.5194/tc-9-881-2015>.
- DeConto, R., and D. Pollard. 2003. Rapid Cenozoic glaciation of Antarctica induced by declining atmospheric CO_2 . *Nature* 421:245–249, <https://doi.org/10.1038/nature01290>.
- DeConto, R., D. Pollard, and D. Harwood. 2007. Sea ice feedback and Cenozoic evolution of Antarctic climate and ice sheets. *Paleoceanography* 22(3), <https://doi.org/10.1029/2006PA001350>.
- DeConto, R., and D. Pollard. 2016. Contribution of Antarctica to past and future sea-level rise. *Nature* 531(7596):591–597, <https://doi.org/10.1038/nature17145>.
- De Vleeschouwer, D., M. Vahlenkamp, M. Crucifix, and H. Pälike. 2017. Alternating Southern and Northern Hemisphere climate response to astronomical forcing during the past 35 m.y. *Geology* 45(4):375–378, <https://doi.org/10.1130/G38663.1>.
- Dolan, A.M., B. de Boer, J. Bernales, D.J. Hill, and A.M. Haywood. 2018. High climate model dependency of Pliocene Antarctic ice-sheet predictions. *Nature Communications* 9:2799, <https://doi.org/10.1038/s41467-018-05179-4>.
- Dowdeswell, J.A., C.L. Batchelor, A. Montelli, D. Ottesen, F.D.W. Christie, E.K. Dowdeswell, and J. Evans. 2020. Delicate seafloor landforms reveal past Antarctic grounding-line retreat of kilometers per year. *Science* 368(6494):1,020–1,024, <https://doi.org/10.1126/science.aaz3059>.
- Drews, R., F. Pattyn, I. Hewitt, F.S.L. Ng, S. Berger, K. Matsuoka, V. Helm, N. Bergeot, L. Favier, and N. Neckel. 2017. Actively evolving subglacial conduits and eskers initiate ice shelf channels at an Antarctic grounding line. *Nature Communications* 8:15228, <https://doi.org/10.1038/ncomms15228>.
- Dumitru, O.A., J. Austermann, V.J. Polyak, J.J. Fornós, Y. Asmerom, J. Ginés, A. Genés, and B.P. Onac. 2019. Constraints on global mean sea level during Pliocene warmth. *Nature* 574(7777):233–236, <https://doi.org/10.1038/s41586-019-1543-2>.
- Dutton, A., A.E. Carlson, A.J. Long, G.A. Milne, P.U. Clark, R. DeConto, B.P. Horton, S. Rahmstorf, and M.E. Raymo. 2015. Sea-level rise due to polar ice-sheet mass loss during past warm periods. *Science* 349(6244):aaa4019, <https://doi.org/10.1126/science.aaa4019>.
- Edwards, T.L., M.A. Brandon, G. Durand, N.R. Edwards, N.R. Golledge, P.B. Holden, I.J. Nias, A.J. Payne, C. Ritz, and A. Wernecke. 2019. Revisiting Antarctic ice loss due to marine ice-cliff instability. *Nature* 566:58–64, <https://doi.org/10.1038/s41586-019-0901-4>.
- Escutia, C., R.M. DeConto, R. Dunbar, L. De Santis, A. Shevenell, and T. Naish. 2019. Keeping an eye on Antarctic Ice Sheet stability. *Oceanography* 32(1):32–46, <https://doi.org/10.5670/oceanog.2019.117>.
- Expedition 318 Scientists. 2010. Wilkes Land glacial history: Cenozoic East Antarctic Ice Sheet evolution from Wilkes Land margin sediments. *Integrated Ocean Drilling Program Preliminary Report*, volume 318, <https://doi.org/10.2204/iodp.pr.318.2010>.
- Feakins, S.J., S. Warny, and J.E. Lee. 2012. Hydrologic cycling over Antarctica during the middle Miocene warming. *Nature Geoscience* 5:557–560, <https://doi.org/10.1038/ngeo1498>.
- Foster, G.L., C.H. Lear, and J.W.B. Rae. 2012. The evolution of pCO_2 , ice volume and climate during the middle Miocene. *Earth and Planetary Science Letters* 341–344:243–254, <https://doi.org/10.1016/j.epsl.2012.06.007>.
- Foster, G.L., and E.J. Rohling. 2013. Relationship between sea level and climate forcing by CO_2 on geological timescales. *Proceedings of the National Academy of Sciences of the United States of America* 110(4):1,029–1,214, <https://doi.org/10.1073/pnas.1216073110>.
- Fretwell, P., H.D. Pritchard, D.G. Vaughan, J.L. Bamber, N.E. Barrand, R. Bell, C. Bianchi, R.G. Bingham, D.D. Blankenship, G. Casassa, and others. 2013. Bedmap2: Improved ice bed, surface and thickness datasets for Antarctica. *The Cryosphere* 7(1):375–393, <https://doi.org/10.5194/tc-7-375-2013>.
- Fürst, J.J., G. Durand, F. Gillet-Chaulet, L. Tavaré, M. Rankl, M. Braun, and O. Gagliardini. 2016. The safety band of Antarctic ice shelves. *Nature Climate Change* 6(5):479–482, <https://doi.org/10.1038/nclimate2912>.
- Galeotti, S., R. DeConto, T. Naish, P. Stocchi, F. Florindo, M. Pagani, P. Barrett, S.M. Bohaty, L. Lanci, D. Pollard, and others. 2016. Antarctic Ice Sheet variability across the Eocene-Oligocene boundary climate transition. *Science* 352(6281):76–80, <https://doi.org/10.1126/science.aab0669>.
- Gasson, E., R.M. DeConto, and D. Pollard. 2016a. Modeling the oxygen isotope composition of the Antarctic ice sheet and its significance to Pliocene sea level. *Geology* 44(10):827–830, <https://doi.org/10.1130/G38104.1>.
- Gasson, E., R.M. DeConto, D. Pollard, and R.H. Levy. 2016b. Dynamic Antarctic Ice Sheet during the early to mid-Miocene. *Proceedings of the National Academy of Sciences of the United States of America* 113(13):3,459–3,464, <https://doi.org/10.1073/pnas.1516130113>.
- Goldner, A., N. Herold, and M. Huber. 2014. The challenge of simulating the warmth of the mid-Miocene climatic optimum in CESM1. *Climate of the Past* 10(2):523–536, <https://doi.org/10.5194/cp-10-523-2014>.
- Golledge, N.R. 2020. Long-term projections of sea-level rise from ice sheets. *WIREs Climate Change* 11(2):e634, <https://doi.org/10.1002/wcc.634>.
- Golledge, N.R., D.E. Kowalewski, T.R. Naish, R.H. Levy, C.J. Fogwill, and E.G.W. Gasson. 2015. The multi-millennial Antarctic commitment to future sea-level rise. *Nature* 526(7573):421–425, <https://doi.org/10.1038/nature15706>.
- Golledge, N.R., Z.A. Thomas, R.H. Levy, E.G.W. Gasson, T.R. Naish, R.M. McKay, D.E. Kowalewski, and C.J. Fogwill. 2017. Antarctic climate and ice-sheet configuration during the early Pliocene interglacial at 4.23 Ma. *Climate of the Past* 13:959–975, <https://doi.org/10.5194/cp-13-959-2017>.
- Golledge, N.R., E.D. Keller, N. Gomez, K.A. Naughten, J. Bernales, L.D. Trusel, and T.L. Edwards. 2019. Global environmental consequences of twenty-first-century ice-sheet melt. *Nature* 566(7742):65–72, <https://doi.org/10.1038/s41586-019-0889-9>.
- Grant, G.R., T.R. Naish, G.B. Dunbar, P. Stocchi, M.A. Kominz, P.J.J. Kamp, C.A. Tapia, R.M. McKay, R.H. Levy, and M.O. Petterson. 2019. The amplitude and origin of sea-level variability during the Pliocene epoch. *Nature* 574(7777):237–241, <https://doi.org/10.1038/s41586-019-1619-z>.
- Greenop, R., G.L. Foster, P.A. Wilson, and C.H. Lear. 2014. Middle Miocene climate instability associated with high-amplitude CO_2 variability. *Paleoceanography and Paleoclimatology* 29(9):845–853, <https://doi.org/10.1002/2014PA002653>.
- Greenop, R., S.M. Sossdian, M.J. Henehan, P.A. Wilson, C.H. Lear, and G.L. Foster. 2019. Orbital forcing, ice volume, and CO_2 across the Oligocene-Miocene Transition. *Paleoceanography and Paleoclimatology* 34(3):313–328, <https://doi.org/10.1029/2018PA003420>.
- Gulick, S.P.S., A.E. Shevenell, A. Montelli, R. Fernandez, C. Smith, S. Warny, S.M. Bohaty, C. Sjunneskog, A. Leventer, B. Frederick, and D.D. Blankenship. 2017. Initiation and long-term instability of the East Antarctic Ice Sheet. *Nature* 552(7684):225–229, <https://doi.org/10.1038/nature25026>.
- Hill, D., A. Haywood, R. Hindmarsh, and P. Valdes. 2007. Characterising ice sheets during the mid Pliocene: Evidence from data and models. Pp. 517–538 in *Deep Time Perspectives on Climate Change: Marrying the Signal from Computer Models and Biological Proxies*, M. Williams, A. Haywood, F. Gregory, and D. Schmidt, eds, Geological Society of London.

- Holbourn, A., W. Kuhnt, M. Schulz, and H. Erlenkeuser. 2005. Impacts of orbital forcing and atmospheric carbon dioxide on Miocene ice-sheet expansion. *Nature* 438(7067):483–487, <https://doi.org/10.1038/nature04123>.
- Huber, M., and R. Caballero. 2011. The early Eocene equable climate problem revisited. *Climate of the Past* 7(2):603–633, <https://doi.org/10.5194/cp-7-603-2011>.
- Huybrechts, P. 1993. Glaciological modelling of the late Cenozoic East Antarctic Ice Sheet: Stability or dynamism? *Geografiska Annaler: Series A, Physical Geography* 75(4):221–228, <https://doi.org/10.2307/521202>.
- John, C.M., G.D. Karner, E. Browning, R.M. Leckie, Z. Mateo, B. Carson, and C. Lowery. 2011. Timing and magnitude of Miocene eustasy derived from the mixed siliciclastic-carbonate stratigraphic record of the northeastern Australian margin. *Earth and Planetary Science Letters* 304(3–4):455–467, <https://doi.org/10.1016/j.epsl.2011.02.013>.
- Kennett, J.P. 1977. Cenozoic evolution of Antarctic glaciation, the circum-Antarctic Ocean, and their impact on global paleoceanography. *Journal of Geophysical Research* 82(27):3,843–3,860, <https://doi.org/10.1029/JC082i027p03843>.
- Kennett, J., and N. Shackleton. 1976. Oxygen isotopic evidence for the development of the psychrosphere 38 Myr ago. *Nature* 260(8):513–515, <https://doi.org/10.1038/260513a0>.
- Kennicutt, M.C., S.L. Chown, J.J. Cassano, D. Liggett, L.S. Peck, R. Massom, S.R. Rintoul, J. Storey, D.G. Vaughan, T.J. Wilson, and others. 2015. A roadmap for Antarctic and Southern Ocean science for the next two decades and beyond. *Antarctic Science* 27(1):3–18, <https://doi.org/10.1017/S0954102014000674>.
- Kingslake, J., J.C. Ely, I. Das, and R.E. Bell. 2017. Widespread movement of meltwater onto and across Antarctic ice shelves. *Nature* 544:349–352, <https://doi.org/10.1038/nature22049>.
- Kominz, M.A., J.V. Browning, K.G. Miller, P.J. Sugarman, S. Mizintseva, and C.R. Scotese. 2008. Late Cretaceous to Miocene sea-level estimates from the New Jersey and Delaware coastal plain coreholes: An error analysis. *Basin Research* 20(2):211–226, <https://doi.org/10.1111/j.1365-2117.2008.00354.x>.
- Langebroek, P.M., A. Paul, and M. Schulz. 2009. Antarctic ice-sheet response to atmospheric CO₂ and insolation in the Middle Miocene. *Climate of the Past* 5(4):633–646, <https://doi.org/10.5194/cp-5-633-2009>.
- Langebroek, P.M., A. Paul, and M. Schulz. 2010. Simulating the sea level imprint on marine oxygen isotope records during the middle Miocene using an ice sheet-climate model. *Paleoceanography* 25(4), <https://doi.org/10.1029/2008PA001704>.
- Lear, C.H., E.M. Mawbey, and Y. Rosenthal. 2010. Cenozoic benthic foraminifer Mg/Ca and Li/Ca records: Toward unlocking temperatures and saturation states. *Paleoceanography* 25(4):PA4215, <https://doi.org/10.1029/2009PA001880>.
- Lenaerts, J.T.M., S. Lhermitte, R. Drews, S.R.M. Ligtenberg, S. Berger, V. Helm, C.J.P.P. Smeets, M.R. van den Broeke, W.J. van de Berg, E. van Meijgaard, and others. 2017. Meltwater produced by wind-albedo interaction stored in an East Antarctic ice shelf. *Nature Climate Change* 7(1):58–62, <https://doi.org/10.1038/nclimate3180>.
- Levy, R., D. Harwood, F. Florindo, F. Sangiorgi, R. Tripati, H. von Eynatten, E. Gasson, G. Kuhn, A. Tripati, R. DeConto, and others. 2016. Antarctic ice sheet sensitivity to atmospheric CO₂ variations in the early to mid-Miocene. *Proceedings of the National Academy of Sciences of the United States of America* 113(13):3,453–3,458, <https://doi.org/10.1073/pnas.1516030113>.
- Levy, R.H., S.R. Meyers, T.R. Naish, N.R. Golledge, R.M. McKay, J.S. Crampton, R.M. DeConto, L. De Santis, F. Florindo, E.G.W. Gasson, and others. 2019. Antarctic ice-sheet sensitivity to obliquity forcing enhanced through ocean connections. *Nature Geoscience* 12:132–137, <https://doi.org/10.1038/s41561-018-0284-4>.
- Lewis, A.R., D.R. Marchant, D.E. Kowalewski, S.L. Baldwin, and L.E. Webb. 2006. The age and origin of the Labyrinth, western Dry Valleys, Antarctica: Evidence for extensive middle Miocene subglacial floods and freshwater discharge to the Southern Ocean. *Geology* 34(7):513–516, <https://doi.org/10.1130/G22145.1>.
- Lewis, A.R., D.R. Marchant, A.C. Ashworth, L. Hedenäs, S.R. Hemming, J.V. Johnson, M.J. Leng, M.L. Machlus, A.E. Newton, J.I. Raine, and others. 2008. Mid-Miocene cooling and the extinction of tundra in continental Antarctica. *Proceedings of the National Academy of Sciences of the United States of America* 105(31):10,676–10,680, <https://doi.org/10.1073/pnas.0802501105>.
- Liebrand, D., A.T.M. de Bakker, H.M. Beddow, P.A. Wilson, S.M. Bohaty, G. Ruessink, H. Pälike, S.J. Batenburg, F.J. Hilgen, D.A. Hodell, and others. 2017. Evolution of the early Antarctic ice ages. *Proceedings of the National Academy of Sciences of the United States of America* 114(15):3,867–3,872, <https://doi.org/10.1073/pnas.1615440114>.
- Littler, K., T. Westerhold, A.J. Drury, D. Liebrand, L. Lisiecki, and H. Pälike. 2019. Astronomical time keeping of Earth history: An invaluable contribution of scientific ocean drilling. *Oceanography* 32(1):72–76, <https://doi.org/10.5670/oceanog.2019.122>.
- Lunt, D., F. Bragg, W.-L. Chan, D. Hutchinson, J.-B. Ladant, I. Niezgodzki, S. Steinig, Z. Zhang, J. Zhu, A. Abe-Ouchi, and others. 2020. DeepMIP: Model intercomparison of early Eocene climatic optimum (EEO) large-scale climate features and comparison with proxy data. *Climate of the Past Discussions*, <https://doi.org/10.5194/cp-2019-149>, in review.
- Lunt, D.J., T. Dunkley Jones, M. Heinemann, M. Huber, A. LeGrande, A. Winguth, C. Loptson, J. Marotzke, C.D. Roberts, J. Tindall, and others. 2012. A model-data comparison for a multi-model ensemble of early Eocene atmosphere-ocean simulations: EoMIP. *Climate of the Past* 8(5):1,717–1,736, <https://doi.org/10.5194/cp-8-1717-2012>.
- Martínez-Botí, M.A., G.L. Foster, T.B. Chalk, E.J. Rohling, P.F. Sexton, D.J. Lunt, R.D. Pancost, M.P.S. Badger, and D.N. Schmidt. 2015. Plio-Pleistocene climate sensitivity evaluated using high-resolution CO₂ records. *Nature* 518(7537):49–54, <https://doi.org/10.1038/nature14145>.
- McKay, R.M., P.J. Barrett, R.S. Levy, T.R. Naish, N.R. Golledge, and A. Pyne. 2016. Antarctic Cenozoic climate history from sedimentary records: ANDRILL and beyond. *Philosophical Transactions of the Royal Society A* 374(2059), <https://doi.org/10.1098/rsta.2014.0301>.
- McKay, R.M., L. De Santis, D.K. Kulhanek, and the Expedition 374 Scientists. 2019. Ross Sea West Antarctic Ice Sheet history. *Proceedings of the International Ocean Discovery Program*, Volume 374, College Station, TX, <https://doi.org/10.14379/iodp.proc.374.2019>.
- Mengel, M., A. Levermann, K. Frieler, A. Robinson, B. Marzeion, and R. Winkelmann. 2016. Future sea level rise constrained by observations and long-term commitment. *Proceedings of the National Academy of Sciences of the United States of America* 113(10):2,597–2,602, <https://doi.org/10.1073/pnas.1500515113>.
- Mercer, J. 1978. West Antarctic ice sheet and CO₂ greenhouse effect: A threat of disaster. *Nature* 271(26):321–325, <https://doi.org/10.1038/271321a0>.
- Meredith, M., M. Sommerkorn, S. Cassotta, C. Derksen, A. Ekaykin, A. Hollowed, G. Kofinas, A. Mackintosh, J. Melbourne-Thomas, M.M.C. Muelbert, and others. 2019. Polar regions. Pp. 203–320 in *IPCC Special Report on the Ocean and Cryosphere in a Changing Climate*. H.-O. Pörtner, D.C. Roberts, V. Masson-Delmotte, P. Zhai, M. Tignor, E. Poloczanska, K. Mintenbeck, A. Alegria, M. Nicolai, A. Okem, J. Petzold, B. Rama, and N.M. Weyer, eds.
- Miller, K.G., J.D. Wright, and R.G. Fairbanks. 1991. Unlocking the ice house: Oligocene-Miocene oxygen isotopes, eustasy, and margin erosion. *Journal of Geophysical Research* 96:6,829–6,848, <https://doi.org/10.1029/90JB02015>.
- Miller, K.G., J.D. Wright, J.V. Browning, A. Kulpecz, M. Kominz, T.R. Naish, B.S. Cramer, Y. Rosenthal, W.R. Peltier, and S. Sosdian. 2012. High tide of the warm Pliocene: Implications of global sea level for Antarctic deglaciation. *Geology* 40(5):407–410, <https://doi.org/10.1130/G32869.1>.
- Miller, K.G., J.V. Browning, W.J. Schmelz, R.E. Kopp, G.S. Mountain, and J.D. Wright. 2020. Cenozoic sea-level and cryospheric evolution from deep-sea geochemical and continental margin records. *Science Advances* 6(20):eaaz1346, <https://doi.org/10.1126/sciadv.aaz1346>.
- Morlighem, M., E. Rignot, T. Binder, D. Blankenship, R. Drews, G. Eagles, O. Eisen, F. Ferraccioli, R. Forsberg, P. Fretwell, and others. 2020. Deep glacial troughs and stabilizing ridges unveiled beneath the margins of the Antarctic ice sheet. *Nature Geoscience* 13(2):132–137, <https://doi.org/10.1038/s41561-019-0510-8>.
- Moucha, R., A.M. Forte, J.X. Mitrovica, D.B. Rowley, S. Quere, N.A. Simmons, and S.P. Grand. 2008. Dynamic topography and long-term sea-level variations: There is no such thing as a stable continental platform. *Earth and Planetary Science Letters* 271(1–4):101–108, <https://doi.org/10.1016/j.epsl.2008.03.056>.
- Mudelsee, M., T. Bickert, C.H. Lear, and G. Lohmann. 2014. Cenozoic climate changes: A review based on time series analysis of marine benthic δ¹⁸O records. *Reviews of Geophysics* 52(3):333–374, <https://doi.org/10.1002/2013RG000440>.
- Parizek, B.R., K. Christianson, R.B. Alley, D. Voytenko, I. Vaňková, T.H. Dixon, R.T. Walker, and D.M. Holland. 2019. Ice-cliff failure via retrogressive slumping. *Geology* 47(5):449–452, <https://doi.org/10.1130/G45880.1>.
- Pattyn, F. 2018. The paradigm shift in Antarctic ice sheet modelling. *Nature Communications* 9(1):10–12, <https://doi.org/10.1038/s41467-018-05003-z>.
- Paxman, G.J.G., S.S.R. Jamieson, F. Ferraccioli, M.J. Bentley, N. Ross, E. Armadillo, E.G.W. Gasson, G. Leitchenkov, and R.M. DeConto. 2018. Bedrock erosion surfaces record former East Antarctic Ice Sheet extent. *Geophysical Research Letters* 45(9):4,114–4,123, <https://doi.org/10.1029/2018GL077268>.
- Paxman, G.J.G., S.S.R. Jamieson, K. Hochmuth, K. Gohl, K., M.J. Bentley, G. Leitchenkov, and F. Ferraccioli. 2019. Reconstructions of Antarctic topography since the Eocene-Oligocene boundary. *Palaeogeography, Palaeoclimatology, Palaeoecology* 535:109346, <https://doi.org/10.1016/j.palaeo.2019.109346>.
- Pearson, P.N., G.L. Foster, and B.S. Wade. 2009. Atmospheric carbon dioxide through the Eocene-Oligocene climate transition. *Nature* 461(7267):1,110–1,113, <https://doi.org/10.1038/nature08447>.
- Pekar, S.F., and R.M. DeConto. 2006. High-resolution ice-volume estimates for the early Miocene: Evidence for a dynamic ice sheet in Antarctica. *Palaeogeography, Palaeoclimatology, Palaeoecology* 231(1–2):101–109, <https://doi.org/10.1016/j.palaeo.2005.07.027>.
- Pierce, E.L., T. van de Fliedert, T. Williams, S.R. Hemming, C.P. Cook, and S. Passchier. 2017. Evidence for a dynamic East Antarctic ice sheet during the mid-Miocene climate transition. *Earth and Planetary Science Letters* 478:1–13, <https://doi.org/10.1016/j.epsl.2017.08.011>.
- Pollard, D., and R. DeConto. 2005. Hysteresis in Cenozoic Antarctic ice-sheet variations. *Global and Planetary Change* 45(1–3):9–21, <https://doi.org/10.1016/j.gloplacha.2004.09.011>.

- Pollard, D., and R.M. DeConto. 2009. Modelling West Antarctic ice sheet growth and collapse through the past five million years. *Nature* 458:329–332, <https://doi.org/10.1038/nature07809>.
- Pollard, D., R.M. DeConto, and R.B. Alley. 2015. Potential Antarctic Ice Sheet retreat driven by hydrofracturing and ice cliff failure. *Earth and Planetary Science Letters* 412:112–121, <https://doi.org/10.1016/j.epsl.2014.12.035>.
- Raymo, M.E., R. Kozdon, D. Evans, L. Lisiecki, and H.L. Ford. 2018. The accuracy of mid-Pliocene $\delta^{18}\text{O}$ -based ice volume and sea level reconstructions. *Earth-Science Reviews* 177:291–302, <https://doi.org/10.1016/j.earscirev.2017.11.022>.
- Rignot, E., J. Mouginot, B. Scheuchl, M. van de Broeke, M. van Wessen, and M. Morlighem. 2019. Four decades of Antarctic Ice Sheet mass balance from 1979–2017. *Proceedings of the National Academy of Sciences of the United States of America* 116(4):1,095–1,103, <https://doi.org/10.1073/pnas.1812883116>.
- Rintoul, S.R., S.L. Chown, R.M. DeConto, M.H. England, H.A. Fricker, V. Masson-Delmotte, T.R. Naish, M.J. Siegert, and J.C. Xavier. 2018. Choosing the future of Antarctica. *Nature* 558(7709):233–241, <https://doi.org/10.1038/s41586-018-0173-4>.
- Robel, A.A., and A.F. Banwell. 2019. A speed limit on ice shelf collapse through hydrofracture. *Geophysical Research Letters* 46(21):12,092–12,100, <https://doi.org/10.1029/2019GL084397>.
- Rohling, E.J., F.D. Hibbert, K.M. Grant, E.V. Galaasen, N. Ival, H.F. Kleiven, G. Marino, Y. Ninnemann, A.P. Roberts, Y. Rosenthal, and others. 2019. Asynchronous Antarctic and Greenland ice-volume contributions to the last interglacial sea-level highstand. *Nature Communications* 10:5040, <https://doi.org/10.1038/s41467-019-12874-3>.
- Rose, K.C., F. Ferraccioli, S.S.R. Jamieson, R.E. Bell, H. Corr, T.T. Creyts, D. Braaten, T.A. Jordan, P.T. Fretwell, and D. Damaske. 2013. Early East Antarctic Ice Sheet growth recorded in the landscape of the Gamburtsev Subglacial Mountains. *Earth and Planetary Science Letters* 375:1–12, <https://doi.org/10.1016/j.epsl.2013.03.053>.
- Sagoo, N., P. Valdes, R. Flecker, and L.J. Gregoire. 2013. The early Eocene equable climate problem: Can perturbations of climate model parameters identify possible solutions? *Philosophical Transactions of the Royal Society A* 371(2001), <https://doi.org/10.1098/rsta.2013.0123>.
- Sangiorgi, F., P.K. Bijl, S. Passchier, U. Salzmann, S. Schouten, R. McKay, R.D. Cody, J. Pross, T. van de Fliert, S.M. Bohaty, and others. 2018. Southern Ocean warming and Wilkes Land ice sheet retreat during the mid-Miocene. *Nature Communications* 9:317, <https://doi.org/10.1038/s41467-017-02609-7>.
- Schoof, C. 2007. Ice sheet grounding line dynamics: Steady states, stability, and hysteresis. *Journal of Geophysical Research* 112(F3), <https://doi.org/10.1029/2006JF000664>.
- Seroussi, H., and M. Morlighem. 2018. Representation of basal melting at the grounding line in ice flow models. *The Cryosphere* 12:3,085–3,096, <https://doi.org/10.5194/tc-12-3085-2018>.
- Shackleton, N. 1967. Oxygen isotope analyses and Pleistocene temperatures re-assessed. *Nature* 215(5096):15–17, <https://doi.org/10.1038/215015a0>.
- Shakun, J.D., L.B. Corbett, P.R. Bierman, K. Underwood, D.M. Rizzo, S.R. Zimmerman, M.W. Caffee, T. Naish, N.R. Golledge, and C.C. Hay. 2018. Minimal East Antarctic Ice Sheet retreat onto land during the past eight million years. *Nature* 558:284–287, <https://doi.org/10.1038/s41586-018-0155-6>.
- Shevenell, A.E., J.P. Kennett, and D.W. Lea. 2004. Middle Miocene Southern Ocean cooling and Antarctic cryosphere expansion. *Science* 305(5691):1,766–1,770, <https://doi.org/10.1126/science.1100061>.
- Shevenell, A.E., J.P. Kennett, and D.W. Lea. 2008. Middle Miocene ice sheet dynamics, deep-sea temperatures, and carbon cycling: A Southern Ocean perspective. *Geochemistry, Geophysics, Geosystems* 9(2), <https://doi.org/10.1029/2007GC001736>.
- Simkins, L.M., J.B. Anderson, S.L. Greenwood, H.M. Gonnermann, L.O. Prothro, A.R.W. Halberstadt, L.A. Stearns, D. Pollard, and R.M. DeConto. 2017. Anatomy of a meltwater drainage system beneath the ancestral East Antarctic Ice Sheet. *Nature Geoscience* 10(9):691–697, <https://doi.org/10.1038/ngeo3012>.
- Spears, A., M. West, M. Meister, J. Buffo, C. Walker, T.R. Collins, A. Howard, and B. Schmidt. 2016. Under ice in Antarctica. *IEEE Robotics and Automation Magazine* 23(4):30–41, <https://doi.org/10.1109/MRA.2016.2578858>.
- Stap, L.B., J. Sutter, G. Knorr, M. Stürz, and G. Lohmann. 2019. Transient variability of the Miocene Antarctic Ice Sheet smaller than equilibrium differences. *Geophysical Research Letters* 46(8):4,288–4,298, <https://doi.org/10.1029/2019GL082163>.
- Stocchi, P., C. Escutia, A.J.P. Houben, B.L.A. Vermeersen, P.K. Bijl, H. Brinkhuis, R.M. DeConto, S. Galeotti, S. Passchier, D. Pollard, and others. 2013. Relative sea-level rise around East Antarctica during Oligocene glaciation. *Nature Geoscience* 6(5):380–384, <https://doi.org/10.1038/NNGEO1783>.
- Treasure, A.M., F. Roquet, I.J. Ansoorge, M.N. Bester, L. Boehme, H. Bornemann, J.-B. Charrassin, D. Chevallier, D.P. Costa, M.A. Fedak, and others. 2017. Marine mammals exploring the oceans pole to pole: A review of the MEOP consortium. *Oceanography* 30(2):132–138, <https://doi.org/10.5670/oceanog.2017.234>.
- Trusel, L.D., K.E. Frey, S.B. Das, P.K. Munneke, and R.M. Van Den Broeke. 2013. Satellite-based estimates of Antarctic surface meltwater fluxes. *Geophysical Research Letters* 40(23):6,148–6,153, <https://doi.org/10.1002/2013GL058138>.
- Turney, C.S.M., C.J. Fogwill, N.R. Golledge, N.P. McKay, E. van Sebille, R.T. Jones, D. Etheridge, M. Rubino, D.P. Thornton, S.M. Davies, and others. 2020. Early Last Interglacial ocean warming drove substantial ice mass loss from Antarctica. *Proceedings of the National Academy of Sciences of the United States of America* 117(8):3,996–4,006, <https://doi.org/10.1073/pnas.1902469117>.
- Warny, S., R.A. Askin, M.J. Hannah, B.A.R. Mohr, J.I. Raine, D.M. Harwood, and F. Florindo. 2009. Palynomorphs from a sediment core reveal a sudden remarkably warm Antarctica during the middle Miocene. *Geology* 37(10):955–958, <https://doi.org/10.1130/G30139A.1>.
- Whitehouse, P.L., N. Gomez, M.A. King, and D.A. Wiens. 2019. Solid Earth change and the evolution of the Antarctic Ice Sheet. *Nature Communications* 10(503), <https://doi.org/10.1038/s41467-018-08068-y>.
- Wilson, D.J., R.A. Bertram, E.F. Needham, T. van de Fliert, K.J. Welsh, R.M. McKay, A. Mazumder, C.R. Riesselman, F.J. Jimenez-Espejo, and C. Escutia. 2018. Ice loss from the East Antarctic Ice Sheet during late Pleistocene interglacials. *Nature* 561(7723):383–386, <https://doi.org/10.1038/s41586-018-0501-8>.
- Winkelmann, R., A. Levermann, A. Ridgwell, and K. Caldeira. 2015. Combustion of available fossil fuel resources sufficient to eliminate the Antarctic Ice Sheet. *Science Advances* 1(8):e1500589, <https://doi.org/10.1126/sciadv.1500589>.
- Winnick, M.J., and J.K. Caves. 2015. Oxygen isotope mass-balance constraints on Pliocene sea level and East Antarctic Ice Sheet stability. *Geology* 43(10):879–882, <https://doi.org/10.1130/G36999.1>.
- Wise, M.G., J.A. Dowdeswell, M. Jakobsson, and R.D. Larer. 2017. Evidence of marine ice-cliff instability in Pine Island Bay from iceberg-keel plough marks. *Nature* 550(7677):506–510, <https://doi.org/10.1038/nature24458>.
- Young, D.A., A.P. Wright, J.L. Roberts, R.C. Warner, N.W. Young, J.S. Greenbaum, D.M. Schroeder, J.W. Holt, D.E. Sugden, D.D. Blankenship, and others. 2011. A dynamic early East Antarctic Ice Sheet suggested by ice-covered fjord landscapes. *Nature* 474(7349):72–75, <https://doi.org/10.1038/nature10114>.
- Zachos, J.C., J.R. Breza, and S.M. Wise. 1992. Early Oligocene ice-sheet expansion on Antarctica: Stable isotope and sedimentological evidence from Kerguelen Plateau, southern Indian Ocean. *Geology* 20(6):569–573, [https://doi.org/10.1130/0091-7613\(1992\)020<0569:EOISEO>2.3.CO;2](https://doi.org/10.1130/0091-7613(1992)020<0569:EOISEO>2.3.CO;2).
- Zachos, J.C., G.R. Dickens, and R.E. Zeebe. 2008. An early Cenozoic perspective on greenhouse warming and carbon-cycle dynamics. *Nature* 451(7176):279–283, <https://doi.org/10.1038/nature06588>.
- Zelinka, M.D., T.A. Myers, D.T. McCoy, S. Po-Chedley, P.M. Caldwell, P. Ceppi, S.A. Klein, and K.E. Taylor. 2020. Causes of higher climate sensitivity in CMIP6 models. *Geophysical Research Letters* 47(1):e2019GL085782, <https://doi.org/10.1029/2019GL085782>.
- Zhang, Y.G., M. Pagani, Z. Liu, S.M. Bohaty, and R. DeConto. 2013. A 40-million-year history of atmospheric CO₂. *Philosophical Transactions of the Royal Society A* 371:20130096, <https://doi.org/10.1098/rsta.2013.0096>.
- Zhu, J., C.J. Poulsen, and J.E. Tierney. 2019. Simulation of Eocene extreme warmth and high climate sensitivity through cloud feedbacks. *Science Advances* 5(9):eaax1874, <https://doi.org/10.1126/sciadv.aax1874>.
- Zhu, J., C.J. Poulsen, and B.L. Otto-Bliesner. 2020. High climate sensitivity in CMIP6 model not supported by paleoclimate. *Nature Climate Change* 10:378–379, <https://doi.org/10.1038/s41586-020-0764-6>.

ACKNOWLEDGMENTS

E.G. thanks the Royal Society and Natural Environment Research Council (NERC) grant “PLIOAMP” (NE/T007397/1) for financial support. B.K. is funded by a Lamont-Doherty Postdoctoral Fellowship. We thank Bas de Boer and guest editor Amelia Shevenell for comments that greatly improved the manuscript.

AUTHORS

Edward G.W. Gasson (e.gasson@bristol.ac.uk) is Royal Society University Research Fellow, School of Geographical Sciences, University of Bristol, Bristol, UK. **Benjamin A. Keisling** is Postdoctoral Research Scientist, Lamont-Doherty Earth Observatory of Columbia University, Palisades, NY, USA.

ARTICLE CITATION

Gasson, E.G.W., and B.A. Keisling. 2020. The Antarctic Ice Sheet: A paleoclimate modeling perspective. *Oceanography* 33(2):90–100, <https://doi.org/10.5670/oceanog.2020.208>.

COPYRIGHT & USAGE

This is an open access article made available under the terms of the Creative Commons Attribution 4.0 International License (<https://creativecommons.org/licenses/by/4.0/>), which permits use, sharing, adaptation, distribution, and reproduction in any medium or format as long as users cite the materials appropriately, provide a link to the Creative Commons license, and indicate the changes that were made to the original content.

SIDEBAR. The Mid-Pleistocene Enigma

By Heather L. Ford and Thomas B. Chalk

Variations in Earth's orbit affect incoming solar radiation and have guided past glacial-interglacial oscillations. These rhythmic changes in insolation are known as Milankovitch cycles. Approximately 900,000 years ago, Earth's climate pacemaker skipped a beat and switched from the 41,000-year obliquity (Earth's axial tilt) pacing of the Early Pleistocene to ~100,000-year eccentricity (circularity of Earth's orbit around the sun) pacing of the Late Pleistocene. This glacial-to-interglacial shift, called the Mid-Pleistocene Transition (MPT), remains one of the most enduring mysteries of the Quaternary and in the field of paleoceanography. Recent reconstructions of atmospheric and oceanic processes and studies of the dynamic linkages between them have paved the way for a more detailed mechanistic understanding of this climatic transition and of Earth's climate system at large.

Advances in geochemical techniques applied to studies of ocean sediment cores recovered by scientific ocean drilling enable reconstruction of higher-resolution paleoclimatic

records of atmospheric CO₂, ocean remineralized carbon content, ocean circulation change, and ice volume. We now understand that the characteristic timescales of glacial-interglacial variability are primarily linked to dynamical processes modulated by the ocean and its interaction with ice sheets—in particular, we understand much more about the Southern Ocean's role in moderating Earth's climate and its characteristic beats.

The MPT occurred in at least two steps (Figures 1 and 2). The first was the “900 kyr event” around Marine Isotope Stage¹ (MIS) 22, when the quasi-eccentricity signal emerged. The second was MIS 16 when the transition was complete. The first step had the largest impact on ocean carbon cycling and (likely) on atmospheric carbon. The Early Pleistocene had symmetrical ice age cycles and a glacial-to-interglacial atmospheric CO₂ of ~240–285 μatm (Yan et al., 2019, and references within). Between MIS 22 and MIS 16, there were weak interglacial and increasingly severe glacial periods. At MIS 16,

¹ Marine isotope stages are alternating warm and cool periods in Earth history deduced from oxygen isotope ratios of fossil benthic foraminifera shells recovered from deep-sea sediments. Even numbers represent cold glacial periods and odd numbers represent warmer interglacial periods. MIS 1 is the present day.

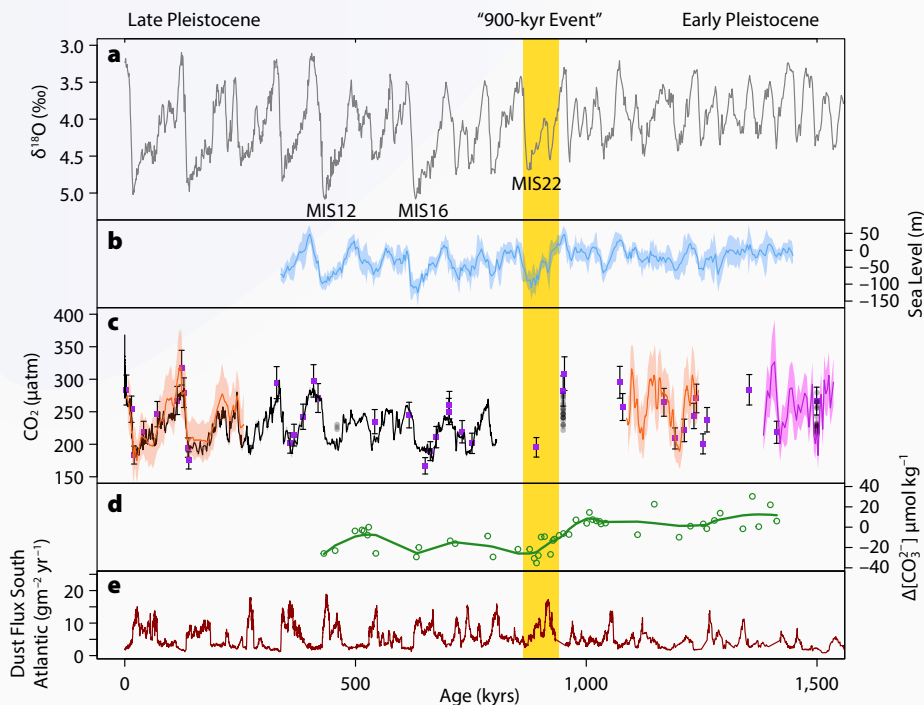


FIGURE 1. A selection of records across the Mid-Pleistocene Transition: (a) Benthic oxygen isotope stack (Lisiecki and Raymo, 2005). (b) Ice volume as a proxy for sea level, derived from $\delta^{18}\text{O}$ of seawater from benthic foraminifera (Ford and Raymo, 2020). The light blue is the 1 sigma error envelope from a Monte Carlo simulation. (c) Atmospheric CO₂ reconstructions, where the black line is the Antarctic ice core record and gray dots are the Antarctic blue ice record. The colored records are from marine sediment reconstructions (Chalk et al., 2017, and references within). Error bars are 2 sigma. (d) Carbonate ion records derived from foraminiferal trace element (B/Ca) (Farmer et al., 2019, and references within). (e) Southern Hemisphere iron dust based on analysis of marine sediments from Ocean Drilling Program Site 1090, located in the Atlantic sector of the subantarctic (Martínez-García et al., 2011). Marine Isotope Stages (MIS) discussed in text are annotated, and the yellow bar highlights the 900 kyr event.

the strong glacial periods of the Late Pleistocene emerged, and after MIS 12, glacial-to-interglacial atmospheric CO₂ ranged from ~200 μatm to 280 μatm.

The role of CO₂ as a driving mechanism for the MPT is debated, largely due to the absence of a continuous high-resolution record over the transition. Within the next few years, ice drilling in Antarctica may yield some of Earth's oldest ice, with potential for recovering a continuous record of ancient atmospheric composition back to 1.5 million years ago (Dahl-Jensen, 2018). Nevertheless, existing high-resolution atmospheric CO₂ snapshots before, during, and after the MPT suggest that a combination of ocean and ice sheet dynamics controls atmospheric CO₂ cycles (e.g., Chalk et al., 2017).

Ocean dynamics played an increasingly important role in sequestering carbon in the deep ocean over the MPT, particularly during the glacial intervals. Neodymium isotopes and benthic foraminifera δ¹³C, which are used as water mass tracers, show that intermediate- to deep-ocean circulation reorganized between MIS 25 and MIS 21 (Pena and Goldstein, 2014; Ford et al., 2016). Prior to the MPT, deep water formed in the polar north extended toward southern subpolar latitudes during glacial and interglacial periods. During the 900 kyr event, southern-sourced deep water flooded the Atlantic, and its spatial range continued to be extensive during subsequent glacial intervals. This southern-sourced deep water is carbon-rich and has low carbonate ion values (e.g., more acidic, higher carbon content water; Farmer et al., 2019, and refer-

ences within) and increased the deep ocean carbon reservoir.

In addition to changing the geometry of major water masses, enhanced biological production changed the carbon content of the water subducting into the ocean's interior from the Southern Ocean, effectively sequestering more carbon in the global deep ocean. During the early stages of the MPT, the amount of iron-bearing dust supplied to the Southern Ocean began to increase (Figure 1), particularly during ice ages (Martínez-García et al., 2011). This iron fertilized the Southern Ocean, increased biological productivity and biological pump efficiency, and contributed to the drawdown of CO₂ (Chalk et al., 2017).

The triggers for these alterations in Southern Ocean circulation and biological dynamics remain unknown. A Southern Hemisphere insolation minimum around the 900 kyr event points toward an Antarctic trigger that allowed sea ice to expand. Raymo et al. (2006) hypothesized that Antarctica's ice sheets transformed from terrestrial-based to marine-based at this time, though there is little physical evidence to support this. Changes in sea ice and ice sheet margins would have altered the freshwater balance of the Southern Ocean, strengthened water-column stratification, and contributed to sequestration of carbon into the ocean's interior (Hasenfratz et al., 2019).

Deciphering when, where, and how much ice volume growth occurred over the MPT from benthic δ¹⁸O records is difficult. An individual record reflects the regional signal from

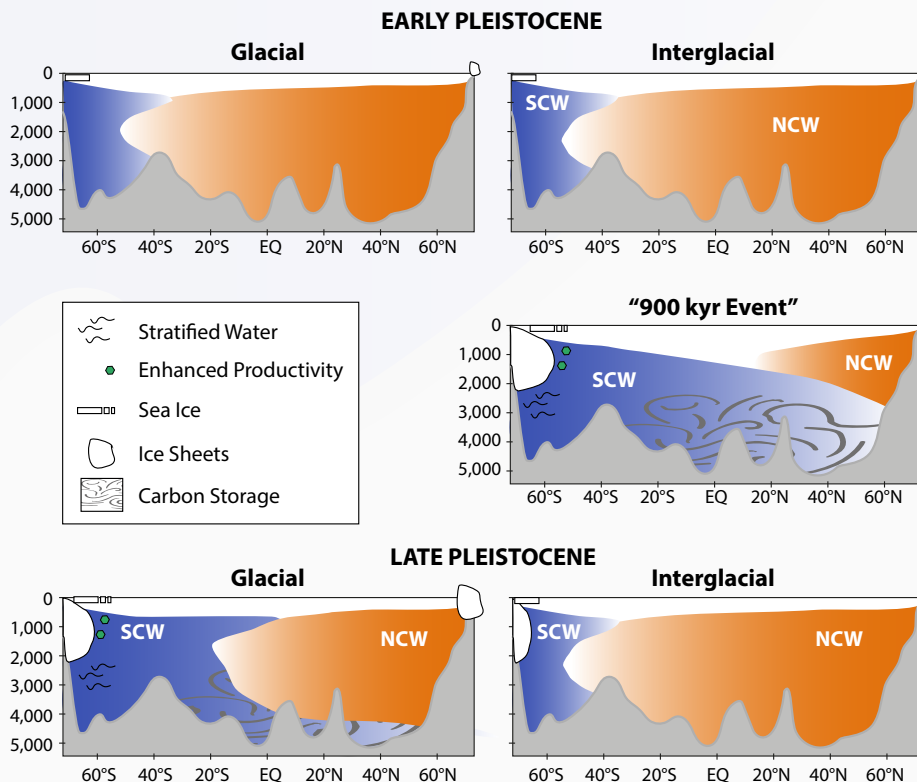


FIGURE 2. Schematic of biological productivity, carbon storage, ocean circulation, sea ice, and ice volume changes over the Mid-Pleistocene Transition derived from data displayed in Figure 1. SCW is southern component water, which is carbon-rich. NCW is northern component water. The 900 kyr event represents a large reorganization of Southern Hemisphere processes. SCW and NCW are derived from Nd and δ¹³C records.

where deep waters are formed (temperature and evaporation and precipitation processes that are imprinted in the $\delta^{18}\text{O}$ of seawater), the circulation history of the water mass, and the global signal of both temperature and ice volume. Lisiecki and Raymo's (2005) original "LR04 stack" (updated by Ahn et al., 2017) was revolutionary because these regional imprints were largely "averaged out," allowing them to create a global picture of temperature and ice volume over the last few million years (Figure 1). The question of *where* ice volume increased can only be inferred, even in a benthic stack.

Isolating $\delta^{18}\text{O}$ of seawater is crucial for reconstructing changes in global ice volume over the MPT. The $\delta^{18}\text{O}$ of benthic foraminifera calcite reflects both the temperature and $\delta^{18}\text{O}$ of seawater in which the calcite formed. The magnesium-to-calcium ratio of benthic foraminifera calcite can be used to independently constrain temperature so that the $\delta^{18}\text{O}$ of seawater can be teased apart. Although early interpretations from individual sediment cores were complicated by changes in ocean circulation, a recent stack of $\delta^{18}\text{O}$ of seawater that includes North Atlantic, South Pacific, and North Pacific sites aims to construct a global picture of ice volume change (Ford and Raymo, 2020). It shows that ice volume grew during both MIS 22 and MIS 16 (Figure 1), though we don't know the precise location of this ice. Given the Southern Hemisphere insolation minimum during the 900 kyr event, ice volume growth likely occurred in Antarctica during MIS 22 and consequently increased the sensitivity to the 100 kyr cycle through hemispheric phase locking (Raymo and Huybers, 2008). Ice volume growth during MIS 16 likely had Northern Hemisphere origins, possibly related to Laurentian regolith removal and ice sheet stability (Clark and Pollard, 1998), and this growth completed the transition.

The MPT is a prime example of a gradual climate transition whereby small, additive changes in Earth's internal climate dynamics can force a large response, and the transition occurs with relatively minor changes to average CO_2 levels (less than 20 year's average at current rates of anthropogenic emissions) and with no apparent changes to the structure of orbital parameters that have governed much of Cenozoic climate change. Studying exactly how these changes were triggered and how they interact with one another is going to be crucial as we enter the next phase of human-caused climate change.

REFERENCES

- Ahn, S., D. Khider, L.E. Lisiecki, and C.E. Lawrence. 2017. A probabilistic Pliocene-Pleistocene stack of benthic $\delta^{18}\text{O}$ using a profile hidden Markov model. *Dynamics and Statistics of the Climate System* 2:91–116, <https://doi.org/10.1093/climsys/dzx002>.
- Chalk, T.B., M.P. Hain, G.L. Foster, E.J. Rohling, P.F. Sexton, M.P.S. Badger, S.G. Cherry, A.P. Hasenfratz, G.H. Haug, S.L. Jaccard, and others. 2017. Causes of ice age intensification across the Mid-Pleistocene Transition. *Proceedings of the National Academy of Sciences of the United States of America* 123, 201702143, <http://doi.org/10.1073/pnas.1702143114>.
- Clark, P.U., and D. Pollard. 1998. Origin of the Middle Pleistocene Transition by ice sheet erosion of regolith. *Paleoceanography and Paleoclimatology* 13:1–9, <https://doi.org/10.1029/97PA02660>.
- Dahl-Jensen, D. 2018. Drilling for the oldest ice. *Nature Geoscience* 11:703–704, <https://doi.org/10.1038/s41561-018-0241-2>.

- Farmer, J.R., B. Hönisch, L.L. Haynes, D. Kroon, S. Jung, H.L. Ford, M.E. Raymo, M. Jaume-Seguí, D.B. Bell, S.L. Goldstein, and others. 2019. Deep Atlantic Ocean carbon storage and the rise of 100,000-year glacial cycles. *Nature Geoscience* 12:355–360, <https://doi.org/10.1038/s41561-019-0334-6>.
- Ford, H.L., S.M. Sosdian, Y. Rosenthal, and M.E. Raymo. 2016. Gradual and abrupt changes during the Mid-Pleistocene Transition. *Quaternary Science Reviews* 148(C):222–233, <https://doi.org/10.1016/j.quascirev.2016.07.005>.
- Ford, H.L., and M.E. Raymo. 2020. Regional and global signals in seawater $\delta^{18}\text{O}$ records across the mid-Pleistocene transition. *Geology* 48(2):113–117, <https://doi.org/10.1130/G46546.1>.
- Hasenfratz, A.P., S.L. Jaccard, A. Martínez-García, D.M. Sigman, D.A. Hodell, D. Vance, S.M. Bernasconi, H.F. Kleiven, F.A. Haumann, and G.H. Haug. 2019. The residence time of Southern Ocean surface waters and the 100,000-year ice age cycle. *Science* 363(6431):1,080–1,084, <https://doi.org/10.1126/science.aat7067>.
- Lisiecki, L.E., and M.E. Raymo. 2005. A Pliocene-Pleistocene stack of 57 globally distributed benthic $\delta^{18}\text{O}$ records. *Paleoceanography and Paleoclimatology* 20(1), <https://doi.org/10.1029/2004PA001071>.
- Martínez-García, A., A. Rosell-Melé, S.L. Jaccard, W. Geibert, D.M. Sigman, and G.H. Haug. 2011. Southern Ocean dust-climate coupling over the past four million years. *Nature* 476:312–315, <https://doi.org/10.1038/nature10310>.
- Pena, L.D., and S.L. Goldstein. 2014. Thermohaline circulation crisis and impacts during the mid-Pleistocene transition. *Science* 345(6194):318–322, <https://doi.org/10.1126/science.1249770>.
- Raymo, M.E., L.E. Lisiecki, and K.H. Nisancioglu. 2006. Plio-Pleistocene ice volume, Antarctic climate, and the global $\delta^{18}\text{O}$ record. *Science* 313(5786):492–495, <https://doi.org/10.1126/science.1123296>.
- Raymo, M.E., and P. Huybers. 2008. Unlocking the mysteries of the ice ages. *Nature* 451:284–285, <https://doi.org/10.1038/nature06589>.
- Yan, Y., M.L. Bender, E.J. Brook, H.M. Clifford, P.C. Kemeny, A.V. Kurbatov, S. Mackay, P.A. Mayewski, J. Ng, J.P. Severinghaus, and J.A. Higgins. 2019. Two-million-year-old snapshots of atmospheric gases from Antarctic ice. *Nature* 574:663–666, <https://doi.org/10.1038/s41586-019-1692-3>.

ACKNOWLEDGMENTS

We are grateful to members of the PAGES Working Group on Quaternary Interglacials (QUIGS), and in particular participants of the workshop on Interglacials of the 41 kyr world and the Mid-Pleistocene Transition, for stimulating discussions. Ford is supported by the Natural Environment Research Council (NE/N015045/1).

AUTHORS

Heather L. Ford (h.ford@qmul.ac.uk) is Lecturer in Environmental Science, Queen Mary University of London, London, UK. **Thomas B. Chalk** (t.chalk@noc.soton.ac.uk) is Postdoctoral Research Fellow, National Oceanography Centre, University of Southampton, Southampton, UK.

Archaeal Membrane Lipid-Based Paleothermometry for Applications in Polar Oceans

By Susanne Fietz, Sze Ling Ho, and Carme Huguet

Investigating the icy waters of
the Southern Ocean aboard
R/V SA Agulhas II.

ABSTRACT. To establish whether ongoing climate change is outside the range of natural variability and a result of anthropogenic inputs, it is essential to reconstruct past oceanic and atmospheric temperatures for comparison with the modern world. Reconstructing past temperatures is a complex endeavor that employs indirect proxy indicators. Over the past two decades, promising paleothermometers have been developed that use isoprenoidal glycerol dialkyl glycerol tetraethers (isoGDGTs) from the membrane lipids of archaea preserved in marine sediments. These proxies are based on the observed relationship between lipid structure and temperature. As with all proxy indicators, observed relationships are often complex. Here, we focus on the application of isoGDGT paleotemperature proxies in the polar oceans, critical components of the global climate system. We discuss the application of and caveats regarding these archaeal membrane lipid-derived proxies and make recommendations to improve isoGDGT-derived polar ocean temperature reconstructions. We also review initial successes using hydroxylated (OH) isoGDGTs proxies in cold Arctic and Southern Ocean regions and recommend that multi-proxy approaches, including both hydroxylated and non-hydroxylated isoGDGTs, be used to contribute to the robustness of paleotemperature reconstructions.

INTRODUCTION

Given the rate and societal impact of ongoing human-caused warming, understanding the geographical extent, magnitude, and frequency of past global climate variations is essential. Ocean temperature is a critical parameter in the climate system. While sea surface temperature reflects heat exchange between the ocean and atmosphere, as well as large-scale ocean circulation, the average temperature of the upper ocean (0–1,000 m) is a useful estimate of upper ocean heat content. Thus, a top priority in paleoceanography is to provide accurate proxy-based ocean temperature reconstructions across all timescales (millions to hundreds of years). This information, gleaned from geological records, is essential for validating numerical models used to project future change and to inform policymakers who are developing strategies for mitigation and adaptation.

Efforts to reconstruct past surface and bottom water temperatures have expanded to include the polar regions (e.g., Shevenell et al., 2011; Fietz et al., 2016), where reliable instrumental temperature data are only available for the past 100 years (e.g., Hansen et al., 2010; IPCC, 2019, and references therein). Part of the impetus for this focus is the rev-

elation that retreating grounding lines accompanied by warming ocean waters are resulting in Antarctic ice sheet mass loss and global sea level rise (Jacob et al., 2012; Rintoul et al., 2018). Furthermore, the Intergovernmental Panel on Climate Change states with high confidence that “both polar oceans have continued to warm in recent years, with the Southern Ocean being disproportionately and increasingly important in global ocean heat increase” (IPCC, 2019).

As calcium carbonate microfossils are not always continuously preserved in high-latitude sediments (e.g., Zamelczyk et al., 2012), paleoceanographers turn to non-carbonate-based molecular fossils to determine past variations in high-latitude ocean water temperatures (e.g., Sluijs et al., 2006; Bijl et al., 2009; Shevenell et al., 2011). Lipids preserved in marine sediments that have been successfully used in paleotemperature reconstructions include algal alkenones and archaeal isoprenoidal glycerol dialkyl glycerol tetraethers (isoGDGTs), which are sensitive to temperature change and relatively resilient to degradation compared to other lipids (e.g., Huguet et al. 2008; Zonneveld et al., 2010; Schouten et al., 2013; Herbert, 2014, and references therein). For example, the most mature of these paleothermometers,

the alkenone unsaturation index U_{37}^K , was developed in 1986 (Brassell et al., 1986) and is widely used to reconstruct sea surface temperatures (e.g., Ho et al., 2013; Herbert, 2014, and references therein). Subsequently, the archaeal isoGDGT-based paleotemperature proxy known as the TetraEther indeX of 86 carbons, TEX_{86} , was proposed (Schouten et al., 2002) and well received by the organic geochemistry community.

One advantage of proxies that employ archaeal membrane lipids is that these molecules are ubiquitous in globally distributed marine sediments, making them useful for calibration and estimating low-to-high latitude thermal gradients (Schouten et al., 2002). However, as with all proxies, researchers have discovered a number of non-thermal factors that affect the distribution of isoGDGTs in marine sediments. Because archaea occupy almost every niche on Earth, a number of studies have been undertaken to improve our understanding of archaeal distribution, ecophysiology (e.g., Hayes, 2000), and membrane molecular structure (e.g., Chugunov et al., 2015).

Here, we review current knowledge of the archaeal isoGDGT paleotemperature proxies, including the recent hydroxylated isoGDGT (OH-isoGDGTs) paleothermometer. We focus our review on recent insights gained from using these archaeal membrane lipid paleothermometers in the polar regions.

ARCHAEOAL MEMBRANE LIPIDS AND PALEOTHERMOMETRY

Membranes are the interfaces between (micro)organisms and their environments. The key roles they play in metabolism (e.g., providing energy to the cell using ion gradients across the membranes; Konings et al., 2002; Zhou et al., 2020) and environmental sensing and signaling (Ren and Paulsen, 2005) require constant composition adjustments (Oger and Cario, 2013). Archaea synthesize tetraether lipids that span the entire mem-

brane and form a monolayer (Koga and Morii, 2007). The isoGDGTs are a subset of these archaeal tetraether lipids, and their composition is group specific; for example, Thaumarchaeota preferentially synthesize isoGDGTs with cyclopentane rings (Sinninghe Damsté et al., 2002). Archaea also produce OH-isoGDGTs (Lipp and Hinrichs, 2009) that were first discovered in methanotrophic archaea (Hinrichs et al., 1999) and later in Thaumarchaeota (Elling et al., 2017; Bale et al., 2019).

The stability of archaeal membranes increases with ambient growth temperature, especially in thermophilic extremophiles (De Rosa et al., 1980). Yet, it was not until the 2000s that geochemists exploited this observation to develop quantitative temperature proxies (e.g., Schouten et al., 2002; Kim et al. 2010; Ho et al., 2014; Tierney and Tingley, 2014). Of particular importance for understanding isoGDGT-based proxies is that, at all temperatures, archaea must maintain semi-permeability without impacting rigidity (e.g., Chugunov

et al., 2015). Most isoGDGTs involved in paleothermometry contain one or more cyclopentane rings, resulting in tighter packing and a more stable membrane (see Figure 1 in Zhou et al., 2020). At low temperatures, archaea reduce the number of cyclopentane rings in their membrane structures, thereby preventing membrane rigidity (Gabriel and Chong, 2000; Schouten et al., 2002). Indeed, Schouten et al. (2002) observed that the cyclization of isoGDGTs in surface marine sediments is correlated globally with measured surface water temperature in mesophilic (non-extreme) environments, resulting in the development of the first archaeal lipid paleothermometer, TEX_{86} (Table 1). In addition, in Thaumarchaeota, hydroxylation increases membrane fluidity and transport (Huguet et al., 2017), which compensates for increased rigidity at lower temperatures. The observation that the number of rings in hydroxylated isoGDGTs changes with temperature led to the development of ring-number-based OH-isoGDGT proxies (Fietz et al., 2013; Lü et al., 2015; Table 1).

TEX₈₆ RECONSTRUCTIONS IN POLAR OCEANS: OPPORTUNITIES AND CHALLENGES

The general relationship between the number of rings in sedimentary GDGTs and the overlying mean annual sea surface temperature is that the warmer the seawater, the more isoGDGTs there are with higher numbers of cyclopentane rings (e.g., isoGDGT-2 and isoGDGT-3), resulting in higher TEX_{86} index values; incorporation of the isomer of crenarchaeol adds accuracy (Sinninghe Damsté et al., 2002). Kim et al. (2010) proposed a variant of TEX_{86} , termed TEX_{86}^L , that employs a different GDGT combination (TEX_{86}^L ; Table 1) and is intended for temperatures below 15°C.

The isoGDGT-derived indices in surface sediments are generally well correlated with seawater temperatures in the overlying upper water column (e.g., Kim et al., 2010; Ho et al., 2014; Tierney and Tingley, 2014; Figure 1). In global calibrations, the standard errors of temperature estimates vary between 4.0°C and

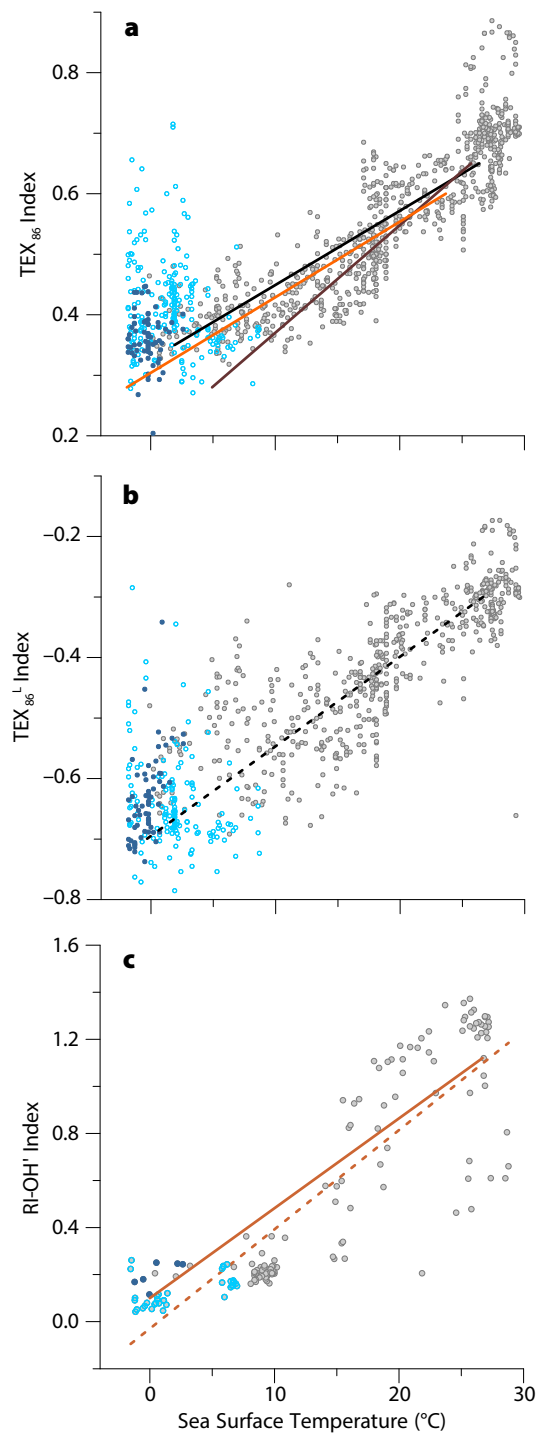
TABLE 1. Isoprenoid and hydroxylated GDGT-derived indices proposed for paleotemperature estimates. In the equations, the abbreviation GDGT*n* represents isoGDGTs with *n* number of cyclopentane rings. For example, isoGDGT-1 represents the non-hydroxylated isoprenoid GDGT with one cyclopentane moiety. The abbreviation OH-isoGDGT*n* stands for hydroxylated isoprenoid GDGTs with *n* number of cyclopentane rings. The term Σ isoGDGTs refers to the sum of all non-hydroxylated isoprenoid GDGTs (e.g., isoGDGT-1, isoGDGT-2, isoGDGT-3, crenarchaeol and its isomer, abbreviated in this table as cren'). The term Σ OH-isoGDGTs refers to the sum of OH-isoGDGT-0, OH-isoGDGT-1 and OH-isoGDGT-2.

INDEX	EQUATION	REFERENCE
TEX_{86}	$\frac{[\text{isoGDGT} - 2] + [\text{isoGDGT} - 3] + [\text{cren}']}{[\text{isoGDGT} - 1] + [\text{isoGDGT} - 2] + [\text{isoGDGT} - 3] + [\text{cren}]}$	Schouten et al., 2002
TEX_{86}^L	$\log \left(\frac{[\text{isoGDGT} - 2]}{[\text{isoGDGT} - 1] + [\text{isoGDGT} - 2] + [\text{isoGDGT} - 3]} \right)$	Kim et al., 2010
OH-GDGT%	$\frac{\Sigma \text{OH} - \text{isoGDGTs}}{(\Sigma \text{OH} - \text{isoGDGTs} + \Sigma \text{isoGDGTs})} \times 100$	Huguet et al., 2013
OH-GDGT _{1318/1316}	$\frac{\text{OH} - \text{isoGDGT} - 0}{\text{OH} - \text{isoGDGT} - 0 + \text{OH} - \text{isoGDGT} - 1}$	Fietz et al., 2013
RI-OH	$\frac{[\text{OH} - \text{isoGDGT} - 1] + 2 \times [\text{OH} - \text{isoGDGT} - 2]}{[\text{OH} - \text{isoGDGT} - 0] + [\text{OH} - \text{isoGDGT} - 1] + [\text{OH} - \text{isoGDGT} - 2]}$	Lü et al., 2015
RI-OH'	$\frac{[\text{OH} - \text{isoGDGT} - 1] + 2 \times [\text{OH} - \text{isoGDGT} - 2]}{[\text{OH} - \text{isoGDGT} - 1] + [\text{OH} - \text{isoGDGT} - 2]}$	Lü et al., 2015
OH ^c	$\frac{[\text{isoGDGT} - 2] + [\text{isoGDGT} - 3] + [\text{cren}'] - [\text{OH} - \text{isoGDGT} - 0]}{[\text{isoGDGT} - 1] + [\text{isoGDGT} - 2] + [\text{isoGDGT} - 3] + [\text{cren}'] + \Sigma \text{OH} - \text{isoGDGTs}}$	Fietz et al., 2016

5.2°C for TEX_{86}^L and TEX_{86} , respectively (Kim et al., 2010). Inter-laboratory error (3°–4°C) for TEX_{86} are the same order of magnitude as other commonly used quantitative temperature proxies (Schouten et al., 2013). There is, however, a larger scatter in the TEX_{86} –sea surface temperature (SST) relationships at the low temperature end of the calibrations (Figure 1; Kim et al., 2010; Ho et al., 2014; Tierney and Tingley, 2014). The scatter is partly due to bias from terrestrial input, especially in the Arctic Ocean (Ho et al., 2014; Y. Park et al., 2014), and potentially from the use of satellite-assigned sea surface temperatures below the seawater freezing point for some calibrations (Pearson and Ingalls, 2013). Large scatter in TEX_{86} –SST relationship is not an issue unique to the polar oceans. It also exists at the high-temperature end in the Red Sea (Figure 1), likely due to an endemic Thaumarchaeota population (Trommer et al., 2009). As such, TEX_{86} and its variants may be affected by environmental conditions other than temperature, such as pH (Elling et al., 2015), oxygen availability (Qin et al., 2015), cellular physiological acclimation including ammonia oxidation rates (Elling et al., 2014; Hurley et al., 2016), and shifts in season and depth of production (Huguet et al., 2007; Ho and Laepple, 2016; Chen et al., 2018). Many of the caveats mentioned above have been reviewed for the global ocean in general (see, for example, comprehensive reviews by Pearson and Ingalls, 2013; Schouten et al., 2013; and Tierney, 2014). Figure 2 illustrates concerns raised for the polar oceans.

A solution for overcoming some of the caveats is to develop a regional calibration. For instance, Shevenell et al. (2011) applied a regionally calibrated TEX_{86} equation instead of TEX_{86}^L to reconstruct Holocene temperature evolution in the Antarctic Peninsula (Figure 1a). Some sources of uncertainty, such as spatial change in the archaeal community, cannot be included in ordinary least squares regression approaches for global calibration. Thus, alternative statistical approaches have also been adopted to improve correlation of TEX_{86} with upper ocean temperature, such as Bayesian regression (BAYSPAR; Tierney and Tingley, 2014) and machine-learning approaches (OPTiMAL; Eley et al., 2019).

Despite calibration challenges, inherent to all paleotemperature proxies, the TEX_{86} paleothermometer revolutionized understanding of past ocean temperature changes in the carbonate-poor polar regions. In the Arctic Ocean, TEX_{86} provided one of the first quantitative temperature estimates for past warm climates characterized by high atmospheric CO_2 , such as the Cretaceous and the Eocene. TEX_{86} revealed that the Arctic surface ocean during these time peri-



- 60°S to 60°N
- >60°N
- >60°S
- Kim et al., 2010, Calibration
SST = $81.5 \times \text{TEX}_{86} - 26.6$, $n = 396$, $R^2 = 0.77$
- Kim et al., 2008, Calibration
SST = $56.2 \times \text{TEX}_{86} - 10.8$, $n = 223$, $R^2 = 0.94$
- Shevenell et al., 2011, Calibration
 $\text{TEX}_{86} = 0.0125 \times \text{SST} + 0.3038$, $n = 230$, $R^2 = 0.82$
- - Kim et al., 2010, Calibration
SST = $67.5 \times \text{TEX}_{86}^L + 46.9$, $n = 396$, $R^2 = 0.86$
- Lü et al., 2015, Calibration
RI-OH' = $0.0382 \times \text{SST} + 0.1$, $n = 107$, $R^2 = 0.75$
- - Linear Fit, This Study
RI-OH' = $0.0422 \times \text{SST} - 0.029$, $n = 167$, $R^2 = 0.76$

FIGURE 1. Selected global calibrations for paleothermometers (a) TEX_{86} (TetraEther index of 86 carbons), (b) TEX_{86}^L (which employs a different combination of glycerol dialkyl glycerol tetraethers from TEX_{86} and is intended for temperatures below 15°C), and (c) RI-OH' (the weighted average number of cyclopentane rings) against sea surface temperatures. The data for the scatterplots in (a) and (b) are sourced from Tierney and Tingley (2015). A new, extended compilation of published data sets is presented here for RI-OH' (Fietz et al., 2013; Huguet et al., 2013; Lü et al., 2015; Kaiser and Arz, 2016). In (c), linear plots illustrate published calibrations for all three indices as well as a new linear fit for the extended RI-OH' data set.

ods was as warm as today's subtropics, a stark contrast to the currently ice-covered Arctic (e.g., Jenkyns et al., 2004; Brinkhuis et al., 2006; Sluijs et al., 2006). Similarly, in the Southern Ocean, TEX₈₆ and its variants have made it possible to reconstruct the temperature evolution from the Jurassic to the Holocene (summarized in Table 2). Thanks to this large body of work, we now know that the surface temperature of the Southern Ocean was once as high as 30°C during the Jurassic (Jenkyns et al., 2012) and has cooled through the Cenozoic, resulting in present-day temperatures surrounding the Antarctic Peninsula (Shevenell et al., 2011; Etourneau et al., 2013). Importantly, TEX₈₆-based reconstructions have helped characterize past greenhouse climates, suggesting that Antarctic surface water temperatures were >10°C during the Early Eocene Climatic Optimum (e.g., Bijl

et al., 2009). These reconstructions also improved understanding of temperature magnitude ranges over major climate transitions, including the >4°C cooling across the Eocene-Oligocene transition (e.g., Bijl et al., 2009; Z. Liu et al., 2009). TEX₈₆-based paleotemperature studies also indicate that in climatically sensitive regions, surface ocean temperatures fluctuated abruptly during the Holocene (Shevenell et al., 2011), suggesting the potential for rapid polar ocean temperature fluctuations with continued warming. Furthermore, both long-term cooling and millennial-scale variability on the western Antarctic Peninsula are similar to changes in the low latitudes (i.e., the tropical Pacific) and in regional ice core records (Mulvaney et al., 2012), suggesting climate teleconnections between the low and high latitudes via the Southern Hemisphere westerlies (Shevenell et al., 2011).

DOES INCLUDING OH-isoGDGTs IN TEMPERATURE PROXY INDEX IMPROVE THE ESTIMATES?

At some sites in the Arctic and Southern Oceans, TEX₈₆ and TEX₈₆^L do not show expected changes. For example, analyses using these proxies do not reflect the warmer conditions during glacial retreat in the Pliocene Arctic (Knies et al., 2014), during the Plio-Pleistocene transition and Pleistocene deglaciations in the Southern Ocean (e.g., McKay et al., 2012; Fietz et al., 2016), and during the late Holocene Arctic sea ice melting (e.g., Fietz et al., 2013). Some inconsistencies in warmer reconstructed temperatures during the deglacials compared to peak interglacials may be attributed to increased meltwater stratification (Shevenell et al., 2011; McKay et al., 2012). Another caveat of particular importance here is the potential lack of TEX₈₆ sensitivity at tempera-

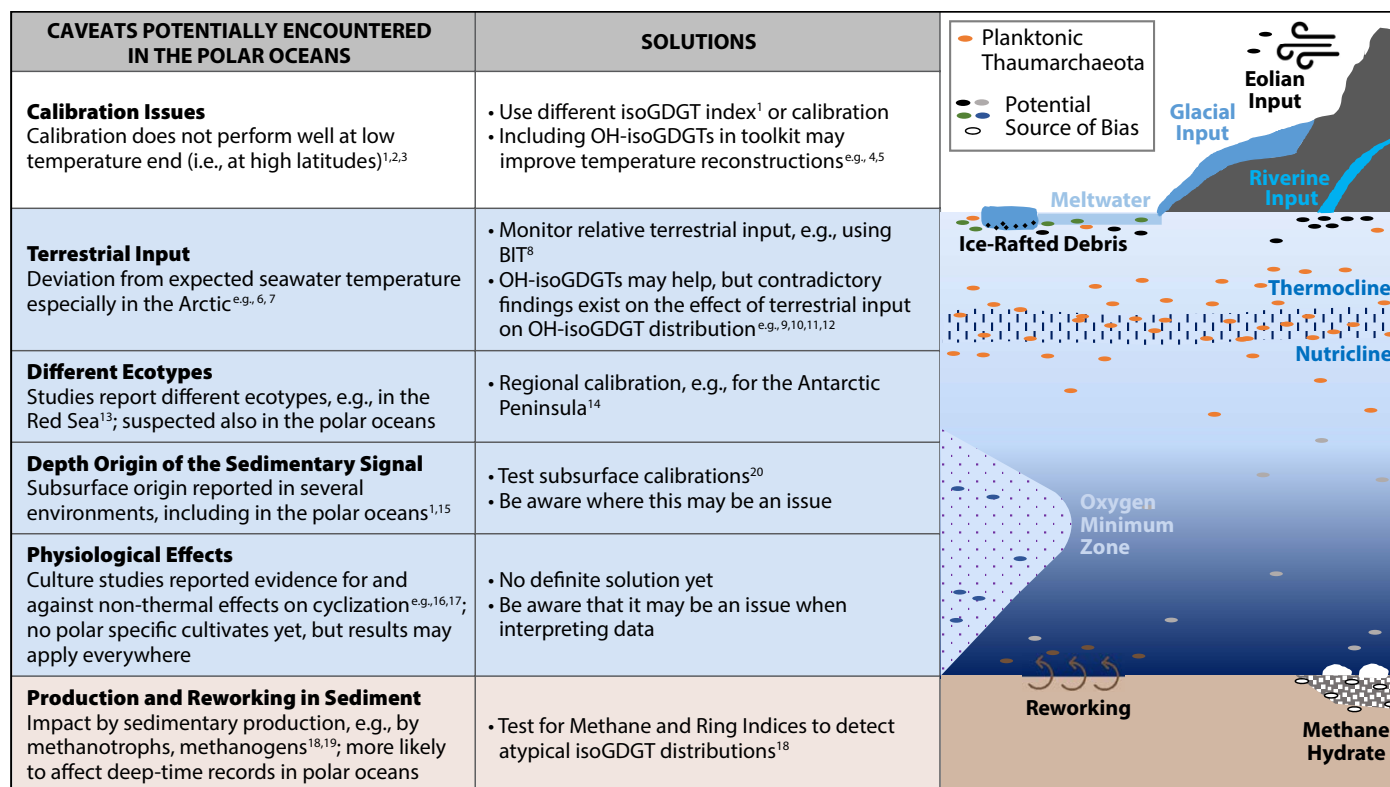


FIGURE 2. Overview of processes in the water column that can bias the isoprenoidal glycerol dialkyl glycerol tetraether (isoGDGT)-based paleotemperature reconstruction, especially in the polar oceans. Recommendations on how to work with such caveats and how including hydroxylated isoGDGTs (OH-isoGDGTs) in the paleothermometry toolbox may help are included. ¹Kim et al. (2010), ²Ho et al. (2014), ³Tierney and Tingley (2014), ⁴Fietz et al. (2013), ⁵Fietz et al. (2016), ⁶Ho et al. (2014), ⁷Y. Park et al. (2014), ⁸Hopmans et al. (2004), ⁹Kaiser and Arz (2016), ¹⁰Lü et al. (2019), ¹¹Kang et al. (2017), ¹²Wei et al. (2019), ¹³Ionescu et al. (2009), ¹⁴Shevenell et al. (2011), ¹⁵Huguet et al. (2007), ¹⁶Wuchter et al. (2004), ¹⁷Qin et al. (2015), ¹⁸Zhang et al. (2016), ¹⁹Shah et al. (2008), ²⁰Ho and Laepple (2016).

tures below 10°C as observed in mesocosms studies (e.g., Wuchter et al., 2004). In cold waters, archaea adjust the permeability of their membranes by changing the number of rings and adding hydroxyl groups. Including only one of the processes in the proxy index may therefore underestimate the full range of temperature acclimations of archaea in polar oceans. Hence, accounting for both processes by adding OH-isoGDGTs to the paleothermometer index should, in principle, improve the sensitivity of the proxy.

Like isoGDGTs, OH-isoGDGTs are globally distributed in the water column and in sediments (X.-L. Liu et al., 2012; Huguet et al., 2013; Figure 3). X.L. Liu et al. (2012) suggested that OH-isoGDGTs had potential for paleothermometry, and Huguet et al. (2013) proposed the first OH-isoGDGTs-based temperature proxy after observing a strong correla-

tion between the relative abundance of OH-isoGDGTs and sea surface temperatures in globally distributed seawater and sediment samples. Thereafter, several indices were proposed for applications in the polar oceans (Table 1). While the addition of hydroxylated isoGDGTs in the isoGDGT toolbox was originally proposed as an alternative for cold water paleothermometry (e.g., Fietz et al., 2013; Huguet et al., 2013), it was later suggested that an OH-isoGDGT-temperature relationship also exists globally (Lü et al., 2015). The finding of OH-isoGDGTs in a large set of surface sediments in Chinese coastal seas (n = 70; Figure 3) led Lü et al. (2015) to propose the weighted average number of cyclopentane rings (RI-OH index) as a proxy for sea surface temperatures, as well as a polar variant, the RI-OH' (Table 1; Figure 1c), with a residual standard error of 6.0°C (compared to

5.2°C for TEX₈₆; Kim et al., 2010). This RI-OH index reasonably reproduced TEX₈₆-derived temperatures dating back 30–40 million years for the US New Jersey shelf (de Bar et al., 2019).

Thus far, OH-isoGDGT-based proxies have been applied to Arctic and Southern Ocean sediments to reconstruct seawater temperatures and to help elucidate ice-ocean dynamics (Fietz et al., 2013, 2016; Knies et al., 2014; Kremer et al., 2018). In these cases, OH-isoGDGT proxies were utilized instead of TEX₈₆ as the latter did not yield changes in accordance with other proxies (Figure 4). For example, in Fram Strait, the gateway to the Arctic Ocean, the OH-isoGDGT-derived indices indicated sea surface cooling of ~5°C (OH-isoGDGT%) and ~3°C (RI-OH') across the Plio-Pleistocene transition, suggesting an increasing influence of polar water masses (Knies et al.,

TABLE 2. isoGDGT-inferred Jurassic-Holocene upper ocean temperature evolution in the Southern Ocean.

TIME PERIOD STUDIED	GDGT INDEX	MAIN FINDING IN TERMS OF TEMPERATURE CHANGE	REFERENCE
Jurassic-Cretaceous	TEX ₈₆	Persistent high temperatures of 26°–30°C ^a	Jenkyns et al., 2012
Eocene	TEX ₈₆	Cooling from ~25°C during early Eocene to ~21°C during late Eocene ^b	Bijl et al., 2009
Eocene-Oligocene	TEX ₈₆	Substantial cooling of >5°C across the Eocene-Oligocene boundary	Z. Liu et al., 2009
Oligocene-Miocene	TEX ₈₆	~5°–6°C cooling from Oligocene to mid-Miocene	Hartman et al., 2018
Miocene	TEX ₈₆ ^L	Cold (–1°–3°C) and warm (6°–10°C) intervals during early to mid Miocene ^c	Levy et al., 2016
Miocene	TEX ₈₆ ^L	~14°C before the mid-Miocene climatic optimum, and ~8°C thereafter ^c	Sangiorgi et al., 2018
Pliocene	TEX ₈₆ ^L	Cooling, from ~5°C during early Pliocene to ~2°C during the late Pliocene ^d	McKay et al., 2012
Pleistocene	TEX ₈₆ ^L	~5°C warming from glacial to deglaciation	Hayes et al., 2014
Last Glacial-Holocene	TEX ₈₆	Warming from ~10°C during the last glacial to ~19°C during the early Holocene ^b	Kim et al., 2009
Holocene	TEX ₈₆ ^L	~3°C of cooling over the Holocene	Etourneau et al., 2013
Holocene	TEX ₈₆	3°–4°C of cooling over the past 12,000 years; superimposed series of millennial-scale warm and cold events	Shevenell et al., 2011
Holocene	TEX ₈₆ ^L	No long-term trend over the Holocene	Kim et al., 2012
Holocene	TEX ₈₆ ^L	Abrupt warming of ~1.5°C in the early Holocene, possibly associated with ice shelf disintegration	Etourneau et al., 2019

^a 5.2°C standard error of the estimate for TEX₈₆ (Kim et al., 2010)

^b 1.7°C standard error of the estimate for TEX₈₆ (Kim et al., 2008)

^c 2.8°C standard error of the estimate for TEX₈₆^L (Kim et al. 2012)

^d 4.0°C standard error of the estimate for TEX₈₆^L (Kim et al. 2010)

2014). In contrast, TEX_{86}^L temperatures did not reveal consistent temporal patterns. Meanwhile, a reconstruction over the past ~120,000 years (Kremer et al., 2018) revealed more reasonable RI-OH'-inferred temperatures (-2.5° to 2.5°C; calibration error of 6°C) than TEX_{86}^L -derived temperatures (-17° to 9°C; calibration error of 4°C). Over the Holocene, temperatures based on the OH-isoGDGT% and RI-OH' indices also followed trends in temperature and water mass changes indicated by multiple proxies, in contrast to the TEX_{86}^L -based temperatures (Fietz et al., 2013; Figure 4).

The reasons for the mismatch between TEX_{86} -related temperatures and other proxies in the Arctic are unknown. The isoGDGT-based Ring Index (Zhang et al., 2016) may shed light on the extent

of non-thermal bias of the TEX_{86} -related reconstructions, especially potential terrestrial input. Ring Index offset values lower than 0.3 at the Plio-Pleistocene transition (Knies et al., 2014) and in the Holocene (Fietz et al., 2013) do not point to a specific non-thermal bias. The factors driving the mismatch between TEX_{86} -related temperatures and other proxies in the Arctic do not seem to affect the utility of OH-isoGDGT proxies, as the reconstruction based on them coevolves with other temperature proxies (Figure 4).

The OH-isoGDGT proxy has not been widely tested in the Southern Ocean. E. Park et al. (2019) recently published the very first sediment trap-based study indicating that several OH-isoGDGT-based proxies show promise as temperature proxies for both the Arctic and the

Southern Oceans. To date, only one study has applied the OH-isoGDGTs for reconstructions in the Southern Ocean (Fietz et al., 2016). Here, in the subantarctic Atlantic, TEX_{86} (Figure 3) suggests warmer conditions during glacials than interglacials in the past 500,000 years, in contrast to other paleotemperature proxies based on the same sediment core (Fietz et al., 2016). Located north of the winter sea ice extent during the last glacial maximum, some inconsistencies of warmer reconstructed temperatures during the glacial and colder temperatures during the interglacial may be attributed to increased meltwater stratification (Shevenell et al., 2011; McKay et al., 2012). Another possible explanation for the “warm” glacial TEX_{86} -temperatures in the subantarctic Atlantic record

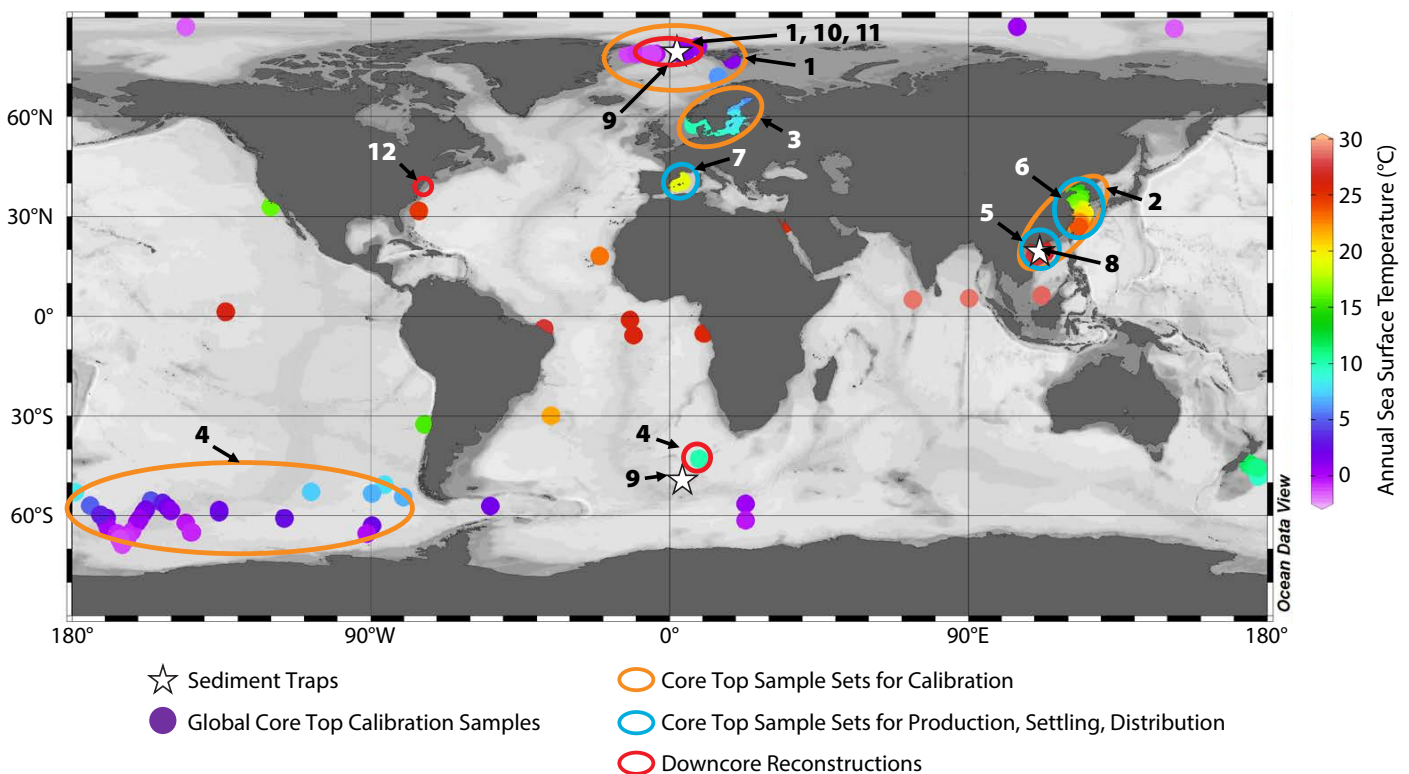


FIGURE 3. An Ocean Data View (Schlitzer, 2018) map illustrates the progress made since the OH-isoGDGTs were first proposed in 2013 as paleotemperature proxies, including surface sediment sample locations used for calibrations of initial OH-isoGDGT% (unlabeled filled circles; Huguet et al., 2013). Orange circles roughly indicate the locations of the additional sample sets for calibrations of cyclization variants, such as OH-isoGDGT_{1318/1316} (Table 1) by Fietz et al. (2013, #1), RI-OH and RI-OH' (Table 1) by Lü et al. (2015; #2), and improved calibrations thereof by Kaiser and Arz (2016; #3), as well as for OH^c index determination (Table 1) by Fietz et al. (2016; #4). Blue circles highlight focus areas of surface sediment studies that improve our understanding of OH-isoGDGT production, settling, and thus ultimately, distribution in the sediment (#5, Lü et al., 2019; #6, Kang et al., 2017; #7, Davtian et al., 2019). White stars indicate two sediment trap studies (#8, Wei et al., 2019, South China Sea; #9, E. Park et al., 2019, Fram Strait and Southern Ocean). Red circles roughly indicate downcore temperature reconstructions (#1, Fietz et al., 2013; #10, Knies et al., 2014; #4, Fietz et al., 2016; #11, Kremer et al., 2018; #12, de Bar et al., 2019). Circles and stars are not to scale and may not represent 100% of the data set.

could be the bias toward warmer TEX_{86} -temperatures caused by low ammonium oxidizing rates (Hurley et al., 2016). However, higher eolian iron input during the glacials (Martinez-Garcia et al., 2009) would contribute to increased oxidation rates (Shafiee et al., 2019) and thus toward a cold bias of the TEX_{86} tempera-

tures and vice versa in the interglacials. This is the opposite of the temporal patterns in the TEX_{86} records and, hence, a bias introduced by such nutrient dynamics does not explain the warm temperatures reconstructed during the glacials.

Adding OH-isoGDGTs in the temperature index improves the reconstruct-

tion to some degree. Unlike their counterparts TEX_{86} and TEX_{86}^L , the OH-isoGDGT indices exhibit temporal patterns that are more consistent with other non-isoGDGT-based proxies (Figure 4) and expectations (lower temperatures during the glacials), with the OH^c index showing the best match in the temporal trend. In the

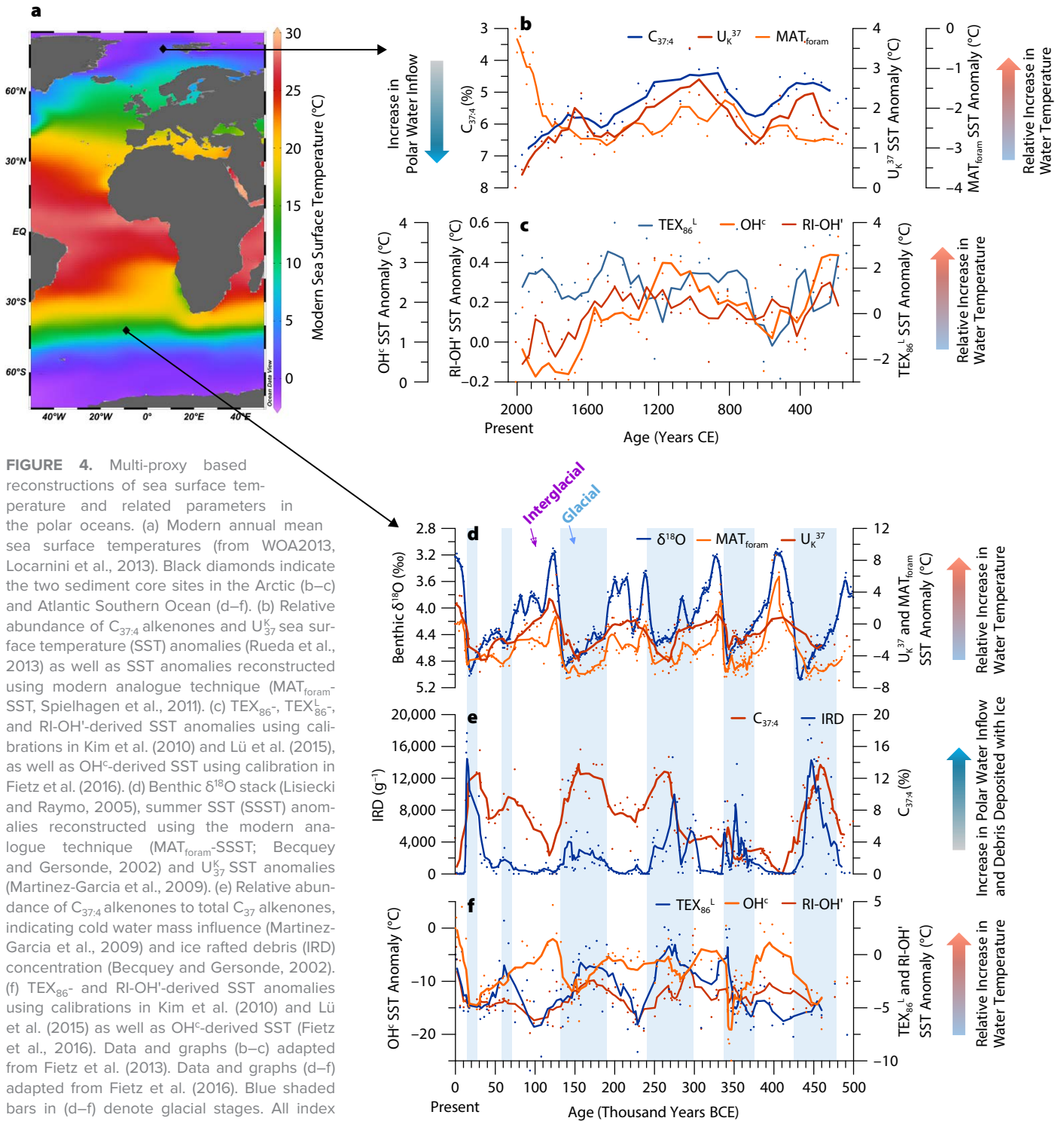


FIGURE 4. Multi-proxy based reconstructions of sea surface temperature and related parameters in the polar oceans. (a) Modern annual mean sea surface temperatures (from WOA2013, Locarnini et al., 2013). Black diamonds indicate the two sediment core sites in the Arctic (b–c) and Atlantic Southern Ocean (d–f). (b) Relative abundance of $C_{37,4}$ alkenones and U_K^{37} sea surface temperature (SST) anomalies (Rueda et al., 2013) as well as SST anomalies reconstructed using modern analogue technique (MAT_{foram} -SST; Spielhagen et al., 2011). (c) TEX_{86}^L , TEX_{86}^L , and RI-OH'-derived SST anomalies using calibrations in Kim et al. (2010) and Lü et al. (2015), as well as OH^c-derived SST using calibration in Fietz et al. (2016). (d) Benthic $\delta^{18}O$ stack (Lisiecki and Raymo, 2005), summer SST (SSST) anomalies reconstructed using the modern analogue technique (MAT_{foram} -SSST; Becquey and Gersonde, 2002) and U_K^{37} SST anomalies (Martinez-Garcia et al., 2009). (e) Relative abundance of $C_{37,4}$ alkenones to total C_{37} alkenones, indicating cold water mass influence (Martinez-Garcia et al., 2009) and ice rafted debris (IRD) concentration (Becquey and Gersonde, 2002). (f) TEX_{86}^L and RI-OH'-derived SST anomalies using calibrations in Kim et al. (2010) and Lü et al. (2015) as well as OH^c-derived SST (Fietz et al., 2016). Data and graphs (b–c) adapted from Fietz et al. (2013). Data and graphs (d–f) adapted from Fietz et al. (2016). Blue shaded bars in (d–f) denote glacial stages. All index equations are provided in Table 1. All anomalies refer to the core top value as "0."

OH^c index, the assumed cold-water end-member OH-isoGDGT-0 is subtracted from the numerator (Table 1). The fact that this approach improves the reconstruction of temperature evolution suggests that the addition of OH-isoGDGT in the temperature index may help to fully capture the temperature responses of archaeal membranes to temperature changes in polar waters. The global calibration of RI-OH (Lü et al., 2015) consists of 107 data points, a far cry from the TEX₈₆ calibration data set (n > 1,000; Tierney and Tingley, 2015). Here, we show that combining recently published surface sediment OH-isoGDGT data (n = 167; Figure 1c) does not change the global calibration equation nor the closeness of fit, but the database should be expanded to improve its robustness. Improvement of both the isoGDGT- and the OH-isoGDGT-based proxy calibrations remains a priority task for the future. As for TEX₈₆, one approach is to develop more regional calibrations or use alternative statistical approaches, such as BAYSPAR (Tierney and Tingley, 2014) and OPTIMAL (Eley et al., 2019).

Nonetheless, some uncertainties remain. Even though OH-isoGDGTs have been found in cultured mesophilic Group I Thaumarchaeota and methanogenic Euryarchaeota (X.-L. Liu et al., 2012), and that OH-isoGDGTs have been proposed to be produced autochthonously in the marine water column (Lü et al., 2015; Kaiser and Arz, 2016; Lü et al., 2019; Davtian et al., 2019) and thus may circumvent the impact of terrestrial bias in TEX₈₆-reconstructions (Figure 1), the possibility of terrestrial influence has recently been put forward (Kang et al., 2017; Wei et al., 2019). In addition, OH-isoGDGT proxies may also respond to environmental factors other than temperature, such as salinity, the presence of sea ice (Fietz et al., 2013), and/or seasonality (Lü et al., 2019; Wei et al., 2019). More ground truthing in water column and surface sediments, and most importantly culture incubation studies, are needed.

CONCLUSIONS

Over the last few decades, the TEX₈₆ paleothermometer has been used to help reconstruct past changes in sea surface temperatures in the polar regions (e.g., Table 2). However, several caveats exist (Figure 2) and structurally different isoGDGTs have been identified, such as OH-isoGDGTs. More work is needed to shed light on these compounds and the proxies based on them, but a few preliminary studies show that incorporating OH-isoGDGTs in the temperature proxy index may lead to improved reconstructions in the polar oceans. We thus recommend that the OH-isoGDGTs be analyzed simultaneously during standard isoGDGTs analysis, as this multi-proxy approach will increase the robustness of paleotemperature reconstructions. 

REFERENCES

- Bale, N.J., M. Palatinszky, W.I.C. Rijpstra, C.W. Herbold, M. Wagner, and J.S. Sinninghe Damsté. 2019. Membrane lipid composition of the moderately thermophilic ammonia-oxidizing archaeon “*Candidatus Nitrosotenuis uzonensis*” at different growth temperatures. *Applied and Environmental Microbiology* 85:e01332-19, <https://doi.org/10.1128/AEM.01332-19>.
- Beccuque, S., and R. Gersonde. 2002. Past hydrographic and climatic changes in the Subantarctic Zone of the South Atlantic: The Pleistocene record from ODP Site 1090. *Palaeogeography, Palaeoclimatology, Palaeoecology* 182:221–239, [https://doi.org/10.1016/S0031-0182\(01\)00497-7](https://doi.org/10.1016/S0031-0182(01)00497-7).
- Bijl, P.K., S. Schouten, A. Sluijs, G.-J. Reichert, J.C. Zachos, and H. Brinkhuis. 2009. Early Palaeogene temperature evolution of the southwest Pacific Ocean. *Nature* 461:776–779, <https://doi.org/10.1038/nature08399>.
- Brassell, S., G. Eglinton, I. Marlowe, U. Pflaumann, and M. Sarnthein. 1986. Molecular stratigraphy: A new tool for climatic assessment. *Nature* 320:129–133, <https://doi.org/10.1038/320129a0>.
- Brinkhuis, H., S. Schouten, M.E. Collinson, A. Sluigs, J.S. Sinninghe Damsté, G.R. Dickens, M. Huber, T.M. Cronin, J. Onodera, K. Takahashi, and others. 2006. Episodic fresh surface waters in the Eocene Arctic Ocean. *Nature* 441:606–609, <https://doi.org/10.1038/nature04692>.
- Chen, L.L., J. Liu, and J.S. Wang. 2018. Sources and distribution of tetraether lipids in sediments from the Zhejiang–Fujian coastal mud area, China, over the past 160 years: Implications for paleoclimate change. *Organic Geochemistry* 121:114–125, <https://doi.org/10.1016/j.orggeochem.2018.03.010>.
- Chugunov, A.O., P.E. Volynsky, N.A. Krylov, I.A. Boldyrev, and R.G. Efremov. 2015. Liquid but durable: Molecular dynamics simulations explain the unique properties of archaeal like membranes. *Scientific Reports* 4:7462, <https://doi.org/10.1038/srep07462>.
- Davtian, N., G. Ménot, Y. Fagault, and E. Bard. 2019. Western Mediterranean Sea paleothermometry over the last glacial cycle based on

the novel RI-OH index. *Paleoceanography and Paleoclimatology* 34:616–634, <https://doi.org/10.1029/2018PA003452>.

- de Bar, M.W., S.W. Rampen, E.C. Hopmans, J.S. Sinninghe Damsté, and S. Schouten. 2019. Constraining the applicability of organic paleotemperature proxies for the last 90 Myrs. *Organic Geochemistry* 128:122–136, <https://doi.org/10.1016/j.orggeochem.2018.12.005>.
- De Rosa, M., E. Esposito, A. Gambacorta, B. Nicolaus, and J.D. Bu'Lock. 1980. Effects of temperature on ether lipid composition of *Caldariella acidophila*. *Phytochemistry* 19:827–831, [https://doi.org/10.1016/0031-9422\(80\)85120-X](https://doi.org/10.1016/0031-9422(80)85120-X).
- Eley, Y.L., W. Thompson, S. E. Greene, I. Mandel, K. Edgar, J.A. Bendle, and T. Dunkley Jones. 2019. OPTIMAL: A new machine learning approach for GDGT-based palaeothermometry. *Climate of the Past – Discussion*, <https://doi.org/10.5194/cp-2019-60>, in review.
- Elling, F.J., M. Könneke, J.S. Lipp, K.W. Becker, E.J. Gagen, and K.-U. Hinrichs. 2014. Effects of growth phase on the membrane lipid composition of the thaumarchaeon *Nitrosopumilus maritimus* and their implications for archaeal lipid distributions in the marine environment. *Geochimica et Cosmochimica Acta* 141:579–597, <https://doi.org/10.1016/j.gca.2014.07.005>.
- Elling, F.J., M. Könneke, M. Mußmann, A. Greve, and K.-U. Hinrichs. 2015. Influence of temperature, pH, and salinity on membrane lipid composition and TEX₈₆ of marine planktonic thaumarchaeal isolates. *Geochimica et Cosmochimica Acta* 171:238–255, <https://doi.org/10.1016/j.gca.2015.09.004>.
- Elling, F.J., M. Könneke, G.W. Nicol, M. Stieglmeier, B. Bayer, E. Spieck, J.R. de la Torre, K.W. Becker, M. Thomm, J.I. Prosser, and others. 2017. Chemotaxonomic characterisation of the thaumarchaeal lipidome. *Environmental Microbiology* 19:2,681–2,700, <https://doi.org/10.1111/1462-2920.13759>.
- Etourneau, J., L.G. Collins, V. Willmott, J.-H. Kim, L. Barbara, A. Leventer, S. Schouten, J.S. Sinninghe Damsté, A. Bianchini, V. Klein, and others. 2013. Holocene climate variations in the western Antarctic Peninsula: Evidence for sea ice extent predominantly controlled by changes in insolation and ENSO variability. *Climate of the Past* 9:1,431–1,446, <https://doi.org/10.5194/cp-9-1431-2013>.
- Etourneau, J., G. Sgubin, X. Crosta, D. Swingedouw, V. Willmott, L. Barbara, M.-N. Houssais, S. Schouten, J.S. Sinninghe Damsté, H. Goosse, and others. 2019. Ocean temperature impact on ice shelf extent in the eastern Antarctic Peninsula. *Nature Communications* 10:304, <https://doi.org/10.1038/s41467-018-08195-6>.
- Fietz, S., C. Huguet, G. Rueda, B. Hambach, and A. Rosell-Melé. 2013. Hydroxylated isoprenoidal GDGTs in the Nordic seas. *Marine Chemistry* 152:1–10, <https://doi.org/10.1016/j.marchem.2013.02.007>.
- Fietz, S., S.L. Ho, C. Huguet, A. Rosell-Melé, and A. Martínez-García. 2016. Appraising GDGT-based seawater temperature indices in the Southern Ocean. *Organic Geochemistry* 102:93–105, <https://doi.org/10.1016/j.orggeochem.2016.10.003>.
- Gabriel, J.L., and P.L.G. Chong. 2000. Molecular modeling of archaeobacterial bipolar tetraether lipid membranes. *Chemistry and Physics of Lipids* 105:193–200, [https://doi.org/10.1016/S0009-3084\(00\)00126-2](https://doi.org/10.1016/S0009-3084(00)00126-2).
- Hansen, J., R. Ruedy, M. Sato, and K. Lo. 2010. Global surface temperature change. *Reviews of Geophysics* 48(4), <https://doi.org/10.1029/2010RG000345>.

- Hartman, J.D., F. Sangiorgi, A. Salabarnada, F. Peterse, A.J.P. Houben, S. Schouten, H. Brinkhuis, C. Escutia, and P.K. Bijl. 2018. Paleoclimatology and ice sheet variability off-shore Wilkes Land, Antarctica: Part 3. Insights from Oligocene–Miocene TEX₈₆-based sea surface temperature reconstructions. *Climate of the Past* 14:1,275–1,297, <https://doi.org/10.5194/cp-14-1275-2018>.
- Hayes, C.T., A. Martínez-García, A.P. Hasenfratz, S.L. Jaccard, D.A. Hodell, D.M. Sigman, G.H. Haug, and R.F. Anderson. 2014. A stagnation event in the deep South Atlantic during the last interglacial period. *Science* 346:1,514–1,517, <https://doi.org/10.1126/science.1256620>.
- Hayes, J.H. 2000. Lipids as a common interest of microorganisms and geochemists. *Proceedings of the National Academy of Sciences of the United States of America* 97:14,033–14,034, <https://doi.org/10.1073/pnas.97.26.14033>.
- Herbert, T.D. 2014. Alkenone paleotemperature determinations. Pp. 399–433 in *Treatise on Geochemistry*, 2nd ed. H.D. Holland and K. Turekian, eds, Elsevier, <https://doi.org/10.1016/B978-0-08-095975-7.00615-X>.
- Hinrichs, K.U., J.M. Hayes, S.P. Sylva, P.G. Brewer, and E.F. DeLong. 1999. Methane consuming archaeobacteria in marine sediments. *Nature* 398:802–805, <https://doi.org/10.1038/19751>.
- Ho, S.L., B.D.A. Naafs, and F. Lamy. 2013. Alkenone paleothermometry based on the haptophyte algae. Pp. 755–764 in *The Encyclopedia of Quaternary Science*. S. Elias, ed., Elsevier.
- Ho, S.L., G. Mollenhauer, S. Fietz, A. Martínez-García, F. Lamy, G. Rueda, K. Schipper, M. Méheust, A. Rosell-Melé, R. Stein, and R. Tiedemann. 2014. Appraisal of TEX₈₆ and TEX₈₆^L thermometries in subpolar and polar regions. *Geochimica et Cosmochimica Acta* 131:213–226, <https://doi.org/10.1016/j.gca.2014.01.001>.
- Ho, S.L., and T. Laepple. 2016. Flat meridional temperature gradient in the early Eocene in the subsurface rather than surface ocean. *Nature Geoscience* 9:606–610, <https://doi.org/10.1038/ngeo2763>.
- Hopmans, E.C., J.W.H. Weijers, E. Schefuß, L. Herfort, J.S. Sinninghe Damsté, and S. Schouten. 2004. A novel proxy for terrestrial organic matter in sediments based on branched and isoprenoid tetraether lipids. *Earth and Planetary Science Letters* 224(1–2):107–116, <https://doi.org/10.1016/j.epsl.2004.05.012>.
- Huguet, C., A. Schimmelmann, R. Thunell, L.J. Lourens, J.S. Sinninghe Damsté, and S. Schouten. 2007. A study of the TEX₈₆ paleothermometer in the water column and sediments of the Santa Barbara Basin, California. *Paleoceanography and Paleoclimatology* 22(3), <https://doi.org/10.1029/2006PA001310>.
- Huguet, C., G.J. de Lange, Ö. Gustafsson, J.J. Middelburg, J.S. Sinninghe Damsté, and S. Schouten. 2008. Selective preservation of soil organic matter in oxidized marine sediments (Madeira Abyssal Plain). *Geochimica et Cosmochimica Acta* 72:6,061–6,068, <https://doi.org/10.1016/j.gca.2008.09.021>.
- Huguet, C., S. Fietz, and A. Rosell-Melé. 2013. Global distribution patterns of hydroxy glycerol dialkyl glycerol tetraethers. *Organic Geochemistry* 57:107–118, <https://doi.org/10.1016/j.orggeochem.2013.01.010>.
- Huguet, C., S. Fietz, A. Rosell-Melé, X. Daura, and L. Costenaro. 2017. Molecular dynamics simulation study of the effect of glycerol dialkyl glycerol tetraether hydroxylation on membrane thermostability. *Biochimica et Biophysica Acta (BBA) – Biomembranes* 1859(5):966–974, <https://doi.org/10.1016/j.bbame.2017.02.009>.
- Hurley, S.J., F.J. Elling, M. Könneke, C. Buchwald, S.C. Wankel, A.E. Santoro, J.S. Lipp, K.-U. Hinrichs, and A. Pearson. 2016. Influence of ammonia oxidation rate on thaumarchaeal lipid composition and the TEX₈₆ temperature proxy. *Proceedings of the National Academy of Sciences of the United States of America* 113:7,762–7,767, <https://doi.org/10.1073/pnas.1518534113>.
- IPCC (Intergovernmental Panel on Climate Change). 2019. *Special Report on the Ocean and Cryosphere in a Changing Climate*. H.-O. Pörtner, D.C. Roberts, V. Masson-Delmotte, P. Zhai, M. Tignor, E. Poloczanska, K. Mintenbeck, A. Alegría, M. Nicolai, A. Okem, J. Petzold, B. Rama, and N.M. Weyer, eds, https://www.ipcc.ch/site/assets/uploads/sites/3/2019/12/02_SROCC_FM_FINAL.pdf.
- Ionescu, D., S. Penno, M. Haimovich, B. Rihtman, A. Goodwin, D. Schwartz, L. Hazanov, M. Chernihovsky, A.F. Post, and A. Oren. 2009. Archaea in the Gulf of Aqaba. *FEMS Microbiology Letters* 69:425–438, <https://doi.org/10.1111/j.1574-6941.2009.00721.x>.
- Jacob, T.J. Wahr, W.T. Pfeffer, and S. Swenson. 2012. Recent contributions of glaciers and ice caps to sea level rise. *Nature* 482:514–518, <https://doi.org/10.1038/nature10847>.
- Jenkyns, H.C., A. Forster, S. Schouten, and J.S. Sinninghe Damsté. 2004. High temperatures in the Late Cretaceous Arctic Ocean. *Nature* 432:888–892, <https://doi.org/10.1038/nature03143>.
- Jenkyns, H.C., L. Schouten-Huibers, S. Schouten, and J.S. Sinninghe Damsté. 2012. Warm Middle Jurassic–Early Cretaceous high-latitude sea-surface temperatures from the Southern Ocean. *Climate of the Past* 8:215–226, <https://doi.org/10.5194/cp-8-215-2012>.
- Kaiser, J., and H.W. Arz. 2016. Sources of sedimentary biomarkers and proxies with potential paleoenvironmental significance for the Baltic Sea. *Continental Shelf Research* 122:102–119, <https://doi.org/10.1016/j.csr.2016.03.020>.
- Kang, S., K.H. Shin, and J.H. Kim. 2017. Occurrence and distribution of hydroxylated isoprenoid glycerol dialkyl glycerol tetraethers (OH-GDGTs) in the Han River system, South Korea. *Acta Geochimica* 36:367–369, <https://doi.org/10.1007/s11631-017-0165-3>.
- Kim, J.-H., S. Schouten, E.C. Hopmans, B. Donner, and J.S. Sinninghe Damsté. 2008. Global sediment core-top calibration of the TEX₈₆ paleothermometer in the ocean. *Geochimica et Cosmochimica Acta* 72:1,154–1,173, <https://doi.org/10.1016/j.gca.2007.12.010>.
- Kim, J.-H., X. Crosta, E. Michel, S. Schouten, J. Duprat, and J.S. Sinninghe Damsté. 2009. Impact of lateral transport on organic proxies in the Southern Ocean. *Quaternary Research* 71:246–250, <https://doi.org/10.1016/j.jyqres.2008.10.005>.
- Kim, J.-H., J. van der Meer, S. Schouten, P. Helmke, V. Willmott, F. Sangiorgi, N. Koç, E.C. Hopmans, and J.S. Sinninghe Damsté. 2010. New indices and calibrations derived from the distribution of crenarchaeal isoprenoid tetraether lipids: Implications for past sea surface temperature reconstructions. *Geochimica et Cosmochimica Acta* 74:4,639–4,654, <https://doi.org/10.1016/j.gca.2010.05.027>.
- Kim, J.-H., X. Crosta, V. Willmott, H. Renssen, G. Masse, J. Bonnin, P. Helmke, S. Schouten, and J.S. Sinninghe Damsté. 2012. Holocene subsurface temperature variability in the eastern Antarctic continental margin. *Geophysical Research Letters* 39:L06705, <https://doi.org/10.1029/2012GL051157>.
- Knies, J., P. Cabedo-Sanz, S.T. Belt, S. Baranwa, S. Fietz, and A. Rosell-Melé. 2014. The emergence of modern sea ice cover in the Arctic Ocean. *Nature Communications* 5:5608, <https://doi.org/10.1038/ncomms5608>.
- Koga, Y., and H. Morii. 2007. Biosynthesis of ether-type polar lipids in archaea and evolutionary considerations. *Microbiology and Molecular Biology Reviews* 71:97–120, <https://doi.org/10.1128/MMBR.00033-06>.
- Konings, W.N., S.V. Albers, S. Koning, and A.J.M. Driessen. 2002. The cell membrane plays a crucial role in survival of bacteria and archaea in extreme environments. *Antonie Van Leeuwenhoek* 81:61–72, <https://doi.org/10.1023/A:1020573408652>.
- Kremer, A., R. Stein, K. Fahl, Z. Ji, Z. Yang, S. Wiers, J. Matthiessen, M. Forwick, L. Löwemark, M. O'Regan, J. Chen, and I. Snowball. 2018. Changes in sea ice cover and ice sheet extent at the Yermak Plateau during the last 160 ka: Reconstructions from biomarker records. *Quaternary Science Reviews* 182:93–108, <https://doi.org/10.1016/j.quascirev.2017.12.016>.
- Levy R., D. Harwood, F. Florindo, F. Sangiorgi, R. Tripati, H. von Eynatten, E. Gasson, G. Kuhn, A. Tripati, R. DeConto, and others. 2016. Antarctic ice sheet sensitivity to atmospheric CO₂ variations in the early to mid-Miocene. *Proceedings of the National Academy of Sciences of the United States of America* 113:3,453–3,458, <https://doi.org/10.1073/pnas.1516030113>.
- Lipp, J.S., and K.-U. Hinrichs. 2009. Structural diversity and fate of intact polar lipids in marine sediments. *Geochimica et Cosmochimica Acta* 73:6,816–6,833, <https://doi.org/10.1016/j.gca.2009.08.003>.
- Lisiecki, L.E., and M.E. Raymo. 2005. A Pliocene–Pleistocene stack of 57 globally distributed benthic δ¹⁸O records. *Paleoceanography* 20(1), <https://doi.org/10.1029/2004PA001071>.
- Liu, X.-L., J.S. Lipp, J.H. Simpson, Y.-S. Lin, R.E. Summons, and K.-U. Hinrichs. 2012. Mono- and dihydroxyl glycerol dibiphytanyl glycerol tetraethers in marine sediments: Identification of both core and intact polar lipid forms. *Geochimica et Cosmochimica Acta* 89:102–115, <https://doi.org/10.1016/j.gca.2012.04.053>.
- Liu, Z., M. Pagani, D. Zinniker, R. DeConto, M. Huber, H. Brinkhuis, S.R. Shah, R.M. Leckie, and A. Pearson. 2009. Global cooling during the Eocene–Oligocene climate transition. *Science* 323:1,187–1,190, <https://doi.org/10.1126/science.1166368>.
- Locarnini, R.A., A.V. Mishonov, J.I. Antonov, T.P. Boyer, H.E. Garcia, O.K. Baranova, M.M. Zweng, C.R. Paver, J.R. Reagan, D.R. Johnson, and others. 2013. World Ocean Atlas 2013, Volume 1: Temperature. S. Levitus, ed., A. Mishonov, tech. ed., NOAA Atlas NESDIS 73, 40 pp.
- Lü, X., X.-L. Liu, F.J. Elling, H. Yang, S. Xie, J. Song, X. Li, H. Yuan, N. Li, and K.U. Hinrichs. 2015. Hydroxylated isoprenoid GDGTs in Chinese coastal seas and their potential as a paleotemperature proxy for mid-to-low latitude marginal seas. *Organic Geochemistry* 89–90:31–43, <https://doi.org/10.1016/j.orggeochem.2015.10.004>.
- Lü, X., J. Chen, T. Han, H. Yang, W. Wu, W. Ding, and K.U. Hinrichs. 2019. Origin of hydroxyl GDGTs and regular isoprenoid GDGTs in suspended particulate matter of Yangtze River Estuary. *Organic Geochemistry* 128:78–85, <https://doi.org/10.1016/j.orggeochem.2018.12.010>.
- Martínez-García, A., A. Rosell-Melé, W. Geibert, R. Gersonde, P. Masqué, V. Gaspari, and C. Barbante. 2009. Links between iron supply, marine productivity, sea surface temperatures and

- CO₂ over the last 11 Ma. *Paleoceanography and Paleoclimatology* 24(1), <https://doi.org/10.1029/2008PA001657>.
- McKay, R., T. Naish, L. Carter, C. Riesselman, R. Dunbar, C. Sjunneskog, D. Winter, F. Sangiorgi, C. Warren, M. Pagani, and others. 2012. Antarctic and Southern Ocean influences on Late Pliocene global cooling. *Proceedings of the National Academy of Sciences of the United States of America* 109:6,423–6,428, <https://doi.org/10.1073/pnas.1112248109>.
- Mulvaney, R., N. Abram, R. Hindmarsh, C. Arrowsmith, L. Fleet, J. Triest, L.C. Sime, O. Alemany, and S. Foord. 2012. Recent Antarctic Peninsula warming relative to Holocene climate and ice-shelf history. *Nature* 489:141–144, <https://doi.org/10.1038/nature11391>.
- Oger, P.M., and A. Cario. 2013. Adaptation of the membrane in Archaea. *Biophysical Chemistry* 183:42–56, <https://doi.org/10.1016/j.bpc.2013.06.020>.
- Park, E., J. Hefter, G. Fischer, M. Iversen, S. Ramondenc, E.M. Nöthig, and G. Mollenhauer. 2019. Seasonality of archaeal lipid flux and GDGT-based thermometry in sinking particles of high latitude regions: Fram Strait (79°N) and Antarctic Polar Front (50°S). *Biogeosciences* 16:2,247–2,268, <https://doi.org/10.5194/bg-2019-34>.
- Park, Y., M. Yamamoto, S. Nam, T. Irino, L. Polyak, N. Harada, K. Nagashima, B. Khim, K. Chikita, and S. Saitoh. 2014. Distribution, source and transport of glycerol dialkyl glycerol tetraethers in surface sediments from the western Arctic Ocean and the northern Bering Sea. *Marine Chemistry* 165:10–24, <https://doi.org/10.1016/j.marchem.2014.07.001>.
- Pearson, A., and A.E. Ingalls. 2013. Assessing the use of archaeal lipids as marine environmental proxies. *Annual Review of Earth and Planetary Sciences* 41:359–384, <https://doi.org/10.1146/annurev-earth-050212-123947>.
- Qin, W., L.T. Carlson, E.V. Armbrust, A.H. Devol, J.W. Moffett, D.A. Stahl, and A.E. Ingalls. 2015. Confounding effects of oxygen and temperature on the TEX₈₆ signature of marine Thaumarchaeota. *Proceedings of the National Academy of Sciences of the United States of America* 112:10,979–10,984, <https://doi.org/10.1073/pnas.1501568112>.
- Ren, Q., and I.T. Paulsen. 2005. Comparative analyses of fundamental differences in membrane transport capabilities in prokaryotes and eukaryotes. *PLoS Computational Biology* 1:e27, <https://doi.org/10.1371/journal.pcbi.0010027>.
- Rintoul, S.R., S.L. Chown, R.M. DeConto, M.H. England, H.A. Fricker, V. Masson-Delmotte, T.R. Naish, M.J. Siebert, and J.C. Xavier. 2018. Choosing the future of Antarctica. *Nature* 558:233–241, <https://doi.org/10.1038/s41586-018-0173-4>.
- Rueda, G., S. Fietz, and A. Rosell-Melé. 2013. Coupling of air and sea surface temperatures in the eastern Fram Strait during the last 2000 years. *The Holocene* 23:692–698, <https://doi.org/10.1177/0959683612470177>.
- Sangiorgi, F., P.K. Bijl, S. Passchier, U. Salzmann, S. Schouten, R. McKay, R.D. Cody, J. Pross, T. van de Fliert, S.M. Bohaty, and others. 2018. Southern Ocean warming and Wilkes Land ice sheet retreat during the mid-Miocene. *Nature Communications* 9:317, <https://doi.org/10.1038/s41467-017-02609-7>.
- Schlitzer, R. 2018. Ocean Data View, Version 5.1.0, <https://odv.awi.de>.
- Schouten, S., E.C. Hopmans, E. Schefuß, and J.S. Sinninghe Damsté. 2002. Distributional variations in marine crenarchaeotal membrane lipids: A new tool for reconstructing ancient sea water temperatures? *Earth and Planetary Science Letters* 204:265–274, [https://doi.org/10.1016/S0012-821X\(02\)00979-2](https://doi.org/10.1016/S0012-821X(02)00979-2).
- Schouten, S., E.C. Hopmans, and J.S. Sinninghe Damsté. 2013. The organic geochemistry of glycerol dialkyl glycerol tetraether lipids: A review. *Organic Geochemistry* 54:19–61, <https://doi.org/10.1016/j.orggeochem.2012.09.006>.
- Shah, S.R., G. Mollenhauer, N. Ohkouchi, T.I. Eglinton, and A. Pearson. 2008. Origins of archaeal tetraether lipids in sediments: Insights from radio-carbon analysis. *Geochimica et Cosmochimica Acta* 72:4,577–4,594, <https://doi.org/10.1016/j.gca.2008.06.021>.
- Shafiee, R.T., J.T. Snow, Q. Zhang, and R.E.M. Rickaby. 2019. Iron requirements and uptake strategies of the globally abundant marine ammonia-oxidising archaeon, *Nitrosopumilus maritimus* SCM1. *The ISME Journal* 13:2,295–2,305, <https://doi.org/10.1038/s41396-019-0434-8>.
- Shevenell, A.E., A.E. Ingalls, E.W. Domack, and C. Kelly. 2011. Holocene Southern Ocean surface temperature variability west of the Antarctic Peninsula. *Nature* 470:250–254, <https://doi.org/10.1038/nature09751>.
- Sinninghe Damsté, J.S., S. Schouten, E.C. Hopmans, A.C. van Duin, and J.A. Geenevasen. 2002. Crenarchaeol: The characteristic core glycerol dibiphytanyl glycerol tetraether membrane lipid of cosmopolitan pelagic crenarchaeota. *Journal of Lipid Research* 43:1,641–1,651, <https://doi.org/10.1194/jlr.M200148-JLR200>.
- Sluijs, A., S. Schouten, M. Pagani, M. Woltering, H. Brinkhuis, J.S. Sinninghe Damsté, G.R. Dickens, M. Huber, G.-J. Reichert, R. Stein, and others. 2006. Subtropical Arctic Ocean temperatures during the Palaeocene/Eocene thermal maximum. *Nature* 441:610–613, <https://doi.org/10.1038/nature04668>.
- Spielhagen, R.F., K. Werner, S.A. Sørensen, K. Zamelczyk, E. Kandiano, G. Budeus, K. Husum, T.M. Marchitto, and M. Hald. 2011. Enhanced modern heat transfer to the Arctic by warm Atlantic water. *Science* 331:450–453, <https://doi.org/10.1126/science.1197397>.
- Tierney, J.E. 2014. Biomarker-based inferences of past climate: The TEX₈₆ paleotemperature proxy. Pp. 379–393 in *Treatise on Geochemistry*, 2nd ed. H.D. Holland, K.K. Turekian, eds, Elsevier, <https://doi.org/10.1016/B978-0-08-095975-701032-9>.
- Tierney, J.E., and M.P. Tingley. 2014. A Bayesian, spatially-varying calibration model for the TEX₈₆ proxy. *Geochimica et Cosmochimica Acta* 127:83–106, <https://doi.org/10.1016/j.gca.2013.11.026>.
- Tierney, J.E., and M.P. Tingley. 2015. A TEX₈₆ surface sediment database and extended Bayesian calibration. *Scientific Data* 2:150029, <https://doi.org/10.1038/sdata.2015.29>.
- Trommer, G., M. Siccha, M.T. van der Meer, S. Schouten, J.S. Sinninghe Damsté, H. Schulz, C. Hemleben, and M. Kucera. 2009. Distribution of Crenarchaeota tetraether membrane lipids in surface sediments from the Red Sea. *Organic Geochemistry* 40:724–731, <https://doi.org/10.1016/j.orggeochem.2009.03.001>.
- Wei, B., G. Jia, J. Hefter, M. Kang, E. Park, and G. Mollenhauer. 2019. Comparison of the U₃₇^H, LDL, TEX₈₆^H and RI-OH temperature proxies in the northern shelf of the South China Sea. *Biogeosciences-Discussion*, <https://doi.org/10.5194/bg-2019-345>, in review.
- Wuchter, C., S. Schouten, M.J.L. Coolen, and J.S. Sinninghe Damsté. 2004. Temperature-dependent variation in the distribution of tetraether membrane lipids of marine Crenarchaeota: Implications for TEX₈₆ paleothermometry. *Paleoceanography and Paleoclimatology* 19(4), <https://doi.org/10.1029/2004PA001041>.
- Zhang, Y.G., M. Pagani, and Z. Wang. 2016. Ring Index: A new strategy to evaluate the integrity of TEX₈₆ paleothermometry. *Paleoceanography and Paleoclimatology* 31:220–232, <https://doi.org/10.1002/2015PA002848>.
- Zhou, A., Y. Weber, B.K. Chiu, F.J. Elling, A.B. Cobban, A. Pearson, and W.D. Leavitt. 2020. Energy flux controls tetraether lipid cyclization in *Sulfolobus acidocaldarius*. *Environmental Microbiology* 22:343–353, <https://doi.org/10.1111/1462-2920.14851>.
- Zonneveld, K.A., G.J. Versteegh, S. Kasten, T.I. Eglinton, K.-C. Emeis, C. Huguet, B.P. Koch, G.J. de Lange, J.W. de Leeuw, J.J. Middelburg, and others. 2010. Selective preservation of organic matter in marine environments: Processes and impact on the sedimentary record. *Biogeosciences* 7:483–511, <https://doi.org/10.5194/bg-7-483-2010>.
- Zamelczyk, K., T.L. Rasmussen, K. Husum, H. Haffidason, A. de Vernal, E. K. Ravna, M. Hald, and C. Hillaire-Marcel. 2012. Paleoclimatographic changes and calcium carbonate dissolution in the central Fram Strait during the last 20 ka. *Quaternary Research* 78:405–416, <https://doi.org/10.1016/j.yqres.2012.07.006>.

ACKNOWLEDGMENTS

The authors thank two anonymous reviewers and guest editor Amelia Shevenell for the thorough review and valuable comments and suggestions. This work is based on the research supported by the National Research Foundation (NRF) of South Africa awarded to SF (#93072, #98905, #110731). CH wishes to acknowledge the Los Andes Faculty of Science INV-2019-84-1814 and the Humboldt Research Fellowship for Experienced Researchers. SLH acknowledges funding from the Ministry of Science and Technology (Taiwan; # 107-2611-M-002-021-MY3).

AUTHORS

Susanne Fietz (sfietz@sun.ac.za) is Senior Lecturer, Department of Earth Sciences, Stellenbosch University, Stellenbosch, South Africa. **Sze Ling Ho** is Assistant Professor, National Taiwan University, Taipei, Taiwan. **Carme Huguet** is Associate Professor, Geoscience Department, Universidad de los Andes, Bogotá, Colombia.

AUTHOR CONTRIBUTIONS

All authors contributed equally to this article.

ARTICLE CITATION

Fietz, S., S.L. Ho, and C. Huguet. 2020. Archaeal membrane lipid-based paleothermometry for applications in polar oceans. *Oceanography* 33(2):104–114, <https://doi.org/10.5670/oceanog.2020.207>.

COPYRIGHT & USAGE

This is an open access article made available under the terms of the Creative Commons Attribution 4.0 International License (<https://creativecommons.org/licenses/by/4.0/>), which permits use, sharing, adaptation, distribution, and reproduction in any medium or format as long as users cite the materials appropriately, provide a link to the Creative Commons license, and indicate the changes that were made to the original content.



Algal strands hang beneath the sea ice in Salmon Bay, western McMurdo Sound, Antarctica. Photo credit: Cecil Shin/B043 archive

SIDEBAR. Diatoms as Sea Ice Proxies

By Amy Leventer

Diatoms can live almost anywhere, but one of the most unusual places is within sea ice. These single-celled algae concentrate in newly forming sea ice and tinge the slushy surface a golden brown. They live in small channels between ice crystals and also on algal strands that hang from the underside of the ice. When the spring melt comes, diatoms in the sea ice serve as the seed population for ice-marginal blooms. The use of polar marine diatoms as a proxy for past sea ice relies upon their abundance, diversity, and preservation. In sediments, the presence of obligate sea ice diatoms, those species whose habitat is limited to within the sea ice, is reliable evidence of overlying sea ice. However, these species tend to be lightly silicified and underrepresented in marine sediments. Hence, while their presence is diagnostic, their absence is more difficult to interpret. Consequently, most sea ice reconstructions rely on species common in the marginal ice zone, seeded from melting sea ice into the adjacent open water. Many of these taxa have robust frustules that are well preserved at the seafloor.

Diatom-based sea ice reconstructions date to the early 1980s, with increasingly quantitative work beginning in the mid-1990s and continuing today. Reconstructing past Southern Ocean sea ice presence is most readily accomplished in sediments with extant species, ground truthed by modern observations. Thus, it is more difficult to use diatom-based sea ice proxies for time periods that harbored extinct species because the paleoenvironmental affiliation of these species is uncertain. Several approaches, in combination, are possible to circumvent this issue. First, diagnostic evolutionary lineages can be traced (e.g., at present, many

small pennate taxa within the genus *Fragilariopsis* are associated with sea ice)—but can we assume their ancestors had the same preferences? Second, specific morphologic characteristics (e.g., the development of resting spores or more heavily silicified winter stages) may have evolved following the initial or persistent occurrence of annual sea ice.

The use of diatom proxies for paleo sea ice extent also has its shortcomings, including biases associated with preferential grazing, water column dissolution, horizontal displacement by surface and bottom currents, and degradation within the sediments. Thus, while diatom assemblages reveal important clues to past sea ice presence, the imperfect sedimentary record of diatom assemblages has motivated development of new complementary biomolecular sea ice proxies.

REFERENCES

- Leventer, A. 1998. The fate of sea ice diatoms and their use as paleoenvironmental indicators. Pp. 121–137 in *Antarctic Sea Ice: Biological Processes, Interactions and Variability*. M.P. Lizotte and K.R. Arrigo, eds. Antarctic Research Series, vol. 73, American Geophysical Union, Washington, DC.
- Armand, L., and A. Leventer. 2010. Palaeo sea ice distribution and reconstruction derived from the geological record. Pp. 469–530 in *Sea Ice: An Introduction to its Physics, Biology, Chemistry, and Geology*. D.N. Thomas and G.S. Dieckmann, eds, Blackwell Science.
- Gersonde, R., and U. Zielinski. 2000. The reconstruction of late Quaternary Antarctic sea-ice distribution—The use of diatoms as a proxy for sea-ice. *Palaeogeography, Palaeoclimatology, Palaeoecology* 162 (3–4):263–286, [https://doi.org/10.1016/S0031-0182\(00\)00131-0](https://doi.org/10.1016/S0031-0182(00)00131-0).

AUTHOR

Amy Leventer (aleventer@colgate.edu) is Professor, Department of Geology, Colgate University, Hamilton, NY, USA.

The Potential of Sedimentary Ancient DNA to Reconstruct Past Ocean Ecosystems

By Linda H. Armbrecht

ABSTRACT. Sedimentary ancient DNA (*sedaDNA*) offers a novel approach to investigating past marine ecosystems—from the smallest bacteria to phytoplankton and their predators—over geological timescales. Knowledge about such paleo-food webs can provide broad-scale biological context to paleoceanographic and environmental reconstructions. However, the field of marine *sedaDNA* research is still in its infancy; community reconstructions are complicated by the minuscule amounts of ancient DNA preserved in the sediments. Consequently, the identification of most prokaryotes and eukaryotes in *sedaDNA* is difficult, and *sedaDNA* sampling, extraction, and analysis require optimized procedures and rigorous contamination control to ensure that the *sedaDNA* signal is authentic and not overridden by modern environmental DNA. This article describes some of the latest developments in marine *sedaDNA* research, including the use of metagenomics to study past marine food webs, and new experimental and computational techniques to maximize taxonomic resolution, particularly that of eukaryotes. An example of bioinformatic techniques designed to increase taxonomic insight is presented, demonstrating the breadth of paleogenetic signals that could be extracted from marine sediments. With ongoing improvements in genetic reference databases, *sedaDNA* extraction techniques, species-specific enrichment approaches, and computational tools, marine *sedaDNA* will continue to improve our understanding of how marine ecosystems evolved in concert with changing environmental conditions.

Piston core recovered during an R/V *Investigator* voyage to East Antarctica in 2017. Photo credit: Asaesja Young, CSIRO



WHAT INFORMATION CAN BE GAINED FROM SEDIMENTARY ANCIENT DNA?

Analysis of marine sedimentary ancient DNA (*sedaDNA*) allows identification of deceased organisms that have sunk from the upper water layers to the bottom of the ocean and become preserved. As a result of the sedimentation process, the remains of deceased organisms accumulate over time, forming a continuous record of past communities that have inhabited the ocean. Marine *sedaDNA* can be used to study a broad variety of taxa, including viruses, archaea, prokaryotes (bacteria), and eukaryotes (phytoplankton to larger predators). Eukaryotic planktonic organisms, such as diatoms, dinoflagellates, coccolithophores, and foraminifers, are particularly interesting targets for *sedaDNA* studies because of their established reliability as environmental indicators. However, the breadth of taxa for which genetic signals are preserved in the sediments—including species that do not fossilize—means that *sedaDNA* holds enormous potential to go beyond these standard environmental proxies and facilitate reconstruction of past marine ecosystems across the food web. Further, in cases where the preservation, or information content, of microfossil, physical, (biogeo)chemical or biomarker proxies is limited, *sedaDNA* can provide novel insights into past oceanographic and environmental conditions.

WHAT MAKES ANCIENT DNA DIFFERENT FROM MODERN DNA?

Ancient DNA is highly fragmented and degraded. Once an organism dies, cellular processes such as DNA repair mechanisms are no longer active, and the unmaintained DNA degrades over time. Previous research has shown that ancient DNA is usually <100 base pairs (bp) long (e.g., Pääbo, 1989; Weyrich et al., 2017), and marine *sedaDNA* fragments also tend to be very short (~69 bp; Armbrrecht et al., 2020). Although ancient DNA extracted from bones and teeth has been used

extensively to study human and megafauna evolution for more than 30 years (Hagelberg et al., 2015), its application to marine settings is still relatively new. Consequently, *sedaDNA* laboratory protocols, as well as downstream bioinformatic processing and analysis of *sedaDNA* data, are not yet well established. This is especially the case for eukaryotes for which only trace amounts of *sedaDNA* are preserved in the forms of both extra- and intracellular DNA (e.g., within robust resting stages such as cysts and spores). Further, ancient DNA fragment size and damage analysis, standard procedures for validating ancient DNA signals in human- and megafauna-related ancient DNA research, have not yet been commonly applied to *sedaDNA*, making it difficult to evaluate *sedaDNA* authenticity across existing studies.

In contrast to ancient DNA, DNA from living organisms (modern DNA) is highly intact and overwhelmingly abundant in the environment, including the ocean. For example, the average size of the small subunit ribosomal RNA gene—SSU rRNA, a gene commonly used as a taxonomic marker—is approximately 20 times that of a typical ancient DNA molecule (~1,800 bp; Tanabe et al., 2016) and can occur in copy numbers of ~12,000 in a single cell of a marine phytoplankter (Zhu et al., 2005). Molecular biological techniques used to detect and investigate marine organisms in present-day ocean settings are well established and have greatly improved our knowledge about the functioning, composition, and dynamics of marine food webs (Amaral-Zettler et al., 2009; De Vargas et al., 2015; Carradec et al., 2018). In addition, metagenomic research of the modern ocean continues to generate invaluable reference sequences of living marine organisms to which ancient sequences can be compared.

Due to the sheer abundance of modern DNA in the ocean, contamination is a negligible issue in contemporary marine genomics because contaminant

sequences are largely outweighed by the target genetic signal. The opposite pattern is the case for *sedaDNA*, however, and thorough contamination control is required at each step along the process of *sedaDNA* acquisition and analysis.

HOW IS *sedaDNA* ACQUIRED FROM THE SEAFLOOR?

The recovery of *sedaDNA* from deep ocean sediments usually involves the acquisition of sediment cores from research vessels or platforms (Figure 1). Armbrrecht et al. (2019) describe in detail such coring operations and best practice techniques. In brief, among the different coring methods currently available, gravity-based coring and advanced piston coring (APC) systems are preferred for *sedaDNA* analyses, as they recover the least disturbed sediments and minimize the likelihood of modern seawater ingress. Gravity-based corers simply “free fall” into the sediment, cutting a core from the seafloor. To trigger the APC system, hydraulic pressure is applied by pumping drill fluid toward the shear pins at the top of the core barrel (Sun et al., 2018). Only small volumes of drill fluid can enter the space between the core barrel and the collar from above after stroking, greatly reducing the risk of contamination. However, because the standard drill fluid is seawater, which inevitably contains vast amounts of modern marine organisms, contamination is still a risk, and strict contamination measures are necessary. This potential contamination source can be tracked by infusing a non-toxic, non-volatile chemical tracer (e.g., perfluoromethyldecalin, PFMD) at a constant rate into the drill fluid and testing sediment subsamples along the length of the core for the presence of the tracer (Figure 1).

When the core is on deck, measures can be taken to prevent contamination derived from core handling and the surrounding environment. Readily applied contamination control measures while working on board a research vessel or

platform include wearing personal protective equipment; decontaminating the working environment, core liners, and cutting and splitting tools; instituting a variety of controls (e.g., air sampling, work bench swabbing, using PFMD controls alongside *sedaDNA* samples), and, if possible, working fast in cold, still-air conditions. Core storage under cold and anoxic conditions and/or freezing of sediment subsamples is also recommended, as well as subsequent sample processing at specialized ancient DNA facilities. The latter comprise ultraclean, low-DNA

environments achieved by following a unidirectional workflow from sample preparation to extraction and sequencing library preparation in separate working areas, and positively pressured and frequently decontaminated laboratories (Fulton and Shapiro, 2019).

ARE THERE OPTIMAL MARINE *sedaDNA* EXTRACTION TECHNIQUES?

While a “one-fits-all” extraction protocol for *sedaDNA* would be highly desirable, optimized protocols are usually required,

depending on the type of sediment and the target organisms to be analyzed. The efficiency of *sedaDNA* extraction can be highly variable, depending on sediment type and composition. Sediments rich in clay, borate, and organic content, and those kept at low temperatures and protected from oxygen and irradiation, usually contain relatively well preserved *sedaDNA* (Armbrecht et al., 2019, and references therein). A recent study showed that extracellular DNA binds well to clay minerals, which may protect it from being degraded by living bacteria in the subseafloor environment, and such DNA-substrate interactions are important to consider during *sedaDNA* extractions (Vuillemin et al., 2019).

Both intra- and extracellular *sedaDNA* can be extracted from sediments using a sequence of chemical and mechanical treatments. At the initial step of *sedaDNA* extractions, shaking the sample in a solution containing small beads (bead-beating) is commonly employed to break robust resting cells and to facilitate the recovery of intracellular as well as extracellular *sedaDNA* (e.g., Shaw et al., 2019). Phosphate-containing buffers have also been incorporated into *sedaDNA* extraction protocols, as phosphate has similar charge and structural properties to DNA so that it creates a competitive environment in which more DNA remains in solution, thereby aiding its isolation (Direito et al., 2012). We recently developed an optimized extraction protocol for marine eukaryote *sedaDNA* that combines two-step DNA-isolation (extracting DNA from fragile as well as robust organisms) with a DNA binding reaction in silica solution (Armbrecht et al., 2020). This technique facilitates recovery of particularly small and degraded DNA fragments (down to 27 bp), which is important for studies of ancient marine deposits, as *sedaDNA* fragmentation is expected to increase with the depth and age of the sediments.

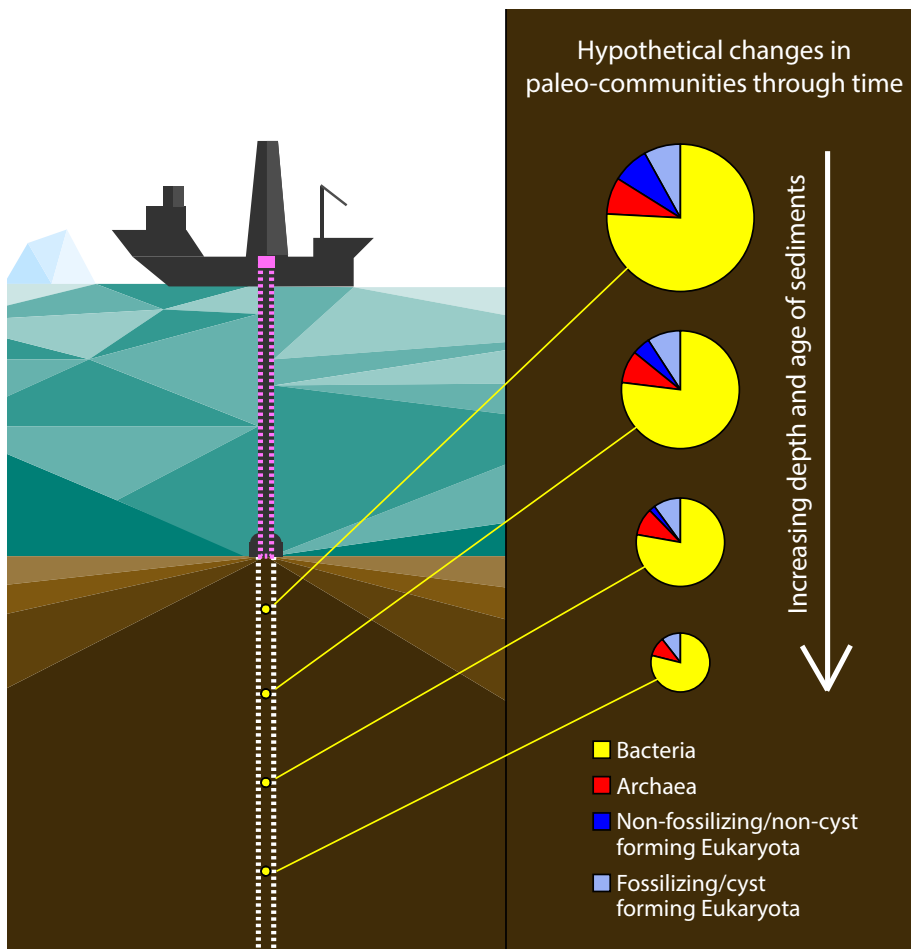


FIGURE 1. Schematic of a drilling vessel recovering a sediment core for *sedaDNA* analysis and hypothetical past marine community composition. The pink dashed line indicates the use of a chemical tracer for contamination tracking during coring. The white dashed line depicts the sediment core. Small yellow circles indicate theoretical *sedaDNA* sampling intervals, corresponding to pie charts on the right. Pie charts represent hypothetical paleo-communities detectable from *sedaDNA* shotgun analysis, where the majority (~75%, see text and Figure 3c) of the recovered *sedaDNA* sequences originate from bacteria, and where *sedaDNA* from fossilizing/cyst-forming taxa increases relative to non-fossilizing/non-cyst-forming taxa with subseafloor depth (assuming that *sedaDNA* of fossilizing/cyst-forming taxa preserves better than that of non-fossilizing/non-cyst-forming taxa). The decreasing size of the pie charts with subseafloor depth indicates an expected decrease in *sedaDNA*. Schematic not to scale.

WHICH GENOMICS AND SEQUENCING APPROACHES ARE SUITABLE FOR STUDYING *seadaDNA*?

Studies that rely on the analysis of *seadaDNA* should demonstrate data authenticity (i.e., the DNA recovered is ancient and free from modern contamination; Willerslev and Cooper, 2005). Validation protocols for ancient DNA include DNA damage analysis—for example, by applying mapDamage software, which was specifically developed to detect nucleotide misincorporations and fragmentation patterns that are characteristic of ancient DNA (Ginolhac et al., 2011; Jónsson et al., 2013). MapDamage has become a routine tool for authenticating ancient DNA across studies focusing on megafauna and humans (e.g., Llamas et al., 2015; Tobler et al., 2017). However, in highly complex metagenomic data, the identification and authentication of ancient sequences of very rare organisms remains challenging, partly due to the lack of high-quality reference sequences for the thousands of marine organisms thriving in the global ocean, and as the threshold of ~250 reads per species required to analyze and plot DNA damage patterns in mapDamage is often not reached (Collin et al., 2020). To overcome this issue, recent studies have focused on developing new bioinformatic techniques suitable for identification and authentication of low abundance ancient DNA in metagenomic data. For example, Hübler et al. (2019) developed HOPS (Heuristic Operations for Pathogen Screening) to screen for ancient pathogens in metagenomic samples, and Collin et al. (2020) described a new approach for processing and analyzing ancient metagenomic shotgun data focusing on the conservation of rare reads. The application and optimization of such tools for identifying and authenticating marine eukaryotes in *seadaDNA* appear highly promising and relevant to future *seadaDNA* research. A much less ideal but simpler authenticity assessment can be achieved through DNA fragment size analysis (as

noted above, fragmentation is expected to increase with age of the sediment sample), which should be the minimum authenticity analysis undertaken in any marine *seadaDNA* study.

To date, however, most *seadaDNA* studies have used a metabarcoding approach to investigate paleocommunities. This commonly used method targets a specific DNA region used as a taxonomic marker to identify different species that are aggregated in a sediment sample (Taberlet et al., 2012). These genetic markers are amplified using primers (short sequences matching the start and end of the target gene) in a polymerase chain reaction (PCR) and are subsequently sequenced (Figure 2). This technique has been shown to be unsuitable for the study of ancient DNA (e.g., Weyrich et al., 2017) for the following reasons:

1. Ancient DNA is typically highly damaged so that primers may not bind.
2. The DNA segments to be amplified are usually longer (>100 bp) than most ancient DNA fragments (<100 bp; Pääbo, 1989), introducing

biases toward longer sequences that favor modern contaminants where present, and skew the taxonomic composition.

3. PCRs are prone to inherent biases such as random amplification in the first few amplification cycles and PCR drift; hence, biases become more severe with increasing numbers of amplification cycles (Wagner et al., 1994; Taberlet et al., 2012) as necessitated with *seadaDNA* protocols.
4. The characteristic DNA damage patterns described above are no longer detectable in metabarcoding data as polymerases correct these patterns during amplification, preventing this mode of authenticity testing.

Studies that have applied metabarcoding should therefore be interpreted with caution unless they have shown authenticity of the *seadaDNA* through complementary analyses (e.g., fossils, biomarkers).

With ongoing increases in sequencing power and decreases in cost (Reuter et al., 2015), metagenomics is becoming

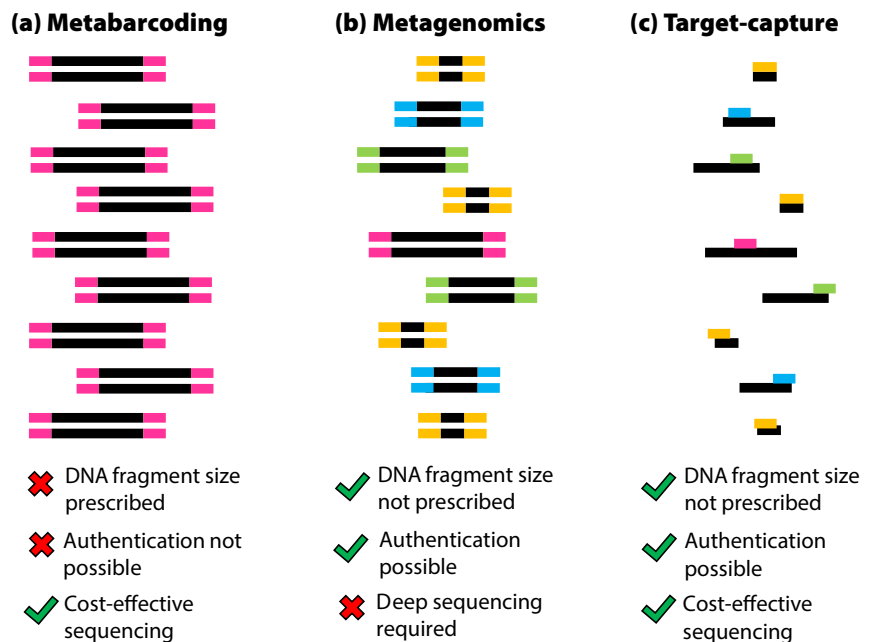


FIGURE 2. Schematic of different methodological approaches in modern and ancient marine genomics. (a) Metabarcoding is the amplification and analysis of equally sized DNA fragments from a total DNA extract. (b) Metagenomics is the extraction, amplification, and analysis of all DNA fragments independent of size. (c) Target-capture describes the enrichment and analysis of specific (chosen) DNA fragments independent of size from a total DNA extract.

a viable alternative to metabarcoding. Metagenomics studies extract and amplify the “total” DNA in a sample (i.e., potentially all species), thereby facilitating the recovery of DNA sequences proportionate to their original representation in that sample and independent of DNA fragment-size (“shotgun sequencing”; **Figure 2**). Thus, metagenomics approaches are better suited to studying *sedaDNA*, as they permit detection of bacteria, archaea, and eukaryotes, and they recover DNA damage patterns and fragment size variability without the biases inherent to metabarcoding. Community composition can then be reconstructed from this large pool of metagenomic data by screening for the occurrence of taxonomic marker genes. Additionally, metagenomic data sets offer the opportunity to draw functional information (“what organisms were doing”), as recently shown by Giosan et al. (2018), through their identification and use of chlorophyll biosynthesis proteins to estimate paleoproductivity. If the representation of the target organisms/genes is relatively low in the pool of total DNA data (e.g., in the case of eukaryote *sedaDNA*), very deep sequencing is required to recover sufficient genetic information to perform meaningful statistical analyses.

An attractive alternative that combines the specificity of the PCR approach but avoids the biases of the PCR method is the targeted enrichment of specific genetic sequences via hybridization-capture techniques (Horn, 2012). This approach uses short RNA probes (also called “baits,” analogous to the baits used in a fishing context) that are designed to be complementary to any DNA sequences the researchers may choose (e.g., specific genes of a target organism). By binding to the target sequence, these genetic baits “capture” DNA fragments in a manner that is akin to the PCR targeting, but independent of fragment size and with the preservation of damage patterns, allowing detailed authenticity testing (**Figure 2**). A recent study successfully applied this capture technique to

Northern Hemisphere permafrost samples by developing PaleoChip Arctic 1.0 for investigating ancient Arctic plants and animals (Murchie et al., 2019).

HOW DETAILED ARE THE COMMUNITY DATA GENERATED FROM *sedaDNA*?

Most marine organisms are known genetically only by short segments of their genome, such as “taxonomic marker genes,” which occur in a large group of organisms but with slight variations in each species that allow taxonomic differentiation. An example are the ribosomal genes: small subunit ribosomal RNA (18S rRNA or SSU rRNA) or large subunit ribosomal RNA (28S rRNA or LSU rRNA). Applying metabarcoding of the 18S rRNA gene (V9 region only, ~130 bp long), De Vargas et al. (2015) estimated a taxa richness of ~150,000 eukaryotes in the modern global surface ocean, detecting over 3,000 diatoms alone (categorizing the latter as a “hyperdiverse” group). This estimate stands in comparison to only 12 complete diatom genomes currently available via the National Center for Biotechnology Information’s (NCBI) Genome database (<https://www.ncbi.nlm.nih.gov/genome/>; search terms: “Eukaryota”[Organism] AND “Bacillariophyta”[Organism], June 16, 2020). The abundance of references for taxonomic marker genes over whole genomes of major marine eukaryotic taxa plainly illustrates why the use of marker genes for community composition assessments is popular.

Two of the best-known curated databases containing marine eukaryote sequences are the Protist Ribosomal Reference Database (PR²; Guillou et al., 2012) and the SILVA ribosomal RNA database (Quast et al., 2013). PR² contains SSU rRNA sequences, while SILVA is split into two separate databases, one containing full-length sequences of the same gene (SSU rRNA) and the other full-length sequences of the LSU rRNA gene. Both SILVA databases contain sequence information from a variety of

marine organisms—the latest release of the SILVA SSU database (SSURef NR 132) contains 592,561 bacterial, 25,026 archaeal, and 77,584 eukaryotic sequences, and the LSU database (LSURef 132) contains 168,075 bacterial, 1,440 archaeal, and 29,319 eukaryotic sequences (<https://www.arb-silva.de/documentation/release-132/>). Although PR² and SILVA comprise extensive resources, it is important to consider the use of additional databases, depending on the target organisms and/or study focus. For example, in *sedaDNA* research, the NCBI database, the largest genetic database available (<https://www.ncbi.nlm.nih.gov/>), may also be considered as well as the Marine Microbial Eukaryote Transcriptome Sequencing Project (MMETSP) database, an extensive resource for marine eukaryote RNA sequences (Keeling et al., 2014). While there is no standard approach to choosing a reference database (or combination of databases) for *sedaDNA* research, it is recommended to use one that is as complete as possible regarding reference sequences of the target organisms (Keeling et al., 2014; Collin et al., 2020).

Despite the usefulness of taxonomic marker genes for investigating marine eukaryotes, some limitations are yet to be overcome to achieve comprehensive community estimates and/or reconstructions. Even in modern marine investigations, part of the detected sequences can remain unidentified due to missing reference sequences, possibly because some organisms are (1) not easy or are impossible to culture and/or sequence, (2) rarely the subject of scientific investigations, or (3) entirely unknown and undescribed. For example, in their global study of marine eukaryotes, De Vargas et al. (2015) were able to assign taxonomy to two-thirds of the generated sequences, with the remaining third falling into the “unknown sequences” category. As a result of this imbalance in reference sequences across eukaryotes, some groups are better represented than others in genetic databases, which in turn

will impact a study's taxonomic resolution. Crucially, low taxonomic resolution can inhibit paleoenvironmental reconstruction efforts, where species-level identification is often pivotal in order to estimate key environmental or oceanographic conditions in a region of interest (Weckström et al., 2020).

An unfortunate consequence when applying taxonomic marker gene filters to metagenomic data is that the majority of the recovered sequencing data is not used. In fact, we recently showed that of a metagenomic marine *sedaDNA* shotgun data set, less than 1% of the quality-filtered sequencing reads were assigned taxonomy after alignment using the SILVA SSU reference database (Armbrecht et al., 2020). With high enough sequencing depth, a sufficient number of reads may remain available for statistical analyses; however, studies may wish to pursue optimizations in the experimental phase (e.g., hybridization-capture), or bioinformatic analysis (e.g., integrating complete databases), or both, where achieving high throughput is of concern.

EXAMPLE OF INCREASING TAXONOMIC RESOLUTION BY COMBINING INFORMATION FROM TWO MARKER GENES

The following example shows how the rarely used LSU, when combined with the more widely used SSU, may provide increased taxonomic resolution in metagenomic *sedaDNA* data. Metagenomic *sedaDNA* sequence data, acquired from a sediment sample collected during the Sabrina Seafloor Survey 2017 (IN2017_V01) off East Antarctica (Armand et al., 2018), was extracted and analyzed using optimized laboratory and bioinformatic procedures described in detail in Armbrecht et al. (2020). The DNA fragment length distribution of the filtered sequences was analyzed and showed a predominance of very short *sedaDNA* fragments (76 bp), as expected (Figure 3a). The filtered sequences were aligned against both the SILVA SSURef NR 132 and the LSURef 132 databases

(Huson et al., 2016). Read counts were determined for the SSU and LSU markers and analyzed separately, and then in combination, to avoid overrepresentation of any given taxon if detected by both. The read counts per taxon were summed if the taxon was identified exclusively by either SSU or LSU, and averaged if identified by both.

Using the combined markers showed a significant improvement in species resolution for eukaryotes (i.e., an increase in the number of eukaryotic taxa detected) relative to single markers (91 taxa determined using combined markers across all three samples vs. 59 and 51 for SSU and LSU alone, respectively; Figure 3b). Approximately 17% of the combined data was of eukaryote origin, including fossilizing as well as non-fossilizing taxa. For example, silica-skeleton-forming diatoms (Bacillariophyta) and Radiolaria were represented in the *sedaDNA* data, while non-fossilizing taxa such as cnidarians, copepods, and molluscs were also present (summarized under Eukaryota in Figure 3c). While the SSU appeared to be better suited for detecting major marine groups such as tintinnids (a group of ciliates), cnidarians, molluscs, and fish, the

LSU provided better resolution for crustaceans (e.g., copepods) and haptophytes (e.g., Phaeophyceae). This example for a single *sedaDNA* sample shows that taxonomic resolution can be considerably improved when merging information from different taxonomic marker genes, and that the latter approach may be helpful for gaining a much more detailed understanding of marine paleocommunities in future *sedaDNA* studies.

WHAT DOES THE FUTURE HOLD FOR MARINE *sedaDNA*...

The emergence of the new marine *sedaDNA* research field has shown that genetic signals preserved in the marine seafloor are a precious reservoir of biological information that can be used for paleoceanographic reconstructions. However, several key points have been identified to consider in future *sedaDNA* research, outlined below.

...In Terms of Reference Sequences and Genetic Databases?

Obtaining a more detailed taxonomic picture of marine paleocommunities will rely closely upon the continuous addition of new reference sequences from

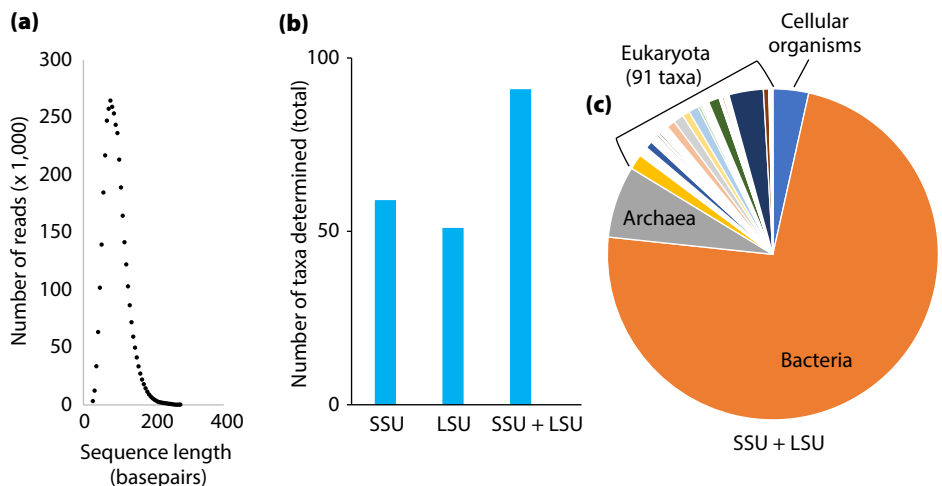


FIGURE 3. Taxonomic resolution achieved through different databases from short reads in metagenomic *sedaDNA* data. (a) Sequence-length distribution of a marine *sedaDNA* sample (counts of filtered reads classified into 51 DNA fragment size classes; sequenced on an Illumina HiSeq [2x 150 bp] at Garvan Institute for Medical Research, Sydney, Australia). (b) Total number of eukaryote taxa determined from metagenomic *sedaDNA* in a marine sediment sample using the SILVA small-subunit ribosomal RNA (SSU), large-subunit ribosomal RNA (LSU), and both SSU and LSU as reference databases. (c) Taxonomic composition derived from metagenomic *sedaDNA* of the same sample based on the combined SILVA SSU+LSU approach.

modern marine organisms to taxonomic databases. This is achieved by both morphological and molecular characterization of individual species (e.g., through the application of single cell genomics), providing modern reference genomes against which ancient specimens can be aligned. Such references will be invaluable in efforts to achieve species-level community estimates and to detect indicator species of paleoenvironments using *sedaDNA*. Additionally, it is important to further optimize and develop bioinformatic tools that enable the streamlined analysis of the vast amounts of genetic data (millions of sequencing reads) generated from highly diverse marine *sedaDNA* samples. Currently, no standard bioinformatic approaches exist for the study of ancient marine *sedaDNA*, and their development should be a focus of future research to facilitate rapid analysis and comparison of results across studies and research groups.

...In Terms of Optimizations of Experimental Procedures?

sedaDNA extraction techniques may need further optimizations, depending on the study organisms. For example, diatoms are one of the most productive classes of phytoplankton in the Southern Ocean and are extremely useful paleoenvironmental indicators due to their sensitivity to changing oceanographic conditions and their excellent preservation as microfossils in marine sediments (Deppeler and Davidson, 2017). In contrast to their prevalence in the microfossil record, diatoms are often underrepresented in *sedaDNA* data (e.g., Shaw et al., 2019), which may be due to biases in DNA extraction methods, relatively poor preservation of ancient diatom DNA possibly linked to physical and chemical sediment characteristics, and/or current limitations in reference databases. Continuous improvement of extraction methods, application of targeted enrichment approaches, and addition of modern diatom sequences to genetic reference databases may help to tackle this

important question in the future and enable detailed investigation of both diatoms and similar keystone marine species over geologic timescales.

...With Regard to Authenticity Testing of the Ancient Signal?

It will be important to move from metabarcoding to metagenomic techniques to allow authentication of ancient signals in genetic data (Taberlet et al., 2012; Weyrich et al., 2017; Collin et al., 2020). If the study organisms are expected to be a rare component of the metagenomic data, sequencing depth should be maximized, and *sedaDNA* damage-preserving target-enrichment techniques should be considered (Horn, 2012). Sequence-length distribution analyses offer a simple measure for assessing authenticity of *sedaDNA* data; however, DNA damage analysis should be applied in the future to test and ensure *sedaDNA* authenticity (Ginolhac et al., 2011; Jónsson et al., 2013; Huebler et al., 2019; Collin et al., 2020), especially when working with increasingly old sediment samples. Additionally, blank and environmental controls should be included in the processing and analysis of *sedaDNA* and lists of contaminant taxa made publicly available alongside each study's results. This will allow interlaboratory comparisons of common contaminants introduced by reagents and/or databases, as well as laboratory or extraction method-specific contaminants, which might otherwise confound the results from which conclusions are drawn.

...For the Investigation of Species- and Location-Specific Degradation Patterns?

Preservation of marine *sedaDNA* in various locations should be investigated alongside environmental variables that might influence preservation and degradation patterns. Taxon-specific degradation patterns and taphonomic biases require in-depth investigation to determine whether calibrations of the community data are required in *sedaDNA* data.

Much more research is required to determine the variations in *sedaDNA* fragment size by location, age, and taxonomic composition, and the environmental factors that contribute to *sedaDNA* degradation.

The points listed above are fundamental aspects to be addressed in future marine *sedaDNA* research, an area that is still in its infancy and that holds great potential for providing novel insights into the evolution and dynamics of marine ecosystems. Keeping these key points in mind is vital to continued efforts to reconstruct past marine communities from *sedaDNA* and will help to generate and authenticate better resolved data for exploring in detail the history of life in our ocean. 🌊

REFERENCES

- Amaral-Zettler, L.A., E.A. McCliment, H.W. Ducklow, and S.M. Huse. 2009. A method for studying protistan diversity using massively parallel sequencing of V9 hypervariable regions of small-subunit ribosomal RNA genes. *PLOS ONE* 4:e6372, <https://doi.org/10.1371/journal.pone.0006372>.
- Armand, L.K., P.E. O'Brien, and On-board Scientific Party. 2018. Interactions of the Totten Glacier with the Southern Ocean through multiple glacial cycles (IN2017-V01): Post-survey report. *Research School of Earth Sciences, Australian National University, Canberra*, <https://doi.org/10.4225/13/5acea64c48693>.
- Armbrecht, L., M.J.L. Coolen, F. Lejzerowicz, S.C. George, K. Negandhi, Y. Suzuki, J. Young, N.R. Foster, L.K. Armand, A. Cooper, and others. 2019. Ancient DNA from marine sediments: Precautions and considerations for seafloor coring, sample handling and data generation. *Earth-Science Reviews* 196:102887, <https://doi.org/10.1016/j.earscirev.2019.102887>.
- Armbrecht, L., S. Herrando-Pérez, R. Eisenhofer, G.M. Hallegraef, C.J.S. Bolch, and A. Cooper. 2020. An optimized method for the extraction of ancient eukaryote DNA from marine sediments. *Molecular Ecology Resources*, <https://doi.org/10.1111/1755-0998.13162>.
- Carradec, Q., E. Pelletier, C. Da Silva, A. Alberti, Y. Seeleuthner, R. Blanc-Mathieu, G. Lima-Mendez, F. Rocha, L. Tirichine, K. Labadie, and A. Kirilovsky. 2018. A global ocean atlas of eukaryotic genes. *Nature Communications* 9:373, <https://doi.org/10.1038/s41467-017-02342-1>.
- Collin, T.C., K. Drosou, J.D. O'Riordan, T. Meshveliani, R. Pinhasi, and R.N.M. Feeney. 2020. An open-sourced bioinformatic pipeline for the processing of Next-Generation Sequencing derived nucleotide reads: Identification and authentication of ancient metagenomic DNA. *bioRxiv*, <https://doi.org/10.1101/2020.04.20.050369>.
- Deppeler, S.L., and A.T. Davidson. 2017. Southern Ocean phytoplankton in a changing climate. *Frontiers in Marine Science*, <https://doi.org/10.3389/fmars.2017.00040>.
- De Vargas, C., S. Audic, N. Henry, J. Decelle, F. Mahé, R. Logares, E. Lara, C. Berney, N. Le Bescot, I. Probert, and others. 2015. Eukaryotic plankton diversity in the sunlit ocean. *Science* 348(6237), <https://doi.org/10.1126/science.1261605>.

- Direito, S.O., A. Marees, and W.F. Röling. 2012. Sensitive life detection strategies for low-biomass environments: Optimizing extraction of nucleic acids adsorbing to terrestrial and Mars analogue minerals. *FEMS Microbiology Ecology* 81:111–123, <https://doi.org/10.1111/j.1574-6941.2012.01325.x>.
- Fulton, T., and B. Shapiro. 2019. Setting up an ancient DNA laboratory. Pp. 1–13 in *Ancient DNA: Methods and Protocols*, 2nd ed. B. Shapiro, A. Barlow, P.D. Heintzman, M. Hofreiter, J.L.A. Pajmans, and A.E.R. Soares, eds., Humana Press, New York, USA.
- Ginolhac, A., M. Rasmussen, M.T.P. Gilbert, E. Willerslev, and L. Orlando. 2011. mapDamage: Testing for damage patterns in ancient DNA sequences. *Bioinformatics* 27(15):2,153–2,155, <https://doi.org/10.1093/bioinformatics/btr347>.
- Giosan, L., W.D. Orsi, M. Coolen, C. Wuchter, A.G. Dunlea, K. Thirumalai, S.E. Munoz, P.C. Clift, J.P. Donnelly, V. Galy, and D.Q. Fuller. 2018. Neoglacial climate anomalies and the Harappan metamorphosis. *Climate of the Past* 14:1,669–1,686, <https://doi.org/10.5194/cp-14-1669-2018>.
- Guillou, L., D. Bachar, S. Audic, D. Bass, C. Berney, L. Bittner, C. Boutte, G. Burgaud, C. de Vargas, J. Decelle, and J. del Campo. 2012. The Protist Ribosomal Reference database (PR2): A catalog of unicellular eukaryote small sub-unit rRNA sequences with curated taxonomy. *Nucleic Acids Research* 41(D1):D597–D604, <https://doi.org/10.1093/nar/gks1160>.
- Hagelberg, E., M. Hofreiter, and C. Keyser. 2015. Ancient DNA: The first three decades. *Philosophical Transactions of the Royal Society B* 370(11660), <https://doi.org/10.1098/rstb.2013.0371>.
- Hübner, R., F.M. Key, C. Warinner, K.I. Bos, J. Krause, and A. Herbig. 2019. HOPS: Automated detection and authentication of pathogen DNA in archaeological remains. *Genome Biology* 20:1–13, <https://doi.org/10.1186/s13059-019-1903-0>.
- Horn, S. 2012. Target enrichment via DNA hybridization capture. Pp. 177–188 in *Ancient DNA (Methods and Protocols)*. B. Shapiro and M. Hofreiter, eds., Methods in Molecular Biology, vol. 840, Humana Press, https://doi.org/10.1007/978-1-61779-516-9_21.
- Huson, D.H., S. Beier, I. Flade, A. Górski, M. El-Hadidi, S. Mitra, H.-J. Ruscheweyh, and R. Tappu. 2016. MEGAN Community Edition - Interactive exploration and analysis of large-scale microbiome sequencing data. *PLOS Computational Biology* 12:e1004957, <https://doi.org/10.1371/journal.pcbi.1004957>.
- Jónsson, H., A. Ginolhac, M. Schubert, P.L.F. Johnson, and L. Orlando. 2013. mapDamage2.0: Fast approximate Bayesian estimates of ancient DNA damage parameters. *Bioinformatics* 29:1,682–1,684, <https://doi.org/10.1093/bioinformatics/btt193>.
- Keeling, P.J., F. Burki, H.M. Wilcox, B. Allam, E.E. Allen, L.A. Amaral-Zettler, E.V. Armbrust, J.M. Archibald, A.K. Bharti, C.J. Bell, and B. Beszteri. 2014. The Marine Microbial Eukaryote Transcriptome Sequencing Project (MMETSP): Illuminating the functional diversity of eukaryotic life in the oceans through transcriptome sequencing. *PLOS Biology* 12:6, <https://doi.org/10.1371/journal.pbio.1001889>.
- Llamas, B., P. Brotherton, K.J. Mitchell, J.E. Templeton, V.A. Thomson, J.L. Metcalf, K.N. Armstrong, M. Kasper, S.M. Richards, A.B. Camens, and M.S. Lee. 2015. Late Pleistocene Australian marsupial DNA clarifies the affinities of extinct megafaunal kangaroos and wallabies. *Molecular Biology and Evolution* 32:574–584, <https://doi.org/10.1093/molbev/msu338>.
- Murchie, T.J., M. Kuch, A. Duggan, M.L. Ledger, K. Roche, J. Klunk, E. Karpinski, D. Hackenberger, T. Sadoway, R. MacPhee, and others. 2019. PalaeoChip Arctic1.0: An optimised eDNA targeted enrichment approach to reconstructing past environments. *bioRxiv*, <https://doi.org/10.1101/730440>.
- Pääbo, S. 1989. Ancient DNA: Extraction, characterization, molecular cloning, and enzymatic amplification. *Proceedings of the National Academy of Sciences of the United States of America* 86:1,939–1,943, <https://doi.org/10.1073/pnas.86.6.1939>.
- Quast, C., E. Priesse, P. Yilmaz, J. Gerken, T. Schweer, P. Yarza, J. Peplies, and F.O. Glöckner. 2013. The SILVA ribosomal RNA gene database project: Improved data processing and web-based tools. *Nucleic Acids Research* 41:D590–D596, <https://doi.org/10.1093/nar/gks1219>.
- Reuter, J.A., D.V. Spacek, and M.P. Snyder. 2015. High-throughput sequencing technologies. *Molecular Cell* 58:586–597, <https://doi.org/10.1016/j.molcel.2015.05.004>.
- Shaw, J.L., L.S. Weyrich, G. Hallegraef, and A. Cooper. 2019. Retrospective eDNA assessment of potentially harmful algae in historical ship ballast tank and marine port sediments. *Molecular Ecology* 28:2,476–2,485, <https://doi.org/10.1111/mec.15055>.
- Sun, Z., Z. Jian, J.M. Stock, H.C. Larsen, A. Klaus, C.A. Alvarez Zarkian, and Expedition 367/368 Scientists. 2018. *South China Sea Rifted Margin*. Proceedings of the International Ocean Discovery Program, 367/368. International Ocean Discovery Program, College Station, TX, <https://doi.org/10.14379/iodp.proc.367368.2018>.
- Taberlet, P., E. Coissac, F. Pompanon, C. Brochmann, and E. Willerslev. 2012. Towards next-generation biodiversity assessment using DNA metabarcoding. *Molecular Ecology* 21:2,045–2,050, <https://doi.org/10.1111/j.1365-294X.2012.05470.x>.
- Tanabe, A.S., S. Nagai, K. Hida, M. Yasuie, A. Fujiwara, Y. Nakamura, Y. Takano, and S. Katakura. 2016. Comparative study of the validity of three regions of the 18S-rRNA gene for massively parallel sequencing-based monitoring of the planktonic eukaryote community. *Molecular Ecology Resources* 16:402–414, <https://doi.org/10.1111/1755-0998.12459>.
- Tobler, R., A. Rohrlach, J. Soubrier, P. Bover, B. Llamas, J. Tuke, N. Bean, A. Abdullah-Highfold, S. Agius, A. O'Donoghue, and I. O'Loughlin. 2017. Aboriginal mitogenomes reveal 50,000 years of regionalism in Australia. *Nature* 544:180–184, <https://doi.org/10.1038/nature21416>.
- Vuillemin, A., S.D. Wankel, Ö.K. Coskun, T. Magritsch, S. Vargas, E.R. Estes, A.J. Spivack, D.C. Smith, R. Pockalny, R.W. Murray, and S. D'Hondt. 2019. Archaea dominate oxic seafloor communities over multimillion-year time scales. *Science Advances* 5:p.eaaw4108, <https://doi.org/10.1126/sciadv.aaw4108>.
- Wagner, A., N. Blackstone, P. Cartwright, M. Dick, B. Misof, P. Snow, G.P. Wagner, J. Bartels, M. Murtha, and J. Pendleton. 1994. Surveys of gene families using polymerase chain reaction: PCR selection and PCR drift. *Systematic Biology* 43:250–261, <https://doi.org/10.1093/sysbio/43.2.250>.
- Weckström, K., B.R. Roche, A. Miettinen, D. Krawczyk, A. Limoges, S. Juggins, S. Ribeiro, and M. Heikkilä. 2020. Improving the paleoceanographic proxy tool kit: On the biogeography and ecology of the sea ice-associated species *Fragilariopsis oceanica*, *Fragilariopsis reginae-jahnica* and *Fossula arctica* in the northern North Atlantic. *Marine Micropaleontology* 157:101860, <https://doi.org/10.1016/j.marmicro.2020.101860>.
- Weyrich, L.S., S. Duchene, J. Soubrier, L. Arriola, B. Llamas, J. Breen, A.G. Morris, K.W. Alt, D. Caramelli, V. Dresely, and M. Farrell. 2017. Neanderthal behaviour, diet, and disease inferred from ancient DNA in dental calculus. *Nature* 544:357–361, <https://doi.org/10.1038/nature21674>.
- Willerslev, E., and A. Cooper. 2005. Ancient DNA. *Proceedings of the Royal Society of London B* 272:3–16, <https://doi.org/10.1098/rspb.2004.2813>.
- Zhu, F., R. Massana, F. Not, D. Marie, and D. Vault. 2005. Mapping of picoeukaryotes in marine ecosystems with quantitative PCR of the 18S rRNA gene. *FEMS Microbiology Ecology* 52:79–92, <https://doi.org/10.1016/j.femsec.2004.10.006>.

ACKNOWLEDGMENTS

I thank Leanne Armand and Phil O'Brien, and the IN2017_V01 science party and crew (Commonwealth Scientific and Industrial Research Organisation [CSIRO]/Marine National Facility [MNF]) for their help in acquiring the *sedaDNA* sample that is exemplified in this article and for their input into this research. I also thank Gustaaf Hallegraef, Chris Bolch, and Alan Cooper for supporting this work, as well as Holly Heiniger and Steve Johnson for technical assistance, and Raphael Eisenhofer, Kieren Mitchell, Laura Weyrich, Bastien Llamas, Ray Tobler, Vilma Pérez, Oscar Estrada-Santamaría, Yasmine Souilmi, Yichen Liu, Steve Richards, João Teixeira, Christian Huber, Angad Johar, Joshua Schmidt, Salvador Herrando-Pérez, Jeremy Austin, Maria Lekis, and Adam Wilkins for many constructive discussions around *sedaDNA*. I am also grateful to Laurie Menviel and Katrin Meissner, the organizers of the International Conference on Paleocyanography 2019 (ICP13), where the idea for this manuscript was conceived. I was supported through the 2017 Australian Research Council Discovery Project DP170102261, by the University of Adelaide School of Biological Sciences, and by Past Global Changes (PAGES). Detailed information on eukaryote, bacterial, and archaeal communities not shown in this paper is available on request.

AUTHOR

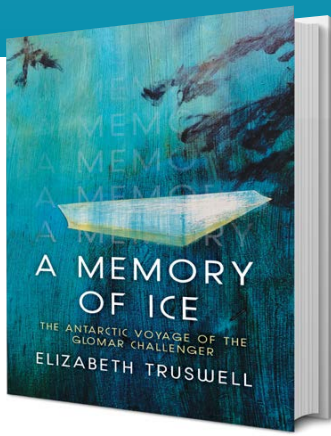
Linda H. Armbricht (linda.armbricht@adelaide.edu.au) is Research Fellow, Australian Centre for Ancient DNA, Department of Ecology and Evolutionary Biology, School of Biological Sciences, Faculty of Science, The University of Adelaide, Adelaide, Australia.

ARTICLE CITATION

Armbricht, L.H. 2020. The potential of sedimentary ancient DNA to reconstruct past ocean ecosystems. *Oceanography* 33(2):116–123, <https://doi.org/10.5670/oceanog.2020.211>.

COPYRIGHT & USAGE

This is an open access article made available under the terms of the Creative Commons Attribution 4.0 International License (<https://creativecommons.org/licenses/by/4.0/>), which permits use, sharing, adaptation, distribution, and reproduction in any medium or format as long as users cite the materials appropriately, provide a link to the Creative Commons license, and indicate the changes that were made to the original content.



SIDEBAR

A Memory of Ice

THE ANTARCTIC VOYAGE OF THE *GLOMAR CHALLENGER*

Book by Elizabeth Truswell

Reviewed by Peter N. Webb and Peter J. Barrett

Deep Sea Drilling Project (DSDP) Leg 28 initiated a new era of seafloor exploration when *Glomar Challenger* departed Fremantle (West Australia) for a 69-day expedition from late December to February in the austral summer of 1972–73. Along with Elizabeth (Liz) Truswell, the author of *A Memory of Ice: The Antarctic Voyage of the Glomar Challenger*, we were members of the shipboard science party, and we value the opportunity to relive this pioneering Antarctic expedition through her account. Not every ocean drilling leg is fortunate enough to have its shipboard and science activities documented in such an interesting, permanent, and colorful fashion, and we feel privileged to have the opportunity here to share a few memories from that spring that surfaced while reading *A Memory of Ice*.

Liz Truswell skillfully interleaves diary-based personal recollections of deep ocean drillship science from five decades ago, the significant events in polar exploration and science of the preceding two centuries, and the more significant south polar Earth science achievements in the time since 1973. As the reader journeys through *A Memory of Ice*, the author discusses a wide spectrum of science topics, with particular attention devoted to her career-long research emphases in paleobotany, palynology, and plant biogeography. The use of high-quality illustrations, many reproduced from archival sources, strengthens the impact of the text. A bibliography and a glossary of terms are also provided.

Why has almost a half-century elapsed before the telling of this expedition's events, its scientific results, and the thoughts surrounding its place in science history? A pre-syn-post approach that spans a few decades allows a much more valuable understanding of how science evolves and progresses. This makes Liz Truswell's presentation a meaningful source for aspiring Earth scientists and perhaps even some experienced researchers. Published expedition accounts from the heroic-era expeditions by Scott, Shackleton, Amundsen, Mawson, and others were usually published shortly after an expedition, emphasizing exploration and the associated suffering and hardships and offering relatively little in the way of scientific information. This latter publication style satisfied the immediate needs of a curious public and the generous expedition sponsors.

The scientific objectives of DSDP Leg 28 were rooted in forging a better understanding of the high-latitude Cenozoic sedimentary record. Let us briefly recall the status of Antarctic

Cenozoic Earth science before the arrival of Leg 28 aboard *Glomar Challenger*. Prior to 1972, the Cenozoic geology of Antarctica was very poorly known. Cenozoic sediments and fossils had been documented at the northern end of the Antarctic Peninsula—West Antarctica—in the early twentieth century. The record in East Antarctica was confined to surficial Quaternary terrestrial glacial deposits along the Ross Sea–Transantarctic Mountains margins together with volcanic rocks, some of which are now known to be late Cenozoic in age. Cenozoic geology was not a primary program during the 1957–1959 International Geophysical Year (IGY) activities in West and East Antarctica. In one of the earlier reviews of Antarctic geology, Harrington (1965) noted: “There is as yet no sedimentary record of the history of East Antarctica from the later Jurassic to the Pliocene.” Cenozoic data from the Antarctic continental shelves and floors of the circum-Antarctic deep ocean were equally absent. In the late 1960s, the association of terrestrial glacial and fjordal marine deposits and volcanic extrusions in the Dry Valleys (now McMurdo Dry Valleys) adjacent to the Ross Sea provided the first concrete evidence that glaciation in the Transantarctic Mountains predated the Quaternary and might span the late Miocene and Pliocene.

Prior to the availability of direct evidence derived from sources in Antarctica, biogeographers, paleontologists, stratigraphers, sedimentologists, and isotope geochemists, among others, working in lower latitude locales, searched for environmental indicators of widely oscillating polar, temperate, and tropical paleoclimate across Southern Hemisphere latitudes in the past. In 1953 and 1962, C.A. Fleming explored the possible impact Late Cenozoic expansion of cool glacial-interglacial water-mass circulation of Antarctic origin had on marine biota, basin histories, and stratigraphy in New Zealand. In 1963, Fleming proposed that Antarctic and subantarctic climate change drove alpine vegetation zones further north and treeline elevations to higher altitudes (including that of the southern beech genus *Nothofagus*) in New Zealand and in the Southwest Pacific. These thoughtful speculations were subtle hints to later investigators that there were indeed paleoclimatically important linkages between the cryogenic terrestrial and marine Antarctic Cenozoic and coeval records in temperate latitudes to the north.

As *Glomar Challenger* recovered Cenozoic biogenic and clastic sedimentary successions from six drillholes in the Southern Ocean and four in the Ross Sea, it was instantly

apparent to the paleontology group that we had entered a distinctly different paleo-biological world from that we were accustomed to back home, way to the north. The high-resolution pelagic and benthic biostratigraphic zonations of New Zealand and Australia could not be applied in these extreme southern high latitudes. The paleontologists of Leg 28 made the first attempts to develop austral biostratigraphic zonations that were based principally on diatoms but that also included other microfossil groups such as foraminifera and radiolaria and the occasional temperate zone invaders from the north. These efforts continue today. Our preliminary time controls proved adequate for contributing to the principal expedition objectives.

The scientific and technical successes of DSDP Leg 28 were many. We quote a few of them directly from Liz's account.

The 69 days at sea that we had enjoyed—or endured, depending on one's experience and point of view—had produced results that were outstanding for the time. Our mandate, when we left Fremantle in December 1972, had been to explore the history of the Antarctic icecap and the high-latitude circulation of the seas surrounding that continent; and to investigate the timing and nature of sea-floor spreading between Australia and Antarctica... Overall, the most demanding of aims was to test the feasibility of drilling the sea floor in high southern latitudes under the constant threat of icebergs and the storms that characterise those regions... By all measures, the voyage had been a success. We had succeeded in pushing back the age of the icecap from the 3–5 million years that was accepted when we left port, to something close to 26 million years... We had tested the age and rates of sea-floor spreading across the Southeast Indian Ridge separating Antarctica and Australia, using ages from tiny fossils in the sediments lying atop the volcanic basement of the sea floor. We confirmed that these were in accord with magnetic ages deduced from earlier seismic mapping... More recent reviews of the whole program of drilling the sea floor of the deep oceans, reviews that can now look back over 50 years, classify the Deep Sea Drilling Project (DSDP), and its rugged Glomar Challenger, as belonging to an initial phase of 'curiosity driven' exploration—a rather simplified 'looking to see what's there' approach. In contrast, according to these reviews, more recent phases have singled out particular issues in Earth science and have sought answers to global problems through focusing on carefully selected drilling programs. Perhaps that is so in general, but the history of the polar ice sheet, an issue to which several DSDP expeditions contributed substantially, is a subject of ongoing scientific concern at a global level.

Successes emanating from DSDP Leg 28 spurred the launching of a number of highly technical deep stratigraphic drilling programs over the last half century, all aimed at sampling and deciphering the Antarctic Cenozoic cryogenic record. These

projects include: Dry Valley Drilling Project (DVDP), McMurdo Sound Sediment and Tectonic Studies (MSSTS), Cenozoic Investigations in the Ross Sea (CIROS), Ross Ice Shelf Project (RISP), Cape Roberts Project (CRP), and ANtarctic DRILLing Project (ANDRILL). All of these programs were international initiatives to some degree. Examination of Leg 28 drill core has continued through the decades and is still being incorporated in research activities today. Countless graduate students prepared theses and dissertations based on Leg 28 core from the Southern Ocean and Ross Sea. Many proceeded on to careers in academia and industry. Some continued to contribute to the Antarctic Earth sciences, often becoming lead investigators of the drilling initiatives noted above.

We conclude by quoting a few lines by Liz Truswell from the prologue of *Memory of Ice*:

The book gives my personal story—that of a young scientist feeling largely unprepared—thrown into the excitement and absorbing interest of field work in one of the most remote regions of the globe... This is a world full of stories. Many have been told before, but fresh details continue to emerge. There are stories of human endurance in encounters with the elements, of competing national and individual ambitions, of dealing with the novel and unexpected in nature and of persistence in the everyday tasks of mapping and recording. It has often proved difficult to separate these different threads that are interwoven with the story of Leg 28.

The often deeply personal recollections that are so central to the success of this account will reverberate with many readers, especially those who have had like experiences in the remotest parts of Earth. This is a truly scholarly contribution and likely to figure prominently in future research by polar historians. The legacy of DSDP Leg 28 is certainly secure.

REFERENCES

- Fleming C.A. 1953. *The Geology of the Wanganui Subdivision*. New Zealand Geological Survey Bulletin, new series number 52, Department of Scientific and Industrial Research, Wellington, New Zealand, 361 pp.
- Fleming C.A. 1962. New Zealand biogeography: A paleontologist's approach. *Tuatara* 10(2):53–108.
- Fleming C.A. 1963. Age of the alpine biota. *Proceedings of the New Zealand Ecological Society* 10:15–18.
- Harrington, H.J. 1965. Geology and morphology of Antarctica. Pp. 1–71 in *Biogeography and Ecology in Antarctica*. J. van Mieghan and P. van Oye, eds, Springer, Dordrecht, the Netherlands.

BOOK INFO

A Memory of Ice: The Antarctic Voyage of the Glomar Challenger by E. Truswell. The Australian National University Press, 2019, 246 pages, free formats available for download, print version available for purchase, <https://doi.org/10.22459/MI.2019>.

REVIEWERS

Peter N. Webb (peternoelwebb@yahoo.com) is Professor Emeritus, School of Earth Sciences, The Ohio State University, Columbus, OH, USA.

Peter J. Barrett (peter.barrett@vuw.ac.nz) is Professor Emeritus, Antarctic Research Centre, Victoria University of Wellington, New Zealand.

The Origins of Oceanography in France

THE SCIENTIFIC EXPEDITIONS OF *TRAVAILLEUR* AND *TALISMAN* (1880–1883)

By John R. Dolan

ABSTRACT. This article describes the earliest French oceanographic expeditions dedicated to investigating the deep sea. Though these expeditions, conducted from 1880 to 1883, were quite successful in terms of both science and what today we call “outreach,” they are often overlooked in histories of oceanography or mentioned only in passing. They produced a substantial literature of over 100 scientific publications. Participants’ descriptions of 176 new species are still considered valid today. Among the remarkable scientific discoveries were culturable and pressure-tolerant bacteria in deep-sea sediment samples, which led to the origin of deep-sea microbiology, and iconic deep-sea fish such as the gulper eel. Specimens, instruments, and equipment from these expeditions were on display for the general public at an exhibition at the National Museum of Natural History in Paris in early 1884. Between 1885 and 1891, expedition scientists authored three mass-market books on deep-sea life and the expeditions. Following a summary of the expeditions and their results, some speculation is provided as to why such an auspicious nineteenth century beginning of oceanography in France did not lead to a sustained interest in oceanography. A supplementary file contains a bibliography of expedition publications and a list of the species described from expedition collections.

THE BEGINNINGS OF SCIENTIFIC STUDY OF THE DEEP SEA

Development of Scientific Interest in the Deep Sea and British Efforts

Histories of scientific interest in the deep sea often, and curiously, give prominence to a proposition credited to Edward Forbes (1844) that the deep sea was a vast lifeless, or azoic, zone (e.g., Rice et al., 1976). In reality, Forbes reported findings only with regard to the vertical distribution of mollusks and echinoderms in the Aegean Sea based on dredging. He found nothing below a depth of 230 fathoms (420 m), and his report included a diagram of faunal depth zones that labeled the layer below 300 fathoms “Zero of Animal Life probably about 300 fathoms.” He did not propose the depth as a general rule, nor did he use the term “azoic”; it appears only once in passing in the posthumously published book, *The Natural History of the European*

Seas (Forbes and Godwin-Austen, 1859, pg. 247). Regardless, testing the idea that no life existed at great depths, despite long-standing but scattered evidence to the contrary (as summarized in Carpenter, 1868), provided a marvelous straw man that justified early explorations for deep-sea life. Additionally, there was great interest in the nature of the seabed and physical conditions in the deep sea as attempts were being made to lay undersea telegraph cables. In fact, some of the early discoveries of deep-sea life forms were made through soundings carried out to determine the depth and nature of the seabed in the North Atlantic by the British (e.g., Wallich, 1860) and during retrieval of broken cables in the Mediterranean by the French (e.g., Milne Edwards, 1861).

The proposition of the deep sea as perhaps azoic provided in no small part the justification for the first systematic explorations of the deep sea led by British biolo-

gists through the expeditions of *Lightning* in 1868 and *Porcupine* in 1869 in the North Atlantic (Thomson, 1873). These first cruises dedicated to dredging the deep sea yielded the conclusions below, presented to the Royal Society of London by William Carpenter, vice president of the society (Carpenter et al., 1870):

1. *That the Ocean bottom, at depths of 500 fathoms or more, presents a vast field for research, of which the systematic exploration can scarcely fail to yield results of the highest interest and importance, in regard alike to Physical, Biological, and Geological Science.*
2. *That the prosecution of such a systematic exploration is altogether beyond the reach of private enterprise, requiring means and appliances which can only be furnished by Government.*

These observations led directly to the first large-scale exploration of the sea, the well-known *Challenger* Expedition of 1872–1876. Preliminary results of the *Challenger* Expedition appeared relatively quickly and were made widely available in 1878 by the chief scientist, Sir Charles Wyville Thomson, in two volumes under the title *The Voyage of the Challenger: The Atlantic: a preliminary account of the general results of the exploring voyage of the H.M.S. Challenger during 1873 and the early part of the year 1876*. The complete scientific results were eventually published from 1885 to 1895 in the famous massive series of over 80 monographs, mostly under the guidance of John Murray following Thomson’s death in 1882.

French Interest in Exploring the Deep Sea

Long-standing French interest in the deep sea is evidenced by Alphonse Milne Edwards's descriptions of organisms attached to the undersea telegraph cables laid between Sardinia and Algeria (Milne Edwards, 1861). In 1867, while Carpenter and Thomson were occupied with planning the *Lightning* expedition, the Marquis Léopold Folin, harbor-master of the Port of Bayonne, founded the first serial publication dedicated to marine sciences, including one focused on the deep sea: *Les Fonds de la Mer* (*The Bottom of the Sea*). A naturalist as well as a harbormaster, Folin specialized in tube-forming mollusks on which he would later contribute to the *Challenger* Reports (Folin, 1886).

Les Fonds de la Mer was originally printed in 16-page issues of text with plates (Figure 1). The first "volume," composed of issues published from 1867 to 1872, contained contributions by George S. Brady, who would later contribute to the *Challenger* Reports (Brady, 1880), and Alphonse Milne Edwards, whose interests included mammals, birds, and crustaceans and who (along with Folin) would later be responsible for the *Travailleur* and *Talisman* expeditions. The first issues also contained early citizen science, as Folin reported extensively on diverse samples of deep-sea soundings and sediment types from around the globe sent to him or delivered by the captains or officers of ships, many traveling to or from Bayonne. Issues of the *Les Fonds de la Mer* appeared irregularly, with the last issues delivered in 1887. While this first marine science serial is very nearly forgotten, it shows that some French scientists had a marked interest in the deep sea well before the *Challenger* Expedition, and that they maintained close relationships with British scientists who would later be involved in analyzing samples from *Challenger*.

Since Thomson's book on the preliminary results of *Challenger* appeared in 1878, it is plausible, and even probable,

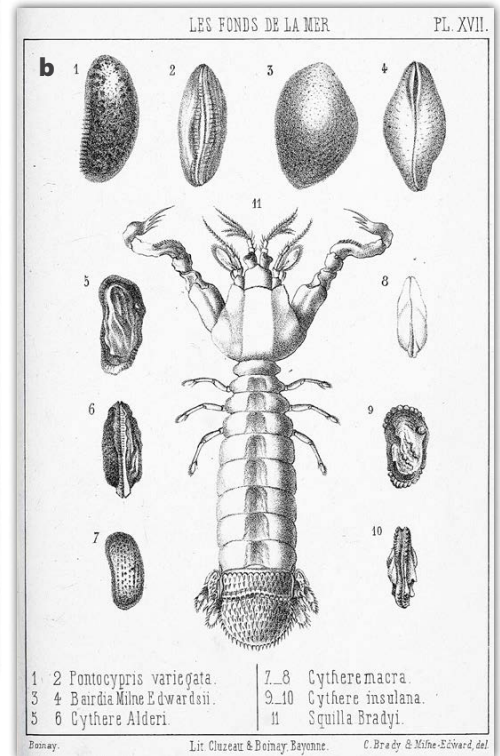
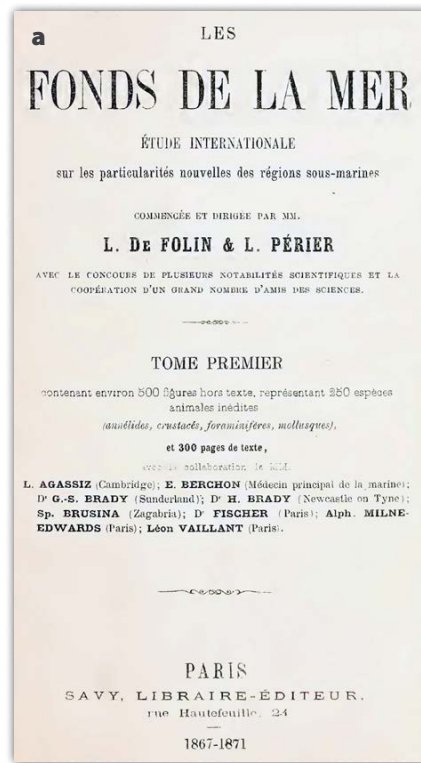


FIGURE 1. (a) The cover of volume one of *Les Fonds de la Mer* published in issues of 16 pages from 1867 to 1871. (b) Plate 17 from an 1869 article in *Les Fonds de la Mer* on fauna of Cape Verde with descriptions of new species by George S. Brady and Alphonse Milne Edwards (Folin et al., 1869).

that the success of the British *Challenger* Expedition prompted, at least in part, Alphonse Milne Edwards to plead in Paris before the Academy of Sciences in 1880 for French expeditions, at the behest of Folin. Milne Edwards had been elected to the academy only the year before at the relatively young age of 43. He successfully argued for government financing for deep-sea expeditions (Milne Edwards, 1881), as many deep-sea expeditions had been carried out in recent years but none in waters near France or by the French, except for private efforts by himself and Folin. With the support of the Academy of Sciences (roughly the French equivalent of the British Royal Society of London), the Ministry of Education named a commission to organize expeditions to explore the deep sea, headed by invertebrate zoologist Henri Milne-Edwards, and including his son Alphonse, Folin, a number of French zoologists, and also the British scientists John Gwyn Jeffreys (who had been



FIGURE 2. The instigators and organizers of the deep-sea expeditions: (a) Leopold Folin (1817–1896) and (b) Alphonse Milne Edwards (1835–1900).

chief scientist aboard *Porcupine* in 1869) and Alfred Norman. Folin and Alphonse Milne Edwards (Figure 2) obtained the use of a navy steamer, *Travailleur*, from the Ministry of Maritime Affairs for an expedition to sample the deep sea.

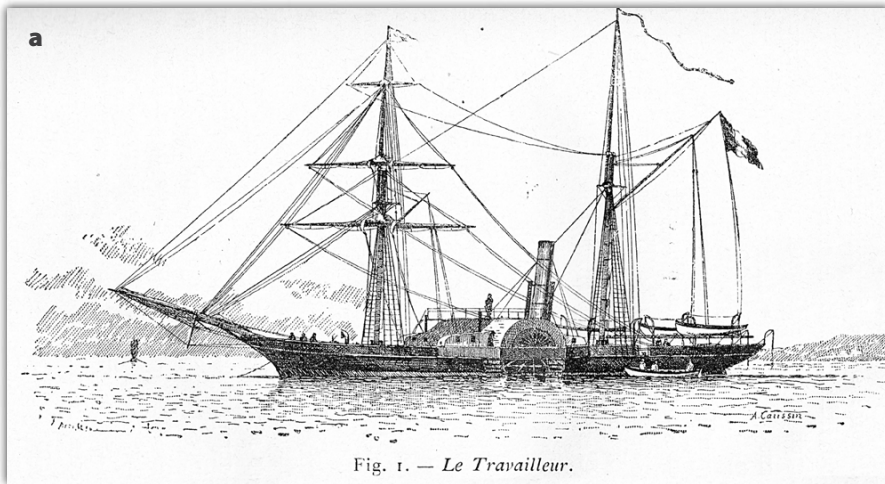
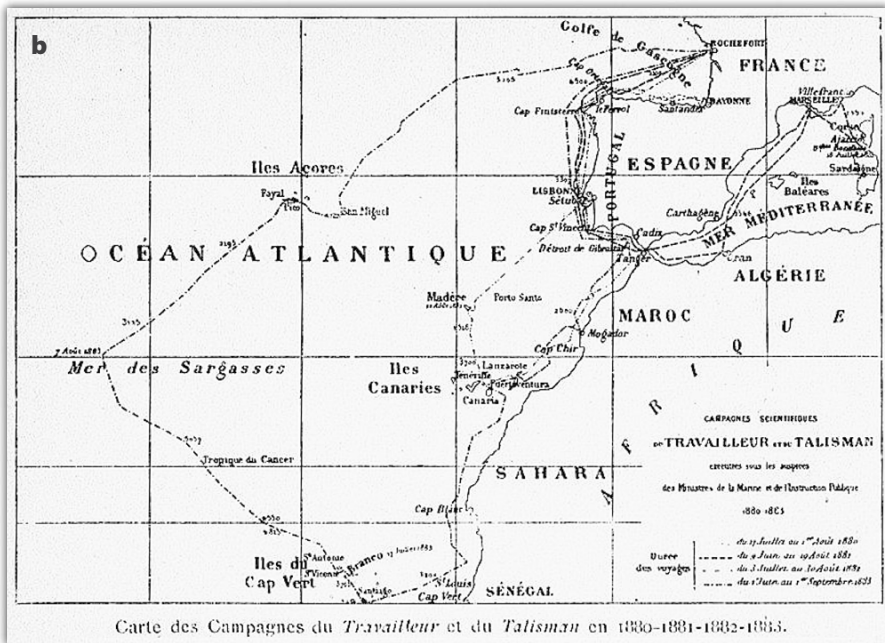


Fig. 1. — *Le Travailleur*.



Carte des Campagnes du *Travailleur* et du *Talisman* en 1880-1881-1882-1883.

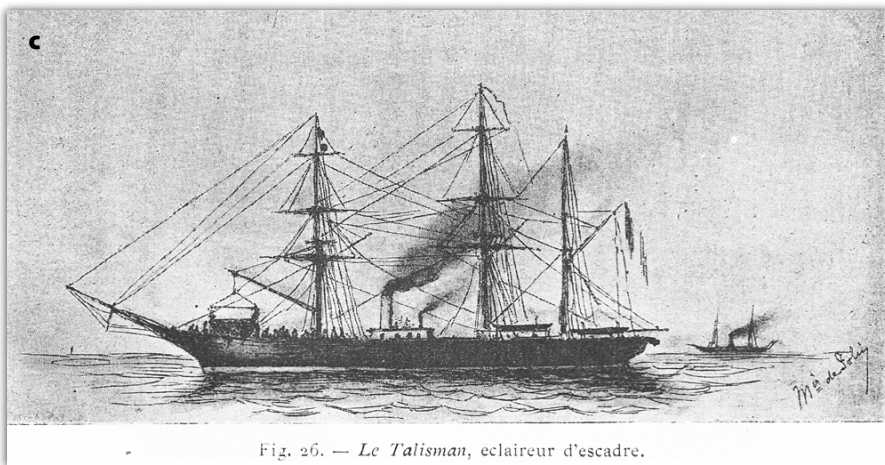


Fig. 26. — *Le Talisman*, éclairer d'escadre.

FIGURE 3. (a) The 45 m long side-wheel steamer *Travailleur* used in 1880, 1881, and 1882. (b) Cruise tracks of *Travailleur* and *Talisman*. (c) The 75 m long steamer *Talisman* used in the 1883 cruise. Ship drawings from Folin, 1887, *Talisman* drawing by Folin, map from Anonymous, 1880–1890

THE EXPEDITIONS OF *TRAVAILLEUR* AND *TALISMAN*

Travailleur was a 45 m long side-wheel steamer (Figure 3a), usually with a crew of about 90, but increased to 128 for the anticipated intensive dredging operations. The dredge used was that designed by the American naturalist Alexander Agassiz: it worked equally well whichever way it fell onto the seabed. The first expedition of two weeks duration in July of 1880 in the Bay of Biscay was basically a shakedown cruise. With 23 dredge hauls made between 300 m and 2,600 m depth, and 103 soundings, the cruise was a resounding success. Preliminary reports by the two British naturalists aboard *Travailleur*, Jeffreys and Norman, appeared very quickly, noting findings of new deep-sea forms and even some mollusks thought to be extinct (Jeffreys, 1880; Norman, 1880).

Based on the success of the first cruise, eight weeks of ship time was granted for the following year to explore the depths of the North Atlantic and the Mediterranean. During the second *Travailleur* expedition in July and August of 1881, the ship, equipped with 15 km of cable for dredging and new samplers for taking discrete depth water samples, traveled from Bayonne on the Atlantic coast to the Mediterranean. Mostly sampling in the Northwest Mediterranean Sea (see Figure 3b), about 50 deepwater dredge hauls were made; the Mediterranean fauna was found to be largely a subset of that known from the depths of the Atlantic, where the deepwater fauna appeared to be much richer. Again, the preliminary scientific results were described as unique and significant (Milne-Edwards, 1882), justifying continuing the explorations the following year.

The third *Travailleur* cruise lasted the entire months of July and August of 1882 and was dedicated to exploration of the seafloor in the North Atlantic between Bayonne and the islands of Madeira and the Canaries, thus ranging much further offshore than the previous cruises. Dredge hauls were made at 71 stations, again

bringing up new species. The ship, however, with its limited range, proved to be less than ideal for open-water sampling. The final expedition the following year therefore employed a larger steamer with a longer range of operation, *Talisman*.

Talisman (Figure 3c) was a 75 m long vessel equipped with a steam-driven propeller as well as a full complement of sails. It sailed from Rochefort (see Figure 3b) on June 1 and returned on August 31, 1883. Sampling was conducted along the Atlantic coasts of Morocco, Sudan, and Senegal, then through the Canaries, the Azores, and out to the edge of the Sargasso Sea. Along the cruise track, 212 soundings and 156 dredge hauls were carried out, some to depths of 5 km. This last cruise with *Talisman* yielded some of the more spectacular finds such as the iconic deep-sea fish, the gulper eel, and decapod crustaceans with odd morphologies, one named after *Talisman* (Figure 4). Jeffreys (1884) reported on the *Talisman* cruise, and the participants were honored by the Academy of Sciences with medals of honor. A popular account of the expedition by Filhol was serialized in the French journal *La Nature* (Filhol, 1884); excerpts were translated into English and published in installments in the American journal *Science* (Anonymous, 1884a).

SUMMARY OF THE SCIENTIFIC RESULTS OF THE TRAVAILLEUR AND TALISMAN EXPEDITIONS

Many new species were described from the material gathered during the expeditions. However, as is often the case, most forms described as new eventually turned out to have been previously described under another name. For example, in his monographic treatment of mollusks from the expeditions, Locard (1897–1898) described 163 forms as new, and of those, only 56 are currently credited as valid original descriptions. Likewise, only 7 of the 70 species of bryozoans described as new by Calvet (1906) are currently credited to him. Nonetheless, a large number, at least 176 species descriptions based on expedition material, are still recognized

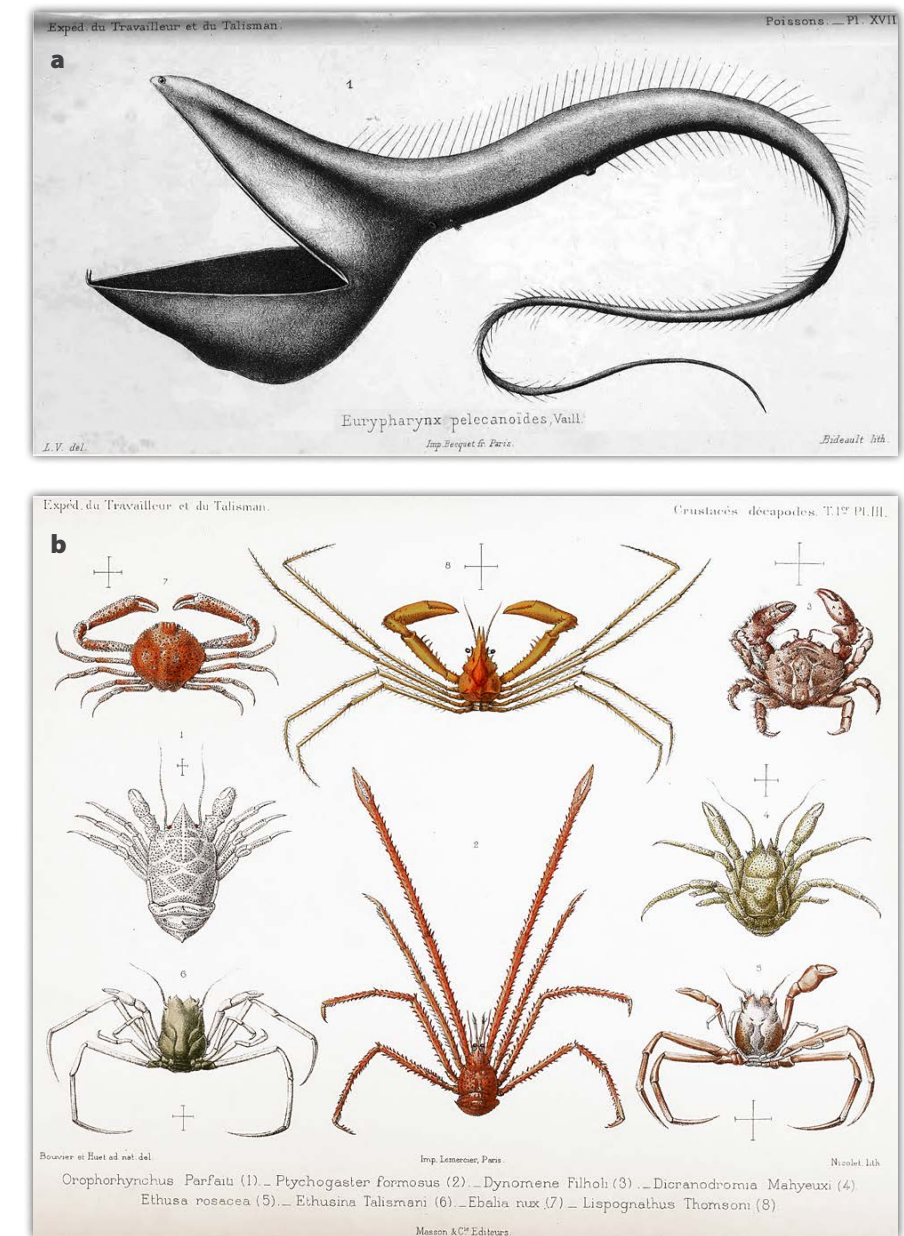


FIGURE 4. The surprising morphologies of deep-sea fauna found during the expeditions. (a) The iconic deep-sea fish, the gulper eel. (b) Deep-sea crustaceans, including a new species named for *Talisman*, *Ethusina talismani*.

as valid. This estimate is conservative as it is not always clear from the descriptions if the specimens used were from the expeditions or from other collections (e.g., Milne Edwards and Bouvier, 1900). Most of the new forms found were benthic macrofauna, shelled mollusks, echinoderms, and crustaceans (Figure 5).

A substantial literature concerning the expeditions themselves, or the material collected, was produced totaling at least 126 works. It is probable that my

searches did not uncover all the publications, but of those found, almost half concern the benthic megafauna, mirroring to a large extent the descriptions of new species (Figure 5). In addition, there were also technical accounts: cruise narratives destined for a professional audience (e.g., geographers) and official cruise accounts (e.g., for the Maritime Ministry). The most cited publications (according to Google Scholar) are those on the taxonomic groups, with many new

species described, again mollusks and crustaceans. Exceptions are well-cited publications that describe bacteria cultured from deep Mediterranean Sea sediment samples collected during the 1881 *Travailleur* expedition and early experiments examining the tolerance of a variety of microbes for high pressure, like that of the deep sea. The papers by Adrian Certes (1884a,b; Certes and Cochin 1884), based on work he carried out in the laboratory of Louis Pasteur, are well recognized as the beginnings of deep-sea microbiology (e.g., Zobell, 1952; Jannasch and Taylor, 1984; Levin and Gooday, 2003; Bartlett,

2008; Adler and Dücker, 2018). Thus, ironically, the scientific results of the expeditions of *Travailleur* and *Talisman* likely are better known to microbiologists than to oceanographers.

POPULARIZATION OF THE DEEP SEA BY EXPEDITION PARTICIPANTS

Just a few months after *Talisman* returned to its homeport of La Rochelle, a large public exhibition was installed in the National Museum of Natural History in Paris: *L'Exposition Sous-Marine du Travailleur et du Talisman* (The Undersea Exhibition

of the *Travailleur* and *Talisman*). Organized by Milne Edwards with other staff of the museum's Laboratory of Zoological Anatomy and Physiology, the exhibition was opened with great ceremony by the Minister of Education in the company of a variety of politicians and the captains of both *Travailleur* and *Talisman*, as well as all the museum professors (Anonymous, 1884b). From January to March 1884, the public was invited to admire not only specimens of the odd fauna found but also to examine for themselves some of the instruments and equipment used to explore the deep sea (Figure 6). The exhibit was enormously successful, described as drawing crowds not previously seen at the museum (Lacroix, 1926). The exhibition appears to be one of the earliest efforts of outreach in oceanography.

In addition to the exhibition, the expedition participants also wrote books, aimed at general audiences, about the deep sea in general and the expeditions in particular. The first and most spectacular to appear, as it included four color plates (e.g., Figure 7), was by Henry Filhol in 1885, *La Vie au Fonds Des Mer: Les explorations sous-marines et les voyages du Travailleur et du Talisman* (Life at the bottom of the sea: The under-sea explorations and voyages of the *Travailleur*

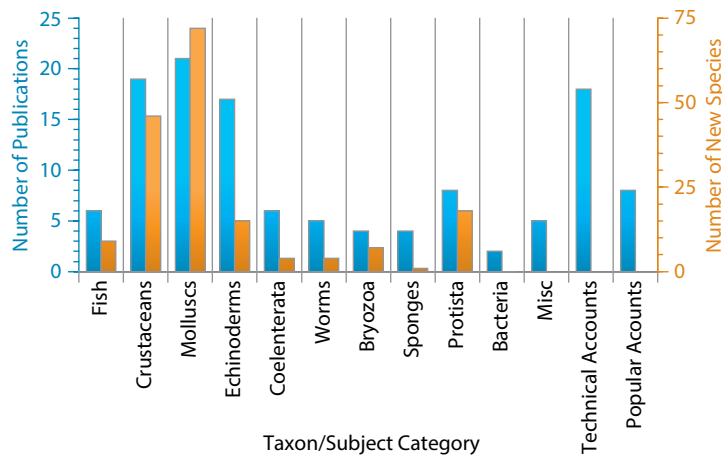


FIGURE 5. Numbers of new species described from expedition material pooled into large taxonomic groups and numbers of expedition publications pooled by subject.

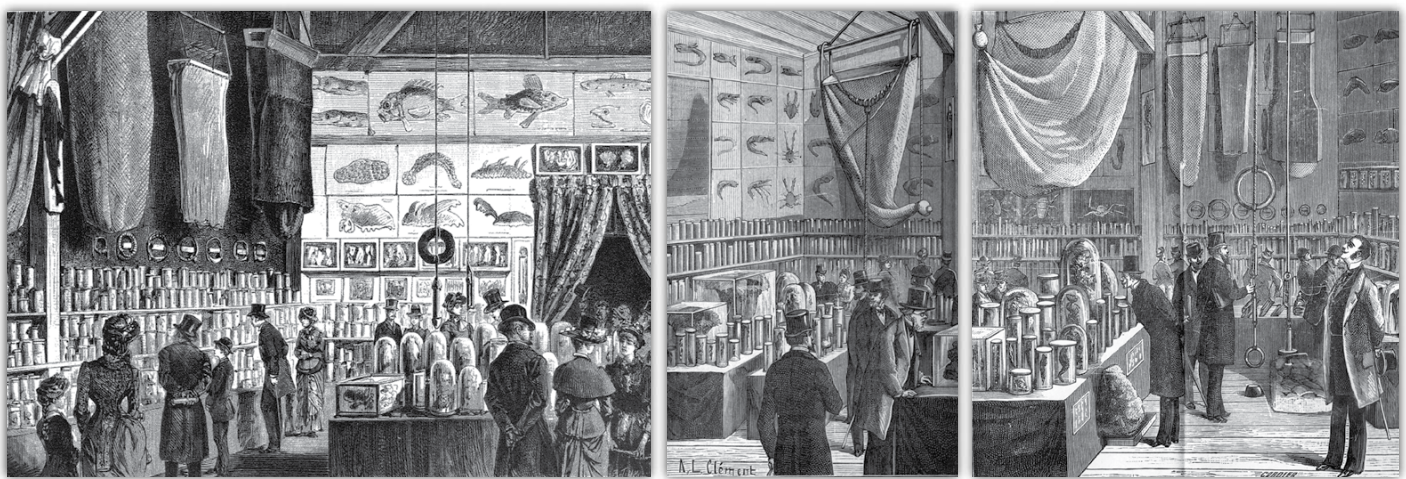


FIGURE 6. Illustrations show scenes of *L'Exposition Sous-Marine du Travailleur et du Talisman*, which ran at the National Museum of Natural History (Paris) from January 26 to March 16, 1884. The exhibition included specimens and illustrations of deep-sea fauna as well as, importantly, the equipment and instruments used in oceanographic studies. Thus, the exhibit displayed not only the deep-sea creatures found but also how the creatures were found. Illustrations from Filhol, 1884, and Dollo, 1891

and of the *Talisman*). Henry Filhol would later hold the Chair of Comparative Anatomy at the Museum of Natural History and be elected to the French Academy of Sciences.

The second book, by Edmond Perrier, subsequently to become the director of the National Museum of Natural History, was published a year later, in 1886. From its title, *Les Explorations Sous-Marin* (Undersea Explorations), the book was clearly not focused exclusively on the *Travailleur* and *Talisman* expeditions nor on the deep sea. But, as noted in the preface, Perrier relied considerably on the expeditions' results and the contributions of other cruise participants, including both Folin and Filhol. Second and third editions were published in 1891 and 1899 (Perrier, 1891, 1899). The third popular book appeared in 1887: *Sous les Mers: Campagnes d'explorations du Travailleur et du Talisman* (Under the Sea: The campaigns of exploration of the *Travailleur* and of the *Talisman*) by the instigator of the expeditions, Léopold Folin. By then age 70, Folin dedicated the book to his grandson "hoping he also will be interested in the study of the sea" (Folin, 1887). The fact that these books appeared in such quick succession (i.e., 1885, 1886, 1887, 1891, and 1899) suggests that the publishers found a solid market for popular books on the deep sea.

NEGLECT OF THE EXPEDITIONS DUE TO THE SLOW DEVELOPMENT OF OCEANOGRAPHY IN FRANCE?

The *Travailleur* and *Talisman* expeditions were scientific and public relations successes, an auspicious beginning to oceanography in France. However, with the singular exception of Saldanha (2002), in accounts of the history of oceanography, they are either mentioned only in passing (e.g., Deacon, 1971; Menzies et al., 1973) or neglected (e.g., Wüst, 1964; Sears and Merriman, 1980) as pointed out by Mills (1983). This is likely due, at least in part, to the fact that the expeditions were not followed by sustained

development of oceanography in France. This was largely true until the 1960s. This is not to say that there were no French oceanographic expeditions; there were, for example, the early twentieth century voyages of Jean-Baptist Charcot to the Arctic and Antarctic, but they were conducted without the direct support of governmental agencies (Laubier, 1992). Meanwhile in other countries, such as the United States, Germany, and the United Kingdom, oceanography grew

rapidly in the first half of the twentieth century with the establishment by the 1930s of oceanographic institutions and graduate programs in oceanography (Vaughn, 1937). Admittedly, assessing why oceanography failed to develop similarly in France is largely speculation. Nonetheless, a few non-exclusive explanations can be offered.

One factor may have been a lack of scientists of stature advocating for oceanography. The instigators of the expedi-



FIGURE 7. Plate 2 of *La Vie au Fonds des Mer: Les explorations sous-marines et les voyages du Travailleur et du Talisman* (Life at the bottom of the sea: The undersea explorations and voyages of the *Travailleur* and of the *Talisman*; Filhol, 1885) depicts organisms from depths between 1,000 m and 1,500 m.

tions, Folin and Milne Edwards, both died by 1900. Although the other scientists involved eventually acquired considerable stature, they were classic zoologists working on a variety of taxa and not focused on studies of the sea. There were no French personalities comparable to John Murray in the United Kingdom, Alexander Agassiz in the United States, Johan Schmidt in Denmark, or Victor Hensen in Germany. Another possible factor is that the oceanographic institute created by the Prince of Monaco in Paris, along with his voyages (which furnished specimens for researchers in France), reduced impetus and need for the establishment of a French oceanographic institution. Ironically, the Prince of Monaco is said to have been greatly inspired to create the Musée Océanographique in Monaco by the *Travailleur* and *Talisman* exhibition at the National Museum of Natural History (Carpine-Lancre, 2001). The Institute Océanographique in Paris employed some research staff, and classes were given, but it did not confer diplomas.

Another aspect is that marine science in France was, by the early 1900s, overwhelmingly dominated by marine biologists working on littoral habitats in a large number of marine stations, part of what Antony Adler (2019) termed “The Marine Station Movement.” Charles Kofoid’s 1910 book, *The Biological Stations of Europe*, listed 14 marine stations in France (excluding fisheries laboratories) compared to eight in the United Kingdom and only three in Germany. Thus, in France, there was a relatively large population of shore-based biologists perhaps nearly monopolizing available resources. Eric Mills (2009) discussed “the failure of French oceanography” and pointed out that for a variety of reasons, French physical oceanographers in the early 1900s were few in number and appear to have been isolated from scientific currents in other countries. Regardless of the reasons, oceanography, although today quite strong, was undeniably slow to develop in France.

The first French vessel specifically

built for deepwater oceanographic work was *Président Théodore Tissier* in 1933 (Le Danois, 1948), but by 1938 it was transferred to the merchant marine for use as a training vessel. In the Cold War era, the strong ties of ocean scientists with the navy that characterized the development of oceanography in the United States (i.e., the Office of Naval Research) apparently did not exist in France. It was not until 1968 that another deepwater oceanographic vessel, *Jean Charcot*, was launched; the vessel was described as “designed with the ambition of allowing our country to recover its place among the leading nations of oceanography” (Laubier, 1985). Some of the first oceanographic campaigns of both *Président Théodore Tissier* and *Jean Charcot* were dedicated to sampling the benthos of the Bay of Biscay (Le Danois, 1948; Laubier, 1985) as was the first expedition of *Travailleur*. Although courses in ocean sciences were offered in the universities, degree programs were not created in France until the late 1960s, at about the same time that the national science organization, the Centre National de la Recherche Scientifique (the largest employer of research scientists in France), formally recognized oceanography as a distinct scientific discipline (Geistdoerfer, 2015).

CONCLUSION

On the heels of the *Challenger* Expedition, the early French deep-sea explorations of *Travailleur* and *Talisman*, while not of the same magnitude as the *Challenger* Expedition, uncovered a large number of novel organisms, including the first deep-sea bacteria and the ever-popular gulper eel (e.g., https://www.youtube.com/watch?v=iT_EMK12A3Y). The scientists involved in the explorations produced not only a considerable number of scientific publications, many still cited today, but also a museum exhibition, articles in the popular press, and several general audience books, all on the deep sea. Despite their scientific and popular successes, the *Travailleur* and *Talisman* voy-

ages are rarely remembered. I hope that, with the story told here of the remarkable expeditions of Léopold Folin and Alphonse Milne Edwards, they will perhaps be less neglected. 

SUPPLEMENTARY MATERIALS

A file containing lists of publications from the expeditions and of species described from expedition material, currently recognized as valid first descriptions, is available online at <https://doi.org/10.5670/oceanog.2020.202>.

REFERENCES

- Adler, A. 2019. *Neptune’s Laboratory: Fantasy, Fear, and Science at Sea*. Harvard University Press, Cambridge MA, 241 pp.
- Adler, A., and E. Dücker. 2018. When Pasteurian science went to sea: The birth of marine microbiology. *Journal of the History of Biology* 51:107–138, <https://doi.org/10.1007/s10739-017-9477-8>.
- Anonymous. 1880–1890. *Cahiers d’enseignement illustrés. no 4: Explorations sous-marines du Travailleur et du Talisman*. L. Basset, Paris, 16 pp.
- Anonymous. 1884a. The deep-sea dredging apparatus of the *Talisman*; The deep-sea fishes collected by the *Talisman*; The deep-sea crustacea dredged by the *Talisman*; The echinoderms dredged by the *Talisman*. *Science*, 3:448–455; 3:623–628; 3:713–716; 4:102–105.
- Anonymous. 1884b. Un monde sous-marin. *Le Temps*, number 8314, February 1, 1884, p. 2.
- Bartlett, D.H. 2008. Introduction to deep-sea microbiology. Pp 195–201 in *High Pressure Microbiology*. C. Michaels, D.H. Bartlett, and A. Aertsen, eds, American Society for Microbiology, Washington, DC.
- Brady, G.S. 1880. Report on the Ostracoda dredged by H.M.S. *Challenger* during the years 1873–1876. Pp. 1–184 in *Report on the Scientific Results of the Voyage of H.M.S. Challenger*. *Zoology*, Volume 1.
- Calvet, L. 1906. Bryozoaires. Pp. 355–495 in *Expéditions scientifiques du ‘Travailleur’ et du ‘Talisman’ pendant les années 1880, 1881, 1882, 1883*, vol. 7.
- Carpenter, W.B. 1868. Preliminary report of dredging operations in the seas to the North of the British Islands, carried on in Her Majesty’s Steam-vessel *Lightning* by Dr. Carpenter and Dr. Wyville Thomson. *Proceedings of the Royal Society of London* 17:168–200, <https://doi.org/10.1098/rspl.1868.0026>.
- Carpenter, W.B., J.G. Jeffreys, and C.T.W. Thomson. 1870. Preliminary report of the scientific exploration of the deep sea in HM surveying-vessel *Porcupine*, during the summer of 1869. *Proceedings of the Royal Society of London* 18:397–492, <https://doi.org/10.1098/rspl.1869.0084>.
- Carpine-Lancre, J. 2001. Oceanographic sovereigns: Prince Albert I of Monaco and King Carlos I of Portugal. Pp. 56–68 in *Understanding the Oceans*. M. Deaco, T. Rice, and C. Summerhayes, eds, UCL Press, London.
- Certes, A. 1884a. Sur la culture, à l’abri des germes atmosphériques, des eaux et des sédiments rapportés par les expéditions du *Travailleur* et du *Talisman*. *Comptes Rendue Hebdomadaire des Séances de l’Académie des Sciences* 98:690–693.
- Certes, A. 1884b. Note relative à l’action des hautes pressions sur la vitalité des microorganismes d’eau douce et d’eau de mer. *Comptes Rendue Hebdomadaire des Séances de l’Académie des Sciences* 99:385–388.

- Certes, A., and D. Cochin. 1884. Action des hautes pressions sur la vitalité de la levure et sur les phénomènes de la fermentation. *Comptes Rendue Hebdomadaires des Séances et Mémoires de la Société de Biologie, Série 8*, n° 36:639–640.
- Deacon, M. 1971. *Scientists and the Sea 1650–1900: A Study of Marine Science*. Aberdeen University Press, Aberdeen, UK, 445 pp.
- Dollo, L. 1891. *La Vie au Sein des Mers: La faune marine et les grandes profondeurs, les grandes explorations sous marin, les conditions d'existence dans l'abysses, la faune abyssale*. Librairie J.-B. Baillière et Fils, Paris, 300 pp.
- Filhol, H. 1884. Explorations sous-marines, Voyage du "Talisman". *La Nature*, Year 12, 119–122, 134–138, 147–151, 161–164, 182–186, 198–202, 230–234, 278–282, 391–394.
- Filhol, H. 1885. *La vie au fonds des mers: les explorations sous-marine et les voyages due "Travailleur" et du "Talisman."* Paris, Masson, 301 pp.
- Folin, L. 1886. Appendix B. Report on the Caecidae collected by H.M.S. *Challenger* during the years 1873–76. In *Report on the Scientific Results of the Voyage of H.M.S. Challenger During the Years 1873–1876*. *Zoology* 15:681–689.
- Folin, L. 1887. *Sous les mers Campagnes d'explorations du "Travailleur" et du "Talisman."* Librairie J.-B. Baillière et Fils, Paris, 340 pp.
- Folin, L., G.S. Brady, and A. Milne-Edwards. 1869. La rade de Saint-Vincent du Cap-Vert (supplément). *Les Fonds de la Mer* 1:136–146.
- Forbes, E. 1844. Report on the Mollusca and Radiata of the Aegean Sea, and on their distribution, considered as bearing on Geology. Pp. 130–193 in *Report of the Thirteenth Meeting of the British Association for the Advancement of Science, Cork, August 1883*.
- Forbes, E., and R. Godwin-Austen. 1859. *The Natural History of the European Seas*. John Van Voorst, London, 306 pp.
- Geistdoerfer, P. 2015. *Histoire de l'océanographie: De la surface aux abysses*. Nouveau Monde Editions, Paris, 235 pp.
- Jannasch, H.W., and C.D. Taylor. 1984. Deep-sea microbiology. *Annual Review of Microbiology* 38:487–514, <https://doi.org/10.1146/annurev.mi.38.100184.002415>.
- Jeffreys, J.G. 1880. The deep-sea Mollusca of the Bay of Biscay. *The Annals and Magazine of Natural History* 6:315–319.
- Jeffreys, J.G. 1884. The French deep-sea expedition of 1883. *Nature* 29:216–217, <https://doi.org/10.1038/029216b0>.
- Kofoed, C.A. 1910. *The Biological Stations of Europe*. United States Bureau of Education, Bulletin No. 4, Whole Number 400. Government Printing Office, Washington, DC, 360 pp.
- Laubier, L. 1985. Le program Biogas. Pp. 13–24 in *Peuplements Profonds du Golfe de Gascogne*. L. Laubier and C. Monniot, eds, Ifremer, Paris, 629 pp.
- Laubier, L. 1992. *Vingt mille vies sous la mer*. Editions Odile Jacob, Paris, 332 pp.
- Lacroix, A. 1926. Notice historique sur Alphonse Milne Edwards. *Mémoires de l'Académie des Sciences de l'Institut de France* 58:LXXIV.
- Le Danois, E. 1948. *Les Profondeurs de la Mer: Trente ans de recherches sur la faune sou-marine au large des côtes de France*. Payot, Paris, 303 pp.
- Levin, L.A., and A. Gooday. 2003. The deep Atlantic Ocean. Pp 111–178 in *Ecosystems of the Deep Oceans*. P.A. Tyler, ed., Elsevier, Amsterdam.
- Locard, A. 1897–1898. Mollusques testacés. *Expéditions scientifiques du Travailleur et du Talisman pendant les Années 1880, 1881, 1882, et 1883*, Masson. vol. 1 [1897], p. 1–516; vol. 2 [1898], p. 1–515.
- Menzies, R.J., R.Y. George, and G.T. Rowe. 1973. *Abyssal Environment and Ecology of the World Oceans*. John Wiley & Sons, New York, 488 pp.
- Mills, E.L. 1983. Problems of deep-sea biology: An historical perspective. Pp 1–79 in *The Sea*. G.T. Rowe, ed., John Wiley & Sons, San Francisco.
- Mills, E.L. 2009. *The Fluid Envelope of Our Planet: How the Study of Currents Became a Science*. University of Toronto Press, Toronto, 433 pp.
- Milne Edwards, A. 1861. Observations sur l'existence de divers mollusques et zoophyes à de très grandes profondeurs dans la Mer Méditerranée. *Annales des Sciences Naturelles, Serie 4, Zoologie* 15:149–157.
- Milne Edwards, A. 1881. Rapport sur les travaux de la commission chargé par M. le Ministre de l'Instruction Publique d'étudier la faune sous-marine dans les grandes profeneurs du Golfe de Gascogne. *Archives des Missions Scientifiques et Littéraires* 7:421–431.
- Milne-Edwards, A. 1882. Les explorations sous-marines du *Travailleur* dans l'Océan Atlantique et dans la Méditerranée en 1880 et 1881. *Bulletin de la Société de Géographie* 3:93–130.
- Milne Edwards, A., and Bouvier, E.L. 1900. *Heterocarpus grimaldii*, espèce nouvelle recueillie par le "Talisman," "l'Hirondelle" et la "Princesse Alice." *Bulletin de la Société Zoologique de France* 25:58.
- Norman, A.M. 1880. Notes on the French explorations of "Le Travailleur" in the Bay of Biscay. *Annals and Magazine of Natural History* 36:430–436.
- Perrier, E. 1886. *Les Explorations Sous-Marines*. Hachette, Paris, 352 pp.
- Perrier, E. 1891. *Les Explorations Sous-Marines*, 2nd ed. Paris, Hachette, 352 pp.
- Perrier, E. 1899. *Les Explorations Sous-Marines*, 3rd ed. Paris, Hachette, 352 pp.
- Rice, A.L., H.L. Burstyn, and A.G.E. Jones. 1976. G.C. Wallich M.D. – megalomaniac or mis-used oceanographic genius? *Journal of the Society for the Bibliography of Natural History* 7:423–450, <https://doi.org/10.3366/jbnh.1976.7.4.423>.
- Saldanha, L. 2002. The discovery of the deep-sea Atlantic fauna. Pp. 235–247 in *Oceanographic History: The Pacific and Beyond*. K.R. Benson and P.F. Rehbock, eds, University of Washington Press, Seattle.
- Sears, M., and D. Merriman, eds. 1980. *Oceanography: The Past*. Springer-Verlag, New York, 812 pp.
- Thomson, C.W. 1873. *The Depths of the Sea: An Account of the General Results of the Dredging Cruises of H.M.S.S. Porcupine and Lightning During the Summer of 1868, 1869, and 1870, Under the Scientific Direction of Dr. Carpenter, F.R.S., J. Gwyn Jeffreys, F.R.S., and Dr. Wyville Thomson, F.R.S.* Macmillan, London, 527 pp.
- Thomson, C.W. 1878. *The Voyage of the Challenger: The Atlantic: A preliminary Account of the General Results of The Exploring Voyage of H.M.S. Challenger During the Year 1873 and the Early Part of the Year 1876*. Harper, New York, vol. 1, 391 pp., vol. 2, 340 pp.
- Vaughan, T.W. 1937. *International Aspects of Oceanography*. Oceanographic Data and Provisions for Oceanographic Research. National Academy of Sciences, Washington, DC, 225 pp.
- Wallich, G.C. 1860. *Notes on the Presence of Animal Life at Vast Depths in the Sea; With Observations on the Nature of the Sea Bed, as Bearing on Submarine Telegraphy*. Taylor and Francis, London, 38 pp.
- Wüst, G. 1964. The major deep-sea expeditions and research vessels 1873–1960: A contribution to the history of oceanography. *Progress in Oceanography* 2:1–52, [https://doi.org/10.1016/0079-6611\(64\)90002-3](https://doi.org/10.1016/0079-6611(64)90002-3).
- Zobell, C.E. 1952. Bacterial life at the bottom of the Philippine Trench. *Science* 115:507–508, <https://doi.org/10.1126/science.115.2993.507>.

ACKNOWLEDGMENTS

I am grateful to the editor for her patience. The remarks of Antony Adler, Robert Carney, Eric Mills, an anonymous reviewer, but most especially Tony Rice, on previous versions led to great improvements in the manuscript. However, I retain full responsibility for all errors of fact and interpretation.

AUTHOR

John R. Dolan (dolan@obs-vlfr.fr) is a research scientist at the Laboratoire d'Océanographie de Villefranche-sur-Mer, Sorbonne Université CNRS UMR 7093, Villefranche-sur-Mer, France.

ARTICLE CITATION

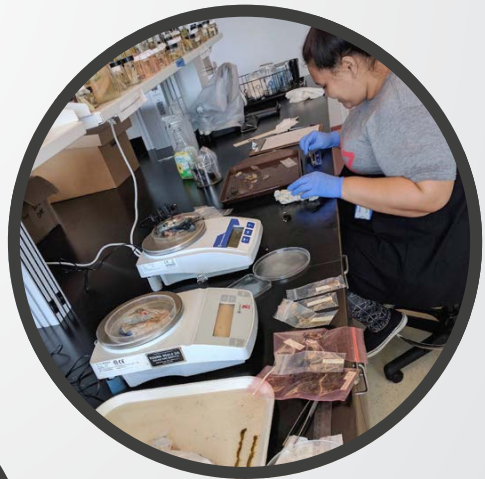
Dolan, J.R. 2020. The origins of oceanography in France: The scientific expeditions of *Travailleur* and *Talisman* (1880–1883). *Oceanography* 33(2):126–133, <https://doi.org/10.5670/oceanog.2020.202>.

COPYRIGHT & USAGE

This is an open access article made available under the terms of the Creative Commons Attribution 4.0 International License (<https://creativecommons.org/licenses/by/4.0/>), which permits use, sharing, adaptation, distribution, and reproduction in any medium or format as long as users cite the materials appropriately, provide a link to the Creative Commons license, and indicate the changes that were made to the original content.

How Do Advisor Assessments of Diverse Undergraduate Researchers Compare with the Students' Self-Assessments? And What Does This Imply for How We Train and Assess Students?

By Barbara C. Bruno, Cherryle Heu, and Grady Weyenberg



ABSTRACT. This study involves survey data collected from 30 diverse undergraduates and their research advisors in oceanography and related fields who participated in the SOEST Scholars Program at the University of Hawai'i in 2016–17 and 2017–18. At the end of the research experience, students and their advisors each complete online surveys to evaluate student performance and growth over the course of the program on a scale of 1 (low) to 5 (high). The results indicate that, on average, (1) the students (4.06) underrate their performance relative to their advisors' assessments (4.24), a difference ($D = 0.18$) that is highly significant ($p = 0.005$), and (2) there is no statistically significant difference between student and advisor assessments of student growth ($p = 0.25$). Further analysis by student demographics reveals distinct differences by gender and ethnicity. In particular, women of Native Hawaiian and Pacific Islander ancestry showed the greatest ($D = 0.36$) and most significant ($p = 0.02$) underrating of their own performances relative to their advisors' assessments. In contrast, the mean student-advisor differences obtained for men and non-indigenous students were statistically insignificant ($p = 0.31$ and 0.18 , respectively). This paper explores various possible interpretations of these results and their implications for how we train and assess students, and it includes recommendations for undergraduate research programs in oceanography. Specifically, we recommend intentionally focusing on building student self-efficacy alongside technical training, designing evaluation instruments that avoid the use of self-promoting language, and scheduling—or at least revisiting—discussions on STEM pathways and careers toward the end of the undergraduate research experience.

INTRODUCTION

The SOEST Scholars program is an undergraduate research program at the School of Ocean and Earth Science and Technology (SOEST) at the University of Hawai'i (UH) that runs throughout the academic year. Like many undergraduate research programs, it includes closely mentored research experiences, professional development training, and cohort-building activities. Originally developed by the Center for Microbial Oceanography: Research and Education (C-MORE) to train students in biological oceanography, the program later evolved into the SOEST Scholars Program in 2016 and now spans a wider variety of disciplines, including chemical and physical oceanography, Earth science, and environmental science.

There is a continuing lack of diversity

in the field of oceanography. Although the number of PhDs awarded in oceanography has risen sharply in the last decade, those awarded to ethnic and racial minorities have remained stagnant (Bernard and Cooperdock, 2018). Thus, one of our key program goals is to broaden participation among students from groups that have been traditionally underrepresented in STEM, including women, indigenous students, and other ethnic and racial minorities. Toward this goal, we established recruiting partnerships with various Native Hawaiian and minority-serving organizations, including community colleges, and this has led to a diverse cohort of undergraduate SOEST Scholars. However, for these students to persist on a STEM pathway and ultimately diversify the field of oceanography, developing research and other

technical skills is not enough: they also need to develop self-efficacy.

Self-efficacy (a person's belief that they can accomplish a given task or achieve a desired outcome) has been shown to be a key factor in successful academic performance that can help motivate students to persist in the face of adversity (Bandura, 1977; Multon et al., 1991; Zimmerman, 2000), including in the ocean and Earth sciences (Kortz et al., 2019) and across STEM fields (Andrew, 1998; Williams and George-Jackson, 2014). In some studies (Zusho et al., 2003), self-efficacy predicted student performance and persistence better than other cognitive variables, even when controlling for prior achievement (Lent et al., 1986). Studies of indigenous students have similarly shown significant, positive relationships between self-efficacy and academic success (Bryan, 2004; Frawley et al., 2017) and between self-efficacy and persistence (Gloria and Robinson Kurpius, 2001).

The motivation of this study is to see how student self-evaluations of their own skills and performances compare with their advisors' evaluations. This analysis could potentially shed light on student self-efficacy. Further, this paper explores any potential differences between student vs. advisor assessments through a demographic lens, as prior research studies indicate that students from underrepresented groups—such as women (Hackett, 1985; Falk et al., 2016), Native Americans (Brown and Lavish, 2016), and other underrepresented minorities (Carpi et al., 2017)—tend to report lower self-efficacy. Thus, these results can inform how we train diverse undergraduate researchers in oceanography.

DATA AND METHODS

Survey data were collected from 30 diverse undergraduates and their research advisors who participated in the SOEST Scholars Program in 2016–17 and 2017–18 (response rate of 83%). **Figure 1** summarizes student demographics.

We collected two types of survey data, which we term “Absolute” and “Growth.” In the Absolute set, students and advisors evaluate the students’ skills and performances at the end of the research experience in 10 areas (e.g., amount of work accomplished, quality of work performed) along a five-point Likert scale ranging from Unsatisfactory to Excellent. In the Growth set, students and advisors evaluate the extent to which the students changed or grew over the course of the research experience in nine areas (e.g., works more

independently, takes more initiative to problem-solve) along a five-point Likert scale ranging from Strongly Disagree to Strongly Agree. (**Table 1**)

Our null hypothesis is that there is no statistically significant difference between student vs. advisor assessments of students’ skills and performances, as measured by Absolute and Growth survey items. We test this hypothesis in two ways: (1) comparing the student vs. advisor responses to each individual survey item, and (2) comparing the student vs. advisor responses to each data set (Absolute and Growth) as a whole. For the former analysis, we perform a paired, two-tailed t-test. For the latter, we apply a non-parametric permutation test.

We then examined any differences in student-advisor ratings by gender, ethnicity, and the intersectionality of these

identities. This analysis was motivated by previous studies that found that women and certain minority groups—and particularly students at the intersection of those identities—often report lower self-efficacy (see Introduction). For gender, we compared men vs. women, as none of the students reported a non-binary gender. For ethnicity, we compared Native Hawaiians and Pacific Islanders (NHPI) vs. non-indigenous students (non-NHPI); this choice was determined by the data set rather than a priori, as 50% of our students were NHPI. For the intersectionality analysis, we compared four categories: NHPI women, NHPI men, non-NHPI women, and non-NHPI men.

Further details on data and methods are provided in the online supplementary materials.

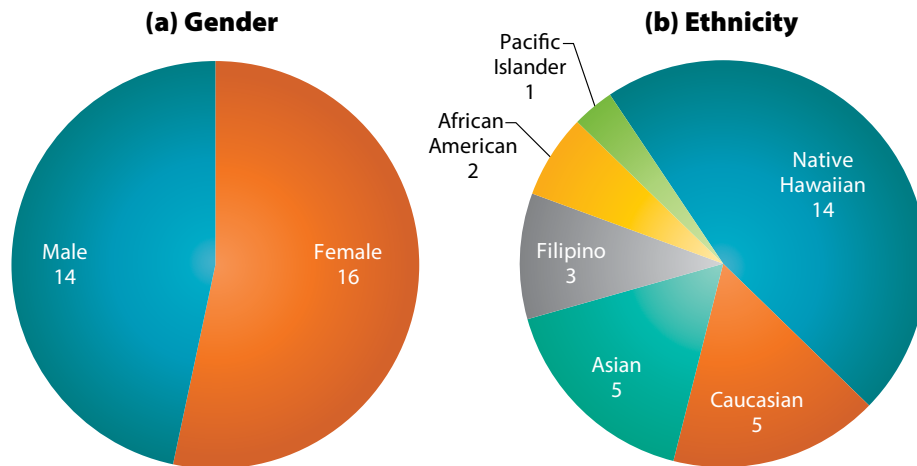


FIGURE 1. Gender and ethnicity demographics of 30 SOEST Scholars involved in the study described here. Half (15) are Native Hawaiians and Pacific Islanders (NHPI); the other half represent a range of non-indigenous identities.

TABLE 1. Quantification of Likert responses to Absolute and Growth survey items on a scale of 1 to 5.

LIKERT SCALE RESPONSES					
	1	2	3	4	5
ABSOLUTE SURVEY ITEMS	Unsatisfactory	Fair	Satisfactory	Very Good	Excellent
GROWTH SURVEY ITEMS	Strongly Disagree	Disagree	Not Sure	Agree	Strongly Agree

RESULTS

Absolute Results (All Students and Advisors)

As a group, the 30 SOEST Scholars consistently underrated their Absolute skills and performances relative to their advisors' ratings (Table 2 and Figure 2). For eight of 10 survey items, D values were positive, ranging from 0.03 to 0.40, indicating that the students' mean self-ratings were lower than the advisors' mean ratings. The remaining two items yielded $D = 0$ and $D = -0.03$, respectively indi-

cating that the mean student self-rating was identical or very slightly higher than the mean advisor rating. T-test results for each survey item indicate that most of these student-advisor differences were not statistically significant (defined as $p < 0.05$): the only survey items found to have significant student-advisor differences were *Quality of work performed* (Absolute Item 2) and *Organizing tasks in an efficient manner* (Absolute Item 4).

These data raise the question: Even though the advisor-student differences

(D) for individual Absolute survey items are generally not statistically significant, does the general pattern of positive D values indicate that the students are statistically significantly underrating themselves relative to their advisors' assessments on Absolute survey items as a whole? To answer this question, we performed a permutation test, and the answer is a resounding yes. We found $p = 0.005$, indicating that the advisor-student differences are highly significant (Figure 3 and last row of Table 2).

TABLE 2. Comparison of advisor vs. student responses to 10 Absolute survey items assessing student skills and performances at the end of the undergraduate research experience.

ABSOLUTE SURVEY ITEMS	S	S SEM	A	A SEM	D	p
1. Amount of work accomplished	3.87	0.13	4.07	0.17	0.20	0.28
2. Quality of work performed	3.93	0.13	4.33	0.14	0.40	0.04
3. Self-motivation & willingness to take initiative	4.30	0.15	4.33	0.17	0.03	0.87
4. Organizing tasks in an efficient manner	3.87	0.11	4.23	0.19	0.37	0.05
5. Verbal and written communication skills	3.63	0.13	3.93	0.16	0.30	0.12
6. Behaving in a professional manner	4.30	0.13	4.43	0.15	0.13	0.40
7. Working as a member of a research team	4.40	0.12	4.40	0.14	0.00	1.00
8. Working independently as appropriate	4.23	0.16	4.20	0.18	-0.03	0.89
9. Analyzing my performance & trying to improve	4.03	0.15	4.10	0.16	0.07	0.75
10. Maintaining research hours and schedule	4.07	0.17	4.33	0.18	0.27	0.17
All Absolute Survey Items	4.06	0.05	4.24	0.05	0.18	0.005

S = Mean student self-assessment.
S SEM = Standard Error of S.
A = Mean advisor assessment.
A SEM = Standard Error of A.

$D = A - S$.
p = Probability value. For individual survey items, p is calculated from a two-tailed, paired t-test. For all Absolute survey items combined, p is calculated empirically from a permutation test.

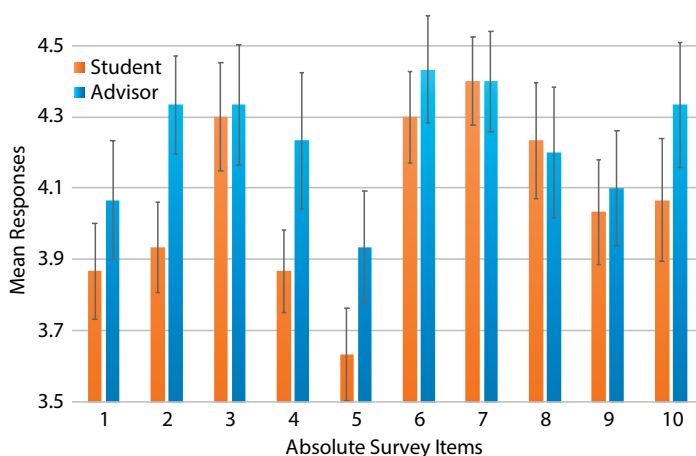


FIGURE 2. Histogram of student (orange) vs. advisor (blue) responses to Absolute survey items. Error bars represent ± 1 one standard error of the mean. In eight of 10 survey items, the advisors rate the students more highly than the students rate themselves; however, most of these differences are not statistically significant.

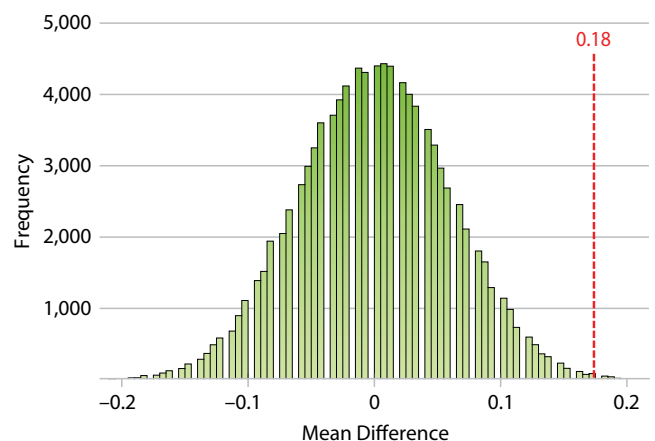


FIGURE 3. Distribution of permutation test results for the Absolute data set (10 survey items combined), showing highly significant student-advisor differences (observed mean difference = 0.18; $p = 0.005$).

Growth Results (All Students and Advisors)

In contrast to the Absolute survey items, there is no systematic pattern of students' underrating their Growth over the course of the research experience relative to their advisors' ratings, let alone a statistically significant one (Table 3 and Figure 4). In fact, for six of the nine Growth items, students self-ranked their Growth higher than did their advisors ($D < 0$). Applying a paired, two-tailed t-test to each Growth survey item, none of these differences were statistically significant at $\alpha = 0.05$ and only

two $p < 0.10$ (p ranged from 0.06 to 0.75).

The two greatest—and most statistically significant—disparities between student vs. advisor mean ratings (both $D < 0$) pertained to the two survey items that concerned students' future plans: Growth Item 5. *Compared to before I started the program, I now am more interested in attending graduate school* ($D = -0.30$; $p = 0.06$). Growth Item 9. *Compared to before I started the program, I now am more interested in pursuing a STEM career* ($D = -0.37$; $p = 0.08$). For both survey items, the students, on aver-

age, self-reported greater Growth during the course of the undergraduate research experience than did their advisors, resulting in $D < 0$.

Performing a permutation test on the complete Growth data set (all nine survey items combined) yielded $p = 0.25$. That is, 25% of the 100,000 permutations were tailward of the observed mean difference (-0.07 ; Figure 5). The low significance of this p -value is unsurprising, given the lack of systemic differences between the student vs. advisor responses to the Growth survey items (Figure 4).

TABLE 3. Comparison of advisor vs. student responses to nine Growth survey items assessing growth during the undergraduate research experience. On the student survey, all Growth items begin with the phrase: "Compared to before I started the Scholars Program, I now..." On the advisor survey, the wording is "Compared to when s/he started the Scholars Program, the student now..."

GROWTH SURVEY ITEMS	S	S SEM	A	A SEM	D	p
1 Work more independently	3.93	0.17	4.07	0.15	0.13	0.51
2 Take more initiative to problem-solve	4.13	0.16	4.07	0.15	-0.07	0.75
3 Am more confident about my STEM abilities	4.17	0.10	4.30	0.15	0.13	0.38
4 Have a larger professional network	4.47	0.13	4.33	0.14	-0.13	0.35
5 Am more interested in attending graduate school	4.20	0.15	3.90	0.16	-0.30	0.06
6 Am more excited about STEM	4.13	0.12	4.03	0.14	-0.10	0.40
7 Have a better understanding of how to succeed in school	4.17	0.14	4.13	0.14	-0.03	0.87
8 Have a better understanding of how to conduct research	4.47	0.11	4.60	0.10	0.13	0.35
9 Am more interested in pursuing a STEM career	4.30	0.14	3.93	0.16	-0.37	0.08
All Growth Survey Items	4.22	0.05	4.15	0.05	-0.07	0.25

S = Mean student self-assessment.

S SEM = Standard Error of S.

A = Mean advisor assessment.

A SEM = Standard Error of A.

$D = A - S$.

p = Probability value. For individual survey items, p is calculated from a two-tailed, paired t-test. For all Growth survey items combined, p is calculated empirically from a permutation test.

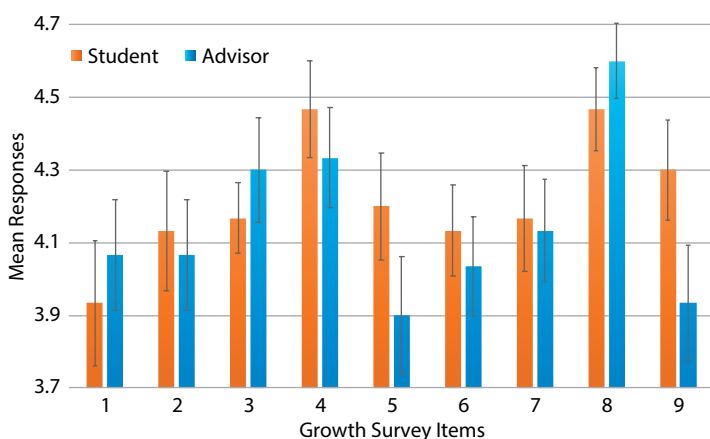


FIGURE 4. Histogram of student (orange) vs. advisor (blue) responses to Growth survey responses. Error bars represent ± 1 one standard error of the mean. In contrast to the Absolute data, in six of nine Growth survey items, the advisors rate student growth lower than the students rate themselves, although these differences are generally not statistically significant.

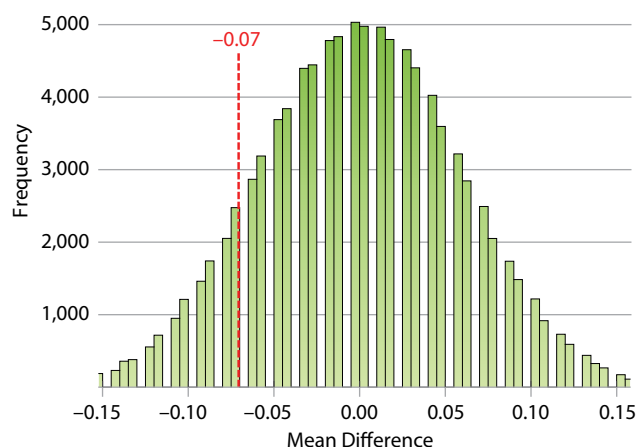


FIGURE 5. Distribution of permutation test results for the Growth data set (nine survey items combined), showing that the observed student-advisor differences are statistically insignificant (observed mean difference = -0.07 ; $p = 0.25$).

Demographic Analyses

Here, we present the results of our demographic analyses by gender (men and women), ethnicity (NHPI and non-NHPI), and the intersection of gender and ethnicity (NHPI women, NHPI men, non-NHPI women, and non-NHPI men). For each analysis, we applied the permutation test methodology described above to the entire sets of Absolute and Growth survey items.

GENDER

We found that both male (3.97) and female (4.14) students' mean responses to Absolute survey items were lower than the corresponding advisors' assessments (4.06 and 4.39, respectively). However, only the female students' self-assessments were significantly less than their advisors' assessments. The difference between ratings given by male students and their advisors on Absolute survey items was smaller in magnitude ($D = 0.09$ male vs. 0.24 female) and much less significant ($p = 0.31$ male vs. 0.01 female) (Table 4a).

For Growth survey items, the male students' mean self-assessments (4.01) were again slightly lower but statistically indistinguishable ($p = 0.69$) from their advisors' assessments (4.05). However, for female students, a different pattern emerged. The female students, as a group, self-rated their Growth more highly (4.41) than did their advisors (4.24), and this difference was reasonably significant ($p = 0.06$) (Table 4b).

Together, the Growth and Absolute permutation analyses indicate that female SOEST Scholars, on average, significantly underrated their skills and performances at the end of a research experience relative to their advisors' assessments, but self-reported more Growth. In contrast, mean differences between male SOEST Scholars self-assessments vs. their advisors' assessments were much smaller and within the range of error (not statistically significant).

ETHNICITY

We found that both NHPI (3.91) and non-NHPI (4.21) students' mean responses to Absolute survey items were lower than the corresponding advisors' assessments (4.15 and 4.32, respectively). However, only the NHPI students' mean self-assessments were significantly less than their advisors' mean assessments ($p = 0.01$). The difference between ratings

given by non-NHPI students and their advisors on Absolute survey items was much less significant ($p = 0.18$) (Table 5a).

For Growth survey items, both NHPI (4.24) and non-NHPI (4.21) students' mean self-assessments were slightly higher but statistically indistinguishable ($p = 0.31$ and 0.60 , respectively) from their advisors' assessments (4.15 and 4.16, respectively) (Table 5b).

TABLE 4. Comparison of advisor vs. student responses to (a) Absolute and (b) Growth survey items by gender (men and women) and ethnicity (NHPI and non-NHPI). No students reported other genders.

CATEGORY	VARIABLE	n	S	S SEM	A	A SEM	D	p
(a) Demographic Analysis of Absolute Survey Items								
Gender	Men	14	3.97	0.06	4.06	0.08	0.09	0.31
	Women	16	4.14	0.07	4.39	0.07	0.24	0.01
Ethnicity	NHPI	15	3.91	0.06	4.15	0.08	0.24	0.01
	Non-NHPI	15	4.21	0.06	4.32	0.06	0.11	0.18
All Data		30	4.06	0.05	4.24	0.05	0.18	0.005
(b) Demographic Analysis of Growth Survey Items								
Gender	Men	14	4.01	0.07	4.05	0.07	0.04	0.69
	Women	16	4.41	0.06	4.24	0.07	-0.17	0.06
Ethnicity	NHPI	15	4.24	0.05	4.15	0.07	-0.09	0.31
	Non-NHPI	15	4.21	0.08	4.16	0.07	-0.05	0.60
All Data		30	4.22	0.05	4.15	0.05	-0.07	0.25

S = Mean student self-assessment.
 S SEM = Standard Error of S.
 A = Mean advisor assessment.
 A SEM = Standard Error of A.

$D = A - S$.
 p = Probability value calculated empirically from permutation test.

TABLE 5. Comparison of advisor vs. student responses to (a) Absolute and (b) Growth survey items by gender (men and women) and ethnicity (NHPI and non-NHPI) through an intersectionality analysis.

	n	S	S SEM	A	A SEM	D	p
(a) Intersectionality Analysis of Absolute Survey Items							
NHPI Women	8	3.80	0.10	4.16	0.11	0.36	0.02
NHPI Men	7	4.04	0.07	4.14	0.12	0.10	0.43
Non-NHPI Women	8	4.49	0.08	4.61	0.07	0.12	0.18
Non-NHPI Men	7	3.90	0.09	3.99	0.10	0.09	0.59
All	30	4.06	0.05	4.24	0.05	0.18	0.005
(b) Intersectionality Analysis of Growth Survey Items							
NHPI Women	8	4.25	0.07	4.18	0.09	-0.07	0.63
NHPI Men	7	4.23	0.07	4.11	0.10	-0.12	0.38
Non-NHPI Women	8	4.57	0.09	4.31	0.10	-0.26	0.04
Non-NHPI Men	7	3.79	0.11	3.98	0.10	0.19	0.13
All	30	4.22	0.05	4.15	0.05	-0.07	0.25

S = Mean student self-assessment.
 S SEM = Standard Error of S.
 A = Mean advisor assessment.
 A SEM = Standard Error of A.

$D = A - S$.
 p = Probability value calculated empirically from permutation test.

Together, these results indicate that NHPI SOEST Scholars, on average, significantly underrate their skills and performances at the end of a research experience relative to their advisors' assessments and report slightly (but not significantly) more Growth. Mean differences between non-NHPI SOEST Scholars vs. their advisors' assessments for both Growth and Absolute survey items were small and not statistically significant.

INTERSECTIONALITY

We explored the interplay between gender and ethnicity through an intersectionality analysis of four subgroups of students: NHPI women, NHPI men, non-NHPI women, and non-NHPI men. Although all subgroups, on average, underrated their Absolute skills relative to their advisors' ratings (all $D > 0$), the magnitude and significance of the mean advisor-student difference varied greatly (Table 5a). NHPI women had the greatest ($D = 0.36$) and most significant ($p = 0.02$) underreporting of their Absolute skills and performances. Conversely, non-NHPI men had the smallest, least significant student-advisor difference ($D = 0.09$, $p = 0.59$). Assessments of Growth during the research experience were mixed, with all students except non-NHPI men self-reporting greater Growth than did their advisors, at greatly varying significant levels (0.04 to 0.63). Non-NHPI women reported the highest Growth ($S = 4.31$), the greatest disparity with their advisors' ratings ($D = -0.26$), and the most significant differences ($p = 0.04$). Non-NHPI men were the only group of students to self-assess their mean Growth during the research experience as lower than did their advisors ($D = 0.19$, $p = 0.13$) (Table 5b).

DISCUSSION AND RECOMMENDATIONS

As a group, the SOEST Scholars significantly underrated their Absolute skills and performances relative to their advisors' assessments ($D = 0.18$; $p = 0.005$). The advisor-student difference was most pronounced among NHPI women ($D = 0.36$; $p = 0.02$). As a group, the students were much more likely to rate themselves "very good" when their advisors rated them as "excellent" (Figure 6)—and this pattern was driven by the responses of NHPI women (Figure 7a) and NHPI men (Figure 7b). In this section, we explore possible interpretations of these results and their implications for training and assessing undergraduate researchers.

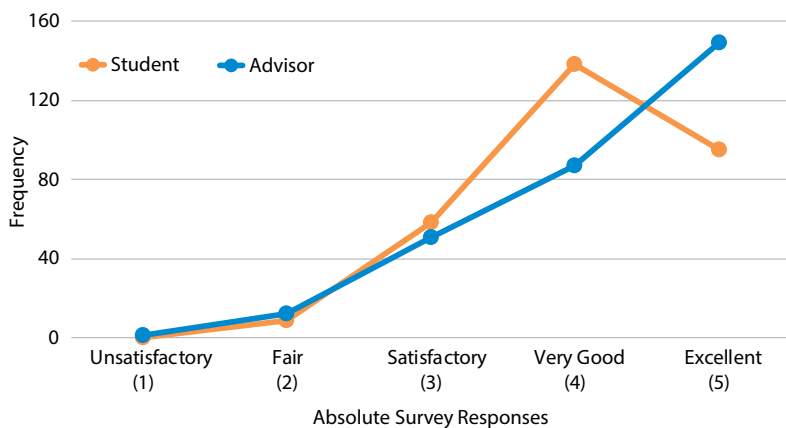


FIGURE 6. Line graph of Absolute survey responses (all students and advisors) showing that students' underrating of their own research performances relative to their advisors' assessments was largely due to students rating themselves "very good" in cases where their advisors rated them "excellent."

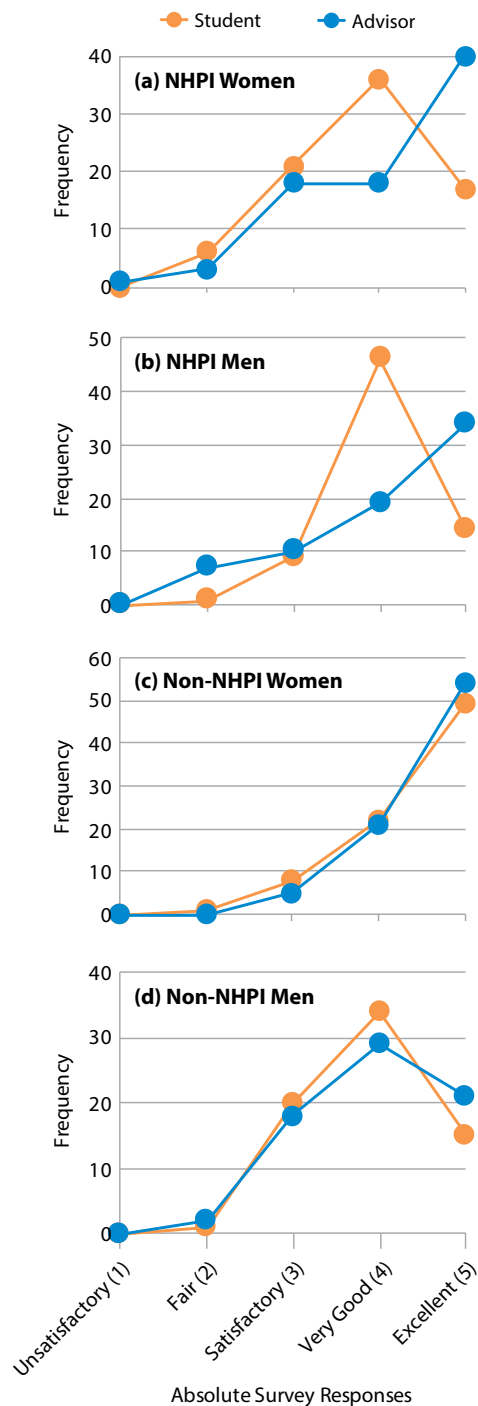


FIGURE 7. Line graphs of Absolute survey responses for (a) NHPI women, (b) NHPI men, (c) non-NHPI women, and (d) non-NHPI men. In many cases, NHPI students rated themselves "very good" in cases where their advisors rated them "excellent." This pattern was not seen among non-NHPI students.

Recommendation 1. Intentionally Focus on Building Student Self-Efficacy

One explanation for mean student Absolute survey responses being lower, on average, than mean advisor ratings could be low student self-efficacy. If true, this would suggest that the SOEST Scholars program, and perhaps undergraduate oceanography research programs in general, could be improved by intentionally focusing on building student self-efficacy, which has been linked to academic and career success. Here are a few examples of how this could be done in the context of undergraduate research training in oceanography (based on Bandura, 1977, and Kortz et al., 2019).

- Design research projects (e.g., field and laboratory work) such that some degree of troubleshooting is required. Rather than handing students a perfected methodology, leave some issues for the students to encounter that are within their skill sets to solve. Developing mastery by overcoming progressively more difficult obstacles through perseverance and hard work is a highly effective way of building self-efficacy.
- Students also build self-efficacy through vicarious experiences: “If they can do it, I can too.” This is particularly effective when the person observed to be succeeding is of a similar background (e.g., gender, racial, or socioeconomic) to the student observer. For example, women mentoring women has been shown to significantly benefit women’s confidence, persistence, and performance in STEM (Bettinger and Long, 2005; Drury et al., 2011; Dawson et al., 2015; Thomas et al., 2015; Herrmann et al., 2016). It can sometimes be challenging, however, to find women, minority, and low-income role models and mentors in oceanography. Until the oceanography profession reflects our nation’s diversity, we recommend employing diverse near-peer mentors (e.g., graduate stu-

dents) as well as professionals in other STEM fields (e.g., biology, engineering) to contribute relevant expertise.

- In addition to mastery and vicarious experiences, students build self-efficacy through social persuasion (e.g., being assured that success is possible) and reducing physical or emotional stress (e.g., through physical activity, positive environment; Bandura, 1977; Kortz et al., 2019). Service learning projects that address real-world needs (Astin et al., 2000; Eyler et al., 2001; Boyle et al., 2007; Celio et al., 2011), especially when combined with structured reflections (Conway and Amel, 2009) and outdoor activities (Stokes et al., 2015), invoke many of these strategies. Thus, incorporating these approaches into undergraduate research programs is highly recommended.

Recommendation 2. Design Evaluation Instruments to Avoid Use of Self-Promoting Language

A second, possibly related, interpretation for student Absolute survey responses being lower, on average, than the advisor ratings could be that students in general—and perhaps female and/or indigenous students in particular—may be less comfortable describing themselves or their research performances with self-promoting language. Lerchenmueller et al. (2019) found gender differences in how scientists present the importance of their research. Their textual analysis of over six million scientific research articles revealed that male-led research teams were 12% more likely to use glowing terms (e.g., “novel,” “unique,” “excellent”) to describe their research than female-led teams, and that such self-promotion was associated with greater numbers of citations. Kolev et al. (2019) similarly found gender differences in language use among scientists when communicating about their research. This is consistent with our findings that (particularly female NHPI) students are much more likely to rate

themselves “very good” when their advisors rate them as “excellent.”

In contrast to the Absolute data, students’ mean ratings of their Growth over the undergraduate research experience exceeded their advisors’ ratings. One explanation for this disparity is that a different Likert Scale was used, this time ranging from Strongly Disagree to Strongly Agree. Perhaps students, on average, felt more comfortable Strongly Agreeing with a statement that they improved considerably in a given skill set over the course of a research experience, compared with saying they were Excellent at the end of the research experience. Thus, it could be valuable to reframe survey item language to enable use of a Likert Scale ranging from Strongly Disagree to Strongly Agree, rather than from Unsatisfactory to Excellent.

Recommendation 3. Discuss STEM Pathways and Careers at the End of the Research Experience

Interestingly, the two greatest—and most statistically significant—disparities between student vs. advisor mean ratings on Growth survey items pertained to the two survey items that concerned students’ future plans: Growth Item 5. *Compared to before I started the program, I now am more interested in attending graduate school* ($D = -0.30$; $p = 0.06$). Growth Item 9. *Compared to before I started the program, I now am more interested in pursuing a STEM career* ($D = -0.37$; $p = 0.08$). For both survey items, the students, on average, self-reported considerably more Growth than did their advisors (hence $D < 0$). This suggests that discussions and professional development on these topics may be more impactful if they are scheduled—or at least revisited—toward the end of the undergraduate research experience.

Limitations of This Study

Both the t-test and permutation analyses are based on quantification of the Likert scale responses to integers. A short-

coming of this approach is the inherent assumption of equal spacing between successive responses—for example, that the distance between “Strongly Disagree” and “Disagree” is the same as the distance between “Disagree” and “Not Sure.” For

groups that have been traditionally underrepresented (e.g., African-American, Hispanic, Filipino) and overrepresented (e.g., Caucasian, Asian) in STEM fields. Therefore, caution is advised when interpreting these combined results.

men and women) were much more likely to rate themselves “very good” when their advisors rated them as “excellent” than non-NHPI students. These differences in advisor-student ratings may be due to low student self-efficacy and/or discomfort in



“Specifically, we recommend intentionally focusing on building student self-efficacy alongside technical training, designing evaluation instruments that avoid the use of self-promoting language, and scheduling—or at least revisiting—discussions on STEM pathways and careers toward the end of the undergraduate research experience.”

the t-test, this quantification is required. For the permutation test, it is possible to avoid this quantification by only considering the sign (not the magnitude) of the advisor-student difference. This sign-only approach would entail assigning one of three sign values to each student-advisor pair, -1 ($S > A$), 0 ($S = A$), and $+1$ ($A > S$), computing the mean, and comparing this observed mean value to that obtained from (say, 100,000) permutations of the original data set. However, doing so loses key information, thereby drastically reducing the power of the test. Therefore, we instead opted to quantify the Likert Scale and acknowledge this underlying assumption.

A second limitation of the study is rooted in the small size of our data set (30 student-advisor pairs) and the fact that SOEST Scholars represent numerous ethnicities. This combination precluded analysis of each individual ethnicity and limited our ethnicity analysis to comparing the responses of indigenous Native Hawaiian and Pacific Islander (NHPI) students with those of non-NHPI students. The latter category includes students from

Finally, we recognize that students and advisors have access to different information. For some Growth survey items (e.g., Question 3. *Compared to before I started the program, I now am more confident about my STEM abilities*), advisors may have little or no knowledge. Thus, we do not interpret student-advisor differences in responses to Growth survey items in terms of self-efficacy.

CONCLUSIONS

As a group, the undergraduate researchers consistently underrated their Absolute skills and performances relative to their advisors’ ratings. For all 10 Absolute survey items combined, the mean student and advisor ratings were 4.06 and 4.24, respectively—a difference that is highly significant ($p = 0.005$). Much of this advisor-student difference was driven by the responses of NHPI women ($D = 0.36$; $p = 0.02$). While men and non-indigenous students also rated themselves lower than did their advisors, the differences were considerably less ($D: 0.09$ – 0.12) as well as less significant ($p: 0.18$ – 0.59). NHPI students (both

describing oneself with self-promoting language. The former explanation would lead to a recommendation to intentionally build student self-efficacy alongside technical training in undergraduate research programs, while the latter would suggest a need to reframe survey items to avoid the use of self-promoting language (e.g., using a Likert Scale ranging from Strongly Disagree to Strongly Agree, rather than from Unsatisfactory to Excellent). In contrast to the Absolute survey items, there was no statistically significant difference between student and advisor assessments on Growth survey items as a whole ($p = 0.25$).

However, for both Growth survey items pertaining to students’ interest in pursuing graduate school and STEM careers, the students self-reported greater mean Growth during the course of the undergraduate research experience than did their advisors ($D = -0.30$ and $D = -0.37$, respectively). This suggests that conversations with students about STEM pathways and careers should be held—or at least revisited—toward the end of the undergraduate research experience. 

ONLINE SUPPLEMENTARY MATERIALS

Data and Methods (detailed information) and the Student and Advisor Surveys are available online at <https://doi.org/10.5670/oceanog.2020.210>.

REFERENCES

- Andrew, S. 1998. Self-efficacy as a predictor of academic performance in science. *Journal of Advanced Nursing* 27(3):596–603, <https://doi.org/10.1046/j.1365-2648.1998.00550.x>.
- Astin, A.W., L.J. Vogelgesang, E.K. Ikeda, and J.A. Yee. 2000. How service learning affects students. University of California, Los Angeles, <https://heri.ucla.edu/PDFs/HSLAS/HSLAS.PDF>.
- Bandura, A. 1977. Self-efficacy: Towards a unifying theory of behavioral change. *Psychological Review* 84(2):191–215, <https://doi.org/10.1037/0033-295X.84.2.191>.
- Bernard, R.E., and E.H.G. Cooperdock. 2018. No progress on diversity in 40 years. *Nature Geoscience* 11(5):292–295, <https://doi.org/10.1038/s41561-018-0116-6>.
- Bettinger, E.P., and B.T. Long. 2005. Do faculty serve as role models? The impact of instructor gender on female students. *American Economic Review* 95(2):152–157, <https://doi.org/10.1257/000282805774670149>.
- Boyle, A., S. Maguire, A. Martin, C. Milsom, R. Nash, S. Rawlinson, A. Turner, and S. Wurthmann. 2007. Fieldwork is good: The student perception and the affective domain. *Journal of Geography in Higher Education* 31(2):299–317, <https://doi.org/10.1080/03098260601063628>.
- Brown, C., and L.A. Lavish. 2016. Career assessment with Native Americans: Role salience and career decision-making self-efficacy. *Journal of Career Assessment* 14(1):116–129, <https://doi.org/10.1177/1069072705281368>.
- Bryan, M.T. 2004. *An Examination of Navajo Cultural Identity and its Relationship to Academic Achievement*. Doctoral dissertation, Brigham Young University, Utah.
- Carpi, A., D.M. Ronan, H.M. Falconer, and N.H. Lents. 2017. Cultivating minority scientists: Undergraduate research increases self-efficacy and career ambitions for underrepresented students in STEM. *Journal of Research in Science Teaching* 54(2):169–194, <https://doi.org/10.1002/tea.21341>.
- Celio, C.I., J. Durlak, and A. Dymnicki. 2011. A meta-analysis of the impact of service-learning on students. *Journal of Experiential Education* 34(2):164–181, <https://doi.org/10.1177/105382591103400205>.
- Conway, J.M., E.L. Amel, and D.P. Gerwien. 2009. Teaching and learning in the social context: A meta-analysis of service learning's effects on academic, personal, social, and citizenship outcomes. *Teaching of Psychology* 36(4):233–245, <https://doi.org/10.1080/00986280903172969>.
- Dawson, A.E., B.L. Bernstein, and J.M. Bekki. 2015. Providing the psychosocial benefits of mentoring to women in STEM: CareerWISE as an online solution. *New Directions for Higher Education* 2015(171):53–62, <https://doi.org/10.1002/he.20142>.
- Drury, B.J., J.O. Siy, and S. Cheryan. 2011. When do female role models benefit women? The importance of differentiating recruitment from retention in STEM. *Psychological Inquiry* 22(4):265–269, <https://doi.org/10.1080/1047840X.2011.620935>.
- Eyler, J.S., D.E.J. Giles, C.M. Stenson, and C.J. Gray. 2001. *At a Glance: What We Know About the Effects of Service-Learning on College Students, Faculty, Institutions and Communities, 1993–2000: Third Edition*. Vanderbilt University, 121 pp.
- Falk, N.A., P.J. Rottinghaus, T.N. Casanova, F.H. Borgen, and N.E. Betz. 2016. Expanding women's participation in STEM. *Journal of Career Assessment* 25(4):571–584, <https://doi.org/10.1177/1069072716665822>.
- Frawley, J., R. Ober, M. Olcay, and J.A. Smith. 2017. *Indigenous Achievement in Higher Education and the Role of Self-Efficacy: Rippling Stories of Success*. National Centre for Student Equity in Higher Education, Curtin University, Perth, 31 pp.
- Gloria, A.M., and S.E. Robinson Kurpius. 2001. Influences of self-beliefs, social support, and comfort in the university environment on the academic nonpersistence decisions of American Indian undergraduates. *Cultural Diversity and Ethnic Minority Psychology* 7(1):88–102, <https://doi.org/10.1037/1099-9809.7.1.88>.
- Hackett, G. 1985. Role of mathematics self-efficacy in the choice of math-related majors of college women and men: A path analysis. *Journal of Counseling Psychology* 32(1):47–56, <https://doi.org/10.1037/0022-0167.32.1.47>.
- Herrmann, S.D., R.M. Adelman, J.E. Bodford, O. Graudejus, M.A. Okun, and V.S. Kwan. 2016. The effects of a female role model on academic performance and persistence of women in STEM courses. *Basic and Applied Social Psychology* 38(5):258–268, <https://doi.org/10.1080/01973533.2016.1209757>.
- Kolev, J., Y. Fuentes-Medel, and F. Murray. 2019. *Is Blinded Review Enough? How Gendered Outcomes Arise Even Under Anonymous Evaluation*. National Bureau of Economic Research (NBER) Working Paper No. 25759, 42 pp.
- Kortz, K.M., D. Cardace, and B. Savage. 2019. Affective factors during field research that influence intention to persist in the geosciences. *Journal of Geoscience Education* 68(2):133–151, <https://doi.org/10.1080/10899995.2019.1652463>.
- Lent, R.W., S.D. Brown, and K.C. Larkin. 1986. Self-efficacy in the prediction of academic performance and perceived career options. *Journal of Counseling Psychology* 33(3):265–269, <https://doi.org/10.1037/0022-0167.33.3.265>.
- Leichenmueller, M.J., O. Sorenson, and A.B. Jena. 2019. Gender differences in how scientists present the importance of their research: Observational study. *BMJ* 367(8227):470–476, <https://doi.org/10.1136/bmj.l6573>.
- Multon, K.D., S.D. Brown, and R.W. Lent. 1991. Relation of self-efficacy beliefs to academic outcomes: A meta-analytic investigation. *Journal of Counseling Psychology* 38(1):30–38, <https://doi.org/10.1037/0022-0167.38.1.30>.
- Stokes, P.J., R. Levine, and K.W. Flessa. 2015. Choosing the geoscience major: Important factors, race/ethnicity, and gender. *Journal of Geoscience Education* 63(3):250–263, <https://doi.org/10.5408/14-038.1>.
- Thomas, N., J. Bystydziński, and A. Desai. 2015. Changing institutional culture through peer mentoring of women STEM faculty. *Innovative Higher Education* 40(2):143–157, <https://doi.org/10.1007/s10755-014-9300-9>.
- Williams, M.M., and C.E. George-Jackson. 2014. Using and doing science: Gender, self-efficacy, and science identity of undergraduate students in STEM. *Journal of Women and Minorities in Science and Engineering* 20(2):99–126, <https://doi.org/10.1615/JWomenMinorScienEng.2014004477>.
- Zimmerman, B.J. 2000. Self-efficacy: An essential motive to learn. *Contemporary Educational Psychology* 25(1):82–91, <https://doi.org/10.1006/ceps.1999.1016>.
- Zusho, A., P.R. Pintrich, and B. Coppola. 2003. Skill and will: The role of motivation and cognition in the learning of college chemistry. *International Journal of Science Education* 25(9):1,081–1,094, <https://doi.org/10.1080/0950069032000052207>.

ACKNOWLEDGMENTS

The SOEST Scholars program is supported by the National Science Foundation (NSF/OIA #1557349 and NSF/GEO #1565950) and Kamehameha Schools (KS#12662304). Maria Daniella Douglas and S. Anne Wallace contributed to the literature review. The authors thank two anonymous reviewers for input that improved this manuscript.

AUTHORS

Barbara C. Bruno (barb@hawaii.edu) is Faculty Specialist and **Cherryle Heu** is Undergraduate Research Assistant, both at the Hawai'i Institute of Geophysics and Planetology, School of Ocean and Earth Science and Technology, University of Hawai'i at Mānoa, Honolulu, HI, USA. **Grady Weyenberg** is Assistant Professor, Department of Mathematics, College of Natural and Health Sciences, University of Hawai'i at Hilo, Hilo, HI, USA.

ARTICLE CITATION

Bruno, B.C., C. Heu, and G. Weyenberg. 2020. How do advisor assessments of diverse undergraduate researchers compare with the students' self-assessments? And what does this imply for how we train and assess students? *Oceanography* 33(2):134–143, <https://doi.org/10.5670/oceanog.2020.210>.

COPYRIGHT & USAGE

This is an open access article made available under the terms of the Creative Commons Attribution 4.0 International License (<https://creativecommons.org/licenses/by/4.0/>), which permits use, sharing, adaptation, distribution, and reproduction in any medium or format as long as users cite the materials appropriately, provide a link to the Creative Commons license, and indicate the changes that were made to the original content.

Deep Ocean Passive Acoustic Technologies for Exploration of Ocean and Surface Sea Worlds in the Outer Solar System

By Robert Dziak, Don Banfield, Ralph Lorenz, Haruyoshi Matsumoto, Holger Klinck, Richard Dissly, Christian Meinig, and Brian Kahn

ABSTRACT. Ocean worlds are numerous in our solar system. Here, we present an overview of how passive acoustic monitoring (PAM) and signal detection systems, developed for acoustic sensing in Earth's ocean, might be used to explore an ocean and/or surface sea world in the outer solar system. Three potential seagoing mobile platforms for a PAM system are considered: a saildrone or surface buoy for exploring Saturn's largest moon, Titan, and an autonomous underwater vehicle for exploring the sub-ice oceans of Enceladus, one of Saturn's smaller moons, or Europa, one of Jupiter's larger moons. We also evaluate preparation of an acoustic system and electronics for the rigors of spaceflight and the challenging environments of outer solar system planetary bodies. The relatively benign Europa/Enceladus ocean thermal environment (-40° to 40°C) suggests a standard commercial acoustic product may meet system design needs. In comparison, a PAM system for Titan's hydrocarbon seas must function at -180°C temperatures, necessitating testing in liquid nitrogen. We also discuss adapting for outer ocean world exploration, acoustic signal detection, and classification algorithms used widely in ocean research on Earth, as well as data compression methods for interplanetary transmission. The characteristics of geophysical, cryogenic, and meteorological acoustic signals expected in an ocean or surface sea world, including signals from seafloor cold seeps and/or hydrothermal vents, are considered because of their potential to harbor chemosynthetic life.

INTRODUCTION

Spacecraft exploration of the outer solar system over the last three decades has led to the discovery of several planetary bodies that likely have liquid water oceans beneath a shell of ice that covers the planetary surface (Nimmo and Pappalardo, 2016; Lunine, 2017). For example, Jupiter's moon Europa has a relatively thin (<10 km) icy shell that exhibits a variety of tectonic features, and Saturn's small but geologically active moon Enceladus also has a global ocean. Enceladus's ocean is relatively deep beneath the planetary surface, but surface fractures at the south pole allow ice and gas from the ocean to escape into space (Lunine, 2017). Saturn's moon Titan is the only planetary body with an atmosphere and liquid hydrocarbon seas and lakes (Stofan et al., 2007).

In situ exploration of these outer solar system ocean and surface sea worlds might benefit from technologies and techniques that oceanographers have developed to explore Earth's ocean. Earth-focused oceanographers may also benefit from exploration of other ocean worlds because it will further our understanding of ocean creation, dynamics, and the development of hydrologic cycles on these planetary bodies, and provide insight into similar systems on Earth. Moreover, the dynamics of global oceans beneath tidally flexing ice shells represents a rich set of problems that have barely begun to be explored (Nimmo and Pappalardo, 2016) and may provide insights into the dynamics of ice caps and ice sheets in Earth's polar regions. Continued exploration of ocean and surface sea worlds is criti-

cal for one of the most compelling reasons of all: these ocean worlds could harbor life. Ocean worlds have the necessary combination of factors (liquid water, heat energy, chemical nutrients) that can lead to the development of life as we know it on Earth (Nimmo and Pappalardo, 2016). Indeed, it is recognized that these ocean worlds likely have developed analogs to Earth's deep-ocean hydrothermal systems (Vance et al., 2007). On Earth, in the absence of sunlight and hence photosynthesis, chemosynthetic organisms use the various chemicals coming out of hydrothermal vents to create energy. Chemosynthesis generally requires a redox gradient but not necessarily with oxygen (Chyba and Phillips, 2001), implying chemosynthetic life could have developed on other planets without the presence of oxygen.

In this study, we consider how hydrophone and passive acoustic recording technology developed for use in Earth's ocean might be applied to ocean research in the outer solar system. As for potential vehicles, or seagoing platforms, we consider a saildrone/submarine for Titan and a submarine for exploration of the subsurface oceans of Europa or Enceladus (Figures 1 and 2). For example, the saildrone may mirror similar designs used on Earth (Figure S1). A range of possible mission architectures already considered for exploring Titan's seas include (1) a capsule serving as a free-drifting buoy (Stofan et al., 2013; Lorenz and Mann, 2015), (2) propelled surface vessels (i.e., boats; Lorenz et al., 2018), and (3) submersibles with buoyancy control

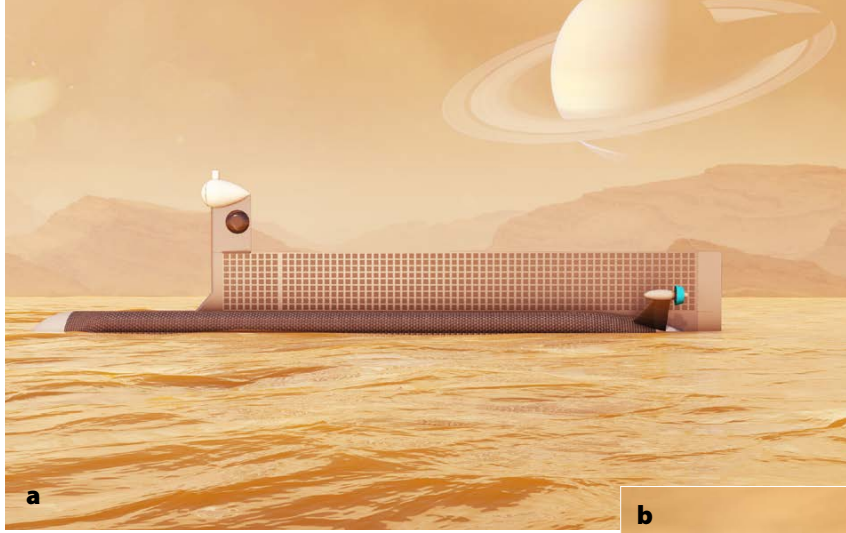


FIGURE 1. (a) Artist's rendition of a submarine conceptual design deployed at Kraken Mare on Titan. To meet science exploration objectives, a submarine must be autonomous, ballasted for stability at the sea surface and at depth, withstand fluid pressures up to 10 bars, traverse large distances using low power, and be capable of tolerating 94 K liquid hydrocarbons (Hartwig et al., 2016). *Image courtesy of NASA.* (b) Artist's rendition of the Titan Mare Explorer (TiME) capsule. The capsule design acts as a drifter buoy, allowing for sea surface stability in a wind wave environment, while enduring spaceflight, hypersonic atmospheric entry, and splash down. A passive acoustic recording system (outlined in this article), would be a key component of the instrument payload for either of these missions. *After Lorenz and Mann (2015).*



FIGURE 2. Artist's conception of one possible autonomous underwater vehicle (AUV) system approaching a volcanic vent in Europa's ocean. A passive acoustic hydrophone system would be a critical instrument for such an outer world probe not only for finding sub-ice volcanic centers and seafloor hydrothermal systems but also for determining spatial distribution of volcanic centers and their seismo-acoustic activity levels prior to direct sampling. *Image courtesy of NASA Jet Propulsion Laboratory (<https://www.jpl.nasa.gov/spaceimages/>)*

(Hartwig et al., 2016). We also briefly discuss preparation of the hydrophone technology for the rigors of spaceflight, the challenging outer solar system environments, and the required planetary protection considerations. We present an overview of instrument back-end electronics and signal classification algorithms for efficient use of the limited downlink bandwidth expected from exploration vehicles. Acoustic signals from seafloor hydrothermal vents are of particular scientific interest because of the vents' potential to harbor extant life. Thus, passive acoustic techniques may be uniquely poised to detect these astrobiologically relevant phenomena.

CHARACTERISTICS OF OUTER SOLAR SYSTEM OCEANS AND SEAS

Table 1 lists several of the essential physical characteristics of Europa, Enceladus, and Titan, the three outer solar system bodies that are the focus of proposed/planned exploration missions. All three of these planetary satellites have thin

atmospheres and low atmospheric pressure (relative to Earth) as well as very low surface temperatures that enable the formation of a thick ice shell on the planetary surface. Internal heating driven by gravity-induced tidal stresses suggests that these worlds also harbor deep oceans beneath their surface ice shells; however, because the oceans are hidden, their thicknesses and compositions are not well known (e.g., Iess et al., 2012). For Europa, the inferred moment of inertia and presumption that the icy shell is not more than a few tens of kilometers thick implies an ocean thickness of <150 km (Schubert et al., 2004). The Galileo spacecraft survey indicated Europa's sub-ice ocean is composed of a water-brine mixture, with magnesium sulfate salt (McCord and Hansen, 1998). On Enceladus, the ocean is perhaps 10 km thick on average but greater at the south pole, reaching depths of <30 km (e.g., Cadec et al., 2016). The Cassini mission sampled the geyser plumes at Enceladus that originate from its sub-ice ocean and found the plumes to be composed of water vapor with a mix-

ture of salts and ice particles (Postberg et al., 2018). Because pure water has very low conductivity, dissolved ions must be present at some level in the oceans of Jupiter's larger icy moons, where induction signals have been detected.

The evolution models for Titan suggest a <400 km thick water-ammonia ocean beneath a <100 km ice shell (e.g., Vance et al., 2017). Compared with Earth, satellite sub-ice oceans are not only poorly characterized but are also driven by a different set of forces. On Earth, wind stresses and salinity variations play a major role in ocean dynamics (e.g., Schmitz and McCartney, 1993); for ice-covered satellite oceans, wind stresses are certainly negligible, and salinity's role is uncertain (see below).

Titan also hosts a methane-based hydrologic cycle that supports standing bodies of liquid hydrocarbons on the planetary surface. Observations from Cassini have revealed more than 650 lakes and seas scattered throughout the north and south polar regions (Hayes, 2016). Cassini surveys also revealed that the

depths of Titan's seas and lakes can exceed 100 m (e.g., Mastrogiuseppe et al., 2019). It is thought the seas are composed of ethane, with ~10% methane and smaller amounts of dissolved nitrogen and propane (e.g., Cordier et al., 2009). Kraken Mare and Ontario Lacus, the largest seas in the south, may have a similar composition. In contrast, comparison of the small observed radar attenuation with laboratory data suggests that the northernmost seas, Ligeia and Punga Mare, are almost pure liquid methane (e.g. Mastrogiuseppe et al., 2019). Indeed, there may be a compositional variation across the linked Ligeia/Kraken system that is similar to the Black Sea/Mediterranean Sea gradient, forced by methane precipitation with involatile

ethane analogous to salt in Earth's ocean (Lorenz, 2014). In addition to the fundamental differences in physical properties of hydrocarbons compared to water, a notable peculiarity of Earth's ocean and lakes is that at freezing temperatures, terrestrial bodies of liquid become stably stratified by density, causing sound speed to increase with depth. This does not happen on Titan, nor does ice form at the sea surface. Because the solid phase of hydrocarbons is denser than the liquid phase, if freezing should occur, the solids will generally sink to the seafloor.

Arvelo and Lorenz (2013) modeled temperature, density, sound speed, and sound absorption for Titan's seas (Figure S2) and found that even with

off-the-shelf piezoelectric sonar transducers, a relatively simple sonar system should generate sufficient acoustic power to enable good sound propagation and enable sensing of the environment in a 1 km deep cryogenic hydrocarbon sea. In Titan's low gravity (1.35 m s^{-2}), the pressure variation with depth in the sea is an order of magnitude weaker than that of Earth. Thus, while atmospheric pressure at sea level is higher on Titan (1.49 bar) than on Earth, at 1 km depth, the pressure is ~11.5 bars on Titan as compared to 101 bars on Earth. Sound speeds in methane and ethane are $1,498.2 \text{ m s}^{-1}$ and $1,971.0 \text{ m s}^{-1}$, respectively, at 95 K (<https://webbook.nist.gov/>). Figure S2 shows an example temperature, density, and sound speed profile for Titan. Note that the vertical extent of a 1 km hydrocarbon sea is small enough compared with Titan's radius (2,575 km) that gravity g can be considered constant with depth, in contrast to the deeper (~100 km) liquid water oceans of icy satellites like Europa, where g varies appreciably with depth (Leighton et al., 2013). Arvelo and Lorenz (2013) estimate acoustic signal loss due to sound absorption α in Titan's methane seas is expected to be very low (~0.035 dB km^{-1} measured at 20 kHz) and likely to have little effect on sound propagation.

TABLE 1. Essential physical characteristics for Europa, Enceladus, and Titan.

	EUROPA	ENCELADUS	TITAN
ICE SHELL THICKNESS	15–25 km ^a	30–40 km; <10 km at poles ^b	<200 km ^c
OCEAN/SEA DEPTH	Ocean: 60–150 km ^d	Ocean: 26–31 km ^e	Sub-Ice Ocean: <400 km ^f Seas and Lakes: 2.9–160 m ^{g,h}
OCEAN/SEA COMPOSITION	Water-Brine: –40°C to 40°C ⁱ (for example, magnesium sulfate (MgSO ₄), sulfuric acid hydrate (H ₄ O ₅ S)) ^j	Water with Salts (–Na, –Cl, –CO ₃)	Sub-Ice Ocean: water/ammonia ^k Surface Lakes and Seas: ~79% ethane (C ₂ H ₆), ~8% propane (C ₃ H ₈), ~10% methane (CH ₄), ~3% hydrogen cyanide (HCN), ~1% butane, acetylene ^l
SURFACE TEMPERATURE	Equator: –160°C Poles: –220°C	Equator: –128°C Poles: –240°C	Equator: –179.5°C ^m
ATMOSPHERIC SURFACE PRESSURE	10–12 bars ⁿ	Variable (Plumes) ^o	1.47 bars
ATMOSPHERIC COMPOSITION	O ₂	91% water vapor, 4% N, 3.2% CO ₂ , 1.7% CH ₄	95%–98% N ₂ , 1.4%–4.9% CH ₄ , 0.2% H ₂ ^p
PROPORTION TO EARTH DIAMETER^q	25%	4%	40.4%
SURFACE GRAVITY	1.314 m s ^{–2}	0.113 m s ^{–2}	0.138 m s ^{–2}
DISTANCE FROM SUN	7.8 × 10 ⁸ km	1.4 × 10 ⁹ km	1.2 × 10 ⁹ km
TRAVEL TIME FROM EARTH	6 years	2.3–6 years ^r	2.3–6 years ^r

^a Nimmo et al. (2003)

^b Cadek et al. (2016)

^c Hemingway et al. (2013)

^d Pappalardo et al. (1999)

^e Choblet et al. (2017)

^f Vance et al. (2017)

^g Mastrogiuseppe et al. (2014)

^h Hayes (2016)

ⁱ Melosh et al. (2004)

^j McCord et al. (1998)

^k Iess et al. (2012)

^l Cordier et al. (2009)

^m Mitri et al. (2007)

ⁿ McGrath (2009)

^o Dougherty et al. (2006)

^p Niemann et al. (2005)

^q https://ssd.jpl.nasa.gov/?sat_phys_par

^r Depending on direct trajectory or gravity assist. Pioneer 11 = 6.5 years. Voyager 1 = 3.2 years. Voyager 2 = 4 years. Cassini = 6.75 years. New Horizons = 2.3 years.

OCEAN WORLD GEOPHYSICAL SIGNALS RECORDED ON A HYDROPHONE

On an ocean world, whether ice-covered or open, acoustic waves propagating through water or ice provide a very effective means for detecting and evaluating mega-sources of fracturing and volcanism on a planetary scale, thus giving an “over-the-horizon” sense of the world that is not available at a single landing site (Lee et al., 2003; Leighton et al., 2013). A variety of environmental acoustic signal sources can be expected in an ocean world. These sources should be similar to those common on Earth and include fracturing of cryo- and/or lithic-crust

(quakes), explosive volcanism, debris flows/landslides, meteor impacts, and buoyant hydrothermal fluid plumes. Moreover, as is the case on Titan where there are open fluid lakes or seas, meteorological sound sources from precipitation, surface wave breaking, waterfalls, and wind-wave interaction can also be expected (Arvelo and Lorenz, 2013). Thus, the unique scientific contribution achieved by using hydrophones and hydroacoustic signal detection techniques on Earth is likely to be the same for other ocean worlds. Hydrophones are relatively inexpensive to build, and the low acoustic wave attenuation characteristics in the ocean permit hydrophones to detect much weaker acoustic signals originating from geophysical phenomena than can be detected by seismometers on the planetary surface (Dziak et al., 2015).

In our experience, it is not uncommon to detect acoustic signals (broadband and single tone) that are not easily classified. This issue raises an important question: given the expected uncertainty in interpreting sound signals and sources occurring in the waters of an outer ocean world, how useful will omnidirectional passive acoustics be? The ocean science community's long experience in identifying the wide variety of underwater sound sources recorded by hydrophones on Earth suggests this problem is manageable. In the past several decades, great strides have been made by the ocean acoustics community in identifying the unique signal characteristics of vocal marine animals using single omnidirectional hydrophones on moorings and mobile platforms (e.g., Baumgartner et al., 2019; Au et al., 2000). This is also true for geophysical sounds, and we think it will be possible to identify natural sound sources where there are clear analogs on Earth.

Cryogenic Seismo-Acoustic Sources

For ocean worlds with ice shells, we expect to record two basic types of cryogenic sources on a sub-ice hydrophone that should be similar to signals recorded in Earth's polar oceans. The first

is "icequakes," where fracturing of large sections (meters to kilometers) of ice generate strong seismo-acoustic waves (Figure 3a,b; Dziak et al., 2015). The second is ice tremors, the harmonic signals produced when large blocks (several kilometers long) of ice impact one another, remain in contact, then slide in stick-slip fashion past each other (Figure 3c; MacAyeal et al., 2008).

There are a number of potential source mechanisms for seismo-acoustic signals generated by the breakup of sea surface ice on Earth. Podolskiy and Walter (2016) provide an extensive review of this literature. To summarize, possible source mechanisms include rifting, near-surface crevassing, stick-slip motion/rupture of an ice-bedrock interface, collision and sliding between two adjacent ice masses, and sea surface ice sheet flexures

caused by ocean tides and waves. Indeed, large sea surface ice mass (iceberg) collisions, grounding, and breakup on Earth have been shown to generate energetic hydroacoustic harmonic tremor as well as cryogenic icequake events detected both by in situ seismometers (MacAyeal et al., 2008) and hydrophones at distances of 10–1,000 km from the iceberg source (Talandier et al., 2002; Royer et al., 2015). Seismo-acoustic signals generated by icequakes on Earth are typically in the ~10 Hz to ~500 Hz frequency band, while ice tremors can exhibit fundamental frequencies of ~1 Hz with multiple overtones of up to several hundred hertz.

Previous studies of Europa and Enceladus show that the ice surfaces of these worlds exhibit large-scale faulting and fracturing due to tidal stress from Jupiter and Saturn (e.g., Smith-Konter

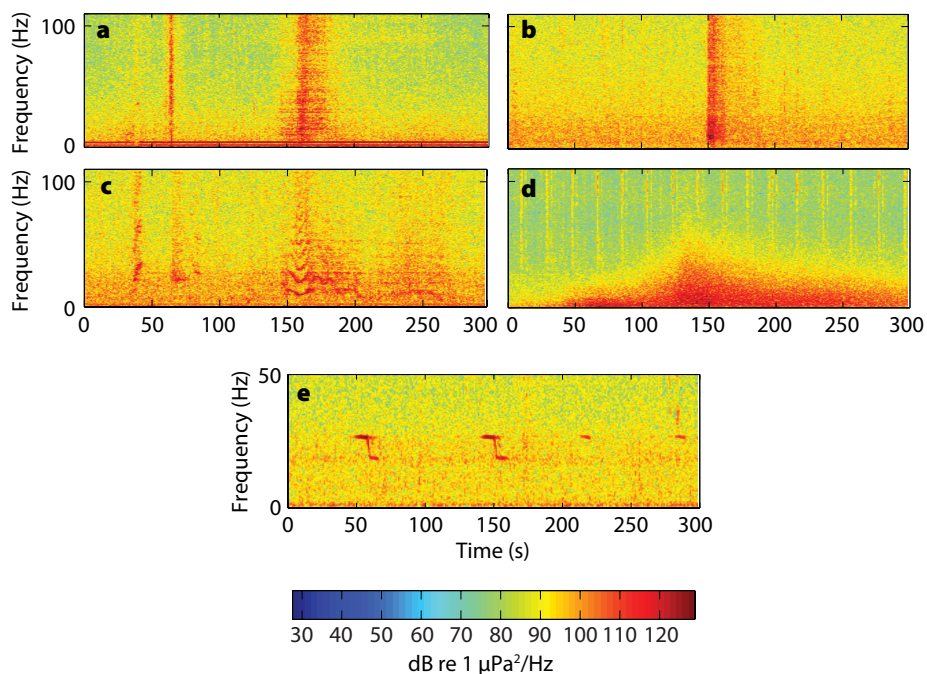


FIGURE 3. Frequency-time displays (spectrograms) of various sound sources recorded in the Southern Ocean near the Antarctic Peninsula (~900 m depth). The sound energy level is roughly equivalent for all sources; however, each varies in prevalence through the year. (a) A record of an emergent (i.e., the signal is spread out in time), broadband icequake acoustic arrival caused by fracturing of sea ice or a nearby iceberg. (b) A record of an impulsive, short-duration icequake signal indicating that the icequake may be closer to the recorder, exhibiting less attenuation than the emergent record shown in (a). (c) A record showing fundamental and harmonic overtones of an iceberg harmonic tremor caused by grounding and scraping of an iceberg keel along the seafloor (MacAyeal et al., 2008). (d) A record showing emergent, long-duration seismo-acoustic energy (<50 Hz) from a nearby earthquake (body wave magnitude ~4). An example of anthropogenic signals from a nearby seismic survey ship can also be seen as broadband signals repeating every 30 seconds in the background. (e) A recording showing a bioacoustic signal from an Antarctic blue whale. Antarctic blue whale vocalizations are identifiable as a series of band-limited, down-swept frequency tones from 28 Hz to 22 Hz. *After Dziak et al. (2015)*

and Pappalardo, 2008; Vance et al., 2018). Thus, the ice shells on Europa and Enceladus will very likely produce icequakes with a wide range of magnitudes (acoustic source levels). The magnitude range of icequakes will likely follow a power-law distribution in number and size as quakes do on Earth (Panning et al., 2006), which will allow assessment of the dynamics of ice shell movement and breakup in response to tidal forcing. It may also be possible to use icequakes to detect the explosions of water vapor through the ice shell observed on Enceladus. The cryo-volcanic and water plume systems on Enceladus are thought to exhibit similar geometries and acoustic sources as Earth's hydrothermal geyser systems, with volatile flow through a conduit system producing cavitation and chamber resonance (Vance et al., 2018). Tidal fracturing of the ice shell will also likely generate substantial ice tremor signals. The magnitude and frequency bands of ice tremors are directly proportional to the sizes of the ice blocks (or plates) that impact one another. Thus, monitoring tremors will provide insights into the dynamics of ice shell breakup. On Earth, large icebergs can generate ice tremors as they impact and grind against the shallow seafloor (Dziak et al., 2015). We do not anticipate the oceans on Europa or Enceladus will be shal-

low enough for their ice shells to impact their sub-ocean lithic crusts. Interestingly, in contrast to the polar regions on Earth, seismic noise due to thermal expansion/contraction of the ice shells is not likely to be substantial due to the great distances of Europa and Enceladus from the sun, resulting in smaller diurnal and seasonal temperature variations (Vance et al., 2018).

Geophysical Seismo-Acoustic and Meteorological Sources

We expect to detect four main types of geophysical acoustic sources generated from ocean lithic floor on ocean worlds. We assume these geophysical signals occur in or near the sub-ocean lithic crust and include quakes due to crustal fracturing (e.g., Figure 3d), volcanic (harmonic) tremor caused by magma flowing in the shallow crust, explosions from violent degassing of lava erupting on the ocean floor (e.g., Caplan-Auerbach et al., 2017), and resonant and broadband noise associated with hydrothermal fluid vents (Figure 4). Volcanic eruptions on Earth are typically associated with substantial amounts of earthquake activity (e.g., Klein et al., 1987), but volcanic earthquakes tend to be much smaller in magnitude than events produced by large plate boundary faults. Thus, these two types of quakes should be distinguishable on an ocean world. Moreover, meteorite impacts, both on an open sea surface and on lithic/ice crust, should also be sources of detectable seismo-acoustic waves, as their high-velocity collisions can cause massive fracturing and generate significant pressure-wave energy.

When magma erupts on the seafloor on Earth or flows through a lithic crust, it can also produce very distinctive resonant tremor signals (e.g., Dziak et al., 2012). Volcanic tremor acoustic signals are similar to those of ice tremor, exhibiting both fundamental and multiple overtones (e.g., Figure 3c) but typically lower frequencies (<20 Hz). Volcanic tremor also tends to be very low amplitude and attenuates rapidly, necessitating the employment of hydroacoustic detection methods to record these signals at tens of kilometers and over-the-horizon distances. Additionally, it would seem that an under-ice hydrophone would have a better chance of detecting the relatively low-amplitude seismic/tremor signals from sub-ocean volcanic sources than seismometers on the outer surface of a planetary ice shell. The upward-propagating ocean acoustic phases would scatter when they encountered the ocean ice-shell interface (Keenan and Merriam, 1991), and attenuation would increase as the signals propagated through the thick, icy crust.

If we can detect volcanic explosions and seismic and/or tremor events, we may be able to use these signals to localize volcanic centers (i.e., large areas of magmatic activity on the sub-ocean floor). On Earth, seafloor volcanic centers can host vigorous high-temperature (>200°–300°C) fluid vents. Water, heated by subsurface magma bodies, exits the seafloor through fractures, building polymetallic sulfide chimneys as the metals precipitate from the super-heated fluid upon contact with the

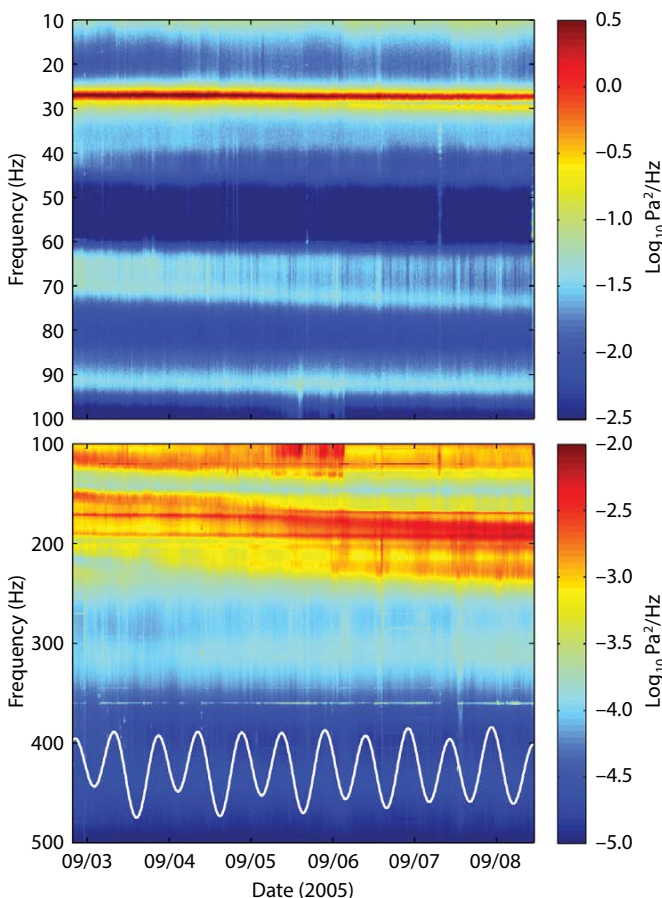


FIGURE 4. Spectrogram of the temporal evolution of the acoustic power spectrum of a “black smoker” hydrothermal vent. The narrowband tones at 25 Hz, ~100 Hz, and ~200 Hz are from the vent source. The white lines at the bottom show the tidal phase, indicating tides modulate this vent’s acoustic signature at ~200 Hz. *After Crone et al. (2006)*

near-freezing seawater. The fluid flowing through these chimneys can be turbulent, producing seismo-acoustic harmonic tones (tremor) through resonance of the chimney conduit and oscillations at the chimney nozzle (Figure 4). Although the amplitude of these signals is not expected to be large (e.g., Crone et al., 2006), because of the astrobiological significance of these chimneys, they are the most interesting sources to use to establish the sensitivity of our instruments (see Table 2). Detection ranges of ~1 km are possible on Earth in the 5–500 Hz band (Crone et al., 2006) despite high ambient noise from ship traffic and microseisms.

On the outer ocean worlds, we might expect hydrothermal vent detectability at much farther distances, depending on the actual ambient noise characteristics. Titan is the only satellite in the solar system with a dense atmosphere and hydrocarbon seas. Its undersea noise is expected to be dominated by molecular agitation, sea surface dynamics, and occasional precipitation. The sea surface noise should vary with wind speed, due to the entrainment and ringing of bubbles by sea surface wave breakers. Surface wind on Titan has been shown to be $\leq 2 \text{ m s}^{-1}$, which may generate waves up to ~1 m high (Lorenz et al., 2012). Estimates are that wind speed and wave height would produce 40 dB re $1 \mu\text{Pa}^2/\text{Hz}$ of noise at 20 kHz in Titan's seas, but it is also likely this noise will be broadband in the tens of hertz to kilohertz range as it is on Earth (Arvelo and Lorenz, 2013). Sound can also be generated by precipitation (e.g., Ma and Nystuen, 2005), which is a possibility for Ligeia Mare. Arvelo and Lorenz (2013) suggest rainfall is likely to occur at rates of tens of millimeters per hour. This rainfall would be methane, and its impact on the sea surface would produce broadband sounds (tens of hertz to kilohertz). Thus, we anticipate using an undersea hydrophone to record time variation in rainfall and wind-wave noise on the sea surface to provide insights into Titan's weather dynamics and climate conditions. Moreover, because Kraken

Mare is composed of two basins separated by a narrow (~17 km wide) strait, it is thought that current velocity in this strait may be high (~0.5 m s^{-1}). Acoustic flow noise could also be a significant source of ambient sound in these methane/ethane seas (Lorenz., 2014).

Bubble streams emanating from cold seeps and hydrothermal systems on the ocean floor are other potential sources of ambient sound in the Titan seas. Methane seep bubble streams are a fairly common feature on Earth's shallow (50–1,725 m) continental shelves (Johnson et al., 2015). These bubble streams produce a series of broadband (0.5–4.5 kHz) acoustic pulses of short duration (~0.2–0.5 msec) that occur in clusters of pulses that last two to three seconds (e.g., Figure S5; Dziak et al., 2018). The bubble streams generate sound during bubble formation; detachment of the gas bubble from the end of a tube or conduit causes the bubble to oscillate, producing sound (Leifer and Tang, 2007). Titan may also be cryo-volcanically active (e.g., Lopes et al., 2013), and it is possible that some form of thermal-fluid vents may also exist on the bottoms of Titan's seas, similar to systems discussed for the lithic seafloors of Europa and Enceladus. Indeed, Cassini radar showed evidence of ephemeral “bright features” at the surface of Ligeia Mare, interpreted as rising gas bubbles (Hofgartner et al., 2014). Modeling of thermodynamic instabilities indicates N_2 can be exsolved in the Titan seas, producing streams of centimeter-sized bubbles (Cordier et al., 2017). Thus, seismic and tremor signals from cryo-volcanic activity, as well as the harmonic tones from fluid flow at hydrothermal vents, are all potential sources of sound in Titan's seas. Lastly, as both cold and hot vents are sources of chemosynthetic life on Earth, and if found on Titan, they may also host extant life.

Biological Acoustic Signals

We think the most likely places for life to thrive on ocean-ice worlds like Europa and Enceladus are thermal hot springs associated with ocean-floor volcanic centers or, as may be the case for Titan, cold seeps in the shallow seas. As on Earth, the hot springs and cold seeps provide the energy source for chemosynthetic ecosystems to develop and thrive. These vent ecosystems can exhibit a diverse range of biota (e.g., microbes, tube worms, mussels, shrimp, and crabs). Thus, one method to find life would be to detect and locate these volcanic centers/hotsprings and/or cold seeps using the geophysical acoustic signals they produce, then directly sample these chemosynthetic environments to search for chemical evidence of life (e.g., Figure 2).

The majority of marine vertebrates on Earth has evolved to use sound to navigate, orient, and find food (Au et al., 2000). Large baleen whales (e.g., blue, fin, and right) exhibit vocal ranges from 10 Hz to 1 kHz (e.g., Figure 3e). Toothed whales, dolphins, porpoises, and pinnipeds vocalize and echolocate in the tens of hertz to hundreds of kilohertz range, while vocal fish species (e.g., cod, pollack, salmon, herring) can produce sounds ranging from 20 Hz to as high as 8 kHz (Web et al., 2008). Even animals as small as snapping shrimp are capable of producing source levels in excess of 190 dB $1 \mu\text{Pa}$ at 1 m (in the 5–20 kHz band) by collapsing a cavitation bubble when clos-

TABLE 2. Notional requirements for hydrophone.

		EUROPA/ ENCELADUS	TITAN
OPERATIONAL	Temperature	-40°C to 40°C	-230°C to 40°C
	Static Pressure	1–1,300 bars	1–10 bars
	Acidity	3–8 pH	N/A
	Sensitivity Floor	-200 dB V/uPa	-200 dB V/uPa
	Saturation	150 dB	150 dB
	Bandwidth	0.01–40 kHz	0.01–40 kHz
SURVIVAL	Temperature	-50°C to 150°C	-196°C to 50°C
	Pressure	0–1,300 bars	0–20 bars
	Radiation (TID)	200 krad	20 krad
	Outgassing	TBD	TBD
	Acceleration	25 g	25 g

ing their larger claws (Bohnenstiehl et al., 2016). Snapping shrimp use this sound to stun their prey (typically small fish). It thus seems plausible that if life exists and thrives in these ocean worlds, even very simple creatures may have developed an acoustic-based means to sense and interact with their surroundings. We don't know the exact character and frequency band these biotic sounds may take, but if they are higher amplitude than ambient background noise levels, they can be detected, categorized, and quantified.

INCLUSION OF PAM SYSTEMS ON OCEAN WORLD EXPLORATION VEHICLES

The hydrophone system described in this article could be used for a near-term mission that inserts a vehicle into a Titan sea (e.g., Figure 1). One option would be to mount the hydrophone to the hull of a saildrone or submarine. We know from saildrone deployments on Earth that hull-mounted acoustic systems are subjected to large hull vibrations associated with vehicle movement across the sea surface. A better option would be to position the hydrophone on a tether, or possibly use a winch system to deploy an array of hydrophones some distance from the vehicle's hull, while the electronics would remain inside and thermally controlled. A recent study of flow noise on ocean gliders demonstrated that lower vehicle speeds ($<25 \text{ cm s}^{-1}$) result in lower ambient noise levels in the 50–200 Hz band, to the point where ambient noise levels were comparable to fixed acoustic recorders (Fregosi et al., 2020). In contrast, increased vehicle speeds will increase flow noise energy. Thus, recording relatively high-energy geophysical or cryogenic sound sources may be possible from a surface vehicle, while seafloor bubble streams will likely be difficult to detect, given their low expected source levels. Bubble detection may only be possible with relatively low vehicle speed, low ambient sound conditions, and proximity to the bubble source.

The hydrophone could also be a can-

didate for an initial Europa lander mission (staying on the frozen surface) or a follow-on mission to Europa or Enceladus that would endeavor to enter a fluid sea, either via cracks in the surface ice or melting through the ice shell (e.g., Figure 2). This ocean worlds hydrophone system may potentially enable detection and monitoring of geophysical acoustic sources occurring within and at the boundaries of the oceans and seas on these moons. On Earth, underwater sound (especially low frequency) propagates very efficiently in dense media such as seawater, where acoustic signatures associated with geophysical events, meteorological events (e.g., high winds and waves caused by storms), or biological sources (e.g., infrasonic baleen whales calls) are often detectable at distances of tens to hundreds of kilometers (e.g., Dziak et al., 2015). Thus, acoustic sensing might also be an effective exploration tool within the exotic ocean worlds of the solar system. The acoustic recording system would need to be broadband enough to enable detection and identification of acoustic signals from a wide range of sources from these outer worlds and capable of parameterization of the signals for transmission back to Earth.

In the following sections, we consider development of a passive acoustic recording module that might feasibly be included on a future mission to Europa, Enceladus, or Titan. The instrument design seeks to minimize its resource footprint to roughly match that available for realistic mission scenarios. An autonomous signal processing capability would be built in as well to reduce the volume of acoustic data for transmission back to Earth. To assess the feasibility of including a passive acoustic system on a future ocean worlds exploration mission, we have taken the baseline Europa Lander resource budget to estimate instrument design limitations. Detailed payload and power considerations, as well as the use of outer world acoustic records for public engagement, are discussed further in the online supplementary materials.

TECHNICAL DEVELOPMENT OF AN OCEAN WORLDS PASSIVE ACOUSTIC SYSTEM

We think autonomous hydrophone systems that could be used to explore an ocean world already exist. Passive acoustic monitoring (PAM) systems have been installed on an ocean glider and a profiler float (Matsumoto et al., 2011, 2013), successfully recording, detecting, and classifying deep-ocean geophysical and biological sounds. These instruments are useful analogs for what can be achieved on an ocean world in that they operate in remote, inhospitable environments, are very low-power, and perform without human intervention for long periods. These oceanographic mobile platforms also have minimal downlink bandwidth through which to communicate (via Iridium satellite connection).

The hydrophone technology will need to be tested for the rigors of spaceflight, including materials selected for outgassing concerns, extreme temperatures that will be encountered on outer solar system worlds, and shock and vibration conditions during launch (Table 2). The signal processing electronics are not a difficult design problem, but re-casting the autonomous processing electronics into a system that can endure spaceflight, yet retain the minimal power requirements, is critical. Lastly, the signal identification and classification algorithms needed to reduce the transmitted data sizes to meet downlink requirements for an ocean world exploration mission will be derived from similar concepts already used on mobile marine instruments and platforms on Earth. However, the bandwidth of potential signals of interest may be much wider on outer solar system worlds than it is on Earth (all signals are of interest, both geophysical and biological), and signal ranking system would need to be developed.

Ocean World Hydrophone Overview

The three developmental components of an ocean worlds passive acoustic technology project are (1) the hydrophone element, (2) signal-processing electronics,

and (3) signal identification/classification algorithms. The hydrophone and processing electronics could be built together to enable laboratory testing, and hydrophone designs (for Titan, Europa, and Enceladus), electronics, and identification/classification algorithms could be tested in sea trials on Earth. It is assumed that the signal-processing electronics would be held within the hull of the exploration vehicle to maintain a relatively hospitable temperature (e.g., -40°C or above). This separation between the hydrophone sensor and instrument electronics will not be a problem (e.g., due to signal attenuation) for distances up to ~ 10 m, which is significantly longer than expected for the size of an ocean world exploration vehicle.

Table 2 shows the estimated requirements for the successful performance of a hydrophone meeting our planetary exploration science goals. This exercise serves to show the different thermal environments that the Titan hydrophone must survive. The temperature requirements are based on the expected ambient conditions in the target body's seas, as well as survival requirements expected during deep-space cruise conditions and NASA's planetary protection thermal-sterilization requirements to prevent contamination. The pressure limits are set by the expected depth of the seas. We assumed the vehicle would remain within the top 10 km of the Europa or Enceladus oceans but may be at the floor of a Titan sea. The pH requirements were set to account for potentially inhospitable acidic seas (Towner et al., 2006). The hydrophone sensitivity floor was set to enable detection of acoustic signals from a hydrothermal vent sound source at distances of tens to hundreds of meters, assuming terrestrial-ocean spherical spreading and transmission loss. We assumed an ambient noise floor similar to a quiet ice-covered sea (as in Antarctica; Dziak et al., 2015) and a hydrothermal vent acoustic source level (**Figure 4**; Crone et al., 2006) caused by cavitation due to turbulent fluid flow through a vent chimney. The high signal saturation level is required to enable a high dynamic

range because of the uncertainty in the noise spectral level and the likelihood of a highly red spectral character.

Lastly, the high sample rate for both Europa/Enceladus and Titan hydrophones (0.01–40 kHz; **Table 2**) were selected to include a wide variety of potential signal sources. Types and frequencies of these sources as observed on Earth range from high-temperature hydrothermal vent systems (≤ 200 Hz) to seismo-acoustic volcano and cryogenic signals (10–500 Hz), seafloor bubble streams (max ≤ 45 kHz), and potential bioacoustics signals, which could be broadband and high frequency as well (10 Hz to tens of kilohertz). A 40 kHz sample rate would create 2.56 TB of acoustic data over a one-year recording period, which should be an easily manageable data volume, given current commercially available solid-state-drive storage capacities. However, given that the data will be processed in real time for transmission of detected events back to Earth, there really is no need to retain the data onboard the vehicle, enabling use of lower-capacity, lower-power data storage systems. This data archive will also only be needed for the duration of the vehicle's mission on an outer world, as the data will be used by embedded identification and classification algorithms that will parameterize signals of value for transmission back to Earth (see following sections).

Hydrophone Requirements for Europa/Enceladus

The relatively benign thermal environment (by outer solar system standards) needed for a Europa/Enceladus hydrophone suggests that a standard commercial product may be suitable. Deepwater, omnidirectional transducers are available from several manufacturers (e.g., Teledyne Reson; **Figure 5**). Many commercial entities that supply hydrophones for oceanographic applications are already familiar with designing transducers capable of thermal sterilization for medical applications. Whether the materials encasing the hydrophone sensor head are compatible with spaceflight will still need to be examined. Also, the stringent NASA planetary protection requirements for Europa and Enceladus missions mean that outgassing and cold performance of the materials chosen need to be considered, as well as the material's ability to survive thermal sterilization. Outgassing characteristics are driven by the requirement to not contaminate other instruments during spaceflight while in a hard vacuum for several years. The shock and vibration requirements needed for spaceflight may necessitate some redesign of an off-the-shelf transducer head. However, piezoelectric transducers are often robust where mechanical shock and vibration are unlikely to damage the device.

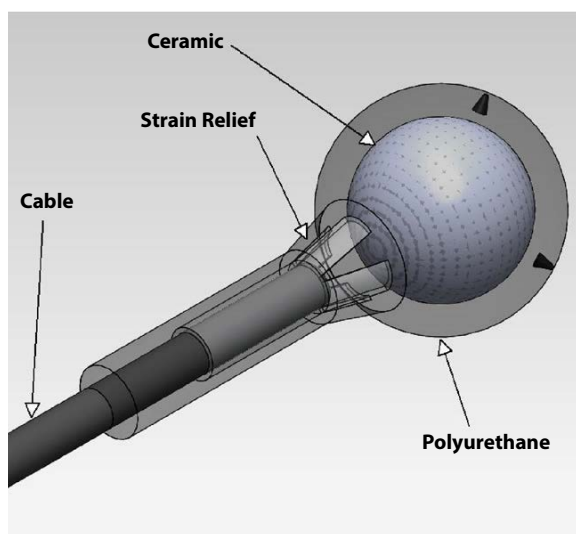


FIGURE 5. Schematic of an example hydrophone for spaceflight development. Shock and vibration requirements for spaceflight may necessitate transducer redesign; however, piezoelectric transducers are often robust when subjected mechanical shock. As transducers are capable of both receiving and emitting sound, it is possible this sensor could also serve engineering roles on a future vehicle as an active sonar, or possibly even as an acoustic modem for a communication network composed of nearby seafloor sensors.

Hydrophone Requirements for Titan

Meeting hydrophone design requirements for Europa/Enceladus would be the first step in adapting a hydrophone for survival and performance under the environmental conditions needed for Titan. Principally, this would involve increasing the cold tolerance of the hydrophone from that acceptable for Europa/Enceladus down to -183°C for Titan's surface temperatures. Also, depending on how the platform is delivered, for example, in slow parachute descent, the vehicle could experience the Titan tropopause minimum temperature of -203°C . To ensure continued performance at these very low temperatures would take further redesign of the mechanical structures of the hydrophone and careful selection of materials. Simpler narrowband transducers have been sent to Titan (e.g., Towner et al., 2006), and Arvelo and Lorenz (2013) successfully tested another narrowband transducer to liquid nitrogen (LN_2) temperatures of 77 K, colder than Titan's 90–94 K surface temperatures. Thus, it appears that a material solution for a broadband sensor would be available. The acoustic impedance of Titan's seas is different than in Earth's ocean, of course, but not so dramatically that it is expected to be a driver in the redesign. The difference in the fluid properties could be accommodated to optimize the hydrophone for Titan's ethane/methane seas. Lastly, an important simplification exists for Titan instrumentation, in that the ocean is electrically insulating. Many of the reliability issues that confound terrestrial electronics in marine applications are obviated, and electrical conductors can be exposed without issue.

One approach to laboratory testing a Titan hydrophone would be to immerse the hydrophone in a Dewar of LN_2 , similar to the approach used by Arvelo and Lorenz (2013). The LN_2 temperature would slightly exceed the extremely cold surface temperature of Titan, and LN_2 differs from seawater in acoustic impedance. The biggest challenge in designing a Titan hydrophone is the

extreme temperature, so this approach would constitute a strong test of the design presented.

Signal Processing Electronics

Passive acoustic recording and processing electronics that have been built for deep-sea mobile platforms (Matsumoto et al., 2011, 2013) would need to be adapted to enable them to survive spaceflight and yet retain the high performance and extremely low power requirements that an ocean worlds exploration mission would require. Here, we address two aspects of this adaptation. The first is whether the system architecture for terrestrial deep-sea instrumentation is compatible with deep-space flight, typically meaning that it is radiation-hardened against cosmic ray hits. Until recently, this would have meant a redesign of the architecture (now using ARM microprocessors and digital signal processors, or DSPs). However, in the last year, likely because of pressure from the CubeSat community, radiation-hardened ARM processors are now available (e.g., Vorago Technologies), and radiation-hardened DSPs have also existed for somewhat longer. Thus, adapting the existing terrestrial signal processing electronics will not be a difficult process.

A second area of significant concern in designing signal processing electronics for making acoustic recordings in any new environment is to properly anticipate the different ambient noise levels that will occur in the various outer-world environments and how the levels will differ from Earth's ocean. Models of the expected noise levels on the ocean and surface sea worlds (Arvelo and Lorenz, 2013) allow us to anticipate to some extent ocean and sea noise acoustic environments on Europa and Titan. In our view, it will be critical to develop an amplifier with automatic gain control (AGC) to avoid saturating our analog-to-digital converters (ADC) if the noise environment is vastly different than the predictions. Adjustable gain amplifiers can be controlled by the processor to avoid signal saturation,

which will make the best use of the 148 dB dynamic range of the 24-bit ADC. As an example of the wide range of noise levels possible, Figure 6 shows the observed noise spectra in a variety of conditions in Earth's ocean, where ambient noise from natural sources can range in power spectral density by ~ 100 dB re $\mu\text{Pa}^2/\text{Hz}$.

Signal Identification and Classification Algorithms

Acoustic signal detection and classification algorithms are used widely in oceanographic research to automate evaluation of long-term acoustic data sets for geophysical and biological signals of interest in the ocean (for a review, see Mellinger et al., 2016). Over the last decade, acoustic near-real-time applications have become important tools in the detection of marine mammal vocalizations for use in assessing their population sizes and geographic distributions (e.g., Klinck et al., 2012). Significant advancements have been made in the development and operation of stationary and mobile autonomous systems that screen the underwater soundscape continuously for signals of interest and report the occurrence of such signals back to shore, commonly through an Iridium satellite link (Klinck et al., 2012; Matsumoto et al., 2013; Baumgartner et al., 2019). The software implemented on these systems is typically multilayered. In the initial stage, a detection algorithm flags general sounds of interest. First-stage detectors are often very simple in nature (e.g., band-limited energy detector) and generate a significant amount of false positive detections; however, they are very efficient energy-wise, with a low-computational load (Mellinger et al., 2016) and can even be analog in nature (e.g., analog filter banks). If acoustic signals of interest are detected, they are parsed into a second-stage classifier for verification and identification (Klinck and Mellinger, 2011). As the occurrence ratio of interesting signals versus noise is usually heavily skewed toward noise, this helps to keep the overall power consumption low.

This is a key feature as these systems are always power limited, with a finite battery storage capacity.

Single Versus Multiple Sensors

In our experience, it is very common to detect signals (broadband and single tone) that are not easily classified as geophysical, meteorological, cryogenic, or biological and that may have characteristics of all three. One aspect that is of tremendous aid in evaluating the source mechanism of a given signal is to determine the location of the source (e.g., seafloor or water column, fault line or seamount, ice edge or open ocean). Having the ability to estimate the location, or at least the direction, of the acoustic source will greatly aid in determining the nature of the source. To achieve this capability may require having multiple sensors (separated by a short distance proportional to the wavelength of signals to be recorded), or employing a single vector hydrophone to derive signal directionality. Indeed, employing vector sensors for directionality may help differentiate between noise generated by the lander and actual environmental signals. However, because of design complications associated with a vector sensor (added weight, need for a compass, and three-axis accelerometer), it would still seem best to use either a single hydrophone sensor element or potentially employ two to three hydrophones on the lander. Further detailed discussions on (1) signal identification and classification algorithms, (2) data transmission considerations from Titan to Earth, and (3) planetary protection tests (spaceflight shock and vibration) needed for a hydrophone system to be included on a Europa/Enceladus lander or Titan saildrone are presented in the online supplementary material.

SUMMARY

We presented an overview of hydrophone sensor systems and signal processing techniques developed for underwater acoustic research on Earth and described

how these sound sensing technologies might be used to explore ocean and surface sea worlds in the outer solar system. Passive acoustic recording and processing electronics that have been built for deep-sea mobile platforms (Matsumoto et al., 2011, 2013) could be adapted to survive spaceflight and yet retain the high performance and extremely low power requirements of an ocean worlds exploration mission. The hydrophone, microprocessor, and system electronics will also need to withstand the thermal sterilization required under NASA's planetary protection requirements. Both of these hydrophone designs could be tested in deep-ocean conditions on Earth by lowering the instrument to 1,300 m, equivalent to ~10 km depth on Europa and ~120 km depth on Enceladus, sufficient for exploration beneath the ice shell on these worlds. The Titan hydrophone would need to be tested in an LN₂ tank, a proxy for the thermal conditions of Titan's seas.

The acoustic monitoring system proposed here could be a candidate for a Europa or Enceladus mission that would seek a means to enter fluid oceans, via

either cracks or melting through the ice shell. The Europa/Enceladus oceans should be dominated by cryogenic sounds from the ice shell and geophysical sound sources generated in the sub-ocean lithic crust. An under-ice hydrophone should have a much better chance of detecting acoustic signals from a sub-ocean volcano-tectonic source than seismometers on the ice shell surface. However, passive acoustic systems might best be used for a near-term mission to a Titan surface sea. The hydrophone sensor could be deployed on a tether, or possibly use a winch system to deploy a hydrophone array some distance from a vehicle. Previous studies (e.g., Arvelo and Lorenz, 2013; Lopes et al., 2013) assert that Titan should have a dynamic undersea soundscape where signals from cryo-volcanic activity, and harmonic tones from fluid flow at hydrothermal vent chimneys, are all potentially detectable sources of sound.

An accepted possible scenario for life to thrive on worlds like Europa, Enceladus, and Titan is at hydrothermal fluid springs near seafloor volcanic centers or, as may be the case for Titan, associated with

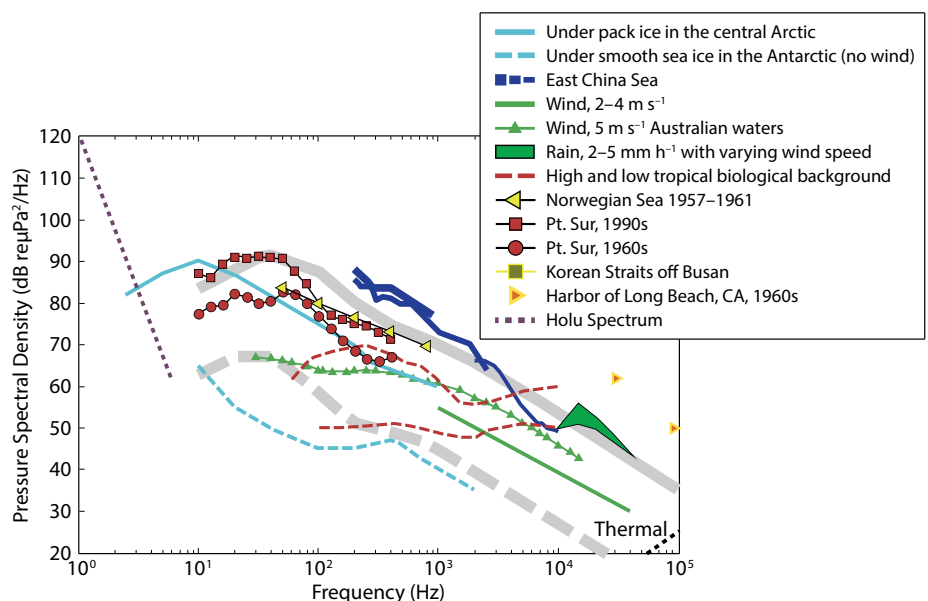


FIGURE 6. Diagram showing various noise spectra from different conditions in Earth's ocean, ranging from under sea ice (quietest) to high sea states and busy shipping channels (noisiest). The red dashed lines indicate high and low biological background noise levels. Predictions of these noise levels on the ocean worlds are preliminary at best, and combined with the variability that may occur from place to place, it is critical that a passive acoustic recording system can dynamically alter gain settings. *After Dahl et al. (2007)*

cold seeps in the shallow seas. These hot/cold springs could provide the energy source for chemosynthetic ecosystems to develop. Thus, one method to find life would be to detect and locate these volcanic centers or cold seep sources using their geophysical acoustic signals, then directly sample the fluids to search for chemical evidence of life. Alternatively, it is not out of the realm of possibility that if extant macro-life has evolved on these ocean worlds, it may also produce some sort of detectable acoustic signal.

Our goal was to describe methods on how to design and protect a passive acoustic monitoring and signal detection system for the rigors of spaceflight and planetary exploration. We think it may be achievable with the methods outlined here. 

ONLINE SUPPLEMENTARY MATERIALS

The supplementary materials are available online at <https://doi.org/10.5670/oceanog.2020.221>.

REFERENCES

- Arvelo, J., and R. Lorenz. 2013. Plumbing the depths of Ligeia: Considerations for depth sounding in Titan's hydrocarbon seas. *Journal of the Acoustical Society of America* 134:4335, <https://doi.org/10.1121/1.4824908>.
- Au, W.W.L., A.N. Popper, and R.R. Fay. 2000. *Hearing by Whales and Dolphins*. Springer-Verlag, New York, 485 pp.
- Baumgartner, M.F., J. Bonnell, S.M. Van Parijs, P.J. Corkeron, C. Hotchkiss, K. Ball, L.P. Pelletier, J. Partan, D. Peters, J. Kemp, and others. 2019. Persistent near real-time passive acoustic monitoring for baleen whales from a moored buoy: System description and evaluation. *Methods in Ecology and Evolution* 10(9):1476–1489, <https://doi.org/10.1111/2041-210X.13244>.
- Bohnenstiehl, D.R., A. Lillis, and D.B. Eggleston. 2016. The curious acoustic behavior of estuarine snapping shrimp: Temporal patterns of snapping shrimp sound in sub-tidal oyster reef habitat. *PLOS ONE* 11(1):e0143691, <https://doi.org/10.1371/journal.pone.0143691>.
- Cadek, O., G. Tobie, T. Van Hoolst, M. Massé, G. Choblet, A. Lefèvre, G. Mitri, R.-M. Baland, M. Behoukova, O. Bourgeois, and A. Trinh. 2016. Enceladus's internal ocean and ice shell constrained from Cassini gravity, shape, and libration data. *Geophysical Research Letters* 42(11):5,653–5,660, <https://doi.org/10.1002/2016GL068634>.
- Caplan-Auerbach, J., R.P. Dziak, J. Haxel, D.R. Bohnenstiehl, and C. Garcia. 2017. Explosive processes during the 2015 eruption of Axial Seamount, as recorded by seafloor hydrophones. *Geochemistry, Geophysics, Geosystems* 18(4):1761–1774, <https://doi.org/10.1002/2016GC006734>.
- Choblet, G., G. Tobie, C. Sotin, M. Behoukova, O. Cadek, F. Postberg, and O. Soucek. 2017. Powering prolonged hydrothermal activity inside Enceladus. *Nature Astronomy* 1:841–847, <https://doi.org/10.1038/s41550-017-0289-8>.
- Chyba, C.F., and C.B. Phillips. 2001. Possible ecosystems and the search for life on Europa. *Proceedings of the National Academy of Sciences of the United States of America* 98(3):801–804, <https://doi.org/10.1073/pnas.98.3.801>.
- COLDTech. 2016. Concepts for Ocean Life Detection, NASA Research Announcement in Space and Earth Sciences, ROSES-2016, <https://nspires.nasaprs.com>.
- Cordier, D., O. Mousis, J.I. Lunine, P. Lavvas, and V. Vuitton. 2009. An estimate of the chemical composition of Titan's lakes. *The Astrophysical Journal Letters* 707(2):L128–L131, <https://doi.org/10.1088/0004-637X/707/2/L128>.
- Cordier, D., F. Garcia-Sanchez, D.N. Justo-Garcia, and G. Liger-Belair. 2017. Bubble streams in Titan's seas as a product of liquid N₂ + CH₄ + C₂H₆ cryogenic mixture. *Nature Astronomy* 1:0102, <https://doi.org/10.1038/s41550-017-0102>.
- Crone, T.J., W.S.D. Wilcock, A.H. Barclay, J.D. Parsons. 2006. The sound generated by mid-ocean ridge black smoker hydrothermal vents. *PLOS ONE* 1(1):e133, <https://doi.org/10.1371/journal.pone.0000133>.
- Dahl, P.H., J.H. Miller, D.H. Cato, and R.K. Andrew. 2007. Underwater ambient noise. Pp. 23–33 in *Acoustics Today*, January 2007.
- Dougherty, M.K., K.K. Khurana, F.M. Neubauer, C.T. Russell, J. Saur, J.S. Leisner, and M.E. Burton. 2006. Identification of a dynamic atmosphere at Enceladus with the Cassini Magnetometer. *Science* 311(5766):1,406–1,409, <https://doi.org/10.1126/science.1120985>.
- Dziak, R.P., J.H. Haxel, D.R. Bohnenstiehl, W.W. Chadwick Jr., S.L. Nooner, M.J. Fowler, H. Matsumoto, and D.A. Butterfield. 2012. Seismic precursors and magma ascent before the April 2011 eruption at Axial Seamount. *Nature Geoscience* 5:478–482, <https://doi.org/10.1038/ngeo1490>.
- Dziak, R.P., D.R. Bohnenstiehl, K.M. Stafford, H. Matsumoto, M. Park, W.S. Lee, M.J. Fowler, T.-K. Lau, J.H. Haxel, and D.K. Mellinger. 2015. Sources and levels of ambient ocean sound near the Antarctic Peninsula. *PLOS ONE* 10(4):e0123425, <https://doi.org/10.1371/journal.pone.0123425>.
- Dziak, R.P., J.H. Haxel, H. Matsumoto, T.-K. Lau, S. Heimlich, S. Nieuwkerk, D. K. Mellinger, J. Osse, C. Meinig, N. Delich, and S. Stalín. 2017. Ambient sound at Challenger Deep, Mariana Trench. *Oceanography* 30(2):186–197, <https://doi.org/10.5670/oceanog.2017.240>.
- Dziak, R.P., H. Matsumoto, R.W. Embley, S.G. Merle, T.-K. Lau, T. Baumberger, S.R. Hammond, and N. Rainault. 2018. Passive acoustic records of seafloor methane bubble streams on the Oregon continental margin. *Deep Sea Research Part II* 150:210–217, <https://doi.org/10.1016/j.dsr2.2018.04.001>.
- Erbe, C., and A.R. King. 2008. Automatic detection of marine mammals using information entropy. *Journal of the Acoustical Society of America* 124:2,833–2,840, <https://doi.org/10.1121/1.2982368>.
- Fregosi, S., D.V. Harris, H. Matsumoto, D.K. Mellinger, C. Negretti, D.J. Moretti, S.W. Martin, B. Matsuyama, P.J. Dugan, and H. Klinck. 2020. Comparison of fin whale 20 Hz call detections by deep-water mobile autonomous and stationary recorders. *Journal of the Acoustical Society of America* 147:961, <https://doi.org/10.1121/10.0000617>.
- Hartwig, J.W., A. Colozza, R.D. Lorenz, S. Oleson, G. Landis, P. Schmitz, M. Paul, and J. Walsh. 2016. Exploring the depths of Kraken Mare—Power, thermal analysis, and ballast control for the Saturn Titan submarine. *Cryogenics* 74:31–46, <https://doi.org/10.1016/j.cryogenics.2015.09.009>.
- Hayes, A.G. 2016. The lakes and seas of Titan. *Annual Review of Earth and Planetary Science* 44:57–83, <https://doi.org/10.1146/annurev-earth-060115-012247>.
- Hemingway, D., F. Nimmo, H. Zebkar, and L. Less. 2013. A rigid and weathered ice shell on Titan. *Science* 500(7464):550–442, <https://doi.org/10.1038/nature12400>.
- Hood, J., D.G. Fløgera, and J.A. Theriault. 2016. Improved passive acoustic band-limited energy detection for cetaceans. *Applied Acoustics* 106:36–41, <https://doi.org/10.1016/j.apacoust.2015.12.011>.
- Hofgartner, J.D., A.G. Hayes, J.I. Lunine, H. Zebkar, B.W. Stiles, C. Sotin, J.W. Barnes, E.P. Turtle, K.H. Baines, R.H. Brown, and others. 2014. Transient features in a Titan sea. *Nature Geoscience* 7:493–496, <https://doi.org/10.1038/ngeo2190>.
- Less, L., R.A. Jacobson, M. Ducci, D.J. Stevenson, J.I. Lunine, J.W. Armstrong, S.W. Asmar, P. Racioppa, N.J. Rappaport, and P. Tortora. 2012. The tides of Titan. *Science* 337(6093):457–459, <https://doi.org/10.1126/science.1219631>.
- Johnson, H.P., U.K. Miller, M.S. Salmi, and E.A. Solomon. 2015. Analysis of bubble plume distributions to evaluate methane hydrate decomposition on the continental slope. *Geochemistry, Geophysics, Geosystems* 16:3,825–3,839, <https://doi.org/10.1002/2015GC005955>.
- Keenan, R.E., and L.R.L. Merriam. 1991. Arctic abyssal T phases: Coupling seismic energy to the ocean sound channel via under ice scattering. *Journal of the Acoustical Society of America* 89:128, <https://doi.org/10.1121/1.400648>.
- Klein, F.W., R.Y. Koyanagi, J.S. Nakata, and W.R. Tanigawa. 1987. The seismicity of Kilauea's magma system. Pp. 1,019–1,186 in *Volcanism in Hawaii: Papers to Commemorate the 75th Anniversary of the Founding of the Hawaiian Volcano Observatory*. R.W. Decker, T.L. Wright, and P.H. Stauffer, eds. US Geological Survey Professional Paper 1350.
- Klinck, H., and D.K. Mellinger. 2011. The energy ratio mapping algorithm: A tool to improve the energy-based detection of odontocete echolocation clicks. *Journal of the Acoustical Society of America* 129:1,807–1,812, <https://doi.org/10.1121/1.3531924>.
- Klinck, H., D.K. Mellinger, K. Klinck, N.M. Bogue, J.C. Luby, W.A. Jump, G.B. Shilling, T. Litchendorf, A.S. Wood, G.S. Schorr, and R.W. Baird. 2012. Near-real-time acoustic monitoring of beaked whales and other cetaceans using a Seaglider. *PLOS ONE* 7(5):e36128, <https://doi.org/10.1371/journal.pone.0036128>.
- Lee, S., M. Zanolin, A.M. Thode, R.T. Pappalardo, and N.C. Makris. 2003. Probing Europa's interior with natural sound sources. *Icarus* 165:144–167, [https://doi.org/10.1016/S0019-1035\(03\)00150-7](https://doi.org/10.1016/S0019-1035(03)00150-7).
- Leifer, I., and D. Tang. 2007. The acoustic signature of marine seep bubbles. *Journal of the Acoustical Society of America* 121(1), <https://doi.org/10.1121/1.2401227>.
- Leighton, T.G., P.R. White, and D.C. Finfer. 2013. The opportunities and challenges in the use of extra-terrestrial acoustics in the exploration of the oceans of ice planetary bodies. *Earth, Moon, and Planets* 109:91116, <https://doi.org/10.1007/s11038-012-9399-6>.
- Lopes, R.M.C., R.L. Kirk, K.L. Mitchell, A. LeGall, J.W. Barnes, A. Hayes, J. Kargel, L. Wye, J. Radebaugh, E.R. Stofan, and others. 2013. Cryovolcanism on Titan: New results from Cassini RADAR and VIMS. *Journal of Geophysical Research* 118:416–435, <https://doi.org/10.1002/jgre.20062>.
- Lorenz, R.D., T. Tokano, and C. Newman. 2012. Winds and tides of Ligeia Mare, with application to the drift of the proposed TiME (Titan Mare Explorer) capsule. *Planetary and Space Science* 60:72–85, <https://doi.org/10.1016/j.pss.2010.12.009>.
- Lorenz, R.D. 2014. The flushing of Ligeia: Composition variations across Titan's seas in a simple hydrological model. *Geophysical Research Letters* 41(16):5,764–5,770, <https://doi.org/10.1002/2014GL061133>.

- Lorenz, R.D., and J.L. Mann. 2015. Seakeeping on Ligeia Mare: Dynamic response of a floating capsule to waves on the hydrocarbon seas of Saturn's moon Titan. *John's Hopkins/APL Technical Digest* 33(2), <https://www.jhuapl.edu/Content/techdigest/pdf/V33-N02/33-02-Lorenz.pdf>.
- Lorenz, R.D., S.R. Oleson, A.J. Colozza, R. Jones, T. Packard, J. Hartwig, J.M. Newman, J.Z. Gyekenyesi, P. Schmitz, and J. Walsh. 2018. Exploring Titan's cryogenic hydrocarbon seas with boat deployed expendable dropsondes. *Advances in Space Research* 62(4):912–920, <https://doi.org/10.1016/j.asr.2018.05.030>.
- Lunine, J.I. 2017. Ocean worlds exploration. *Acta Astronautica* 131:123–130, <https://doi.org/10.1016/j.actaastro.2016.11.017>.
- Ma, B.B., and J.A. Nystuen. 2005. Passive acoustic detection and measurement of rainfall at sea. *Journal of Atmospheric and Oceanic Technology* 22:1,225–1,248, <https://doi.org/10.1175/JTECH1773.1>.
- MacAyeal, D.R., E.A. Okal, R. Aster, and J.N. Bassis. 2008. Seismic and hydroacoustic tremor generated by colliding icebergs. *Journal of Geophysical Research* 113(F3), <https://doi.org/10.1029/2008jf001005>.
- Mastrogioseppe, M., V. Poggiali, A. Hayes, R. Lorenz, J. Lunine, G. Picardi, R. Seu, E. Flamini, G. Mitri, P. Paillou, and H. Zebker. 2014. The bathymetry of a Titan sea. *Geophysical Research Letters* 41:1,432–1,437, <https://doi.org/10.1002/2013GL058618>.
- Mastrogioseppe, M., V. Poggiali, A.G. Hayes, J.I. Lunine, R. Seu, G. Mitri, and R.D. Lorenz. 2019. Deep and methane-rich lakes on Titan. *Nature Astronomy* 3:535–542, <https://doi.org/10.1038/s41550-019-0714-2>.
- Matsumoto, H., D.R. Bohnenstiehl, J.H. Haxel, R.P. Dziak, and R.W. Embley. 2011. Mapping the sound field of an erupting submarine volcano using an acoustic glider. *Journal of the Acoustical Society of America* 129(3), <https://doi.org/10.1121/1.3547720>.
- Matsumoto, H., C. Jones, H. Klinck, D.K. Mellinger, R.P. Dziak, and C. Meinig. 2013. Tracking beaked whales with a passive acoustic profiler float. *Journal of the Acoustical Society of America* 133:731–740, <https://doi.org/10.1121/1.4773260>.
- McCarthy, C., K.L. Craft, C.R. German, M.V. Jakuba, R.D. Lorenz, G.W. Patterson, and A. Rhoden. 2019. Europa STI: Exploring communication techniques and strategies for sending signals through the Ice (STI) for an Ice-Ocean probe. *Ocean Worlds 2019*, May 21–22, Columbia, Maryland, Contribution No. 2168 (extended abstract).
- McCord, T.B., and G.B. Hansen. 1998. Salts on Europa's surface detected by Galileo's near infrared mapping spectrometer. *Science* 280(5367):1,242–1,245, <https://doi.org/10.1126/science.280.5367.1242>.
- McGrath, M.A., C.J. Hansen, and A.R. Hendrix. 2009. Observations of Europa's tenuous atmosphere. Pp. 485–506 in *Europa*. R.T. Pappalardo, W.B. McKinnon, and K. Khurana, eds, University of Arizona Press.
- Meinig, C., E.F. Burger, N. Cohen, E.D. Cokelet, M.F. Cronin, J.N. Cross, S. de Halleux, R. Jenkins, A.T. Jessup, C.W. Mordy, and others. 2019. Public-private partnerships to advance regional ocean observing capabilities: A saildrone and NOAA-PMEL case study and future considerations to expand to global scale observing. *Frontiers in Marine Science* 6:448, <https://doi.org/10.3389/fmars.2019.00448>.
- Mellinger, D.K., M.A. Roch, E.M. Nosal, and H. Klinck. 2016. Signal Processing. Pp. 359–411 in *Listening in the Ocean*. W.W.L. Au and M.O. Lammers, eds, Springer, New York.
- Melosh, H.J., A.G. Ekholm, A.P. Showman, and R.D. Lorenz. 2004. The temperature of Europa's subsurface water ocean. *Icarus* 168:498–502, <https://doi.org/10.1016/j.icarus.2003.11.026>.
- Merchant, N.D., T.R. Barton, P.M. Thompson, and E. Pirotta. 2013. Spectral probability density as a tool for ambient noise analysis. *Journal of the Acoustical Society of America* 133:EL262, <https://doi.org/10.1121/1.4794934>.
- Mitri, G., A.P. Showman, J.I. Lunine, and R.D. Lorenz. 2007. Hydrocarbon lakes on Titan. *Icarus* 186(2):385–394, <https://doi.org/10.1016/j.icarus.2006.09.004>.
- Niemann, H.B., S.K. Atreya, S.J. Bauer, G.R. Carignan, J.E. Demick, R.L. Frost, D. Gautier, J.A. Haberman, D.N. Harpold, D.M. Hunten, and others. 2005. The abundances of constituents of Titan's atmosphere from the GCMS instrument on the Huygens probe. *Nature* 438(7069):779–784, <https://doi.org/10.1038/nature04122>.
- Nimmo, F., B. Giese, and R.T. Pappalardo. 2003. Estimates of Europa's ice shell thickness from elastically supported topography. *Geophysical Research Letters* 30(5), <https://doi.org/10.1029/2002GL016660>.
- Nimmo, F., and R.T. Pappalardo. 2016. Ocean worlds in the outer solar system. *Journal of Geophysical Research* 121(8):1,378–1,399, <https://doi.org/10.1002/2016JE005081>.
- Panning, M., V. Lekic, M. Manga, F. Cammarano, and B. Romanowicz. 2006. Long-period seismology on Europa: Part 2. Predicted seismic response. *Journal of Geophysical Research* 111(E12), <https://doi.org/10.1029/2006JE002712>.
- Pappalardo, R.T., M.J.S. Belton, H.H. Breneman, M.H. Carr, C.R. Chapman, G.C. Collins, T. Denk, S. Fagents, P.E. Geissler, B. Giese, and others. 1999. Does Europa have a subsurface ocean? Evaluation of the geological evidence. *Journal of Geophysical Research* 104:24,015–24,055, <https://doi.org/10.1029/1998JE000628>.
- Podolskiy, E.A., and F. Walter. 2016. Cryoseismology. *Review of Geophysics* 54:708–758, <https://doi.org/10.1002/2016RG000526>.
- Postberg, F., N. Kawajia, B. Abel, G. Choblet, C.R. Glein, M.S. Gudipati, B.L. Henderson, H.-W. Hsu, S. Kempf, F. Klenner, and others. 2018. Macromolecular organic compounds from the depths of Enceladus. *Nature* 558:564–568, <https://doi.org/10.1038/s41586-018-0246-4>.
- Royer, J.-Y., R. Chateau, R.P. Dziak, and D.R. Bohnenstiehl. 2015. Seafloor seismicity, Antarctic ice-sounds, cetacean vocalizations and long-term ambient sound in the Indian Ocean basin. *Geophysical Journal International* 202:748–762, <https://doi.org/10.1093/gji/ggv178>.
- Schmitz, W.J. Jr., and M.S. McCartney. 1993. On the North Atlantic Circulation *Reviews of Geophysics* 31(1):29–49, <https://doi.org/10.1029/92RG02583>.
- Schubert, G., J.D. Anderson, T. Spohn, and W.B. McKinnon. 2004. Pp. 263–280 in *Jupiter: The Planet, Satellites and Magnetosphere*. F. Bagenal, T.E. Dowling, and W.B. McKinnon, eds, Cambridge University Press.
- Smith-Konter, B., and R.T. Pappalardo. 2008. Tidally driven stress accumulation and shear failure of Enceladus's tiger stripes. *Icarus* 198:435–451, <https://doi.org/10.1016/j.icarus.2008.07.005>.
- Stofan, E., C. Elachi, J.I. Lunine, R.D. Lorenz, B. Stiles, K.L. Mitchell, S. Ostro, L. Soderblom, C. Wood, H. Zebker, and others. 2007. The lakes of Titan. *Nature* 445:61–64, <https://doi.org/10.1038/nature05438>.
- Stofan, E.C., R. Lorenz, J. Lunine, E.B. Bierhaus, B. Clark, P.R. Mahaffy, and M. Ravine. 2013. TIME—The Titan Mare Explorer. 2013 *IEEE Aerospace Conference*, March 2–9, AERO, 2013.6497165, <https://doi.org/10.1109/AERO.2013.6497165>.
- Talandier, J., O. Hyvernaud, E.A. Okal, and P.F. Piserchia. 2002. Long range detection of hydroacoustic signals from large icebergs in the Ross Sea, Antarctica. *Earth and Planetary Science Letters* 203:519–534, [https://doi.org/10.1016/s0012-821x\(02\)00867-1](https://doi.org/10.1016/s0012-821x(02)00867-1).
- Towner, M.C., J.R.C. Garry, R.D. Lorenz, A. Hagermann, B. Hathi, H. Svedhem, B.C. Clark, M.R. Leese, and J.C. Zarnecki. 2006. Physical properties of Titan's surface at the Huygens landing site from the Surface Science Package Acoustic Properties sensor (API-S). *Icarus* 185:457–465, <https://doi.org/10.1016/j.icarus.2006.07.013>.
- Vance, S., J. Harmmeijer, J. Kimura, H. Hussmna, B. deMartin, and J.M. Brown. 2007. Hydrothermal systems in small ocean planets. *Astrobiology* 7(6), <https://doi.org/10.1089/ast.2007.0075>.
- Vance, S.D., M.P. Panning, S. Stähler, F. Cammarano, B.G. Bills, G. Tobie, S. Kamata, S. Kedar, C. Sotin, W.T. Pike, and others. 2017. Geophysical investigations of habitability in ice-covered ocean worlds. *Journal of Geophysical Research* 123(1):180–205, <https://doi.org/10.1002/2017JE005341>.
- Vance, S.D., S. Kedar, M.P. Panning, S.C. Stähler, B.G. Bills, R.D. Lorenz, H.-H. Huang, W.T. Pike, J.C. Castillo, P. Lognonné, and others. 2018. Vital signs: Seismology of icy ocean worlds. *Astrobiology* 18(1), <https://doi.org/10.1089/ast.2016.1612>.

ACKNOWLEDGMENTS

The authors wish to thank the editor and two anonymous reviewers for their very helpful comments. Thanks also to D. Butterfield for perspectives on the oxygen requirements of chemosynthetic life. The research in this paper was sponsored by the NOAA/Pacific Marine Environmental Laboratory, PMEL paper contribution number 5086. All data are available from the authors upon request, without undue reservation, to any qualified researcher.

AUTHORS

Robert Dziak (robert.p.dziak@noaa.gov) is Acoustics Program Manager, NOAA/Pacific Marine Environmental Laboratory (PMEL), Newport, OR, USA. **Don Banfield** is Principal Research Scientist, Cornell Center for Astrophysics and Planetary Science, Cornell University, Ithaca, NY, USA. **Ralph Lorenz** is Planetary Scientist, Applied Physics Laboratory, Johns Hopkins University, Baltimore, MD, USA. **Haruyoshi Matsumoto** is Research Associate, Cooperative Institute for Marine Resources Studies, Oregon State University, Newport, OR, USA. **Holger Klinck** is Director, Center for Conservation Bioacoustics, Cornell Lab of Ornithology, Cornell University, Ithaca, NY, USA. **Richard Dissly** is Advanced Systems Manager for Solar System Exploration, Ball Aerospace & Technologies Corporation, Boulder, CO, USA. **Christian Meinig** is Director, Engineering Development Division, NOAA/PMEL, Seattle, WA, USA. **Brian Kahn** is Computer Systems Manager, Cooperative Institute for Marine Resources Studies, Oregon State University, Newport, OR, USA.

ARTICLE CITATION

Dziak, R., D. Banfield, R. Lorenz, H. Matsumoto, H. Klinck, R. Dissly, C. Meinig, and B. Kahn. 2020. Deep ocean passive acoustic technologies for exploration of ocean and surface sea worlds in the outer solar system. *Oceanography* 33(2):144–155, <https://doi.org/10.5670/oceanog.2020.221>.

COPYRIGHT & USAGE

This is an open access article made available under the terms of the Creative Commons Attribution 4.0 International License (<https://creativecommons.org/licenses/by/4.0/>), which permits use, sharing, adaptation, distribution, and reproduction in any medium or format as long as users cite the materials appropriately, provide a link to the Creative Commons license, and indicate the changes that were made to the original content.

The Pressure of In Situ Gases Instrument (PIGI) for Autonomous Shipboard Measurement of Dissolved O₂ and N₂ in Surface Ocean Waters

By Robert W. Izett and Philippe D. Tortell

ABSTRACT. We describe an autonomous flow-through system capable of continuous, unattended measurements of oxygen (O₂) and nitrogen (N₂) concentrations in surface seawater. The derived biological O₂ saturation anomaly, $\Delta\text{O}_2/\text{N}_2$, can be used to estimate mixed-layer net community production (NCP) in place of $\Delta\text{O}_2/\text{Ar}$ -based estimates obtained via mass spectrometry. Our Pressure of In situ Gases Instrument (PIGI) consists of two parallel flow-through chambers: the first contains a buoyancy-driven debubbler, and the second houses an Aanderaa optode and Pro-Oceanus gas tension device (GTD). Custom-designed software is provided to visualize and record observations in real time and to post-process data. The system has been tested in the laboratory and on more than 15 deployments in various ocean regions. The PIGI has average optode and GTD response times of ~ 1.1 min and 1.6 min, respectively; it shows good calibrated accuracy based on comparisons with discrete samples; and the derived $\Delta\text{O}_2/\text{N}_2$ exhibits strong coherence with independent $\Delta\text{O}_2/\text{Ar}$ measurements from mass spectrometry. We conclude with recommendations for successful field use and potential future modifications to support a range of deployments strategies. Overall, the system can be used as a cost-effective tool for increasing global coverage of NCP estimates from research vessels, volunteer observing ships, and land-based observatories.

BACKGROUND

Marine net community production (NCP; i.e., photosynthesis minus respiration) is a critical ecological variable that constrains the ocean's capacity for biomass production and carbon export via the biological pump. Ocean metabolism is reflected in surface O₂ variability, such that NCP can be estimated from in situ O₂ measurements obtained along ship tracks, at fixed sites, and on autonomous profilers (e.g., Kaiser et al., 2005; Emerson et al., 2008; Yang et al., 2017). However, physical processes, including temperature-dependent solubility changes and bubble injection, also influence O₂ budgets, and these effects can bias NCP estimates.

For this reason, underway ship-based measurements of biological O₂ saturation anomalies ($\Delta\text{O}_2/\text{Ar}$) have become increasingly common as tracers of mixed-layer NCP, where argon (Ar) is a biologically inert O₂ analog that corrects for physically induced changes in gas saturation states (Craig and Hayward, 1987).

Presently, underway measurements of $\Delta\text{O}_2/\text{Ar}$ are obtained using ship-based mass spectrometry, and this technique has yielded many important data sets. Yet, these instruments may be cost-prohibitive for some researchers and require significant power and operator oversight, making mass spectrometry poorly suited for long-term data

collection without significant support infrastructure. This limits the capacity for truly autonomous NCP derivation from underway platforms and volunteer observing ships (VOS). Recent technological advances in O₂ optodes and gas tension devices (GTDs; Tengberg et al., 2006; Reed et al., 2018) have enabled high-resolution, unattended measurements of seawater O₂ and N₂ (McNeil et al., 2005). Ongoing work by our group has evaluated the potential to estimate NCP from O₂/N₂ ratios (i.e., $\Delta\text{O}_2/\text{N}_2$) in a manner analogous to $\Delta\text{O}_2/\text{Ar}$ (manuscripts in preparation). Although the solubility properties of N₂ and O₂ somewhat differ, and N₂ is subject to minor biological influences (e.g., N₂-fixation), $\Delta\text{O}_2/\text{N}_2$ approximates $\Delta\text{O}_2/\text{Ar}$ under many conditions. Oxygen and N₂ measurements have been combined to infer gas dynamics (Zhou et al., 2014; Tortell et al., 2015) and NCP from refined O₂ budgets (Emerson et al., 2019), but NCP derivation from underway $\Delta\text{O}_2/\text{N}_2$ remains largely underexploited. The development of a robust system for continuous O₂/N₂ measurement thus has the potential to significantly expand oceanic NCP estimates.

In this article, we describe a system for autonomous, flow-through O₂/N₂ measurements. We provide an overview of this system, named PIGI (Pressure of In situ Gases Instrument), with validation

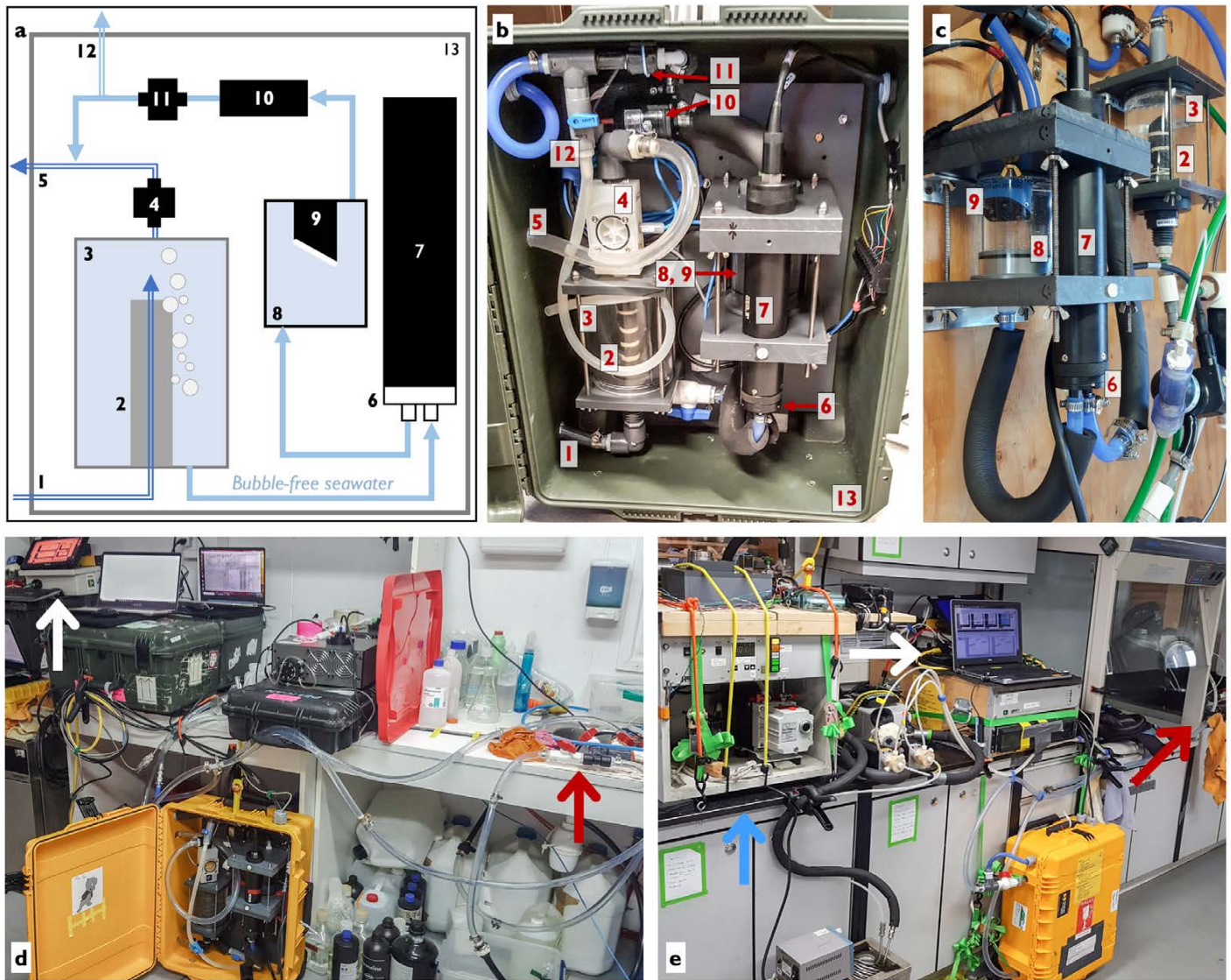


FIGURE 1. A schematic (a) and photographs (b–e) of the flow-through Pressure of In situ Gases Instrument (PIGI) system. Panels (b), (d), and (e) show the system installed in a Pelican case, while (c) shows a wall-mounted version at the Hakai Institute’s Quadra Island Ecological Observatory. Seawater flow paths are represented by blue lines in (a). Labeled parts in (a)–(c) are: system inflow (1), debubbler (2), primary chamber (3), primary chamber flowmeter (4), system outflow (5), TDGP (total dissolved gas pressure)-mini plenum (6), TDGP-mini GTD (gas tension device) (7), optode chamber (8), optode (sensing foil shown in white) (9), centrifugal pump (10), instruments flowmeter (11), discrete sampling line (12), and Pelican case (13). Not all components are shown in (c). PIGI deployments at Base Prat, Antarctica, and on CCGS *Amundsen* are shown in (d) and (e), respectively. The white and red arrows show the locations of the electronics box and the seawater supply. The blue arrow in (e) points to a membrane inlet mass spectrometry (MIMS) system.

results from field deployments and laboratory testing, followed by recommendations for successful field use. Detailed assembly, deployment, and data processing instructions are available in the online supplementary materials.

SYSTEM OVERVIEW

The PIGI is an autonomous measurement system consisting of an electronics box and a flow-through wet box connected to a continuous seawater supply. The wet box (Figure 1) comprises a pri-

mary chamber (~600 mL) containing a custom-built buoyancy-driven debubbler and an instrument loop containing an Aanderaa Data Instruments Optode 4330 (standard sensing foil) and a Pro-Oceanus Systems Inc. mini-TDGP (total dissolved gas pressure) GTD. Seawater entering the system from the ship’s supply first passes through the debubbler to minimize measurement contamination by trapped air. Bubble-free water is then pulled from the primary chamber and past the gas sensors using a centrifugal pump installed

downstream of the instruments.

In the instrument loop, seawater first passes the GTD sensing membrane through a manufacturer-supplied plenum before entering a flow-through cell (~250 mL) containing the optode. Best results (i.e., reduced data noise and optimal instrument response times) are obtained when seawater flows directly onto the sensing faces. Water exiting both chambers merges to form a single outflow line, and check valves are installed to prevent recirculation or drainage of the

centrifugal pump head. Discrete calibration samples can be obtained via a separate line at the outflow of the instrument loop. Flow measurements from both chambers facilitate system monitoring and quality control. Flow rates through the instrument loop should be held constant within 10% of a nominal value, with target rates of $\sim 1.5\text{--}3\text{ L min}^{-1}$ providing optimal data quality.

The wet box components can be mounted directly onto a wall or grating (Figure 1c) or installed on a baseplate secured within a Pelican case (Figure 1b) for protection and easy transport. In either configuration, the system can be disassembled for easy cleaning (see supplemental video) and should be oriented vertically (intake at bottom) so that entrained bubbles escape via the top of the primary chamber (Figure 1a).

The electronics box (Figure S1) runs LabVIEW and AutoIt programs to automate data acquisition and instrument control. AutoIt is used to restart data collection at user-defined intervals.

The LabVIEW program (Figure 2) displays and logs data at a frequency of up to 1 Hz and automatically turns off the instrument's pump to prevent damage during interruptions of seawater flow to the system (e.g., during sea ice blockages). Uncalibrated gas signals (optode O_2 and GTD total dissolved gas pressure), ancillary measurements (temperature and flow rates), and raw sensor signals (e.g., optode phase shift) are saved to a continuously updated ASCII file. Deployment metadata and instrument settings are logged separately at the beginning of each acquisition. The LabVIEW program interfaces with the instruments (e.g., turn pump on/off, set sampling rate), acquires ship GPS information, and performs satellite data transmissions during remote deployments with an optional Iridium transducer module. Data acquisition software and post-processing MATLAB scripts (details in the online supplementary materials) are provided at https://github.com/rizett/PIGI_system.

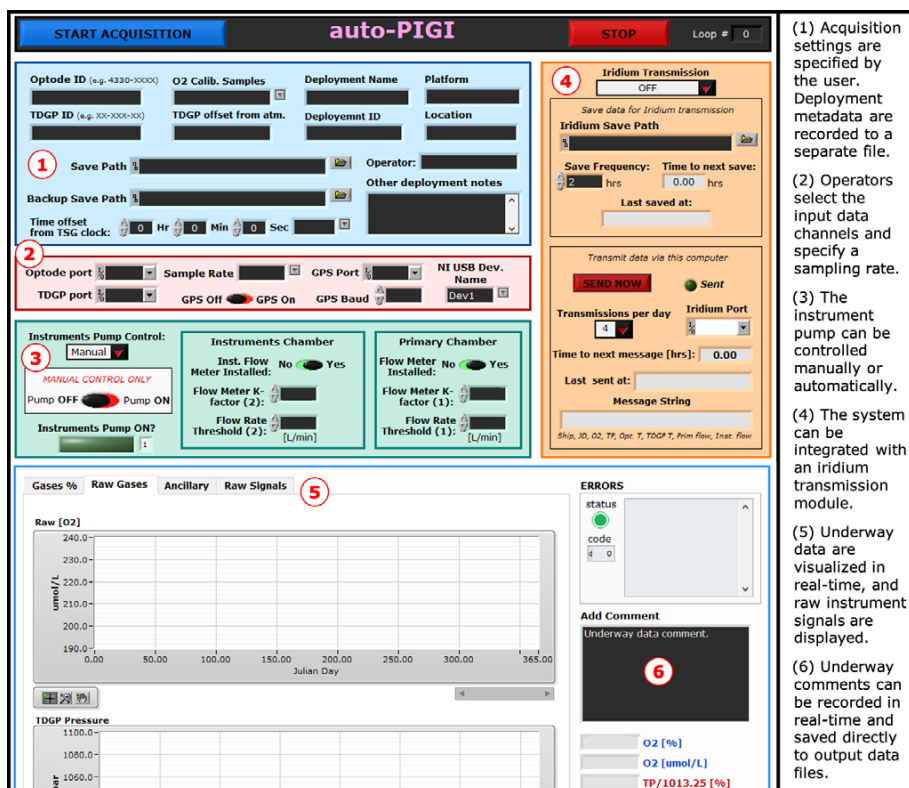
MATERIALS AND COSTS

The PIGI system can be constructed from readily available materials with relatively basic knowledge of electronic systems. The components of the flow-through chambers are machined from durable PVC and acrylic. Detailed technical drawings and assembly instructions are provided in the online supplementary materials and at <https://seawize.weebly.com/pigi-system.html> (refer to this website for potential future updates). The electronics box contains an Intel Nuc mini-processor, data acquisition board, DC relays, and power supplies. Table 1 summarizes component expenses, and Table S1 provides a comprehensive parts list (including recommended suppliers). Notably, the cost of the optode and GTD sensors (combined $< \$12,000$ US) is significantly less than the cost of a mass spectrometer.

Our system consists of an Aanderaa Optode 4330 and Pro-Oceanus TDGP-mini, but other sensors, such as units Aanderaa designed for shallow water deployments (e.g., models 4531 or 4835; $\sim \$2,700$ and $\$4,775$ US, respectively) or the RBRcoda T.ODO O_2 sensor package ($\sim \$4,500$ US), can be incorporated with only minor adjustments for cost savings. Although users require a LabVIEW license (Table 1) to modify the software we provide, we have also produced a stand-alone version of the data acquisition program that can be used with the free run-time LabVIEW engine (details in the online supplementary materials). Data may also be acquired or processed using alternative open-source software (e.g., Python, Inlino; Haëntjens and Boss, 2020); the online supplementary materials include a description of the workflow required for autonomous operation.

FIELD APPLICATIONS AND LABORATORY AND IN SITU TESTING

Various iterations of the PIGI system have been tested on 19 field deployments since 2016 (Table 2). Our system has been deployed frequently on La Perouse and Line P cruises in the subarctic Northeast



- (1) Acquisition settings are specified by the user. Deployment metadata are recorded to a separate file.
- (2) Operators select the input data channels and specify a sampling rate.
- (3) The instrument pump can be controlled manually or automatically.
- (4) The system can be integrated with an Iridium transmission module.
- (5) Underway data are visualized in real-time, and raw instrument signals are displayed.
- (6) Underway comments can be recorded in real-time and saved directly to output data files.

FIGURE 2. A screenshot of the PIGI LabVIEW interface. Data are displayed in real time in the figure panels, and comments corresponding with observations can be recorded to the data file in real time.

Pacific, while a second unit has collected data continuously at the Hakai Institute's Quadra Island Ecological Observatory (in British Columbia's Discovery Islands) for over a year (Figure 1). We have deployed a third system throughout the Canadian Arctic and at a coastal station in Antarctica. A fourth unit will be deployed

on a 2021–2022 R/V *Tara* expedition.

During field deployments, the system was evaluated for underway data accuracy, ease-of-use, and integration with existing instrumentation. Salinity-compensated optode O₂ measurements (see below) were calibrated using discrete samples obtained from the PIGI sampling

line (Figure 1) or surface rosette bottles, and analyzed by Winkler titration. We observed linear relationships between sensor and discrete O₂, with offsets in the uncalibrated data typical of Aanderaa optodes whose accuracy decays over time (Bittig et al., 2018). The strong linearity between sensor and discrete data enables calibration with an average accuracy of 1%, which is required for successful field deployments (Emerson et al., 2019). Optode and GTD-derived N₂ also showed strong coherence with discrete Niskin bottle samples analyzed by mass spectrometry and could be validated to within ~1.2%. The GTD signal shows significantly less drift than optode measurements, so routine calibration with mass spectrometry samples may not be necessary. These results are consistent across multiple deployments and demonstrate that PIGI measurements are not biased by sampling artifacts. Moreover, GTD pressure measurements on air-equilibrated freshwater circulated through the PIGI

TABLE 1. Abbreviated list of expenses of the PIGI system. Full details are provided in the online supplementary materials. Costs are based on quotations obtained in June/July 2020 and exclude local taxes, shipping, and machining expenses. The cost of the wet box includes the gas sensors and additional flow-through parts, while the electronics box expenses include a Windows operating system required to run the automation software, which is quoted separately.

COMPONENT	~ COST (USD)
Calibrated Aanderaa Optode 4330 with cable	\$6,750
Pro-Oceanus mini-TDGP GTD with cable	\$5,000
Wet box total	\$13,500
Electronics box total	\$1,650
System total	\$15,150
LabVIEW Base license (optional)	\$400 (1 yr) / \$3,500 (life)
MATLAB license (optional)	\$860 (1 yr) / \$2,150 (life)

TABLE 2. List of PIGI system deployments between 2016 and present. Cruise IDs are included, where available, in the first column. NCP = net community production.

PROGRAM / CRUISE	SHIP	LOCATION	DURATION (DAYS)	PURPOSE
Line P (2016-001) La Perouse (2016-047) Line P (2016-006) Line P (2016-008) Line P (2017-001) La Perouse (2017-005) Line P (2017-006)	CCGS <i>J.P. Tully</i>	Northeast Pacific/ West Coast Vancouver Island	~100 (total)	testing
2018 ArcticNet Amundsen Expedition (1802 and 1803) ¹	CCGS <i>Amundsen</i>	Labrador Sea, Baffin Bay, Canadian Arctic Archipelago	42 (Jul–Sep 2018)	NCP survey, testing
Line P (2017-008) La Perouse (2017-009) La Perouse (2018-039) Line P (2018-026) Line P (2018-040) Line P (2019-001) Line P (2019-006) La Perouse (2019-023)	CCGS <i>J.P. Tully</i> , CCGS <i>Laurier</i>	Northeast Pacific/ West Coast Vancouver Island	>100 (total)	NCP survey
Hakai Institute coastal monitoring	N/A	Quadra Island Ecological Observatory	Jun 2019–present	NCP time series
2019 ArcticNet Amundsen Expedition (1902) ¹	CCGS <i>Amundsen</i>	Baffin Bay, Canadian Arctic Archipelago	43 (Jul–Aug 2019)	NCP survey
W. Antarctic greenhouse gas survey	N/A	Base Prat, Greenwich Island, Antarctica (Chile)	60 (Jan–Mar 2020)	NCP time series

¹ Data available at https://www.polardata.ca/pdcsearch/PDCSearch.jsp?doi_id=13172

trace atmospheric pressure within $\sim 0.1\%$ across multiple instruments and laboratory tests. We thus conclude that our system is able to accurately determine both O_2 and N_2 concentrations in seawater, provided that necessary calibrations are conducted (see below).

We performed laboratory tests to evaluate PIGI response times by circulating water with contrasting gas compositions (air-equilibrated freshwater and a 1:1 solution of carbonated soda and N_2 -bubbled deionized water) through the primary and instrument chambers at various temperatures and flow rates (Figure 3c). We

determined response times (e-folding time, t_{63}) of O_2 and gas tension signals in the PIGI system ranging from ~ 0.9 min to 1.6 min and 1.0 min to 2.2 min, respectively, based on the time when the water source changed until signals restabilized. These response times are similar to those of a membrane inlet mass spectrometry (MIMS) system used to measure O_2/Ar (Tortell, 2005), and thus permit observations of small-scale oceanic features (Figures 3c and 4). Notably, the instrument response times are shorter at higher temperatures and faster flow rates (lower range of error bars in Figure 3c).

The reported response times reflect the time required to flush the wet box chambers and the water residence time within the optode cell. As a result, the optode response in our PIGI system is longer than the manufacturer's specifications (~ 25 sec) or values reported in different systems (e.g., Bittig et al., 2014). Despite this difference, the GTD signal, with a response time similar to the manufacture specification of 1.5 min, still lags behind O_2 (Figure 4a), so that additional data processing is required when encountering very strong frontal features. Nonetheless, our testing demonstrated that flow rates greater than 1.5 L min^{-1} through the instrument loop (water residence times <1 and <10 sec within the GTD plenum and optode chamber, respectively) produce high-quality data with good spatial resolution. Increasing the seawater flow rates should further improve instrument response times.

Testing also showed that inclusion of a debubbler significantly reduced data noise and contamination from bubbles entrained in ships' seawater lines. Bubble effects are particularly problematic during elevated sea states and, to a lesser extent, in calmer conditions if the seawater intake depth is shallow. Commonly used vortex debubblers increase the water residence time in flow-through systems, thereby leading to excess gas dissolution between the seawater intake and the measurement interface. In the PIGI, we thus designed an upward-oriented debubbler that enables rapid escape of bubbles via buoyant rising (Figure 1). The sampling line leading to the optode and the GTD is installed at the bottom of the debubbling chamber so that bubble-free water is drawn toward the sensors. This approach is very effective in diverting bubbles away from the instruments, even during high sea states. Anomalously high O_2 and N_2 signals can still be measured during elevated sea states, but these result from bubble dissolution in the seawater lines upstream of the PIGI system.

The installation of the pump downstream of the gas sensors and the direc-

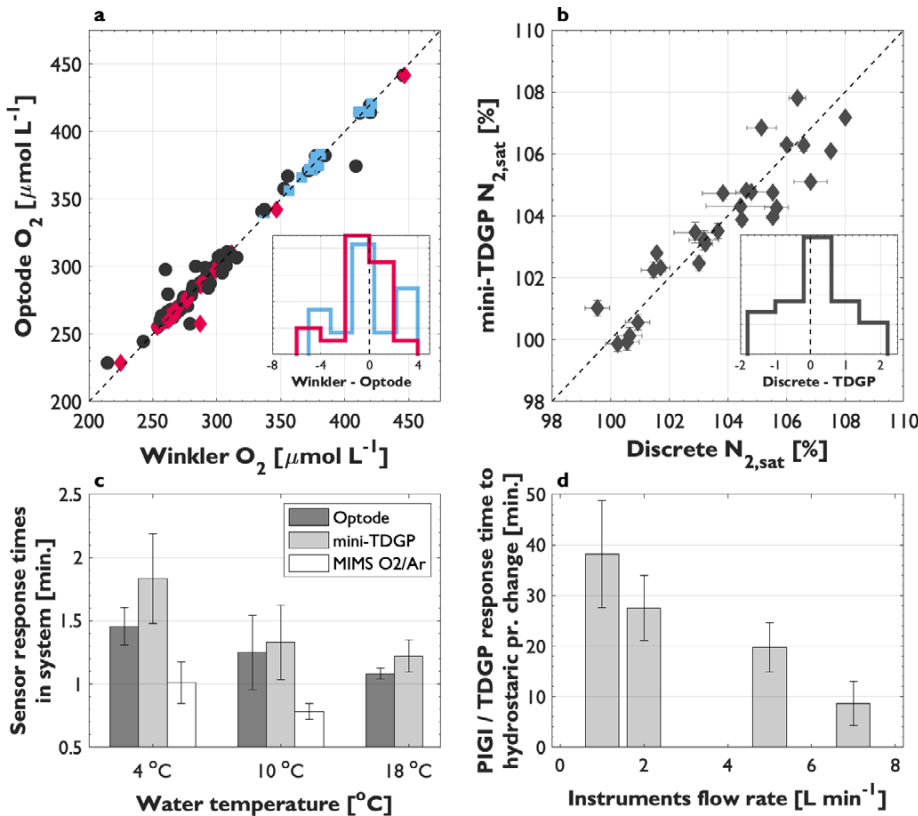


FIGURE 3. Field validation of PIGI-derived O_2 (a) and N_2 (b) against discrete samples. Black markers represent samples obtained from Niskin bottles, and colored markers (blue = Arctic; red = Subarctic Northeast Pacific) are for samples obtained from the PIGI system discrete sampling line. Sensor data have been adjusted for offsets using the discrete samples. The insets in (a) and (b) show the residuals between sensor-derived and discrete gas data, with the y-axis representing the proportion of data points. N_2 saturation ($N_{2,sat}$) represents the seawater concentration normalized to the equilibrium concentration at one standard atmosphere. Panel (c) shows the instrument response times in the PIGI system determined in the laboratory as those required for re-equilibration after a change in the inflowing sample water composition. The response time of a MIMS system, determined under the same conditions, is shown for reference. Error bars represent the range of values recorded during repeat experiments and at different instrument flow rates ($1\text{--}3 \text{ L min}^{-1}$). Panel (d) shows the response time of the mini-TDGP in the PIGI to changes in hydrostatic pressure caused by altering the flow rate through the system. The x-axis corresponds with the flow rate through the instrument chamber during re-equilibration, and error bars represent the standard deviation of values at 4 $^{\circ}$, 10 $^{\circ}$, and 18 $^{\circ}$.

tion of flow onto the instruments' sensing faces (Figure 1) are important for minimizing response times and maintaining neutral hydrostatic pressure within the system. Flow rate changes through the instrument loop following pulses in the discharge from the ship's seawater supply induce hydrostatic effects on GTD measurements analogous to pressure changes during depth profiling (Reed et al., 2018). The PIGI system was designed to minimize these flow-dependent effects and includes flow-rate monitoring for diagnosing such artifacts. Laboratory tests show that GTD response times following such disturbances range between ~10 min and 1 hr, depending on flow rate (Figure 3d). For this reason, it is important to maintain system flow rates as high and as constant as possible.

We also performed side-by-side field deployments of PIGI and MIMS systems (Figure 1e). The results (Figure 4) demonstrate strong coherence between $\Delta O_2/N_2$ and $\Delta O_2/Ar$ across small-scale hydrographic frontal features in Canadian Arctic waters. Offsets between the NCP tracers result from the relatively slow GTD signal and from the slightly different solubility properties of N_2 and Ar . These offsets can be minimized, however, through simple time-response corrections on underway signals (e.g., Bittig et al., 2014; Hamme et al., 2015) and careful evaluation of physical contributions to excess N_2 saturation (manuscript in preparation; Tortell et al., 2015). These results show significant promise for the widespread application of PIGI systems to increase spatial coverage of NCP estimates.

RECOMMENDATIONS AND FUTURE MODIFICATIONS

Throughout system development and testing, we made modifications to PIGI hardware and software to improve overall performance and ease of deployment. Based on our field and laboratory testing of previous versions of the system, we find that the present configuration maximizes data quality. Importantly, the PIGI

was designed for unattended use by operators with little or no previous experience with the relevant instruments. We suggest that future deployments of optode/GTD systems follow similar principles to those discussed here, while considering several recommendations for additional improvements.

Accurate quantification of NCP from O_2/N_2 measurement systems requires ancillary temperature and salinity (T/S) data sets and O_2 calibrations to achieve a desired accuracy of 1%. The latter can be achieved through Winkler analyses on discrete seawater samples or in-air measurements following the approach used on biogeochemical Argo floats (Bittig and Körtzinger, 2015). Nitrogen derivation relies on accurate O_2 and GTD pressure observations, which can be calibrated from in-air measurements made prior to and following deployments. Future PIGI

designs may incorporate an air-pumping system (Bushinsky and Emerson, 2013), so that air-based calibrations could be performed during deployments.

Moreover, T/S data are necessary for performing post-processing calculations on PIGI measurements, including O_2 salinity compensation and the determination of gas partial pressures (details in the online supplementary materials). While optodes include a temperature sensor, salinity measurements must be obtained from separate sensors. If T/S measurements are not made elsewhere on the deployment platform, a salinity sensor can be incorporated in the PIGI instrument loop.

Future systems may also benefit from a smaller optode chamber, which would decrease the optode response time (at a given flow rate) by reducing the optode chamber flushing time. We note, how-

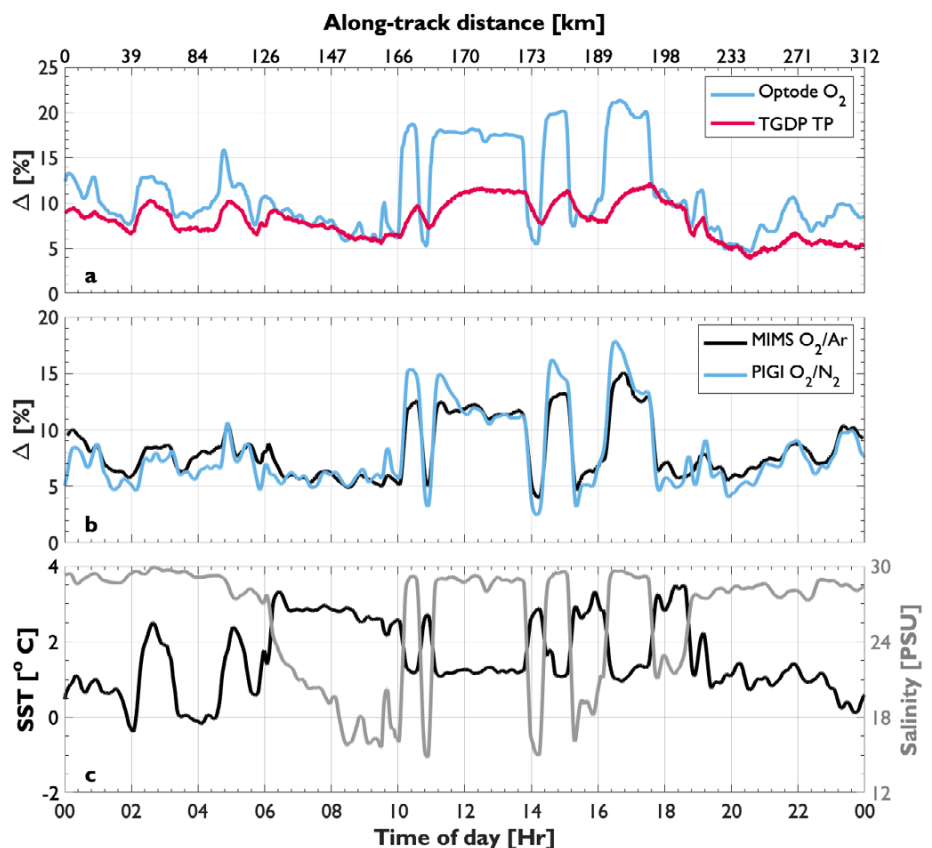


FIGURE 4. One day of field observations from side-by-side deployments of PIGI and MIMS systems near a fjord in the Canadian Arctic. Panel (a) shows the calibrated optode and GTD measurements (normalized to the O_2 equilibrium concentration at ambient sea level pressure and 1013.25 mbar, respectively), with Pro-Oceanus GTD signals seen to lag behind O_2 in strong frontal regions. Derived NCP tracers, $\Delta O_2/N_2$ and $\Delta O_2/Ar$, are presented in (b) and hydrographic data are shown in (c).

ever, that the response time of the GTD in our system remains most limiting to higher resolution $\Delta O_2/N_2$ measurements. In addition, seawater should be pumped rapidly through the primary chamber to reduce overall system response times and minimize the impact of potential bubble dissolution. To limit hydrostatic pressure effects on GTD measurements, a flow controller may be installed in the instrument loop. In its absence, a stable flow rate through the instrument loop should be measured and maintained in order to minimize excursions in the GTD data.

CONCLUSIONS

We describe an automated, user-friendly optode/GTD system capable of high-resolution and accurate O_2/N_2 measurements from a continuous seawater supply. The system has been tested and deployed under a wide range of laboratory and oceanographic conditions and has produced high-quality data from deployments on various platforms. Based on insights from these deployments, we provide recommendations for successful PIGI operation and include detailed designs for the system hardware and software in the online supplementary materials. The system we describe here may be deployed on research vessels and voluntary observing ships or at land-based field stations with a continuous seawater supply. Widespread deployment of the underway PIGI system would lead to a significant expansion of global NCP measurements, providing better understanding of large-scale oceanic responses to ongoing climate variability. 

ONLINE SUPPLEMENTARY MATERIALS

The supplementary materials are available online at <https://doi.org/10.5670/oceanog.2020.214>.

REFERENCES

- Bittig, H.C., and A. Körtzinger. 2015. Tackling oxygen optode drift: Near-surface and in-air oxygen optode measurements on a float provide an accurate in situ reference. *Journal of Atmospheric and Oceanic Technology* 32:1,536–1,543, <https://doi.org/10.1175/JTECH-D-14-00162.1>.
- Bittig, H.C., B. Fiedler, R. Scholz, G. Krahnmann, and A. Körtzinger. 2014. Time response of oxygen optodes on profiling platforms and its dependence on flow speed and temperature. *Limnology and Oceanography: Methods* 12:617–636, <https://doi.org/10.4319/lom.2014.12.617>.
- Bittig, H.C., A. Körtzinger, C. Neill, E. van Ooijen, J.N. Plant, J. Hahn, K.S. Johnson, B. Yang, and S.R. Emerson. 2018. Oxygen optode sensors: Principle, characterization, calibration, and application in the ocean. *Frontiers in Marine Science* 4(429):1–25, <https://doi.org/10.3389/fmars.2017.00429>.
- Bushinsky, S.M., and S. Emerson. 2013. A method for in-situ calibration of Aanderaa oxygen sensors on surface moorings. *Marine Chemistry* 155:22–28, <https://doi.org/10.1016/j.marchem.2013.05.001>.
- Craig, H., and T. Hayward. 1987. Oxygen supersaturation in the ocean: Biological versus physical contributions. *Science* 235(4785):199–202, <https://doi.org/10.1126/science.235.4785.199>.
- Emerson, S., C. Stump, and D. Nicholson. 2008. Net biological oxygen production in the ocean: Remote in situ measurements of O_2 and N_2 in surface waters. *Global Biogeochemical Cycles* 22(GB3023):1–13, <https://doi.org/10.1029/2007GB003095>.
- Emerson, S., B. Yang, M. White, and M. Cronin. 2019. Air-sea gas transfer: Determining bubble fluxes with in situ N_2 observations. *Journal of Geophysical Research* 124(4):2,716–2,727, <https://doi.org/10.1029/2018JC014786>.
- Haëntjens, N., and E. Boss. 2020. Inlinino: A modular software data logger for oceanography. *Oceanography* 33(1):80–84, <https://doi.org/10.5670/oceanog.2020.112>.
- Hamme, R.C., J.E. Berry, J.M. Klymak, and K.L. Denman. 2015. In situ O_2 and N_2 measurements detect deep-water renewal dynamics in seasonally-anoxic Saanich Inlet. *Continental Shelf Research* 106:107–117, <https://doi.org/10.1016/j.csr.2015.06.012>.
- Kaiser, J., M.K. Reuer, B. Barnett, and M.L. Bender. 2005. Marine productivity estimates from continuous O_2/Ar ratio measurements by membrane inlet mass spectrometry. *Geophysical Research Letters* 32:L19605, <https://doi.org/10.1029/2005GL023459>.
- McNeil, C., D. Katz, R. Wanninkhof, and B. Johnson. 2005. Continuous shipboard sampling of gas tension, oxygen and nitrogen. *Deep Sea Research Part I* 52(9):1,767–1,785, <https://doi.org/10.1016/j.dsr.2005.04.003>.
- Reed, A., C. McNeil, E. D'Asaro, M. Altabet, A. Bourbonnais, and B. Johnson. 2018. A gas tension device for the mesopelagic zone. *Deep Sea Research Part I* 139:68–78, <https://doi.org/10.1016/j.dsr.2018.07.007>.
- Tengberg, A., J. Hovdenes, H.J. Andersson, O. Brocandel, R. Diaz, D. Hebert, T. Arnerich, C. Huber, A. Körtzinger, A. Khripounoff, and others. 2006. Evaluation of a lifetime-based optode to measure oxygen in aquatic systems. *Limnology and Oceanography: Methods* 4(2):7–17, <https://doi.org/10.4319/lom.2006.4.7>.
- Tortell, P.D. 2005. Dissolved gas measurements in oceanic waters made by membrane inlet mass spectrometry. *Limnology and Oceanography: Methods* 3:24–37, <https://doi.org/10.4319/lom.2005.3.24>.
- Tortell, P.D., H.C. Bittig, A. Körtzinger, E.M. Jones, and M. Hoppema. 2015. Biological and physical controls on N_2 , O_2 , and CO_2 distributions in contrasting Southern Ocean surface waters. *Global Biogeochemical Cycles* 29:994–1,013, <https://doi.org/10.1002/2014GB004975>.
- Yang, B., S.R. Emerson, and S.M. Bushinsky. 2017. Annual net community production in the subtropical Pacific Ocean from in-situ oxygen measurements on profiling floats. *Global Biogeochemical Cycles* 31:728–744, <https://doi.org/10.1002/2016GB005545>.
- Zhou, J., B. Delille, F. Brabant, and J.L. Tison. 2014. Insights into oxygen transport and net community production in sea ice from oxygen, nitrogen and argon concentrations. *Biogeosciences* 11:5,007–5,020, <https://doi.org/10.5194/bg-11-5007-2014>.

ACKNOWLEDGMENTS

We would like to thank C. McNeil (University of Washington); R. McCulloch, J. Unger, and D. Lovrity (University of British Columbia); and M. Barry (Pro-Oceanus) for their input on instrument design, testing, and technical support. We thank R. McCulloch, H. Bittig, and one anonymous reviewer for their valuable feedback, and many additional colleagues at DFO Canada, Amundsen Science, Hakai Institute, and INACH (including M. Robert, D. Yelland, C. Manning, W. Burt, Z. Zheng, J. Shiller, T. Venello, A. Timmerman, M. Ahmed, R. Hamme, A. Bourbonnais, W. Evans, K. Pocock, C. Weekes, M. Galbraith, T. Fraser, and M. Belton) for their assistance during field deployments. Funding was provided by NSERC, MEOPAR, and ArcticNet.

DECLARATION OF INTEREST

We declare that there are no known conflicts of interest associated with this work. We have not received financial support from Aanderaa Data Instruments AS or Pro-Oceanus Systems Inc.

AUTHORS

Robert W. Izett (rizzett@eoas.ubc.ca) is PhD Candidate, Department of Earth, Ocean and Atmospheric Sciences, University of British Columbia, Vancouver, BC, Canada. **Philippe Tortell** is Professor and Department Head, Department of Earth, Ocean and Atmospheric Sciences, and Professor, Department of Botany, University of British Columbia, Vancouver, BC, Canada.

ARTICLE CITATION

Izett, R.W., and P.D. Tortell. 2020. The Pressure of In Situ Gases Instrument (PIGI) for autonomous shipboard measurement of dissolved O_2 and N_2 in surface ocean waters. *Oceanography* 33(2):156–162, <https://doi.org/10.5670/oceanog.2020.214>.

COPYRIGHT & USAGE

This is an open access article made available under the terms of the Creative Commons Attribution 4.0 International License (<https://creativecommons.org/licenses/by/4.0/>), which permits use, sharing, adaptation, distribution, and reproduction in any medium or format as long as users cite the materials appropriately, provide a link to the Creative Commons license, and indicate the changes that were made to the original content.

Project EDDIE

Using Real Data in Science Classrooms

By Dax Soule

How does the earth speak to you? Or, perhaps even more importantly, how do you get the earth to speak to your students? As oceanographers, and more broadly as Earth scientists, we know that our planet has a fascinating story to tell, one that is full of an amazing array of interconnected facets. What language does it speak? How do we connect students to this story under normal educational circumstances? How about in the middle of a pandemic?

If you have found yourself suddenly needing to revise how you teach your classes and are interested in incorporating more open inquiry using real data, I would like to introduce you to Project EDDIE (Environmental Data-Driven Inquiry and Exploration; <http://www.projecteddie.org>), funded by the National Science Foundation. (Full disclosure: I am a principal investigator of the project.) Project EDDIE is organized by a community of STEM disciplinary and educational researchers dedicated to providing an onramp for the scaffolded¹ analysis of data in the classroom. Participants include faculty from a wide range of STEM disciplines who serve a broad range of student populations at two- and four-year colleges. They create focused lesson plans using EDDIE modules that are designed to be scalable across different skill levels. An “A-B-C” structure based on how students naturally progress through learning objectives of increasing sophistication (Bybee et al., 2006) allows students to develop quantitative skills while making choices about how to use data when addressing aspects of the questions posed. In comparison

to a procedure-driven laboratory where we give students questions and tell them how to answer them, EDDIE modules are structured to compel students to ask their own questions and thus become invested in finding the answers through the exploration of a publicly available data set.

I have used EDDIE modules in a variety of contexts, ranging from large enrollment, multisection courses to small intensive classes focused on time-series analysis. Most recently, I used the climate change module (https://serc.carleton.edu/eddie/enviro_data/activities/climate_change.html) with ~300 students in the lab sections of our non-majors environmental science and geology courses at Queens College (New York City) this past fall. Our students explored the topic of climate change through the analysis of global temperature and atmospheric CO₂ concentrations using data compiled by the Earth Policy Institute (http://www.earth-policy.org/data_center/). In this lesson, students start by downloading and plotting the average global temperature from 1880 to the present (Figure 1a) using Microsoft Excel. In part A, students are prompted to calculate the rate of change and the R² value for the entire time series to determine if they would conclude that the earth appears to be warming currently. To consider the hypothesis that drastic rises in temperature began in the mid-1900s, students can compare the slope and the R² values for the earlier and later portions of the data set. In part B, we remove some scaffolding, and students do a similar analysis of annual mean CO₂ data from

the Mauna Loa observatory (Figure 1b) with the goal of establishing a modern rate of change for atmospheric CO₂. In part C, students working as almost independent scientists continue to explore how CO₂ and temperature have varied together during modern times. At this point, they make all the choices about which data to analyze in order to expand their analyses into how these trends compare to pre-historic rates of change recorded in Vostok ice cores using data available through the Carbon Dioxide Information Analysis Center (CDIAC, <https://ess-dive.lbl.gov/>).

Project EDDIE provides instructors with a framework for successful lessons that use data while allowing flexibility for adapting the structure for different learning environments or student populations. All modules are anchored in a relevant scientific question, use real data, and are structured in such a way that students become progressively more independent as they are asked to make increasingly sophisticated choices about how to use their data to address questions and communicate results. Each module contains a set of learning objectives, a student handout, an instructor handout, and a slide set with presentation notes. EDDIE modules also include curated data for instructors who choose not to have students access the public data portals. Our studies demonstrate that in the context of Project EDDIE modules, undergraduates are able to work with large data sets to explore both scientific and quantitative concepts. This opportunity results in significant gains in confidence and technical

¹“Scaffolding” breaks learning down into manageable chunks to help students progress toward stronger understanding and ultimately greater independence.

ability, a greater appreciation for large data sets and computer software, and a stronger understanding of the associated scientific concepts. As an instructor, Project EDDIE has helped me introduce students to using data through guided inquiry and provided a structure for communicating the overarching theme that we are here to do hard things. The more I have incorporated data into my teaching, the more my classroom environment and the process of learning has evolved to resemble the actual scientific process.

The sudden disruption of the status quo brought on by the COVID-19 pandemic can be a catalyst for examining new strategies for engaging your students. Project EDDIE is a vehicle for transitioning students from studying our ocean as an assignment to exploring it as an extension of their own curiosity. The vast wealth of publicly available sensor data available through networks such as the Ocean Observatories Initiative (OOI) can take students beyond the idealized figures and plots typical of an oceanography textbook into a world where the inherent messiness of real data is part of the story. EDDIE modules can compel students to question what they see in a fundamentally more engaged way than a textbook alone can provide as context for developing an understanding of statistics and numeracy.

Perhaps the question is not how you get the earth to speak to our students; the earth speaks continuously. Perhaps the real question is, how do we equip a much broader portion of our society to hear what the planet has to say and do the work of trying to understand what it means? As scientists, we have made a lot of progress in making data available, and the Project EDDIE community is currently developing new modules covering oceanography topics ranging from tides to hypoxia in the coastal environment. If you have an oceanographic module you would like to contribute, join our community and apply to attend one of the forthcoming module development workshops. (Go to the Project EDDIE webpage,

<https://serc.carleton.edu/eddie/>, and sign up for announcements.) Engaging students in the study of our ocean is a way to develop quantitative reasoning skills that have broad relevance, and now more than ever we have an opportunity to use sensor networks as a window to the ocean and seafloor. I invite you to join Project EDDIE and help us figure out how to give students real access to authentic, data-rich learning experiences—even in the middle of a pandemic. 📧

REFERENCE

Bybee, R.W., J.A. Taylor, A. Gardner, P. Van Scotter, J.C. Powell, A. Westbrook, and N. Landes. 2006. *The BSCS 5E Instructional Model: Origins and Effectiveness*. BSCS, Colorado Springs, CO, 43 pp.

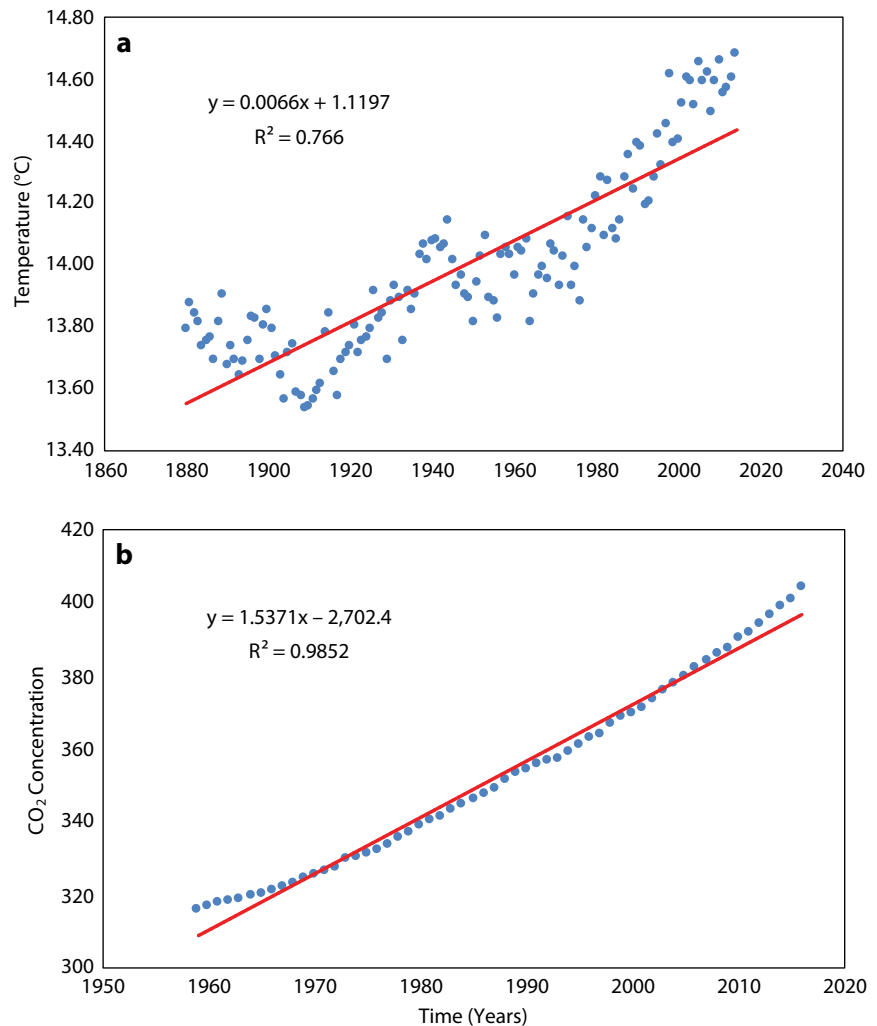


FIGURE 1. Two plots that students are asked to create using Excel in the Project EDDIE climate change module. (a) The average global temperature from 1880 to 2014 using data compiled by the Earth Policy Institute shows variability in its rate of change. (b) Atmospheric data from 1960 to 2016 gathered at the Mauna Loa Observatory in Hawai'i shows a steady increase in CO₂ concentrations over that period.

ACKNOWLEDGMENTS

I'd like to thank Michelle Weirathmueller, Catherine O'Reilly, Rebekka Darner, Megan Kelly, William Wilcock, and Kristin Hunter-Thompson for providing feedback and helping shape this column.

AUTHOR

Dax Soule (dax.soule@qc.cuny.edu) is Assistant Professor, School of Earth and Environmental Sciences, Queens College, Flushing, NY, USA.

ARTICLE CITATION

Soule, D. 2020. Project EDDIE: Using real data in science classrooms. *Oceanography* 33(2):163–164, <https://doi.org/10.5670/oceanog.2020.201>.

COPYRIGHT & USAGE

This is an open access article made available under the terms of the Creative Commons Attribution 4.0 International License (<https://creativecommons.org/licenses/by/4.0/>), which permits use, sharing, adaptation, distribution, and reproduction in any medium or format as long as users cite the materials appropriately, provide a link to the Creative Commons license, and indicate the changes that were made to the original content.

CAREER PROFILES Options and Insights

STEPHANIE WEAR | Senior Scientist and Strategy Advisor,
Global Science, The Nature Conservancy

swear@tnc.org

Degree: When, where, what, and what in?

I earned my BA in environmental science from the University of Virginia in 1996, my master's in marine sciences from the University of North Carolina (UNC), Chapel Hill, in 2000, and my PhD in marine Sciences from UNC Chapel Hill in 2015.

Did you stay in academia at all, and if so, for how long?

No. I had originally intended to get a PhD and go the academic route when I started graduate school, but after taking my comps and completing course work, my advisor moved to a new university. I had the choice of following my advisor and starting over or finishing up and seeing what I could do with a master's degree. I opted for the latter. I didn't return to school to complete my PhD for another 13 years, but fortunately when I did, my credits and requirements were satisfied so I was able to finish very quickly. I hadn't really planned to return for a PhD because my career was very satisfying, and I had been able to get the positions I sought—but then things evolved, and getting my PhD made sense.

How did you go about searching for a job outside of the university setting?

After earning my master's, I wasn't really sure if I wanted to go into conservation, education, or government work. There were not many job options when I was looking in 2000, so I had to get strategic. I took a job doing GIS work for a health research project that I saw as a placeholder, something I wasn't really interested in so that I didn't get stuck in it (inertia tends to get the best of us). So, during

about eight months in that job, I explored all sorts of possibilities, applied for many of them, and saved money. I found that without any experience, it was difficult to land a job, and I wasn't sure what would be interesting and fun. I was offered some positions in outreach and education, but they were not "career" jobs, and I turned them down. I kept looking and finally found a couple of unpaid internships and volunteer opportunities in the US Virgin Islands. I had enough savings to scrape by and keep my student loans from defaulting, so I headed to the Virgin Islands for what was supposed to be three or four months. I didn't know anything about conservation and was hoping to learn. It was baptism by fire—and I was hooked. I loved the work. I loved the people. I loved the place and the challenge, so I stayed. After about five months, I took a full-time position with The Nature Conservancy (TNC) in 2001 and have been working there ever since.

Is this the only job (post-academia) that you've had? If not, what else did you do?

Besides my eight-month stint working on that GIS project, I have been a lifer at The Nature Conservancy.

What is your current job? What path did you take to get there?

I am a senior scientist and strategy advisor on our Global Science Team. The path I took to my current job was always guided by one question: "Will it be fun?" I chose an internship in the Caribbean over a paid position in Rhode Island. I chose a global job that would teach me about the world. I chose working with engaging people in interesting places with a lit-



tle bit of adventure sprinkled in here and there. I often get asked how I got to my position, and to be sure, there is no tried and true way of getting to any job in the environmental space. It was a serendipitous adventure! I started as an intern, then took a position as a protected area specialist that evolved into running the conservation programs for the Virgin Islands and Eastern Caribbean Program. Next, I ran a global coral reef and climate change project, and that evolved into becoming Director of Coral Reef Conservation. At some point in the middle there, I started doing spokesperson work on all topics ocean and nature for TNC. Then I burned out because, well, I go overboard sometimes. So, I stepped back, got my PhD, and now I work on ocean pollution and continue to do spokesperson work for TNC.

What did your oceanographic education (or academic career) give you that is useful in your current job?

My training in oceanography has been the foundation for all of my work. I often say my work is about people, and that is very true. But the ocean science background I have is so important as we work to determine the best strategies, how we measure success, and what sort of questions to ask. It generally helps to have a good understanding of how the system you are working to protect works.

Is there any course or other training you would have liked to have had as part of your graduate education to meet the demands of the job market?

I would encourage students to find ways to get real-world experience outside graduate school and textbook learning. For example, supporting ongoing conservation work, either directly through your studies or in addition to them, will help you better understand the realities of the work as well as begin to build your network before graduation.

Is the job satisfying? What aspects of the job do you like best/least?

I have been at TNC for 19 years, so I would say, my job is satisfying, to be sure. I knew from the beginning that I would

stick around for a long time. There are so many things I love about my job that it is hard to list them, but I would start with the awesome people of TNC. It is very cool to work in a mission-driven environment with people who share your values. I also have loved the diversity of the work—which is pretty much thanks to how messed up our planet is, so I guess that is a mixed bag. The challenge is intense, and there are a million opportunities to be creative and entrepreneurial. In terms of what I like the least, it is really hard to say no, and it feels impossible at times because everything feels important and urgent. Discipline is required to stay sane. I am not very disciplined and have had a few periods of burnout because of it. I always feel like I need a bigger team to

get the job done. But I have learned to be efficient and to maximize the resources available—good life lessons.

Do you have any recommendations for new grads looking for jobs?

My advice is to seek jobs that you think you will enjoy, that will be fun, because you are going to spend a lot of time doing them. Be open to a range of possibilities because there really is no single path to the job of your dreams, and as long as you keep that intent front and center, you will find your way there. I very much believe in the power of setting intentions and then allowing nature to take its course. ☺

KIM I. MARTINI | Senior Oceanographer, Sea-Bird Scientific

kmartini@seabird.com, <https://twitter.com/rejectedbanana>

Degree: When, where, what, and what in?

I completed my undergraduate degrees at the State University of New York at Albany, where I double majored in physics and fine art. After graduation, I stayed in the same department, planning to get a PhD in physics. About a year and a half into it, I realized I didn't want a career where I was trapped in a lab and decided to leave with just a master's degree. After working and figuring out what to do, I moved to Seattle in 2003 to start graduate school (again!) in physical oceanography at the University of Washington. I received my PhD in 2010.

Did you stay in academia at all, and if so, for how long?

After graduating, I moved to the University of Alaska Fairbanks for my first postdoc, researching internal waves and turbulence in the Arctic. In 2013, I returned to Seattle for another postdoc at the University of Washington and NOAA/Pacific Marine Environmental Laboratory, working with the interdisciplinary EcoFOCI group. Its members are oceanographers and fisheries scien-

tists who monitor the Bering Sea ecosystem. The plan when I took the position was to eventually transition to a permanent position within EcoFOCI.

How did you go about searching for a job outside of the university setting?

When I started hunting for jobs during my postdoc years, I knew that I was not going to go down the traditional academic route. Because I had been active on social media and in science communication, I had already seen many of the career opportunities for scientists that existed outside of academia. One of the first things that I did was to make two lists: things in science that I liked to do and things I did not. When I started searching, these lists not only helped me to narrow down which jobs I should apply for, but also to understand whether I was a good fit for positions outside of environmental science.

Another important step was talking to my network outside of oceanography and academia. I would ask my friends questions like: *How did you get your job? What was the application and hiring process like? What do you and don't you like about your*



job? What was your career trajectory to get to this point? Because they had been through the process, they were a wonderful resource for understanding it.

I did my homework. I had a great CV, but that is a highly specialized document intended for other academics and not broadly understood outside of academic settings. Quite honestly, I spent a lot of time googling questions such as: *How do I write a resume? What does a good cover letter look like? How do I translate my skill set for this job? What to do during the interview process?* There are so many great examples out there that can be used as models when you start applying for jobs. Scientists are pretty good at doing research. In this case, I just pivoted

to address the current task of searching for a job.

Lastly, I phoned a friend. After preparing my application, I asked a colleague to review it. We all have strong points, but sometimes we aren't that good at highlighting them. An outside perspective can remind you of the strengths that make you a great fit for the job.

Is this the only job (post-academia) that you've had? If not, what else did you do?

It really depends on your definition of academic. Long-term monitoring with a group based at a government institution has a lot of similarities with a career at a university, but it's not strictly academic with regards to funding and possible career trajectories.

What is your current job? What path did you take to get there?

In simplest terms, my job is to make your data better. But a lot of what I do still mirrors the daily life of an academic. I work at Sea-Bird Scientific, a company that makes instrumentation to study the physical and biogeochemical properties of the ocean. If you have ever used a CTD on a ship, you've used one of our instruments. As Senior Oceanographer, my main responsibility is to be an expert on CTD design and function. I work with engineering to design sensors and with production to streamline manufacturing. I develop processing and analysis tools to improve sensors and data. I collaborate with scientists at various institutions and write peer-reviewed papers. I even design and teach courses.

At the time that I applied for my current job, I wasn't planning on leaving NOAA. But I had been gently exploring other options and applying to a handful of jobs that interested me. I was downloading a manual on the Sea-Bird website and thought, "Why don't I just look if they have any positions available?" And they did! Because I had already been applying, I had practice with the process, and it didn't take long to tailor my resume and cover letter for the application. I also applied even when I didn't have all the

experience listed on the advertisement. I knew that I was bringing a lot of expertise in other areas and could learn the rest when I got the job.

What did your oceanographic education (or academic career) give you that is useful in your current job?

My most useful experience in academia comes from what I call "the year of odd jobs." Between my postdocs, I took on two projects very different from my previous trajectory as an oceanographer. One was designing a data acquisition system for a novel observation platform. The other was mining buoy data to understand sea ice deformation in the Arctic. Both really broadened my skill set and also gave me confidence that I could successfully take on and complete tasks outside my training.

Is there any course or other training you would have liked to have had as part of your graduate education to meet the demands of the job market?

I can only speak for my current position, but I would have liked to have more training in business and managing people. But don't worry if there are gaps in your education when moving outside of academia. When you work in industry, you will often be provided with the training you need to succeed. It's simply not cost-effective for you to spend the time to learn it on your own.

Is the job satisfying? What aspects of the job do you like best/least?

I love my job! I help people with their science, solve difficult problems, and get to work with a lot of very smart and nice people. The atmosphere at Sea-Bird is very social and collaborative. It's rare that I get to spend a day at my desk just quietly doing research. Because we make so many of the instruments that people use to study the ocean, it's really satisfying to know that as a scientist behind the science, even small changes will have a big impact on science globally.

It has not always been an easy transition moving from a research to a manufacturing and business environment.

We use many of the same tools, but the methods and vocabulary are often different. Initially, I was reluctant to learn new processes because I felt it was slowing down my work. But after chatting with a friend who works at another company in the Seattle area, I gave incorporating new approaches into my work a chance. In the end, I found I came up with better solutions and was able to communicate them faster and more clearly among my colleagues. I still struggle sometimes, but it has become easier as I realize that being flexible and open to new ways of doing things can lead to better outcomes overall.

Do you have any recommendations for new grads looking for jobs?

As a person who has left academia, I get asked this question a lot. While I can't say that I am an expert, I have applied for and gotten a job outside academia, I've interviewed over a dozen people for multiple positions across my organization in the past three years, and I've asked people the same question. This is my short summary, written up as a useful to-don't list.

- Don't wait for the perfect job to start applying. In this case, practice does make perfect. If you have already gone through the process, you will be ready when the perfect job does come up.
- Don't ignore the Internet. Get a profile on LinkedIn. Fill out your profile completely. Make a website. Employers do their homework, too.
- Don't be afraid to take risks. Sometimes a different path ends up being the most fruitful.
- Don't do this alone. Lean on your network inside and outside academia. And once you succeed, make sure to pay it forward.
- Don't underestimate yourself. You are all highly capable people. It just doesn't always feel that way when you are in a room full of other highly capable people.
- Don't give up. It takes work to find the job that's right for you. You may not immediately find the right job. You may not. But keep trying—you can do it! 📍

A Tribute to Thomas B. Sanford (1940–2020)

Tom Sanford brought an innovative mind to ocean science. His passion was measuring ocean currents with electromagnetic sensors. This interest led him first to develop a theory for electric currents driven by the flow of conductive seawater in Earth's magnetic field so that measurements could be correctly interpreted, then to design sensors that could measure down to nanovolt accuracy through clever electrode configurations and state-of-the-art low-noise amplifiers using cutting-edge 1970s transistors and integrated circuits.

Throughout his career, Tom always sought ways to improve electrode performance and make measurements that were inaccessible to standard ocean instruments and sampling. He conceived and deployed over a dozen instrument platforms to measure the vertical, horizontal, and temporal structure of ocean flows in the surface mixed layer, stratified interior, and bottom boundary layer, and devised a means to directly measure vorticity and vorticity flux in turbulent boundary layers. Tom proved the feasibility of using a seafloor cable to monitor Florida Current transport, demonstrating its large intra- and inter-annual variability, and leading to long-term monitoring of the Atlantic Meridional Overturning Circulation.

While most of the community was focusing on moored time series in the 1970s, Tom built profilers to uncover the rich vertical and horizontal structure of internal wave motions in groundbreaking work that refined the shape of the internal wave spectrum, established the vertical asymmetry of near-inertial waves from the spiraling of the horizontal velocity vector with depth that has been called the “double helix of physical oceanography,” and described the three-dimensional velocity structure of meso- and submesoscale eddies and boundary currents. His full-depth profilers were later used to study internal tide generation and propagation, identifying the Hawaiian Ridge as a major source of internal tide energy in the North Pacific, and he helped to establish a widespread relationship between finescale internal waves and

ocean turbulence.

Recognizing the limitations of a recoverable profiler, Tom designed an expendable profiler that could be rapidly deployed in heavy seas from ships underway and aircraft. This instrument gained wide use as a submesoscale survey tool for studying the upper ocean's response to storms and hurricanes, near-inertial wave interactions with fronts and eddies, flow-topography interactions such as the impacts of bottom drag and interfacial mixing on the Mediterranean and Denmark Strait outflow plumes, and turbulent dissipation and mixing inferred from a finescale parameterization.

In the last decade, Tom's projects included (but were by no means limited to) augmenting arrays of autonomous profiling floats to measure velocity electromagnetically (EM-APEX) and turbulence with temperature microscale sensors, adding electromagnetic sensors to pressure-gauge-inverted echo sounders (PIES) to measure depth-averaged velocities remotely, and designing an electromagnetic source and sensor array to remotely measure salt wedge variability in river estuaries. His EM-APEX profiling floats have seen wide use, deployed in arrays to make four-dimensional measurements of the submesoscale partition between internal waves and balanced flow, wind generation of internal waves, the evolution of the surface boundary layer, and motions under Antarctic ice. After retiring at 75, he bicycled into the office almost every day to continue developing innovative instruments and conduct fundamental oceanographic research from their data.

Tom earned his undergraduate degree in physics in 1962 and his PhD in mathematics and oceanography with Bill von Arx in 1967. For his scientific and engineering contributions, as well as service on numerous professional committees and as a founding editor for the *Journal of Atmospheric and Oceanic Technology*, Tom was made a fellow of both the American Geophysical Union and American Meteorological Society. He received the AMS Henry Stommel Research Award and IEEE/OES Distinguished Technical Achievement Award, and was



Tom Sanford aboard R/V *Wecoma* with his full-depth absolute velocity profiler during the 2000 Hawaii Ocean Mixing Experiment (HOME).

the Secretary of the Navy/Chief of Naval Operations Chair in Ocean Sciences. Tom was among those who formed The Oceanography Society in 1988, joining as a life member.

For those fortunate to be his collaborators, Tom was an insightful, generous, and kind colleague. Three of his engineers, John Dunlap, Bob Drever, and Art Bartlett, left New England to join him in Seattle, later to be joined by Jim Carlson and Avery Snyder, drawn by the exciting challenges he posed them and the professional rewards of working in his group. He valued all of his many collaborations but perhaps especially those with Tom Rossby, Jim Larsen, Mike Gregg, Jim Price, Rolf Käse, Ann Gargett, Eric D'Asaro, and Peter Spain. He had high standards and pushed everyone around him to do their best, particularly when it came to making the most of seagoing data collection. Tom always acknowledged credit where it was due and tirelessly did everything he could to help his 14 graduate students, nine postdoctoral advisees, and many other early career colleagues get their professional start. As an advisor, Tom gave students and postdocs opportunities to collect their own data and find their own scientific paths. As a collaborator, he did more than his share. As a friend, he could be counted on for advice and support. Tom pulled back the curtain of theory and equations to show us the rich variability of the real ocean. The oceanographic community and world are smaller without him. 📷

Contributed by Eric Kunze and Ren-Chieh Lien

A brilliant oxygen sensor.



Discover how the RBR*concerto*³ CTD and RBR*coda* T.ODO dissolved oxygen optode can improve your profiling, mooring, and vehicle measurements. Available with faster sampling, lower power consumption, and wipeable foils.

RBR
rbr-global.com

SENSORS | LOGGERS | SYSTEMS | OEM



The Oceanography Society
1 Research Court, Suite 450
Rockville, MD 20850, USA

Non Profit Org.
U.S. Postage
PAID
Washington, DC
Permit No. 251

ADDRESS SERVICE REQUESTED



OCEAN SCIENCES

MEETING | FEBRUARY 27 – MARCH 4, 2022
HONOLULU, HI, USA

IMPORTANT DATES:

March 2021

Call for Session Proposals

May 2021

Deadline for Submitting
Session Proposals

June 2021

Session Proposers Notified

July 2021

Call for Abstracts Posted

September 2021

Deadline for
Abstract Submission

November 2021

Presenters Notified
of Acceptance

SPONSORED BY:

